UNIVERSITÀ DEGLI STUDI DI TORINO

DIPARTIMENTO DI PSICOLOGIA

DOTTORATO DI RICERCA IN SCIENZE PSICOLOGICHE, ANTROPOLOGICHE E DELL'EDUCAZIONE

CICLO XXXIV

TITOLO DELLA TESI

Reconceptualizing the Neuroanatomical Landscape of Psychiatric Disorders Using Coordinate-Based Meta-Analytic and Bayesian Approaches

TESI PRESENTATA DA: Donato Liloia

TUTOR: Prof. Tommaso Carlo Brischetto Costa

COORDINATORE DEL DOTTORATO: Prof. Marco Tamietto

ANNI ACCADEMICI: 2018-2022

SETTORE SCIENTIFICO-DISCIPLINARE DI AFFERENZA:

M-PSI/01

Ad Alessandra,

Il mio tutto.

Non ti ringrazierò mai abbastanza.

Table of contents

List of Publications

The present thesis is constituted by an accumulation of peer-reviewed publications accepted and published:

CHAPTER 2

Updating and characterizing neuroanatomical markers in high-risk subjects, recently diagnosed and chronic patients with schizophrenia: A revised coordinate-based meta-analysis. **Liloia, D.**, Brasso, C., Cauda, F., Mancuso, L., Nani, A., Manuello, J., Costa, T., Duca, S., & Rocca, P. 2021. Published in *Neuroscience & Biobehavioral Reviews* 123, 83-103. DOI: 10.1016/j.neubiorev.2021.01.010

CHAPTER 3

Seeking Overlapping Neuroanatomical Alterations between Dyslexia and Attention-Deficit/Hyperactivity Disorder: A Meta-Analytic Replication Study. **Liloia, D.**, Crocetta, A., Cauda, F., Duca, S., Costa, T., & Manuello, J. 2022. Published in *Brain Sciences* 12, 1367. DOI: 10.3390/brainsci12101367

CHAPTER 4

Gray matter abnormalities follow non-random patterns of co-alteration in autism: Meta-connectomic evidence. **Liloia, D.**, Mancuso, L., Uddin, L.Q., Costa, T., Nani, A., Keller, R., Manuello, J., Duca, S., & Cauda, F. 2021. Published in *NeuroImage: Clinical* 30, 102583. DOI: 10.1016/j.nicl.2021.102583

CHAPTER 5

Revealing the Selectivity of Neuroanatomical Alteration in Autism Spectrum Disorder via Reverse Inference. **Liloia, D.**, Cauda, F., Uddin, L.Q., Manuello, J., Mancuso, L., Keller, R., Nani, A., & Costa, T. 2022. Published in *Biological Psychiatry: Cognitive Neuroscience and Neuroimaging*. DOI: 10.1016/j.bpsc.2022.01.007

Other Publications

Atypical local brain connectivity in pediatric autism spectrum disorder? A coordinate-based meta-analysis of regional homogeneity studies. **Liloia, D.**, Manuello, J., Costa, T., Keller, R., Nani, A., & Cauda, F. Published in *European Archives of Psychiatry and Clinical Neuroscience.* DOI: 10.1007/s00406-022-01541-2

Linking neuroanatomical abnormalities in autism spectrum disorder with gene expression of candidate ASD genes: A meta-analytic and network-oriented approach. Camasio, A., Panzeri, E., Mancuso, L., Costa, T., Manuello, J., Ferraro, M., Duca, S., Cauda, F., & **Liloia, D.** 2022. Published in *PloS ONE* 17, e0277466. DOI: 10.1371/journal.pone.0277466

Six actions to improve detection of critical features for neuroimaging coordinate-based meta-analysis preparation. Manuello, J., Costa, T., Cauda, F., & **Liloia, D.** 2022. Published in *Neuroscience & Biobehavioral Reviews* 137, 104659. DOI: 10.1016/j.neubiorev.2022.104659

Retrospective Bayesian Evidence of Null Effect in Two Decades of Alzheimer's Disease Clinical Trials. Costa, T., Manuello, J., Cauda, F., & **Liloia, D.** 2022. Published in *Journal of Alzheimer's Disease*, 1-5. DOI: 10.3233/JAD-220942

Sex differences in brain homotopic co-activations: a meta-analytic study. Bonelli, C., Mancuso, L., Manuello, J., **Liloia, D.**, Costa, T., & Cauda, F. 2022. Published in *Brain Structure and Function* 227, 2839-55. DOI: 10.1007/s00429-022-02572-0

A co-alteration parceling of the cingulate cortex. Manuello, J., Mancuso, L., **Liloia, D.**, Cauda, F., Duca, S., & Costa, T. 2022. Published in *Brain Structure and Function* 227, 1803-16. DOI: 10.1007/s00429-022-02473-2

Tasks activating the default mode network map multiple functional systems. Mancuso, L., Cavuoti-Cabanillas, S., **Liloia, D.**, Manuello, J., Buzi, G., Cauda, F., & Costa, T. 2022. Published in *Brain Structure and Function* 227, 1711-34. DOI: 10.1007/s00429-022-02467-0

Interhemispheric co-alteration of brain homotopic regions. Cauda, F., Nani, A., **Liloia, D.**, Gelmini, G., Mancuso, L., Manuello, J., Panero, M., Duca, S., Zang, Y.-F., & Costa, T. 2021. Published in *Brain Structure and Function* 226, 2181-204. DOI: 10.1007/s00429-021-02318-4

Disentangling predictive processing in the brain: a meta-analytic study in favour of a predictive network. Ficco, L., Mancuso, L., Manuello, J., Teneggi, A., **Liloia, D.**, Duca, S., Costa, T., Kovacs, G.Z., & Cauda, F. 2021. Published in *Scientific Reports* 11, 16258. DOI: 10.1038/s41598-021-95603-5

BACON: A tool for reverse inference in brain activation and alteration. Costa, T., Manuello, J., Ferraro, M., **Liloia, D.**, Nani, A., Fox, P.T., Lancaster, J., & Cauda, F. 2021. Published in *Human Brain Mapping* 42, 3343-51. DOI: 10.1002/hbm.25452

The pathoconnectivity network analysis of the insular cortex: A morphometric fingerprinting. Nani, A., Manuello, J., Mancuso, L., **Liloia, D.**, Costa, T., Vercelli, A., Duca, S., & Cauda, F. 2021. Published in *NeuroImage* 225, 117481. DOI: 10.1016/j.neuroimage.2020.117481

A meta-analytic approach to mapping co-occurrent grey matter volume increases and decreases in psychiatric disorders. Mancuso, L., Fornito, A., Costa, T., Ficco, L., **Liloia, D.**, Manuello, J., Duca, S., & Cauda, F. 2020. Published in *NeuroImage* 222, 117220. DOI: 10.1016/j.neuroimage.2020.117220

Finding specificity in structural brain alterations through Bayesian reverse inference. Cauda, F., Nani, A., **Liloia, D.**, Manuello, J., Premi, E., Duca, S., Fox, P.T., & Costa, T. 2020. Published in *Human Brain Mapping* 41, 4155-72. DOI: 10.1002/hbm.25105

Hubs of long-distance co-alteration characterize brain pathology. Cauda, F., Mancuso, L., Nani, A., Ficco, L., Premi, E., Manuello, J., **Liloia, D.**, Gelmini, G., Duca, S., & Costa, T. 2020. Published in *Human Brain Mapping* 41, 3878-99. DOI: 10.1002/hbm.25093

The Neural Correlates of Time: A Meta-analysis of Neuroimaging Studies. Nani, A., Manuello, J., **Liloia, D.**, Duca, S., Costa, T., & Cauda, F. 2019. Published in *Journal of Cognitive Neuroscience* 31, 1796-1826. DOI: 10.1162/jocn_a_01459

The homotopic connectivity of the functional brain: a meta-analytic approach. Mancuso, L., Costa, T., Nani, A., Manuello, J., **Liloia, D.**, Gelmini, G., Panero, M., Duca, S., & Cauda, F. 2019. Published in *Scientific Reports* 9, 3346. DOI: 10.1038/s41598-019-40188-3

The Neural Correlates of Consciousness and Attention: Two Sister Processes of the Brain. Nani, A., Manuello, J., Mancuso, L., **Liloia, D.**, Costa, T., & Cauda, F. 2019. Published in *Frontiers in Neuroscience* 13, 1169. DOI: 10.3389/fnins.2019.01169

The alteration landscape of the cerebral cortex. Cauda, F., Nani, A., Manuello, J., **Liloia, D.**, Tatu, K., Vercelli, U., Duca, S., Fox, P.T., & Costa, T. 2019. Published in *NeuroImage* 184, 359-71. DOI: 10.1016/j.neuroimage.2018.09.036

Low entropy maps as patterns of the pathological alteration specificity of brain regions: A meta-analysis dataset. **Liloia, D.**, Cauda, F., Nani, A., Manuello, J., Duca, S., Fox, P.T., Costa, T. 2018. Published in *Data in Brief* 21, 1483-95. DOI: 10.1016/j.dib.2018.10.142

The Pathoconnectivity Profile of Alzheimer's Disease: A Morphometric Coalteration Network Analysis. Manuello, J., Nani, A., Premi, E., Borroni, B., Costa, T., Tatu, K., **Liloia, D.**, Duca, S., & Cauda, F. 2018. Published in *Frontiers in Neurology* 8, 739. DOI: 10.3389/fneur.2017.00739

Neuropsychological aspects of Asperger Syndrome in adults: a review. Brighenti, S., Schintu, S., **Liloia, D.**, & Keller, R. 2018. Published in *Neuropsychological Trends*. DOI: 10.7358/neur-2018-024-brig

CHAPTER 1

Introduction and Background

1.1. Context, knowledge gap, and motivation

The human brain is one of the most complex systems in the known universe. Although this organ accounts for only two percent of body weight, it receives about 10 percent of cardiac output and consumes 20 percent of the total oxygen supply (Gusnard et al., 2001). The brain controls cognition, emotion, and sensorimotor domains, to name a few. On the other hand, it is a vulnerable system that can potentially be targeted by several pathological conditions that differ in terms of causes, phenotypic expression, and outcome (Fornito and Bullmore, 2015).

Magnetic resonance imaging (MRI) is a noninvasive imaging technique that has greatly improved our understanding of brain structure and function. MRI is based on the phenomenon of nuclear magnetic resonance and allows us to obtain images of biological tissue with a high spatial resolution, capturing the physical and chemical properties of molecules (Brown et al., 2014). The popular use of MRI in both clinical and experimental settings is due to a number of methodological factors, including the high contrast sensitivity of soft tissue, the non-radioactive nature of in-vivo examination, and the relatively rapid data acquisition (Mulert and Shenton, 2014). Over the last two decades or so, MRI has emerged as an important tool for studying the neuroanatomy of psychiatric disorders in independent cohorts worldwide. In particular, the development of MRI-based analysis techniques with statistical parametric mapping (Friston et al., 1994a), such as voxel-based morphometry (VBM) (Ashburner and Friston, 2000, 2001), has allowed scientists to assess the presence of focal gray and white matter abnormalities in the clinical group of interest compared to the normative population.

Overall, there is a substantial body of VBM literature supporting the notion that the neuroanatomical substrate is altered in individuals with psychiatric conditions (e.g., Birur et al., 2017; Bruin et al., 2020; Davies et al., 2020; Ecker et al., 2015; Madonna et al., 2019; Pereira-Sanchez and Castellanos, 2021; Qiu and Li, 2018; Siehl et al., 2020; Van den Eynde et al., 2012). However, the reproducibility of these results is far from satisfactory. As a result, there is a limited translational impact of MRI findings into clinical practice, and validation of brain-based biomarkers remains an open challenge (Kraguljac et al., 2021; Uddin et al., 2017; Zhuo et al., 2019). A plethora of factors play a role in this knowledge gap. A major issue is that neuroimaging experiments, including VBM, have low statistical power due to a limited

sample size (Samartsidis et al., 2017). Other confounding factors can be attributed to the impact of methodological choices, including image acquisition procedures (e.g., MRI scanner session and sequences, field strengths) (Tardif et al., 2009, 2010), statistical thresholding approaches (Bennett et al., 2009), preprocessing software packages (Diaz-de-Grenu et al., 2014), and pipelines (Zhou et al., 2022). Moreover, the heterogeneity of patients in terms of duration of illness (Meisenzahl et al., 2008a), type of symptomatology (McAlonan et al., 2008), medication status (Chang et al., 2021), neurodevelopmental stage (Ecker et al., 2015), and medical comorbidities (Niedtfeld et al., 2013), makes it challenging to detect a sound neuronal signature for the clinical population of interest. Therefore, rigorous statistical tools are needed to systematically evaluate the findings of previous research on psychiatric disorders.

The term *meta-analysis*, coined by Gene V. Glass (1976), refers to a set of quantitative and data-driven techniques capable of integrating the analytical results of independent investigations on the same topic. The meta-analytic approach is widely used in psychological and biomedical research because it generally ensures high statistical power and reliability (O'Rourke, 2007). In recent years, the so-called coordinate-based meta-analysis (CBMA) has become a valuable tool in the field of brain mapping; its continuous development is justified by the vast but often conflicting body of neuroimaging literature. CBMA aims to identify brain areas of consistent alteration or activation across selected structural or functional neuroimaging experiments. For this purpose, it operates on the list of x-y-z *foci*, namely the three-dimensional spatial coordinates corresponding to the local maximum of brain cluster effects reported by the considered experiments (Manuello et al., 2022). This approach is not only beneficial from a computational perspective but also allows for the reconstruction of original data (i.e., maps with whole-brain image statistics) that are rarely shared by researchers in their published articles (Müller et al., 2018). At the same time, it should be noted that CBMA tools differ from canonical meta-analytic tools.

Consequently, the unique environment of CBMA requires the development of methods capable of addressing the many challenges of brain research. With respect to the clinical population, there is a growing consensus that meta-level investigation of the neural substrate of mental disorders can play an important role in improving diagnosis, prediction, and outcomes (Crossley et al., 2016; Liu et al., 2022; Vanasse et al., 2021). This viewpoint is particularly relevant for neuropsychiatric pathology. For example, the National Institute of

Mental Health (NIMH) Research Domain Criteria (RDoC) project seeks to introduce a novel classification system for psychiatric nosology and diagnosis in which neurobiological measures integrate behavioral signs and symptoms (Cuthbert, 2015; Insel, 2014). On the other hand, a number of researchers question the use of current MRI-based approaches as necessary tools to establish the neural pathophysiology of mental illness because of their limited predictive power (Henson, 2006; Poldrack, 2006), which does not allow for inferences about the disorder-specific neuroanatomical pattern of the illness under study (Cauda et al., 2020b; Sprooten et al., 2017; Zhuo et al., 2021).

The main goal of this dissertation is to design, develop, and apply CBMA tools to study the neuroanatomical landscape of some major psychiatric and neurodevelopmental disorders. More specifically, the present work is an attempt to recharacterize more than 20 years of peer-reviewed VBM literature in the psychiatric context from a meta-analytic perspective. Based on the idea that the development of the CBMA framework would improve our ability to identify core features of the psychiatric brain, this work aims to overcome some drawbacks of clinical neuroimaging in general, and the CBMA environment in particular, by:

- Reviewing the current VBM literature on schizophrenia, attention-deficit/hyperactivity disorder, and autism spectrum disorder. In this way, the merits and limitations of such a popular structural MRI technique for the study of these disabling conditions will be evaluated.
- Using best practice protocols and current state-of-the-art methods in the field of CBMA to establish robust neuroanatomical signatures of the disorders of interest.
- Evaluating the consistency of results between available CBMA methods. Thus, examining the potential impact of key clinical, methodological, and socio-demographic variables on single study outcomes.
- Developing and applying a CBMA framework that enables meta-connectomics, the network analysis of published VBM data.
- Developing and applying a CBMA framework that enables reverse inference reasoning from neuroimaging data. Such inference may be useful to determine the selective neuroanatomical alteration profile of a particular brain disorder.

1.2. Thesis roadmap

This thesis gradually incorporates a selection of peer-reviewed articles that I co-authored during the Ph.D. program in Psychological, Anthropological and Educational Sciences (SPAE) at the University of Turin and Koelliker Hospital. These efforts are both methodological and applied in nature. The first part of the dissertation presents two articles using state-of-the-art CBMA methods that provide a foundation for the following chapters. The second part focuses on the development of innovative CBMA-related tools based on Bayesian statistics and their use in the context of autism spectrum disorder research. A graphical overview of the flow chart of the thesis is given in Fig. 1.1.

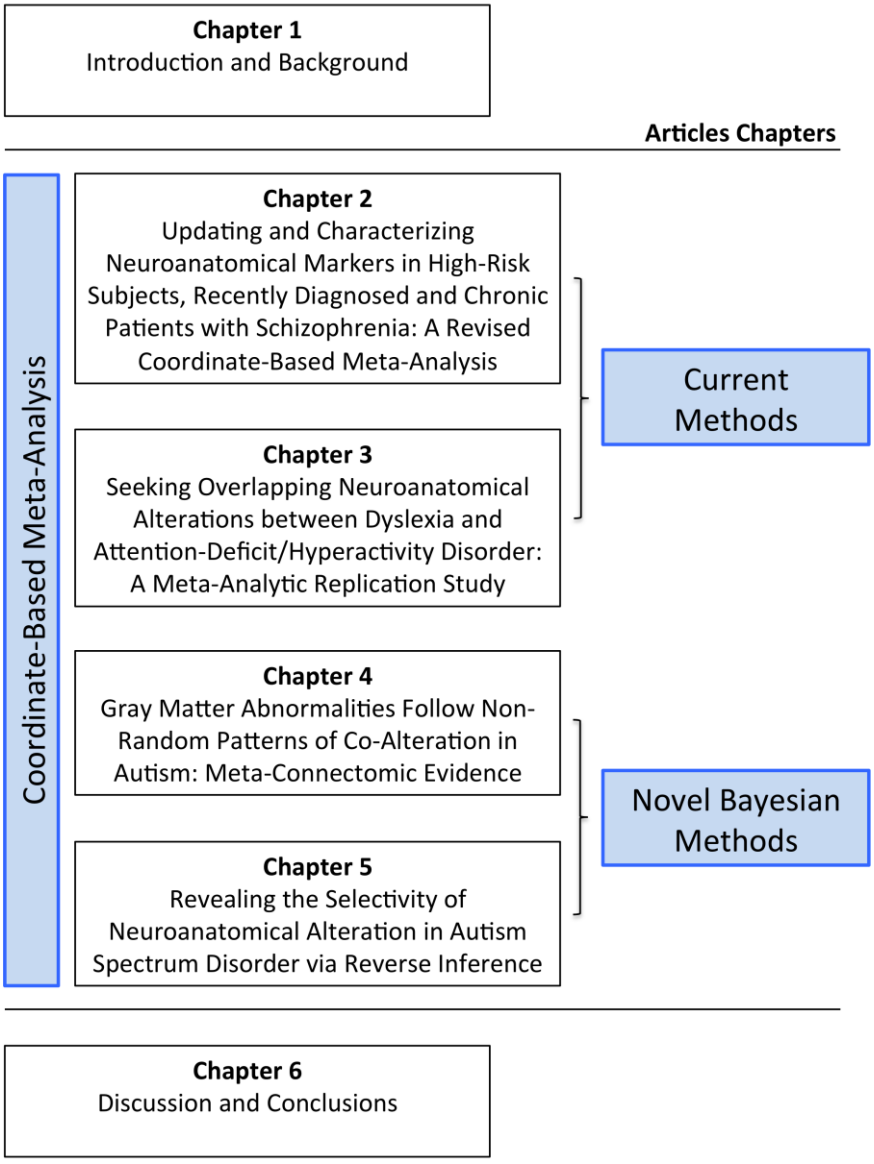

Figure 1.1. Flow chart of thesis chapters.

In the following pages of this Chapter, the role of the voxel-based morphometry technique in understanding the neuroanatomical substrate of major psychiatric disorders is reviewed. As will become apparent, findings in this area of research are largely inconsistent. A discussion of the most likely explanations for these inconsistencies is provided. Thereafter, existing methods for neuroimaging meta-analysis are briefly introduced. Chapter 1 ends with a description of promising directions in the study of the neuroanatomy of psychiatric disorders, particularly with regard to the use of meta-connectomics and reverse inference approaches in neuroimaging.

Chapter 2 introduces the CBMA technique called activation likelihood estimation (ALE), its principles and methodology. The application of ALE to the study of subsequent stages of schizophrenia disorder is presented. Moreover, other corollary neuroimaging CBMA-related techniques are described and applied. The results are discussed in the context of current and conflicting pathophysiological models of the disorder. Chapter 3 evaluates the results in terms of spatial convergence between ALE and another CBMA approach called signed differential mapping-permutation of subject images (SDM-PSI). Here, the current VBM literature on dyslexia and attention-deficit/hyperactivity disorder is considered. A discussion highlighting the strengths and weaknesses of these two approaches is also provided.

Chapter 4 and Chapter 5 are devoted to the study of the complex neuronal substrate of autism spectrum disorder. In both Chapters, special attention is paid to some open questions in autism neuroimaging research and to introduce novel CBMA-based tools based on Bayesian statistics that may overcome them. Specifically, the former presents a meta-connectomics method that aims to identify the largely unclear neuroanatomical co-alteration network that underlies the disorder and characterize it from a graph-theoretic perspective. The latter proposes instead a posterior probability analysis on a massive VBM dataset enriched with published findings on 132 different clinical conditions to identify the selective gray matter profile in ASD. Limitations of the method and possible future clinical applications are discussed.

Chapter 6 concludes by summarizing the main contributions of the selected articles and by reflecting on the long-term challenges of the CBMA approach in the psychiatric context.

1.3. VBM and brain disorders: still an open issue

MRI has evolved extensively over the past three decades, offering an unprecedented array of digital techniques for the study of the human brain. VBM is probably the most popular technique of structural MRI analysis in the experimental field, with more than 6,000 peer-reviewed studies published to date (Zhou et al., 2022). The main goal of VBM is to detect voxel-wise focal differences in brain gray and white matter composition (i.e., tissue concentration or regional volume) by means of a between-group comparison (Ashburner and Friston, 2000); VBM has gained popularity in the human brain mapping community because it has several advantages over previous manual region-of-interest delineation techniques, including the hypothesis-free, whole-brain, and data-driven nature of the investigation accompanied by high spatial accuracy, even for complex or deep brain structures (Ashburner and Friston, 2001; Ridgway et al., 2008).

Standard VBM analysis is based on the frequentist approach to inference (Costa et al., 2021). It uses parametric statistics such as the two-sample t-test, thus brains of the subjects must be sampled from a normally distributed population. VBM takes advantage of T1-weighted MRI scans that detect signals based on the T1 relaxation time of the different body tissues (Scarpazza and De Simone, 2016). Net of differences among publicly available software packages (e.g., SPM-VBM, Statistical Parametric Mapping; FSL-VBM, FMRIB Software Library voxel-based morphometry), VBM preprocessing consists of three basic steps. For a detailed technical description see also Mechelli et al. (2005) and Whitwell (2009).

First, T1-weighted brain data of the subjects are normalized in a common stereotactic space (i.e., customized templates, Talairach - TAL (Talairach and Tournoux, 1988) or Montreal Neurological Institute - MNI (Evans et al., 1993)). This step is necessary to correct for inhomogeneities or differences in brain size between subjects. Second, the normalized images are segmented into three different tissue components (i.e., gray matter, white matter, and cerebrospinal fluid) using Bayesian cluster analyses that assess the different signal intensities of each voxel (Watkins et al., 2001). It is important to note that at this level of preprocessing, the researcher may decide to modulate the data to compensate for volumetric differences created during the normalization step. In this case, it is possible to measure the absolute volume of both gray matter and white matter. In contrast, non-modulation of the data allows the evaluation of the relative concentration of gray matter or white matter (Kurth et al., 2015). The third and final preprocessing step is the application of an isotropic Gaussian

smoothing kernel to the images to ensure the normal distribution of the data and thus increase the validity of subsequent parametric tests (Mechelli et al., 2005). The smoothing process is also useful to compensate for the spatial normalization variability across analyzed brains (Salmond et al., 2002).

After these steps, the voxel-wise statistical analysis between the experimental group and the control group is performed. Here, parametric statistics using the Gaussian random field (GRF) or general linear model (GLM) are often used to identify potential differences in gray/white matter volume or concentration between groups (Whitwell, 2009). Importantly, although VBM performs an operator-independent and largely automated analysis, each preprocessing step adds sources of variability that can lead to Type I errors. Another potential source of false positives comes from multiple testing of parametric statistics performed over 100,000 voxels (Scarpazza et al., 2015). Therefore, results are usually corrected for multiple comparisons, including corrections for false discovery rate (FDR) (Genovese et al., 2002) and family-wise error (FWE) (Friston et al., 1994b).

The output is a statistical parametric map (Friston et al., 1994a), a three-dimensional image of t-statistics, which reveals voxel-wise clusters of the brain where the null hypothesis is rejected. Specifically, VBM can be used to detect two types of focal effects or changes in the brain: the so-called morphometric reduction/atrophy (or *decrease* in gray/white matter; experimental group < control group) (Nani et al., 2021) and increment (or *increase* in gray/white matter; experimental group > control group) (Mancuso et al., 2020), respectively. A number of pathophysiological mechanisms have been proposed that may underlie the changes detected with VBM, such as deficits in synaptogenesis (Sarrazin et al., 2019), neuronal or glial genesis (Eriksson et al., 1998; Rocha et al., 1998), dendritic spine stability or density (Buoli et al., 2017; Grutzendler et al., 2002), and neurovasculature (Reiss et al., 2004; Zatorre et al., 2012). However, this highly relevant topic continues to be under investigation (Naegel et al., 2017), especially in the context of mental and neurological disorders (Mancuso et al., 2020).

Since its initial application in 1995 (Wright et al., 1995), VBM has been used in many different areas of research, from biological sex differences (e.g., Good et al., 2001a), learning and practice (e.g., Maguire et al., 2000), structural plasticity (e.g., Zou et al., 2012) to healthy aging (e.g., Good et al., 2001b) and forensic sciences (e.g., Puri et al., 2008). In particular, the study of brain disorders has benefited tremendously from the advent of this technique. An

impressive number of studies have investigated the presence of neuroanatomical patterns of decrease in neurological disorders compared to healthy controls. For this group of conditions, other VBM-oriented work has also examined distinct and common focal degenerations between two or more clinical phenotypes, as well as assessed the neural substrate that underlies the transition from subclinical or mild to the full-blown manifestation of the disease (Scarpazza and De Simone, 2016).

Alzheimer's disease is a paradigmatic case. A substantial body of studies has found that a set of temporoparietal areas typically show a volume and concentration decrease in this common form of dementia, including the medial temporal lobe, entorhinal cortex, hippocampus, posterior cingulate cortex, and thalamus (Li et al., 2012; Manuello et al., 2018). In order to better define the neuroanatomical aberrations underlying clinical stage or differential symptomatology, part of this literature has also compared Alzheimer's disease with mild cognitive impairment (Ribeiro and Busatto, 2016), frontotemporal lobar degeneration (Rabinovici et al., 2007), dementia with Lewy bodies (Colloby et al., 2014), or hippocampal sclerosis (Woodworth et al., 2020), to name a few. However, a similar use of the VBM approach can be also found in other neurological and neurodegenerative disorders, such as Parkinson's disease and atypical parkinsonian syndromes (Saeed et al., 2020), epilepsy (Yasuda et al., 2010), chronic pain conditions (Kang et al., 2010), multiple sclerosis (Barbi et al., 2022), and amyotrophic lateral sclerosis (Grolez et al., 2016).

VBM is considered one of the most influential neuroimaging tools that have challenged the historically dominant perspective of psychiatric disorders as functional impairments with no demonstrable abnormal organic substrate (Beer, 1996; Berrios and Beer, 1994; Crossley et al., 2018; Kendler, 2012; Reynolds, 2018). In fact, starting from the seminal work of Wright et al. (1995), VBM has been employed extensively to examine the neuroanatomical landscape of psychiatric disorders, a clinically heterogeneous group of disabling conditions characterized by apparent impairments in behavior, cognition, and emotion domains due to biopsychosocial dysfunction of mental operation (American Psychiatric Association, 2013). Schizophrenia (SZ), attention-deficit/hyperactivity disorder (ADHD), and autism spectrum disorder (ASD) are three major neurodevelopmental and psychiatric disorders that have increased in prevalence in recent decades (Chiarotti and Venerosi, 2020; Chung et al., 2019; Wu et al., 2018) and impose a significant economic burden on society, both directly and indirectly (Christensen et al., 2020; Trautmann et al., 2016). Because of their unclear etiology,

complex symptomatology and neurodevelopmental trajectories, they are considered prototypical disorders in the human brain mapping community.

At the time of writing, VBM research on SZ counts more than 90 peer-reviewed studies (see Chapter 2 for a systematic review and description) indicating consistent focal gray and white matter reductions in widespread neuronal networks compared to healthy controls, encompassing a range of high-level, sensorimotor, cerebellar, and limbic territories (Birur et al., 2017; Isobe et al., 2016; Shepherd et al., 2012). On the other hand, a small subset of this literature has also found increases in gray matter volume and concentration (Bassitt et al., 2007; Giuliani et al., 2005; Henze et al., 2011; Horacek et al., 2012; Oertel-Knöchel et al., 2012; Poeppl et al., 2014; Sheng et al., 2013; Wagshal et al., 2015) that are likely due to medication usage (Mancuso et al., 2020). Available etiological models of SZ hypothesize that both neurodevelopmental and progressive pathogenic factors play a role in the etiology of the disorder (Altamura et al., 2014; Anderson et al., 2014), with specific epicenters of brain damage occurring at the preclinical stage and atrophy accelerating at the chronic stage (Buoli et al., 2017; Nenadić et al., 2017). However, there is limited direct, and conflicting, evidence for this from VBM and other neuroimaging techniques adopting a longitudinal or a cross-sectional stage-based design (Asami et al., 2012; Chang et al., 2016; Lei et al., 2015; Nenadic et al., 2015; Schaufelberger et al., 2011; Torres et al., 2016; Zhao et al., 2018).

Abnormalities in neuroanatomy have been repeatedly observed in different cohorts of individuals with ADHD (Castellanos, 2002; Pereira-Sanchez and Castellanos, 2021). A number of VBM studies reveal consistent patterns of gray matter decrease in early childhood and adolescence, particularly in the basal ganglia, orbitofrontal area, and cingulate cortex (He et al., 2015; Johnston et al., 2014; Kumar et al., 2017; Overmeyer et al., 2001); hence in nodes considered to be forming part of the functionally defined salience (Seeley et al., 2007) and default-mode (Raichle et al., 2001) networks. On the other hand, no changes (Saad et al., 2017; Villemonteix et al., 2015a) or atypical increases in gray matter (Brieber et al., 2007; Iannaccone et al., 2015; Kappel et al., 2015; Sutcubasi Kaya et al., 2018) were also observed in ADHD subjects compared with age-matched controls. VBM, which focuses on ADHD in adulthood, is an area of research that has received less attention (Moreno-Alcázar et al., 2016). Here, results are inconclusive and often do not show significant structural changes (Amico et al., 2011; Onnink et al., 2014; Seidman et al., 2011). For a more detailed discussion, see Chapter 3. Overall, the trend of results from the VBM literature suggests a

lack of reliable neuroanatomical effects in ADHD, possibly due to age and other clinical and socio-demographic variables.

Starting with the pioneering work of Abell et al. (1999), VBM has produced more than 50 peer-reviewed studies on ASD (details in Chapter 4 and Chapter 5). The broad spectrum of clinical manifestations of this cluster of neurodevelopmental conditions has its counterpart in the heterogeneous neuroanatomic signature. Several studies comparing pediatric individuals with ASD to age-matched neurotypical control subjects show a significant increase in gray matter in prefrontal, temporoparietal, limbic, and occipital areas in the disorder (Cheng et al., 2011; Foster et al., 2015; Mengotti et al., 2011; Pappaianni et al., 2018; Salmond et al., 2005; Waiter et al., 2004; Wang et al., 2016a). However, a closer examination reveals results without significant (Albajara Sáenz et al., 2020; Groen et al., 2011; Poustka et al., 2012) or opposite effects at the level of the cerebellum, precuneus, frontal lobe, fusiform gyrus, cingulate, and occipital cortices (Bryńska et al., 2021; Cai et al., 2018; McAlonan et al., 2005; Ni et al., 2018; Yang et al., 2018). Other studies shed light on the relationship between neuroanatomy and the autistic phenotype in adulthood. Also for this developmental stage, VBM has noticed mixed patterns of gray matter decreases and increases in a variety of associative, perceptual, and cerebellar areas (Ecker et al., 2012; Lai et al., 2015; McAlonan et al., 2002; Mueller et al., 2013; Sato et al., 2017; Toal et al., 2010). Despite the neuroimaging literature on ASD has largely relied on analysis of high-functioning and male individuals (Müller, 2014), some studies have also explored the relationship between focal variations detected with VBM and biological sex (Beacher et al., 2012; Lai et al., 2013; Retico et al., 2016) or symptom severity (Contarino et al., 2016; Riva et al., 2013; Riva et al., 2011), for example using multiple regression analysis with standardized assessment scores (Eilam-Stock et al., 2016; Rojas et al., 2006). In summary, VBM research on ASD has produced an extensive body of evidence; nevertheless, inconsistencies and unanswered questions remain. Methodological and conceptual improvements are sorely needed to unravel the close relationship between the neuroanatomical substrate and the disordered behavioral manifestations in ASD.

1.4. The need for a CBMA approach

Taken together, VBM-based findings on neuroanatomy in SZ, ADHD, ASD, and other brain disorders suggest widespread but frequently inconsistent patterns of gray matter

impairment across the lifespan. This complex background inevitably affects the implementation of VBM insights into daily clinical practice. In other words, existing primary neuroimaging findings have no relevant applications for early disease detection, diagnostic assessment, and treatment outcome evaluation in single individuals with mental illness (First et al., 2018; Scarpazza et al., 2020; Uddin et al., 2017; Woo et al., 2017). There are many reasons that at least partially explain this translational gap. The small sample size of single studies in brain research (i.e., median sample sizes of 14.5 and 47-50 subjects in clinical fMRI and VBM studies, respectively (Fusar-Poli et al., 2015; Szucs and Ioannidis, 2020)) has historically been considered a critical source of low statistical power, reducing the likelihood of detecting true effects (Button et al., 2013; Carp, 2012; Samartsidis et al., 2017) and inflating the number of false positive outcomes (Fusar-Poli et al., 2015; Lorca-Puls et al., 2018; Szucs and Ioannidis, 2020). Over the past 15 years, however, the substantial increase in sample size in neuroimaging investigations has mitigated this issue (Woo et al., 2017). The analysis of thousands of clinical subjects per study has become feasible thanks to the development of multi-site large-scale MRI data sharing initiatives, such as SchizConnect (Wang et al., 2016b), Autism Brain Imaging Data Exchange (ABIDE) (Di Martino et al., 2014), ADHD-200 Consortium (2012), Alzheimer's Disease Neuroimaging Initiative (ADNI) (Weiner et al., 2017), international Study to Predict Optimized Treatment for Depression (iSPOT-D) (Williams et al., 2011), Parkinson's Progression Markers Initiative (PPMI) (Marek et al., 2011), Pain and Interoception Imaging Network (PAIN) (Labus et al., 2016), and Enhancing NeuroImaging Genetics through Meta-Analysis (ENIGMA) Consortium (Thompson et al., 2014).

In recent years, a number of authors have pointed out other causes of poor reproducibility in the VBM environment that are attributable to methodological factors. In particular, it has been adequately demonstrated that the use of different available processing pipelines, statistical thresholding strategies, and software packages for the same dataset impact profoundly on scientific results, both in terms of spatially distributed overlap and between-pipeline/algorithm reliability (Cheng et al., 2011; Contarino et al., 2016; Li et al., 2020; Popescu et al., 2016; Rajagopalan and Pioro, 2015; Rajagopalan et al., 2014; Scott-Wittenborn et al., 2017; Senjem et al., 2005; Yankowitz et al., 2021; Zhou et al., 2022). In addition, clinical and socio-demographic characteristics are known to influence VBM results when focusing on pathological populations. This is exactly the case of the biological sex

recruitment (i.e., sex-stratified vs. sex-mixed analysis), type of symptomatology, medication status of clinical subjects (i.e., drug naïve vs. treated vs. mixed), duration of illness (i.e., recent diagnosis vs. chronic stage vs. mixed stage), presence/absence of medical comorbidities, and developmental stage of the clinical group (i.e., age-stratified vs. age-mixed analysis) (Anagnostou and Taylor, 2011; Davies et al., 2020; Evans et al., 2014; Gupta et al., 2014; John et al., 2015; Kappel et al., 2015; Kraguljac et al., 2021; Lai et al., 2013; Linke et al., 2017; Meisenzahl et al., 2008a; Villemonteix et al., 2015b; Wang et al., 2022; Wilson et al., 2009).

Against this background, the meta-analytic approach provides a powerful assessment that can combine available VBM data in a quantitative and spatially unbiased manner. In the field of human brain mapping, there are two main categories for meta-analysis of published results, namely image-based meta-analysis (IBMA) and coordinate-based meta-analysis (CBMA). Collectively, these methods are considered voxel-based analyses and thus are capable of performing a statistical calculation for each brain voxel; however, they differ in terms of spatial accuracy (Radua and Mataix-Cols, 2012a). Whereas IBMA uses the statistical parametric maps of the original studies to perform the quantitative synthesis (Lazar et al., 2002), CBMA analyzes the three-dimensional spatial coordinates (also called stereotactic coordinates or x-y-z foci) corresponding to the local maximum of brain cluster effects reported in the original study (Wager et al., 2007). By definition, ICBMA methods operate at a more precise level of information than CBMA and should therefore be preferred (Salimi-Khorshidi et al., 2009). However, their use is severely hampered by the fact that authors rarely provide the voxel-wise whole-brain statistical maps in their articles and no effective system for published data sharing exists. On the other hand, stereotactic coordinates of interest can usually be retrieved from peer-reviewed articles indexed in scientific resources and databases (Manuello et al., 2022; Müller et al., 2018; Salimi-Khorshidi et al., 2009; Samartsidis et al., 2017).

In light of this, CBMA has become the most employed meta-analytic approach in the field of neuroimaging (Müller et al., 2018), including for the study of the neuroanatomical alteration substrate in psychiatric disorders (Tahmasian et al., 2019). Over the past two decades, several CBMA-based techniques have been developed, including activation likelihood estimation (ALE) (Turkeltaub et al., 2002), analysis of brain coordinates (ABC) (Tench et al., 2022), clustering the brain (CluB) (Berlingeri et al., 2019), gaussian-process

regression (GPR) (Salimi-Khorshidi et al., 2011), multilevel kernel density analysis (MKDA) (Wager et al., 2007), parametric voxel-based meta-analysis (PVM) (Costafreda et al., 2009), and signed differential mapping (SDM) (Albajes-Eizagirre et al., 2019; Radua and Mataix-Cols, 2009; Radua et al., 2012).

As evidenced by the more than 1,250 publications in scientific peer-reviewed journals (see http://brainmap.org/pubs/ for the complete list), ALE is the most widely used CBMA technique in the world (Acar et al., 2018; Tahmasian et al., 2019) and the one that provides us a more precise spatial similarity to the IBMA results (Salimi-Khorshidi et al., 2009). Although ALE was originally conceived to summarize task-based findings from positron emission tomography (PET) and functional MRI studies, it has been successfully applied in VBM and clinical contexts (Vanasse et al., 2018). Statistical details of the ALE algorithm and a methodological comparison of ALE with other CBMA approaches can be found in the following Chapters. Briefly, the main objective of this technique is to evaluate "if" and "where" the spatial convergence of activation/alteration effects reported in the studies examined is greater than chance. To achieve this goal, a likelihood map is constructed around the foci of activation/alteration for each study. It must be specified that these maps, called modeled activation/alteration (MA) (Laird et al., 2005a), are based on a three-dimensional Gaussian density distribution of (effect) likelihood with kernel variance inversely proportional to the study sample size: a larger sample size corresponds to a smaller kernel and *vice versa* (Eickhoff et al., 2009). Finally, computing the probability of a union, MA maps are merged into the final ALE map, which should be corrected for multiple comparisons, possibly with the family-wise error (FWE) rate and cluster-level inference (Eickhoff et al., 2016). Another feature of this technique is the statistical determination of common and divergent spatial patterns between two or more different ALE maps using a subtraction algorithm (Eickhoff et al., 2011).

The use of ALE has recently gained popularity thanks to the development of GingerALE (https://brainmap.org/ale/), a user-friendly and free software package for implementing the ALE algorithms (Eickhoff et al., 2012). In parallel with the continuous improvements and updates of the ALE environment (Eickhoff et al., 2012; Eickhoff et al., 2011; Eickhoff et al., 2017; Eickhoff et al., 2009; Eickhoff et al., 2016; Frahm et al., 2022; Turkeltaub et al., 2012; Vanasse et al., 2018), the BrainMap project has made available an electronic coordinate-based archive containing peer-reviewed English-language experiments

on functional and structural neuroimaging: the BrainMap database (Fox et al., 2005; Fox and Lancaster, 2002). Although BrainMap contains only a subset of the literature under consideration in this field (Derrfuss and Mar, 2009; Laird et al., 2008; Samartsidis et al., 2020) (at the time of writing, 4,362 VBM experiments, 115,023 subjects, and 29,016 x-y-z foci), it allows us to build search queries according to a standardized taxonomy scheme and extract meta-data of interest in an automated manner, including foci in stereotactic space that are adopted for subsequent ALE analysis (Laird et al., 2005b). Overall, using the BrainMap database whenever possible is a valuable choice because it overcomes the disadvantages of user-based search and selection, which by definition are time-consuming and error-prone (Manuello et al., 2022).

There are five key steps required to perform a CBMA correctly. See Fig. 1.2. for a graphical overview. First, a systematic literature search in scientific databases and resources (e.g., BrainMap, PubMed, Web of Science, Scopus, Google Scholar, etc.) should be conducted based on a clearly defined research question and a combination of appropriate keyword queries. The correct and transparent execution of this step is crucial in order to have high sensitivity with respect to the research question or to ensure the reproducibility of the search process. In this context, best practices, checklists, and reporting guidelines have recently been proposed. Detailed reports can be found in Manuello et al. (2022), Müller et al. (2018), Page et al. (2021), and in Tahmasian et al. (2019).

Second, the literature identified should be systematically assessed. Records that are not primary research articles (e.g., reviews, letters to the editor, commentaries, etc.) are usually excluded after being evaluated at the title or abstract level. Therefore, the full texts of the remaining articles should be checked. Several rules have been proposed to minimize errors at this stage. For instance, two authors can make an independent assessment, and any discrepancies can be resolved by consulting a third author (Müller et al., 2018). Another key rule is to avoid repeated selection of coordinates from the same group of subjects, both within an article (e.g., two or more experiments in a single publication) and between different articles (e.g., the same group in different publications). Effective control of this problem is important because these types of effects are known to influence the results of CBMA (Müller et al., 2018; Turkeltaub and Coslett, 2010; Turkeltaub et al., 2012). Although the specific inclusion/exclusion criteria are necessarily based on the specific research question, the design of CBMA approaches dictates that the x-y-z foci analyzed are from whole-brain imaging

studies. A key methodological assumption of CBMA is that each brain voxel has an equal chance of being active/altered (Eickhoff et al., 2012; Müller et al., 2018; Radua and Mataix-Cols, 2012a). Therefore, the meta-analysis of foci derived from region-of-interest (ROI) or small volume correction (SVC) studies violates this assumption and may introduce bias for specific brain areas (Manuello et al., 2022).

The third step is to collect and organize the meta-data under consideration. Net of differences among the specific CBMA algorithms employed, a file containing the exact x-y-z foci and the number of subjects per study is mandatory. In contrast, other characteristics of the dataset depend on the technique. For example, to minimize spatial dissimilarity between experiments, ALE requires that foci be analyzed in a common stereotactic space (i.e., MNI or TAL); therefore, it is strongly recommended to convert the original foci from TAL to MNI space or vice versa (Laird et al., 2010; Lancaster et al., 2007). Instead, the SDM technique also requires a T-value for each focus (Albajes-Eizagirre et al., 2019). For details, see Chapter 2 and Chapter 3. Moreover, collecting additional meta-data may be useful to perform subanalyses of interest. In the clinical context, this could be the case for clinical and demographic variables, such as stage of development, type of symptomatology, male-female ratio, and level of functioning. This step also requires a transparent organization to ensure the reproducibility of the research and usually consists of reporting meta-data in the form of tables and the availability of foci in supplementary materials (Manuello et al., 2022; Tahmasian et al., 2019).

The fourth and fifth steps consist of a meta-analysis of foci and reporting of results, respectively. Apart from the analytical differences between the available techniques, CBMA requires correction for multiple comparisons in the same way as for between-group studies. This is a necessary step because uncorrected findings have good sensitivity but also a high false positive rate (Müller et al., 2018). There are several corrections in the field of CBMA, but overall it is recommended to find a balance between sensitivity and susceptibility to Type I errors. In this context, empirical simulation work (Eickhoff et al., 2016) has shown that cluster-level FWE correction is the most appropriate method for statistical inference for the ALE environment; in contrast, FDR-based corrections are not recommended. For the SDM environment, Albajes-Eizagirre et al. (2019) recently recommended instead the use of threshold-free cluster enhancement (TFCE) correction in statistical thresholding because FWE-based correction is generally more conservative. After CBMA calculation, statistically

significant brain clusters must be labeled based on a standardized anatomical atlas (e.g., Talairach Daemon, MNI 152 standard, Harvard/Oxford cortical and subcortical atlases, Julich atlases, etc.). Tables should also be created that include important information about the identified clusters, including anatomical location, stereotactic coordinates of maximum value, cluster size (mm^3 or number of voxels), and studies that contribute to the result (Tahmasian et al., 2019).

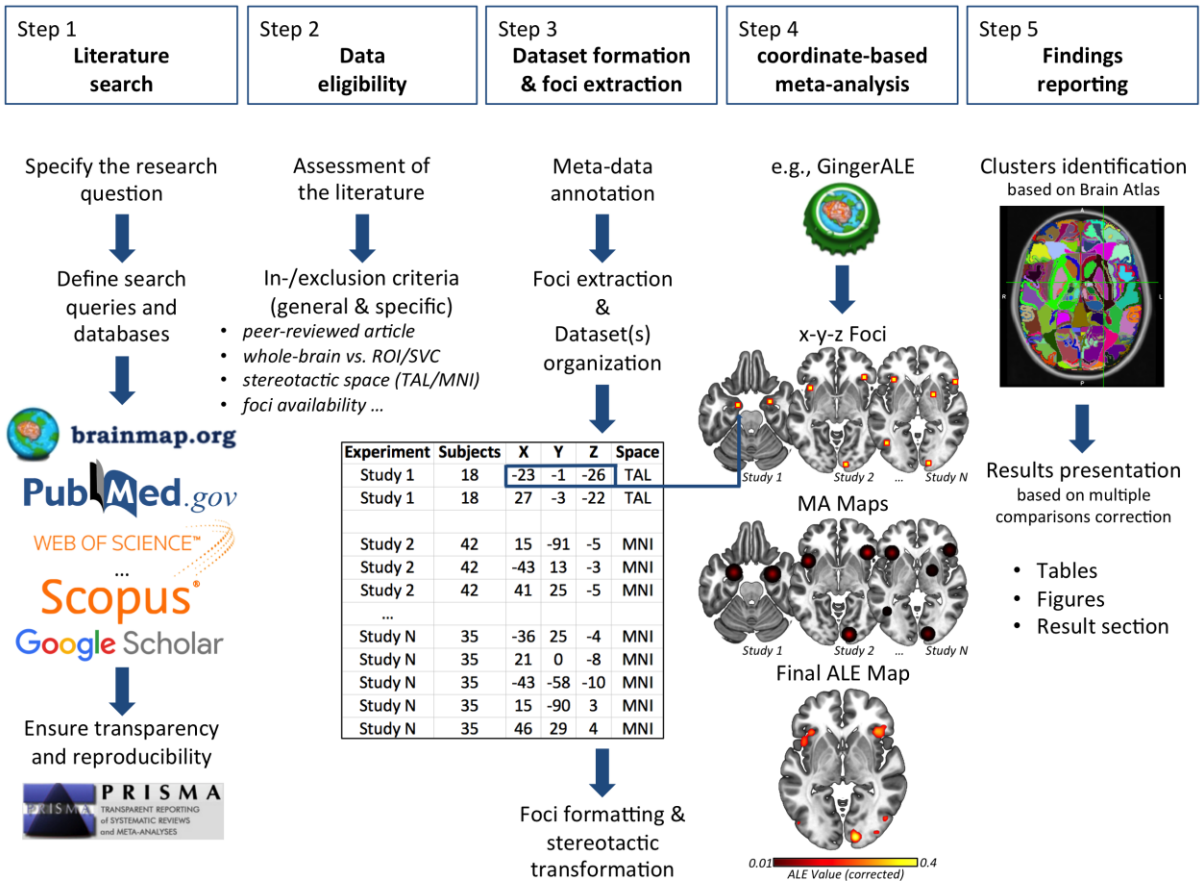

Figure 1.2. Pipeline workflow of coordinate-based meta-analysis (CBMA) method.

Foci, MA maps, and ALE map are shown for illustrative purposes only and are not based on actual data. ALE, activation likelihood estimation; MA, modeled activation; MNI, Montreal Neurological Institute space; PRISMA, Preferred Reporting Items for Systematic Reviews and Meta-Analyses; ROI, region-of-interest; SVC, small volume correction; TAL, Talairach space.

1.5. The need for development of the CBMA approach: meta-connectomics

CBMA has proven to be a powerful and user-friendly tool capable of identifying, in a fully automated and replicable manner, reliable neuronal patterns across brain imaging studies examined. From a structural and clinical point of view, CBMA findings can be interpreted as spatially consistent patterns of neuroanatomical co-alteration in a given brain disorder (Manuello et al., 2022; Müller et al., 2018; Vanasse et al., 2018). It is necessary to note, however, that this type of secondary-level evidence (Fusar-Poli and Radua, 2018) cannot provide information about existing co-alteration patterns at the level of individual studies. As Caspers et al. (2014) have elegantly shown, the final meta-analytic pattern of co-alteration (e.g., *a* = brain cluster 1; *b* = brain cluster 2; *c* = brain cluster 3; *d* = brain cluster 4) might come from one pool of studies identifying the co-alteration between *a*, *b*, *c* and another pool reporting the co-alteration between *b*, *c*, *d*. As a result, no effective co-alteration between *a* and *d* might exist. Overall, this issue makes challenging the study of the existing mutual relationships between two or more brain areas and their topological network organization (Fox et al., 2014). However, the collection of such information could be particularly useful in better characterizing the human brain, with potentially significant implications for understanding brain disorders.

Coined by Olaf Sporns, Giulio Tononi, and Rofl Kötter (2005), the term *connectomics* refers to the "comprehensive structural description of the network of elements and connections forming the human brain" (Sporns et al., 2005) or the so-called connectome. Currently, imaging connectomics refers to a range of neuroimaging approaches that aim to map the complex architecture of the brain at both the micro (Schröter et al., 2017) and macro (Rubinov and Sporns, 2010) levels of resolution. To this end, the brain is conceived as a highly interconnected graph consisting of a series of neuronal units (i.e., nodes) and their functional, structural, or statistical connections (i.e., edges) (Sporns, 2013). Although the "omic" perspective is not new in many areas of biological research (e.g., proteomics, genomics, transcriptomics) (Anderson and Anderson, 1998; Lander, 1996; Milward et al., 2016), it has only been systematically applied to the field of human brain mapping in the last 15 years. Here, methodological advances in functional and structural MRI sequences, combined with the use of graph-theoretic network modeling constructs, have allowed us to identify large-scale features of the brain system, including its small-word architecture (Bassett

and Bullmore, 2017), functional segregation of information (Jbabdi et al., 2013), and rich-club hub organization (van den Heuvel and Sporns, 2011), just to name a few.

The connectome-based approach has also emerged as a valid option for studying whole-brain architecture in psychiatric disorders and has led to the new corollary field of *pathoconnectomics* (Rubinov and Bullmore, 2013). Pathoconnectomics postulates that psychiatric conditions can be viewed as disorders of brain networks by virtue of their anatomically distributed alterations in neural systems (Deco and Kringelbach, 2014; Filippi et al., 2013; Fornito and Bullmore, 2015; Fornito et al., 2017; Fornito et al., 2015; Lord et al., 2017). This view is not without foundation; in fact, it is well known that psychiatric disorders tend to exhibit both structural and functional impairments in brain connectivity (Greicius, 2008; Kumar and Cook, 2002; Woodward and Cascio, 2015). However, canonical connectivity approaches provide only a partial account of brain alteration complexity because of their voxel-wise and localized mapping (Fornito et al., 2015). In contrast, pathoconnectomics has the potential to provide a more detailed high-dimensional mapping, taking advantage of a wide armamentarium of graph-theoretic metrics for characterizing the aberrant topology of neural infrastructure (Fornito and Bullmore, 2015; van den Heuvel and Sporns, 2019).

An important finding from this new area of research is that focal damages are rarely confined to isolated neuronal territories but, instead, tend to exhibit a non-random patterning of diffusion that resembles the connectivity pathways of the brain (Buckholtz and Meyer-Lindenberg, 2012; Cauda et al., 2018; Fornito et al., 2015; Iturria-Medina and Evans, 2015; Iturria-Medina et al., 2014; Warren et al., 2013; Yates, 2012; Yuan et al., 2017). It should be noted that multidisciplinary efforts have suggested several pathophysiological mechanisms that may mediate the large-scale distribution of neuronal alterations in various clinical conditions and influence the progression of injury and associated clinical course.

For example, transneuronal or “prion-like” degenerative mechanisms are thought to underlie the network-like structural atrophy typical of chronic conditions such as tauopathies, synucleinopathies, and amyloidopathies (e.g., Alzheimer’s disease, amyotrophic lateral sclerosis, frontotemporal dementia, Lewy body dementia, Parkinson’s disease) (Bourdenx et al., 2017; Clavaguera et al., 2013; Goedert et al., 2010) as well as psychiatric disorders such as schizophrenia (Korth, 2012). Here, misfolded toxic proteins tend to initially accumulate at specific sites in the brain and spread via synaptic pathways or extracellular uptake, leading to

progressive neuronal shrinkage or death (Fornito et al., 2015; Raj et al., 2012; Warren et al., 2013; Zhou et al., 2012). Two other maladaptive mechanisms are also frequently cited in the pathoconnectomics literature, namely shared vulnerability and nodal stress. The first mechanism relies on evidence that structural deterioration of distributed, but also unconnected, brain areas may result from their shared genetic expression vulnerability (Cioli et al., 2014; Prieto et al., 2008). This type of mechanism has recently been linked to connectome-wide dysconnectivity in patients with neurodevelopmental and psychiatric disorders (de Lange et al., 2019; Radonjić et al., 2021; Romme et al., 2017). The latter mechanism is based on evidence that brain nodes with heavy network traffic in the form of structural connections or functional co-activations (i.e., network hubs) are the most stressed from a functional (Buckner et al., 2009) and metabolic (Tomasi et al., 2013) perspective. As a result, the hubs of the human connectome are extremely susceptible to structural damage in neurological and psychiatric disorders (Cauda et al., 2018; Crossley et al., 2014; Zhou et al., 2012).

Overall, the pathoconnectomics construct has been shown to be highly suitable for primary neuroimaging MRI-based datasets of various types to capture network-like abnormalities in the connectome in individual psychiatric disorders (e.g., Breukelaar et al., 2021; Cao et al., 2014; Collantoni et al., 2022; Di Martino et al., 2017; Narr and Leaver, 2015; Perry et al., 2019). In more recent years, it has been shown to be no less appropriate for CBMA datasets. The concept of *meta-connectomics* was introduced by Crossley et al. (2014; 2016). In their seminal study (Crossley et al., 2014), the authors collected VBM-based foci of alteration from 392 studies (26 different brain disorders; 21,376 subjects) and examined them via ALE technique and structural connectome-wide analysis. The hub areas of the human connectome (i.e., the anterior cingulate cortex, insula, superior temporal gyrus, thalamus, dorsolateral prefrontal cortex, caudate, putamen, and superior parietal cortex) were found to be structurally damaged in many psychiatric and neurological disorders considered. In contrast, areas with non-hub features were generally spared.

The meta-connectomics approach can be considered conceptually similar to the primary large-scale connectomics approach because it takes advantage of voxel-wise neuroimaging maps for subsequent detection of nodes (i.e., brain areas) and their edges (i.e., statistical relationships or connections). However, whereas in primary connectomics approaches the units of analysis are subjects, in a meta-connectomics approach the units of analysis are

studies. Therefore, this exciting analytic extension can leverage large existing neuroimaging datasets to provide attractive perspectives for a deep understanding of the connectome architecture and shed new light on network-level aberrations associated with the psychiatric brain (Crossley et al., 2016). At the same time, however, it is necessary to note that innovative and sound computational CBMA-based methodologies should be developed to achieve these goals.

In this context, one of the main aims of my Ph.D. project was to develop and apply a meta-connectomics method capable of investigating the presence of neuroanatomical co-alteration networks and their aberrant topology in psychiatric disorders. Statistical details and in-depth methodological considerations of this novel approach can be found in Chapter 4. Thus, a short overview is given here.

Called Morphometric Co-alteration Networking analysis (MCN), this CBMA-based approach can be defined as a method able to identify the network-like architecture formed by focal gray matter co-altered neuronal areas. To this end, it uses ALE-derived findings as priors for an unbiased and connectome-wide analysis based on Bayesian statistics. In other words, MCN considers spatially consistent neuroanatomical abnormalities (i.e., nodes) and their statistical co-occurrence across published VBM studies (i.e., edges) as a network unit. This shift also allows the application of a series of graph-theoretic *post hoc* analyses for a topological characterization of the pathological network. Although MCN was originally designed to study the neuroanatomical substrate of single brain disorders, my research group has recently extended its use to other areas of connectomics research, including functional and homotopic connectivity (Bonelli et al., 2022; Cauda et al., 2021; Mancuso et al., 2019), transdiagnostic analysis (Cauda et al., 2020; Mancuso et al., 2020), and parcellation of single brain structures (Nani et al., 2021).

Apart from the differences in its current use, the MCN method consists of three main steps. The first one concerns the preparation of the dataset and the computation of the ALE map, as described in the previous paragraph. It is worth noting that other CBMA or IBMA techniques could also be used; however, they must produce a voxel-wise whole-brain map for each study and a final meta-analytic map of the effect under investigation. Second, network nodes should be generated. For this purpose, the MCN approach uses a peak detection algorithm that identifies the local maxima of spatial convergence of the final ALE map and superimposes spherical regions-of-interest on them, respectively. This data-driven step is

crucial for subsequent analyses because it accounts for focal alterations with very high agreement among the selected studies. Finally, the statistical relationship of co-alteration for each pair of nodes is assessed using Patel's κ index (Patel et al., 2006; Smith et al., 2011). Although this empirical Bayesian technique was originally developed for measuring functional connectivity patterns of the brain (Patel et al., 2006), its data-driven and hypothesis-unconstrained nature also makes it suitable for the meta-analytic and structural neuroimaging research areas. Here, Patel's κ index assesses the likelihood that two nodes can be structurally co-altered against the likelihood of their independent alteration. After assessing the likelihood of co-alteration between each pair of nodes, a general network matrix of neuroanatomical co-alteration is constructed.

From a methodological point of view, an attractive aspect of treating neuroanatomical alterations as a biological network is that graph theory provides a wide range of user-independent and data-driven metrics for identifying the hierarchical position of network elements. For example, measures of node centrality are extremely useful in capturing the *hubness* profile of some network units, namely their central position and associated strong influence on system communication due to the highest degree of connectivity (Hagmann et al., 2008; Rubinov and Sporns, 2010). In particular, degree, closeness, and betweenness are three relatively simple but effective measures of node centrality that are employed collectively for hub detection in human connectomics research (Sporns et al., 2007; van den Heuvel and Sporns, 2013). Statistical details of these metrics can be found in Chapter 4. Importantly, network hubs in the pathoconnectomics scenario should be characterized as *pathological* or *pathoconnectivity hubs* (van den Heuvel and Sporns, 2013, 2019; Worbe, 2015) because they represent areas that play a critical role in propagating neuronal alteration within the network of damage (Fornito et al., 2015; Raj et al., 2012; Zhou et al., 2012).

1.6. The need for development of the CBMA approach: reverse inference

Various neuroimaging approaches, including CBMA, have undoubtedly driven many advances in understanding the neurobiological basis of brain disorders. However, despite considerable effort and important achievements, this decades-long field of research has not yielded significant insights for clinical practice (Etkin, 2019; First et al., 2018; Henderson et al., 2020a; Henderson et al., 2020b; Martinelli and Shergill, 2018). Psychiatric disorders are an exemplary case. Although complementary biological tests are usually performed, the

diagnosis of this group of mental illness conditions is based solely on the assessment of clinical symptoms and signs rather than measurable biomarkers (Iorio-Morin et al., 2022). Furthermore, traditional classification systems such as the diagnostic and statistical manual of mental disorders (DSM) (American Psychiatric Association, 2013) and the international classification of diseases (ICD) (World Health Organization, 1992) define psychiatric disorders as distinct and clearly delineated categories (Tyrer, 2018), even though that several different phenotypes may co-occur in each disorder (Henderson et al., 2020b).

In recent years, this notion has been repeatedly challenged by multidisciplinary evidence, which demonstrated that the biological substrate of psychiatric disorders might not support the current mental illness nosology. Genome-wide association research has revealed a common pattern of genetic activity in psychiatric disorders, with a number of pleiotropic genes that tend to play prominent roles in their neurodevelopment (Anttila et al., 2018; Bulik-Sullivan et al., 2015; Cross-Disorder Group of the Psychiatric Genomics Consortium, 2013; Doherty and Owen, 2014; Gandal et al., 2018; Lee et al., 2019; Lee et al., 2021; Radonjić et al., 2021). From a psychopathological point of view, several authors have proposed a hierarchical phenotypic dimensional approach to explain the nature of psychiatric disorders because it can overcome many limitations of traditional categorical taxonomies, including the inability to account for comorbidities, subthreshold cases, and symptomatic heterogeneity (Caspi et al., 2014; Kotov et al., 2017; Lahey et al., 2017; Ruggero et al., 2019; Waszczuk et al., 2020).

CBMA research also plays a central role in this heated debate. Starting from the aforementioned work of Crossley et al. (2014) and that of Goodkind et al. (2015), a growing body of transdiagnostic CBMAs has identified a shared neuronal abnormal substrate for psychiatric and neurological disorders (Cauda et al., 2017; Dugré et al., 2022; McTeague et al., 2016; McTeague et al., 2017; McTeague et al., 2020; Opel et al., 2020). For example, two articles I co-authored during my Ph.D. program (Cauda et al., 2019b; Liloia et al., 2018) analyzed the entire VBM dataset stored in the BrainMap database (i.e., 82 disorders affecting the nervous system, 1,827 experiments, 19,325 subjects, and 20,238 x-y-z foci of gray matter alteration) using the ALE technique and alteration entropy metric (Shannon, 1948). The main objective was to identify the potential presence of neuronal territories that show a high level of alteration overlap between disorders. Findings suggest that a wide set of multimodal areas are altered in many (if not all) of the disorders under consideration, thus highlighting a high

degree of alteration entropy. This is exactly the case of the insular cortex, anterior/posterior cingulate cortex, hippocampal-amygdala complex, basal ganglia, temporal cortex, cuneus, prefrontal lobe, fusiform gyrus, thalamus, and orbitofrontal cortex (Cauda et al., 2019b). Instead, only a circumscribed set of areas tend to show a low degree of alteration entropy, encompassing visual, cerebellar, parietal, and sensorimotor areas (Liloia et al., 2018).

These results, together with those of previous transdiagnostic CBMAs, have raised the question of the extent to which neuroimaging results could decipher the disorder-specific neuronal substrate and thus effectively contribute to the improvement of current diagnostic strategies. In this context, another critical point should be mentioned, namely the type of inferences that can be drawn from neuroimaging data.

Brain mapping analysis methods, including VBM, generally rely on frequentist inference such as t-test statistics (Friston et al., 2007; Friston et al., 1994a). This type of inferential statistical approach is commonly used in quantitative research to determine significant differences between the means of two normally distributed groups by making a dichotomous decision about a particular null hypothesis. Specifically, a null hypothesis (e.g., no neuroanatomical differences between groups) is rejected at a user-dependent significance level or alpha value, which is the probability of rejecting the null hypothesis when it is actually true. With this definition in mind, no conclusion can be drawn about the *force of evidence* for the two hypotheses under investigation (Kass and Raftery, 1995) or the exact probability distribution of the competing hypothesis (Friston et al., 2002). Therefore, the frequentist approach makes it difficult to detect double dissociation or selectivity of the effect/phenomenon of interest (Friston et al., 2002). In the clinical VBM context, this means that researchers can only detect the presence of a neuroanatomical pattern of variation in the disorder under study compared to the control group (i.e., brain voxels in which the null hypothesis is rejected), but not "whether" and "to what extent" this pattern is selectively abnormal in the disorder under study, or also altered in other disorders (Costa et al., 2021). In other words, researchers perform a disease-to-alteration estimation, also known as *forward inference* (Henson, 2006).

A different kind of inference is required to directly decipher the degree of selectivity of an identified neuroanatomical alteration pattern in the disorder under study and, thus make an alteration-to-disease estimation (i.e., *reverse inference*) (Aguirre et al., 2003). As Russel A. Poldrack has pointed out in his influential work (Poldrack, 2006), the use of Bayesian

statistics, an alternative method of statistical inference used to calculate conditional probabilities, can enable us to make reverse inferences in the context of neuroimaging. In particular, the author performed a Bayesian analysis of the entire BrainMap fMRI database to determine the selective activation of Brodmann's area 44 (i.e., Broca's area) for the language domain (Poldrack, 2006). Starting from this pioneering research, a number of authors have applied the Bayesian reverse inference approach to the field of neuroimaging and discussed its strengths and weaknesses (Bourgeois-Gironde, 2010; Calzavarini and Cevolani, 2022; Coraci and Cevolani, 2022; Del Pinal and Nathan, 2013; Montagna et al., 2018; Poldrack, 2008, 2011; Wager et al., 2015; Yarkoni et al., 2011), with a particular emphasis on the setting of the prior probability distribution of hypotheses (Hutzler, 2014; Machery, 2014). Technical details on this issue in the field of neuroimaging can be found in Chapter 5 and in Cauda et al. (2020b). Overall, Bayesian reverse inference has provided important new information about the functional architecture of the human brain in normative populations by revealing in a quantitative manner the extent to which brain areas are selectively activated by a particular mental function or cognitive processes such as memory, emotion, and pain (Yarkoni et al., 2011). In contrast, the application of this type of inferential reasoning has been systematically neglected in the field of structural and clinical neuroimaging. However, its rigorous and user-friendly application could pave the way for groundbreaking research on possible disorder-specific brain markers for psychiatric disorders.

In this context, another main goal of my Ph.D. project was to develop and apply a method capable of drawing reverse inferences from clinical VBM data to investigate the presence of selective patterns of neuroanatomical alteration in individual brain disorders. Statistical details and methodological explanations of this novel approach are provided in Chapter 5. A brief overview can be found here.

Called Bayes fACtor mOdeliNg (BACON), this CBMA-based approach can be defined as a method able to identify the degree to which a gray matter pattern identified by the VBM technique is selectively altered in the brain disorder of interest (Costa et al., 2021). To this end, it uses ALE-derived findings for a data-driven, quantitative, and voxel-wise analysis based on Bayesian statistics. Although BACON was originally developed to study the selective neuroanatomical substrate of brain disorders, it is possible to extend its application to other areas of neuroimaging research, such as task-based fMRI in normative populations. BACON consists of two main steps. The first concerns the preparation of two datasets and the

computation of two ALE maps, as described in paragraph 1.5. This should be precisely the case for the disorder under study (i.e., the *IS-DISORDER* dataset) and its negation (i.e., the *IS NOT-DISORDER* dataset), which consists of VBM-derived x-y-z foci of gray matter alteration related to other real-world brain disorders. It is important to point out that the systematic selection of the entire eligible VBM literature on brain disorders is a major challenge. Fortunately, there is a way to alleviate this issue by using freely available and online neuroimaging databases (Cauda et al., 2020b; Costa et al., 2021; Poldrack, 2006). Once again, the BrainMap database is the perfect candidate for this scientific purpose. By means of the Sleuth software package (https://www.brainmap.org/sleuth/) and its articulated taxonomy scheme, it is possible to retrieve and download x-y-z foci of alteration associated with over 190 clinical conditions reporting appreciable gray matter changes. The second phase involves the estimation of the selectivity map of neuroanatomical alteration. For this purpose, BACON takes advantage of Bayesian statistics and, in particular, the Bayes' Factor (Jeffreys, 1961). This Bayesian alternative to classical hypothesis testing provides a powerful approach for determining the ratio of the likelihood of one hypothesis of interest to the likelihood of the competing hypothesis. Thus, by performing a posterior probability analysis on two ALE maps (i.e., one representing the disorder under study and the second one being its negation), BACON can quantify the likelihood that brain voxels are altered due to the disorder under study and the likelihood that they are altered due to other disorders.

CHAPTER 2

Updating and Characterizing Neuroanatomical Markers in High-Risk Subjects, Recently Diagnosed and Chronic Patients with Schizophrenia: A Revised Coordinate-Based Meta-Analysis[1]

Abstract

Background: Characterizing neuroanatomical markers of different stages of schizophrenia (SZ) to assess pathophysiological models of how the disorder develops is an important target for the clinical practice. *Methods:* We performed a meta-analysis of voxel-based morphometry studies of genetic and clinical high-risk subjects (g-/c-HR), recently diagnosed (RDSZ) and chronic SZ patients (ChSZ). We quantified gray matter (GM) changes associated with these four conditions and compared them with contrast and conjunctional data. We performed the behavioral analysis and networks decomposition of alterations to obtain their functional characterization. *Results:* Results reveal a cortical-subcortical, left-to-right homotopic progression of GM loss. The right anterior cingulate is the only altered region found altered among c-HR, RDSZ and ChSZ. Contrast analyses show left-lateralized insular, amygdalar and parahippocampal GM reduction in RDSZ, which appears bilateral in ChSZ. Functional decomposition shows involvement of the salience network, with an enlargement of the sensorimotor network in RDSZ and the thalamus-basal nuclei network in ChSZ. *Conclusion:* These findings support the current neuroprogressive models of SZ and integrate this deterioration with the clinical evolution of the disease.

2.1. Introduction

Schizophrenia (SZ) is a severe psychiatric disorder with a typical onset in late adolescence or early adulthood (Owen et al., 2016). The disability-associated burden of SZ was 13.4 million years lived with disability (YLDs) worldwide, equivalent to 1.7% of global YLDs in 2016 (Charlson et al., 2018). Considered the heavy burden of SZ, a better comprehension of the pathophysiology of this disorder is needed to improve treatments and outcomes (Wojtalik et al., 2017). Various current pathophysiological paradigms consider SZ

[1] This study was published in *Neuroscience & Biobehavioral Reviews* in 2021 (Volume 123, April 2021, Pages 83-103, doi: 10.1016/j.neubiorev.2021.01.010). Authors: Liloia D., Brasso C., Cauda F., Mancuso L., Nani A., Manuello J., Costa T., Duca S., Rocca P.

as a neurodevelopmental disease with a progressive peculiar neurodegenerative component characterized by reduced dendritic spines density, altered synaptic homeostasis and glial dysfunction in the absence of gliosis and neuronal necrosis (Andreasen, 2010; Ashe et al., 2001; Buoli et al., 2017; Velakoulis et al., 2000). According to this hypothesis, specific abnormalities, taking place in precise brain development stages, are associated with SZ onset and followed by processes of brain aging acceleration (Buoli et al., 2017; Nenadic et al., 2017). This type of brain alteration can manifest as a progressive reduction in the gray matter (GM) volume of specific neural territories. SZ could be staged from an increased risk of developing psychosis, with milder observable neurobiological and clinical expressions, to a persistent and unremitting condition with more evident signs of neurodegeneration (Davis et al., 2014; McGorry et al., 2006; Ortiz et al., 2017; Wood et al., 2011).

In-vivo neuroimaging techniques have provided an unprecedented insight into the brain alterations underlying neuropsychiatric disorders. Among them, one of the most employed approaches is the structural magnetic resonance imaging (sMRI) with voxel-based morphometry (VBM) (Isobe et al., 2016). VBM allows the detection of GM focal variations (i.e. volume or concentration) between-subject groups comparisons by means of a quantitative and voxel-wise analysis (for a detailed explanation of the method see Ashburner and Friston, 2000). Starting from the seminal work of Wright et al. (1995), widespread morphometric reductions have been repeatedly reported in groups of patients with SZ compared to healthy controls (HC). Importantly, some abnormalities have been observed both at first presentation and in the chronic stage of illness. In this regard, the systematic review of Shepherd et al. (2012) suggested that multiple GM degenerations occur regardless of SZ stages, encompassing the insulae, frontal gyri (particularly the inferior and medial ones), right anterior cingulate and superior temporal cortices. However, the conclusive picture of shared brain markers was limited by the heterogeneity quality of voxel-based investigations being reviewed (Shepherd et al., 2012). Moreover, some authors detected volumetric loss only in isolated cerebral loci (Ferri et al., 2012; Nakamura et al., 2013; Zhang et al., 2015) or even clusters of GM increase (Oertel-Knöchel et al., 2012; Sheng et al., 2013; Watson et al., 2012).

Despite substantial advances in sMRI research on SZ, replicability of results is still far from satisfactory (Hager and Keshavan, 2015; John et al., 2015; Kochunov et al., 2019). Potential sources of variability in findings may be partially due to differences in the assessed clinical population in terms of duration of illness (recently diagnosed or chronic SZ vs.

mixed) (Torres et al., 2016), diagnoses included (only SZ vs. SZ spectrum disorders) (Fervaha and Remington, 2013; Rink et al., 2016; Velakoulis et al., 2006), medical comorbidities or substance abuse (Bora et al., 2017; Koenders et al., 2015), gender distribution (Bora et al., 2012), medication status (antipsychotic-naïve vs. -treated) (Torres et al., 2013), age and type of symptomatology (Koutsouleris et al., 2014). Other confounding factors could derive from methodological choices regarding the type of analysis (whole-brain vs. region of interest - ROI or small volume correction -SVC) (McDonald et al., 2008; Voormolen et al., 2010), acquisition protocols (Jovicich et al., 2009), preprocessing software packages (Li et al., 2019a), sample size (small vs. multicenter mega-analyses) (Torres et al., 2016) and statistical thresholding procedures (Bennett et al., 2009; Vijayakumari et al., 2015).

Given these many confounding factors in the between-group comparisons, an objective assessment is needed to provide robust findings and summarize the recent growing literature about neuroanatomical alterations in SZ. A powerful approach is the quantitative synthesis of published neuroimaging results by means of coordinate-based meta-analysis (CBMA). In particular, the anatomical likelihood estimation (ALE) represents the most widely employed technique in the CBMA field (Tahmasian et al., 2019) and is able to quantify convergent morphometric alterations of neuropsychiatric disorders in a fully automated and replicable manner (Eickhoff et al., 2012). The ALE provides a rigorous environment to estimate the probability of spatial-unbiased distribution maps across experiments, mitigating the laboratory and group-level inhomogeneity (Fox et al., 2014).

This technique and other CBMA approaches have been usefully employed in the last two decades, suggesting that distributed cortical, subcortical and cerebellar GM alterations are involved in SZ spectrum disorders (Bora et al., 2011; Chan et al., 2011; Ellison-Wright and Bullmore, 2010; Ellison-Wright et al., 2008; Fornito et al., 2009; Glahn et al., 2008; Li et al., 2018; Nickl-Jockschat et al., 2011). Also, the presence of aberrations in unaffected relatives of patients with SZ (genetic-risk) and in individuals at risk of psychosis (clinical-risk) has been convincingly highlighted (Fusar-Poli et al., 2011a; Fusar-Poli et al., 2014; Saarinen et al., 2020). Although these meta-analytic findings are relevant, a considerable variability and inconsistency persist due to heterogeneity in the examined hypothesis and/or clinical sub-populations, different inclusion/exclusion criteria and, consequently, in the number of the analyzed experiments. In addition, certain important issues remain to be addressed.

Previous CBMAs systematically included several VBM experiments comparing HC with a mixed experimental group composed of individuals with SZ and of others with diagnoses belonging to the SZ spectrum disorders (SSD), so that the "pure" contribution of the diagnosis of SZ in GM alterations was not completely explored. For this reason, samples including patients diagnosed with SSD were not included in the present CBMA. The choice to focus on the SZ diagnosis only meets the need for identifying patterns of GM alterations that are specific to SZ. Furthermore, given that SZ is the most represented mental disorder in terms of number of sMRI studies and SZ diagnostic criteria are relatively stable over time and between nosological classifications, samples studied in different periods tend to be homogeneous.

We also decided to examine genetic and clinical high-risk (HR) states for psychosis because these two pre-psychotic conditions, albeit not necessarily evolving to psychosis, are characterized by GM alterations, which are not always consistent across studies (Cooper et al., 2014; Saarinen et al., 2020). From a clinical perspective, the detection of consensual neuroanatomical modifications can facilitate a prompt identification of these conditions by assessing their role in the transition to full-blown psychosis, as well as allow more effective strategies for prevention and care. Moreover, a number of studies on these HR samples are now available and sufficient to perform a robust CBMA.

Observer-independent functional characterization of the GM loss in different stages of SZ is essential in order to better understand how large-scale brain networks are involved in different periods of the disease progression. It is also of fundamental importance to control clinical, socio-demographic and methodological effects on VBM results in SZ (John et al., 2015; Kakeda and Korogi, 2010; Kambeitz et al., 2015; Vijayakumari et al., 2015). To our knowledge, no previous CBMAs on aberrant morphometric patterns linked to mental domains have been carried out so far. This line of research would provide a quantitative description of the functional and behavioral impact of anatomical variations at different stages of the disorder.

Another important aspect concerns the recent methodological innovations for the CBMA and the publication of best-practice protocols for this field. In 2017 the BrainMap team reported some technical errors affecting the ALE algorithm as implemented in GingerALE software, whose codes for the thresholding procedure may have increased the rate of false positives (Eickhoff et al., 2017). Still, different authors (Eickhoff et al., 2017;

Eickhoff et al., 2016; Müller et al., 2017; Samea et al., 2019) have strongly discouraged the use of the previously customary false discovery rate (FDR) voxel-level thresholding in the context of ALE meta-analyses, advising instead the use of cluster-level family-wise error (FWE) thresholding, given its better sensitivity to true effects. Great care was recommended regarding the inclusion of studies to enhance reliability and reproducibility, as well as to facilitate subsequent research efforts (Müller et al., 2018; Nichols et al., 2017; Tahmasian et al., 2019). In light of this, computational, statistical and reporting advances support the need to carry out a novel meta-analytic investigation. This is particularly true for an updated and extended estimation on different SZ stages, as the most recent ALE analysis on this topic dates back to 2011 (Chan et al., 2011) and many new relevant VBM studies were published since then.

We therefore conducted an exhaustive systematic search to revisit and characterize spatially consistent GM variations in four clinical groups: genetic high-risk subjects (g-HR), clinical high-risk subjects (c-HR), patients recently diagnosed with SZ (RDSZ, with a duration of illness - DOI < 2 years), and chronic SZ patients (ChSZ, DOI ≥ 2 years). The present ALE study is based on the largest data set of whole-brain VBM results included so far about this topic, on restrictive inclusion criteria, on stringent statistical procedure and on the most recent consensus-based protocols. Our aim has been to establish the most consistent neuroanatomical abnormalities related to the subsequent phases of the SZ. In order to derive common and potentially distinctive brain markers, contrast meta-analyses were conducted between the different groups. We also examined the effects of socio-demographic, clinical and methodological variables through voxel-wise meta-regressions. Finally, we assessed the cognitive/behavioral profiles associated with the GM clusters of alteration identified by the ALE. This combination of morphometric localization and functional characterization allowed for observer-independent inference, thus linking statistically the SZ pathophysiology to its clinical manifestations.

2.2. Methods

2.2.1. Data identification

The study protocol adhered to the PRISMA Statement international guidelines (Moher et al., 2009) and current consensus recommendations for neuroimaging CBMA (Müller et al., 2018; Tahmasian et al., 2019). We employed the software application Sleuth (v.3.0.3) to

query the VBM database of BrainMap (December 1, 2019) (Vanasse et al., 2018). We assembled a standardized search algorithm as follow:

"Experiments Context IS Disease Effects" AND "Subjects Diagnosis IS Schizophrenia" AND "Experiments Contrast IS Gray Matter" AND "Experiments Observed Changes IS Controls > Patients AND Controls < Patients".

We also employed the PubMed search engine to perform a systematic literature search on the MEDLINE database. We used the Advanced Search Builder adopting the following terms to search in title/abstracts:

("voxel-based morphometry" OR "VBM" OR "voxel-wise") AND ("schizophrenia" OR "chronic schizophrenia" OR "SZ" OR "first episode schizophrenia" OR "first episode psychosis" OR "high risk schizophrenia" OR "siblings schizophrenia" OR "first degree relatives" OR "genetic risk schizophrenia" OR "at risk of mental state" OR "ARMS" OR "ultra-high risk").

As final step, we screened references consulting previous review articles (Birur et al., 2017; Shepherd et al., 2012) and CBMAs about the conditions of interest (Chan et al., 2011; Ellison-Wright et al., 2008; Fusar-Poli et al., 2011a; Fusar-Poli et al., 2014).

2.2.2. Data selection

The identified articles were systematically reviewed. Inclusion criteria for neuroimaging experiments were: (a) to be included in a research article published in a peer-review journal; (b) to use a specified whole-brain VBM analysis; (c) to report GM variations in HR subjects and/or patients with RDSZ and/or patients with ChSZ by means of a between-group comparison with healthy controls; (d) to report results in the form of stereotactic space (i.e. x,y,z coordinates in Talairach or MNI space); (e) to adopt analyses corrected for multiple comparisons or cluster-wise extent thresholds >100 voxels; (f) experimental group without other medical comorbidities; (g) diagnosis of SZ based on fulfilling ICD or DSM criteria.

Moreover, we applied rigorous and restrictive exclusion criteria according to which we excluded the articles with one or more of the following characteristics: (a) experimental groups with a sample size < 10 subjects; (b) use of ROI or SVC analysis; (c) mixed experimental sample (i.e. SZ and other SDDs and/or RDSZ and ChSZ). Still, to avoid the possibility of analyzing the same subjects several times in a single study, we selected only the

alteration foci reported by the analysis with the largest sample of that study. Furthermore, to prevent redundancy of subjects and related results across studies by the same authors we selected only the last study (more recent publication date) published by the same research group with the same sample. Detailed reporting of inclusion and exclusion criteria can be found in the best-practice checklist (Table S2.1).

2.2.3. Clinical groups definition

Following the seminal ALE study of Chan et al. (2011), we partitioned our data set into distinct clinical groups: HR, RDSZ and ChSZ. However, we divided HR subjects into two groups (genetic and clinical HR) according to the model proposed by Fusar Poli et al. (2011a). The HR sample consisted of subjects at risk of developing SZ and was composed by the genetic HR group (g-HR) represented by monozygotic twins, siblings and first/second-degree relatives of patients with SZ and the clinical HR group (c-HR) of individuals at risk mental state (ARMS) meeting the criteria of either the Personal Assessment and Crisis Evaluation (PACE) (Yung et al., 1998), the Comprehensive Assessment of At-Risk Mental States (CAARMS) (Yung et al., 2005) or the Structured Interview for Prodromal Symptoms (SIPS) (Miller et al., 2003). The RDSZ group was composed of subjects with DOI less than 2 years. In the ChSZ group, patients had DOI equal or greater than 2 years. We included investigations that, though not reporting the DOI, referred clearly to a whole RDSZ or ChSZ sample.

2.2.4. Anatomical likelihood estimation

A series of ALE meta-analyses was conducted to determine a consistent pattern of GM variations for each of the four clinical groups and for all schizophrenia patients. A revised version of the ALE algorithm implemented in GingerAle (v.3.0.2) was applied (Turkeltaub et al., 2012). Following the recently recommended ALE setting (Eickhoff et al., 2017; Eickhoff et al., 2016), ALE results were family-wise error-corrected (FWE-c) for multiple comparisons, with a cluster-level inference of $p < .05$ and a cluster-forming threshold of $p < .001$ on the voxel-level. We conducted analyses in Talairach space. Thus, we used the icbm2tal algorithm to convert the MNI coordinates into TAL space, improving the accuracy of meta-analysis (Lancaster et al., 2007).

The ALE technique provides information about the spatial convergence of results of the existing literature, considering every coordinate reported in a given study as being the center of a Gaussian probability distribution calculated as:

$$p(d) = \frac{1}{\sigma^3\sqrt{(2\pi)^3}} e^{-\frac{d^2}{2\sigma^2}}$$

in which d is the Euclidean distance between the coordinate and the surrounding voxels, and σ represents the spatial uncertainty. For each experiment, we calculated a modeled alteration (MA) map, considered as the union of every Gaussian distribution of probability related to a given experiment. The combination of all the MA maps resulted in the final ALE map. The significance of each voxel was then tested against a null hypothesis obtained by an iterative random distribution of the foci, and the cluster-level threshold was determined with a Monte Carlo simulation of a cluster size distribution (10,000 permutations).

Finally, contrast analyses were performed (Eickhoff et al., 2011) in order to identify statistically significant differences and convergence between the clinical groups using a $p < .01$ and a minimum cluster-size of 10 mm^3 (10,000 permutations).

2.2.5. Standard voxel-wise permutation tests

We further interrogated the presence of GM variations in our clinical groups by using voxel-wise permutation tests as implemented in the FSL's randomise algorithm (https://fsl.fmrib.ox.ac.uk/fsl/fslwiki/Randomise; Winkler et al., 2014). Starting from the unthresholded MA maps, this algorithm was able to conduct a standard permutation of subject-based images (PSI) to test the presence/absence of the effect in a given voxel, rather than testing the convergence of independent findings around the voxel as implemented in the current CBMA methods (Albajes-Eizagirre and Radua, 2018; Albajes-Eizagirre et al., 2019). For each clinical group, results of test statistics were family-wise error-corrected (FWE-c) for multiple comparisons on the cluster-level with 5,000 permutation runs. Maps were thresholded at $p < .05$, corresponding to a z-score value ≥ 2.3.

2.2.6. Behavioral characterization

Analysis of behavioral domain profiles aims to statistically link morphometric clusters with corresponding physiological mental processes by testing which functional neuroimaging task is more likely to activate a given cluster. The rationale behind this approach is to provide a

quantitative and data-driven attribution of psychological processes to neural subpopulations, respect to a qualitative interpretation of structural results.

We functionally characterized areas of alteration derived by our ALE meta-analyses using the Behavioral plugin (v.3.1) implemented in the Mango software package (Lancaster et al., 2012), capable of testing activation foci of the BrainMap database. At the time of analysis, BrainMap contained over 9400 functional experiments in healthy subjects, each of which has been classified according to the specific mental operations isolated by its experimental contrast into five behavioral domains: (1) cognition, which comprises neuro- and social cognition, with special attention to two cognitive processes: memory and language; (2) perception, referred to external stimuli such as auditory and visual stimuli; (3) interoception, referred to internal stimuli such as hunger, heartbeat and sexual libido; (4) emotion, comprising positive and negative emotions; and (5) action, defined as mental faculty associated with overt movements of the body. Mental operations are further divided into 51 subdomains (see full taxonomy list at http://brainmap.org/taxonomy/behaviors.html) belonging to the five aforementioned domains. Behavioral analyses were performed separately on each clinical group both on the entire pattern of alteration at a whole-brain level and on each derived ALE cluster. A threshold of $p < .05$ with Bonferroni correction for multiple comparisons was applied, corresponding to a subdomain z-score ≥ 3.

2.2.7. Network decomposition

We investigated the impact of GM alterations on functional large-scale networks, detecting how many altered volumes (mm^3) derived from the ALE map of each clinical group fell within different networks. The rationale behind this approach is to provide a quantitative description of the functional localization of anatomical variations, as well as to evaluate a possible evolution and enlargement of the pattern at different stages of the disorder. We applied the 20-network parcellation proposed by Biswal et al. (2010), which parceled human brain cortex using resting-state functional MRI data from 1414 healthy subjects. Decomposition analyses were carried out separately for each clinical group, calculating the number of altered volumes belonging to each of the 20 functional networks and the percentage of alterations of each network, defined as the ratio between the number of altered voxels belonging to a given network and the total number of altered voxels of the ALE map of GM decrease of that clinical group.

2.2.8. Meta-regression

Using the Signed Differential Mapping software (i.e., anisotropic kernel effect sizes version, AES-SDM, v.6.12) (Radua et al., 2014), a series of voxel-wise meta-regression analyses were conducted to explore the potential effects of gender, positive and negative symptoms, age and antipsychotic treatment in the whole SZ sample. Effects of sample size, MRI field strength, slice thickness and image smoothing level were also examined. VBM experiments that did not report these measures were excluded from analyses. A voxel-level threshold of $p < .0005$ with a minimum cluster size of 10 voxels was adopted as proposed by Radua et al. (2012), to offer an optimal balance of specificity and sensitivity in terms of results.

AES-SDM is a relatively new CBMA method that borrows several characteristics from ALE, particularly the kernel-based rationale and the implementation of the coordinate-based random-effects approach; it is therefore able to combine the information of alteration foci in stereotactic space across independent experiments (for a detailed explanation of the methods see also Radua and Mataix-Cols 2012; Samartsidis et al., 2017). The novelty of SDM consists in incorporating t-value statistics related to alteration foci (i.e., effect size estimation), and in the possibility of addressing the confounding effect of potential moderators across included experiments. Meta-regression investigation was conducted via AES-SDM, as we thought it could complement our main analyses for two reasons: (a) meta-regression is to date a largely unexplored topic in CBMA research, particularly valuable when meta-analyzed experiments exhibit an appreciable heterogeneity (Samartsidis et al., 2017), as it is the case of SZ; (b) the comparison between the ALE and SDM yielded similar results in term of spatial convergence for both simulated and empirical data sets (Albrecht et al., 2019; Eickhoff et al., 2016; Enge et al., 2020; Radua and Mataix-Cols, 2012; Samartsidis et al., 2017; Vitolo et al., 2017). We thus expect that ALE map related to the whole SZ group is indicative of AES-SDM method as well.

2.3. Results

Based on the search strategy, 113 peer-reviewed VBM articles were included, for a total of 124 between-group experiments, 11,270 subjects (5,263 in the four clinical groups and 6,007 HC) and 1,104 coordinates of GM variation (1,042 of decrease and 62 of increase) (Fig. 2.1). In details, the g-HR group (average age = 28.7 years) included 18 experiments, 927

subjects compared with 910 HC and 76 coordinates of alteration (64 of GM decrease and 12 of GM increase). The c-HR group (average age = 22.4 years) included 16 experiments, 580 subjects compared with 621 HC and 67 coordinates of alteration (59 of GM decrease and 8 of GM increase). The RDSZ group (average age = 22.8 years; mean illness duration = 0.8 years) included 41 experiments, 1,636 subjects, 1,953 HC and 388 coordinates of alteration (359 of GM decrease and 29 of GM increase). The ChSZ group (average age = 38.6 years; mean illness duration = 15.0 years) included 49 experiments, 2,120 subjects, 2,563 HC and 573 coordinates of alteration (560 of GM decrease and 13 of GM increase). The best-practice checklist for CBMA (Müller et al., 2018) was reported in Table S2.1. Detailed information about the sample of each included experiment is summarized in Table S2.2 and Table S2.3. Distribution of the included experiments in the four clinical groups is summarized in Table S2.4. ALE analysis was performed only for GM reduction foci, as the number of VBM experiments reporting GM increases (i.e., g-HR = 6 experiments; c-HR = 4; RDSZ = 7; ChSZ = 7; Table S2.3) was insufficient to achieve robust ALE estimates (Eickhoff et al., 2016).

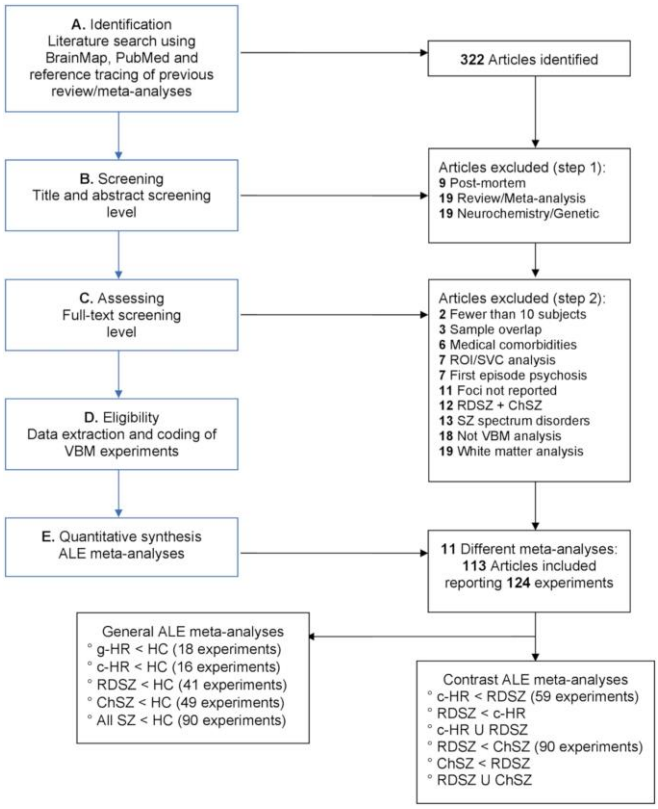

Figure 2.1. Study selection overview and meta-data organization - PRISMA flow chart.

g-HR: genetic high-risk; c-HR: clinical high-risk; RDSZ: recently diagnosed schizophrenia; ChSZ: chronic schizophrenia.

2.3.1. ALE meta-analyses on different stages of schizophrenia

GM reductions in g-HR, c-HR, RDSZ and ChSZ groups relative to HC are shown in Table 2.1 and Fig. 2.2, Fig. 2.3 and Fig .2.4. Results of the ALE meta-analysis performed on the whole sample of patients diagnosed with schizophrenia (RDSZ and ChSZ groups pooled together) are shown in Table S2.5 and Fig. S2.1.

g-HR vs. controls

The g-HR group showed no significant cluster of variation.

c-HR vs. controls

The c-HR group showed a single cluster of GM reduction (altered volume = 800 mm^3), with the ALE maximum value located in the right anterior cingulate cortex (R-ACC, Brodmann area -BA 32).

RDSZ vs. controls

The RDSZ group showed seven clusters of GM reduction involving both cortical and subcortical regions with total altered GM volume of 8,360 mm^3. ALE maxima were found in the: (a) left precentral gyrus (L-PrCG, BA 6), (b) left inferior frontal gyrus (L-IFG, BA 47), (c) bilateral superior temporal gyrus (STG, BA 22), (d) bilateral transverse temporal gyrus (TTG, BA 41), (e) right middle temporal gyrus (R-MTG, BA 21), (f) bilateral insular cortex (BA 13), (g) bilateral ACC (BA 32), (h) left parahippocampal gyrus (L-PHG, BA 34), and (i) left amygdala (L-Amy).

ChSZ vs. controls

Patients of the ChSZ group differed from HC in GM reduction in several cortical and subcortical regions grouped into seven clusters with a total altered GM volume of 14,912 mm^3. ALE maxima were found in the: (a) right medial frontal gyrus (R-MFG, BA 11), (b) L-IFG (BA 47), (c) L-STG (BA 22), (d) bilateral anterior insula (AI, BA 13), (e) bilateral ACC (BA 32/25), (f) bilateral amygdala, (g) head of the left caudal nucleus (L-Caud) and (h) medial dorsal nucleus (MDN) of the left thalamus (L-Thal).

Table 2.1. Clusters of gray matter reduction derived from the Anatomical Likelihood Estimation (ALE) analyses. For each cluster obtained, cluster size (mm^3), extrema ALE values, anatomical labels of the peaks of probability and their Talairach brain atlas coordinates were provided.

Cluster #	Volume (mm^3)	Talairach Daemon Label (Brodmann's Area)	Extrema Value	Talairach x	y	z
g-HR < HC						
No cluster found						
c-HR < HC (tot. 800 mm^3)						
1	800	Right Anterior Cingulate Cortex (BA 32)	0.016	4	36	-6
RDSZ < HC (tot. 8,360 mm^3)						
1	1776	Left Precentral Gyrus (BA 6)	0.025	-48	-10	24
		Left Inferior Frontal Gyrus (BA 44)	0.024	-48	4	18
2	1624	Right Transverse Temporal Gyrus (BA 41)	0.025	48	-24	16
		Right Middle Temporal Gyrus (BA 21)	0.018	54	-26	-2
3	1296	Right Middle Temporal Gyrus (BA 22)	0.023	50	-8	-8
		Right Insula (BA 13)	0.022	40	-10	-6
4	1096	Left Insula (BA 13)	0.031	-32	22	4
5	1032	Left Transverse Temporal Gyrus (BA 41)	0.024	-46	-18	10
		Left Superior Temporal Gyrus (BA 22)	0.020	-52	-8	6
6	784	Left Anterior Cingulate (BA 32)	0.022	-2	34	-4
		Right Anterior Cingulate (BA 32)	0.020	2	40	2
7	752	Left Amygdala	0.023	-20	-4	-18
		Left Parahippocampal Gyrus (BA 34)	0.015	-12	0	-14
ChSZ < HC (tot. 1,4912 mm^3)						
1	4928	Left Insula (BA 13)	0.042	-34	18	6
		Left Superior Temporal Gyrus (BA 22)	0.035	-48	4	2
		Left Insula (BA 13)	0.027	-44	12	0
		Left Inferior Frontal Gyrus (BA 47)	0.020	-40	20	-6
2	3056	Right Insula (BA 13)	0.037	40	14	2
		Right Insula (BA 13)	0.035	32	18	8
3	2312	Left Thalamus (Medial Dorsal Nucleus)	0.036	-2	-16	6
4	1656	Right Medial Frontal Gyrus (BA 11)	0.032	4	36	-14
		Right Anterior Cingulate (BA 32)	0.031	4	32	-6
5	1224	Left Caudate (Nucleus Head)	0.036	-4	6	-4
6	1056	Left Amygdala	0.036	-20	-6	-12
7	680	Right Amygdala	0.026	16	-4	-16

g-HR, genetic high-risk; c-HR, clinical high-risk; RDSZ, recently diagnosed schizophrenia; ChSZ, chronic schizophrenia; HC, healthy controls.

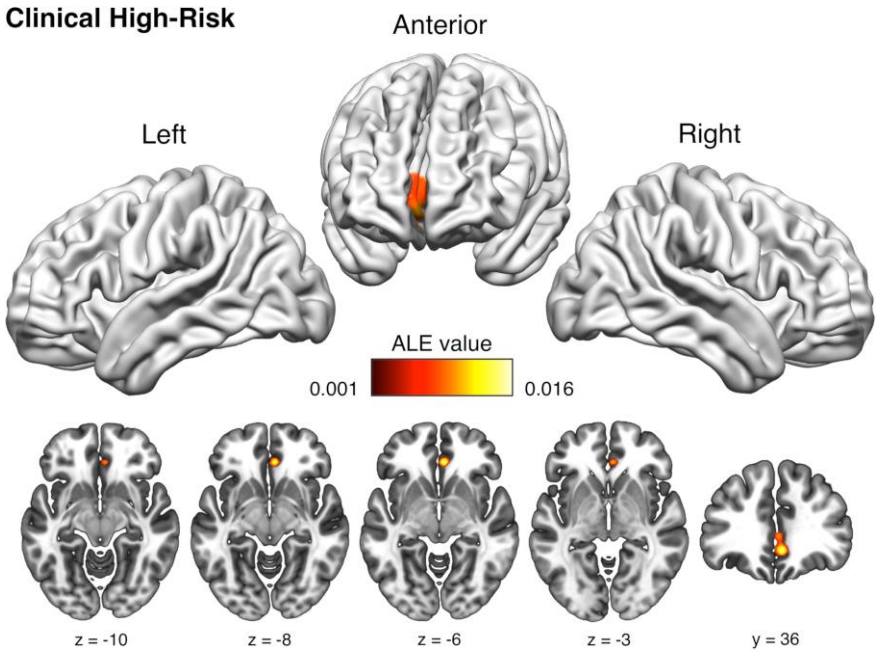

Figure 2.2. Brain clusters of convergent GM reduction in the clinical high-risk (c-HR) group compared to healthy controls (HC). Results are FWE-corrected at .05 with cluster-forming value at $p < .001$. The ALE maps are visualized as three hemispheric surfaces (3-D cortical view) and five axial slices (2-D cortical and subcortical view). Brain templates are in neurological convention (i.e., R is right, L is left).

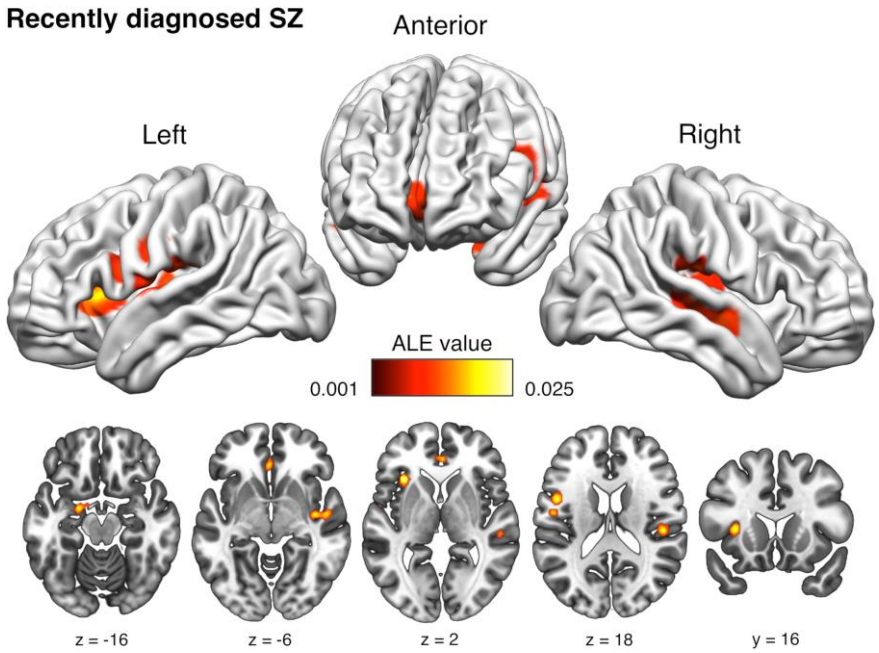

Figure 2.3. Brain clusters of convergent GM reduction in the recently diagnosed schizophrenia (RDSZ) group compared to healthy controls (HC). Results are FWE-corrected at .05 with cluster-forming value at $p < .001$. The ALE maps are visualized as three hemispheric surfaces (3-D cortical view) and five

axial slices (2-D cortical and subcortical view). Brain templates are in neurological convention (i.e., R is right, L is left).

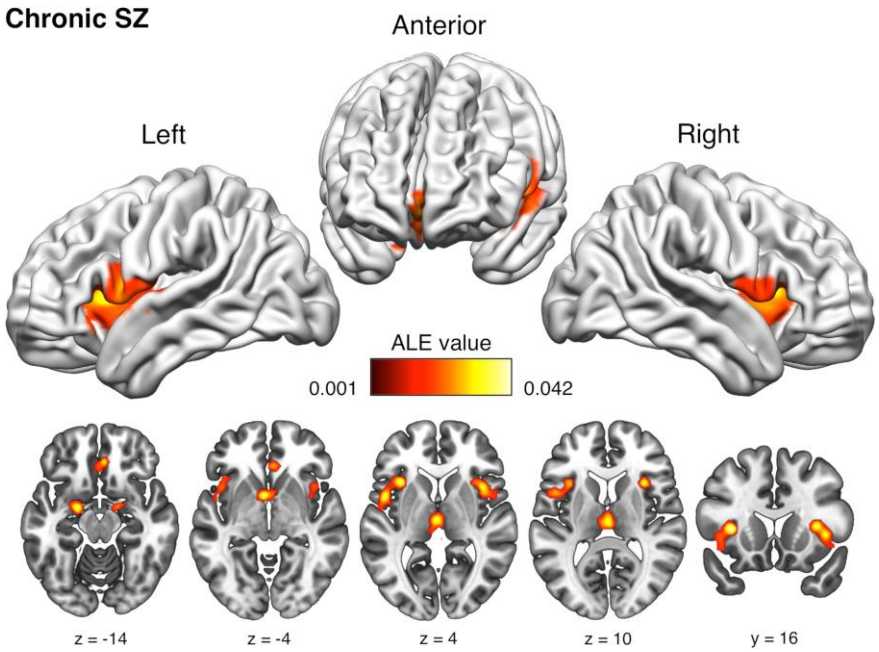

Figure 2.4. Brain clusters of convergent GM reduction in the chronic schizophrenia (ChSZ) group compared to healthy controls (HC). Results are FWE-corrected at .05 with cluster-forming value at $p < .001$. The ALE maps are visualized as three hemispheric surfaces (3-D cortical view) and five axial slices (2-D cortical and subcortical view). Brain templates are in neurological convention (i.e., R is right, L is left).

2.3.2. Between-groups comparisons and conjunction analyses

Results of contrast and conjunction ALE analyses are shown in Table 2.2 and Fig. 2.5.

c-HR vs. RDSZ

c-HR U RDSZ: the conjunction analysis of c-HR and RDSZ groups showed a significant convergence of GM reductions in the R-ACC (BA 32) with a volume of common GM reduction of 144 mm^3.

c-HR < RDSZ: in the between-group comparison there were not significant GM reduction present exclusively in the c-HR as compared to the RDSZ group.

RDSZ < c-HR: contrariwise, there were significant reductions in four clusters regarding the RDSZ group as compared to the c-HR group. The total GM volume altered exclusively in

the RDSZ group was 2,600 mm^3 with ALE maxima located in the left hemisphere, principally in cortical areas in the frontal lobe: (a) in the L-IFG (BA 44) and (b) in the L-PrCG (BA 4); (c) in the left postcentral gyrus (L-PoCG, BA 43); (d) in the L-STG (BA 22); in (e) the L-AI (BA 13) and (f) in the left claustrum (L-Clau).

RDSZ vs. ChSZ

RDSZ U ChSZ: the conjunction analysis of RDSZ and ChSZ groups showed five significant clusters of convergence of GM reductions in the left hemisphere (total volume of common GM reduction: 1,184 mm^3), namely (a) the L-PrCG (BA 6) and (b) the orbital part of the L-IFG (L-IFG, BA 44) in the frontal pole, (c) the L-AI (BA 13), (d) the L-ACC (BA 32), extending to right ACC and (e) the L-Amy.

RDSZ < ChSZ: in the between-group comparison there were three clusters of significant reduction regarding the RDSZ group as compared to the ChSZ group (total volume of altered GM present exclusively in the RDSZ: 672 mm^3), with ALE maxima located in the: (a) L-IFG (BA 44), (b) L-PrCG (BA 6), (c) L-PoCG (BA 43), (d) L-AI (BA 13); and right temporal lobe (e) in the R-MTG (BA 21).

ChSZ < RDSZ: conversely, ChSZ group as compared to RDSZ group showed significant GM decreases in five clusters (total volume of altered GM present exclusively in the ChSZ: 1,464 mm^3) with ALE maxima located both in the left and right hemispheres in cortical and sub-cortical encephalic regions. In particular, ChSZ specific peaks of alteration were found in the: (a) L-IFG (BA 44), (b) L-STG (BA 22); (c) in bilateral AI (BA 13), (d) R-PHG (BA 34), (e) the right uncus (R-Unc, BA 34); (f) MDN and (g) pulvinar (Pulv) of the L-Thal, and (h) Pulv of the R-Thal.

Table 2.2. Clusters of gray matter difference and conjunction derived from the Anatomical Likelihood Estimation (ALE) analyses. For each cluster obtained, cluster size (mm3), extrema values, anatomical labels of the peaks of probability and their Talairach brain atlas coordinates were provided.

Cluster #	Volume (mm^3)	Talairach Daemon Label (Brodmann's Area)	Extrema Value	Talairach x	y	z
c-HR ∪ RDSZ (tot. 144 mm^3)						
1	144	Right Anterior Cingulate Cortex (BA 32)	0.014	2	36	-6
c-HR < RDSZ						
		No cluster found				
RDSZ < c-HR (tot. 2,600 mm^3)						
1	1032	Left Superior Temporal Gyrus (BA 22)	p < .001	-50.2	-13.3	8.4
		Left Insula (BA 13)	p < .001	-47.3	-18.7	16
2	768	Left Postcentral Gyrus (BA 43)	p < .001	-50	-10	16
		Left Precentral Gyrus (BA 4)	p = .001	-51.6	-12	24.4
3	576	Left Insula (BA 13)	p = .001	-32	12	8
		Left Insula (BA 13)	p = .002	-36	13	5
		Left Claustrum	p = .005	-30	18	2
		Left Inferior Frontal Gyrus (BA 45)	p = .009	-32	24	6
4	224	Left Insula (BA 13)	p = .002	-46	4	14
		Left Inferior Frontal Gyrus (BA 44)	p = .003	-49.5	1	15.5
RDSZ ∪ ChSZ (tot. 1,184 mm^3)						
1	680	Left Insula (BA 13)	0.029	-32	20	4
2	304	Left Amygdala	0.023	-20	-4	-16
3	120	Left Anterior Cingulate (BA 32)	0.020	0	34	-4
4	56	Left Precentral Gyrus (BA 6)	0.018	-52	-6	6
5	24	Left Inferior Frontal Gyrus, orbital part (BA 47)	0.016	-48	6	14
RDSZ < ChSZ (tot. 672 mm^3)						
1	520	Left Precentral Gyrus (BA 6)	p = .001	-49	-5	24.4
		Left Postcentral Gyrus (BA 43)	p = .002	-50	-8.5	17.5
		Left Inferior Frontal Gyrus (BA 44)	p = .004	-49	0	20
2	136	Left Postcentral Gyrus (BA 43)	p = .006	-47	-17	14
		Left Insula (BA 13)	p = .007	-46	-14	10
3	16	Right Medial Temporal Gyrus (BA 21)	p = .006	44	-8	-12
ChSZ < RDSZ (tot. 1,464 mm^3)						
1	672	Right Parahippocampal Gyrus (BA 34)	p < .001	12.8	-3.6	-16
		Right Uncus (BA 34)	p = .001	17.7	-4.4	-19
2	480	Left Thalamus (Medial Dorsal Nucleus)	p = .001	-7	-20	11
		Right Thalamus (Pulvinar)	p = .002	4	-24	9
		Left Thalamus (Pulvinar)	p = .003	-3.5	-23	4.5
3	256	Left Precentral Gyrus (BA 44)	p = .001	-46	12	8
		Left Insula (BA 13)	p = .005	-44	0	2
4	40	Right Insula (BA 13)	p = .003	36	20	2
5	16	Left Superior Temporal Gyrus (BA 22)	p = .01	-51	8	4

g-HR, genetic high-risk; c-HR, clinical high-risk; RDSZ, recently diagnosed schizophrenia; ChSZ, chronic schizophrenia; HC, healthy controls. **<**, *Indicates that the gray matter (GM) reduction is wider in the group to the left of the symbol.* **U**, *indicates the clusters of GM volume reduction found in the groups both to the left and to the right of the symbol.*

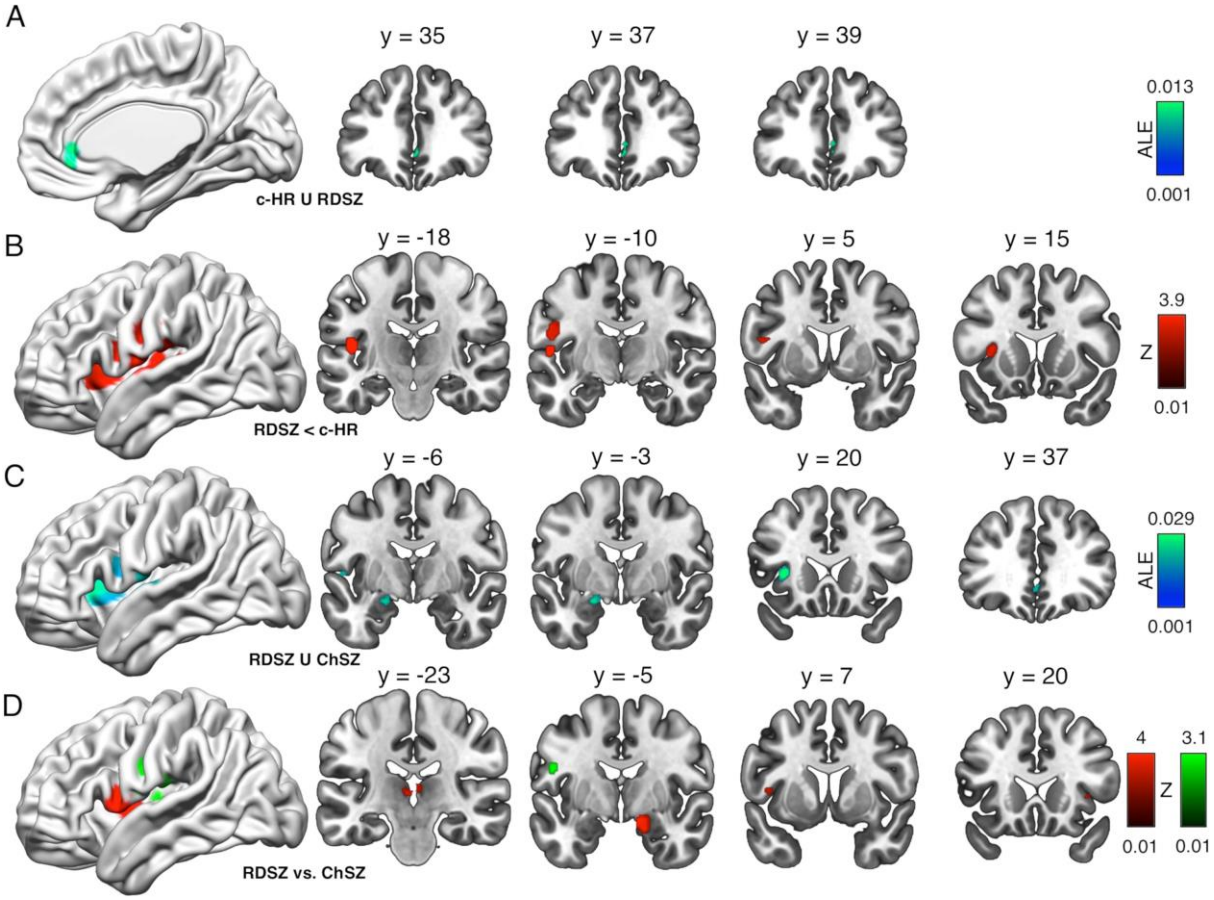

Figure 2.5. Conjunction and contrast analyses between clinical groups. (A) Convergence of GM reduction between clinical-high risk and recently diagnosed schizophrenia groups (colors from dark to light blue represent increasing ALE values). (B) Compared to the clinical-high risk group, GM reductions are exclusively present in the recently diagnosed schizophrenia patients (colors from dark to light red represent increasing z-point values). (C) Convergence of GM reduction between recently diagnosed and chronic schizophrenia groups (colors from dark to light blue represent increasing ALE values). (D) Compared to the chronic schizophrenia group, GM reductions are exclusively present in the recently diagnosed patients (colors from dark to light green represent increasing z-point values). Compared to the recently diagnosed schizophrenia group, GM reductions are exclusively present in the chronic patients (colors from dark to light red represent increasing z-point values). ALE results were computed using a p value < .01 and minimum cluster-size > 10 mm^3.

2.3.3. Standard voxel-wise permutation tests

GM reductions in HR and SZ groups relative to HC are shown in Table S2.6 and Fig. S2.2.

HR groups vs. controls

The g-HR group showed no significant cluster of variation. With regard to the c-HR group, a very small cluster was detected in the R-ACC.

SZ groups vs. controls

Overall, results reported statistically significant clusters largely overlapping with those identified by ALE. The RDSZ group showed eight clusters of GM reduction involving both cortical and subcortical regions with total altered GM volume of 2,246 mm^3. Maximum values were found in the: (a) L-IFG (BA 45), (b) L-AI (BA 13), (c) L-TTG (BA 41), (d) R-MTG (BA 22), (e) bilateral ACC (BA 32/24), and (f) L-PHG (BA 35). The ChSZ group showed eight clusters of GM reduction involving both cortical and subcortical regions with total altered GM volume of 17,913 mm^3. Maximum values were found in the: (a) L-MFG (BA 10), (b) bilateral AI (BA 13), (c) bilateral ACC (BA 32), (d) MDN of the L-Thal, and (e) bilateral PHG (BA 34), extending to the (f) amygdalar complex.

2.3.4. Behavioral characterization

Data-driven behavioral analysis revealed that aberrant ALE-derived patterns found in the clinical groups can be quantitatively associated with a wide range of functional neuroimaging tasks as shown in Fig. 2.6 and Table S2.7 (RDSZ group) and Table S2.8 (ChSZ group).

We found no significant results associated with the R-ACC cluster in the c-HR group, whereas the whole-brain patterns of GM loss in the RDSZ and in the ChSZ groups were characterized by a statistically significant involvement of numerous different subdomains belonging to all five studied domains: cognition, perception, emotion, action and interoception. General distribution of the number of subdomains involved in each domain in the two clinical conditions is shown in the radar chart of Fig. 2.6. The ChSZ group, compared to the RDSZ group, displayed a higher number of involved subdomains (33 vs. 23). The main difference concerned the emotional domain with nine subdomains involved in the ChSZ

group compared to the five of the RDSZ one. Fig. 2.6 (bottom panel) shows the ranking of the involved subdomains of the ChSZ group in decreasing order of z-score, coupled with the z-score of the corresponding subdomain in the RDSZ group. All the 23 functional subdomains found the RDSZ group were also present in the ChSZ group. The 10 subdomains exclusively associated with the GM loss in the ChSZ group were negative emotions (i.e. sadness, anger, unspecified negative emotions), positive emotions (i.e. happiness and unspecified positive emotions) of the emotion domain; “social cognition” and “memory” of the cognitive domain; “olfaction” of the perceptive domain; “inhibition of movement” of the action domain; and “sexuality (libido)” of the interoception domain.

Subdomains associated with single ALE-derived clusters are represented in Fig. S2.3 (RDSZ group) and in Fig. S2.4 (ChSZ group). Of the seven ALE-derived clusters of GM reduction found in both the RDSZ and ChSZ groups, five clusters in each clinical group were significatively associated with at least one functional subdomain. In the RDSZ condition, the L-IFG was principally associated with action subdomains, bilateral TTG with perceptive subdomains, L-Ins with cognitive and action subdomains, and the L-Amy with emotional sub-domains. In the ChSZ group, bilateral insulae were principally associated with cognitive (including social cognitive), perceptive, action and interoceptive subdomains, L-Amy with emotional and perceptive sub-domains, L-Thal with cognitive subdomains and the L-Caud with reward/gain positive emotion subdomain.

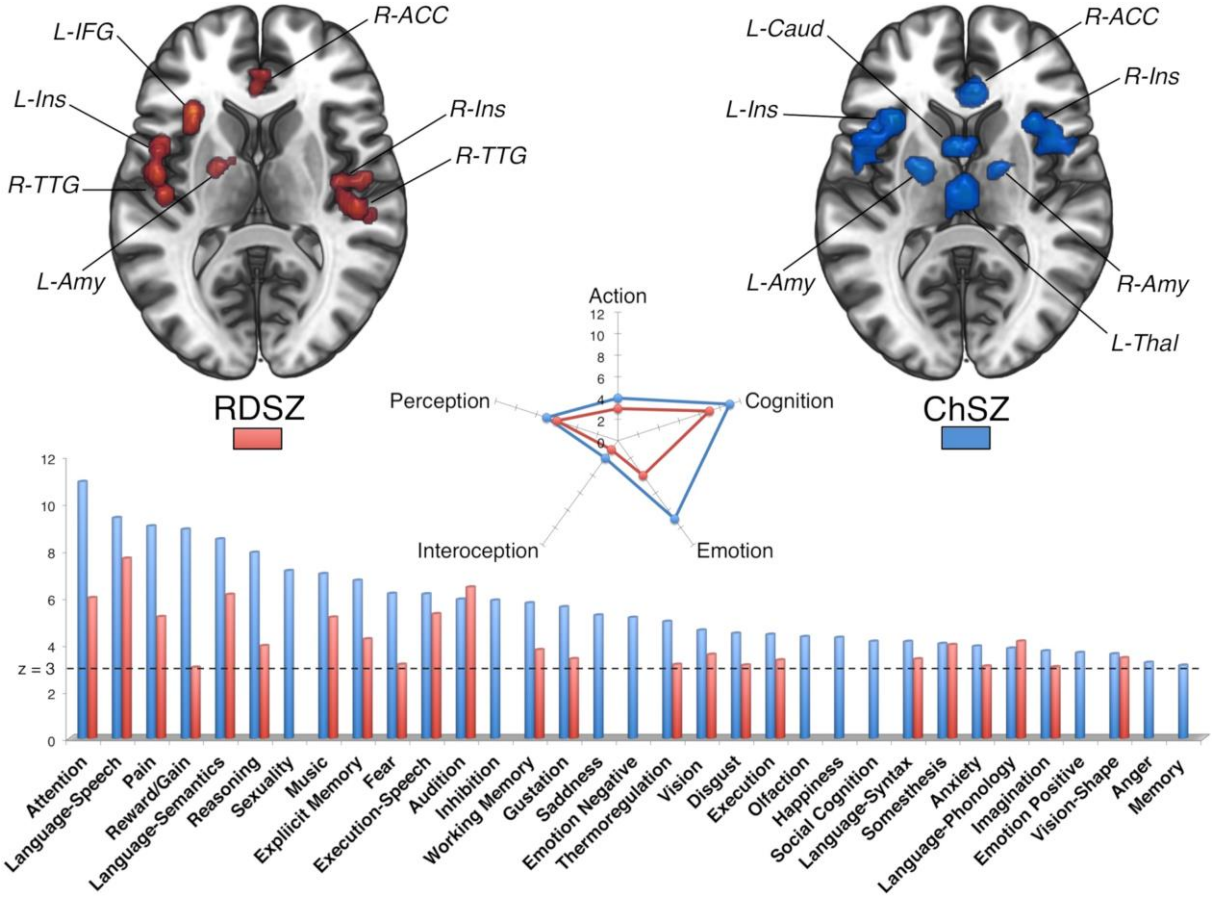

Figure 2.6. Behavioral characterization results of whole ALE-derived brain maps of GM reduction obtained in the RDSZ and ChSZ groups. (Upper panel) Alteration patterns are visualized as two axial slices (3-D cortical and subcortical view). (Central panel) Number of subdomains significantly associated in each domain. (Bottom panel) Z-scores of significant subdomains. A threshold of $p < .05$ with Bonferroni correction for multiple comparisons was applied, corresponding to a subdomain z-scores ≥ 3.

GM, gray matter; ACC, anterior cingulate cortex; Ins, insula; IFG, inferior frontal gyrus; TTG, transverse temporal gyrus; Amy, amygdala; Caud, caudate; Thal, thalamus.

2.3.5. Network decomposition

The results of the functional network decomposition analysis are shown in Fig. 2.7 and in Table S2.9. Fig. 2.7 (A and B panels) shows the subdivision of the morphometric alteration of the clinical groups into the different functional networks, while Fig. 2.7C depicts the percentage of altered GM volume in each network (i.e. proportional to the total altered GM volume in each clinical group).

In the c-HR group the ALE-derived cluster of GM alteration belonged to (a) the orbitofrontal cortex network - OFC-N (548 mm^3, 68.5% of the total altered volume) and to (b) the salience network - SN (252 mm^3, 31.5%). Most of the altered GM volume of the RDSZ fell within (a) the SN (2710 mm^3, 32.4%), (b) the OFC-N (1217 mm^3, 14.6%), (c) the left ventral attention network - L-VAN (1198 mm^3, 14.3%), (d) the motor network - MN (1115 mm^3, 13.3%), and (e) the sensorimotor network - SMN (932 mm^3, 11.2%). In the ChSZ the most involved networks were: (a) the SN (4956 mm^3, 33.2%), (b) the OFC-N (3971 mm^3, 26.6%), and (c) the thalamus/basal nuclei network - Th-BN-N (2667 mm^3, 17.9%).

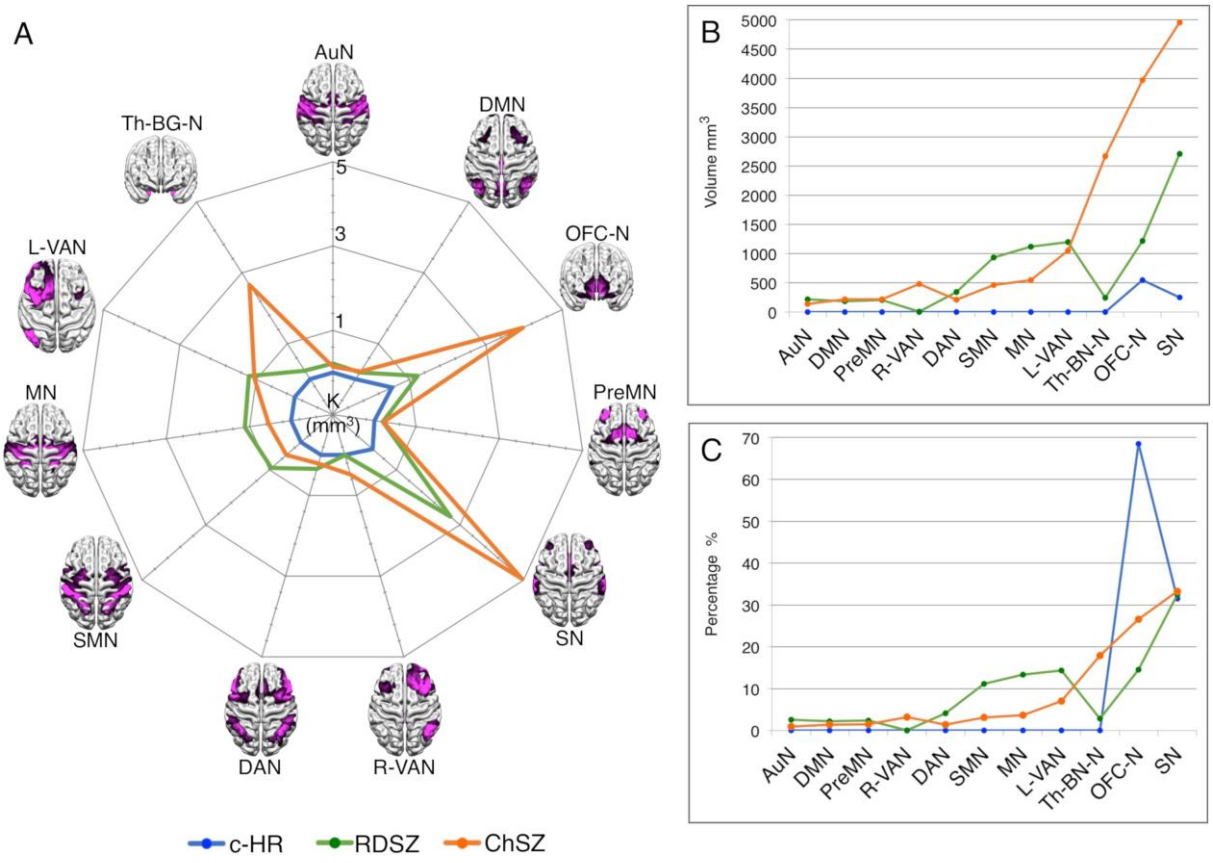

Figure 2.7. Functional network decomposition of the ALE-derived clusters of GM reduction obtained in the c-HR, RDSZ and ChSZ groups. (A and B) Graphical representations of the number of altered volumes (mm^3) falling within a functional network. (C) Graphical representation of the altered volumes falling within a functional network (percentage).

AuN, auditory network; DMN, default mode network; preMN, premotor network; R-VAN, right ventral attention networks; DAN, dorsal attention network; SMN, sensorimotor network; MN, motor network; L-VAN, left ventral attention networks; Th-BN-N, thalamus-basal nuclei subcortical network; OFC-N, orbito-frontal cortex network; SN, salience network.

2.3.6. Effects of meta-regression on GM reduction

Linear associations between selected clinical and methodological variables and VBM data of the included experiments of the whole SZ group are shown in Fig. S2.5 (lower panel), Table S2.10 (demographic and clinical variables) and Table S2.11 (methodological variables) and summarized as follows. As expected, the ALE results related to the whole SZ group were very similar in terms of spatial convergence with those of the AES-SDM (Fig. S2.5**,** upper panel). Voxel-wise correlation (i.e. Pearson's *r*) between the unthresholded ALE and AES-SDM z-score maps was *r* = .64 (calculated excluding the non-brain voxels).

Effects of demographic and clinical variables

Effect of sex: experiments with higher percentage of male patients were associated with a widespread GM loss in the: (a) L-STG (p = 1.0e-5, 52 voxels); (b) left inferior temporal gyrus (L-ITG; p = 1.0e-4, 46 voxels); (c) R-Ins (p = 6.0e-5, 50 voxels); (d) bilateral thalami (p = 5.0e-6, 94 voxels).

Effect of antipsychotic treatment: in experiments with higher percentage of medicated patients compared with studies with a higher percentage of drug-naïve patients at the scan time, we found a more widespread decrease of the GM volumes of (a) the L-MFG (p = 2.0e-4, 39 voxels) and of (b) the R-STG (p = 2.0e-5, 127 voxels).

Antipsychotic dosage, age at scan and positive and negative symptoms: no linear associations with age at scan, medication dosage (chlorpromazine mg equivalents), positive and negative symptoms (PANSS positive and negative scores) were found.

Effects of methodological variables

Sample size: experiments with smaller sample size showed a more widespread GM decrease volume in (a) the right STG (R-STG), extending to (b) the R-Ins (p = 4.0e-7, 293 voxels) and in a small cluster located (c) in the L-ACC (p = 1.0e-5, 28 voxels).

Image smoothing level (FWHM): higher smoothing was significantly associated with GM reduction in (a) the R-Ins, extending to (b) the R-PrCG (p = 1.0e-4, 86 voxels) and in the (c) L-STG (p = 1.0e-4, 27 voxels).

Field strength and slice thickness: linear associations with VBM data and these variables were not found.

2.4. Discussion

By reviewing a vast literature of voxel-based neuroimaging studies about schizophrenia, this meta-analysis offers the most overarching picture of morphometric changes of GM currently available and lends support to pathophysiological models, which combine progressive brain alterations with the clinical evolution of SZ. Using a conservative study selection and the current state-of-the-art methods in the CBMA field, we have identified GM alterations associated with clinical high-risk subjects, recently diagnosed and chronic patients with SZ, providing meta-analytical evidence of progressive brain morphometric changes after prodromal symptoms and signs onset. As a distinguishing feature of this study, we have established an objective link between the SZ symptomatology and the underlying neural pathophysiology, associating the resulting GM changes with data-driven functional profile characterizations. Our findings also demonstrate between-study effects of sex, sample size and medication on published VBM results.

2.4.1. GM alterations partly reproduce previous CBMA results on SZ stages

Our findings are only in part consistent with those of the previous meta-analyses on the different stages of SZ, providing new important information about the progression of GM alteration during the course of the disorder. Interestingly, our analyses showed that there were no morphometric differences between g-HR and HC groups. This result is in line with a recent CBMA of VBM studies on first degree relatives of patients with SZ (Saarinen et al., 2020), but not with previous investigations reporting GM tissue loss at the level of the R-ACC and L-PHG (Fusar-Poli et al., 2011a; Fusar-Poli et al., 2014). The lack of significant findings may be explained by a variety of factors. For example, as early meta-analytic syntheses have been published with significant smaller data sets (i.e. less than 10 VBM experiments each) due to the limited availability of research data, our results are particularly robust and reasonably non-driven by singly experiments (Eickhoff et al., 2016). It is worth noting that the mean age at the scan of the first/second degree relative varies widely across experiments (Table S2.2), which increases the between-study variability. Also, it has been suggested that specific morphometric brain variations in g-HR subjects may be present only in those who develop psychosis later in life (Smieskova et al., 2010; Smieskova et al., 2013). However, as these subjects represent a small portion of the g-HR population (Fusar-Poli et al.,

2012), their contribution could be covered by the substantial number of the non-transitioning subjects.

Regarding c-HR group, we confirmed the GM loss in the R-ACC found in previous CBMAs (Chan et al., 2011; Fusar-Poli et al., 2011a). However, the R-AI, L-Amy and L-IFG clusters found by Chan et al. (2011), and the R-STG, L-PHG, L-AI, R-IFG ones found by Fusar-Poli et al. (2011a) have not survived our rigorous thresholding procedure. Moreover, unlike early meta-analyses (Boos et al., 2007), we have not replicated the hippocampal reduction in HR groups, probably due to our whole-brain approach, which has selectively excluded studies using ROI or SVC analyses on this region (McDonald et al., 2008).

In the RDSZ group, we confirmed the findings that the L-IFG, L-Amy and bilateral ACC show GM decreases (Chan et al., 2011; Ellison-Wright et al., 2008), but not the findings of GM reduction in the caudate, thalamus and cerebellum. In this group, we have also revealed GM alterations in the temporal cortices, bilateral insula and L-PHG, which were associated with ChSZ patients only in those previous investigations. For what concerns the ChSZ group, we confirmed the presence of bilateral GM alterations in the AI, ACC, and amygdala. The left IFG was also found by early CBMAs (Chan et al., 2011; Ellison-Wright et al., 2008). Furthermore, we revealed a cluster of GM reduction in the bilateral thalamus, which was only left-lateralized in Chan et al. (2011), and in the left caudate head, which was not found in the previous ALE studies. It should be noted that the involvement of the aforementioned regions in SZ groups was confirmed by the standard voxel-wise permutation tests. Taking this into account, it is reasonable to assume that our state-of-the-art multiple-comparison corrections ensure an adequate type I error control than the liberal (but previously employed) FDR correction, as the latter is prone to reveal false positive findings in meta-analytic neuroimaging investigations (Eickhoff et al., 2016; Eickhoff et al., 2017; Müller et al., 2017; Nani et al., 2019; Samea et al., 2019).

Another important result of the present work that contrasts with previous ALE investigations (Chan et al., 2011; Ellison-Wright and Bullmore, 2010; Fornara et al., 2017; Fornito et al., 2009) is the systematic absence of the lingual and fusiform gyri, cuneus, posterior cingulate and cerebellum in the SZ clinical groups. As to this aspect, we note that these posterior areas were found altered in a relatively small number of included studies. Therefore, the discrepancy may be due to the fact that our statistical inference was more

sensitive to large effects, and less affected by individual experiments (Eickhoff et al., 2017; Eickhoff et al., 2016).

Finally, our results fit well with findings of white matter (WM) degeneration. In previous studies (Bora et al., 2011; Vitolo et al., 2017) the anterior part of the corpus callosum, the anterior thalamic radiation, inferior longitudinal and fronto-occipital fasciculi, cingulate bundle and fornix were associated to SZ. Notably, these tracts connect GM regions that have been found to be decreased in at least one of the stages. For instance, the anterior corpus callosum might contribute to abnormalities in interhemispheric communication between the AIs during the progression of the disorder, in agreement with studies reporting volumetric alteration of right deep prefrontal-insular WM and a widespread disruption of right genu of the corpus callosum in ChSZ individuals (Mitelman et al., 2009; Spalletta et al., 2015; Sugranyes et al., 2012). To note, long association tracts connecting bilateral ACC, AI and medial prefrontal cortex have been found altered in SZ (Bora et al., 2011; Reid et al., 2016), and also the aberration of bilateral anterior thalamic radiation is a well-replicated finding in chronic stage of the disease (Canu et al., 2015; Li et al., 2017). Taken in this context, GM findings of the present study are in line with fronto-striatal and temporo-limbic systems disruption as well as evidence regarding progressive disconnection of the brain in SZ.

2.4.2. Differences and overlaps between clinical groups: evidence for a typical progression of the GM loss

While none of the meta-analytic works to date assessed an objective overlap estimation between the c-HR, RDSZ and ChSZ groups, here we have quantitatively evaluated the conjunction areas of alteration, in parallel with the differential areas emerging from the between groups comparisons. The contrast ALE analyses showed that the RDSZ group report a larger brain volume characterized by GM reduction compared to c-HR group, suggesting an important enlargement of altered encephalic areas during the first period of full-blown non-affective psychosis. We found a similar trend in the second comparison: recently diagnosed versus chronic SZ. In this case, the two groups differ significantly for mean age, duration of illness and for the total volume of GM decrease.

The strong increment in the GM reduction found in the post-onset phase of SZ may be explained by the fact that the c-HR groups include heterogeneous subclinical psychopathological states that not necessarily, and in a relatively small proportion

(approximately 36% after 3 years from the first evaluation), will transition into a diagnosis of SZ (Falkenberg et al., 2015; Fusar-Poli et al., 2012). In addition, the first months after the onset of the disorder are considered the most critical in influencing prognosis and the most correlated to neurotoxic processes, especially if the patient is not correctly and promptly diagnosed and treated (Anderson et al., 2014).

The R-ACC is the only cluster found among c-HR subjects and is also present in the SZ groups, suggesting a potential significant role of this area in the development and progression of the disorder. Both structural and functional aberrations of the R-ACC are well-replicated findings in different cohorts of individuals at high clinical-risk for psychosis (Allen et al., 2010; Fornito et al., 2008; Fusar-Poli et al., 2011a; Fusar-Poli et al., 2011b; Fusar-Poli et al., 2014; Jessen et al., 2006; Shim et al., 2010; Takayanagi et al., 2017). Moreover, this anatomical region was recently proposed as being the epicenter of neuronal volume loss in SZ (Shafiei et al., 2020). Therefore, the ACC volumetric loss could represent a neuroimaging marker of SZ both before (that is, in the prodromal phase with a putative prognostic significance of transition to SZ) and after the onset of the disorder. However, further research is needed to unravel this issue, especially on patients who later develop psychosis and with the help of harmonized longitudinal protocols to increase comparability across multiple sites (Andreou and Borgwardt, 2020; Cannon et al., 2014; Fusar-Poli et al., 2012).

When compared to the c-HR group, the RDSZ condition shows 4 leftward clusters of higher GM reduction, located in the frontal, parietal, temporal, insular cortices and in the subcortical region of the claustrum (Table 2.2). These results suggest a typical diffusion of GM decrease across left hemispheric cortical areas, which can be detected in the first months after the onset of the disorder (Takahashi and Suzuki, 2018). Interestingly, our findings align with both theoretical and experimental proposals suggesting a prominent abnormal left asymmetry of neural systems in SZ driven by volumetric reductions (Oertel et al., 2010; Oertel-Knöchel and Linden, 2011; Ribolsi et al., 2014). The cortical involvement of the left hemisphere in early stages of SZ was also described by recent resting-state functional connectivity MRI studies (Li et al., 2019c; Li et al., 2017; Wang et al., 2019), which outlined a prevalence of reduced leftward interactions between the functional networks involved in language, interoceptive awareness, auditory and sensory processing. Furthermore, the volumetric reduction of highly connected anatomical structures (such as the AI, STG, IFG and claustrum) is consistent with the pathophysiological model proposed by Palaniyappan

(2017), according to which a GM dysfunctional remodeling takes place in topologically important hubs of the brain, mostly in the immediate post-onset phase of SZ, thus representing an adaptive but inefficient compensatory response to the disorder itself.

RDSZ and ChSZ conditions share convergent patterns of volumetric GM loss preferentially in the left hemisphere (i.e. IFG, PrCG, AI and Amy), except for the bilateral cluster of ACC (Fig. 2.5**)**. These higher-order integration areas were repeatedly found altered in both the recently diagnosed and chronic populations, and related to the wide range of signs and symptoms of SZ (Jeong et al., 2009; Killgore et al., 2009; Shepherd et al., 2012; Wylie and Tregellas, 2010; Yan et al., 2012). It is worth noting that these regions partially overlap with the cortical distribution of the Von Economo Neurons (VENs), large spindle-bipolar neuronal cells, mostly located in layer V of the AI and of the ACC (Allman et al., 2010, 2011). VENs are also present in great apes and other mammalians and are associated with "social brain" abilities (Butti et al., 2013; Cauda et al., 2014b). Alterations of this neuronal subpopulation in post-mortem histological studies were associated with SZ (Brüne et al., 2010; Brüne et al., 2011; Krause et al., 2017). Overall, results are to be interpreted with caution as these neuroanatomical regions were also recently classified as brain hubs with *high structural alteration variety*, which is to say that they can be affected by a wide range of psychiatric and neurological disorders (Cauda et al., 2019b; Crossley et al., 2014; Liloia et al., 2018). Following this view, the development of 'reverse inference' methodologies (e.g., advanced computational tools based on Bayesian statistic inference) is needed to better define neural substrates that are specific to SZ.

Contrast analyses between SZ groups highlight the presence of areas of volumetric loss, which are specific to either the recent diagnosis or to the chronic conditions. A selective GM reduction, found in the RDSZ group only, belongs to cortical areas of the frontal, parietal and insular lobes of the left hemisphere and, to a lesser extent, to the right temporal lobe. The leftward temporal and prefrontal clusters observed in the RDSZ patients might suggest some form of dysfunctional compensation or reorganization mechanism that might take place just after the disruption caused in the acute phase of the first episode of psychosis (Palaniyappan, 2017).

In the ChSZ group five clusters of more marked GM reduction have been found in both cerebral hemispheres, showing a left-to-right and cortical-to-subcortical enlargement that appears to affect the bilateral AI, PHG, Amy, Thal (pulvinar and medial dorsal nuclei) and the

STG. This robust finding is significant, given that GM reductions occurring homotopically have been underemphasized by previous voxel-based investigations. It also worth noting that both cross-sectional and longitudinal approaches have so far collected conflicting results for parahippocampal and amygdalar involvement at different phases of SZ (Shepherd et al., 2012). In accordance with some studies (Asami et al., 2012; Chan et al., 2011; Davidson and Heinrichs, 2003; Velakoulis et al., 2000; Wright et al., 2000), our results underline that abnormalities of the left amygdala-parahippocampal complex are present during the first stages of SZ and that the involvement of the right complex is likely to reflect the chronicity of the disorder. Furthermore, recent studies reported a disrupted interhemispheric coordination in terms of altered functional connectivity and white matter tracts in subjects with SZ (Hoptman et al., 2012; Liu et al., 2018; Sun et al., 2015). Interestingly, new lines of research support the idea that GM tissue damage in SZ is constrained by brain pathways (Cauda et al., 2018b; Shafiei et al., 2020), and intimately related to homotopic interactions (Mancuso et al., 2019). These findings emphasize the role of aberrant connections linking homotopic areas in the development of SZ.

Although thalamic anomalies are well known to be implicated in the SZ condition (Pergola et al., 2015), some meta-analytical investigations found significant volumetric reductions of this diencephalic structure starting from the early phase of illness (Adriano et al., 2010; Ellison-Wright et al., 2008), and others in the chronic stage only (Bora et al., 2011) or exclusively left-lateralized in ChSZ (Chan et al., 2011). This inconsistency is not entirely surprising: different results could be due to the limited MRI resolution, heterogeneity in meta-data selection, study design, as well as to different methodological procedures. The present ALE meta-analysis highlights a selective involvement of L-MDN and bilateral pulvinar in the ChSZ condition, which accords well with some neuroimaging and post-mortem studies (Brickman et al., 2004; Byne et al., 2001; Byne et al., 2009; Horga et al., 2011; Kemether et al., 2003; Pergola et al., 2015; Shimizu et al., 2008).

Even if the neurobiological agents underlying these changes remain largely unknown and the role of structural and functional connectivity in the GM progression is still an open issue in SZ and other neuropsychiatric disorders (Cauda et al., 2019a), the marked increase of the GM volume reduction found in the three stages of the disorder here analyzed (c-HR < RDSZ < ChSZ) is consistent with the contemporary pathophysiological models of SZ, which

describe altered neurodevelopmental long term processes accompanied by neuroprogression phenomena (Andreasen, 2010; Ashe et al., 2001; Keshavan, 1999; Palaniyappan, 2017).

2.4.3. Behavioral characterization: unbiased evidence for a link between GM alterations and psychological features of the disorder

The progression of GM alteration from the RSDZ condition to the ChSZ one has its counterpart in the functional characterization, as all the behavioral subdomains found in the RDSZ group are shared by the ChSZ subjects, who show many other involved mental processes.

Auditive perceptive and phonologic linguistic subdomains exhibit the higher z-scores in the RDSZ condition. The GM reduction associated with the auditive alteration is in agreement with a higher prevalence of positive symptoms in the first months after the onset of the disorder, such as paracusia (Fountoulakis et al., 2019; Fountoulakis et al., 2020), while the phonologic linguistic involvement may be lead to the negative symptoms affecting language processes (Compton et al., 2018). Among these symptoms, aprosody, a specific aspect of the vocal blunted affect, defined as the reduced ability to produce the melodic line of speech thanks to variations in pitch, rhythm, and stress of pronunciation, has been recently associated with patients with a shorter DOI (Compton et al., 2018).

Focusing on GM alteration at a single cluster-level in RDSZ, we find the involvement of linguistic and action speech subdomains associated with the GM reduction in the L-IFG cluster, and of perceptive subdomains (audition and pain) connected with the bilateral TTG clusters. The L-IFG is considered a central node of human brain, implicated in semantic and affective integration during communication (Belyk et al., 2017); its volumetric reduction and dysconnectivity in the first phases of SZ has been associated to linguistic, memory and encoding impairment (Bonner-Jackson et al., 2005; Chen et al., 2014; Jeong et al., 2009).

With regard to common subdomains shared by the two SZ groups, two clusters of GM reduction emerge: L-Ins and L-Amy. The L-Ins cluster suggests an involvement of several cognitive functions, including attention, reasoning, language, working and explicit memory and music comprehension, as well as of action subdomains like execution of speech and inhibition of movement. These data-driven associations accord well with the findings of Liao et al. (2015), who found positive correlations between the GM volume of the L-Ins and

performance at the Digit Symbol Substitution Test (DSST; Jaeger, 2018) in a large cohort of patients with SZ.

To note, this region has been recently found to predict treatment response and clinical prognosis of both RDSZ and ChSZ patients (Li et al., 2019b; Mikolas et al., 2016), showing an important role in the pathophysiology of SZ. In both SZ groups, the L-Amy cluster was linked to negative emotional, explicit memory and visual perception functions. Functional MRI studies report aberrant amygdalar activation in SZ, showing patterns of hypo-connectivity with the insula and IFG during emotional and social recognition tasks (Mier et al., 2019; Mukherjee et al., 2014).

In ChSZ several mental processes, relating to neurocognition (i.e. attention and reasoning), language (i.e. speech and semantics), reward/gain positive emotion and sexuality (i.e. libido) show a high z-score at cluster-level. The neurocognitive impairment, especially the deficits in attentional functions, is a typical trait of SZ (Green et al., 2019; Kahn and Keefe, 2013), which is present since the prodromal phase with important worsening at the illness onset and a slower increment during its progression (Seidman and Mirsky, 2017). In this regard, we observe that a previous voxel-based investigation of ChSZ subjects (Schiffer et al., 2010) showed significant associations between GM volume of frontal/cingulate cortex and planning performance, reasoning, and executive inhibition.

The involvement of cognitive functions related to language production can partially explain the negative symptomatology of SZ, in particular some expression deficits like alogia, and aprosody (Compton et al., 2018). We suppose a similar correlation between the involvement of the reward/gain emotional processes and the pole of reduced motivation of the negative symptoms, interpreted as a product of the reduced ability to expect and feel pleasure during activities (anhedonia) and the reduced ability to start actions and projects (avolition) (Lee et al., 2015). The high engagement of emotional subdomains, defined as the "mental faculty of experiencing an affective state of consciousness" (http://brainmap.org/taxonomy/behaviors.html), including positive and negative emotion like reward/gain, happiness, fear, sadness, disgust, anxiety and anger, may represent a neuroanatomical counterpart of the blunted affect dimension of negative symptoms. More generally, the significant involvement in the ChSZ group of mental processes theoretically related to negative symptoms is concordant with the high prevalence of this type of symptoms in the chronic condition (Fountoulakis et al., 2019; Fountoulakis et al., 2020). Indeed, primary

persistent negative symptoms still represent an unmet need in the care of patients with SZ (Mucci et al., 2017). Finally, the GM reduction of cerebral areas correlated with sexual interoception is in line with the evidence of deficits in sexual cognition and fantasy arousal found in unmedicated patients with SZ: these deficits, therefore, are not necessarily secondary to the antipsychotic treatment (Dembler-Stamm et al., 2018).

2.4.4. Functional networks and their relationship with different SZ stages

Most of the altered GM volume in each clinical group belongs to encephalic regions that are key nodes of the SN, which is composed by the ACC, the ventral part of the PrCG (BA 6, pre-SMA) and the AI (Seeley et al., 2007). The pivotal role played by this functional network in the psychopathology of SZ is supported by numerous studies that found associations between structural and functional alteration of the SN and the core symptoms and the prognosis of the disorder (Li et al., 2019b; Palaniyappan and Liddle, 2012). Moreover, in agreement with our results, alteration of the SN was found in all the SZ stages (Mallikarjun et al., 2018; Spreng et al., 2019; Wang et al., 2016). The SN is thought to be responsible for dynamic switching between default mode and task-related states of the brain, and is engaged in a plethora of tasks involving interoceptive, action, perceptive and cognitive domains (Menon and Uddin, 2010; Uddin, 2015). Our behavioral characterization accords well with this evidence.

In terms of absolute number of volumes associated, the OFC-N was the most functional network involved in the c-HR group, with the following progression between the three clinical groups: c-HR < RDSZ < ChSZ. The importance of the OFC-N in the prodromal phase of SZ was emphasized by Collin et al. (2018), who found that the OFC resting-state functional connectivity (rsFC) is a distinctive trait of the c-HR subjects that, after the MR scan, transition into overt psychosis. The OFC-N is involved in the inference of the expected outcomes' values. This inference ability is impaired when the rsFC of the OFC is reduced with targeted transcranial magnetic stimulation (Howard et al., 2020). Therefore, a GM decrease of OFC-N cortical areas could be related to the prodromal negative symptoms, particularly to the motivational deficits that are frequently found in c-HR subjects and heavily impact on quality of life (Glenthoj et al., 2020).

Morphometric variations of RDSZ appear to accumulate preferentially in specific functional systems, namely L-VAN, MN and SMN. GM reductions of the BA 44, 45 and 47

located in the L-IFG correspond to a selective involvement of the L-VAN, that is thought to be involved in reorienting attention toward unattended stimuli (Corbetta et al., 2002). This result accords well with the evidence of altered connectivity of the VAN in patients in the SZ early-stage (Hummer et al., 2020). However, it should be noted that the involvement of the R-VAN is almost exclusive to the ChSZ condition; it might therefore be considered as the functional counterpart of the homotopic progression (from left to right) of the GM alteration.

A significant GM decrease of the BAs 6 and 4, which are parts of the MN, is specifically found in the RDSZ condition. In particular, the primary motor area (M1) corresponds to the BA 4 and the premotor area (PMA), while the supplementary motor area (SMA) and the pre-SMA partly belong to the BA 6. Our findings are in agreement with previous studies showing alteration of M1 and SMA connectivity in SZ, after controlling for age and antipsychotic medications (Bernard et al., 2017), as well as alteration of the BA 6 correlated with abnormal involuntary movements in RDSZ patients (Kindler et al., 2019).

The specific GM reduction of the *pars opercularis* of the PoCG (BA 43), which constitutes part of the secondary somatosensory area (S2), corresponds to the selective involvement of the SMN found in the RDSZ group. This network is involved in auditory, visual, tactile and direct pain perception, social perception (observation of the stimulus percepted by others), and empathetic accuracy tasks (judging the meaning of the social stimulus) (Keysers et al., 2010; Paracampo et al., 2017). The SMN dysconnectivity has been associated with multiple transdiagnostic dimensions of psychopathology in different major psychiatric disorders, including SZ (Kebets et al., 2019). Furthermore, a recent study on RDSZ subjects demonstrated how, in this specific phase of the disorder, sensorimotor conflictual stimuli could induce failure in bodily self-monitoring by generating presence hallucination, that is, by making patients wrongly perceive a person standing behind themselves (Salomon et al., 2020).

GM reductions in the bilateral thalami (MDN and pulvinar) and in the head of the left caudate have been specifically associated with the ChSZ group. In this group such GM loss may reflect the greater involvement of the Th-BN-N at both absolute and relative levels. This result is in line with a recent study on ChSZ patients (mean DOI > 15 years) that reported a hypo-connection of the SN with the MDN of the thalamus, the ventral parts of striatum and the pallidum, and a hyper-connection of the SMN with the anterior ventral nucleus of the thalamus and the dorsal striatum, which includes the caudate nucleus (Avram et al., 2018).

Thus, according to this evidence and to our results, it is likely a progressive involvement of subcortical "relays" structures as SZ develops. This engagement might play a role in the dysconnectivity and altered integration of other functional networks, such as the SN, MN and the SMN (Ferri et al., 2018; Hua et al., 2019; Skåtun et al., 2018).

2.4.5. Effects of clinical and methodological variables

Our voxel-wise meta-regression approach suggests that gender, antipsychotics, sample size and imaging smoothing level had significant effects on GM alterations across experiments. The result of widespread brain abnormalities in patients' groups with higher percentage of male is not surprising in SZ literature. Similarly to Bora et al. (2011), our results reveal a GM negative relationship related to the L-IFG, R-Ins, and bilateral thalamus in samples with a higher percentage of male patients. Volumetric variations have been related to different GM decreases in male/female patients with SZ (Mendrek and Mancini-Marïe, 2016), which to some extent may reflect different gender health development (Lotze et al., 2019).

Groups with a high percentage of patients undergoing antipsychotic treatment have been associated with more severe GM loss in the L-MFG, R-STG, and R-Ins. At present, the association between the antipsychotic medication and regional anatomical changes in SZ remains inconsistent (Lawrie, 2018). Taken in this context, our results provide voxel-based evidence of localized effects related to antipsychotic drug usage. Cautious interpretations are needed due to the lack of longitudinal approach and the unappreciated contribution of other variables such as the severity of symptoms, which could variously correlate with an antipsychotic treatment and its duration, dosage and typology, as well as a more or less marked GM alteration (Fusar-Poli et al., 2013; Vita et al., 2015).

Small sample size impacts on GM findings in a double cluster of alteration, corresponding to the R-STG and the L-ACC. This result is consistent with a number of studies highlighting the importance of sufficiently large sample sizes in neuroimaging investigations in order to enhance reproducibility and decrease between-study heterogeneity (Chen et al., 2018; Ingre, 2013; Lorca-Puls et al., 2018). Although the CBMA approach tends to mitigate these issues, our findings further highlight that it is advisable to increase the number of patients to provide more robust results.

The absence of significant linear effect on GM volumes with chlorpromazine equivalents

could be explained by the heterogeneity of antipsychotic drugs and of the times of exposure to the drugs (Vita et al., 2015). A similar explanation concerns the absence of linear association between positive and negative symptoms and GM alterations. These two dimensions of symptoms were evaluated with the PANSS positive and negative subscales, that include many items poorly correlated with these two symptomatic constructs, therefore introducing "noise" in the data (Fountoulakis et al., 2019). More specific and targeted evaluations of signs and symptoms of SZ, possibly based on the factor analysis of the PANSS (Kay et al., 1987) and taking into account also disorganized, depressive and cognitive symptoms, should be recommended in all neuroimaging studies on SZ in order to better detect significant correlation between imaging and specific aspects of the disorder.

2.4.6. Innovation and strengths

Our work partially confirms the results of the previous CBMAs about SZ stages and provides new evidence for their better characterization. First, we were able to include the largest number of published experiments due to the rapid growth of the field. The balance between sensitivity and susceptibility to false positive effects was therefore maximized and the power of the meta-analysis increased (Müller et al., 2018).

Second, published articles that pooled together both patients with short and long duration of illness were excluded and studies about HR were included, allowing us to study morphological and functional patterns related to specific stages of the disorder, including the prodromal phase, so as to exclude possible confounding elements derived from other diagnosis belonging to the SSD. For the comparisons between clinical groups we added a set of conjunction and contrast analyses, allowing us to statistically derive common and potentially distinctive neuroanatomical markers.

Third, we employed a new revised version of the ALE method and implemented a conservative thresholding. To our knowledge, this is the first ALE study on SZ using both the corrected GingerALE version and cluster-level FWE correction, ensuring an adequate type I error control and the maximum statistical rigor (Eickhoff et al., 2017; Eickhoff et al., 2016). Importantly, the involvement of ALE-derived brain regions was further demonstrated via voxel-wise permutation tests.

Fourth, we found the neuroanatomical effects of male sex, sample size, image smoothing level and medication. Although these results should be interpreted with caution, as

meta-regression tested the mean-relation between samples (Radua et al., 2012) and a different algorithm than ALE was employed, they might shed light on the impact of certain variables on GM findings, as well as improve future sampling and methodological strategies.

Fifth, the quantitative functional characterization used in this study ensured a comprehensive and objective behavioral association to GM findings, and explored mental functions prominently linked to different stages of SZ. This choice was motivated by the long-standing debate concerning the limits of observer-dependent and region-to-behavior inference in the field of neuroimaging (Scarpazza and De Simone, 2016).

2.4.7. Limitations and challenges

The present study has general limitations inherent to meta-analytic approach. The ALE technique is based on stereotactic foci reported by published articles and, therefore, may be potentially affected by the publication bias against null results (i.e. file-drawer problem) (Müller et al., 2018). Other bias could relate to the selective local maxima evaluation, excluding the remaining significant voxels of variation. However, it should be noted this standardized procedure in the neuroimaging field and in CBMA, can decrease the probability of making spatial errors (Eickhoff et al., 2009; Radua et al., 2012). We also note that the incomplete reporting of included investigations data may hamper some meta-regression results. For instance, a number of studies do not provided information about medication dosage (49/90 studies, 54.5% of the total) or PANSS positive and negative scores (34/90 studies, 37.7% of the total).

Finally, it is important to point out that our approach cannot determine causality of illness progression due to the lack of longitudinal design. However, robust cross-sectional meta- and mega-analyses are also essential to further clarify this issue and build a more integrative view (Meisenzahl et al., 2008a; Pantelis et al., 2005; Torres et al., 2016; Zhao et al., 2018). In this regard, our approach has been highly sensitive in quantifying more widespread structural changes in the chronic condition than in the first period after the onset of the disorder; in addition, it has been able to identify certain common alteration patterns that could represent critical starting points in the propagation of damage and clinical manifestations of the disease.

Although we have consolidated the existing literature by identifying the ‘if’ and ‘where’ of GM changes in SZ, future investigations are needed to detect ‘how’ these changes co-occur

in a network-like architecture and diffuse at different stages of disease. Moreover, the development of novel 'reverse inference' methodologies is greatly needed in order to disentangle the pathological brain landscape, as well as to identify the cerebral regions exhibiting high alteration specificity for the SZ condition.

2.5. Conclusion

This meta-analysis provides a quantitative summary of voxel-based results on different stages of SZ published over the last two-decades. Our findings support the current framework that considers SZ as a neurodevelopmental disease with a neuroprogressive component, but also update and characterize the pathological landscape of SZ stages. The heterogeneity in the underlying literature notwithstanding, we have found high-quality evidence for convergent GM loss in cortico-striatal-limbic hub regions. It is worth noting that the GM reduction in the R-ACC is present both in the c-HR group and in SZ groups; if confirmed, this result would make the alteration of R-ACC a possible marker of disease progression. A widespread GM loss has been found in the RDSZ patients, mainly in frontal and temporal areas of the left cerebral hemisphere. A further spread of the GM reduction in homotopic areas of the right hemisphere as well as into subcortical region has been found in the ChSZ subjects. Albeit in cross-sectional and meta-analytic manner, these results are likely to reflect the temporal progression of SZ and the interhemispheric and subcortical diffusion of its neuroanatomical alteration. The development of novel neuroimaging methodologies and of longitudinal multicenter and multimodal studies is needed to advance in this field. We are therefore hopeful that the approach employed here may pave the way for research on possible diagnostic and neuroimaging biomarkers of SZ staging, as well as on the identification of new therapeutics target that could be addressed not only with psychopharmacological treatments but also with focused magnetic and/or non-invasive electric stimulation and with evidence-based psychosocial rehabilitation programs.

2.6. Supplementary material

2.6.1. Supplementary tables

Table S2.1. Checklist for neuroimaging coordinate-based meta-analysis (adapted from Muller et al. 2018).

1 The research question is specifically defined	**YES** and it includes the following contrasts: **General Meta-Analyses:** a) g-HR group < HC group; b) c-HR group < HC group; c) RDSZ group < HC group; d) ChSZ group < HC group. **Contrast Meta-Analyses:** e) (c-HR group < HC group) < (RDSZ group < HC group); f) (RDSZ group < HC group) < (c-HR group < HC group); g) (c-HR group < HC group) U (RDSZ group < HC group); h) (RDSZ group < HC group) < (ChSZ group < HC group); i) (ChSZ group < HC group) < (RDSZ group < HC group); j) (RDSZ group < HC group) < (ChSZ group < HC group); k) (RDSZ group < HC group) U (ChSZ group < HC group).
2 The literature search was systematic	**YES**, it includes the following keywords in the following databases **(PRISMA international guidelines used)**: **Databases**: BrainMap (http://www.brainmap.org/), PubMed MEDLINE (https://www.ncbi.nlm.nih.gov/pubmed/), reference within the selected literature. **Keywords BrainMap**: [Experiments Contrast is Gray Matter] AND [Experiments Context is Disease Effects] AND [Subjects Diagnosis is Schizophrenia] AND [Subjects Diagnosis is NOT Schizotypal Personality Disorder] AND [Subjects Diagnosis is NOT Schizoaffective Disorder] AND [Experiments Observed Changes is Controls > Patients] AND [Experiments Observed Changes is Controls < Patients]. **Keywords PubMed**: ("voxel-based morphometry" OR "VBM" OR "voxel-wise") AND ("schizophrenia" OR "chronic schizophrenia" OR "SZ" OR "first episode schizophrenia" OR "first episode psychosis" OR "high risk schizophrenia" OR "siblings schizophrenia" OR "first degree relatives" OR "genetic risk schizophrenia" OR "at risk of mental state" OR "ARMS" OR "ultra-high risk").
3 Detailed inclusion and exclusion criteria are included	**YES**, and reason for non-standard criterion was: **Standard inclusion criteria applied:** a) Only experiments that used whole-brain analysis; b) Only experiments published in a peer-review journal; c) Only experiments that reported results in a stereotactic space. **Non standard inclusion criteria applied:** d) Only experiments that used VBM - in order to maximize the power of the meta-analysis and to exclude meta-data with other structural and functional MRI methods, whose results have a different meaning;

	e) Only experiments that performed a between-group comparison with clinical groups of interest and healthy controls - in accordance with research question; f) Only experiments (i.e., g-HR group) that included subjects that were monozygotic twins, siblings and first/second-degree relatives of patients with SZ - in accordance with research question; g) Only experiments (i.e., c-HR group) that included at risk of mental state subjects based on PACE, CAARMS or SIPS criteria - in order to specifically study the clinical risk contribution according to the model proposed by Fusar-Poli et al. (2011a); h) Only experiments (i.e., RDSZ and ChSZ groups) that included subjects with diagnosis of SZ based on DSM and ICD criteria - in order to specifically address the contribution of SZ (diagnosed with the most employed and stable over time diagnostic criteria) to neuroimaging alteration and not that of the whole SSD; i) Only experiments (i.e., RDSZ and ChSZ groups) that included in the experimental group subjects with specific a specified duration of illness (DOI) in order to study the disorder at different stages (i.e. RDSZ = DOI < 2 years and ChSZ = DOI ≥ 2 years); j) Only experiments (i.e., RDSZ and ChSZ groups) that included subjects without other medical comorbidities - in order to exclude confounding factors and to increase the specificity of the coordinate-based meta-analysis; k) Only experiments that adopted analyses corrected for multiple comparisons or cluster-wise extent thresholds >100 voxels, in order to reduce the likelihood to include experiments presenting false positives; l) Only experiments with sample size ≥ 10 participants (per group) - in order to reduce the likelihood to include experiments presenting false positives, according to previous coordinate-based meta-analyses; m) Only experiments with non-mixed experimental sample (i.e., RDSZ + ChSZ subjects) - in order to exclude confounding factors related to the stage of illness and to increase the specificity of the coordinate-based meta-analysis; n) Only more recent experiments published by the same research group with the same sample - in order to prevent redundancy of subjects and related results.
4 Sample overlap was taken into account	**YES**, using the following method: For each selected article, only the contrast of interest that the meta-analysis aims to investigate has been included. In some cases, more contrasts were selected for a single article: in all these cases, the authors run the analysis on two or more independent samples (i.e., g-HR, C-HR, RDSZ and/or ChSZ vs HC) and this is clearly stated in the article.
5 All experiments use the same search coverage	**YES**, the search coverage is the following: **Whole-brain voxel-based morphometry analysis**. If an experiment reported whole brain + ROI or SVC analysis, the whole-brain analysis only has been included in the meta-analysis; if an experiment reported the ROI analysis or SVC only, the experiment was excluded from the meta-analysis in accordance with our inclusion/exclusion criteria. Experiments reporting only conjunctional analysis have been excluded.
6	**YES**, using the following conversion:

Studies are converted to a common space	**Meta-analyses were conducted in Talairach (TAL) space.** The icbm2tal algorithm, as implemented in GingerALE software (v.3.0.2), was used to convert the native Montreal Neurological Institute (MNI) coordinates into TAL space.
7 Data extraction have been conducted by two investigators	**YES**, the following authors: DL, CB and PR checked inclusion criteria; DL, CB extracted coordinates; DL, CB extracted other info: clinical, socio-demographic and methodological meta-data reported in Supplementary tables S2.2 and S2.3.
8 The paper includes a table with basic study descriptions	**YES**, and also the following data: Article reference; number of subjects included; sex distribution, mean age at scan, classification and instrument of classification (i.e., PACE, CAARMS, SIPS, DSM or ICD) for experimental subjects (i.e., g-HR, c-HR, RDSZ and ChSZ groups), duration of illness, percentage of subjects on antipsychotic treatment, contrast performed, number of foci of GM variation for each experiment included, type of VBM software, p value threshold, MRI static field, smoothing, slice thickness and coordinate system.
9 The study protocol was previously registered and all analyses planned	a) The present coordinate-based meta-analysis was not registered before starting the search. According with PROSPERO database (https://www.crd.york.ac.uk/prospero/), both systematic and scoping literature review and meta-analysis should be not registered, which is the present case; b) We declared that we planned all the analysis before starting the literature search and that we did not run any non-planned or non-prespecified analysis; c) The meta-analysis used the default methods and parameters of the software with the following exceptions: none.
10 The meta-analysis includes diagnostics	**YES**, we used post hoc analyses providing more detailed information on the revealed clusters of convergence or effect: Voxel-wise meta-regression analyses, using the Signed Differential Mapping software (SDM v.6.12).

Table S2.2. Articles included in the meta-analysis: demographic and clinical meta-data.

Study	Subjects			Classification or Instrument	DOI	Antipsychotic treatment (%)	Healthy Controls		
	N	M(F)	Age				N	M(F)	Age
Genetic and Clinical High-Risk Group									
Benetti et al. (2013)	21	9 (12)	22.1 (3.3)	cHRS (PACE)	N.A.	9%	23	12 (11)	24.2 (4.2)
Bogwardt et al. (2007a)	12	9 (3)	24.6 (5.3)	cHRS (PACE)	N.A.	8%	22	13 (9)	23.0 (4.3)
Bogwardt et al. (2007b)	35	22 (13)	23.7 (5.6)	cHRS (PACE)	N.A.	9%	22	13 (9)	23.0 (4.3)
Bogwardt et al. (2008)	10	7 (3)	25.2 (6.7)	cHRS (PACE)	N.A.	10%	10	5 (5)	24.2 (6.1)
Bogwardt et al. (2010)	28	22 (6)	37.7 (9.1)	F-RELATIVE	N.A.	N.A.	34	24 (10)	39.3 (9.5)
Chang et al. (2016) (HR exp.)	31	21 (10)	18.4 (3.4)	F-RELATIVE	N.A.	3%	71	27 (44)	20.6 (3.5)
Dukart et al. (2017)	59	43 (16)	24.7 (5.7)	cHRS (PACE)	N.A.	23%	26	12 (14)	27.7 (4.5)
Fusar-Poli et al. (2011a)	15	N.A.	N.A.	cHRS (PACE)	N.A.	0%	15	N.A.	N.A.
Fusar-Poli et al. (2011b)	39	24 (15)	24.5 (4.5)	cHRS (PACE)	N.A.	46%	41	33 (8)	25.9 (5.2)
Guo et al. (2014)	25	17 (8)	23.2 (3.3)	F-RELATIVE	N.A.	0%	43	25 (18)	23.7 (2.8)
Guo et al. (2015) (HR exp.)	46	29 (17)	22.9 (4.0)	F-RELATIVE	N.A.	0%	46	23 (23)	23.3 (2.3)
Honea et al. (2008)	213	87 (126)	36.5 (9.7)	F-RELATIVE	N.A.	0%	212	101 (111)	33.3 (9.9)
Hu et al. (2013) (HR exp.)	48	30 (18)	22.3 (3.9)	F-RELATIVE	N.A.	0%	59	38 (21)	23.2 (2.6)
Hulshoff Pol et al. (2006)	22	12 (10)	39.0 (11.7)	F-RELATIVE	N.A.	N.A.	22	11 (11)	37.0
Jacobson et al. (2010)	11	N.A.	12.0	cHRS (CAARMS)	N.A.	0%	14	N.A.	11.0
Job et al. (2003) (HR exp.)	146	74 (72)	21.2 (2.9)	F/S RELATIVE	N.A.	0%	36	17 (19)	21.2 (2.4)
Jung et al. (2012)	16	9 (7)	21.6 (4.1)	cHRS (CAARMS)	N.A.	19%	23	13 (10)	22.9 (3.7)
Lee et al. (2013)	32	22 (10)	20.6 (2.5)	cHRS (SIPS)	N.A.	0%	32	20 (12)	21.9 (2.4)
Lei et al. (2015) (HR exp.)	44	26 (18)	23.1 (6.9)	F-RELATIVE	N.A.	0%	44	26 (18)	22.5 (6.2)
Li et al. (2012)	21	7 (14)	21.1 (5.5)	F-RELATIVE	N.A.	0%	48	24 (24)	22.0 (5.1)
Lincoln et al. (2014)	22	N.A.	22.0 (4.5)	cHRS (SIPS)	N.A.	N.A.	21	N.A.	22.2 (3.0)
Lui et at al. (2009a) (HR exp.)	10	4 (6)	41.4 (3.7)	F/S-REALTIVE	N.A.	0%	10	4 (6)	43.2 (6.3)
Marcelis et al. (2003)	32	14 (18)	35.5 (10.0)	F-RELATIVE	N.A.	N.A.	27	12 (15)	35.5 (9.8)
McIntosh et al. (2006)	50	N.A.	38.9 (12.9)	F/S-RELATIVE	N.A.	0%	48	N.A.	N.A.
McIntosh et al. (2007)	75	57 (20)	22.0	F/S-RELATIVE	N.A.	N.A.	15	9 (6)	21.8

Study	Subjects			Classification or Instrument	DOI	Antipsychotic treatment (%)	Healthy Controls		
	N	M(F)	Age				N	M(F)	Age
Mechelli et al. (2011)	182	66 (116)	23.0	cHRS (PACE)	N.A.	8%	167	104 (63)	23.5
Meisenzahl et al. (2008b)	40	25 (15)	25.0 (5.6)	cHRS (PACE)	N.A.	0%	75	46 (29)	25.1 (3.8)
Nenadic et al. (2015)	43	21 (22)	23.7 (3.3)	cHRS (CAARMS)	N.A.	0%	49	26 (23)	23.8 (3.0)
Oertel-Knochel et al. (2012) (HR exp.)	29	14 (15)	40.4 (15.8)	F-RELATIVE	N.A.	0%	37	17 (20)	39.9 (10.5)
Pantelis et al. (2003)	23	13 (10)	19.3 (3.7)	cHRS (PACE)	1.8 (2.1)	N.A.	52	30 (22)	21.6 (3.3)
Sugranyes et al.(2015)	38	25 (13)	11.0 (3.3)	F-RELATIVE	N.A.	56%	83	44 (39)	11.8 (3.2)
Tian et al. (2011)	55	27 (28)	50.3 (5.1)	F-RELATIVE	N.A.	0%	29	14 (15)	51.8 (5.6)
Wagshal et al. (2015)	14	8 (6)	12.1 (2.4)	F-RELATIVE	N.A.	0%	46	25 (21)	12.9 (2.6)
Witthaus et al. (2009) (HR exp.)	30	20 (10)	25.1 (4.3)	cHRS (SIPS)	N.A.	40%	29	17 (12)	25.7 (5.2)
Recently Diagnosed Schizophrenia Group									
Asami et al. (2012)	33	28 (5)	22.5 (6.7)	DSM-III-R DSM-IV	0.4 (0.4)	100%	36	30 (6)	22.9 (3.8)
Chang et al. (2016) (RDSZ exp.)	60	29 (31)	18.3 (3.4)	DSM-IV	0.7 (1.1)	45%	71	27 (44)	20.6 (3.5)
Chen et al. (2014)	86	47 (39)	24.5 (0.9)	DSM-IV	0.9 (0.2)	0%	86	46 (40)	25.0 (1.0)
Douaud et al. (2007)	25	18 (7)	16.5 (1.3)	DSM-IV	1.4 (0.7)	100%	25	16.2 (1.7)	17 (8)
Farrow et al. (2005)	25	18 (7)	20.0 (3.0)	DSM-III	0.6	100%	22	13 (9)	20.0 (4.0)
Ferri et al. (2012)	19	14 (5)	27.2 (5.4)	DSM-IV	0.6 (0.4)	100%	19	11 (8)	28.7 (5.0)
Guo et al. (2013)	33	16 (17)	24.3 (8.8)	DSM-IV	0.5 (0.2	100%	33	16 (17)	23.8 (8.4)
Guo et al. (2015) (RDSZ exp.)	49	30 (19)	22.7 (4.6)	DSM-IV	1.8 (0.5)	0%	46	23 (23)	23.3 (2.3)
Guo et al. (2019)	33	16 (17)	24.3 (8.8)	DSM-5	0.4 (0.1)	100%	33	16 (17)	23.8 (8.4)
Henze et al. (2011)	13	8 (5)	17.1 (0.5)	ICD-10	0.6 (0.6)	100%	13	8 (5)	17.6 (0.5)
Hu et al. (2013) (RDSZ exp.)	55	34 (17)	22.3 (3.9)	DSM-IV-TR	0.1 (0.6)	0%	59	38 (21)	23.2 (2.6)
Huang et al. (2015)	18	12 (6)	22.5 (4.5)	DSM-IV	0.7 (0.4)	0%	26	17 (9)	23.1 (5.4)
Jayakumar et al. (2005)	18	9 (9)	24.9 (6.3)	DSM-IV	0.9 (0.4)	0%	18	9 (9)	25.7 (7.5)
Janssen et al. (2008)	25	19 (6)	15.4 (1.8)	DSM-IV	0.3 (0.2)	100%	51	35 (16)	15.4 (1.6)
Job et al. (2003) (RDSZ exp.)	34	23 (11)	21.3 (3.6)	DSM-IV	< 1	0%	36	17 (19)	21.2 (2.4)
Kasparek et al. (2009)	32	32 (0)	23.8 (4.7)	ICD-10	0.7 (1.1)	100%	18	18 (0)	24.1 (1.6)
Kubicki et al. (2002)	16	14 (2)	26(7.5)	DSM-III-R	0.1	100%	18	16 (2)	24(4.5)

Study	Subjects			Classification or Instrument	DOI	Antipsychotic treatment (%)	Healthy Controls		
	N	M(F)	Age				N	M(F)	Age
Lei et al. (2015) (RDSZ exp.)	88	52 (36)	23.0	DSM-IV	1.8 (0.6)	9%	44	26 (18)	22.5 (6.2)
Lei et al. (2019)	14	10 (4)	21.8 (5.3)	DSM-IV	< 1	0%	32	23 (9)	21.6 (4.6)
Li et al. (2019)	86	46 (40)	23.5 (6.9)	DSM-5	1.1 (1.2)	100%	86	45 (41)	24.0 (6.3)
Liao et al. (2015)	93	57 (36)	27.0 (6.6)	DSM-IV-TR	1.7 (1.4)	100%	99	53 (46)	25.8 (5.4)
Lui et al. (2009a) (RDSZ exp.)	10	5 (5)	21.2 (7.5)	DSM-IV	0.4 (0.2)	N.A.	10	5 (5)	23.0 (7.9)
Lui et al. (2009b)	68	30 (38)	24.2 (8.6)	DSM-IV	0.7 (1.2)	0%	68	31 (37)	24.7 (8.8)
Meda et al. (2008) (RDSZ exp.)	22	14 (8)	25.1 (7.0)	DSM-III-R DSM-IV	< 2	0%	21	13 (8)	26.2 (7.5)
Meisenzahl et al. (2008a) (RDSZ exp.)	93	67 (26)	28.2 (7.6)	DSM-IV	0.7 (1.0)	85%	177	123 (54)	31.5 (9.2)
Molina et al. (2010)	30	20 (10)	25.8 (5.0)	DSM-IV	1.4 (0.9)	0%	40	23 (17)	29.4 (9.0)
Nakamura et al. (2013)	34	20 (14)	24.7 (5.5)	ICD-10	< 1	0%	51	30 (21)	23.9 (1.8)
Poeppl et al. (2014)	20	15 (5)	27.7 (7.1)	DSM-IV-TR ICD-10	0.1 (0.1)	100%	30	19 (119	30.2 (7.6)
Price et al. (2010)	41	N.A.	26.2	DSM-IV	0.2	100%	47	27 (20)	24.8
Ren et al. (2013)	100	41 (59)	24.3 (7.4)	DSM-IV	0.5 (0.9)	0%	100	41 (59)	24.4 (7.6)
Schaufelberger et al. (2007)	62	44 (18)	27.6 (8.0)	DSM-IV	0.5 (1.2)	39%	94	53 (41)	30.2 (8.4)
Sheng et al. (2013)	33	15 (18)	22.8 (3.5)	DSM-IV	0.7 (0.8)	100%	41	25 (16)	23.5 (2.8)
Tang et al. (2012)	29	13 (16)	16.5 (0.9)	DSM-IV-TR	0.8 (0.4)	83%	34	16 (18)	16.6 (0.8)
Torres et al. (2016) (RDSZ exp.)	62	44 (18)	27.7 (8.1)	DSM-IV	0.5 (1.2)	100%	151	N.A.	N.A.
Voets et al. (2008)	25	18 (7)	16.0 (1.4)	DSM-IV	1.4 (0.7)	100%	25	17 (8)	16.0 (1.5)
Wang et al. (2017a)	18	7 (11)	24.5 (6.7)	DSM-IV	0.6 (0.5)	N.A.	21	10 (11)	22.4 (3.9)
Watson et al. (2012)	25	19 (6)	28.8 (9.0)	ICD-10	1.6 (0.7)	100%	25	19 (6)	28.2 (8.5)
Whitford et al. (2005)	31	20 (11)	19.3 (3.5)	DSM-IV	0.5 (0.7)	87%	30	20 (10)	19.3 (3.0)
Witthaus et al. (2009) (RDSZ exp.)	23	16 (7)	26.4 (6.1)	DSM-IV	0.7	26%	29	17 (12)	25.7 (5.2)
Yoshihara et al. (2008)	18	9 (9)	15.8 (1.8)	DSM-IV	1.2 (0.9)	94%	18	9 (9)	15.8 (1.3)
Zhang et al. (2015)	37	17 (20)	15.5 (1.8)	DSM-IV-TR	1.3 (1.2)	0%	30	17 (13)	15.3 (1.6)
Chronic Schizophrenia Group									
Amann et al. (2016)	45	26 (19)	43.2 (9.1)	DSM-IV	21.5 (9.8)	100%	45	26 (19)	43.3 (9.9)

Study	Subjects			Classification or Instrument	DOI	Antipsychotic treatment (%)	Healthy Controls		
	N	M(F)	Age				N	M(F)	Age
Ananth et al. (2002)	20	10 (10)	37.8 (9.5)	ICD-10-R	15.8	100%	20	10 (10)	38.6 (9.7)
Anderson et al. (2015)	15	13 (2)	34.3 (7.1)	DSM-IV	11.4 (4.5)	100%	20	17 (3)	33.3 (8.4)
Bassitt et al. (2007)	50	38 (12)	31.7 (7.1)	DSM-IV	11.4 (7.4)	100%	30	21 (9)	31.2 (7.6)
Brown et al. (2011)	17	8 (9)	44.8 (6.8)	DSM-IV	19.1 (6.2)	100%	21	10 (11)	45.0 (10.2)
Cascella et al. (2010)	50	37 (13)	39.7	DSM-IV	15.7	100%	90	43 (47)	46.3 (12.7)
Delvecchio et al. (2017)	61	36 (25)	40.8 (11.2)	DSM-IV	14.6 (11.2)	100%	59	35 (24)	40.2 (11.3)
Donohoe et al. (2011)	70	46 (24)	40.4 (11.7)	DSM-IV	17.8 (10.6)	100%	38	20 (18)	32.5 (12.7)
Egashira et al. (2014)	24	8 (16)	58.2 (8.4)	DSM-IV-TR	34.6 (10.3)	N.A.	41	8 (33)	58.8 (8.8)
Garcia-Marti et al. (2008)	17	17 (0)	35.7 (6.1)	DSM-IV	18.8 (7.7)	100%	19	19 (0)	33.1 (7.6)
Giuliani et al. (2005)	41	32 (12)	39.0 (5.6)	DSM-III-R DSM-IV	17.3 (7.6)	N.A.	34	17 (17)	34.7 (7.2)
Hidese et al. (2018)	83	47 (36)	38.6 (11.2)	DSM-IV	14.5 (9.8)	91%	130	67 (63)	42.1 (15.2)
Hirao et al. (2008)	20	10 (10)	36.7 (7.6)	DSM-IV	10.6 (7.4)	100%	20	10 (10)	35.0 (7.1)
Horacek et al. (2011)	44	22 (22)	30.8 (9.8)	DSM-IV	6.6 (4.4)	91%	56	23 (33)	27.9 (7.3)
Jiang et al. (2018)	30	29 (1)	49.0 (8.3)	DSM-IV	> 20	100%	126	84 (42)	38. (14.9)
Kenneth Martin et al. (2014)	26	N.A.	44.6 (10.7)	DSM-IV	22.8	N.A.	50	28 (22)	46.5 (9.6)
Kim et al. (2017b)	22	12 (10)	31.7 (10)	DSM-IV-TR	9.2 (6.6)	91%	22	12 (10)	31.6 (9.5)
Kong et al. (2015)	22	16 (6)	53.9 (8.5)	DSM-IV	31.5 (13)	100%	20	12 (8)	52.7 (8.1)
Koutsouleris et al. (2007)	175	130 (45)	31.7 (10.2)	DSM-IV	4.3	81%	177	123 (54)	31.5 (9.2)
Martì-Bonmatì et al. (2007)	21	21 (0)	39 (10)	DSM-IV	15.0 (8.0)	100%	10	10 (0)	35.0 (7.0)
McDonald et al. (2005)	25	18 (7)	37.3 (10.2)	DSM-IV	20.0 (5.0)	100%	52	24 (28)	39.3 (14.8)
Meda et al. (2008) (ChSZ exp.)	34	24 (10)	41.3 (5.3)	DSM-III-R DSM-IV	> 2	100%	34	17 (17)	42.5 (6.7)
Meisenzahl et al. (2008a) (ChSZ exp.)	72	56 (16)	35.6 (10.3)	DSM-IV	9.5	86%	177	123 (54)	31.5 (9.2)
Molina et al. (2010)	26	17 (9)	36.3 (11.6)	DSM-IV	10.9 (7.9)	100%	41	23 (18)	29.4 (9.0)
Neugebauer et al. (2019)	18	11 (7)	36.9 (9.9)	ICD-10	12.6 (9.6)	100%	19	12 (7)	35.8 (11.6)
Oertel-Knochel et al. (2012) (ChSZ exp.)	31	16 (15)	38.0 (11.2)	DSM-IV	13.7 (6.8)	100%	37	17 (20)	39.4 (9.9)
Ortiz-Gil et al. (2011)	23	17 (6)	40.1 (10.2)	DSM-IV	18.3 (10.0)	100%	39	30 (9)	40.1 (11.6)

Study	Subjects			Classification or Instrument	DOI	Antipsychotic treatment (%)	Healthy Controls		
	N	M(F)	Age				N	M(F)	Age
Poletti et al. (2016)	96	67 (29)	37.2 (9.3)	DSM-IV	12.6 (8.6)	100%	136	68 (68)	33.3 (12.9)
Pomarol-Clotet et al. (2010)	31	21 (11)	41.5 (8.8)	DSM-IV	21.7 (9.0)	100%	31	21 (11)	41.0 (11.0)
Rametti et al. (2010)	23	11 (12)	32.1 (7.1)	DSM-IV	10.5 (5.9)	96%	23	11 (12)	31.6 (7.1)
Rose et al. (2014)	163	55 (108)	38.5 (10.8)	DSM-IV	15.1	100%	150	84 (66)	33.5 (13.1)
Salgado-Pineda et al. (2011)	14	9 (5)	37.3 (8.9)	DSM-IV	14.0 (6.7)	100%	14	9 (5)	34.6 (6.0)
Sans-Sansa et al. (2013)	31	24 (7)	40.7 (8.6)	DSM-IV	23.8 (7.8)	100%	59	42 (17)	38.3 (10.5)
Sarro et al. (2013)	81	59 (24)	42.9	DSM-IV	21.6	100%	61	44 (17)	40.7 (10.1)
Schiffer et al. (2010)	12	12 (0)	37.5 (8.4)	DSM-IV	16.8 (7.2)	100%	14	14 (0)	36.7 (11.4)
Schuster et al. (2012)	27	14 (13)	59.9 (9.1)	DSM-IV	29.2 (9.6)	93%	40	17 (23)	62.2 (7.8)
Shapleske et al. (2002)	72	72 (0)	34.1 (8.5)	DSM-IV	11.5 (7.8)	N.A.	32	32 (0)	33.3 (8.7)
Sigmussond et al. (2002)	27	26 (1)	34.9 (7.6)	DSM-IV	13.9 (6.6)	N.A.	27	25 (2)	32.2 (6.7)
Singh et al. (2014)	14	8 (6)	34.1 (9.9)	DSM-IV	9.6 (4.3)	100%	14	7 (7)	32.6 (7.6)
Singh et al. (2015)	14	11 (3)	31.5 (9.4)	DSM-IV	9.3 (6.4)	100%	14	10 (4)	27.2 (4.8)
Spalthoff et al. (2018)	51	34 (17)	35.2 (10.9)	DSM-IV	8.8	91%	102	69 (33)	33.1 (9.6)
Tan et al. (2015)	18	11(7)	40.5 (5.5)	DSM-IV	15.9(6.3)	100%	17	10 (7)	41.2 (3.8)
Torres et al. (2016) (ChSZ exp.)	99	67 (32)	32.1 (8.0)	DSM-IV	11.0 (8.2)	100%	151	N.A.	N.A.
Tregellas et al. (2007)	32	21 (11)	39.6 (8.8)	DSM-IV	12.0	100%	32	14 (18)	35.3 (9.3)
van Tol et al. (2014)	51	44 (7)	34.0 (11.4)	DSM-IV	8.8	100%	51	37 (14)	36.1 (10.9)
Venkatasubramanian et al. (2010)	30	21 (9)	30.1 (8.3)	DSM-IV	3.5	0%	27	19 (8)	27.4 (7.0)
Yang et al. (2019)	37	21 (16)	42.0 (8.4)	DSM-IV	18.4 (8.9)	100%	28	16 (12)	40.5 (10.9)
Yamada et al. (2007)	20	10 (10)	38.8 (7.2)	DSM-IV	11.6 (8.7)	100%	20	10 (10)	39.1 (7.1)
Zhuo et al. (2017)	95	54 (41)	33.6 (7.8)	DSM-IV	10.1 (7.7)	90%	93	45 (48)	33.0 (10.2)

M(F), male and female; Age, mean age and standard deviation in years; Classification criteria PACE, Personal Assessment and Crisis Evaluation; CAARMS, Comprehensive Assessment of At-Risk Mental States; SIPS, Structured Interview for Prodromal Symptoms; DSM, Diagnostic and Statistical Manual of Mental Disorders; ICD, International Classification of Diseases; DOI, mean duration of illness and standard deviation in years;

cHRS, clinical high-risk subjects; F-RELATIVE, first relative subjects; F/S-RELATIVE, first and second relative subjects; N.A., meta-data not associated.

Table S2.3. Articles included in the meta-analysis: foci of alteration and methodological meta-data.

Study	GM variations		p value (correction)	VBM software	Slice thickness (mm^3)	Smoothing (FWHM)	Scanner (Tesla)	Space
	HC> SZ	SZ> HC						
Benetti et al. (2013)	3	0	P<0.001 (multiple comparisons)	SPM8	1.1	6	3	MNI
Bogwardt et al. (2007a)	7	0	P<0.05 (cluster-level)	BAMM	1	5	1.5	TAL
Bogwardt et al. (2007b)	8	1	P<0.05 (cluster-level)	SPM2	1	5	1.5	TAL
Bogwardt et al. (2008)	7	0	P<0.05 (cluster-level)	SPM5	1	5	1.5	TAL
Bogwardt et al. (2010)	11	0	P<0.05 (multiple comparisons)	SPM2	1.5	8	1.5	MNI
Chang et al. (2016) (HR exp.)	1	3	P<0.01 (AlphaSim)	SPM8	1	8	3	MNI
Dukart et al. (2017)	2	2	P<0.05 (FWE)	SPM12	N.A.	8	3	MNI
Fusar-Poli et al. (2011a)	5	0	P<0.05 (FWE)	SPM5	1.5	10	1.5	MNI
Fusar-Poli et al. (2011b)	4	0	P<0.05 (FWE)	SPM5	1.5	8	1.5	MNI
Guo et al. (2014)	1	0	P<0.001 (cluster-level)	SPM8	1.1	8	3	MNI
Guo et al. (2015) (HR exp.)	2	1	P<0.005 (GRF)	SPM8	N.A.	N.A.	3	MNI
Honea et al. (2008)	3	0	P<0.05 (FDR)	SPM2	1.5	6	1.5	MNI
Hu et al. (2013) (HR exp.)	1	0	P<0.05 (FDR)	SPM8	1.1	8	3	TAL
Hulshoff Pol et al. (2006)	1	0	P<0.05 (multiple comparisons)	SPM2	N.A.	8	1.5	TAL
Jacobson et al. (2010)	1	4	P<0.05 (multiple comparisons)	FSL-VBM	0.9	4.2	3	TAL
Job et al. (2003) (HR exp.)	6	0	P<0.05 (multiple comparisons)	SPM99	1.88	8	1	TAL
Jung et al. (2012)	3	0	P<0.05 (FDR)	SPM8	N.A.	10	1.5	MNI
Lee et al. (2013)	1	0	P<0.05 (FWE)	FSL-VBM	N.A.	3	3	MNI
Lei et al. (2015) (HR exp.)	1	0	P<0.05 (FWE)	SPM8	1	6	3	MNI
Li et al. (2012)	0	3	P<0.05 (FDR)	SPM8	N.A.	8	1.5	MNI
Lincoln et al. (2014)	1	0	P<0.05 (FWE)	SPM8	N.A.	8	3	MNI
Lui et at al. (2009a) (HR exp.)	2	0	P<0.05 (multiple comparisons)	SPM2	1	8	3	TAL
Marcelis et al. (2003)	5	1	P<0.005 (cluster-level)	BAMM	3	4.2	1.5	TAL
McIntosh et al. (2006)	5	0	P<0.05 (multiple comparisons)	SPM99	1.7	8	1.5	TAL
McIntosh et al. (2007)	2	0	P<0.05 (multiple comparisons)	SPM99	1.88	8	1	TAL

Study	GM variations		p value (correction)	VBM software	Slice thickness (mm^3)	Smoothing (FWHM)	Scanner (Tesla)	Space
	HC> SZ	SZ> HC						
Mechelli et al. (2011)	5	0	P<0.05 (FWE)	SPM8	N.A.	8	3/1.5	MNI
Meisenzahl et al. (2008a)	5	0	P<0.05 (FWE)	SPM2	1.5	12	1.5	MNI
Nenadic et al. (2015)	1	1	P<0.05 (FWE)	SPM8	N.A.	12	3	MNI
Oertel-Knochel et al. (2012) (HR exp.)	4	2	P<0.01 (cluster-level)	SPM8	1	8	3	TAL
Pantelis et al. (2003)	4	0	P<0.001 (cluster-level)	SPM2	3	N.A.	N.A.	TAL
Sugranyes et al.(2015)	1	0	P<0.05 (FWE)	SPM8	N.A.	4	3	MNI
Tian et al. (2011)	9	0	P<0.05 (AlphaSim)	SPM5	1	6	3	MNI
Wagshal et al. (2015)	9	2	P<0.05 (FWE)	FSL-VBM	1	3	3	MNI
Witthaus et al. (2009) (HR exp.)	2	0	P<0.05 (FWE)	SPM2	1	12	1.5	TAL
Asami et al. (2012)	6	0	P<0.05 (FDR)	SPM5	1.5	8	1.5	MNI
Chang et al. (2016) (RDSZ exp.)	9	0	P<0.01 (AlphaSim)	SPM8	1	8	3	MNI
Chen et al. (2014)	2	0	P<0.05 (FWE)	SPM2	1	8	3	MNI
Douaud et al. (2007)	23	0	P<0.01 (multiple comparisons)	FSL-VBM	1	8	1.5	MNI
Farrow et al. (2005)	19	0	P<0.001 (multiple comparisons)	SPM99	N.A.	12	1.5	TAL
Ferri et al. (2012)	1	0	P<0.01 (FWE)	SPM8	N.A.	8	1.5	MNI
Guo et al. (2013)	6	0	P<0.01 (AlphaSim)	SPM8	1.8	8	1.5	MNI
Guo et al. (2015) (RDSZ exp.)	6	0	P<0.005 (GRF)	SPM8	N.A.	N.A.	3	MNI
Guo et al. (2019)	21	0	P<0.05 (FWE)	FSL-VBM	1	3	3	MNI
Henze et al. (2011)	2	4	P<0.05 (FWE)	SPM5	1	10	1.5	TAL
Hu et al. (2013) (RDSZ exp.)	6	0	P<0.05 (FDR)	SPM8	1.1	8	3	TAL
Huang et al. (2015)	3	0	P<0.001 (cluster-level)	SPM8	1	8	3	MNI
Jayakumar et al. (2005)	10	0	P<0.05 (FDR)	SPM2	1	8	1.5	TAL
Janssen et al. (2008)	2	0	P<0.05 (multiple comparisons)	SPM2	1.5	8	1.5	MNI
Job et al. (2003) (RDSZ exp.)	8	0	P<0.05 (multiple comparisons)	SPM99	1.88	8	1	TAL
Kasparek et al. (2009)	5	0	P<0.05 (FWE)	SPM2	N.A.	12	1.5	TAL
Kubicki et al. (2002)	1	0	P<0.05 (multiple comparisons)	SPM99	N.A.	12	1.5	TAL
Lei et al. (2015) (RDSZ exp.)	1	0	P<0.05 (FWE)	SPM8	1	6	3	MNI
Lei et al. (2019)	1	0	P<0.05 (FWE)	SPM8	1	6	3	MNI
Li et al. (2019)	34	7	P<0.05 (FDR)	FSL-VBM	N.A.	3	3	MNI
Liao et al. (2015)	12	0	P<0.05 (FWE)	SPM8	N.A.	8	3	MNI
Lui et al. (2009a) (RDSZ exp.)	3	0	P<0.05 (multiple comparisons)	SPM2	1	8	3	TAL
Lui et al. (2009b)	9	0	P<0.05 (multiple	SPM2	1	8	3	TAL

comparisons)

Study	GM variations		p value (correction)	VBM software	Slice thickness (mm^3)	Smoothing (FWHM)	Scanner (Tesla)	Space
	HC> SZ	SZ> HC						
Meda et al. (2008) (RDSZ exp.)	31	0	P<0.05 (FWE)	SPM2	1.5	8	1.5	TAL
Meisenzahl et al. (2008a) (RDSZ exp.)	48	0	P<0.05 (FWE)	SPM2	1.5	12	1.5	MNI
Molina et al. (2010)	3	0	P<0.05 (FDR)	SPM5	1.1./1.5	6	1.5	MNI
Nakamura et al. (2013)	1	0	P<0.05 (FWE)	SPM8	1	10	1.5	MNI
Poeppl et al. (2014)	3	5	P<0.05 (FWE)	SPM8	N.A.	8	1.5	MNI
Price et al. (2010)	4	3	P<0.05 (FWE)	SPM2	1.2	12	1.5	TAL
Ren et al. (2013)	6	2	P<0.05 (FDR)	SPM8	N.A.	N.A.	3	MNI
Schaufelberger et al. (2007)	6	0	P<0.05 (FWE)	SPM2	N.A.	8	1.5	TAL
Sheng et al. (2013)	15	6	P<0.05 (FWE)	SPM8	N.A.	6	1.5	MNI
Tang et al. (2012)	1	0	P<0.05 (FDR)	SPM5	1.8	8	1.5	MNI
Torres et al. (2016) (RDSZ exp.)	5	0	P<0.05 (FWE)	SPM8	1	8	1.5	MNI
Voets et al. (2008)	20	0	P<0.05 (multiple comparisons)	FSL-VBM	N.A.	8	1.5	MNI
Wang et al. (2017a)	3	0	P<0.05 (AlphaSim)	SPM8	1	8	3	MNI
Watson et al. (2012)	2	2	P<0.05 (FDR)	SPM5	1.5	4	1.5	TAL
Whitford et al. (2005)	12	0	P<0.05 (multiple comparisons)	SPM99	N.A.	12	1.5	TAL
Witthaus et al. (2009) (RDSZ exp.)	7	0	P<0.05 (FWE)	SPM2	1	12	1.5	TAL
Yoshihara et al. (2008)	1	0	P<0.01 (FWE)	BAMM	3	2	1.5	TAL
Zhang et al. (2015)	1	0	P<0.05 (AlphaSim)	SPM8	N.A.	8	3	MNI
Amann et al. (2016)	9	0	P<0.01 (FWE)	FSL-VBM	1	9.4	1.5	MNI
Ananth et al. (2002)	13	0	P<0.05 (FWE)	SPM99	1.5	8	2	MNI
Anderson et al. (2015)	7	0	P<0.05 (FWE)	FSL-VBM	N.A.	7	3	MNI
Bassitt et al. (2007)	4	1	P<0.05 (FWE)	SPM2	1.2	7	1.5	MNI
Brown et al. (2011)	9	0	P<0.05 (multiple comparisons)	SPM5	1	8	1.5	MNI
Cascella et al. (2010)	12	0	P<0.05 (FWE)	SPM5	1.5	8	1.5	TAL
Delvecchio et al. (2017)	1	0	P<0.05 (FWE)	SPM12	5	6	1.5	MNI
Donohoe et al. (2011)	10	0	P<0.05 (FWE)	SPM6	1	8	1.5	MNI
Egashira et al. (2014)	5	0	P<0.05 (FWE)	SPM8	1	8	1.5	MNI
Garcia-Marti et al. (2008)	5	0	P<0.05 (FDR)	SPM2	1.25	12	1.5	TAL
Giuliani et al. (2005)	14	3	P<0.005 (FDR)	SPM2	1.5	12	1.5	TAL
Hidese et al. (2018)	8	0	P<0.05 (FWE)	SPM12	N.A.	8	1.5	MNI
Hirao et al. (2008)	6	0	P<0.05 (FDR)	SPM2	1	6	3	TAL
Horacek et al. (2011)	13	1	P<0.05 (FWE)	SPM5	1	8	1.5	TAL
Jiang et al. (2018)	26	0	P<0.00001 (FDR)	SPM12	1	8	3	MNI

Study	GM variations		p value (correction)	VBM software	Slice thickness (mm^3)	Smoothing (FWHM)	Scanner (Tesla)	Space
	HC> SZ	SZ> HC						
Kenneth Martin et al. (2014)	9	0	P<0.05 (FWE)	SPM8	3	8	3	TAL
Kim et al. (2017b)	4	0	P<0.05 (FWE)	SPM8	N.A.	6	3	MNI
Kong et al. (2015)	17	0	P<0.05 (FDR)	SPM8	1	8	3	TAL
Koutsouleris et al. (2007)	34	0	P<0.05 (FWE)	SPM2	1.5	12	1.5	MNI
Martì-Bonmatì et al. (2007)	8	0	P<0.005 (FDR)	SPM2	1.25	12	1.5	TAL
McDonald et al. (2005)	12	0	P<0.01 (cluster-level)	SPM99	1.5	8	1.5	TAL
Meda et al. (2008) (ChSZ exp.)	37	0	P<0.05 (FWE)	SPM2	1.5	8	1.5	TAL
Meisenzahl et al. (2008a) (ChSZ exp.)	67	0	P<0.05 (FWE)	SPM2	1.5	12	1.5	MNI
Molina et al. (2010)	11	0	P<0.01 (FWE)	SPM8	1	6	1.5	MNI
Neugebauer et al. (2019)	21	0	P<0.01 (FWE)	SPM12	1	6	3	MNI
Oertel-Knochel et al. (2012) (ChSZ exp.)	8	4	P<0.01 (cluster-level)	SPM8	1	8	3	TAL
Ortiz-Gil et al. (2011)	1	0	P<0.05 (multiple comparisons)	SPM5	N.A.	4	1.5	MNI
Poletti et al. (2016)	8	0	P<0.05 (FWE)	SPM8	0.8	8	3	MNI
Pomarol-Clotet et al. (2010)	3	0	P<0.05 (multiple comparisons)	FSL-VBM	N.A.	5	1.5	MNI
Rametti et al. (2010)	1	0	P<0.05 (FWE)	SPM5	1.5	8	1.5	MNI
Rose et al. (2014)	15	0	P<0.05 (FWE)	SPM5	0.9	8	3/1.5	MNI
Salgado-Pineda et al. (2011)	5	0	P<0.05 (FDR)	SPM5	3	6	3	MNI
Sans-Sansa et al. (2013)	5	0	P<0.05 (multiple comparisons)	FSL-VBM	1	4	1.5	MNI
Sarro et al. (2013)	3	2	P<0.05 (multiple comparisons)	FSL-VBM	1	4	1.5	MNI
Schiffer et al. (2010)	11	0	P<0.05 (FDR)	SPM5	1	14	1.5	MNI
Schuster et al. (2012)	16	0	P<0.05 (FDR)	SPM2	N.A.	8	1.5	TAL
Shapleske et al. (2002)	9	1	P<0.005 (cluster-level)	AFNI	3	4.2	1.5	TAL
Sigmussond et al. (2002)	4	1	P<0.001 (cluster-level)	N.A.	3	N.A.	1.5	TAL
Singh et al. (2014)	3	0	P<0.05 (FWE)	SPM8	3	10	3	MNI
Singh et al. (2015)	22	0	P<0.05 (FWE)	SPM8	3	10	3	MNI
Spalthoff et al. (2018)	6	0	P<0.05 (FWE)	SPM12	N.A.	8	3	MNI
Tan et al. (2015)	5	0	P<0.01 (AlphaSim)	SPM5	1	8	2	MNI
Torres et al. (2016) (ChSZ exp.)	15	0	P<0.05 (FWE)	SPM8	1	8	1.5	MNI
Tregellas et al. (2007)	9	0	P<0.05 (FDR)	SPM2	1.5	12	1.5	MNI
van Tol et al. (2014)	7	0	P<0.05 (FWE)	SPM8	N.A.	8	3	MNI
Venkatasubramanian et al. (2010)	14	0	P<0.05 (FDR)	SPM2	1	8	1.5	TAL
Yang et al. (2019)	12	0	P<0.001 (AFNI 3D cluster)	SPM12	1	8	3	MNI

Study	GM variations		p value (correction)	VBM software	Slice thickness (mm^3)	Smoothing (FWHM)	Scanner (Tesla)	Space
	HC> SZ	SZ> HC						
Yamada et al. (2007)	6	0	P<0.05 (FDR)	SPM2	1	12	3	TAL
Zhuo et al. (2017)	10	0	P<0.05 (FDR)	SPM8	1	6	3	MNI

HC, healthy controls; FWHM, full width at half maximum; N.A., meta-data not associated.

Table S2.4. Statistical distribution of the experiments included in the meta-analysis.

Group	VBM Experiments		Subjects (Patients)		Average (Years)		GM decrease (Foci)	
	(N)	(%)	(N)	(%)	Mean Age	Mean DOI	(N)	(%)
g-HRS	18	14.5	927	17.6	28.7	-	64	6.0
c-HRS	16	12.9	580	11.0	22.4	-	59	5.7
RDSZ	41	33.0	1,636	31.1	22.8	0.8	359	34.5
ChSZ	49	39.6	2,120	40.3	38.6	15.0	560	53.8
TOTAL	124	100	5,263	100	-	-	1,042	100

g-HRS, genetic high-risk subjects; c-HRS, clinical high-risk subjects; RDSZ, recently diagnosed schizophrenia; ChSZ, chronic schizophrenia; DOI, duration of illness.

Table S5. ALE results for general meta-analysis on schizophrenia (RDSZ and ChSZ groups pooled together). For each cluster obtained, cluster size (mm^3), extrema ALE values, anatomical labels of the peaks of probability and their Talairach brain atlas coordinates were provided.

Cluster #	Volume (mm^3)	Talairach Daemon Label (Brodmann's Area)	Extrema Value	Talairach		
				x	y	z
1	10,024	Left Insula (BA 13)	0.065	-34	18	6
		Left Superior Temporal Gyrus (BA 22)	0.041	-50	4	0
		Left Superior Temporal Gyrus (BA 22)	0.037	-52	-6	4
		Left Inferior Frontal Gyrus (BA 44)	0.035	-50	6	16
		Left Inferior Temporal Gyrus (BA 21)	0.032	-40	-4	-10
		Left Insula (BA 48)	0.032	-44	12	-2
		Left Superior Temporal Gyrus (BA 38)	0.030	-40	4	-10
		Left Insula (BA 13)	0.029	-40	-10	-4
		Left Precentral Gyrus (BA 6)	0.028	-50	4	26
		Left Claustrum	0.024	-36	-8	6
2	3,488	Right Medial Frontal Gyrus (BA 11)	0.044	4	36	-14
		Left Anterior Cingulate (BA 32)	0.043	0	34	-6
		Left Anterior Cingulate (BA 10)	0.038	-6	42	2
3	3,392	Right Insula (BA 13)	0.049	40	12	2
		Right Insula (BA 13)	0.042	34	16	10
		Right Precentral Gyrus (BA 44)	0.024	50	0	6
4	2,840	Right Transverse Temporal Gyrus (BA 41)	0.037	44	-22	14
		Right Insula (BA 40)	0.035	54	-20	16
		Right Superior Temporal Gyrus (BA 22)	0.031	54	-26	0
5	2,120	Left Thalamus (Medial Dorsal Nucleus)	0.050	0	-16	6
6	1,872	Left Amygdala	0.053	-20	-4	-14
7	1,120	Left Anterior Cingulate (BA 25)	0.043	-4	6	-4
8	1,040	Right Superior Temporal Gyrus (BA 21)	0.030	50	-8	-8
		Right Insula (BA 13)	0.026	40	-10	-4
		Right Insula (BA 13)	0.023	40	-8	4
9	816	Right Anterior Cingulate (BA 32)	0.033	8	40	16

Table S2.6. Standard univariate voxel-wise tests: GM results. For each clinical group, results of test statistics were family-wise error-corrected (FWE-c) for multiple comparisons on the cluster-level with 5,000 permutation runs. Maps were thresholded at $p < .05$, corresponding to a z-score value ≥ 2.3.

Cluster #	Volume (mm^3)	Talairach Daemon Label (Brodmann's Area)	Maximum Value (Z-points)	Talairach		
				x	y	z
g-HR < HC						
No cluster found						
c-HR < HC						
1	10	Right Anterior Cingulate (BA 32)	2.516	8	42	0
RDSZ < HC						
1	1,028	Left Transverse Temporal Gyrus (BA 41)	2.776	-50	-10	17
2	447	Right Middle Temporal Gyrus (BA 22)	2.976	48	-18	2
3	261	Left Insula (BA 13)	2.843	-32	17	3
4	171	Left Anterior Cingulate (BA 32)	2.393	-4	42	8
5	96	Left Inferior Frontal Gyrus (BA 45)	2.408	-42	20	12
6	93	Left Parahippocampal Gyrus (BA 35)	2.680	-26	-12	-22
7	79	Right Anterior Cingulate (BA 32)	2.683	8	34	26
8	71	Right Anterior Cingulate (BA 24)	2.301	8	28	8
ChSZ < HC						
1	6,594	Left Insula (BA 13)	3.671	-36	16	0
2	4,376	Right Insula (BA 13)	3.280	42	10	-4
3	3,243	Left Thalamus (Medial Dorsal Nucleus)	3.068	-4	-16	14
4	1,921	Right Anterior Cingulate (BA 32)	3.065	4	32	-10
5	1,042	Left Amygdala	3.012	-25	-5	-11
6	335	Left Medial Frontal Gyrus (BA 10)	2.693	-6	48	6
7	218	Right Insula (BA 13)	2.891	44	-18	6
8	184	Right Parahippocampal Gyrus (BA 34)	2.653	14	-6	-20
All SZ <HC						
1	12,854	Left Insula (BA 13)	4.336	-36	16	0
2	8,864	Right Insula (BA 13)	3.507	38	10	-4
3	5,257	Left Anterior Cingulate (BA 32)	3.315	-6	46	16
4	3,192	Left Parahippocampal Gyrus (BA 35)	3.395	-26	-12	-20
5	3,012	Right Thalamus (Medial Dorsal Nucleus)	3.254	6	-16	8
6	128	Left Anterior Cingulate (BA 32)	2.969	-2	6	40
7	116	Right Superior Temporal Gyrus (BA 38)	2.950	42	12	-16
8	86	Left Anterior Cingulate (BA 24)	2.881	-4	-8	42

g-HR, genetic high-risk; c-HR, clinical high-risk; RDSZ, recently diagnosed schizophrenia; ChSZ, chronic schizophrenia; HC, healthy controls.

Table S2.7. Behavioral characterization results of the whole ALE pattern of RDSZ group. Colors from red to blue represent different behavioral domains. A threshold of $p < .05$ with Bonferroni correction for multiple comparisons was applied, corresponding to a subdomain z-scores ≥ 3.

Category (sub-category)	Domain	Z-score
Language (Speech)	Cognition	7.644
Audition	Perception	6.423
Language (Semantics)	Cognition	6.110
Attention	Cognition	5.972
Execution (Speech)	Action	5.287
Somesthesis (Pain)	Perception	5.165
Music	Cognition	5.143
Memory (Expliicit)	Cognition	4.221
Language (Phonology)	Cognition	4.124
Somesthesis (Unspecified)	Perception	3.978
Reasoning	Cognition	3.934
Memory (Working)	Cognition	3.761
Vision (Unspecified)	Perception	3.564
Vision (Shape)	Perception	3.419
Gustation	Perception	3.380
Language (Syntax)	Cognition	3.370
Execution (Unspecified)	Action	3.325
Negative (Fear)	Emotion	3.139
Thermoregulation	Interoception	3.136
Negative (Disgust)	Emotion	3.108
Negative (Anxiety)	Emotion	3.064
Imagination	Action	3.034
Positive (Reward/Gain)	Emotion	3.015

Table S2.8. Behavioral characterization results of the whole ALE pattern of ChSZ group. Colors from red to orange represent different behavioral domains. A threshold of $p < .05$ with Bonferroni correction for multiple comparisons was applied, corresponding to a subdomain z-scores ≥ 3.

Category (sub-category)	Domain	Z-score
Attention	Cognition	10.901
Language (Speech)	Cognition	9.371
Somesthesis (Pain)	Perception	9.018
Positive (Reward/Gain)	Emotion	8.882
Language (Semantics)	Cognition	8.464
Reasoning	Cognition	7.895
Sexuality	Interoception	7.118
Music	Cognition	6.991
Memory (Expliicit)	Cognition	6.708
Negative (Fear)	Emotion	6.151
Execution (Speech)	Action	6.131
Audition	Perception	5.904
Inhibition	Action	5.862
Memory (Working)	Cognition	5.749
Gustation	Perception	5.583
Negative (Saddness)	Emotion	5.232
Negative (Unspecified)	Emotion	5.132
Thermoregulation	Interoception	4.963
Vision (Unspecified)	Perception	4.593
Negative (Disgust)	Emotion	4.461
Execution (Unspecified)	Action	4.414
Olfaction	Perception	4.318
Positive (Happiness)	Emotion	4.284
Social Cognition	Cognition	4.118
Language (Syntax)	Cognition	4.113
Somesthesis (Unspecified)	Perception	4.025
Negative (Anxiety)	Emotion	3.913
Language (Phonology)	Cognition	3.826
Imagination	Action	3.711
Positive (Unspecified)	Emotion	3.641
Vision (Shape)	Perception	3.586
Negative (Anger)	Emotion	3.224
Memory (Unspecified)	Cognition	3.100

Table S2.9. Network-based decomposition results. For each clinical group the number of voxels has been reported, as well as the relative percentages of alterations of the ALE maps and network ROIs defined by the Biswal's parcellation.

c-HRS group	Voxel (N)	ALE map (%)	ROI map (%)	RDSZ group	Voxel (N)	ALE map (%)	ROI map (%)	ChSZ group	Voxel (N)	ALE map (%)	ROI map (%)
AuN	0	0	0	*AuN*	214	2.56	0.81	*AuN*	138	0.92	0.52
Cerebel-N	0	0	0	*Cerebel-N*	0	0	0	*Cerebel-N*	0	0	0
DAN	0	0	0	*DAN*	342	4.09	0.22	*DAN*	209	1.4	0.13
DMN	0	0	0	*DMN*	186	2.22	0.09	*DMN*	214	1.43	0.1
MN	0	0	0	*MN*	1115	13.34	1.22	*MN*	543	3.64	0.59
OFC-N	548	68.5	0.68	*OFC-N*	1217	14.56	1.51	*OFC-N*	3971	26.63	4.92
PreMN	0	0	0	*PreMN*	202	2.41	0.77	*PreMN*	220	1.47	0.84
SN	252	31.5	0.32	*SN*	2710	32.42	3.42	*SN*	4956	33.24	6.25
SMN	0	0	0	*SMN*	932	11.15	3.10	*SMN*	463	3.1	1.54
Th-BN-N	0	0	0	*Th-BN-N*	240	2.87	0.34	*Th-BN-N*	2667	17.9	3.75
L-VAN	0	0	0	*L-VAN*	1198	14.33	0.85	*L-VAN*	1051	7.05	0.74
R-VAN	0	0	0	*R-VAN*	4	0.05	0.003	*R-VAN*	480	3.22	0.41
Visual-N	0	0	0	*Visual-N*	0	0	0	*Visual-N*	0	0	0
TOTAL	800	100	1	***TOTAL***	8360	100	12.33	***TOTAL***	14912	100	19.79

AN, auditory network; Cerebel-N, cerebellar network; DAN, dorsal attention network; DMN, default mode network; MN, motor network; OFC-N, orbito-frontal cortex network; PreMN, premotor network; SN, salience network; SMN, sensorimotor network; Th-BN-N, thalamus-basal nuclei subcortical network; L-VAN, left ventral attention network; R-VAN, right ventral attention network; Visual-N, visual network.

Table S2.10. Gray matter abnormalities in the whole SZ group (RDSZ and CHSZ groups pooled together): meta-regression results of demographic and clinical variables.

Voxel-wise results and peaks	Talairach (x,y,z)	Z Value	P Value	No. of voxels	Cluster (No. Of voxels)
EFFECT OF SEX					
(male patients < female patients and controls)					
Bilateral thalami	-1,-9.6,7	-4.379	0.000005	94	Right thalamus (48)
					Left thalamus (46)
Left superior temporal gyrus	-51,-30.7,13	-4.128	0.00001	52	Left BA 42 (32)
					Left BA 48 (20)
Right insula	32,14.7,8	-3.819	0.00006	50	Right BA 48 (39)
					Right BA 47 (11)
Left inferior temporal gyrus	-30,-9,-35	-3.611	0.0001	46	Left BA 34 (46)
EFFECT OF MEDICATION (PERCENTAGE OF)					
(medicated patients < naive patients and controls)					
Right superior temporal gyrus	43.6,14,-8	-4.039	0.00002	127	Right BA 38 (62)
					Right BA 13 (15)
					Right BA 47 (13)
Left medial frontal gyrus	-3.5,-19.5,51	-3.530	0.0002	39	Left BA 6 (39)
EFFECT OF AGE, SYMPTOMS, DOSAGE MEDICATION	No clusters found				

Table S2.11. Gray matter abnormalities in the whole SZ group (RDSZ and CHSZ groups pooled together): meta-regression results of methodological variables.

Voxel-wise results and peaks	Talairach (x,y,z)	Z Value	P Value	No. of voxels	Cluster (No. Of voxels)
EFFECT OF SAMPLE SIZE					
(small < big sample size)					
Right superior temporal gyrus	38,11,-12	4.892	0.0000004	293	Right BA 38 (213)
					Right BA 48 (42)
					Right BA 21 (36)
Left anterior cingulate cortex	-4.9,37.3,27	3.636	0.0001	28	Left BA 32 (28)
EFFECT OF SMOOTHING (FWHM)					
(high < low smoothing)					
Right insula	46.9,-22,17	-3.661	0.0001	86	Right BA 48 (76)
					Right BA 42 (10)
Left superior temporal gyrus	-47.4,5,13	-3.709	0.0001	39	Left BA 38 (27)
					Left BA 48 (12)
EFFECT OF MRI FIELD STRENGHT, SLICE THICKNESS	No clusters found				

2.6.2. Supplementary figures

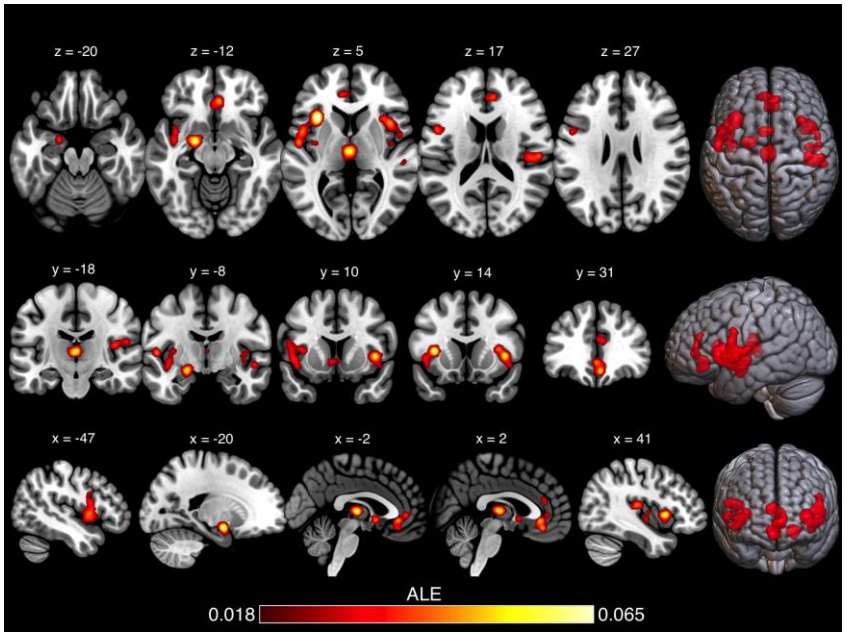

Figure S2.1. ALE results: GM reductions in the whole SZ group. ALE results were family-wise error corrected with a cluster-forming threshold of $p < 0.001$ and cluster-level inference of 0.05. Colors from red to yellow represent increasing ALE values. Slices are shown in neurological convention.

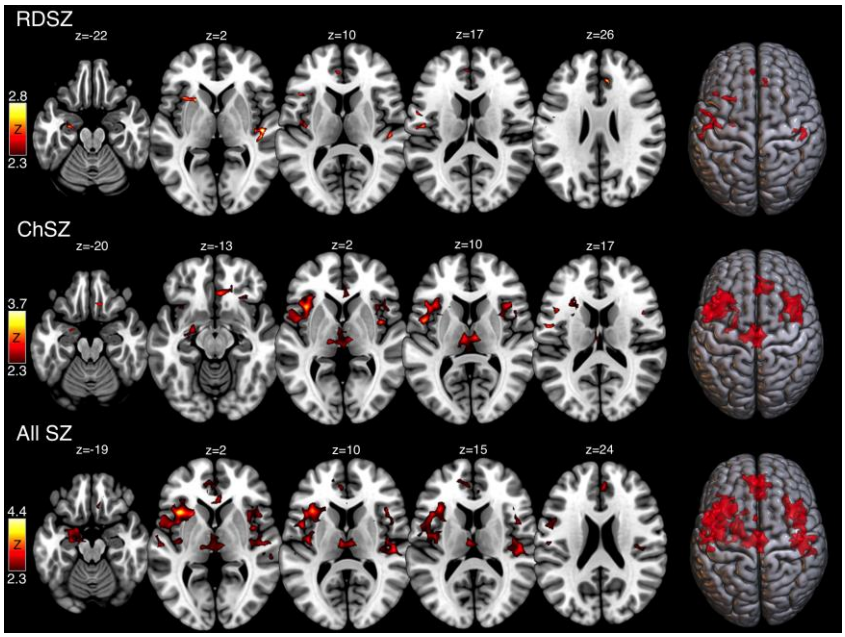

Figure S2.2. Standard univariate voxel-wise tests: GM reductions in the RDSZ, ChSZ and whole SZ groups. Results were family-wise error corrected with a threshold of $p < 0.05$. Colors from red to yellow represent increasing z values. Slices are shown in neurological convention.

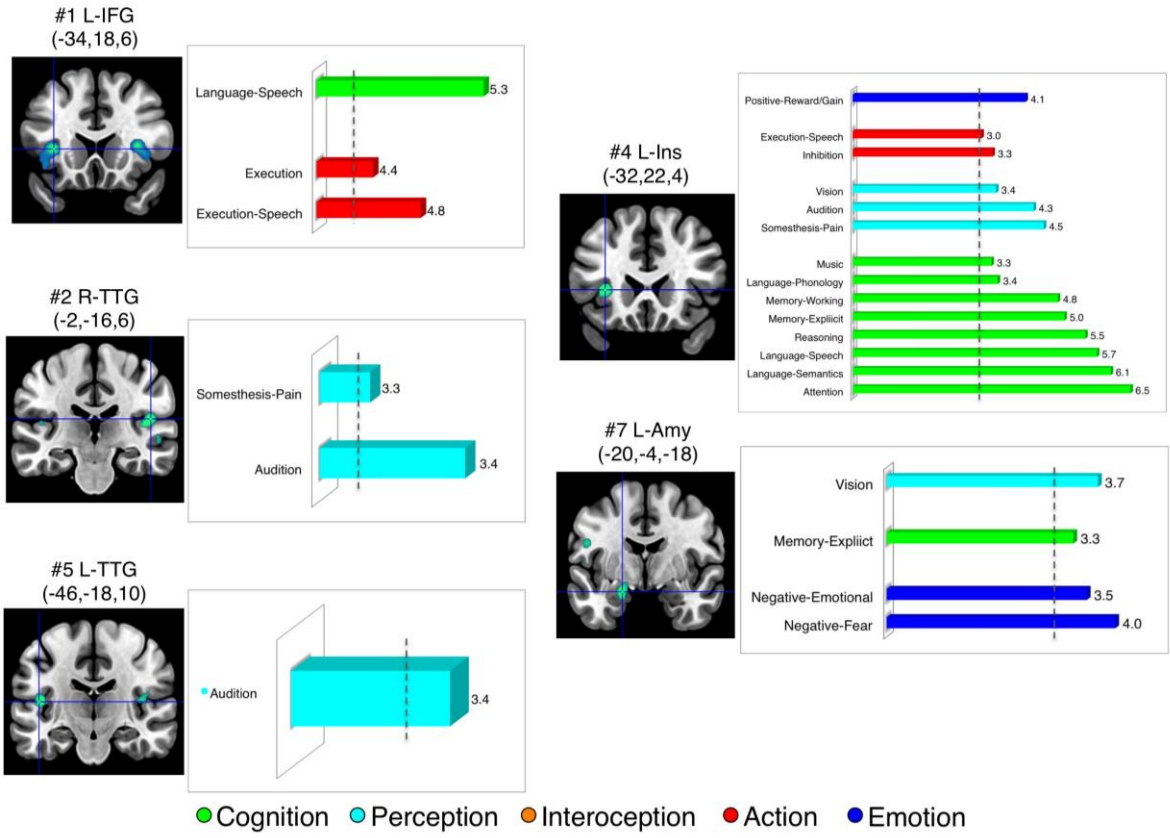

Figure S2.3. Behavioral characterization results of the ALE-derived clusters of GM loss in the RDSZ group. The dashed line indicates the threshold of statistical significance for each functional subdomain (z-point value ≥ 3). Colors refer to different behavioral domains. Cluster 3 and 6 show no significant effects.

L, left; R, right; IFG, inferior frontal gyrus; TTG, transverse temporal gyrus; Ins, insula; Amy, amygdala

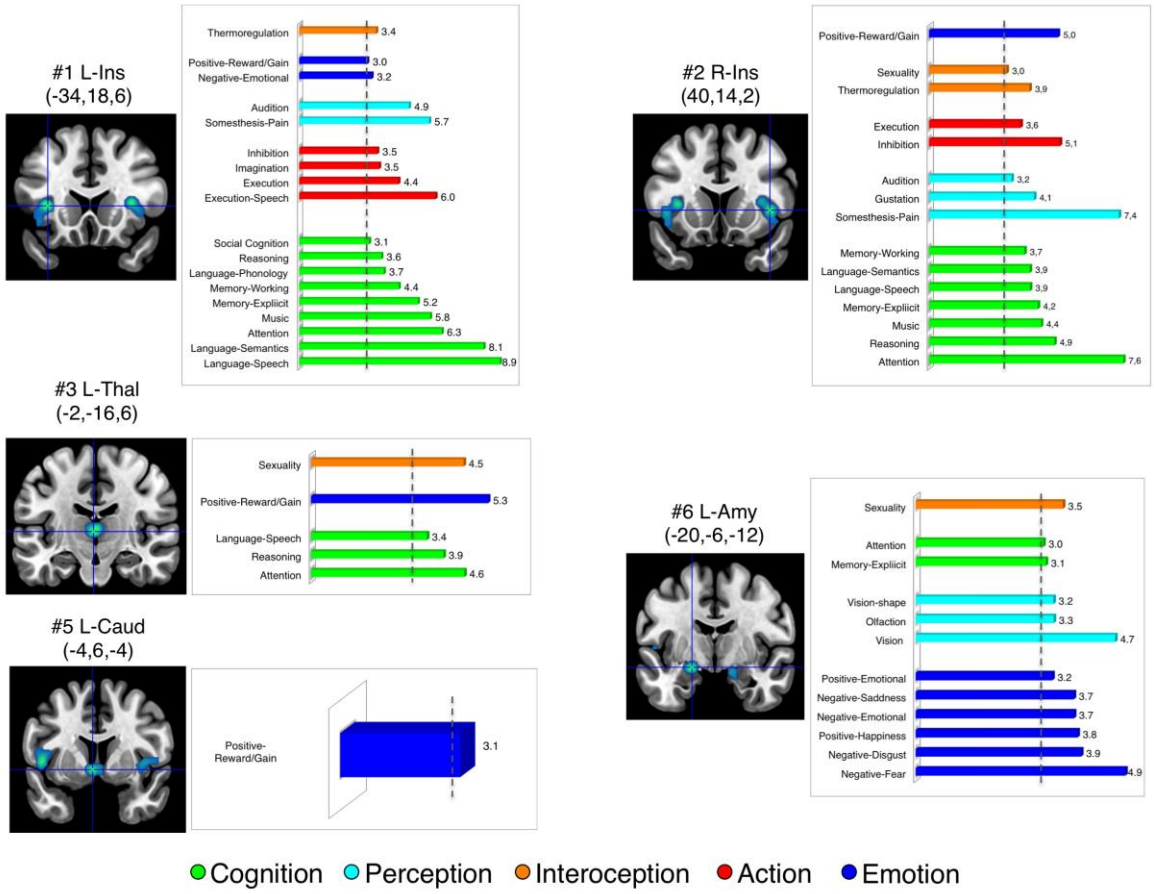

Figure S2.4. Behavioral characterization results of the ALE-derived clusters of ChSZ group. The dashed line indicates the threshold of statistical significance for each functional subdomain (z-point value ≥ 3). Colors refer to different behavioral domains. Cluster 4 and 7 show no significant effects.

L, left; R, right; Ins, insula; Thal, thalamus; Caud, caudatus; Amy, amygdala.

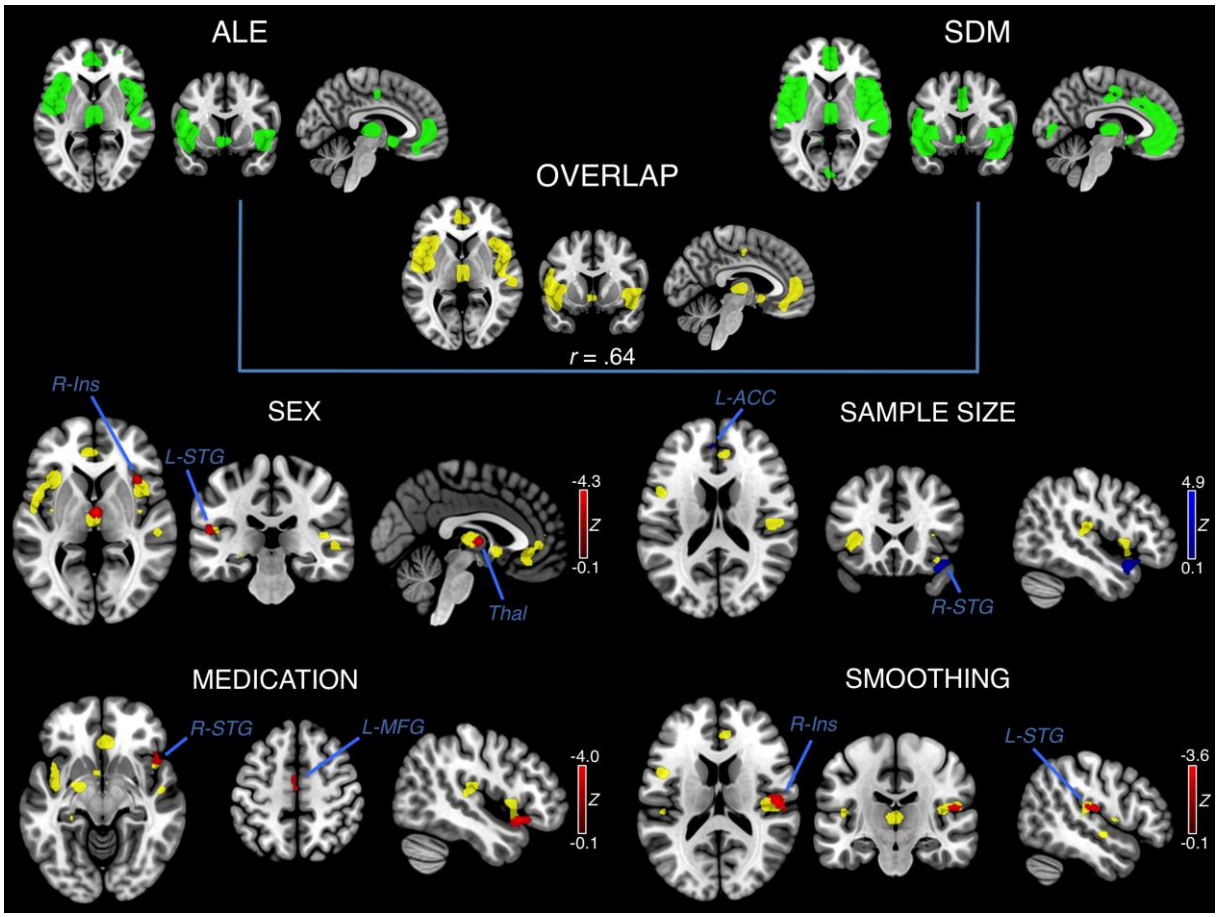

Figure S2.5. Results of meta-regression analyses in the whole SZ group. Upper panel: Spatial comparison between ALE and AES-SDM unthresholded results. Lower panel: Gender results (% of males in each study); Medication results (% of subjects taking antipsychotics in each study); Sample size results; Image smoothing level results (Full Width Half Maximum). Red represents lower volume in patients relative to controls and negative relationships with the variables in meta-regressions; blue represents lower volume relative to controls and positive relationships with variables in the meta regression; yellow represents volume shared by ALE and AES-SDM thresholded maps. Meta-regression results are voxel-level thresholded at $p < .0005$ with a minimum cluster-size > 10 voxels.

.

CHAPTER 3

Seeking for Overlapping Neuroanatomical Alteration Between Dyslexia and Attention-Deficit/Hyperactivity Disorder: A Meta-Analytic Replication Study[2]

Abstract

Background: The present work is a replication article based on the paper "Are there shared neural correlates between dyslexia and ADHD? A meta-analysis of voxel-based morphometry studies" by McGrath and Stoodley (2019). In the original research, the authors used Activation Likelihood Estimation (ALE), a technique to perform coordinate-based meta-analysis (CBMA), to investigate the existence of brain regions undergoing gray matter alteration in association with both attention-deficit/hyper-activity disorder (ADHD) and dyslexia. *Methods:* Here, the same voxel-based morphometry dataset was analysed, while using Permutation-Subject Images version of Signed Differential Mapping (PSI-SDM) in place of ALE. *Results:* Overall, the replication converged with the original paper in showing a limited overlap between the two conditions. In particular, no significant effect was found for dyslexia, therefore precluding any form of comparison between the two disorders. The possible influence of biological sex, age and medication status was also rule out. *Conclusion:* Our findings are in line with literature about gray matter alteration associated with ADHD and dyslexia, often showing conflicting results. Therefore, although neuropsychological and clinical evidence suggest some convergence between ADHD and dyslexia, more future research is sorely needed to reach a consensus on the neuroimaging domain in terms of patterns of gray matter alteration.

3.1. Introduction

In their original research, McGrath and Stoodley (2019) aimed to identify regions of altered gray matter shared between dyslexia and attention-deficit/hyper-activity disorder (ADHD). The conjoint investigation of these two neurodevelopmental disorders (NDDs) is

[2] This study was published in *Brain Sciences* in 2022, as part of the special issue T*he Brain Imaging Replication Crisis* (Volume 12, Articles 1367, Pages 1-20, doi: 10.3390/brainsci12101367). Authors: Liloia D., Crocetta A., Cauda F., Duca, S., Costa, T., Manuello, J.

not only supported by their frequently reported comorbidity, but also by shared genetic and neural pathomechanism risk factors. In this regard, converging evidence suggests that NDDs tend to report a shared etiological basis in neurodevelopment abnormality caused by complex multifactorial interactions of genetic defects, as well as of environmental, epigenetic, cognitive, and behavioral factors (Battaglia et al., 2022; Carlsson et al., 2020; Micai et al., 2020; Parenti et al., 2020; Sánchez-Morán et al., 2018; Tanaka et al., 2022). New potential metabolic targets and neuroprotective agents against NDDs, including ADHD and learning disorders, are starting to appear in the animal model research literature (Salem et al., 2022; Tanaka et al., 2022; Tanaka et al., 2021), thereby opening perspectives for future treatment.

The advent of magnetic resonance imaging (MRI) technologies has provided an unprecedented opportunity to assess the neurophysiological underpinnings of these two NDDs in vivo and noninvasively. Numerous studies about pediatrics and adults with ADHD suggest functional abnormalities in fronto-striatal and fronto-limbic systems (Bush et al., 2005; Cubillo et al., 2012; Rubia, 2018; Sebastian et al., 2014) that may underlie impulsivity, hyperactivity, and inattention deficits typical of the disorder (American Psychiatric Association, 2013). By contrast, subjects suffering from dyslexia tend to report deficits in orthographic and visuo-phonological domains, in which the occipito-temporal functional network seems to have a pivotal role (Maisog et al., 2008; Paulesu et al., 2014; Richlan et al., 2009). From the structural point of view, abnormalities in brain morphology have been reported in both disorders, encompassing multiple areas such as the basal ganglia, cerebellum, parietal cortex, corpus callosum, prefrontal-cingulate cortex, and parieto-temporal regions (Cubillo et al., 2012; Eckert, 2004; Elnakib et al., 2014). However, this voluminous literature remains largely inconclusive. Moreover, only a limited pool of studies has examined neuroanatomical convergence across disorders reporting conflicting findings (Goradia et al., 2016; Jagger-Rickels et al., 2018; Kibby et al., 2009; Langer et al., 2019).

To fill this gap, McGrath and Stoodley (2019) realized a coordinate-based meta-analysis (CBMA) of previously published voxel-based morphometry (VBM) findings. VBM is a widely used MRI technique in the field of human brain mapping, which allows the identification of focal differences in volume or concentration between the brains of two groups of subjects (Ashburner and Frinston, 2000). In the specific case of McGrath and Stoodley (2019), the considered experiments had compared either subjects diagnosed with dyslexia against typically developing controls (TDCs), or subjects diagnosed with ADHD

against TDCs. The dataset was then processed according to the CBMA approach. In general terms, this class of techniques allows us to quantify the consensus between multiple experiments based on structural or functional neuroimaging techniques (Caspers et al., 2014; Salimi-Khorhidi et al., 2009). Therefore, they represent a valuable tool for human brain mapping, offering a way to overcome the variability frequently found among single experiments (Samartsidis et al., 2017; Smith et al., 2005). Unlike image-based meta-analyses, which take in three-dimensional (3D) maps representing the results, CBMAs process instead the so-called "list of foci". Here, each focus is a peak of the maximum measured cluster effect, localized through a triplet of stereotactic coordinates (x,y,z) (Manuello et al., 2022). CBMAs makes therefore possible to recover the full 3D information starting from a much sparser (but often the only available) representation of the data (Müller et al., 2018).

Among the various CBMA algorithms, McGrath and Stoodley (2019) resorted to the activation likelihood estimation (ALE) technique (Eickhoff et al., 2009; Eickhoff et al., 2012). Notably, this approach uses a Gaussian kernel to model the effect, adjusting the full-width half-maximum (FWHM) of the Gaussian based on the sample size of the experiment considered time to time. This means that the higher the number of subjects analyzed in the experiment, the more spatially precise (and reliable) are considered the related results, and therefore smoothed through a tighter Gaussian (Turkeltaub et al., 2002).

In the original paper, a two-step procedure was followed. First, the ALE analysis was separately applied to estimate the spatial convergence associated with each of the four possible conditions: dyslexia < TDCs; ADHD < TDCs; dyslexia > TDCs; ADHD > TDCs. The first two contrasts investigated the so-called decrease effect (Nani et al., 2021), meaning that the pathological state is associated with a reduction in gray matter; conversely, the remaining two targeted the increase effect, where an increment of gray matter is searched for instead (Mancuso et al., 2020). The obtained ALE maps were thresholded using both a more conservative option (i.e., $p_{\text{uncorrected}} < 0.001$; minimum cluster size k = 50 mm^3) and a less conservative one (i.e., $p_{\text{uncorrected}} < 0.005$; k = 50 mm^3). In the second step, a conjunction analysis was implemented between the previously obtained dyslexia < TDCs and ADHD < TDCs maps (separately for the conservative and lenient thresholding). This allowed us to identify voxels with a statistically significant overlap between the two disorders (Eickhoff et al., 2011). The resulting conjunction maps were thresholded using a false discovery rate (FDR) of $p < 0.05$ (based on 5000 permutations) and k = 50 mm^3 as above. No conjunction

analysis was run for the increase condition due to lack of any overlap already at visual inspection. McGrath and Stoodley (2019) did not find any overlap between dyslexia and ADHD when using ALE maps thresholded at $p_{uncorrected} < 0.001$; k = 50 mm^3 (i.e., the most conservative option). A sole cluster in the right caudate was instead observed for $p_{uncorrected} < 0.005$; k = 50 mm^3. In addition to the described main analyses, the authors aimed to assess the possible effect of brain volume and age on the results. Since ALE technique does not allow us to model confounding variables during the estimation of the spatial convergence, different subsets of the original dataset were extracted and separately analyzed. In the first case, only those VBM experiments that originally controlled for total brain volume or total gray matter volume were retained. In the second case, VBM experiments were divided into two groups based on the reported mean age of subjects (≤12 years; ≥18 years). Experiments were discarded if the necessary information was missing. The previously observed cluster in the right caudate was still significant in the brain volume-controlled subset. On the contrary, no overlap was found between dyslexia and ADHD in the adult subgroup. In children, a cluster of overlap was observed in the left middle frontal gyrus/supplementary motor area, for ALE map thresholded at $p_{uncorrected} < 0.005$; k = 50 mm^3.

In the present paper, we first aimed to test the original dataset analyzed by McGrath and Stoodley (2019) using a different CBMA technique. Specifically, permutation-subject images version of signed differential mapping (PSI-SDM) (Albajes-Eizagirre et al., 2019) was employed as an alternative to ALE. To the best of our knowledge, no previous study has evaluated the constancy in terms of results between the two algorithms despite substantial methodological differences. From the clinical point of view, we expected limited or completely absent neuroanatomical overlap between disorders in line with the limited available literature on the topic (McGrath and Stoodley, 2019; Samea et al., 2019; Stoodley, 2014). Given the peculiar nature of PSI-SDM, additional analyses were also performed. In fact, we directly estimated the possible interfering effect of key socio-demographic and clinical variables via voxel-wise meta-regression approach (Radua et al., 2012). Finally, an additional analysis was made including in the dataset the nine VBM experiments with null results that were identified but excluded by McGrath and Stoodley (2019).

3.2. Methods

As mentioned above, the core element of this replication attempt is the change of technique used to compute the CBMA. This implied several methodological differences that are detailed below.

3.2.1. Dataset construction

The present replication used exactly the same set of VBM experiments analyzed by McGrath and Stoodley (2019). The lists of foci necessary as input to run any CBMA was retrieved from the Supplementary Files of the original paper. The following adjustments were necessary due to technical differences between ALE and PSI-SDM. First, while the list of foci used by ALE only contains the stereotactic coordinates (x,y,x) of the peaks of effect, the PSI-SDM method also requires a measure of effect size. Therefore, the T-value of each focus was retrieved from the original manuscripts. When missing, these were computed from Z-values or *p*-values, as implemented in the dedicated conversion utility of SDM (https://www.sdmproject.com/utilities/?show=Statistics).

To note, McGrath and Stoodley (2019) designed four different main contrasts: ADHD < TDCs (23 experiments; 718 subjects; 128 foci); dyslexia < TDCs (18 experiments; 388 subjects; 81 foci of variation); ADHD > TDCs (5 experiments; 75 subjects; 21 foci); dyslexia > TDCs (5 experiments; 101 subjects; 16 foci). Because of the inclusion of T-values, PSI-SDM does not require separate inputs for gray matter increase and decrease. Therefore, only ADHD vs. TDCs (24 experiments; 1661 subjects; 149 foci) (Table 3.1 A and B for socio-demographic and clinical details; Table S3.1 for methodological details), and dyslexia vs. TDCs (18 experiments; 833 subjects; 97 foci) (Table 3.1 A and B for socio-demographic and clinical details; Table S3.1 for methodological details) were needed for the replication.

Table 3.1. Voxel-based morphometry experiments included in the original coordinate-based meta-analysis by McGrath and Stoodley (2019): demographic and clinical details for the attention-deficit/hyper-activity disorder (A) and dyslexia (B) datasets.

VBM Experiments (Group)	Clinical Group						Control Group				Brain volume analysis	Co-morbid disorders reported in sample
	N	% Male	Mean Age (yrs)	Age SD (yrs)	FSIQ	% Medication	N	% Male	Mean Age (yrs)	Age SD (yrs)		
(A) ADHD												
Ahrendts et al. (2011)	31	65%	31.2	9.7	N/A	0%	31	65%	31.5	8.6	yes	Anxiety
Bonath et al. (2018)	18	100%	13.6	1.7	N/A	55.6%	18	100%	14.1	1.3	yes	1 ODD
Bralten et al. (2016)	307	68%	17.1	3.4	97.08	88.6%	196	51%	16.7	3.1	no	-
Brieber et al. (2007)	15	100%	13.1	1.4	N/A	66.7%	15	100%	13.3	1.8	yes	-
Carmona et al. (2005)	25	84%	10.8	3.0	> 80	100%	25	84%	11.2	3.2	yes	11 anxiety, 2 MDD, 4 phobias, 6 tics, 7 obsessions
He et al. (2015)	37	100%	9.9	2.4	> 90	0%	35	100%	10.7	2.6	yes	-
Iannaccone et al. (2015)	20	61%	14.5	1.5	108.46	65%	20	50%	14.8	1.2	yes	2 affective disorder, 3 AD, 3 anxiety/phobia, 2 dyscalculia, 2 CD
Johnston et al. (2014)	34	100%	12.5	2.3	N/A	29.4%	34	100%	13.2	1.0	no	1 dyslexia, 3 ODD/CD
Kappel et al. (2015)(adults)	16	94%	23.5	4.1	N/A	0%	20	100%	23.7	3.4	no	2 alcohol abuse, 1 multiple drug abuse
Kappel et al. (2015)(children)	14	71%	9.8	1.3	N/A	0%	10	80%	11.0	1.3	no	-
Kaya et al. (2018)	19	71%	10.3	2.0	N/A	0%	18	67%	10.2	2.0	no	-
Kobel et al. (2010)	14	100%	10.4	1.3	N/A	100%	12	100%	10.9	1.6	yes	3 OCD-CD, 2 GAD, 2 OCD-GAD
Kumar et al. (2017)	18	100%	9.6	1.8	N/A	0%	18	100%	9.7	1.9	yes	-
Lim et al. (2013)	29	100%	13.8	1.8	N/A	20%	29	100%	14.4	2.5	no	-
McAlonan et al. (2007)	28	100%	9.9	2.0	N/A	100%	31	100%	9.6	1.8	yes	16 OCD, 2 CD
Montes et al. (2010)	20	50%	29.0	4.0	N/A	N/A	20	50%	27.6	2.6	no	-
Moreno-Alcazar et al. (2016)	44	66%	31.6	11.4	N/A	65.9%	44	66%	32.6	10.6	no	-
Overmeyer et al. (2001)	18	83%	10.4	1.7	N/A	N/A	16	94%	10.3	2.2	yes	1 dyslexia, 2 ODD, 2 CD
Roman-Urrestarazu et	49	76%	22.2	0.7	96.4	0%	34	50%	22.9	0.4	no	-

al. (2016)

VBM Experiments (Group)	Clinical Group						Control Group				Brain volume analysis	Co-morbid disorders reported in sample
	N	% Male	Mean Age (yrs)	Age SD (yrs)	FSIQ	% Medication	N	% Male	Mean Age (yrs)	Age SD (yrs)		
Sasayama et al. (2010)	18	72%	10.6	2.9	90.05	0%	17	71%	10.0	2.4	yes	6 ODD, 4 CD
van Wingen et al. (2013)	14	100%	32.0	7.0	N/A	0%	15	100%	37.0	6.0	yes	-
Villemonteix et al. (2015a) (naïve)	33	55%	10.3	1.4	N/A	0%	24	50%	10.0	1.2	no	-
Villemonteix et al. (2015a) (medicated)	20	80%	10.4	1.4	N/A	100%	24	50%	10.0	1.2	no	-
Yang et al. (2008)	57	61%	11.1	N/A	97.9	87.7%	57	60%	11.7	N/A	yes	5 LD, 14 ODD, 1 tic, 1 GAD
Totals, sample size, averages	898	76%	16.5	-	-	-	763	71%	16.6	-	-	-
(B) Dyslexia												
Brambati et al. (2004)	10	50%	31.6	N/A	107,1	N/A	11	45%	27.4	N/A	yes	-
Brown et al. (2001)	16	100%	24.0	5.0	> 90	N/A	14	100%	N/A	N/A	no	-
Eckert et al. (2005)	13	100%	11.4	0.7	N/A	N/A	13	100%	11.3	0.7	yes	-
Evans et al. (2013)(male adults)	14	100%	42.9	10.4	108.0	0%	14	100%	41.1	9.0	yes	-
Evans et al. (2013)(female adults)	13	0%	34.0	11.6	99.6	0%	13	0%	27.9	9.7	yes	-
Evans et al. (2013)(male children)	15	100%	9.6	1.3	101.7	0%	15	100%	8.3	2.1	yes	-
Evans et al. (2013)(female children)	17	0%	10.1	2.1	101.9	0%	17	0%	9.1	3.0	yes	-
Hoeft et al. (2007)	19	53%	14.4	1.9	N/A	N/A	19	53%	14.4	2.4	yes	-
Jednorog et al. (2015)	130	57%	10.3	0.9	> 85	N/A	106	48%	10.2	0.9	yes	-
Kronbichler et al. (2008)	13	100%	15.9	0.8	N/A	N/A	15	100%	15.5	0.6	yes	-
Liu et al. (2013)	18	72%	11.8	0.6	> 90	0%	18	83%	11.8	0.3	yes	-
Silani et al. (2005)	32	100%	24.4	5.0	110	N/A	32	100%	26.3	5.0	no	-
Siok et al. (2008)	16	50%	11.0	0.5	N/A	N/A	16	81%	11.0	0.6	yes	-
Steinbrink et al. (2008)	8	75%	20.1	3.9	N/A	N/A	8	75%	23.7	4.3	yes	-
Tamboer et al. (2015)	37	16%	20.6	1.5	N/A	N/A	57	12%	20.3	1.1	yes	-
Vinckenbosch et al. (2005)	13	100%	N/A	N/A	N/A	N/A	10	100%	N/A	N/A	yes	-

VBM Experiments (Group)	Clinical Group						Control Group				Brain volume analysis	Co-morbid disorders reported in sample
	N	% Male	Mean Age (yrs)	Age SD (yrs)	FSIQ	% Medication	N	% Male	Mean Age (yrs)	Age SD (yrs)		
Xia et al. (2016)	24	58%	12.5	0.7	> 80	N/A	24	50%	12.5	0.4	no	-
Yang et al. (2016)	9	33%	12.6	0.6	N/A	N/A	14	43%	12.3	1.0	yes	-
Totals, sample size, averages	417	61%	16.4	-	-	-	416	57%	16.5	-	-	-

ADHD, attention-deficit/hyper-activity disorder; anxiety, anxiety disorders; CD, conduct disorder; FSIQ, full-scale intelligent quotient; GAD, generalized anxiety disorder; LD, learning disability; MDD, major depressive disorder; N, sample size; N/A, data not available; ODD, oppositional defiant disorder; psychiatric, no history of psychiatric disorders; SD, standard deviation; yrs, years; VBM, voxel-based morphometry.

3.2.2. Coordinate-based meta-analysis via PSI-SDM

As mentioned above, this replication used the PSI-SDM method in place of the ALE originally applied by McGrath and Stoodley (2019). While ALE computes for each voxel the likelihood to find a statistically significant effect in it, based on the spatial convergence among the considered experiments (Eickhoff et al., 2009; Eickhoff et al., 2012), PSI-SDM evaluates the presence or absence of the effect for each brain voxel performing standard univariate voxel-wise tests (Albajes-Eizagirre et al., 2019; Winkler et al., 2014). In other words, PSI-SDM estimates the effect size. To do so, the lower and upper bounds of possible effect sizes for all voxels were evaluated with multiple imputations. Then, a map of brain alteration was reconstructed for each experiment. This was made by means of an anisotropic Gaussian kernel, which attributes higher effect sizes to the voxels that appear to be more correlated with the peak coordinates. This step is conceptually similar to the creation of the modelled activation (MA) maps in ALE, although values in the MA maps represent the likelihood of finding an effect, rather than the estimated effect size. As a further difference, in ALE the FWHM of the Gaussian kernel is changed based on the sample size of each experiment (Eickhoff et al., 2009). On the contrary, PSI-SDM keeps a fixed FWHM, typically set at 20 mm (Albajes-Eizagirre et al., 2019). Continuing with the PSI-SDM procedure, the most likely effect size (based on the level of statistical significance and its standard error, the coordinates and effect sizes of the reported peaks, and the anisotropic covariance between adjacent voxels) was computed for each included experiment through the maximum likelihood techniques (Radua et al., 2013). At this point, the obtained effect size maps of each

imputation dataset were combined with a random-effects model. Then, the obtained maps were combined in a final meta-analytic map by applying Rubin's rules. Briefly, this technique allows us to impute the overall effect sizes for each brain voxel, based on the possible different effect sizes that voxels may have had in the original unavailable 3D maps associated with each experiment. Finally, the meta-analytic map was thresholded applying a family-wise error (FWE) correction for multiple comparisons, with 1000 permutations, and the threshold-free cluster enhancement (TFCE) statistic ($p \leq 0.05$; minimum cluster size = 10 voxels) (Albajes-Eizagirre et al., 2019).

These steps were repeated twice, for dyslexia vs. TDCs, and ADHD vs. TDCs contrasts. The PSI-SDM algorithm was set to the default parameters (i.e., VBM—gray matter modality; SDM gray matter mask; anisotropy = 1; isotropic FWHM = 20 mm; voxel size = 2 mm; number of imputations = 50).

Finally, we aimed to formally test whole-brain communalities in gray matter variation between dyslexia and ADHD by calculating the overlap between both conditions in each brain voxel. To do so, the two TFCE-corrected maps (i.e., dyslexia vs. TDCs and ADHD vs. TDCs, respectively) have to be added on top of each other and compared via the multimodal function of PSI-SDM software that calculate the most probable gray matter overlap taking into account the presence of noise in the estimation of the *p*-values of each meta-analytic map (Albajes-Eizagirre et al., 2019).

3.2.3. Impact of socio-demographic and clinical variables

While ALE does not permit the modelling of additional covariates, these can be included in PSI-SDM to perform meta-regression analyses (Radua et al. 2013). First, in order to test the hypothesis originally made by McGrath and Stoodley (i.e., the influence of subjects' age for ADHD and dyslexia on gray matter differences), one variable was created to account for age, taking the mean age of the clinical groups as reported in the original Table 1 of McGrath and Stoodley (2019), as to obtain the overall mean age for each experiment. VBM experiments that did not report these data were excluded from this specific analysis. To note, the impact of age was separately tested for ADHD and dyslexia datasets. Therefore, the age variable was treated as independent variable in a univariate linear regression over the voxel-wise magnitude of gray matter brain alteration. The potential impact of biological sex (percentage of male), full-scale intelligence quotient (FSIQ; mean score), and medication

(percentage of medicated subjects at the scan session) was also explored for ADHD and dyslexia datasets when at least 50% of the experiments for each dataset provided the required information.

The results of the meta-regressions were thresholded at $p_{uncorrected} < 0.0005$ and minimum cluster size = 10 voxels, as suggested by the SDM team to reach the optimal balance between specificity and sensitivity (Radua and Mataix-Cols, 2012a).

3.2.4. Brain volume sub-analysis

McGrath and Stoodley (2019) also tested the possible confounding effect of total brain volume, or gray matter volume. To do so, they reduced the dataset to the group of experiments that explicitly corrected results to account for the volumetric difference between the clinical and control groups. Since this kind of hypothesis can't be tested by means of a meta-regression, we followed the same original approach, but using PSI-SDM in place of ALE to analyze the identified subset.

3.2.5. Additional analysis: impact of null experiments

Knowing that some attempts to find a given effect of interest have yielded null results is of great relevance when running a CBMA (Acar et al., 2018; Laitin et al., 2021). Quantifying the exact number of null experiments is generally hard, as formalized in the so-called "file-drawer effect" bias (Acar et al., 2018; Laitin et al., 2021; Müller et al., 2018). Nonetheless, McGrath and Stoodley (2019) identified nine of them during their literature search. However, it is not possible to process null experiments with the ALE method, as this would result into empty MA maps that can't be modelled by the algorithm. On the contrary, PSI-SDM allows the consideration of null results as well. Therefore, an additional analysis was performed after the inclusion of those nine experiments into the dataset, correctly divided between dyslexia and ADHD (see also Table 3.2 for demographic and clinical details; Table S3.2 for methodological details).

Table 3.2. Voxel-based morphometry experiments with null results and therefore not included in the original coordinate-based meta-analysis by McGrath and Stoodley (2019): demographic and clinical details for the attention-deficit/hyper-activity disorder (A) and dyslexia (B) datasets.

VBM Experiments (Group)	Clinical Group						Control Group				Brain volume analysis	Co-morbid disorders reported in sample
	N	% Male	Mean Age (yrs)	Age SD (yrs)	FSIQ	% Medication	N	% Male	Mean Age (yrs)	Age SD (yrs)		
(A) ADHD												
Amico et al. (2011)	20	75%	33.6	10.2	N/A	N/A	20	75%	34.7	10.7	yes	6 MDD, 7 depressive episodes
Depue et al. (2010)	31	61%	20	1.7	114.2	77.4%	21	39%	19.3	1.1	yes	-
Maier et al. (2015)	131	48%	34.5	10.0	113.1	0%	95	47%	37.7	10.5	no	History of depression and/or pharmacotherapy
Onnink et al. (2013)	119	38%	36.29	10.90	107.5	69%	107	42%	36.9	11.54	yes	-
Saad et al. (2017)	34	73%	13.28	2.75	N/A	0%	28	68%	13.09	2.63	yes	ODD
Seidman et al. (2011)	24	51%	37,3	12.6	116.0	87.5%	54	46%	34.3	11.3	yes	LD, MDD
Villemonteix et al. (2015b)	33	54%	10,1	1.3	105.6	0%	27	48%	10.1	1.3	yes	-
Totals, sample size, averages	392	51%	28.4	-	-	-	352	44%	31.6	-	-	-
(B) Dyslexia												
Eckert et al. (2016)	164	60%	10.8	2.59	N/A	N/A	129	60%	10.8	2.73	yes	-
Pernet et al. (2009)	38	89%	27.3	7.9	N/A	0%	39	89%	27.8	5.8	yes	-
Totals, sample size, averages	202	66%	13.9	-	-	-	168	67%	14.7	-	-	-

ADHD, attention-deficit/hyper-activity disorder; FSIQ, full-scale intelligent quotient; LD, learning disability; MDD, major depressive disorder; N, sample size; N/A, data not available; neurological disorder, no history of neurological disorders; ODD, oppositional defiant disorder; psychiatric, no history of psychiatric disorders; SD, standard deviation; yrs, years; VBM, voxel-based morphometry.

3.3. Results

We aimed to replicate each of the analyses described in McGrath and Stoodley (2019). Moreover, we performed some additional analyses that the authors of the original work had been unable to carry out due to methodological limitations.

3.3.1. Gray matter variations in ADHD groups

When looking at the gray matter decrease effect associated with ADHD (i.e., ADHD < TDCs) McGrath and Stoodley (2019) found 11 clusters, encompassing the left frontal gyrus, the right superior orbitofrontal gyrus, the right medial frontal gyrus, the right gyrus rectus, the bilateral cingulate gyrus, the left precentral gyrus, the left superior temporal gyrus, the right putamen, the left amygdala, and the right caudate head. The increase effect (i.e., ADHD > TDCs) was observed instead in 18 clusters, covering the left superior frontal gyrus, the right precentral gyrus, the bilateral postcentral gyrus, the right supplementary motor area, the left paracentral lobule, the left posterior cingulate gyrus, the bilateral precuneus, the left cuneus, the right mid-occipital gyrus, the left medial dorsal nucleus of the thalamus, and the left insula. As highlighted by McGrath and Stoodley, these results were obtained applying a threshold of $p_{uncorrected} < 0.001$. For the sake of clarity, it should be mentioned that the use of the uncorrected thresholding is no longer recommended in the ALE field (Eickhoff et al., 2016). Therefore, any interpretation of the results obtained for individual disorders should be made with caution. The conjunction analysis was FDR corrected instead, in line with current guidelines.

Since PSI-SDM, as mentioned in the Methods section, can analyze decrease and increase effects together, the replication of this step consisted of a unique ADHD vs. TDCs contrast. Our results showed no effect applying a TFCE $p \leq 0.05$; minimum cluster size = 10 voxels thresholding. Five clusters of decrease effect were instead observed at the intermediate step of the analyses when the $p_{uncorrected} < 0.005$; minimum cluster size = 10 voxels threshold was used. Although it is not infrequent in literature to describe results surviving this lenient thresholding, the current recommended statistical standard is TFCE (Albajes-Eizagirre et al., 2019). Therefore, we have decided to include those less robust results in the Supplementary Materials only (Table S3.3 and Figure S3.1, respectively), for the sake of clarity and completeness.

3.3.2. Gray matter variations in dyslexia groups

When looking at the gray matter decrease effect associated with dyslexia (i.e., dyslexia < TDCs) McGrath and Stoodley (2019) found 12 clusters, localized over the right superior frontal gyrus, the right orbitofrontal gyrus, the bilateral supramarginal gyrus, the bilateral superior temporal gyrus, the left middle temporal gyrus, the right inferior occipital gyrus, the bilateral caudate body, the left medial dorsal nucleus of the thalamus, the left insula, and the left lobule VI in the cerebellum. The increase effect (i.e., dyslexia > TDCs) was observed instead in 13 clusters, encompassing the bilateral medial superior frontal gyrus, the right precentral gyrus, the right supplementary motor area, the right paracentral lobule, the right precuneus, the left inferior parietal lobule, the bilateral superior temporal gyrus, the left middle temporal gyrus, and the left crus I in the cerebellum. As for ADHD, a threshold of $p_{uncorrected} < 0.001$ was used.

In our replication, no effect was found for the contrast dyslexia vs. TDCs, neither at TFCE $p \leq 0.05$ nor at $p_{uncorrected} < 0.005$ (Table S3.4).

3.3.3. Common gray matter differences in dyslexia and ADHD groups

Although McGrath and Stoodley (2019) found wide patterns of effect for both ADHD and dyslexia, the conjunction analysis highlighted no convergence between the two neurodevelopmental conditions when considering decrease ALE maps thresholded at $p_{uncorrected} < 0.001$. When the authors lowered the threshold to $p_{uncorrected} < 0.005$ a sole cluster of decrease in the right caudate survived FDR $p < 0.05$ ($k = 50$ mm^3; 5000 permutations) correction. No conjunction analysis for the increase effect was carried out instead.

Concerning our results, since no effect was found in the main PSI-SDM about dyslexia, it was not possible to compute the conjunction analysis, neither at TFCE $p \leq 0.05$ nor at $p_{uncorrected} < 0.005$ thresholding.

3.3.4. Additional results: impact of null experiments

As described in the Methods section, PSI-SDM allows us to also model experiments that found null results. Therefore, we repeated the analyses described above after having complemented the database with the null experiments reported in McGrath and Stoodley (2019). This was an additional analysis, not implemented in the original research due to

methodological constrain. Concerning ADHD, still no effect was found at TFCE $p \leq 0.05$, in line with what observed for the original database. Coherently, four clusters of decrease effect were observed at $p_{uncorrected} < 0.005$ threshold (Table S3.5 and Figure S3.2). The inclusion of the null experiments did not affect dyslexia that still showed no cluster of effect at any level of thresholding (Table S3.6). As in the case of the original database, it was not possible to complete the conjunction analysis due to the lack of effect at previous stages.

3.3.5. Impact of socio-demographic and clinical variables

In order to evaluate the potential effect of age, McGrath and Stoodley (2019) created and separately analyzed subsets of experiments depending on the mean age of the sample. When focusing on the decrease effect in adult groups (i.e., mean age > 18 years), the conjunction analysis showed no convergence between ADHD and dyslexia, irrespective of the threshold level applied to the ALE maps. The same happened for children groups based on the ALE maps thresholded at $p_{uncorrected} < 0.001$. When using the more lenient $p_{uncorrected} < 0.005$, a cluster of convergent decrease was observed in the left middle frontal gyrus and supplementary motor area. The authors did not consider the increase effect for this analysis due to the paucity of data. As explained in the Methods section, we decided to leverage on the features of PSI-SDM and perform a meta-regression, rather than separately analyzing the subset. This was in fact the most direct way to test the potential effect of age, as originally hypothesized by McGrath and Stoodley (2019). Our results showed that no effect of age was found at $p_{uncorrected} \leq 0.0005$ either in ADHD or dyslexia.

Additionally, meta-regression analyses about biological sex and medication indicated no significant effect in both ADHD and dyslexia VBM findings. FSIQ meta-regression was not performed instead due to a large amount of unavailable data about the pertaining variable (Table 3.1).

3.3.6. Brain volume sub-analysis

In order to evaluate the possible effect of total brain volume, McGrath and Stoodley (2019) reduced the analysis to the subset of experiments that explicitly corrected the results for the volumetric difference between the clinical and control group. Even in this condition, convergence was observed in the sole cluster in the right caudate, based on the less conservative version of the maps (i.e., $p_{uncorrected} < 0.005$).

In our replication, as in the case of using the whole dataset, it was not possible to perform the conjunction analysis at TFCE $p \leq 0.05$ since no significant effect was found for dyslexia at that threshold. The only two clusters that survived at this corrected thresholding, based on the subset for ADHD, were localized in the left crus I and crus II of the cerebellum (Table 3.3 and Figure 3.1). It is important to note that no significant heterogeneity of effect size (i.e., $I^2 = 4.5\%$ for the peak 1; $I^2 = 17.9\%$ for the peak 2) and no obvious publication bias (i.e., Egger's test $p = 0.6$ for the peak 1; $p = 0.6$ for the peak 2) (Radua et al., 2013) were found for these brain volume related findings.

At the uncorrected level of statistical significance ($p < 0.005$), we found three clusters of gray matter decrease in dyslexia (Table S3.7; Figure S3.3) and 13 clusters of gray matter decrease in ADHD (Table S3.8; Figure S3.4) respectively, when accounting for brain volume. For the sake of completeness, we ran the conjunction analysis comparing the two maps at the uncorrected level. Results showed no common brain area of variation.

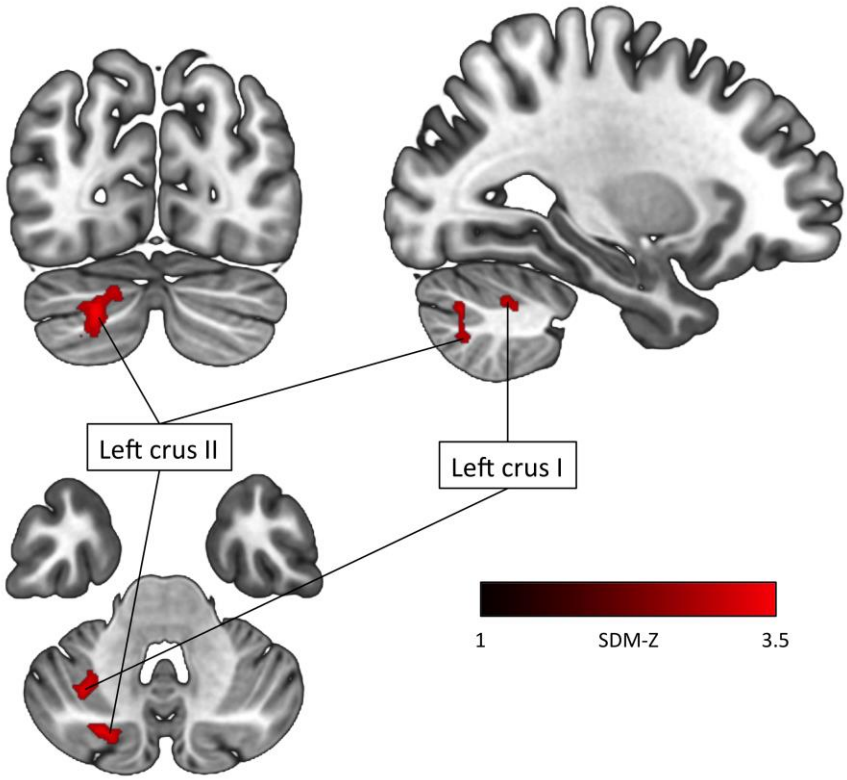

Figure 3.1. Brain cluster of gray matter reduction in subjects with attention-deficit/hyper-activity disorder compared to typically developing controls (brain volume sub-analysis). Results are TFCEbased FWER corrected at 0.05. The PSI-SDM findings are visualized as coronal, sagittal, and axial slices (2-D cortical, subcortical, and cerebellar view).

Table 3.3. Brain clusters of gray matter variation in attention-deficit/hyper-activity disorder compared with typically developmental controls at TFCE corrected p≤0.05 and minimum cluster size = 10 voxels (brain volume sub-analysis).

Region	MNI coordinate			SDM	P ≤ 0.05	Voxels	Cluster breakdown
	x	y	z	Z score	(Corrected)		(Voxels)
ADHD > TDCs							
No cluster found							
ADHD < TDCs							
Left crus II (Cerebellum)	-22	-78	-36	-3.569	0.02	120	Left crus II (73) Left crus I (44) Left lobule VIIB (3)
Left crus I (Cerebellum)	-32	-58	-44	-3.525	0.03	84	Left crus II (51) Left crus I (11) Left lobule VIIB (10) Left lobule VI (9) Left lobule VII (2) Middle cerebellar peduncles (1)

ADHD, attention-deficit/hyper-activity disorder; TDCs, typically developing controls; BA, Brodmann area; MNI, Montreal Neurological Institute; SDM, Seed-based d Mapping.

3.4. Discussion

In the present study, we aimed to replicate the original VBM meta-analysis by McGrath and Stoodley (2019), using PSI-SDM in place of ALE as a method to carry out the analyses. Overall, the current attempt confirmed a limited overlap between the alteration correlates of ADHD and dyslexia. This was primarily due to the lack of significant effects for dyslexia that prevented the execution of the conjunction analysis. Even for ADHD, the only main results were obtained at uncorrected thresholding, and should therefore be interpreted with caution.

Nevertheless, this outcome was not completely surprising. As correctly stated by McGrath and Stoodley (2019) throughout their work, the magnitude of the identified effect was limited. In fact, the conjunction analysis highlighted the only cluster in the right caudate, and only when comparing maps with the more lenient and very liberal thresholding (i.e., $p_{\text{uncorrected}} < 0.005$). The authors did not test their results with more conservative correction thresholds, such as the false discovery rate (Laird et al., 2005), voxel- or cluster-level FWE (Eickhoff et al., 2016). Therefore, any consideration about the behavior of the data in that scenario would be speculative (Eickhoff et al., 2017). As a further and related aspect, it should be noted that the number of experiments originally included in the various analyses

was very close to the lower bound recommended in the ALE literature (Eickhoff et al., 2016; Liloia et al., 2021b; Tahmasian et al., 2019). In similar cases, the stability of the results can be limited, and findings can be driven by single experiments (Eickhoff et al., 2017; Müller et al., 2018; Tahmasian et al., 2019). In light of these considerations, the opposite outcomes we found could be more related with the size of the dataset than with the influence of methodological differences between ALE and PSI-SDM.

Although for some of the additional analyses we performed the null experiments for were included, the particular nature of these studies did not really contribute to expand the dataset. On the contrary, the effect of considering null results is rather to further increase the threshold to be reached by the remaining experiments. In line with this, one cluster of gray matter decrease in ADHD was lost after the inclusion of the seven null experiments. In our analyses, the only two clusters surviving the TFCE corrected $p \leq 0.05$ thresholding were found in the left cerebellar crus II and crus I, based on the subset of ADHD experiments that accounted for total brain volume differences. Although the involvement of the cerebellum in this disorder was not reported by McGrath and Stoodley (2019), this is well described in ADHD literature (Bruchhage et al., 2018; Goetz et al., 2014; Mostofsky et al., 1998; Stoodley, 2014; Stoodley, 2016). The fact that, in our replication, the alteration of the cerebellum only emerged in the sub-analysis could be due to the homogenization induced through the selection process. In fact, an effect of excluding the experiments that had not taken into account differences in total brain volume could be to retain more similar brains, in spatial terms. This could in turn increase the chance of finding convergence among the various experiments, therefore surviving to statistical thresholding. On the other hand, it should also be considered that when reducing the number of experiments analyzed, the chance to find some significant results increases, in virtue of reduced variance (Eickhoff et al., 2017).

A very strict interpretation of the paucity of significant results in our replication would be that neither ADHD nor dyslexia are consistently associated with a pattern of gray matter alteration in the brain. This stance is coherent with a recent ALE cluster-level FWE corrected study by Samea et al. (2019) on pediatric subjects with ADHD. By contrast, prior CBMAs described significant, albeit largely different, patterns of neuroanatomical alteration in dyslexia (Linkersdörfer et al., 2012; Richlan et al., 2013; Yan et al., 2021). The discrepancy in VBM findings between current and early meta-analyses could be explained by a number of factors. First, the CBMAs of Linkersdörfer et al. (2012) and Richlan et al. (2013) analyzed

small datasets due to the limited availability of appropriate data (i.e., nine experiments for a total of 62 gray matter decrease foci and nine experiments for a total of 45 gray matter decrease/increase foci, respectively), hence prone to type I error (Eickhoff et al., 2017). Second, Yan et al. (2021) evaluated the neuroanatomical landscape of dyslexia from a cross-linguistic writing perspective, partitioning the current VBM literature about disorder in two datasets, namely the alphabetic language (21 experiments) and morpho-syllabic (6 experiments) groups. Third, Richlan et al. (2013) and Yan et al. (2021) used the effect-size version of SDM at uncorrected level; Linkersdörfer et al. (2012) used the ALE instead. While these CBMA methods test the spatial convergence across coordinates, our PSI-SDM approach conducts standard univariate voxel-wise tests (Albajes-Eizagirre et al., 2019; Winkler et al., 2014). From a methodological point of view, this means that we were able to overcome certain spatial drawbacks which may have decreased the statistical power of the meta-analysis, leading to either spuriously conservative or spuriously liberal results (Albajes-Eizagirre and Radua, 2018; Albajes-Eizagirre et al., 2019; Winkler et al., 2014). As a further relevant note, the current lack of consensus would be further reinforced by the complex and not fully understood nature of these neurodevelopmental multi-faceted disorders. For example, some authors have suggested that both ADHD and dyslexia might not be discrete entities but, rather, their symptomatology occurs on a continuum (Kern et al., 2015; McLennan, 2016; Peterson et al., 2013; Shaywitz et al., 1992; Whitely, 2015). Moreover, medical comorbidity in these clinically heterogeneous conditions is frequent (Darweesh et al., 2020; Gnanavel et al., 2019). In this regard, we note that 15 out of 31 original VBM experiments about ADHD (i.e., the 48% of the dataset) have recruited at least one subject with other psychiatric and neurological disorders (Table 3.1) (McGrath and Stoodley, 2019). This aspect adds inevitable heterogeneity to the meta-analytic sample.

A further aspect to be mentioned is the role of the gray matter increase. While some clusters of decrease were found at the uncorrected level of thresholding, no increase was detected in our replication. On the contrary, McGrath and Stoodley (2019) found several clusters of increase in both ADHD and dyslexia. As discussed in Mancuso et al. (2020), the biological meaning of the increment of gray matter in the pathological brain remains elusive, as well as its relationship with the opposed phenomenon of decrease. However, the divergent findings could be explained by the different approach followed by ALE and PSI-SDM. While the former analyses increase and decrease separately, PSI-SDM processes the two effects

together. In virtue of this, if the prevalence of experiments reports the decrease of a given brain region, this could hide the presence of some increase effect in that same region. The two directions could also be counterbalancing, showing zero effect in total. Since it is known that increase effect is less represented in literature than decrease one (Mancuso et al., 2020; Nani et al., 2021), the absence of significant increase results should always be considered with caution.

3.4.1 Limitations and future directions

Disorder-specific issues and clinical heterogeneity aside, we should note that the CBMA approach in general, and PSI-SDM technique in particular, have some limitations. By definition, coordinate-based techniques have a limited accuracy because they only consider significant foci (i.e., x,y,z peak values) instead of the entire voxel-wise statistic parametric maps (Manuello et al., 2022). However, we observe that this procedure is standardized in the field and capable of reducing the probability of making spatial errors (Eickhoff et al., 2009; Radua et al., 2012). Second, although McGrath and Stoodley (2019) identified nine VBM studies with null result experiments about ADHD and dyslexia, we cannot exclude that this research topic is affected by the publication bias against null or contra-evidence results (i.e., file-drawer problem) (Manuello et al., 2022; Müller et al., 2018). Third, exploratory meta-regression analyses did not find a significant impact of some key socio-demographic and clinical variables on published findings in both clinical conditions of interest. It is necessary to note that these results are based on a limited number of eligible experiments and, therefore, should be taken with caution and deserves future attention. Fourth, in performing the SDM-PSI analyses we cannot rule out that taking into account a few experiments may slightly bias effect sizes towards zero, even though simulations made by the SDM team with the maximum likelihood/multiple imputation algorithm have already shown that this kind of bias is almost negligible (Albajes-Eizagirre et al., 2019). Lastly, although the meta-analytic approach has permitted a quantitative synthesis of over 20 years of research about the topic, the cross-sectional nature of the data hampers the possibility to characterize possible disorder-specific and common patterns of neuroanatomical variation from a developmental perspective. In this regard, future longitudinal studies scanning the same individuals across the lifespan, along with new reproducible data analytic pipelines, may open new lines of research able to propose new neuroimaging-based targeted interventions.

3.5. Conclusion

Here, we aimed to replicate the important findings pertaining the existence of brain regions undergoing gray matter alteration in association with both ADHD and dyslexia reported in the McGrath and Stoodley study (2019). Using a different state-of-the-art meta-analytic method and additional statistical procedures, we found no significant alteration overlap between these two neurodevelopmental conditions. These results remained unchanged under the addition of nine experiments not included in the original analyses. Furthermore, we have argued that the evidence for the existence of socio-demographic and clinical confounding effects on published findings is not convincingly demonstrated. Despite common genetic, environmental, cognitive, and pathomechanism risk factors between these two NDDs, current outcomes support the existence of a marked distinction at the neural level, which may be useful for a clinical point of view especially when comorbidity is present. In sum, we believe that the overall replication of the original study may be a further step forward that will help us to find precise neural markers of these neurodevelopmental conditions.

3.6. Supplementary material

3.6.1. Supplementary tables

Table S3.1. VBM experiments included in the original coordinate-based meta-analysis by McGrath and Stoodley (2019): methodological details for the attention-deficit/hyper-activity disorder (A) and dyslexia (B) datasets.

Experiments	GM variations		VBM software	Thickness	Smoothing	Scanner	Original
	TDCs > PZ	PZ > TDCs		(mm)	(FWHM)	(Tesla)	data
(A) ADHD							
Ahrendts et al. (2011)	2	0	SPM 2	1	12 mm	1.5	MNI
Bonath et al. (2018)	12	0	SPM 8	1	8 mm	3.0	BRETT
Bralten et al. (2016)	5	0	SPM	N/A	8 mm	1.5	MNI
Brieber et al. (2007)	9	6	SPM 2	1	12 mm	1.5	MNI
Carmona et al. (2005)	17	0	SPM 2	N/A	12 mm	1.5	MNI
He et al. (2015)	4	0	SPM 8	1	8 mm	3.0	MNI
Iannaccone et al. (2015)	3	2	SPM 8	1	8 mm	3.0	MNI
Johnston et al. (2014)	12	0	SPM 8	1	8 mm	1.5	MNI
Kappel et al. (2015) (adults)	4	0	SPM 8	1	6 mm	3.0	MNI
Kappel et al. (2015) (children)	1	4	SPM 8	1	6 mm	3.0	MNI
Kaya et al. (2018)	0	7	SPM 8	N/A	8 mm	1.5	MNI
Kobel et al. (2010)	1	0	SPM 5	N/A	12 mm	3.0	TAL
Kumar et al. (2017)	4	0	SPM 8	N/A	12 mm	3.0	OTHER
Lim et al. (2013)	6	0	SPM 8	N/A	8 mm	3.0	TAL
McAlonan et al. (2007)	8	0	BAMM	3	4.4 mm	1.5	TAL
Montes et al. (2010)	2	0	SPM 5	1	8 mm	1.0	MNI
Moreno-Alcazar et al. (2016)	3	1	FSL	1	9.4 mm	1.5	MNI
Overmeyer et al. (2001)	9	0	N/A	3	N/A	1.5	TAL
Roman-Urrestarazu et al. (2016)	2	0	FSL-VBM	1	3 mm	1.5	MNI
Sasayama et al. (2010)	14	0	SPM 2	1	12 mm	1.5	MNI
van Wingen et al. (2013)	2	2	SPM 8	1.2	8 mm	3.0	MNI
Villemonteix et al. (2015a) (naïve)	2	0	SPM 8	N/A	5 mm	3.0	MNI
Villemonteix et al. (2015a) (medicated)	2	0	SPM 8	N/A	5 mm	3.0	MNI
Yang et al. (2008)	6	0	SPM 2	5	8 mm	1.5	MNI
(B) DYSLEXIA							
Brambati et al., 2004	9	0	SPM 2	1.5	12 mm	1.5	TAL
Brown et al., 2001	8	0	SPM 99	2	8 mm	1.5	TAL
Eckert et al., 2005	5	1	SPM2b	N/A	12 mm	1.5	MNI
Evans et al., 2014 (male adults)	2	0	SPM 8	1	8 mm	1.5/3.0	TAL
Evans et al., 2014 (female adults)	2	0	SPM 8	1	8 mm	1.5/3.0	TAL
Evans et al., 2014 (male children)	1	0	SPM 8	1	8 mm	1.5/3.0	TAL

Experiments	GM variations		VBM software	Thickness	Smoothing	Scanner	Original
	TDCs > PZ	PZ > TDCs		(mm)	(FWHM)	(Tesla)	data
Evans et al., 2014 (female children)	3	0	SPM 8	1	8 mm	1.5/3.0	TAL
Hoeft et al., 2007	6	0	SPM 2	N/A	8 mm	3.0	TAL
Jednoróg et al., 2015	1	0	SPM 8	1	4 mm	1.5/3.0	MNI
Kronbichler et al., 2008	11	8	SPM 2	1.3	12mm	1.5	MNI
Liu et al., 2013	8	0	SPM 5	1	12 mm	3.0	MNI
Silani et al., 2005	1	1	SPM 2	1.5	12 mm	1.5/2.0	TAL
Siok et al., 2008	3	0	SPM 2	2	10 mm	2.0	MNI
Steinbrink et al., 2008	2	0	SPM 5	N/A	12 mm	3.0	MNI
Tamboer et al., 2015	8	3	FSL-VBM	N/A	4 mm	3.0	MNI
Vinckenbosch et al., 2005	1	1	SPM99	1	8 mm	1.5	TAL
Xia et al., 2016	3	0	SPM8	1.33	8 mm	3.0	MNI
Yang et al., 2016	7	3	SPM8	4	8 mm	1.5	MNI

ADHD, attention-deficit/hyper-activity disorder; FWHM, full width at half maximum; MNI, Montreal Neurological Institute; N/A, data not available; PZ, patients; TAL, Talairach; TDCs, typically developing controls; VBM, voxel-based morphometry.

Table S3.2. VBM experiments with null results and not included in the original coordinate-based meta-analysis by McGrath and Stoodley (2019): methodological details for the attention-deficit/hyper-activity disorder (A) and dyslexia (B) datasets.

Experiments	GM variations		VBM software	Thickness	Smoothing	Scanner	Original
	TDCs > PZ	PZ > TDCs		(mm)	(FWHM)	(Tesla)	data
(A) ADHD							
Amico et al. (2011)	0	0	SPM5	1.5	8 mm	1.5	TAL
Depue et al. (2010)	0	0	FSL-VBM	1.7	4.6 mm	N/A	MNI
Maier et al. (2015)	0	0	SPM12	N/A	8 mm	N/A	OTHER
Onnink et al. (2013)	0	0	SPM8	N/A	8 mm	1.5	MNI
Saad et al. (2017)	0	0	SPM8	1	N/A	3.0	MNI
Seidman et al. (2011)	0	0	FSL-VBM	1.33	7.05 mm	1.5	MNI
Villemonteix et al. (2015b)	0	0	SPM8	N/A	12 mm	3.0	MNI
(B) DYSLEXIA							
Eckert et al. (2016)	0	0	SPM8	N/A	8 mm	1.5/3.0	MNI
Pernet et al. (2009)	0	0	SPM5	N/A	8 mm	1.5	MNI

ADHD, attention-deficit/hyper-activity disorder; FWHM, full width at half maximum; MNI, Montreal Neurological Institute; N/A, data not available; PZ, patients; TAL, Talairach; TDCs, typically developing controls; VBM, voxel-based morphometry.

Table S3.3. Brain clusters of gray matter variation in attention-deficit/hyper-activity disorder compared with typically developmental controls at $p_{uncorrected}$ <0.0005 and minimum cluster size = 10 voxels (replication analysis).

Region	MNI coordinate			SDM	*P < 0.005*	Voxels	Cluster breakdown
	x	y	z	*Z* score	*(Uncorrected)*		(Voxels)
ADHD > TDCs							
No cluster found							
ADHD < TDCs							
Right superior frontal gyrus, medial orbital (BA 11)	6	24	-10	-3.708	0.0001	127	Right SFG (66) Right gyrus rectus (32) Right olfactory cortex (15) Bilateral ACC (12) Right Striatum (2)
Right lenticular nucleus (Putamen)	30	0	-2	-3.385	0.0003	82	Right Putamen (65) Right Striatum (17)
Left lobule VI (Cerebellum)	-34	-46	-34	-2.783	0.002	22	Left lobule VI (16) Left crus I (6)
Left postcentral gyrus (BA 6)	-46	-14	50	-2.942	0.001	12	Left PoCG (12)
Right gyrus rectus (BA 11)	4	38	-24	-2.781	0.002	10	Right gyrus rectus (10)

ADHD, attention-deficit/hyper-activity disorder; TDCs, typically developing controls; BA, Brodmann area; MNI, Montreal Neurological Institute; SDM, Seed-based d Mapping; SFG, superior frontal gyrus; ACC, anterior cingulate cortex; PoCG, posterior central gyrus.

Table S3.4. Brain clusters of gray matter variation in dyslexia compared with typically developmental controls at $p_{uncorrected}$ <0.0005 and minimum cluster size = 10 voxels (replication analysis).

Region	MNI coordinate			SDM	*P < 0.005*	Voxels	Cluster breakdown
	x	y	z	*Z* score	*(Uncorrected)*		(Voxels)
Dyslexia > TDCs No cluster found							
Dyslexia < TDCs No cluster found							

TDCs, typically developing controls; SDM, Seed-based d Mapping.

Table S3.5. Brain clusters of gray matter variation in attention-deficit/hyper-activity disorder compared with typically developmental controls at $p_{uncorrected}$ <0.0005 and minimum cluster size = 10 voxels (additional analysis).

Region	MNI coordinate			SDM	*P < 0.005*	Voxels	Cluster breakdown
	x	y	z	*Z* score	*(Uncorrected)*		(Voxels)
ADHD > TDCs No cluster found							
ADHD < TDCs							
Right superior frontal gyrus, medial orbital (BA 11)	6	24	-10	-4.051	0.00002	148	Right SFG (87) Right gyrus rectus (38) Right olfactory cortex (10) Bilateral ACC (9) Right Striatum (4)
Right lenticular nucleus (Putamen)	30	0	-2	-3.817	0.00006	152	Right Putamen (131) Right Striatum (21)
Left lobule VI (Cerebellum)	-34	-46	-34	-3.023	0.001	50	Left lobule VI (29) Left crus I (21)
Right gyrus rectus (BA 11)	4	38	-24	-3.281	0.0005	19	Right gyrus rectus (19)

Abbreviations: ADHD, attention-deficit/hyper-activity disorder; TDCs, typically developing controls; BA, Brodmann area; MNI, Montreal Neurological Institute; SDM, Seed-based d Mapping; SFG, superior frontal gyrus; ACC, anterior cingulate cortex.

Table S3.6. Brain clusters of gray matter variation in dyslexia compared with typically developmental controls at $p_{uncorrected}$ <0.0005 and minimum cluster size = 10 voxels (additional analysis).

Region	MNI coordinate			SDM	*P < 0.005*	Voxels	Cluster breakdown
	x	y	z	*Z* score	*(Uncorrected)*		(Voxels)
Dyslexia > TDCs No cluster found							
Dyslexia < TDCs No cluster found							

TDCs, typically developing controls; SDM, Seed-based d Mapping.

Table S3.7. Brain clusters of gray matter variation in dyslexia compared with typically developmental controls at $p_{uncorrected}$ <0.0005 and minimum cluster size = 10 voxels (brain volume sub-analysis).

Region	MNI coordinate			SDM	*P < 0.005*	Voxels	Cluster breakdown
	x	y	z	*Z* score	*(Uncorrected)*		(Voxels)
Dyslexia > TDCs No cluster found							
Dyslexia < TDCs							
Left superior temporal gyrus (BA 38)	-46	10	-14	-3.578	0.0001	207	Left STG (181) Left MTG (26)
Right lobule VI (Cerebellum)	36	-58	-24	-2.839	0.002	34	Right lobule VI (22) Right crus I (12)
Middle cerebellar peduncles	-24	-44	-32	-2.715	0.003	14	Middle cerebellar peduncles (14)

TDCs, typically developing controls; BA, Brodmann area; MNI, Montreal Neurological Institute; SDM, Seed-based d Mapping; STG, superior temporal gyrus; MTG, middle temporal gyrus.

Table S3.8. Brain clusters of gray matter variation in attention-deficit/hyper-activity disorder compared with typically developmental controls at $p_{uncorrected}$ <0.0005 and minimum cluster size = 10 voxels (brain volume sub-analysis).

Region	MNI coordinate			SDM	*P < 0.005*	Voxels	Cluster breakdown
	x	y	z	*Z* score	*(Uncorrected)*		(Voxels)
ADHD > TDCs							
No cluster found							
ADHD < TDCs							
Left crus II (Cerebellum)	-22	-78	-36	-3.569	0.0001	693	Left crus II (372) Left crus I (199) Left lobule VIIB (52) Left lobule VI (36) Left lobule VIII (34)
Left parahippocampal gyrus (BA 36)	-20	-12	-24	-4.468	0.000003	372	Left parahippocampus (247) Left hippocampus (55) Left medial cingulum (33) Left fusiform gyrus (22) Left amygdala (15)
Right caudate nucleus	16	14	10	-4.509	0.000003	276	Right caudate (276)
Left cuneus cortex (BA 17)	-10	-98	14	-4.362	0.000006	227	Left cuneus (135) Left SOG (78) Left MOG (7)
Left caudate nucleus	-12	20	6	-4.213	0.00001	157	Left caudate (152) Left striatum (5)
Right gyrus rectus (BA 11)	10	38	-24	-3.414	0.0003	165	Right gyrus rectus (153) Right SFG (12)
Right lenticular nucleus (Putamen)	30	-2	-4	-3.400	0.0003	136	Right putamen (108) Right striatum (28)
Left anterior cingulate cortex (BA 32)	-4	40	4	-3.218	0.0006	124	Left ACC (109) Right ACC (15)
Right lobule IX (Cerebellum)	10	-50	-50	-3.343	0.0004	104	Right lobule IX (104)

Region	MNI coordinate			SDM	P < 0.005	Voxels	Cluster breakdown
	x	y	z	Z score	*(Uncorrected)*		(Voxels)
Left lobule IX (Cerebellum)	-10	-48	-52	-3.566	0.0001	58	Left lobule IX (58)
Right superior temporal gyrus (BA 38)	28	8	-26	-3.067	0.0007	38	Right STG (26) Right parahippocampal (12)
Right parahippocampal gyrus (BA 20)	30	-26	-24	-3.013	0.001	17	Right parahippocampal (17)
Left supplementary motor area (BA 6)	-8	-12	50	-3.645	0.0001	14	Left SMA (11)

ADHD, attention-deficit/hyper-activity disorder; TDCs, typically developing controls; BA, Brodmann area; MNI, Montreal Neurological Institute; SDM, Seed-based d Mapping; SOG, superior occipital gyrus; MOG, middle occipital gyrus; ACC, anterior cingulate cortex; STG, superior temporal gyrus; SMA, supplementary motor area.

3.6.2. Supplementary figures

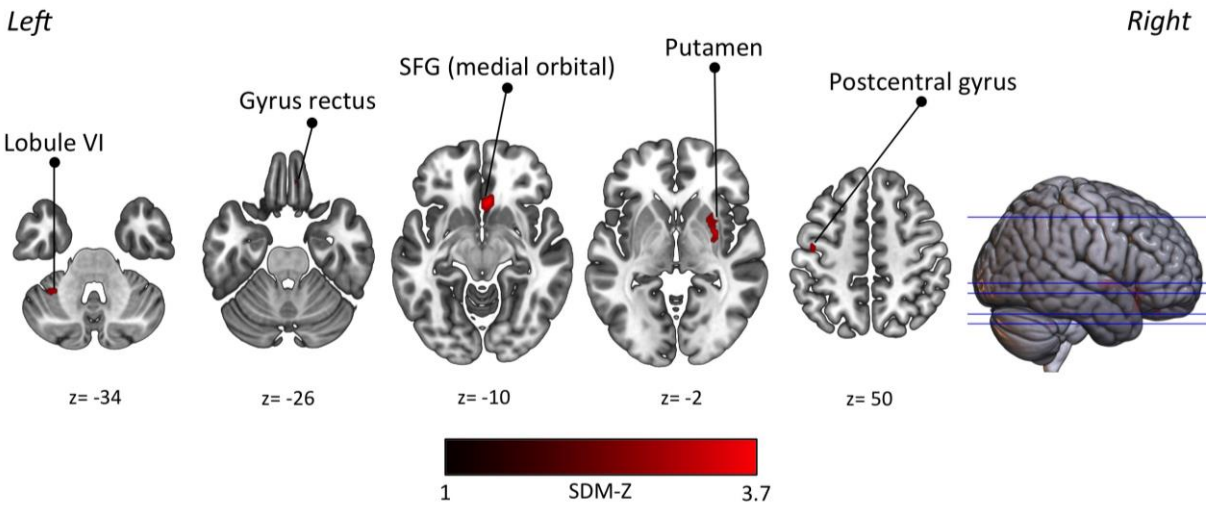

Figure S3.1. Brain clusters of gray matter variation in attention-deficit/hyper-activity disorder compared with typically developmental controls at $p_{uncorrected}$ <0.0005 and minimum cluster size = 10 voxels (replication analysis).

The PSI-SDM map is visualized as six axial slices (2-D cortical, subcortical, and cerebellar view). Colors from dark to light red represent voxels with a common pattern of neuroanatomical reduction (gray matter in attention-deficit/hyper-activity disorder < typically developmental controls). Brain slices are in neurological convention (i.e. Right is right, Left is left). SFG, superior frontal gyrus.

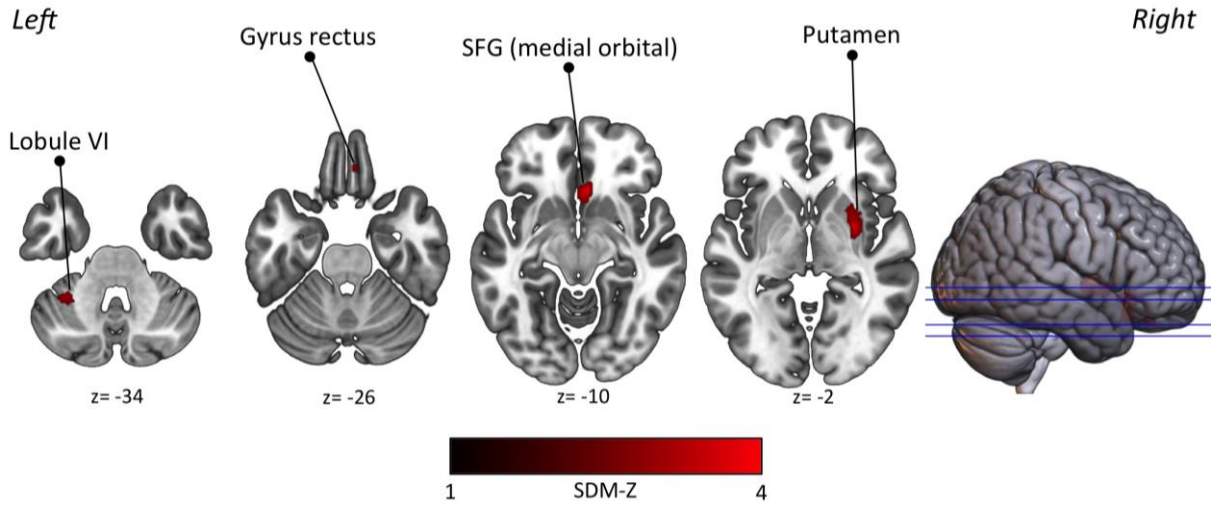

Figure S3.2. Brain clusters of gray matter variation in attention-deficit/hyper-activity disorder compared with typically developmental controls at $p_{uncorrected}$ <0.0005 and minimum cluster size = 10 voxels (additional analysis).

The PSI-SDM map is visualized as six axial slices (2-D cortical, subcortical, and cerebellar view). Colors from dark to light red represent voxels with a common pattern of neuroanatomical reduction (gray matter in attention-deficit/hyper-activity disorder < typically developmental controls). Brain slices are in neurological convention (i.e. Right is right, Left is left). SFG, superior frontal gyrus.

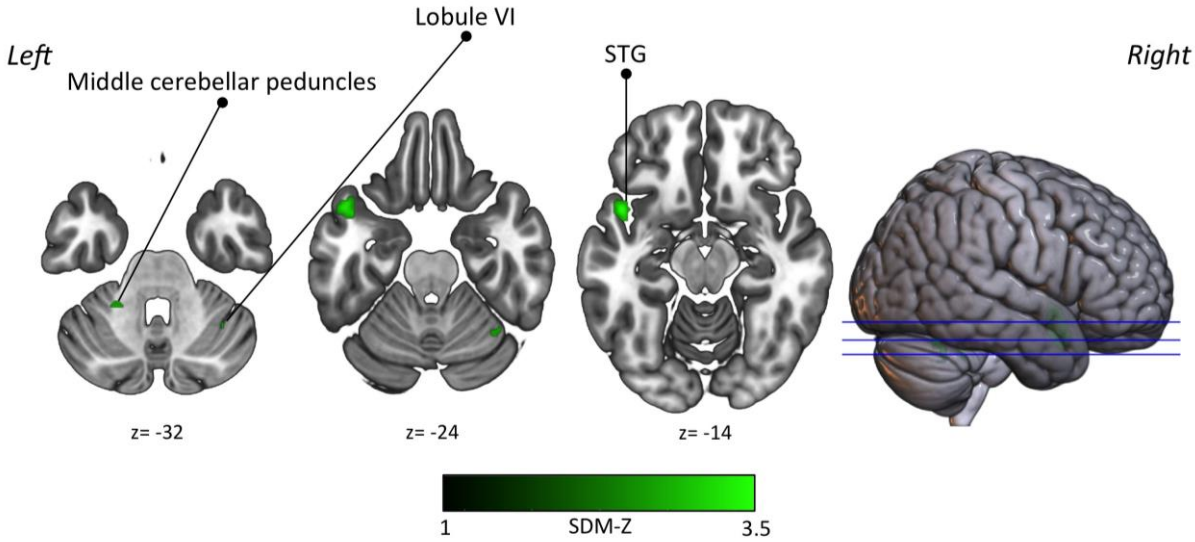

Figure S3.3. Brain clusters of gray matter variation in dyslexia compared with typically developmental controls at $p_{uncorrected}$ <0.0005 and minimum cluster size = 10 voxels (brain volume sub-analysis).

The PSI-SDM map is visualized as six axial slices (2-D cortical, subcortical, and cerebellar view). Colors from dark to light green represent voxels with a common pattern of neuroanatomical reduction (gray matter in dyslexia < typically developmental controls). Brain slices are in neurological convention (i.e. Right is right, Left is left). STG, superior temporal gyrus.

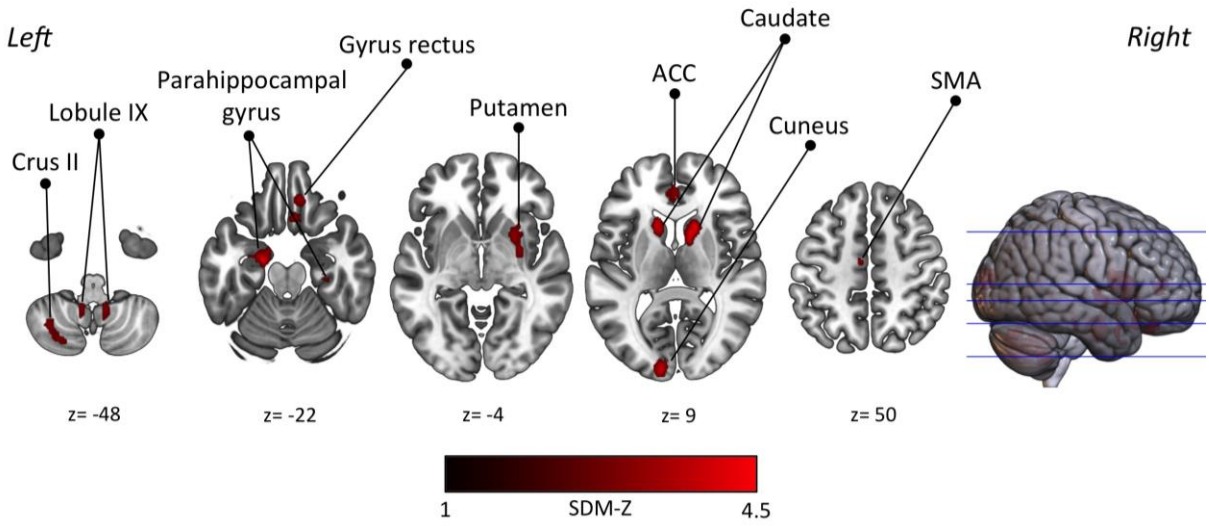

Figure S3.4. Brain clusters of gray matter variation in attention-deficit/hyper-activity disorder compared with typically developmental controls at $p_{uncorrected}$ <0.0005 and minimum cluster size = 10 voxels (brain volume sub-analysis).

The PSI-SDM map is visualized as six axial slices (2-D cortical, subcortical, and cerebellar view). Colors from dark to light red represent voxels with a common pattern of neuroanatomical reduction (gray matter in attention-deficit/hyper-activity disorder < typically developmental controls). Brain slices are in neurological convention (i.e. Right is right, Left is left). ACC, anterior cingulate cortex; SMA, supplementary motor area.

CHAPTER 4

Gray Matter Abnormalities Follow Non-Random Patterns of Co-Alteration in Autism: Meta-Connectomic Evidence[3]

Abstract

Background: Autism spectrum disorder (ASD) is a neurodevelopmental disorder characterized by atypical brain anatomy and connectivity. Graph-theoretical methods have mainly been applied to detect altered patterns of white matter tracts and functional brain activation in individuals with ASD. The network topology of gray matter (GM) abnormalities in ASD remains relatively unexplored. *Methods:* An innovative meta-connectomic analysis on voxel-based morphometry data (45 experiments, 1,786 subjects with ASD) was performed in order to investigate whether GM variations can develop in a distinct pattern of co-alteration across the brain. This pattern was then compared with normative profiles of structural and genetic co-expression maps. Graph measures of centrality and clustering were also applied to identify brain areas with the highest topological hierarchy and *core* sub-graph components within the co-alteration network observed in ASD. *Results:* Individuals with ASD exhibit a distinctive and topologically defined pattern of GM co-alteration that moderately follows the structural connectivity constraints. This was not observed with respect to the pattern of genetic co-expression. Hub regions of the co-alteration network were mainly left-lateralized, encompassing the precuneus, ventral anterior cingulate, and middle occipital gyrus. Regions of the default mode network appear to be central in the topology of co-alterations. *Conclusion:* These findings shed new light on the pathobiology of ASD, suggesting a network-level dysfunction among spatially distributed GM regions. At the same time, this study supports pathoconnectomics as an insightful approach to better understand neuropsychiatric disorders.

4.1. Introduction

Autism spectrum disorder (ASD) is the diagnostic label that refers to a set of neurodevelopmental conditions characterized by impairment in social abilities, repetitive

[3] This study was published in *NeuroImage: Clinical* in 2021 (Volume 30, Article 102583, Pages 1-19, doi: 10.1016/j.nicl.2021.102583). Authors: Liloia D., Mancuso L., Uddin L.Q., Costa T., Nani A., Keller R., Manuello J., Duca S., Cauda F.

behaviors, restricted interests and abnormal sensory processing (American Psychiatric Association, 2013). This cluster of conditions reports clinical features persisting throughout the lifespan (Brighenti et al., 2018; Keller et al., 2020; Lord et al., 2018) and afflicting approximately 1 in 54 children aged 8 years (Baio et al., 2018).

Over the past decades, neuroimaging studies have suggested that ASD is associated with both anatomical and functional brain abnormalities (for a review see Ecker et al., 2015). In particular, voxel-based morphometry (VBM), a univariate technique capable of quantifying morphometric differences between diagnostic groups (Ashburner and Friston, 2000), has been used extensively to elucidate the neuroanatomy of autism. In addition, coordinate-based meta-analyses (CBMAs) have identified concordant structural effects across independent ASD studies, showing focal aberrations in multiple areas such as the cerebellum, amygdala-hippocampus complex, cingulate cortex, parieto-occipital pole, temporal and prefrontal cortices (Carlisi et al., 2017; Cauda et al., 2014a; Cauda et al., 2011; DeRamus and Kana, 2015; Liu et al., 2017; Lukito et al., 2020; Nickl-Jockschat et al., 2012; Via et al., 2011). These important findings notwithstanding, the intrinsic mechanisms and network topological organization that underpin the distribution of gray matter (GM) abnormalities in ASD remains largely unappreciated.

In recent years, advances in graph-theoretical analysis have begun to provide a conceptual framework for studying the topological properties of complex brain systems, which has led to the new field of connectomics. This line of research has been aiming to comprehensively map large-scale brain networks as a collection of nodes (brain regions or sub-areas) and edges (neural pathways or statistical relationships) (Sporns, 2013). The conceptual and empirical development of connectomics presents novel opportunities for understanding neuropsychiatric conditions, which now tend to be conceived of as brain networks disorders (Deco and Kringelbach, 2014; Fornito et al., 2017; Rubinov and Bullmore, 2013; van den Heuvel and Sporns, 2019). Moreover, there is an emerging consensus that the investigation of neuropathological patterns is ever more essential to improve diagnosis and prediction of mental illness (Cao et al., 2015; Huys et al., 2016; Yahata et al., 2017). This view is particularly relevant for psychiatric disorders. The U.S. National Institute of Mental Health's Research Domain Criteria (RDoC) takes into account network-level abnormalities as a core feature for understanding the neurobiology of mental disorders, with the aim to integrate the current symptom-based diagnostic classifications

(Insel et al., 2010; Insel, 2014).

Despite advances in neuroimaging, graphs of GM alterations are particularly difficult to investigate. So far only a few studies have explored differences in GM systems in ASD using source-based morphometry (SoBM) (Grecucci et al., 2016; Pappaianni et al., 2018) and anatomical covariance, an MRI measure of cortical thickness or density relationships between brain areas (Evans, 2013). Although the neurobiological basis of anatomical covariance is still poorly understood (Alexander-Bloch et al., 2013), research on this topic has produced important findings in characterizing abnormal brain structures in ASD that appear to be part of the salience and default mode (Valk et al., 2015; Zheng et al., 2020; Zielinski et al., 2012), fronto-temporal (Bernhardt et al., 2014; Sharda et al., 2017), striatal (Eisenberg et al., 2015), parieto-occipital and limbic (Balardin et al., 2015; Bethlehem et al., 2017; Cardon et al., 2017) networks. A network neuroscience approach can better assess the anatomical alterations of ASD, reporting not only the sites of the alterations but also their mutual relationships.

An innovative computational methodology has been devised recently to perform *morphometric co-alteration networking* (MCN) analysis of human brain pathology, which can be defined as the investigation of abnormal conjoint patterns formed by localized GM co-altered regions (Cauda et al., 2018a). This type of analysis is a meta-connectomic and data-driven method, able to extend the information available from voxel-wise data. MCN can statistically derive the pathological network of a given brain disease using Patel's κ, an empirical Bayesian technique suitable for detecting the probability that alterations of two brain regions can co-occur (Patel et al., 2006; Smith et al., 2011). Different from the anatomical covariance method, MCN can identify a network in which the pathological modifications of GM are statistically related. It is therefore possible to examine the topological properties of GM co-alterations rather than those related to within-group anatomical covariance (Cauda et al., 2018a).

This innovative approach is well-suited to the study of pathophysiological alterations of brain disorders, which tend to be distributed across the brain according to network-like patterns (Fornito and Bullmore, 2015; Iturria-Medina and Evans, 2015; Raj et al., 2012; Stam, 2014). It has been proposed that mutual relationships of morphometric variation between two or more structurally defined regions reflects their shared vulnerability to damage due to processes of neuronal degeneration or neurodevelopmental factors (e.g., atypical dendritic growth, cellular migration, myelination, synaptogenesis and axonal pathfinding), and is

mediated by molecular/cellular trophic and genetic effects (for a review see Fornito et al., 2015; Raj and Powell, 2018). Evidence for such mutual alteration distributions in autism exists (Casanova, 2006; Cauda et al., 2014a; Galvez-Contreras et al., 2017; Nickl-Jockschat and Michel, 2011; Palmen et al., 2004; Wegiel et al., 2014; Zielinski et al., 2012); however, these distributions have not yet been comprehensively understood both from a micro- and macro-level perspective. Therefore, the identification of statistically robust and anatomically plausible co-alteration networks by means of the MCN methodology has the potential to reveal more about ASD pathophysiology than a canonical GM approach, since it better assesses the complex nature of morphometric abnormalities underlying the clinical hallmarks of disease.

Moreover, an emerging literature suggests that certain brain regions are preferentially vulnerable to a wide range of psychiatric and neurological disorders (Cauda et al., 2019b; Crossley et al., 2014; Goodkind et al., 2015; Liloia et al., 2018; Uddin, 2015). Typically, these regions are highly connected and play a pivotal role in supporting the integrity of brain network architecture (Buckholtz and Meyer-Lindenberg, 2012; Bullmore and Sporns, 2012; Crossley et al., 2014). In relation to their high topological centrality, these regions are to be conceived as pathological hubs capable of influencing the distribution of alterations within the cerebral parenchyma (Manuello et al., 2018; van den Heuvel and Sporns, 2013; Worbe, 2015; Zhou et al., 2012).

To date, the MCN methodology has been applied to find evidence of abnormal conjoint patterns in transdiagnostic meta-analyses (Cauda et al., 2020a; Cauda et al., 2018a; Cauda et al., 2018b; Mancuso et al., 2020; Nani et al., 2020) and in studies on single neurological conditions such as Alzheimer's disease (Manuello et al., 2018) and chronic pain (Tatu et al., 2018). However, the presented approach has never been used to analyze data from individuals with ASD or other psychiatric conditions. Following the hypothesis that dysfunction at the systems' level characterizes this neurodevelopmental disorder (Ecker et al., 2013; Geschwind and Levitt, 2007), here we aim to provide a unique and comprehensive description of network topology of regional GM co-alterations in individuals with ASD. To further clarify the neurobiological basis of co-alterations, we also investigate the possible correspondence of MCN with normative structural and genetic co-expression connectivity. This choice is motivated by recent experimental proposals suggesting that the development of pathological alteration patterns are influenced by brain connectivity constraints (Cauda et al., 2020a;

Cauda et al., 2018b; Shafiei et al., 2020), as well as by degeneration processes and maladaptive mechanisms (Fornito et al., 2015; Zhou et al., 2012). Finally, since we believe that the application of network science tools offer a powerful way of better understanding how pathology affects the brain (Filippi et al., 2013; Fornito and Bullmore, 2015; Fornito et al., 2017), this study takes advantage of graph-theoretical measures of centrality and clustering in order to provide new insights into large-scale GM co-alteration patterns in ASD.

4.2. Methods

4.2.1. Data sources and search strategy

Meta-data of interest were identified in BrainMap (Fox et al., 2005; Laird et al., 2005b) and MEDLINE databases. First, the VBM BrainMap sector (Vanasse et al., 2018) was queried employing the software package Sleuth (v.3.0.3). The search logic was composed as follows:

> *[Experiments Contrast is Gray Matter] AND [Experiments Context is Disease Effects] AND [Subjects Diagnosis is Autism Spectrum Disorder] AND [Experiments Observed Changes is Controls > Patients]*

A further systematic search was also carried out on the PubMed search engine (https://www.ncbi.nlm.nih.gov/pubmed/). Keywords terms were used as follows:

> *("Autism spectrum disorder" [title/abstract] OR "ASD" [title/abstract] OR "Autism" [title/abstract]) AND ("voxel-based morphometry" [title/abstract] OR "VBM" [title/abstract]).*

The search protocol adheres to the PRISMA Statement international guidelines (Liberati et al., 2009; Moher et al., 2009). This study is also compliant with the consensus-based rules for neuroimaging CBMA in psychiatric disorders (Muller et al., 2018; Tahmasian et al., 2019).

Up until December 2019, 118 full-text articles were reviewed systematically. We included experiments published in a peer-review journal a) using a whole-brain VBM analysis; b) reporting GM variations (i.e., decreased morphometric values) in subjects with ASD; c) adopting a between-group comparison with healthy controls; d) including stereotactic results in Talairach (TAL) or Montreal Neurological Institute (MNI) space.

We removed all the experimental groups having a sample size smaller than 10

participants as previous recommended (Muller et al., 2018; Norman et al., 2016; Tahmasian et al., 2019). We also excluded experiments based on region-of-interest (ROI) analysis that did not analyze the whole brain (Muller et al., 2018). Additionally, to avoid the possibility of analyzing the same participants several times in a single study, we selected only the alteration foci reported by the largest experiment or the ones divided into diagnostic subcategories (for further details see also Table S4.1).

4.2.2. Morphometric co-alteration network identification

Node definition

The anatomical likelihood estimation (ALE) results were used as priors for the meta-connectomic analysis. ALE is the most employed CBMA technique (Tahmasian et al., 2019); it can identify the spatial concordance of the morphological brain alterations between different neuroimaging experiments (Eickhoff et al., 2012; Eickhoff et al., 2009). For each included experiment, the ALE algorithm generated a modeled alteration (MA) map as the union of the 3-D Gaussian probability distribution of each stereotactic coordinate (Fig. 4.1A). The final ALE map was obtained from the union of the MA maps.

To produce the MCN set of nodes, we individuated the local maxima of the ALE maps using a peak detection algorithm. Only the local maxima exhibiting the highest values survived this stage (i.e., values greater than the 90 percentile of the unthresholded ALE distribution). This step was crucial to consider only the altered loci with a very high consensus among the selected experiments. Thus, we reduced the number of nodes by adding a minimum spatial distance of 10 mm and a spherical ROI with a diameter of 10 mm was superimposed on the resulting peaks. The aforementioned threshold values employed are based on the quantitative estimates of the spatial uncertainty associated with the stereotactic coordinate in CBMA provided by Eickhoff et al. (2009), who evidenced an uncertainty in a spatial location with a mean of 10.2 mm (StDev = 0.4 mm). Therefore, the rationale behind this step is to minimize the redundancy of the co-alterations relating to the same cluster of variation that could potentially affect our subsequent topological analysis (Manuello et al., 2018). The Talairach Daemon (Lancaster et al., 2000) was finally used to label the anatomical areas.

To determine whether these nodes were altered in a given experiment, an MA map was produced for each experiment (Laird et al., 2005a). A 3-D Gaussian distribution of probability

was built around each reported coordinate of a given experiment, for which standard deviation is smaller for a larger number of subjects, as proposed by Eickhoff et al. (2009). Then, MA was thresholded at p = 0.01 and overlaid on the set of nodes. Each node was considered to be altered for that experiment if at least 20% of its volume overlapped with a significant MA voxel. This step was crucial to avoid the detection of a false positive, given the possibility of considering a node as altered if it only includes the periphery of a distribution probability (Mancuso et al., 2019). For an in depth and comprehensive discussion of the methodological steps, see also Manuello et al. (2018).

Co-alteration probability quantification

The set of nodes was used to build the MCN in ASD. We generated an alteration matrix N × M, where each column corresponds to a node and each row represents an included experiment (Fig. 4.1B). By means of a Bernoulli generation data model, we determined the probability distribution of joint values of alteration for each pair of nodes. For each couple of nodes (*a* and *b*) it is possible to describe their state of co-occurrence with two binary variables representing four cases: both *a* and *b* altered; *a* altered and *b* non-altered; *a* non-altered and *b* altered; 4) both *a* and *b* non-altered:

$$\theta_1 = P(a = 1, b = 1)$$

$$\theta_2 = P(a = 1, b = 0)$$

$$\theta_3 = P(a = 0, b = 1)$$

$$\theta_4 = P(a = 0, b = 0)$$

Starting from the marginal probabilities, we calculated the co-alteration probability strength between each pair of nodes using the Patel's κ index (Patel et al., 2006; Smith et al., 2011) as:

$$\kappa = \frac{(\theta_1 - E)}{D(\max(\theta_1) - E) + (1 - D)(E - \min(\theta_1))}$$

where

$$E = (\theta_1 + \theta_2)(\theta_1 + \theta_3)$$

$$\begin{cases} \dfrac{\vartheta_1 - E}{2(max(\vartheta_1) - E)} + 0.5, if\, \vartheta_1 \geq E \\ 0.5 - \dfrac{\vartheta_1 - E}{2\big(E - min(\vartheta_1)\big)}, otherwise \end{cases}$$

$$\min(\theta_1) = \max(0.2\theta_1 + \theta_2 + \theta_3 - 1)$$

$$\max(\theta_1) = \min\left(\theta_1 + \theta_2, \theta_1 + \theta_1 + \theta_3\right)$$

The numerator of the fraction calculates the difference between the probability that a and b occur to be co-altered and the expected probability E that a and b occur to be co-altered independently. E is the prior information of this Bayesian equation, which, in a frequentist framework, would be disregarded or treated as not fixed by the data. The denominator calculates a weighted normalizing constant so as to have the κ ranging from –1 and 1: an index that is close to 1 denotes high co-alteration (i.e., co-occurrence) between the nodes (Fig. 4.1C). The statistical significance of κ is assessed by means of a Monte Carlo simulation algorithm, a multinomial and generative model, which determines an estimate of $p(\kappa|z)$ by sampling a Dirichlet distribution and by calculating the proportion of the samples in which $\kappa > e$, where e is the threshold of statistical significance set to 0.01 (1,000 permutation runs). The obtained co-alteration matrix reports values proportional to the statistical occurrence between the alterations of the brain areas taken into account (Cauda et al., 2018a).

4.2.3. Topological analysis

Nodes and edges are the basic units of every network, and their accurate definition is of fundamental importance for a valid model of a complex system (Butts, 2009). Here, a large-scale brain analysis was employed: every node was defined as a peak of GM alteration, while the undirected binary edges represented the values of the thresholded Patel's κ. To determine the topological properties of the MCN in ASD, the corresponding co-alteration matrix was analyzed with Cytoscape (v.3.7.2.) (https://cytoscape.org/). Cytoscape is a bioinformatics software platform, which allows the analysis, modeling and visualization of biological networks and complex systems (Su et al., 2014). Then, the software application CentiScaPe (v.2.2) (Scardoni et al., 2014) was used to examine the topological properties of the nodes (Fig. 4.1D).

Measures of centrality

For each node of alteration, degree, closeness, and betweenness were determined in order to quantify the relevance of the node in the context of the MCN. These measures are cardinal indices of topological centrality (Freeman, 1978) and have been used collectively to examine the central network position of brain areas in both structural and functional connectomes (for a review see van den Heuvel and Sporns, 2013). Among them, degree centrality (D_C) is the simplest measure, which is formally defined as:

$$C_D(i) = k_i = \sum_{i \neq j} A_{ij}$$

In the formula, A_{ij} is a matrix of adjacency. The D_C is defined as the number of undirected links that are incident to a node, assuming that nodes with high connections exert more influence over network structure and function.

The closeness index can be conceived as the average tendency to node proximity or isolation. The closeness is calculated by determining the shortest path between the given node and all the others in the graph. The reciprocal of the summa is then calculated. Closeness centrality (C_C) is formally defined as the inverse of the average shortest path length:

$$C_C(i) = \frac{N-1}{\sum_{i \neq j} l_{ij}}$$

In the formula, l_{ij} is the shortest path length between nodes i and j. Of note, distance is related to the topological proximity. The C_C reflects the integration capacity of a node, as it can be conceived as the probability of the node to be relevant for several other nodes.

The betweenness index is determined by considering a pair of nodes (i, j) and counting the number of shortest paths connecting i and j that pass through another node (h). Betweenness centrality (B_C) measures the proportion of shortest paths between all pairs of nodes in the network that pass through a given node. Therefore, the B_C of a node i can be formally defined as:

$$C_B(i) = \frac{1}{(N-1)(N-2)} \sum_{h \neq i, h \neq j, j \neq i} l_{ij} \frac{p_{hj}(i)}{p_{hj}}$$

In the formula, $p_{hj}(i)$ indicates the number of shortest paths between h and j going through i, p_{hj} indicates the number of shortest paths between h and j, and $(N-1)(N-2)$

indicates the number of couples of nodes that do not include node i. The normalization by p_{hj} accounts for the possibility that several shortest paths may exist between any couple of nodes. Of note, the B_C value is associated with the total number of shortest paths connecting i and j. However, though a node can be crossed by only one path connecting i and j, if this path is the only one to link i and j, the node will have a high betweenness value. This implies that the node is essential in order to maintain the network connections.

Degree, closeness and betweenness are all measures of node prominence because they indicate which focal points, or brain areas in our case, occupy a central position in the network (i.e., *hubness* profile). Conceptually, these measures exhibit a considerable overlap in both real and simulated networks (Bolland, 1988); however, paying attention to different process by which key nodes might influence the distribution of the network. In particular, degree and closeness tend to be highly intercorrelated because they are directed centrality measures between nodes. By contrast, betweenness remains relatively uncorrelated with the degree and closeness, as it is an inherently asymmetric metric, measuring the frequency with which a node lies along paths that link other nodes (Valente et al., 2008).

Therefore, we defined node centrality on the grounds of different topological properties, aggregating rankings across all the measures to devise a more robust classification (Fornito et al., 2016). Specifically, we considered regions as pathological hubs when they reported the highest level of centrality (i.e., one standard deviation above the mean) across all three metrics (Fornito et al., 2016; van den Heuvel and Sporns, 2013).

Graph clustering

To provide a more specific characterization of the core architecture of the MCN, a network clustering analysis was performed. We applied the k-core decomposition algorithm as implemented in the Brain Connectivity Toolbox (Hagmann et al., 2008; Rubinov and Sporns, 2010), to reveal the hierarchical nucleus organization of the graph by gradually focusing on their central cores. This decomposition consists in identifying specific subsets of the graph (i.e., k-cores), each obtained by recursively eliminating all the nodes with a degree smaller than k, until the degree of all the surviving nodes is higher than or equal to k. Higher values of coreness indicate the nodes having greater degree and a more central position in the network's organization.

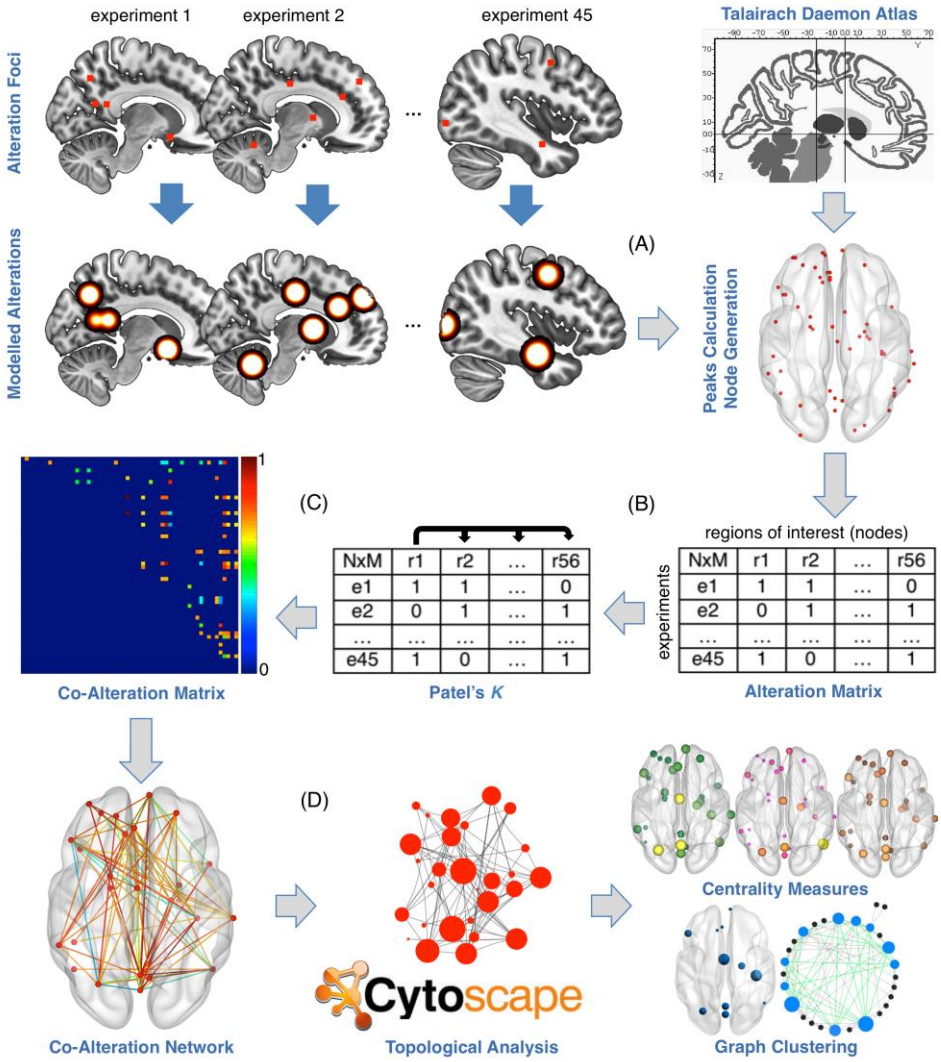

Figure 4.1. Pipeline workflow of the method. (A) Meta-analytic estimation: For each VBM experiment included, the anatomical likelihood estimation (ALE) algorithm generated a modeled alteration (MA) map as the union of the 3-D Gaussian probability distribution of each alteration focus. (B) Alteration matrix creation: The general ALE map was created from the union of the MA maps and was fed to a peak detection algorithm to generate regions of interest (nodes). For each VBM experiment, nodes were considered altered if at least the 20% of their volume overlap with a MA map included. Thus, a binary vector was generated, able to describe if each node is altered/unaltered in each experiment. (C) Network detection: Using the Patel's κ index, the network of co-alteration probability was obtained. Specifically, the co-alteration strength was calculated between each one of such vectors and all the others. (D) Topological analysis: Using the resulting co-alteration matrix, graph-theoretical measures of centrality and clustering were computed.

4.2.4. Correlation with brain connectivity profiles

To determine a possible correspondence of the MCN with normative patterns of brain connectivity, the Mantel's test – MT (Mantel, 1967) was applied. Specifically, we tested the relationship of similarity (i.e., Pearson's *r*) of the ASD co-alteration matrix with the structural and genetic co-expression connectivity matrices, respectively. The MT is a statistical test able to detect the correlation between two distance matrices. By means of a permutation test (i.e., Monte Carlo simulation), the significance of similarity was assessed. This step was crucial to overcome the problem of non-independence of elements in a distance matrix (Mantel, 1967). In this investigation we evaluated the statistical significance of any apparent departure from a zero correlation. To do so, each column and row of one of the two analyzed matrices was randomly permuted 5,000 times. The correlation was recalculated after each permutation, with a statistical significance consisting in the proportion of the permutations leading to a higher correlation coefficient. P-value was estimated after 5,000 permutations.

Analyses of the relationship of similarity between matrices were conducted in MNI space. Thus, we renormalized TAL coordinates of the co-altered nodes using the 'icbm2tal' algorithm developed by Lancaster et al. (2007).

Structural connectivity matrix

The structural connectivity matrix was generated from the diffusion tensor imaging (DTI) data set provided by the WU-Minn Human Connectome Project (900 Subjects data release, 2015 Q4) (Van Essen et al., 2013). DTI data were acquired from 842 healthy subjects using a multishell diffusion scheme (diffusion sampling directions: 90, 90, 90; in-plane resolution and slice thickness: 1.25 mm; b-values: 1000, 2000, 3000 s/mm^2). The spatial normalization of the DTI data was conducted by the q-space diffeomorphic reconstruction method (Yeh and Tseng, 2011), which can obtain the spin distribution function in the MNI stereotactic space (resolution: 1 mm; sampling length ratio: 1.25). Averaging the spike density functions of all subjects, an atlas was created. Thus, the generalized q-sampling imaging (GQI) method (Yeh et al., 2010) was employed to detect the structural pathways. In this investigation the GQI was able to obtain 5,000 seeds in the whole-brain. Only the seeds corresponding to our co-altered nodes, obtained previously with the MCN approach, were employed to calculate the structural matrix by using the numbers of fiber tracts passing between two seeds normalized by the median length of the connecting paths.

Genetic co-expression connectivity matrix

The genetic co-expression connectivity matrix was generated from the microarray data sets provided by the Allen Human Brain Atlas (AHBA) Project (Hawrylycz et al., 2012). Complete normalized microarray data were acquired from six healthy human brains. The AHBA data set was processed using the workflow pipeline for relating brain-wide gene expression profile to neuroimaging results developed by Arnatkeviciute et al. (2019a). The processing steps were performed as implemented in the code available at github (https://github.com/BMHLab/AHBAprocessing) (for an in-depth discussion of the methodological steps, see also Arnatkeviciute et al. 2019a). To note, the differential stability measure (Hawrylycz et al., 2015) of gene filtering was used to derive gene patterns expressed consistently across all AHBA brains. Also, the 1,000 seeds parcellation (Schaefer et al., 2018) was applied to identify regions spatially corresponding to the MCN nodes. Only the seeds corresponding to our nodes were employed to generate the gene expression x node matrix.

4.2.5. Distribution of the nodes across canonical networks

To evaluate the impact of GM alterations on different functional large-scale networks, each co-altered node was assigned in data-driven manner to one of the 7 networks of the parcellation proposed by Yeo et al. (2011), who parceled the human cerebral cortex using resting-state fMRI data from 1000 healthy volunteers. Nodes falling in the basal nuclei and cerebellum were assigned to one of Yeo's networks using the striatal (Choi et al., 2012) and cerebellar (Buckner et al., 2011) parcellations, respectively. We tested if the spatial distribution of the alteration nodes across canonical networks was different from chance by creating 28 random GM nodes (corresponding to the number of the co-altered nodes of our network, see below), and repeating the procedure 1000 times. The significance of the numerosity of each network's nodes was tested against the resulting null distributions.

For each network, its network-betweenness – NB (Cauda et al., 2020a; Mancuso et al., 2020) was estimated as the ratio between the number of co-alteration edges connecting its nodes to the nodes belonging to other networks and the total number of edges incident upon its nodes. To test whether the NB of each network was significantly different from chance, the co-alteration network was randomized 1000 times using a Maslov-Sneppen algorithm (Maslov and Sneppen, 2002; Rubinov and Sporns, 2010); the NB of each network was recalculated in each iteration to obtain 7 NB distributions. A one-sample two-tailed t-test was

used to assess the significance of the 7 NBs (Cauda et al., 2020a).

4.3. Results

We included 42 published articles. Specifically, we analyzed meta-data coming from 45 VBM experiments, including 3,576 subjects (1,786 with diagnosis of ASD and 1790 healthy controls) and 244 coordinates of GM variation. The analysis was carried out in the TAL space. Original MNI coordinates were converted using the 'icbm2tal' algorithm (Lancaster et al., 2007) in order to correct the spatial disparity between coordinate (x-y-z) results (Laird et al., 2010), thus promoting accuracy of the meta-analytic synthesis (Muller et al., 2018; Tahmasian et al., 2019). For the systematic study selection see Fig. S4.1 and Table S4.1. For detailed information about the clinical and methodological characteristics of the selected meta-data, see also Table S4.2 and Table S4.3, respectively.

4.3.1. General characterization of co-alterations

Our meta-connectomic and data-driven approach reveals that it is possible to identify a quantifiable co-alteration network of GM abnormalities in ASD. On the grounds of the ALE meta-data, our ROI generation procedure derived 56 nodes (see also Table 4.1 for the morphometric location of nodes and their coordinates in TAL space). However, only 28 nodes exhibit statistically significant edges of co-alteration, encompassing cortical, basal nuclei and cerebellar regions. With regard to the anatomical distribution of the nodes, we observe that they can be found in both perceptual lower-level and multimodal regions and that some of them show a symmetric position across hemispheres. This is the case of the amygdala, precuneus and the cerebellar crus II.

Fig. 4.2 reports the whole co-alteration pattern showing 91 edges (45 interhemispheric and 46 intrahemispheric). Most of the edges involve fronto-cerebellar, limbic-striatal and fronto-parietal regions. A complex pattern of co-alteration was also detected for occipital and superior temporal nodes. Patel's κ values range from .79 of the right amygdala-parahippocampal-basal ganglia structures to the .23 of the edges of the middle occipital-inferior frontal regions. High κ values are also associated to the left precuneus (PCUN_L), lingual gyrus (LG_L) and posterior cingulate cortex (PCC_L), as well as to the right orbitofrontal gyrus (OFG_R), temporopolar pole (BA_38_R) and posterior cerebellar lobe (Crus2_R) (see Table 4.2 for the κ values graph).

Table 4.1. Brain areas (nodes) of the gray matter morphometric co-alteration network. Node labeling, morphometric location (Talairach Daemon Labels) and Talairach coordinates were expressed for both co-altered and non co-altered nodes.

Node ID	Node label	Anatomical region (Brodmann area)	Hemisphere	Talairach			Co-altered
				x	y	z	
1	Crus2_L	Crus II (cerebellum)	Left	-44	-58	-44	Yes
2	Crus2_R	Crus II (cerebellum)	Right	48	-58	-44	Yes
3	ML9	Medial lobule IX (cerebellum)	Left	-4	-56	-42	No
4	FG	Fusiform gyrus (BA 37)	Right	26	-2	-38	Yes
5	Crus1	Crus I (cerebellum)	Right	48	-54	-32	No
6	Crus1	Crus I (cerebellum)	Left	-44	-40	-32	Yes
7	BA38	Temporopolar cortex (BA 38)	Right	46	12	-30	Yes
8	BA28	Parahippocampal gyrus (BA 28)	Right	26	-12	-28	Yes
9	Unc	Uncus (BA 20)	Right	28	-14	-26	No
10	Dec	Declive (cerebellum)	Right	24	-84	-22	No
11	Amy_R	Amygdala	Right	24	-8	-22	Yes
12	OG	Orbital gyrus (BA 11)	Left	-4	40	-22	No
13	IFG	Inferior frontal gyrus (BA 11)	Left	-12	36	-20	No
14	RG	Rectal gyrus (BA 11)	Left	-6	40	-20	No
15	PHG	Parahippocampal gyrus (BA 34)	Right	20	-12	-14	Yes
16	Hip	Hippocampus	Left	-18	-6	-14	No
17	BA10	Superior frontal gyrus (BA 10)	Left	-10	56	-12	No
18	OFG_R	Orbitofrontal gyrus (BA 10)	Right	6	58	-12	Yes
19	BA37	Fusiform gyrus (BA 37)	Right	48	-60	-10	No
20	MTG	Middle temporal gyrus (BA 37)	Right	60	-48	-10	No
21	Amy_L	Amygdala	Left	-20	-4	-10	Yes
22	BA47	Inferior frontal gyrus (BA 47)	Left	-30	12	-10	No
23	MFG_R	Medial frontal gyrus (BA 10)	Right	6	58	-10	No
24	BA17	Inferior occipital gyrus (BA 17)	Right	16	-88	-8	No
25	Pu	Putamen	Left	-20	4	-8	Yes
26	OFG_L	Middle orbital gyrus (BA 10)	Left	-32	52	-8	No
27	IOG	Inferior occipital gyrus (BA 18)	Right	44	-72	-6	No
28	Cd	Caudate tail	Right	38	-24	-6	Yes
29	BA11	Middle frontal gyrus (BA 11)	Left	-34	52	-6	Yes
30	Cl	Claustrum	Right	38	-26	-4	No
31	AI_R	Anterior insula (BA 13)	Right	40	-26	-4	No
32	STG	Superior temporal gyrus (BA 22)	Right	62	-24	-2	Yes
33	ACC_L	Anterior cingulate cortex (BA 10)	Left	-8	54	-2	No
34	AI_L	Anterior insula (BA 13)	Left	-40	22	0	Yes
35	BA22	Middle temporal gyrus (BA 22)	Right	64	-34	2	No
36	IFG_Tri	Inferior frontal gyrus (BA 47)	Left	-42	22	2	No
37	IFG	Inferior frontal gyrus (BA 45)	Left	-46	28	2	Yes
38	LG	Lingual gyrus (BA 18)	Left	0	-72	8	Yes

Node ID	Node label	Anatomical region (Brodmann area)	Hemisphere	Talairach			Co-altered
				x	y	z	
39	PCC	Posterior cingulate cortex (BA 30)	Left	0	-62	10	Yes
40	Pulv	Pulvinar (thalamus)	Right	12	-22	10	No
41	MDN	Medial dorsal nucleus (thalamus)	Right	2	-16	10	No
42	MFG_L	Middle frontal gyrus (BA 10)	Left	-26	46	10	Yes
43	BA18	Middle occipital gyrus (BA 18)	Left	-28	-92	12	No
44	BA9	Medial frontal gyrus (BA 9)	Left	-16	44	20	Yes
45	IPL	Inferior parietal lobule (BA 40)	Left	-50	-28	22	No
46	SM	Supramarginal gyrus (BA 40)	Left	-54	-42	24	Yes
47	vACC	Ventral anterior cingulate (BA 24)	Left	-2	-4	26	Yes
48	PCG	Precentral gyrus (BA 6)	Left	-48	0	28	No
49	PCUN_R	Precuneus (BA 7)	Right	6	-64	36	Yes
50	BA6	Medial frontal gyrus (BA 6)	Left	-4	34	36	No
51	SFG_R	Superior frontal gyrus (BA 9)	Right	24	46	36	Yes
52	MOG	Middle occipital gyrus (BA 19)	Left	-28	-68	38	Yes
53	PCUN_L	Precuneus (BA 7)	Left	0	-62	38	Yes
54	BA8	Superior medial frontal gyrus (BA 8)	Left	-10	32	38	Yes
55	ACC_R	Anterior cingulate cortex (BA 32)	Right	8	8	40	No
56	SFG_L	Superior frontal gyrus (BA 9)	Left	-4	36	42	Yes

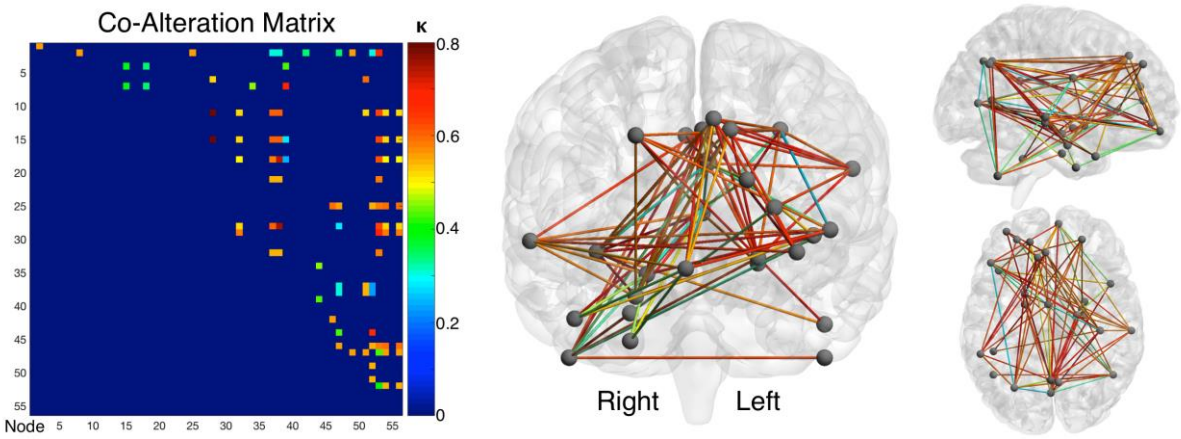

Figure 4.2. The gray matter morphometric co-alteration network of autism spectrum disorder. Both co-alteration matrix and brain network related to gray matter abnormalities are shown. Edge colors from blue to red mean increasing Patel's κ values (i.e., increasing co-alteration probabilities). Unconnected nodes are not reported. The images were generated by the BrainNet application (Xia et al., 2013).

Table 4.2. Edge co-alteration strength between co-altered nodes (Patel's k). Node labeling, Talairach coordinates and Yeo's network classification were expressed for each co-altered node.

Node	Talairach			Yeo's Network	Patel's k	Node	Talairach			Yeo's Network
	x	y	z				x	y	z	
Amy_R	24	-8	-22	Limbic	0.790	Cd_R	38	-24	-6	FPN
PHG_R	20	-12	-14	Limbic	0.790	Cd_R	38	-24	-6	FPN
Cd_R	38	-24	-6	FPN	0.755	LG_L	0	-72	8	Visual
OFG_R	6	58	-12	DMN	0.742	LG_L	0	-72	8	Visual
BA_11_L	-34	52	-6	DMN	0.685	PCUN_L	0	-62	38	DMN
BA_38_R	46	12	-30	DMN	0.669	PCC_L	0	-62	10	DMN
Crus2_R	48	-58	-44	FPN	0.669	PCUN_L	0	-62	38	DMN
BA_9_L	-16	44	20	DMN	0.652	MOG_L	-28	-68	38	Visual
Amy_R	24	-8	-22	Limbic	0.634	PCUN_L	0	-62	38	DMN
PHG_R	20	-12	-14	Limbic	0.634	PCUN_L	0	-62	38	DMN
Cd_R	38	-24	-6	FPN	0.634	PCUN_L	0	-62	38	DMN
OFG_R	6	58	-12	DMN	0.615	PCUN_L	0	-62	38	DMN
Amy_R	24	-8	-22	Limbic	0.602	IFG_L	-46	28	2	FPN
PHG_R	20	-12	-14	Limbic	0.602	IFG_L	-46	28	2	FPN
Cd_R	38	-24	-6	FPN	0.602	IFG_L	-46	28	2	FPN
Amy_R	24	-8	-22	Limbic	0.602	LG_L	0	-72	8	Visual
PHG_R	20	-12	-14	Limbic	0.602	LG_L	0	-72	8	Visual
Pu_L	-20	4	-8	SN/VAN	0.600	SM_L	-54	-42	24	SN/VAN
Crus1_L	-44	-40	-32	SN/VAN	0.600	SFG_R	24	46	36	FPN
Pu_L	-20	4	-8	SN/VAN	0.600	BA_8_L	-10	32	38	FPN
SM_L	-54	-42	24	SN/VAN	0.600	BA_8_L	-10	32	38	FPN
Pu_L	-20	4	-8	SN/VAN	0.600	SFG_L	-4	36	42	DMN
SM_L	-54	-42	24	SN/VAN	0.600	SFG_L	-4	36	42	DMN
OFG_R	6	58	-12	DMN	0.581	IFG_L	-46	28	2	FPN
BA_11_L	-34	52	-6	DMN	0.580	STG_R	62	-24	-2	SMN
Amy_L	-20	-4	-10	Limbic	0.580	PCUN_L	0	-62	38	DMN
Pu_L	-20	4	-8	SN/VAN	0.580	PCUN_L	0	-62	38	DMN
STG_R	62	-24	-2	SMN	0.580	PCUN_L	0	-62	38	DMN
SM_L	-54	-42	24	SN/VAN	0.580	PCUN_L	0	-62	38	DMN
BA_11_L	-34	52	-6	DMN	0.580	BA_8_L	-10	32	38	FPN
BA_11_L	-34	52	-6	DMN	0.580	SFG_L	-4	36	42	DMN
Crus2_L	-44	-58	-44	FPN	0.560	Crus2_R	48	-58	-44	DMN
Crus2_R	48	-58	-44	DMN	0.560	BA_28_R	26	-12	-28	Limbic
Crus2_R	48	-58	-44	DMN	0.560	Pu_L	-20	4	-8	SN/VAN
MFG_L	-26	46	10	DMN	0.560	SM_L	-54	-42	24	SN/VAN
Pu_L	-20	4	-8	SN/VAN	0.560	vACC_L	-2	-4	26	SN/VAN
SM_L	-54	-42	24	SN/VAN	0.560	vACC_L	-2	-4	26	SN/VAN

Node	Talairach			Yeo's Network	Patel's k	Node	Talairach			Yeo's Network
	x	y	z				x	y	z	
Crus2_R	48	-58	-44	DMN	0.560	PCUN_R	6	-64	36	DMN
vACC_L	-2	-4	26	SN/VAN	0.560	PCUN_R	6	-64	36	DMN
vACC_L	-2	-4	26	SN/VAN	0.560	SFG_R	24	46	36	FPN
vACC_L	-2	-4	26	SN/VAN	0.560	BA_8_L	-10	32	38	FPN
vACC_L	-2	-4	26	SN/VAN	0.560	SFG_L	-4	36	42	DMN
Amy_L	-20	-4	-10	Limbic	0.538	IFG_L	-46	28	2	FPN
STG_R	62	-24	-2	SMN	0.538	IFG_L	-46	28	2	FPN
Amy_L	-20	-4	-10	Limbic	0.538	LG_L	0	-72	8	Visual
STG_R	62	-24	-2	SMN	0.538	LG_L	0	-72	8	Visual
IFG_L	-46	28	2	FPN	0.538	SFG_R	24	46	36	FPN
LG_L	0	-72	8	Visual	0.538	SFG_R	24	46	36	FPN
Pu_L	-20	4	-8	SN/VAN	0.538	MOG_L	-28	-68	38	Visual
SM_L	-54	-42	24	SN/VAN	0.538	MOG_L	-28	-68	38	Visual
PCUN_R	6	-64	36	DMN	0.538	MOG_L	-28	-68	38	Visual
SFG_R	24	46	36	FPN	0.538	MOG_L	-28	-68	38	Visual
MOG_L	-28	-68	38	Visual	0.538	BA_8_L	-10	32	38	FPN
MOG_L	-28	-68	38	Visual	0.538	SFG_L	-4	36	42	DMN
Crus1_L	-44	-40	-32	SN/VAN	0.515	Cd_R	38	-24	-6	FPN
Amy_R	24	-8	-22	Limbic	0.515	STG_R	62	-24	-2	SMN
PHG_R	20	-12	-14	Limbic	0.515	STG_R	62	-24	-2	SMN
Cd_R	38	-24	-6	FPN	0.515	STG_R	62	-24	-2	SMN
Amy_R	24	-8	-22	Limbic	0.515	SFG_R	24	46	36	FPN
Amy_R	24	-8	-22	Limbic	0.515	BA_8_L	-10	32	38	FPN
PHG_R	20	-12	-14	Limbic	0.515	BA_8_L	-10	32	38	FPN
Cd_R	38	-24	-6	FPN	0.515	BA_8_L	-10	32	38	FPN
Amy_R	24	-8	-22	Limbic	0.515	SFG_L	-4	36	42	DMN
PHG_R	20	-12	-14	Limbic	0.515	SFG_L	-4	36	42	DMN
Cd_R	38	-24	-6	FPN	0.515	SFG_L	-4	36	42	DMN
OFG_R	6	58	-12	DMN	0.490	STG_R	62	-24	-2	SMN
OFG_R	6	58	-12	DMN	0.490	BA_8_L	-10	32	38	FPN
OFG_R	6	58	-12	DMN	0.490	SFG_L	-4	36	42	DMN
BA_38_R	46	12	-30	DMN	0.461	AI_L	-40	22	0	SN/VAN
AI_L	-40	22	0	SN/VAN	0.461	BA_9_L	-16	44	20	DMN
FFG_R	26	-2	-38	Limbic	0.435	PCC_L	0	-62	10	DMN
PCC_L	0	-62	10	DMN	0.435	BA_9_L	-16	44	20	DMN
BA_9_L	-16	44	20	DMN	0.435	vACC_L	-2	-4	26	SN/VAN
vACC_L	-2	-4	26	SN/VAN	0.435	PCUN_L	0	-62	38	DMN
MOG_L	-28	-68	38	Visual	0.408	PCUN_L	0	-62	38	DMN
FFG_R	26	-2	-38	Limbic	0.379	PHG_R	20	-12	-14	Limbic
BA_38_R	46	12	-30	DMN	0.379	PHG_R	20	-12	-14	Limbic
FFG_R	26	-2	-38	Limbic	0.348	OFG_R	6	58	-12	DMN
BA_38_R	46	12	-30	DMN	0.348	OFG_R	6	58	-12	DMN

Node	Talairach			Yeo's Network	Patel's k	Node	Talairach			Yeo's Network
	x	y	z				x	y	z	
Crus2_R	48	-58	-44	DMN	0.342	MFG_L	-26	46	10	DMN
Crus2_R	48	-58	-44	DMN	0.342	vACC_L	-2	-4	26	SN/VAN
Crus2_R	48	-58	-44	DMN	0.311	IFG_L	-46	28	2	FPN
Crus2_R	48	-58	-44	DMN	0.311	LG_L	0	-72	8	Visual
IFG_L	-46	28	2	FPN	0.311	vACC_L	-2	-4	26	SN/VAN
LG_L	0	-72	8	Visual	0.311	vACC_L	-2	-4	26	SN/VAN
Crus2_R	48	-58	-44	DMN	0.311	MOG_L	-28	-68	38	Visual
PHG_R	20	-12	-14	Limbic	0.277	PCC_L	0	-62	10	DMN
Cd_R	38	-24	-6	FPN	0.277	vACC_L	-2	-4	26	SN/VAN
OFG_R	6	58	-12	DMN	0.242	PCC_L	0	-62	10	DMN
IFG_L	-46	28	2	FPN	0.235	MOG_L	-28	-68	38	Visual
LG_L	0	-72	8	Visual	0.235	MOG_L	-28	-68	38	Visual

4.3.2. Level of the centrality of nodes

Fig. 4.3 illustrates the level of topological position of the nodes. The co-altered nodes are represented in different colors and sizes according to their values of degree, betweenness and closeness centrality. The PCUN_L and ventral anterior cingulate cortex (vACC_L) show the highest values of degree (12 edges), followed by the left middle occipital gyrus (MOG_L, 11 edges) and right Crus2, tail of caudate (Cd_R), left inferior frontal gyrus (IFG_L), LG_L and right parahippocampal area (PHG_R) (10 edges). By contrast, the left anterior insular and cerebellar regions (i.e., AI_L and Crus2_L) exhibit the lowest values of degree. Values of closeness range from .34 to .63, with the highest values associated with the PCUN_L, followed by the vACC_L, MOG_L, IFG_L, Cd_R and PHG_R. Also for this measure, the AI_L and Crus2_L show the lowest values. Relative to the betweenness, the Crus2_R reports the highest value, followed, in order, by the PCUN_L, PHG_R, vACC_L, MOG_L and OFG_R.

Next, we investigated in detail the pathological *hubness* profile of the regions. To do so, we identified the nodes reporting the highest level of centrality (i.e., one standard deviation above the mean) across all three metrics. The analysis reveals a central network position for the PCUN_L [TAL x = 0; y = -62; z = 38], vACC_L [TAL x = -2; y = -4; z = 26] and MOG_L [TAL x = -28; y = -68; z = 38]. For a graphical representation of results and node-specific values of degree, betweenness and closeness of each node of the MCN, see Fig. 4.4.

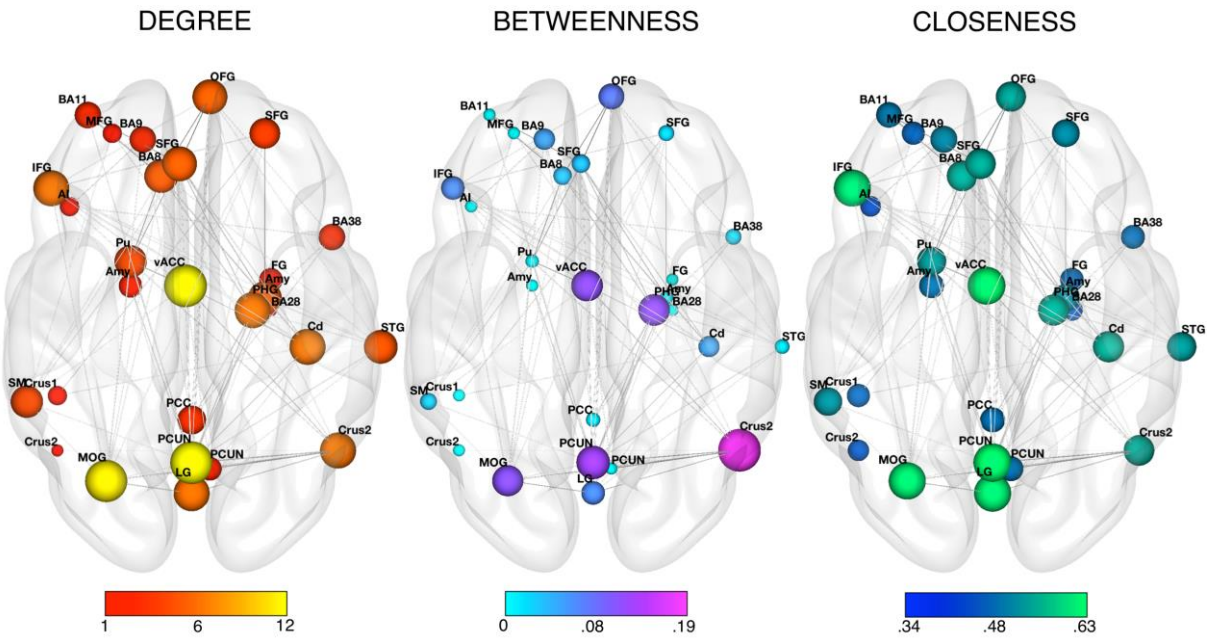

Figure 4.3. Superposition of the topological analysis of the gray matter morphometric co-alteration network (MCN) on 3-D brain axial slices. Left template: Degree centrality values of the MCN in autism spectrum disorder. Central template: Betweenness centrality values of the MCN in autism spectrum disorder. Right template: Closeness centrality values of the MCN in autism spectrum disorder. The colors and dimensions of the nodes indicate their network centrality (bigger node: higher centrality; from red to yellow, from light blue to purple and from dark blue to green: from lower to higher values of degree, betweenness and closeness centrality, respectively). Slices are shown in neurological convention (i.e., right is right, left is left).

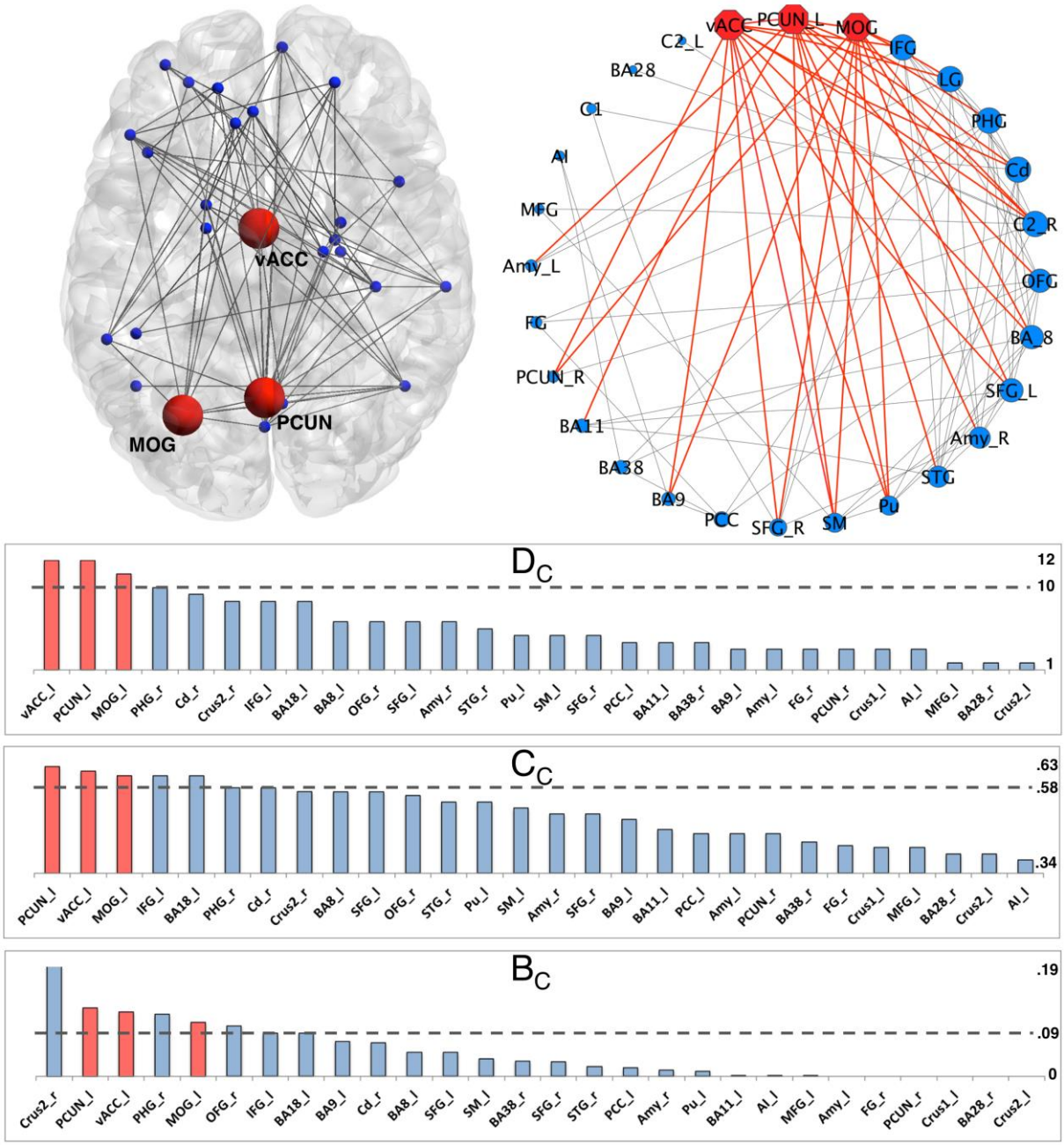

Figure 4.4. Specific centrality values of degree (D_C), closeness (C_C) and betweenness (B_C) of each of the 28 co-altered nodes of the morphometric co-alteration network in ASD. The red nodes and bars mark the brain areas that report the highest level of centrality across all three metrics (i.e., > one standard deviation of the mean). The figure also illustrates the anatomical position of the brain pathological hubs and their co-alterations using the circular layout algorithm of Cytoscape software application (https://cytoscape.org/).

4.3.3. Core sub-graph

Since highly interconnected nodes characterize the MCN of ASD, we investigated the possibility of identifying the most central sub-graph and its hierarchical components. The implementation of the k-core decomposition algorithm allowed us to detect a core nucleus composed of 15 nodes and 57 edges using a k degree = 6, including frontal (i.e., OFG_R, left superior, medial and inferior frontal gyri), subcortical (vACC_L, PHG_R, Cd_R, left putamen and right amygdala), occipital (LG_L and MOG_L), temporo-parietal (PCUN_L, right superior temporal gyrus and left supramarginal gyrus) and cerebellar (Crus2_R) areas (Fig. 4.5).

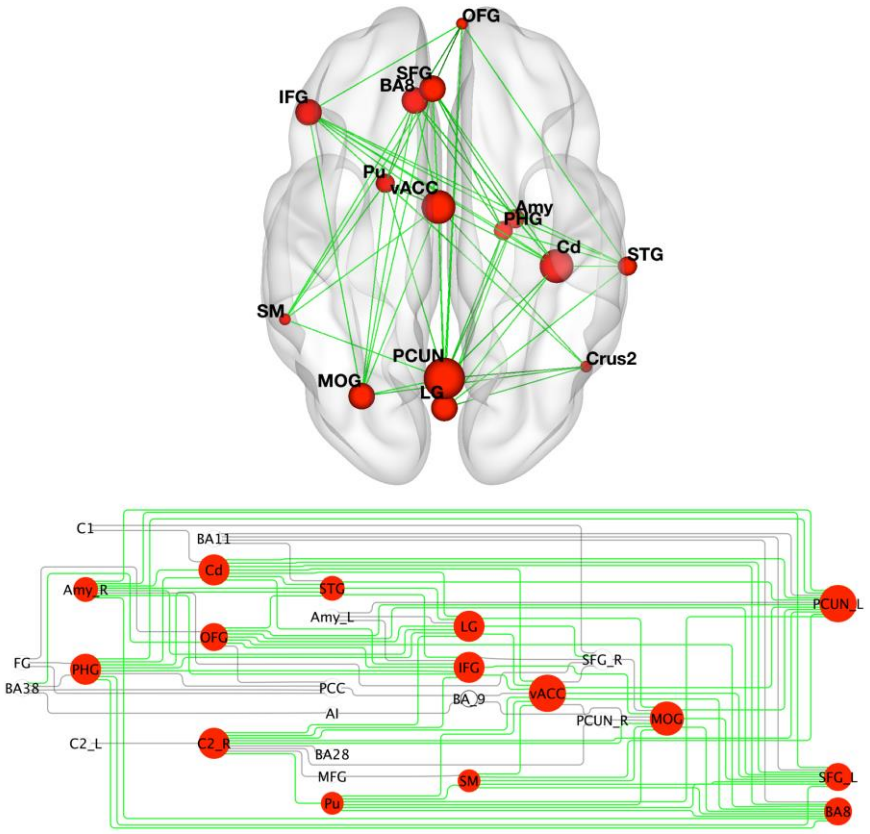

Figure 4.5. Brain network clustering results using the k-core decomposition algorithm. Upper panel: Superposition of the k-core values of the morphometric co-alteration network on 3-D brain template. Bottom panel: Graphical illustration of the clustering values using the hierarchical layout algorithm of Cytoscape software application (https://cytoscape.org/). The colors and dimensions of the nodes indicate their network centrality (red node: brain areas with highest hierarchy; bigger node: higher degree centrality).

4.3.4. Correlation with brain connectivity profiles

The Mantel test employed to investigate whether or not GM co-alterations overlap the structural or genetic connectivity profiles showed that the ASD co-alterations are significantly correlated with the anatomical connectivity (r = 0.14, $p < 0.027$). Finally, the comparison with the genetic co-expression connectivity matrix reports non-significant results at $p = 0.05$.

4.3.5. Distribution of the nodes across canonical networks

The parcellation search revealed the presence of at least one node for six out of seven canonical networks, namely the default mode network (DMN), frontoparietal network (FPN), salience/ventral attentional network (SN/VAN), limbic network, visual network and the sensorimotor network (SMN). In particular, the DMN reports the highest number of co-altered nodes (10/28, 35.7% of the total) mainly located in fronto-parietal areas. The number of nodes of the DMN was greater than a random null model ($p = 0.06$). By contrast, the number of nodes related to the Limbic, SN/VAN FPN and Visual networks was not significantly different from chance. The SMN network showed only a single node located in the right STG (Fig. 4.6 left panel), while in the null model there were significantly more nodes ($p = 0.04$). The dorsal attentional network (DAN) had no co-altered nodes, which was significant when compared to the random extraction ($p = 0.02$). It is important to clarify that these results do not indicate that the functionally defined SMN and DAN regions are not altered in subjects with ASD, but rather that their alterations are not associated with that in other nodes. With regard to the 91 edges, only 17 edges connect nodes of the same functional network, whereas 81.6% of them connect nodes belonging to different networks (Fig. 4.6 right panel). Table 4.3 indicates the NB of each one of the 7 networks identified by Yeo et al. (2011).

With the exception of the DAN, which is not represented by any node of alteration, each one of the canonical networks have a very high NB, that is, the edges of co-alteration often connect nodes that are placed in two different functional networks rather than in the same one. The DMN is the more co-altered with itself, while the nodes belonging to the SMN only connect with nodes of other networks. However, the Maslov-Sneppen null model (Cauda et al., 2020a; Maslov and Sneppen, 2002) indicates that, given our starting nodes, only the DMN-NB is significantly higher than chance ($p < 0.001$). All the other networks' NB, SMN included, are not different from the null model. The apparent contradiction of having the

DMN-NB as the lowest one of the 7 canonical networks, but also significantly higher than chance, is probably due to the fact that the DMN is the most represented network in terms nodes of alteration. Thus, the number of within-DMN co-alteration edges is obviously high (Fig. 4.6 bottom panel); however, given the node distribution across the networks, this is not a surprising result, as it could be expected to be even higher.

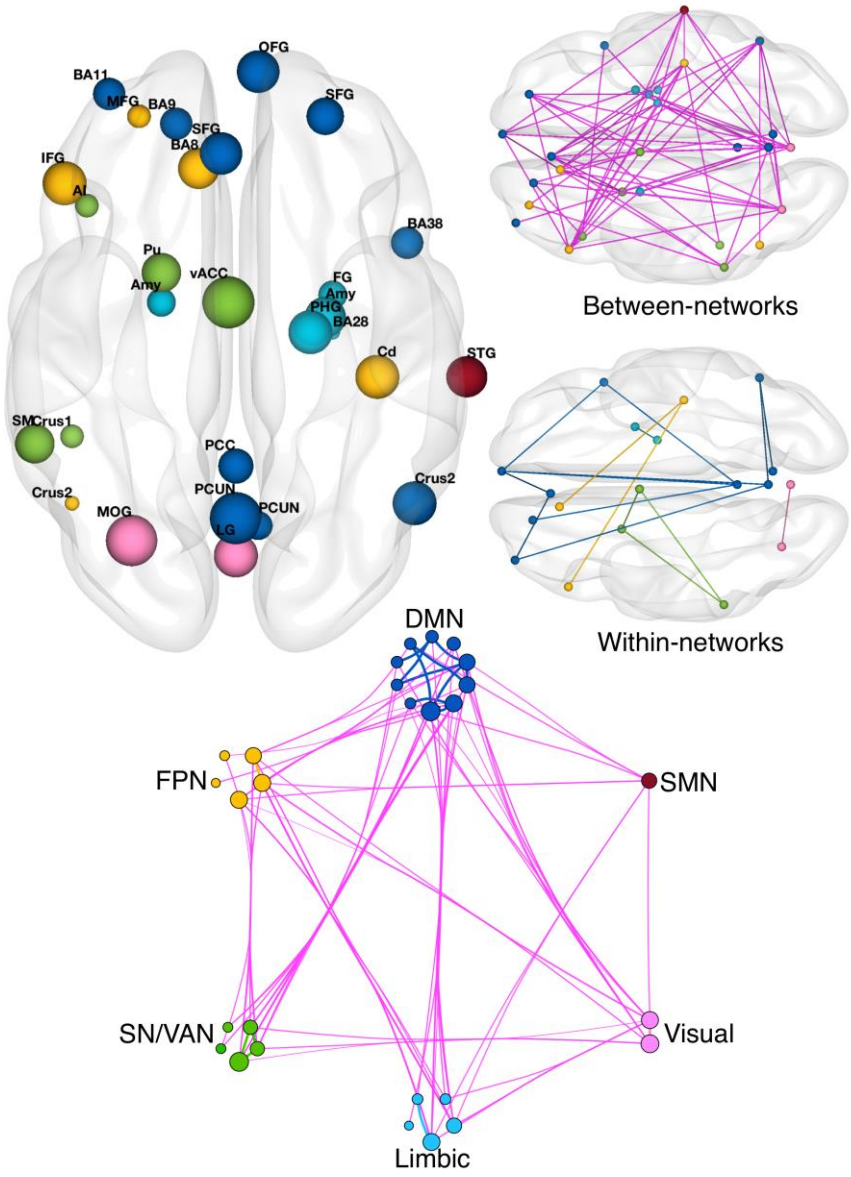

Figure 4.6. Brain templates illustrating the anatomical location of the co-altered nodes within the main human large-scale functional networks (left panel) and the between/within network distribution of the co-alterations (right and bottom panels).

DMN, default mode network; FPN, frontoparietal network; SN/VAN, salience/ventral attentional network; Limbic, limbic network; Visual, visual network; SMN, sensorimotor network.

Table 4.3. The network-betweenness of each one of the Yeo et al. (2011) networks.

Canonical Network	Network Betweenness
DMN	0.82
FPN	0.93
SN/VAN	0.89
DAN	N.A.
Limbic	0.96
Visual	0.95
SMN	1

DMN, default mode network; FPN, frontoparietal network; SN/VAN, salience/ventral attentional network; DAN, dorsal attentional network; Limbic, limbic network; Visual, visual network; SMN, sensorimotor network; N.A., data not associated.

4.4. Discussion

To the best of our knowledge, this is the first meta-analytic study that mapped the unknown GM topology in individuals with ASD, using the canonical ALE framework as priors for an unbiased and connectome-wide analysis. Our findings provide evidence that neuroanatomical variations in ASD tend to form a complex network of co-alteration, encompassing multiple defined cortical, subcortical and cerebellar sites. Within this co-alteration network, certain higher-order areas (i.e., vACC, PCUN and MOG) exhibit a substantial hierarchical profile, and thereby they are conceivable as pathological hubs. Further, we reveal that the organization of co-alterations reflects a biologically plausible distribution, mirroring in part the constraints of brain structural connectivity. Altogether, these results extend previous literature reporting morphometric variations in the ASD pathophysiology, emphasizing the necessity of considering this spectrum of disorders as a network-like dysfunction of spatially distributed GM sites.

Significantly, our findings demonstrate that regional GM abnormalities are not independent in ASD. Instead, multiple neural subpopulations report a morphometric change that statistically co-occurs with an alteration in other brain sites. This result is consistent with recent neuroimaging literature suggesting a structural signature of brain architecture in other psychiatric disorders, such as schizophrenia (Cauda et al., 2020a; Shafiei et al., 2020; van den Heuvel et al., 2010), major depression (Korgaonkar et al., 2014; Zheng et al., 2019), obsessive-compulsive disorder (Cao et al., 2020; Reess et al., 2016) and bipolar disorder

(Ajilore et al., 2015; Collin et al., 2016; Fernandes et al., 2019). Our analysis reveals robust co-alterations between a distinct set of regions that have been consistently reported to be altered and associated with clinical manifestations in previous MRI-based investigations in ASD. However, different from classical anatomical neuroimaging techniques such as VBM or cortical thickness, which do not assess any kind of topological relationship between regions (Ashburner and Friston, 2001), our graphical analysis was able to consider neuroanatomical abnormalities (nodes) and their statistical mutual relationship (edges) as a network unit (Cauda et al., 2018b). Therefore, our results can be understood in the context of a spatially distributed model rather than of isolated neural loci.

Anatomical abnormalities have been observed in different cerebral systems, encompassing a set of multimodal, cerebellar, perceptual and limbic nodes. This large-scale distribution and its conjoint patterns of alteration might be considered as a clinical implication of the phenotypic heterogeneity of ASD (Wylie et al., 2020) and might also derive from an abnormal neural development (Frith, 2004; Kim et al., 2017a; Neniskyte and Gross, 2017; Thomas et al., 2016) or compensatory responses (Fornito et al., 2015; Zhou et al., 2012).

The present findings, along with recent proposals (Balardin et al., 2015; Ecker et al., 2010; Geschwind and Levitt, 2007; Minshew and Williams, 2007; Picci et al., 2016), are largely consistent with the notion of ASD as a syndrome due to perturbations of different cytoarchitectonic and neurocognitive systems. According to this view, a reasonable interpretation of our results is that topological organization of interregional GM co-alterations may arise from volumetric aberrations of the regional-level morphology. This hypothesis accords well with the experimental evidence of Ecker et al. (2013), who, performing measures of cortical separation distances on a sample of adults with ASD, reported an abnormal architecture of GM showing reduced cortico-cortical connectivity and low intrinsic wiring costs of the cortex. Interestingly, these authors observed low intrinsic wiring costs in the fronto-posterior areas that are also key components of our MCN, including the left precuneus (BA 7), right temporal pole (BA 22), bilateral orbitofrontal and dorsolateral prefrontal cortices (BA 10, BA 11).

Moreover, our analysis confirms and extends previous results of altered anatomical covariance patterns as a key mechanism in the ASD condition. For example, in the seminal paper of Zielinski et al. (2012), the authors found distributed abnormal components in GM structure using seed-ROIs anchored in the fronto-insular and posterior cingulate cortices. In

line with their findings, our data show a non-negligible overlap with pathological covariance sites in ASD. Morphometric components with reduced covariance are clearly present and co-altered in our MCN; some of these are *core* units within the co-alteration pattern. This is the case with regard to the left precuneus, right STG, left supramarginal area, left vACC, left IFG, right MFG, right OFG and the left SFG. Similar results obtained with the same seeds were also reported by Palande et al. (2017), who carried out a graph correlation analysis combined with a statistical inference approach in addition to the anatomical covariance analysis. This general overlap is not surprising, as significant correlations between the MCN and anatomical covariance has been recently evidenced by our group (Cauda et al., 2018a). However, we note that the present methodology differs from the anatomical covariance approach because it enables the examination, in a whole-brain and data-driven manner, of multiple large-scale network affected architectures, thus overcoming the limited resolution of network-level effects given by prior ROI correlations (Evans, 2013; Palande et al., 2017; Tatu et al., 2018; Zielinski et al., 2012).

Another important issue addressed by this study concerns the identification of brain sites that have a pivotal position in the MCN of ASD. By combining three different measures of node centrality (i.e., degree, closeness and betweenness), we observe that a subset of areas influences significantly the architecture of co-alterations; for this reason, these multimodal areas can be conceived as pathological hubs (i.e., they are topologically central in the co-alteration network) (Cauda et al., 2018a; Cauda et al., 2018b; Manuello et al., 2018). One of those regions is the left precuneus, a component of the medial posterior parietal cortex, which has been frequently associated with social reasoning and self-reflection (Patriquin et al., 2016). The precuneus has also been reported to be involved in a range of integrated tasks, including awareness information processing, visuospatial imagery, mnemonic retrieval and voluntary attention (Cavanna, 2007; Cavanna and Trimble, 2006; Zhang and Li, 2012). From a clinical point of view, its morphometric alterations and decreased functional connectivity have been linked to autistic symptom severity (Cheng et al., 2017; Fang et al., 2020; Lynch et al., 2013), as well as to dysfunction in mentalizing processes (Wang et al., 2007), attention orienting (Fitzgerald et al., 2015) and empathy (Schulte-Rüther et al., 2011) in different ASD cohorts.

The second pathological hub is the left vACC. Reduced activation of this region has been reported in patients with ASD while playing a social-exchange game (Chiu et al., 2008).

Authors have therefore associated this reduced cingulate response with ASD social impairment. Furthermore, it has been observed that developmental differences in the limbic nodes as well as in other integrative regions such as the cingulate cortex might produce a cascading effect on brain areas mediating social perception (Apps et al., 2013; Baron-Cohen et al., 2000; Rolls, 2019). These findings are in agreement with the pattern of our MCN, and with research finding alterations in the activity of the cingulate cortex in individuals with ASD, especially with regard to a reduced glucose metabolism (Haznedar et al., 2000), functional connectivity (Zhou et al., 2016) and disrupted white matter pathways (Barnea-Goraly et al., 2004). It therefore should not be surprising that this region may be significantly co-altered in ASD, given the essential involvement of the vACC in integrative circuits that are supposed to help the regulation of cognitive, executive and emotional processes (for a review see Stevens et al., 2011). Interestingly, the cingulate cortex and the precuneus were proposed to be part of a whole-brain system of areas involved in joint attention, which disruption is an early and characteristic symptom of ASD (Mundy, 2018).

The third hub node identified in the analysis is the left MOG, a second-order region implicated in the integration of multisensory stimuli (Kravitz et al., 2011). It has been recently suggested that microstructural dendritic dispersion of this site is associated with abnormal visual processing in ASD and also with social interaction dysfunction because of its long-range disconnections (Matsuoka et al., 2020). It is worth noting that the central involvement of the MOG in the MCN may indicate an anatomical damage, which can be typical of the ASD condition. As recently reported by VBM transdiagnostic investigations (Cauda et al., 2019b; Liloia et al., 2018), the left portion of the occipital lobe, including BA 18/19, is usually spared by most psychiatric and neurological disorders, and is thereby considered a region with *low structural alteration variety*. Therefore, the present finding further supports the importance of abnormalities at the perceptual level in ASD, as well as of their fronto-posterior patterns. Those abnormalities have been hypothesized to be the basis of sensory aberrations and of failure in socio-communicative integration (Courchesne and Pierce, 2005; Hadjikhani et al., 2004; Lombardo et al., 2019; Marco et al., 2011).

As the aforementioned nodes are also network hubs in the healthy connectome (van den Heuvel and Sporns, 2013), our results are consistent with a recent line of research showing that morphometric damage of brain disorders preferentially accumulates in areas with greater topological value (Crossley et al., 2014), probably due to their long-range connections (Cauda

et al., 2020a) and related high metabolic cost (Arnatkeviciute et al., 2019b; Liang et al., 2013).

We found that the pathological hubs are selectively located in the left hemisphere. Interestingly, this finding is in line with both experimental and theoretical proposals suggesting a typical leftward asymmetry and volumetric reduction in ASD, particularly in cognitive and linguistic-related areas (De Fossé et al., 2004; Floris et al., 2013; Floris et al., 2020; Kong et al., 2020; Mellet et al., 2014; Postema et al., 2019; Prior and Bradshaw, 1979). Moreover, a recent transdiagnostic study from our group (Cauda et al., 2020a) found that the regional mean physical distance of co-alteration is higher in the left hemisphere compared to the right one. In other words, the GM decreases of the left hemisphere tend to show long-range co-alterations across many psychiatric and neurological diseases. The concurrent existence of GM decreases and GM increases, which might be taken as evidence of functional and structural failures and compensations, has shown to be more lateralized in the left hemisphere in a range of psychiatric and neurodevelopmental diseases, including autism (Mancuso et al., 2020). Therefore, our current findings of ASD hubs mainly located in left-brain sites suggest a left hemisphere dominance in the co-alteration process.

However, this is not to say that the contribution to the MCN of the right hemisphere is negligible. In fact, there is also an important involvement of right-lateralized sites in the MCN, encompassing the cerebellar crus II, caudate, amygdala, STG and orbitofrontal gyrus. These structures and their dysfunctional connections have attracted much attention in ASD research and have been associated with specific features of social, emotional and motor dysfunctions of the disorder (Bachevalier and Loveland, 2006; D'Mello et al., 2016; D'Mello and Stoodley, 2015; Gibbard et al., 2018; Girgis et al., 2007; Hardan et al., 2006; Qiu et al., 2010; Turner et al., 2006).

To further characterize the topological structure of the MCN and to go beyond the peculiarities of the specific hub nodes, we employed k-core decomposition. Our network clustering analysis suggests that the core hierarchy in ASD contains regions predominantly associated with the highest values of node centrality. In particular, several components are higher-order associative areas, namely left precuneus, left superior and medial frontal gyri, left anterior cingulate cortex, right parahippocampus, along with visual regions such as lingual and middle occipital gyri (Fig. 4.5). Interestingly, the aforementioned components were recently categorized as units of high hierarchy within large-scale brain networks (Lahav

et al., 2016) because they essentially support the structural organization of inter-connections and, thereby, can efficiently allow data integration and monitor cognitive processing (Collin et al., 2014; Hagmann et al., 2008). Thus, our findings support the notion that the integration and monitoring of information might be disrupted in ASD, especially with regard to the social and affective domains associated with the DMN (Buckner and DiNicola, 2019; Padmanabhan et al., 2017), whose nodes appear to be the central components within the MCN of ASD.

Overall, our findings emphasize the importance of the DMN in ASD. In fact, many co-altered nodes have been located in this network, indicating its relevance in the system of reciprocal GM modifications produced by ASD. This is also pointed out by the combined centrality measures and the k-core that highlight brain regions associated with the DMN.

Also, the DMN is the only network whose co-alterations are more likely to be between its nodes and those of other networks than within itself (Fig. 4.6). This means that the numerous alterations occurring in the DMN also co-occur with many others in the other networks, suggesting a pivotal role of the DMN in the spatial distribution of GM abnormalities in ASD. Despite the fact that direct associations between functional covariation and underlying morphometric substrates remains an open question in autism research (Uddin et al., 2013), the peculiar topology related to the DMN co-alterations might suggest an atypical morphometric substrate for aberrant between-network functional connectivity, which was found decreased in different age-stratified cohorts of individuals with ASD compared with neurotypical controls (Kennedy and Courchesne, 2008; Nomi and Uddin, 2015; von dem Hagen et al., 2013).

Although it is tempting to speculate that the DMN might exert a causal effect in the development of alterations, our analyses do not provide information about the directionality of the co-alteration edges. Still, regardless of the direction of the pathological influence, the central position of the DMN in the pathoconnectome of ASD is significant. By contrast, other networks, namely the SMN and, in particular, the DAN, appeared to be much less involved in our network of co-alterations (Fig. 4.6 left panel). This seems to indicate that the alterations in these networks do not influence or are not influenced by those in other parts of the brain. It is worth pointing out that the only SMN node is connected to six other nodes spanning across all the remaining networks (Fig. 4.6 right and bottom panels). Considering its location in the right STG, such a node might be associated with auditory functions, thus suggesting an association between auditory dysfunctions such as hypersensitivity and impaired perception

(Marco et al., 2011; Nieto Del Rincón, 2008; Robertson and Baron-Cohen, 2017; Williams et al., 2020). On the contrary, the lack of edges incident upon the DAN nodes might suggest that any top-down attention deficit of ASD patients (Allen and Courchesne, 2001) might be not associated, at least with respect to morphological substrates, with other symptoms.

Another finding of the present study is a rich pattern of co-alterations related to the limbic nodes including fusiform and orbitofrontal gyri, parahippocampal cortex and amygdar nuclear complex. Disrupted communication of these regions is thought to explain some clinical features of ASD, associated with deficits in emotional processing, social cognition and executive function (Ameis and Catani, 2015; Catani et al., 2016; Haznedar et al., 2000). In particular, the PHG_R node showed high centrality in our results, mostly due to several connections with the DMN. This is not a surprising result, as the parahippocampal gyrus is functionally coupled to the DMN and has been found to be involved in social cognition tasks regarding face versus non-face stimuli (Patriquin et al., 2016). The same brain area has been reported to exhibit altered activity in individuals with ASD during social reward learning task (Choi et al., 2015). These results can be understood in light of the evidence that the memory/encoding system supported by the medial temporal lobe represents a functional subnetwork, which is linked to the cortical nodes of the DMN through parahippocampal connections (Ward et al., 2014).

Another intriguing observation is that the right caudate tends to co-alter with prefrontal areas, encompassing both superior and inferior frontal gyri (i.e., SFG_L, BA8_L and IFG_L). These nodes are components of the dorsolateral prefrontal loop, previously associated with a degraded neuronal organization in ASD (Hashemi et al., 2017; Morgan et al., 2012) and involved in a number of high-order cognitive functions deficient in the disorder, such as complex behavioral planning, working memory processing and procedural learning (Çırak et al., 2020).

Our results also highlighted widespread co-alterations of the cerebellum, both between its hemispheres and through long-range pathways. Converging lines of research offer insight into the link between the cerebellum and ASD symptomatology (Becker and Stoodley, 2013), showing the crucial role of the posterior right lobules and their circuits in core deficits, such as those in language and social cognition processing, stereotyped behaviors and impairments in imitation planning and affective regulation (D'Mello and Stoodley, 2015). Our meta-connectomic analysis accords well with these evidences, suggesting a tendency of the

Crus2_R to be co-altered with a set of contralateral fronto-posterior nodes (i.e., IFG, MFG, MOG and PCUN) structurally connected and intrinsically implicated in an abnormal cerebro-cerebellar connectivity in mentalizing, verb generation, attention or resting-state tasks (D'Mello and Stoodley, 2015; Ecker et al., 2010; Itahashi et al., 2015; Khan et al., 2015; Noonan et al., 2009; Verly et al., 2014).

The mechanisms that might explain the observed co-alterations are varied. In fact, the presence of an alteration in a brain region might influence another one due to the long-range effects of diaschisis (Carrera and Tononi, 2014), for instance, through the lack of trophic support to the connected regions (Fornito et al., 2015; Nave, 2010; Perlson et al., 2010; Salehi et al., 2003) via direct axonal fiber tracts. In this regard, previous *in vivo* studies suggest that variations in GM morphometry and white matter connectivity are closely linked in ASD (Ameis and Catani, 2015; Andrews et al., 2017; Bos et al., 2015; Ecker et al., 2016; Schaer et al., 2013), reflecting a consistent number of gray-white matter pathological concordances in several clusters throughout the brain (Cauda et al., 2014a). Therefore, the correlation between the MCN and structural connectivity might support the hypothesis that connected regions tend to be co-altered because they lack neurotrophic regulation, which has been shown to be essential in normal brain development and maintenance of neuronal connections (Nickl-Jockschat and Michel, 2011). Neurotrophic failure has been also linked to the pathophysiology of ASD (Galvez-Contreras et al., 2017; Garcia et al., 2012; Kasarpalkar et al., 2014; Qin et al., 2016; Zheng et al., 2016), which indicates that a neurotrophic factor mechanism may convincingly explain the formation of the MCN pattern of ASD. Instead, the absence of a significant correlation with the genetic connectivity suggests that a model of shared genetic vulnerability to the disease (Zhou et al., 2012) falls short in explaining the development of the MCN pattern of ASD.

4.4.1 Methodological considerations and future perspectives

The present meta-connectomics analysis proposes a statistically robust view on the GM topology of autism, improving on previous works in several ways. The innovative method used here allowed us to extend spatial information given by canonical CBMAs, providing valuable insights on the mutual relationship between regional changes of the ASD phenotype, as well as on the peculiar role of each aberrant component and of brain connectivity. Also, from a network-level perspective, the MCN integrates current anatomical covariance

approaches, exercising a thorough and detailed topological resolution not limited by a prior choice of ROIs or by circumscribed ASD cohort analysis. However, methodologically speaking, it is important to point out that, given the different scale of statistical comparison (i.e., meta-analytic vs. group data level), the two types of analysis should not be confused but, rather, integrated for a better comprehension of the dynamic underlying brain disorders. Finally, although this study proposes a new outlook on the ASD brain architecture, the MCN methodology can be potentially applied to any other condition that reflects morphometric disturbances of the brain, opening attractive prospects for an in-depth comprehension of the human pathoconnectome.

Despite these strengths, we acknowledge that some limitations should be recognized. By definition, meta-connectomic approaches have general limitations inherent to publication biases (i.e., the file-drawer problem) and to the quality/constraints of individual investigations (Crossley et al., 2016). In this regard, we note that our data set reports a certain degree of heterogeneity in terms of clinical- and age-related differences among participants. Specifically, 23 out of 45 VBM experiments contain a mixed (i.e., comprehensive of two or more diagnostic sub-categories) or an unspecified ASD sample (Table S4.2). Still, the marked presence of original experimental groups composed of mixed age-stratified participants or with unspecified age ranges (35.6% of the experiments included), hampers the possibility to interpret developmental co-alteration changes in neuroanatomy of ASD (Table S4.2). In other words, this heterogeneity makes it challenging to discriminate possible differences related to the clinical or age-stratified subpopulations. At the same time, however, it offers important advantages. In fact, in conjunction with the substantial statistical power provided by meta-analytic synthesis (Eickhoff et al., 2016), the meta-level approach tends to afford more robust and reliable results in terms of generalization for the population of interest (Muller et al., 2018).

Another critical element of the present study relates to the continuous dimensionality of the psychopathology of ASD. Since the diagnosis of ASD includes a wide array of clinical manifestations and biological endophenotypes, it might be pointed out that our database could be affected by a large inter-subject variability. This does not constitute a limitation *per se*, as the aim of a meta-analysis is exactly to overcome the heterogeneity of samples in order to discover invariant findings across groups (Tahmasian et al., 2019). However, not considering the peculiarity of each individual or diagnostic subgroup might be simplistic and miss some

critical feature of ASD. Future research might develop subject-level methods to assess co-alteration networks, and eventually investigate whether or not they can help discriminate between different categories or dimensions of ASD. At the moment, the main issue to extend the methodology used here to subject-level data is the identification of focal structural alteration in absence of normative intensity values to discriminate between T1 images of healthy and pathological subjects.

The current work does not assess the directionality of the network co-alterations, but future research might test, for instance, the hypothesis that the DMN alterations may play a role in the distribution of the other GM alterations, or the other way round. Finally, the lack of a significant correlation between the co-alteration network and genetic co-expression connectivity is not indicative of an absence of a genetic role in ASD, but rather, that the genetic influence does not explain the statistical dependence between GM modifications. However, genetic connectivity could have a role in determining the first areas to be affected (Cauda et al., 2019a), while the diaschisis effect might induce other regions to be co-altered (Carrera and Tononi, 2014). Further research is needed to investigate these possibilities.

The long-term aim of the co-alteration approach is to produce valuable insights for clinical practice, in terms of improvement in the diagnostic procedure and in monitoring the disease course. Future investigations may adopt the co-alteration nodes as ROIs to test the generalizability of the MCN pattern on longitudinal native data. In addition, multi-scale research may explore the role of the meta-analytic hubs in different clinical cohorts, testing in detail the impact of these key regions on the ASD pathoconnectome. Finally, a more profound comprehension of the role of brain connectivity could help us understand the maladaptive mechanisms underlying the distribution of co-alterations and could pinpoint how to intervene to halt those mechanisms.

4.5. Conclusion

This study investigated VBM abnormalities of individuals with ASD using a meta-connectomic perspective, demonstrating a topologically characteristic structure of co-alteration underlying a circumscribed set of GM sites in the autistic brain. We found that the co-alteration pattern is influenced in part by structural connectivity, which is in line with the hypothesis that the brain connectome plays an important role in the development of disease-related alterations. Finally, we observed that the regions belonging to the DMN are central in

the topology of co-alterations, thus suggesting a significant contribution of DMN dysfunction in the pathophysiology of ASD. This effect may be due to the strong network-betweenness of the DMN, which makes GM alterations in these network regions to be pathoconnectivity centers. In conclusion, the present study provides new insight into the complex pathophysiology of ASD, emphasizing the need for a more integrative view based on large-scale network dysfunction in order to better understand the complex clinical manifestations of this spectrum of disorders.

4.6. Supplementary material

4.6.1. Supplementary tables

Table S4.1. Checklist for neuroimaging coordinate-based meta-analysis (CBMA) (adapted from Muller et al. 2018).

A The research question is specifically defined	**YES**, and it was clearly reported in the introduction section.
B The literature search was systematic	**YES**, and it follows the **PRISMA international guidelines**. Search includes the following keywords in the following databases: **Databases**: BrainMap (http://www.brainmap.org/); PubMed MEDLINE (https://www.ncbi.nlm.nih.gov/pubmed/). **Keywords BrainMap**: [Experiments Contrast is Gray Matter] AND [Experiments Context is Disease Effects] AND [Subjects Diagnosis is Autism spectrum disorder] AND [Experiments Observed Changes is Controls > Patients]. **Keywords PubMed**: ("Autism spectrum disorder" [title/abstract] OR "ASD" [title/abstract] OR "autism" [title/abstract]) AND ("voxel-based morphometry" [title/abstract] OR "VBM" [title/abstract]).
C Detailed inclusion and exclusion criteria are included	**YES**, and reason was: **Standard inclusion criteria applied:** 1 Only experimental contrasts that used whole-brain analysis of gray matter; 2 Only data reported by articles published in a peer-review journal; 3 Only experimental contrasts that reported results in a stereotactic brain space (i.e., coordinates in TAL or MNI). **Non standard inclusion criteria applied:** 1 Only experimental contrasts that used VBM analysis (in order to maximize the power of the CBMA and to exclude meta-data with other structural and functional MRI-based methods, whose results have a different meaning); 2 Only experimental contrasts that employed a between-group comparison with clinical groups of interest and healthy controls (in accordance with research question); 3 Only experimental contrasts that included subjects with diagnosis of ASD (in accordance with research question); 4 Only VBM contrasts with experimental sample size ≥ 10 subjects (in order to reduce the likelihood to include experiments presenting false positives, according to previous coordinate-based meta-analyses).

D Sample overlap was taken into account	**YES**, using the following criteria: Only VBM results reported by the largest experiment or those divided into diagnostic subcategories published by the same articles (in order to prevent redundancy of subjects and related results).
E All experiments use the same search coverage	**YES**, the search coverage is the following: **Only whole-brain VBM analysis**. 1 If an experimental contrast reported whole-brain + ROI analysis, the whole-brain analysis only has been included in the meta-analysis; 2 If an experimental contrast reported the ROI analysis only, the experimental contrast was excluded from the meta-analysis in accordance with our inclusion/exclusion criteria; 3 Experimental contrasts reporting only conjunctional analysis have been excluded.
F Studies are converted to a common reference space	**YES**, using the following conversion: **CBMA was conducted in Talairach (TAL) space.** We employed the icbm2tal algorithm, as implemented in GingerALE software (v.3.0.2), to convert the native Montreal Neurological Institute (MNI) coordinates into TAL space.
G Data extraction have been conducted by two investigators	**YES**, the following authors: LD, TC, FC checked inclusion criteria; LD, FC extracted coordinates; LD extracted other info: clinical, socio-demographic and methodological meta-data were reported in Supplementary tables S3.2 and S3.3.
H The paper includes a table with basic study description	**YES**, and also the following data: Article reference and MEDLINE id; number of subjects included (clinical and control groups); mean age and age range at scan (clinical and control groups); sex distribution (clinical and control groups); type of VBM software employed; voxel size or slice thickness (mm); smoothing (FWHM); MRI static field; original stereotactic space (coordinates in x, y, z); classification and instrument of classification (i.e., DSM or ICD) for experimental subjects; number of foci of GM variation for each experimental contrast included.
I The study protocol was previously registered and all analyses planned beforehand	**NO**: This CBMA was not registered before starting the search. According with PROSPERO database (https://www.crd.york.ac.uk/prospero/), both systematic and scoping literature review and CBMA should be not registered, which is the present case; We declared that we planned all the analysis before starting the literature search and that we did not run any non-planned or non-prespecified analysis.

Table S4.2. Articles included in the meta-analysis: demographic and clinical meta-data.

First Author	Medline ID	Clinical group					Control group			
		N	F	M	Age* (range)	Diagnosis**	N	F	M	Age * (range)
Abell et al. (1999)	10501551	15	3	12	29±6.6 (N/A)	ASP	15	3	12	25±3.1 (N/A)
Boddaert et al. (2004)	15325384	21	5	16	9.3±2.2 (7-15)	Autism	12	5	7	10.8±2.7 (7-15)
Brieber et al. (2007)	18093031	15	0	15	14.2±1.9 (10-16)	ASP/HFA	15	0	15	13.3±1.8 (10-16)
Cai et al. (2018)	30425664	38	6	32	9.6±3.4 (5-16)	HFA	27	1	26	8.3±2.3 (5-14)
Cheng et al. (2011) (HFA group)	21541322	15	0	15	13.7±2.5 (10-18)	HFA	25	0	25	13.5±2.1 (11-18)
Cheng et al. (2011) (ASP group)	21541322	10	0	10	13.7±2.5 (10-18)	ASP	25	0	25	13.5±2.1 (11-18)
Craig et al. (2007)	17766762	14	14	0	37.9±11.4 (N/A)	ASP/Autism	19	19	0	35±14 (N/A)
D'Mello et al. (2015)	25844317	35	5	30	10.4±1.6 (8-13)	ASD	35	14	21	10.4±1.5 (8-13)
D'Mello et al. (2016)	27868392	18	0	18	11.0±1.6 (8-13)	ASD	35	14	21	10.4±1.5 (8-13)
Ecker et al. (2010)	19683584	22	0	22	27±7 (18-42)	ASD	22	0	22	28±7 (18-42)
Ecker et al. (2012)	22310506	89	0	89	26±7 (18-43)	ASP/HFA	89	0	89	28±7 (18-43)
Eilam-Stock et al. (2016)	27313505	66	6	60	27±8 (18-64)	HFA	66	6	60	27±7 (18-43)
Foster et al. (2015)	26231265	38	0	38	12.4±2.4 (6-17)	ASD	46	0	46	12.6±2.6 (7-17)
Freitag et al. (2008)	18262208	15	2	13	17.6±3.6 (N/A)	ASD	15	2	13	18.6±1.2 (N/A)
Greimel et al. (2013)	22777602	47	0	47	21.4±10.1 (10-50)	ASP/HFA/ Autism	51	0	51	18.3±7.5 (8-47)
Hyde et al. (2010)	19790171	15	0	15	22.7±6.4 (14-33)	Autism	13	0	13	19.2±5 (14-34)
Kaufmann et al. (2013)	23117423	10	2	8	14.7±5.0 (N/A)	ASP	10	2	8	13.8±5.3 (N/A)
Ke et al. (2008)	18520994	17	3	14	8.88±1.96 (6-14)	HFA	15	3	12	9.73±1.67 (6-14)
Kosaka et al. (2010)	20123027	32	0	32	23.8±4.2 (17-32)	ASP/HFA	40	0	40	22.5±4.3 (18-34)
Kurth et al. (2011)	21531390	52	14	38	11.2±3.95 (5.9-20.4)	ASD	52	14	38	11.14±3.58 (6.1-19.7)
Kwon et al. (2004)	15540637	11	0	11	13.6±2.4 (10-18)	ASP/HFA	13	0	13	13.6±3.1 (10-18)
Lai et al. (2013)	23935125	60	30	30	27.5 (18-49)	ASP/Autism	60	30	30	27.8 (18-49)
Lai et al. (2015)	25249409	80	0	80	24.2 (18-41)	ASP/Autism	57	0	57	N/A (N/A)
McAlonan et al. (2002)	12077008	21	2	19	32±10 (18-49)	ASP	24	2	22	33±7 (18-49)
McAlonan et al. (2005)	15548557	17	1	16	12±1.8 (8-14)	Autism	17	1	16	11±1.2 (8-14)
McAlonan et al. (2008)(HFA group)	18673405	17	3	14	11.4±2.5 (7-16)	HFA	55	8	47	10.7±2.7 (7-16)
McAlonan et al. (2008)(ASP group)	18673405	16	3	13	11.7±2.8 (7-16)	ASP	55	8	47	10.7±2.7 (7-16)
Mengotti et al. (2011)	21146593	20	2	18	7.0±2.7 (4-14)	Autism	22	2	20	7.7±2.0 (4-11)
Muller et al. (2013)	23825652	12	3	9	35.5±11.4 (N/A)	HFA	12	4	8	33.3±9 (N/A)

First Author	Medline ID	Clinical group					Control group			
		N	F	M	Age* (range)	Diagnosis**	N	F	M	Age * (range)
Ni et al. (2018)	29129723	81	0	81	12.5±2.1 (7-17)	HFA	61	0	61	12.4±2.4 (7-17)
Osipowicz et al. (2015)	25630444	531	101	430	17.0±8.0 (7-64)	ASD	571	109	462	17.0±8.0 (7-64)
Pereira et al. (2018)	30042724	22	4	18	17.4±3.3 (14-25)	HFA	29	10	19	18.5± 2.8 (14-25)
Radeloff et al. (2014)	25188200	34	3	31	19.06±5.12 (14-33)	ASP/Autism	26	4	22	19.54±3.46 (14-27)
Riedel et al. (2014)	24953998	30	11	19	35.4±9.1 (21-52)	HFA	30	11	19	35.5±8.3 (22-53)
Riva et al. (2011)	21700792	21	8	13	6.6±2.5 (3.3-10.10)	Autism/ PDD-NOS	21	8	13	6.10±2.1 (3.9-10.10)
Riva et al. (2013)	23572290	26	3	23	5.1±2.6 (2.7-10.10)	Autism/ PDD-NOS	21	8	13	6.10±2.1 (3.9-10.3)
Rojas et al. (2006)	17166273	24	0	24	20.79±10.58 (7-47)	Autism	23	0	23	21.41±10.91 (7.8-44)
Salmond et al. (2005)	16101758	14	1	13	12.9±0.7 (8-18)	ASP/HFA	13	0	13	12.1±0.7 (8-18)
Salmond et al. (2007)	17710821	22	2	20	11.8 (8-18)	ASD	22	3	19	12.1 (8-18)
Sato et al. (2017)	28824399	36	11	25	27.0±8.0 (18-53)	ASP/ PDD-NOS	36	11	25	24.9±5.5 (20-43)
Toal et al. (2010) (ASP group)	19891805	39	4	35	32.0±12.0 (16-59)	ASP	33	3	30	30.0±3.0 (19-58)
Toal et al. (2010) (ASD group)	19891805	26	5	21	30.0±8.0 (16-59)	ASD	33	3	30	30.0±3.0 (19-58)
Waiter et al. (2004)	15193590	16	0	16	15.4±2.24 (12-20)	ASP	16	0	16	15.5±1.6 (12-20)
Wilson et al. (2009)	19853418	10	2	8	30.1±9.18 (22.2-47.2)	Autism	10	3	7	29.4±7.91 (21.8-43.8)
Yang et al. (2018)	30001226	16	6	10	10.4± 2.8 (N/A)	ASD	16	6	10	10.5 ± 3.1 (N/A)

** The average age at scan session, its standard deviation and age range are reported on the basis of what is specified by the authors of the original articles. ** Reported diagnosis of clinical groups is based on what is specified by the authors of the original articles. ASP, Asperger's Syndrome; Autism, Primary/Atypical Autism; HFA, High Functional Autism; PDD-NOS, Pervasive Developmental Disorder Not Otherwise Specified; ASD, Autism Spectrum Disorder (diagnosis not specified); N, number of subjects; F, female; M, male; N/A, meta-data not associated.*

Table S4.3. Articles included in the meta-analysis: methodological meta-data.

First Author	*VBM Software*	*Voxel Size (mm)**	*Smoothing (FWHM)*	*Scanner (Tesla)*	*Foci*	*Space*
Abell et al. (1999)	SPM 96	1x1x1.5	12	2	3	TAL
Boddaert et al. (2004)	SPM 99	0.86x1.33x1.20	12	1.5	4	TAL
Brieber et al. (2007)	SPM2	1x1.42x1	12	1.5	6	MNI
Cai et al. (2018)	SPM 8	1x1x1	8	3	3	MNI
Cheng et al. (2011) (HFA group)	SPM 2	Thickness 1.5	8	1.5	2	MNI
Cheng et al. (2011) (ASP group)	SPM 2	Thickness 1.5	8	1.5	10	MNI
Craig et al. (2007)	SPM2	Thickness 1.5	5	1.5	5	TAL
D'Mello et al. (2015)	SPM 8	1x1x1	8	3	3	MNI
D'Mello et al. (2016)	SPM 8	1x1x1	8	3	2	MNI
Ecker et al. (2010)	SPM5	1.09x1.09x1	8	3	14	TAL
Ecker et al. (2012)	FSL-VBM	Thickness 1	3	3	11	MNI
Eilam-Stock et al. (2016)	SPM 8	N/A	8	N/A	3	MNI
Foster et al. (2015)	CIVET	1x1x1	8	3	5	MNI
Freitag et al. (2008)	SPM 99	1x1x1	8	1.5	1	MNI
Greimel et al. (2013)	SPM5	1x1x1	8	1.5/3	3	MNI
Hyde et al. (2010)	CIVET	1x1x1	12	3	3	MNI
Kaufmann et al. (2013)	SPM 8	N/A	6	1.5	1	MNI
Ke et al. (2008)	SPM5	0.94x0.94x1	8	1.5	1	TAL
Kosaka et al. (2010)	SPM5	0.75x1.25x1.06	8	3	5	MNI
Kurth et al. (2011)	SPM 8	Thickness 1.2	8	1.5	1	MNI
Kwon et al. (2004)	SPM99	Thickness 1.5	8	3	3	TAL
Lai et al. (2013)	SPM 8	N/A	4	3	1	MNI
Lai et al. (2015)	SPM 8	1x1x1	4	3	6	MNI
McAlonan et al. (2002)	SMaRT on SPARC	Thickness 1.5	N/A	1.5	9	TAL
McAlonan et al. (2005)	BAMM on SPARC	Thickness 3	4.4	1.5	13	TAL
McAlonan et al. (2008)(HFA group)	BAMM on SPARC	0.86x0.86x3	4.4	1.5	8	TAL
McAlonan et al. (2008)(ASP group)	BAMM on SPARC	0.86x0.86x3	4.4	1.5	4	TAL
Mengotti et al. (2011)	SPM 5	Thickness 5	8	1.5	2	MNI
Muller et al. (2013)	FSL-VBM	0.8x0.8x0.8	4	3	14	MNI
Ni et al. (2018)	SPM 8	1x1x1	4	3	6	MNI
Osipowicz et al. (2015)	SPM 8	1x1x1	8	3	5	MNI
Pereira et al. (2018)	SPM 8	1x1x1	10	3	16	MNI
Radeloff et al. (2014)	SPM 8	Thickness 1	8	3	4	MNI
Riedel et al. (2014)	SPM 8	1x1x1	8	N/A	1	MNI
Riva et al. (2011)	SPM 5	1x1x1	8	1.5	13	TAL
Riva et al. (2013)	SPM 8	Thickness 5	8	1.5	13	TAL
Rojas et al. (2006)	SPM2	0.94x0.94x1.7	8	1.5	4	MNI
Salmond et al. (2005)	SPM99	0.8x0.8x1	12	1.5	2	TAL

First Author	*VBM Software*	*Voxel Size (mm)**	*Smoothing (FWHM)*	*Scanner (Tesla)*	*Foci*	*Space*
Salmond et al. (2007)	SPM99	0.8x0.8x1	12	1.5	6	MNI
Sato et al. (2017)	SPM 8	1x1x1	8	3	19	MNI
Toal et al. (2010) (ASP group)	SPM 2	0.859x0.859x1.5	8	1.5	1	TAL
Toal et al. (2010) (ASD group)	SPM 2	0.859x0.859x1.5	8	1.5	2	TAL
Waiter et al. (2004)	SPM 2	1x1x1	12	1.5	1	TAL
Wilson et al. (2009)	SPM 2	0.94x0.94x1.7	12	1.5	2	MNI
Yang et al. (2018)	FS-VBM	Thickness 1	3	3	3	MNI

** Where no information was provided, the slice thickness was expressed. FWHM, full width at half maximum; TAL, Talairach stereotactic space; MNI, Montreal Neurological Institute stereotactic space; N/A, meta-data not associated.*

4.6.2. Supplementary figure

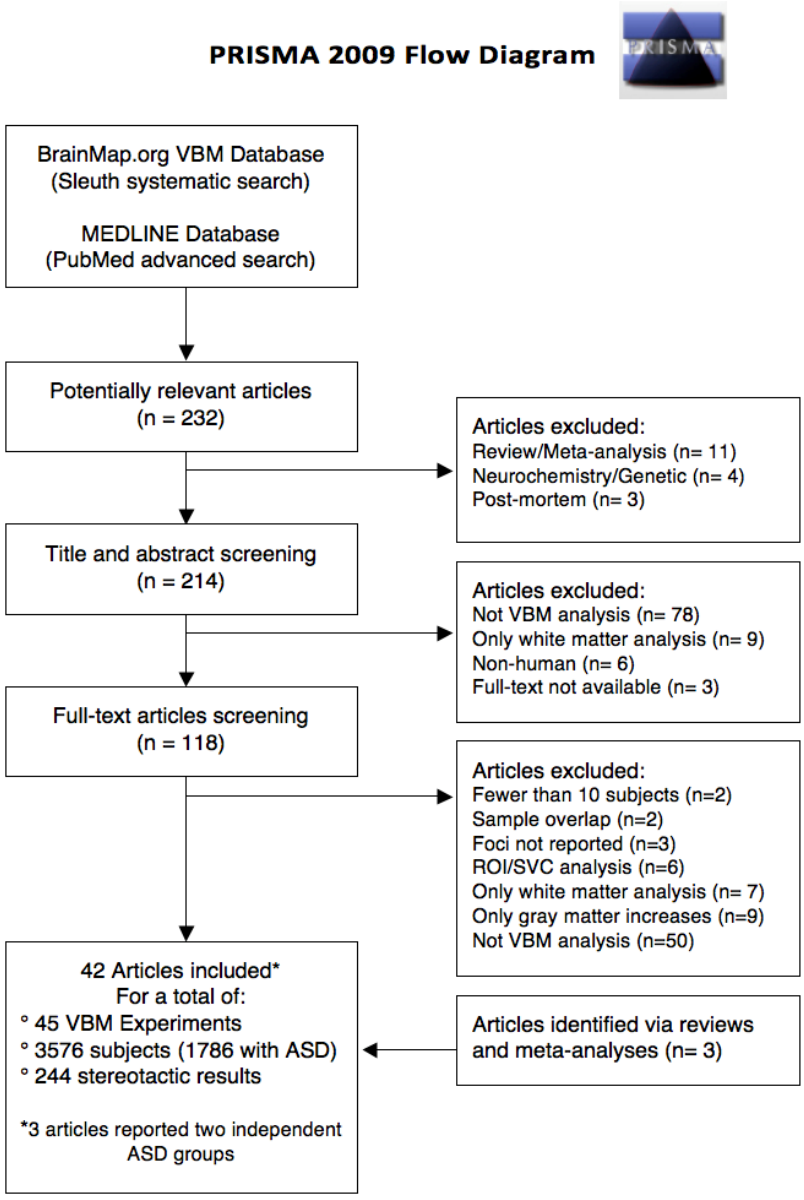

Figure S4.1. PRISMA flow chart of meta-data selection.

CHAPTER 5

Revealing the Selectivity of Neuroanatomical Alteration in Autism Spectrum Disorder via Reverse Inference[4]

Abstract

Background: Although neuroimaging research has identified atypical neuroanatomical substrates in individuals with autism spectrum disorder (ASD), it is at present unclear whether and to what extent disorder-selective gray matter (GM) alterations occur in this spectrum of conditions. In fact, a growing body of evidence shows a substantial overlap between the pathomorphological changes across different brain diseases, which may complicate identification of reliable neural markers and differentiation of the anatomical substrates of distinct psychopathologies. *Methods:* Using a novel data-driven and Bayesian methodology with published voxel-based morphometry data (849 peer-reviewed experiments and 22,304 clinical subjects), this study performs the first *reverse inference* investigation to explore the selective structural brain alteration profile of ASD. *Results:* We found that specific brain areas exhibit a > 90% probability of GM alteration selectivity for ASD: the bilateral precuneus (BAs 7), right inferior occipital gyrus (BA 18), left cerebellar lobule IX and Crus II, right cerebellar lobule VIIIA, and right Crus I. Of note, many brain voxels that are selective for ASD include areas that are posterior components of the default mode network. *Conclusion:* The identification of these spatial GM alteration patterns offers new insights into understanding the complex neurobiological underpinnings of ASD, and opens attractive prospects for future neuroimaging-based interventions.

5.1. Introduction

The ultimate goal of clinical neuroimaging is to elucidate *in-vivo* the relationship between atypicalities in the brain and disease. Structural magnetic resonance imaging (sMRI) methods such as voxel-based morphometry (VBM) (Ashburner and Friston, 2000), have been extensively employed to examine regional brain variations associated with clinical populations by means of voxel-wise intergroup comparison. From this type of data,

[4] This study was published in *Biological Psychiatry: Cognitive Neuroscience and Neuroimaging* in 2022 (doi: 10.1016/j.bpsc.2022.01.007). Authors: Liloia D., Cauda F., Uddin L.Q., Manuello J., Mancuso L., Keller R., Costa T.

researchers typically infer which neuroanatomical correlates are altered in clinical conditions under examination compared with the normative population. In other words, they can help us to draw "disease-to-alteration" estimations, also known as *forward inferences* (Henson, 2006).

Forward inference-based reasoning is widely used in the field of neuroimaging, and has an important role in understanding the neural substrates underlying brain disorders; however, such reasoning suffers from a significant drawback: the lack of selectivity (Poldrack, 2006). From the perspective of clinical sMRI, a critical limitation concerns the impossibility of determining the alteration specificity of brain areas in a given clinical condition (Cauda et al., 2020b). This, and the fact that several psychiatric and neurological disorders tend to exhibit a common substrate of neuroanatomical variation (Cauda et al., 2017; Cauda et al., 2019b; Cole et al., 2014; Crossley et al., 2014; Goodkind et al., 2015; Liloia et al., 2018; McTeague et al., 2016; Radonjić et al., 2021) make "alteration-to-disease" estimation challenging, and limit the effective contribution of sMRI findings to diagnostic and treatment strategies.

Research on autism spectrum disorder (ASD) is an exemplary case. A substantial body of VBM investigations have evidenced that this spectrum of conditions is associated with atypical brain development, which leads to anomalies across widespread neural territories (Ecker et al., 2015). Coordinate-based meta-analyses (CBMAs) have identified aberrant volumetric concordances at the level of the insula, cingulate cortex, thalamus, amygdala, frontal and temporal gyri (Carlisi et al., 2017; DeRamus and Kana, 2015; Lukito et al., 2020). Although these variations are common in ASD, their involvement is not selective to the disorder. For example, prefrontal, cingulo-insular, amygdalar and thalamic alterations are also shared with other conditions, such as schizophrenia (Liloia et al., 2021a), post-traumatic stress disorder (Meng et al., 2016) and chronic pain (Smallwood et al., 2013). Overlapping alterations have been found with attention-deficit/hyperactivity disorder (Brieber et al., 2007), with obsessive-compulsive (Cauda et al., 2017) and social anxiety (Wang et al., 2018) disorders.

A complementary approach is therefore needed to disentangle the alteration landscape of brain pathology. One way to achieve this aim is with analytic tools based on Bayesian statistics, which can apply a form of reasoning leading from alteration data to neural disorders, also known as *reverse inference* (Poldrack, 2006). Since Poldrack's seminal paper (2006), the use of such reasoning in the field of neuroimaging has been explored and

extensively debated (Del Pinal and Nathan, 2013; Hutzler, 2014; Machery, 2014; Poldrack, 2008, 2011; Wager et al., 2016; Yarkoni et al., 2011). Although different efforts highlight the issue of *reverse inference* as necessary for brain research, some challenges remain. For example, the absence of a comprehensive formal cognitive ontology limits the possibility of inferring psychological functions from neuroimaging data (Poldrack and Yarkoni, 2016). Another limitation is due to the extreme difficulty in taking into account the entire body of specialized literature that would permit strong claims about the selective mapping of interest. Fortunately, this issue can be mitigated by the advent of open-access repositories such as BrainMap (Fox et al., 2005; Fox and Lancaster, 2002) and Neurosynth (Yarkoni et al., 2011), which currently contain a broad sample of peer-reviewed experiments (detailed accounts on this topic can be found in (Cauda et al., 2020b; Poldrack, 2011)).

From its earliest implementations in neuroimaging, *reverse inference* approaches have been limited to functional MRI data and to normative populations so as to estimate the selective engagement of a given cognitive function on the basis of the activation of specific neuronal assemblies. Only recently, such approaches have been applied to anatomical alterations associated with brain disorders. Specifically, Cauda et al. (2020b) have explored the alteration profiles of Alzheimer's disease and schizophrenia, applying the calculation of the Bayes' factor (Jeffreys, 1961) to sMRI meta-analytic data.

A further step is the implementation of this technique in a tool called BACON (Bayes fACtor mOdeliNg; (Costa et al., 2021)). This novel resource allows the generation, in a data-driven and replicable manner through posterior probability analyses, of brain maps showing the voxel-wise alteration selectivity landscape of a given neuropathology. Based on the Bayes' factor, BACON calculates the likelihood between two competing hypotheses: the probability that voxels are altered because of the disorder of interest and the probability that they are altered because of another disorder. By switching from *forward* to *reverse inference*, BACON provides different evidence from that obtained with conventional CBMA techniques such as activation likelihood estimation (ALE) (Eickhoff et al., 2012; Eickhoff et al., 2016).

Despite intense effort in sMRI research, the extent of disorder-differentiated morphological alterations occurring in ASD remains unclear. Establishing the neuroanatomical signature of this group of neurodevelopmental conditions may pave the way for future research on neuroimaging-based biomarkers, as well as for devising new-targeted interventions. Here we explore the spatial location of selective brain abnormalities in ASD by

conducting a standardized search of clinical primary data on gray matter (GM) VBM alterations. We analyzed a large amount of data with BACON, which enabled us to assess, for the first time, the posterior probability distribution of GM alterations that are selectively associated with ASD.

5.2. Methods

This research adhered to the PRISMA guidelines (Moher et al., 2009). First, the BrainMap and MEDLINE databases were queried to identify VBM meta-data related to ASD, through January 30, 2021. Another standardized search was carried out on BrainMap to retrieve VBM meta-data related to other conditions reporting appreciable GM changes. For details and search algorithms see Supplementary methods (i.e., data search strategy section).

5.2.1. Data inclusion

Standard criteria

Eligible experiments were published in a peer-reviewed article, statistically contrasted GM brain volume/concentration between a patient group and a healthy control (HC) group, and reported a whole-brain VBM analysis and stereotactic results (x-y-z foci in Talairach or MNI spaces). This preliminary screening was aimed at removing bias related to region-of-interest analysis and to spatial error (Eickhoff et al., 2009; Muller et al., 2018).

Clinical criteria.

Regarding the ASD sample, eligible experimental groups comprised subjects with a diagnosis of ASD that met standardized DSM and/or ICD criteria. Regarding other brain conditions, all eligible experiments that were coded as ‘disease effects context’ in the BrainMap VBM sector were included. There were no restrictions on age, gender or diagnosis of the participants. Inclusion of clinical conditions that may report associations with ASD was allowed (e.g., epilepsy, tuberous sclerosis, Down, Fragile X, and 22q11.2 deletion syndromes), provided that none of the experimental participants had a history of autism. We did not exclude experiments on medicated subjects, as they represent a non-negligible part of the literature. However, inclusion was only permitted when experiments reported between-group differences (i.e., effect of diagnosis) and not effects of pharmacologic treatment (Muller et al., 2018).

Technical criteria.

Potential bias related to overlapping populations was minimized both within and between experiments. When different articles were published by the same first author, making use of the same clinical group and reporting the same stereotactic results, only the earliest published experiment was included. In the case of multiple experiments included in a single article, those carried out on the same patient group or its subgroups were excluded: in other words, we included only those experiments that reported data from non-redundant clinical groups. Post hoc assessments were conducted via GingerALE (v.3.0.2), to exclude duplicate results related to the same clinical group that was included in other studies published by different first authors. Lastly, stereotactic results of hypotrophy and hypertrophy were pooled in a single experiment when the results were related to the same comparison of diagnosed individuals relative to HCs.

5.2.2. Data groupings

Two distinct datasets were created to estimate the selectivity of GM abnormalities in ASD: i) ASD dataset, composed of experiments reporting brain alterations in patients with ASD (vs. HC); ii) non-ASD dataset, composed of experiments reporting brain alterations in all BrainMap conditions (vs. HC) without those reporting brain alterations in ASD (vs. HC). Analyses were conducted in Talairach space. Thus, the spatial accuracy of the data was improved by converting coordinates reported in MNI into Talairach space (Laird et al., 2010).

5.2.3. Statistical methods

Activation likelihood estimation

The calculation of the BF, as implemented in BACON, is based on two unthresholded ALE maps: the first obtained from the ASD dataset, the second from the non-ASD dataset. The ALE algorithm (Eickhoff et al., 2012) (GingerALE software package; v.3.0.2), models each experiment alterations as a series of 3-D Gaussian distribution of probabilities centered on the peaks of alterations reported by the included experiments. This permits generation of a modeled activation (MA) map for each experiment. The size of the Gaussian kernel varies between the MA maps, taking into account the sample size originally used in each experiment (Eickhoff et al., 2009). Every final ALE map can be seen as a union of all per-experiment MA maps (see also Fig. 5.1).

Bayes factor modeling

BACON was devised as a method for obtaining posterior probability distributions on the selectivity alteration with regard to a particular brain disorder (Costa et al., 2021); it implements the BF and uses ALE derived-maps. Formula 1 expresses the Bayes' theorem in terms of relative belief, also referred to as the BF:

$$\frac{P(H_0|D)}{P(H_1|D)} = \frac{P(D|H_0)}{P(D|H_1)}\frac{P(H_0)}{P(H_1)} \qquad (1)$$

Where D is a measurement of structural alteration in a voxel, H_0 is the hypothesis affirming the occurrence of ASD in such voxel, and H_1 is the hypothesis affirming the occurrence of any other disorder (i.e., the negation of H_0). BACON allows us to compute the probability that, given the measurement (D) of a certain voxel, ASD is actually occurring (i.e., H_0 is true). Because knowledge of priors is not available for the two hypotheses, we considered them to be identical (see also Cauda et al. (2020b) for further consideration and validation of this choice). Therefore, the BF_{01} can be expressed as:

$$BF_{01} = \frac{P(D|H_0)}{P(D|H_1)} \qquad (2)$$

Because the sum of the two posterior probabilities must be equal to 1, and based on formula 1, we can re-write formula 2 as:

$$BF_{01} = \frac{P(H_0|D)}{1-P(H_0|D)} \qquad (3)$$

BF_{01} provides the degree of evidence for the two hypotheses: if $BF_{01}$is greater than 1, the evidence favors H_0; if $BF_{01}$is less than 1, the evidence favors H_1. Inverting formula 3, we obtain:

$$P(H_0|D) = \frac{BF_{01}}{BF_{01}+1} \qquad (4)$$

This expression allows us to directly obtain a posterior probability via the BF (see Fig. 5.1 for a graphical interpretation of the formulas).

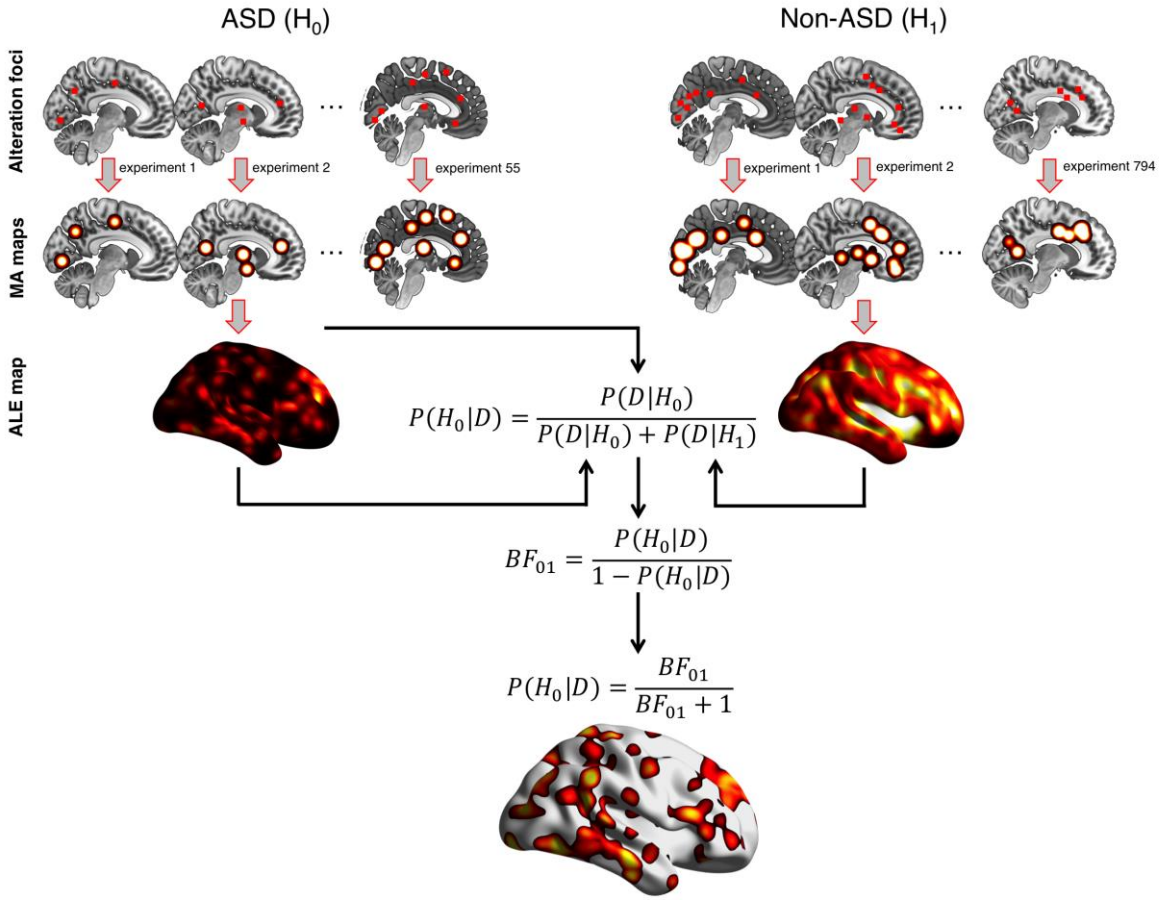

Figure 5.1. Graphical representation of the data analytic pipeline, from the alteration foci to the selectivity map. The final map, which represents the values of the probabilities and is obtained with the BF_{01} computation (as implemented in BACON), can be thresholded depending on the desired level of selective alteration probability.

Functional network decomposition

To determine the functional localization of GM selective patterns in ASD, we applied the 7-networks parcellation of Yeo et al. (2011). Alterations within the cerebellar cortex and striatal nuclei were assigned to each of Yeo's canonical networks according to the cerebellar (Buckner et al., 2011) and striatal (Choi et al., 2012) parcellations, respectively. A data-driven decomposition was undertaken to investigate how many volumes (mm^3) derived from BACON map fell within the following networks: visual network, somatomotor network (SMN), dorsal attention network (DAN), salience/ventral attention network (SN/VAN), limbic network, frontoparietal network (FPN) and default mode network (DMN).

Robustness analyses

CBMA findings can potentially be affected by the file-drawer problem, a literature bias relating to the contra-evidence results that are unpublished (Acar et al., 2018; Samartsidis et al., 2020). To overcome this issue, we tested the robustness of our findings using the Fail-Safe technique for the ALE method (Acar et al., 2018;). According to the simulation study by Samartidis et al. (2020), who estimated the rate of missing experiments in the BrainMap database to be around the 6%, analyses were retested adding the same percentage of "noise" injection for both datasets. Robustness of the findings was also estimated with noise injection up to 30%, as recently proposed (Gray et al., 2020). Details of this analysis can be found in the Fail-Safe analysis section (Supplementary methods).

The ASD dataset included four experiments analyzing subjects from the ABIDE database (Di Martino et al., 2014). Although clinical and sociodemographic differences were found between experiments, we were unable to determine whether and to what extent population overlap occurred between experiments. Therefore, a leave-one-out analysis was performed to test the reproducibility of main findings, which consisted of repeating the BACON analysis after systematically removing each of the four experiments that used the ABIDE dataset.

Age-related and alteration-related contribution to findings

Because the autistic brain architecture may not be static within individuals across the lifespan (Dajani and Uddin, 2016; Lange et al., 2015; Nomi and Uddin, 2015; Nunes et al., 2020), we assessed the contribution of the age-related and alteration-related data to BACON results.

Based on the BF index (Jeffreys, 1961), conceived as the ratio between the likelihoods of two alternative hypotheses, we examined the force of evidence on general alteration selectivity clusters of two subsets of meta-data stratified by age, namely the pediatric group (generated by grouping foci related to ASD subjects with an age < 18 years) and the adult group (age ≥ 18 years). VBM experiments composed of mixed age-stratified individuals were not included in this analysis. Starting from the untresholded *p*-value ALE maps of pediatric and adult groups, the calculus of the BF was performed, capable of reporting an index ranging from 0 to ∞ for each ALE-related voxel and representing how much the age-stratified data could support the BACON clusters. The force of evidence was interpreted following the

Jeffreys' classification scheme (1961) (Table S5.1).

We also evaluated the contribution of the type of alteration (i.e., GM decrease/increase). Following the same steps of the age-related analysis, two subsets of meta-data were organized and analyzed via BF: the GM decrease group (generated by grouping foci of GM decrease related to ASD dataset; ASD < HC) and the GM increase group (generated by grouping foci of GM increase; ASD > HC) (Table S5.2).

5.3. Results

The comprehensive search yielded a total of 849 published experiments including 131 clinical conditions (Fig. 5.2). The distribution of the ASD datasets was: 55 experiments, 2,407 patients, 546 stereotactic coordinates (Table S5.3). No neurological, psychiatric, seizure or genetic comorbidities were identified, except for 18 subjects distributed in three different experiments (details in Table S5.3). The Non-ASD dataset was composed of 794 experiments, 19,897 patients, 8,035 coordinates (Table S5.4). Details about the meta-data distribution are shown in Table S5.5, Table S5.6 and Table S5.7.

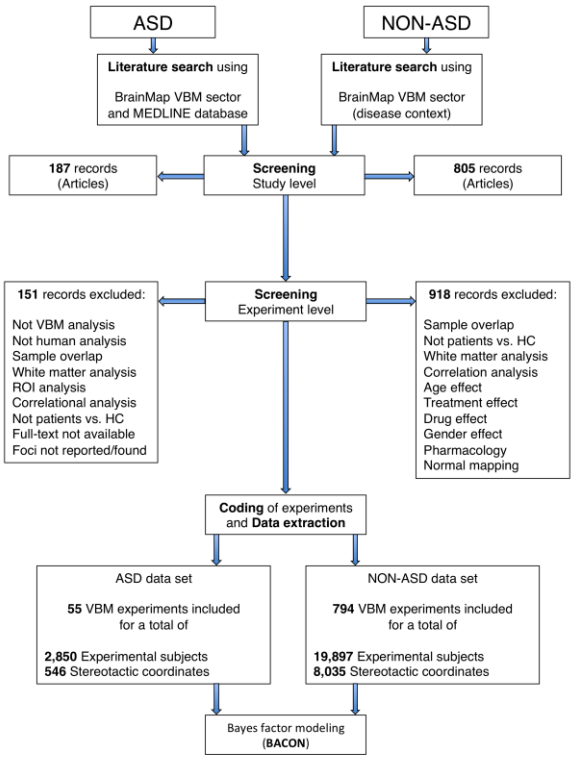

Figure 5.2. PRISMA flowchart: overview of literature selection and coding organization of meta-data.

5.3.1. Selective structural alteration profile of ASD

Our *reverse inference* voxel-wise approach revealed both cortical and cerebellar areas of GM alteration selectivity in ASD. In particular, taking into account a selectivity value of 90% (i.e., map thresholded at p $(ASD|alteration) \geq .90$), eight clusters showed a k size > 100 mm^3 (Fig. 5.3 and Table 5.1). A graphical representation of the results thresholded at different levels of posterior probability is shown in Fig. S5.1. The peak reporting (highest percentage) of morphometric alteration selectivity (i.e., 98%; p $(ASD|alteration) = .98$) was found in the right inferior occipital gyrus (R-IOG; Brodmann area - BA 18), which is part of the largest alteration cluster, along with the right lobule VI of the cerebellum (declive). Other high values of selectivity were found bilaterally in the posterior cerebellar lobes, encompassing the left lobule IX (p = .97), left Crus II (pyramis; p = .97), right Crus I (culmen; p = .96), and the right lobule VIIIA (p = .93). High values were also exhibited by three clusters located bilaterally in the precuneus (PCUNs - BAs 7; p > .92).

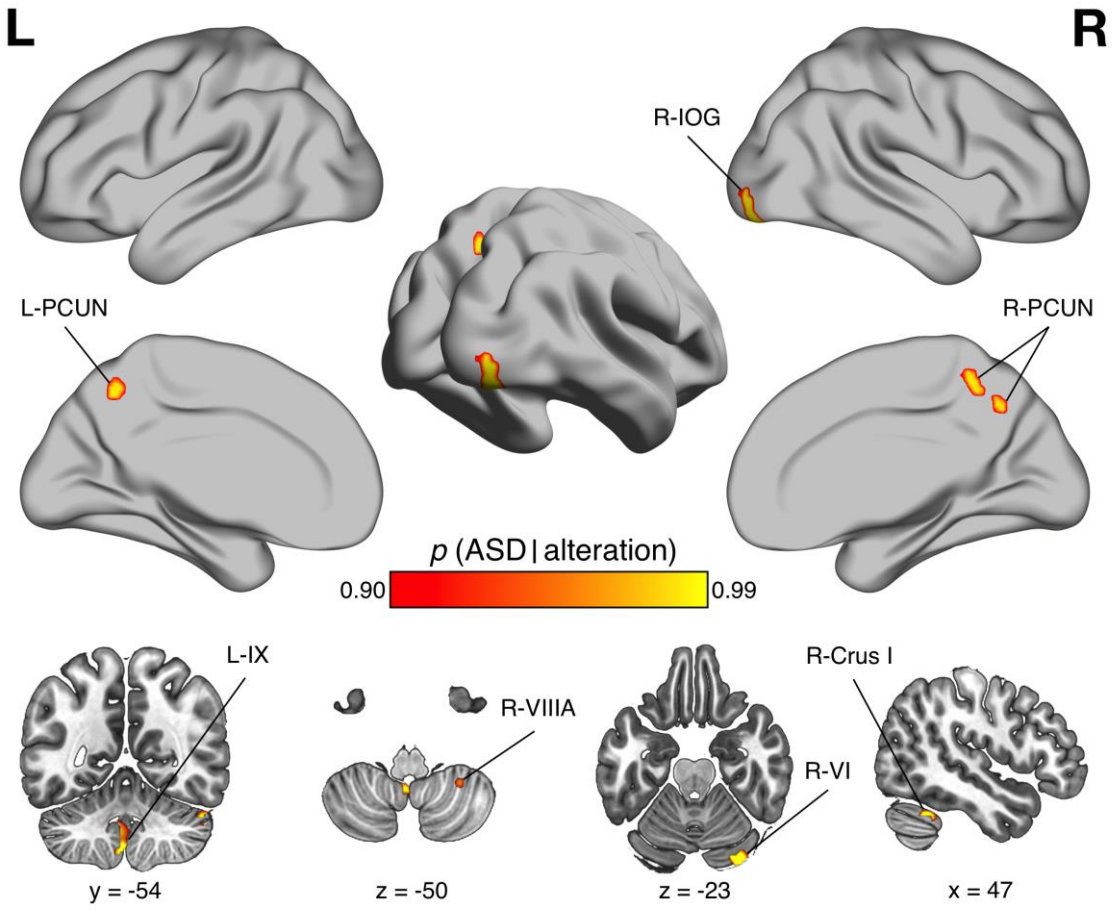

Figure 5.3. Brain clusters of selective gray matter alteration in autism spectrum disorder

(ASD) derived from Bayes factor modeling (BACON) analysis and thresholded at $p(ASD|alteration) = 0.9$ (90%). BACON map is visualized as hemispheric surfaces (3-D cortical view) and coronal/axial/sagittal slices (2-D cortical and cerebellar view). Templates are in neurological convention (L is left; R is right).

IOG; inferior frontal gyrus; PCUN, precuneus; L-IX, lobule IX (cerebellar tonsil); VIIIA, lobule VIIIA; VI, lobule VI (declive); Crus I, Crus I (culmen).

5.3.2. Functional characterization

Most of the ASD-selective volumes fell within the DMN according to the Yeo's parcellation (2011), followed by the visual network, SN/VAN, and FPN. For other networks, no volume of alteration was found at this probability threshold. Detailed representation of the results of network decomposition thresholded at different levels of posterior probability is provided in Table S5.8.

5.3.3. Robustness testing

The Fail-Safe analysis suggests that our findings are sound, as they very well resist injections of contra-evidence data performed concurrently on two datasets (Table 5.1). The percentage of random experiments that could be added without altering the appearance of the alteration peaks ranged from 10% for cluster 5 (R-PCUN) to more than 30% for several brain areas, encompassing the cerebellar regions and the R-IOG. In each case, all identified peaks survived at a 6% injection of noise, corresponding to the missing contrasts estimated for the BrainMap database (Gray et al., 2020).

The leave-one-out analysis showed that the main results were highly robust against the deletion of individual experiments with ABIDE subjects, as the eight clusters were preserved in all combinations of the dataset (Table S5.9).

Table 5.1. Clusters of gray matter alteration selectivity in autism spectrum disorder (ASD) derived from the Bayes factor modeling (BACON) analysis and thresholded at $p(ASD|alteration) = 0.9\ (90\%)$. For each cluster obtained, anatomical location (Talairach Daemon Atlas), stereotactic coordinates, cluster size, BACON value and Fail-Safe results were provided.

	Lobe	Brain Region (Local Maxima)	Talairach			Cluster	BACON Value		Robustness
			x	y	z	Size (mm^3)	Maximum	Minimum	(Fail-Safe)
1	Right Occipital	Inferior Occipital Gyrus (BA 18)	30	-86	-15	1,197	.9868	.90004	> 30%
2	Left Cerebellar	Lobule IX (Tonsil)	-4	-53	-42	640	.97371	.90013	> 30%
3	Right Cerebellar	Crus I (Culmen)	47	-50	-30	421	.96917	.90001	> 30%
4	Left Cerebellar	Crus II (Pyramis)	-2	-83	-31	273	.97031	.90005	> 30%
5	Right Parietal	Precuneus (BA 7)	6	-60	44	201	.92559	.90001	20% > FS > 10%
6	Right Parietal	Precuneus (BA 7)	8	-48	52	140	.93446	.90018	30% > FS > 20%
7	Left Parietal	Precuneus (BA 7)	-8	-58	50	126	.94660	.90015	30% > FS > 20%
8	Right Cerebellar	Lobule VIIIA	30	-50	-50	112	.93605	.90029	> 30%

5.3.4. Contribution of participant age and type of alteration to findings

According to the BF analysis, both the ASD age-stratified groups contribute to the observed BACON findings. The pediatric data exert strong (BF = 10.7), very strong (BF = 30.1) and extreme (BF > 100) evidences on the R-IOG, L-Crus II and L-Lobule IX results, respectively. The adult data exert extreme evidence on the R-Crus I result (BF < .01). The R-Lobule VIIIA shows a BF index around 1, corresponding to the 'no evidence' category. Voxels in the precuneus clusters report a BF index ranging from < .01 to 52, corresponding to extreme/very strong evidence for both pediatric and adult data. This result suggests that foci of both groups, and/or of the experiments with mixed-age ASD subjects, contribute to clusters 5-8.

With regard to the alteration-related analysis, we found that the GM decrease data exert extreme evidences on the L-Lobule IX, R-Crus I and R-PCUN (cluster 5) results. The R-Lobule VIIIA shows a BF index = 32.7, corresponding to a very strong evidence for the GM decrease contribution. The GM increase data exert very strong evidence on the L-Crus II results (BF = 0.018). Voxels in the R-IOG, L-PCUN and R-PCUN (cluster 6) report a BF index ranging from 36 to 0.06, suggesting that both types of alteration contribute to these

clusters.

5.4. Discussion

The current study is the first to reveal the selective GM alteration profile of autism spectrum disorder. We used peer-reviewed VBM data from 22,304 clinical subjects as the basis for our data-driven, whole-brain, and Bayesian analysis. Our CBMA approach shows multiple brain sites of disorder-differentiated morphometric alteration in ASD compared with 131 other clinical conditions. Functional characterization of these abnormalities suggests a significant involvement of the posterior components of the DMN, or medial frontoparietal network (Uddin et al., 2019).

Since Poldrack's seminal paper (Poldrack, 2006), *reverse inference* approaches in neuroimaging research have been employed to estimate the likelihood of a certain cognitive process from a specific pattern of brain activity. Here we shifted the objective, inferring the likelihood of a brain disorder of interest from a specific pattern of brain structural alteration. Our analysis shows that neural territories with high probability of alteration selectivity in ASD exist and tend to concentrate in posterior brain sites. By contrast, other regions that are generally considered neuroanatomical markers of this psychiatric spectrum (e.g., thalamus, prefrontal, superior temporal, insular, and cingulate cortex) (Lukito et al., 2020) exhibit no selectivity voxels at p $(ASD|alteration) \geq .90$, suggesting that these sites are affected not only by ASD, but also by other brain disorders (Cauda et al., 2019b). Note that the present findings accord well with a recent line of research, whereby areas classified as "hub nodes" of the human connectome are generally more susceptible to psychopathology (Buckholtz and Meyer-Lindenberg, 2012; Crossley et al., 2014; Goodkind et al., 2015; McTeague et al., 2017; McTeague et al., 2020; van den Heuvel and Sporns, 2019); as a consequence, alterations of these regions are scarcely informative about the specific development and impact of a single disorder *per se* (Cauda et al., 2020b; Cauda et al., 2019b; Liloia et al., 2018).

The R-IOG exhibits the highest value of alteration selectivity. Abnormal morphometric increases and decreases of this area have been consistently linked to different cohorts of children with ASD (Bonilha et al., 2008; Riva et al., 2013; Zielinski et al., 2014). This is in line with our BF results. Altered functional connectivity of this area has been also documented (Bi et al., 2018; Long et al., 2016). This result is significant, given that the R-IOG does not have an established role in current models of autistic pathophysiology. The IOG

is conventionally related to primary-level sensory aberrations in ASD (Samson et al., 2012). However, a number of studies are now challenging this view, highlighting instead a central role of visual association circuitry in socio-communicative-emotional impairments that are characteristic of ASD (Hadjikhani et al., 2007; Jou et al., 2011; Koshino et al., 2008; Lombardo et al., 2019; Pierce et al., 2004). Convincing evidence now points to the R-IOG being a key brain region involved in ASD and shows that variation in neuroanatomical and functional metrics may be highly relevant to various aspects of the core functional impairments of the spectrum. Further research is needed to directly address this issue, for example by adopting our coordinates as regions-of-interest for structural and functional analyses of pediatric ASD cohorts.

BACON also revealed a selective involvement of the posteromedial parietal cortex in the autistic brain landscape. Three clusters bilaterally encompassing the precuneus (BAs 7) were identified. This is consistent with sMRI investigations over the past 20 years, which show abnormalities in neuronal volume/concentration, thickness and cortical organization of this multimodal region across the lifespan in ASD (Bonilha et al., 2008; Ecker et al., 2013; Foster et al., 2015; Jiao et al., 2010; McAlonan et al., 2005; McAlonan et al., 2002; Riva et al., 2011; Uddin et al., 2011).

Although Brodmann's cytoarchitectonic mapping classified the PCUN as a unitary structure (i.e., medial area 7; Brodmann, 2007), evidence from MRI studies suggests differentiated patterns of functional connectivity associated with anterior, central and posterior subparts of the BA 7 (Margulies et al., 2009). Our functional decomposition reveals that the identified clusters are mainly located in the central portion of the posteromedial cortex, which is functionally associated with the DMN. It is thus not surprising that this region has a pivotal role in ASD pathophysiology and behavioral manifestations (Burrows et al., 2016): it has been related in different age-stratified ASD groups to impairments of social cognition (Patriquin et al., 2016), moral reasoning (Schneider et al., 2012), self-involvement ability (Just et al., 2014), emotion processing (Wang et al., 2004), self-referential cognition and empathy (Schulte-Rüther et al., 2011), as well as to symptom severity (Cheng et al., 2017; Rolls et al., 2020), and to decreased functional connectivity (Jann et al., 2015; Li et al., 2019d; Lynch et al., 2013; Weng et al., 2010). The present results are also reminiscent of those we have recently obtained using a VBM connectomics analysis (Liloia et al., 2021b), which showed a pathological *hubness* position of the PCUN in the morphometric alteration

network of ASD. In sum, the selective involvement of the bilateral central PCUN is a notable finding for both past and future research investigating this cerebral subregion's role in autism, highlighting at the same time the importance of precise anatomical methods in clinical sMRI.

Another finding of this study is that most alteration selectivity results at p $(ASD|alteration) \geq .90$ are in the bilateral posterior lobe of cerebellum. We found a double cluster in the left hemisphere encompassing lobule IX and Crus II, sites that have been correlated with communication-interaction deficits and observed to be altered in volume in children/adolescents with ASD (Becker and Stoodley, 2013; Cauda et al., 2011; Liu et al., 2017; Riva et al., 2013). This is in agreement with our BF analysis, suggesting a decisive contribution of pediatric data to the current results. Lobule IX and Crus II are both involved in social cognition and mentalizing tasks (Becker and Stoodley, 2013; Klucharev et al., 2009; Van Overwalle et al., 2020); they maintain functional connections with prefrontal and temporoparietal nodes of the DMN and areas considered to be part of the social brain network (D'Mello and Stoodley, 2015; Pantelis et al., 2015).

We also found voxels of selective alteration in the right cerebellum, including areas that are associated with different symptomatic features of the disorder. For example, changes in the volume of Purkinje cells in Lobule VIIIA are related to deficits in language function (D'Mello et al., 2016), social interaction, stereotyped behaviors and restricted interests (D'Mello et al., 2015). We identified voxels of alteration at the level of Crus I. In line with previous ASD research (Cauda et al., 2011), the BF analysis suggested that this subunit of Lobule VII shows GM volumetric decreases. Although the largest part of this area is associated with the DMN, our network decomposition suggests that the Crus I cluster correlates with the SN/VAN (Buckner et al., 2011), whose cortical nodes (i.e., anterior insula and dorsal ACC) are significantly associated with cognitive deficits and autistic traits in the neurotypical population (Di Martino et al., 2009; Tu et al., 2016; Uddin, 2015). Our results provide a new characterization of structural atypicalities in the autistic brain by identifying selective cerebellar markers, which are related to core aspects of ASD symptomatology.

5.4.1. Limitations

Several limitations should be considered when interpreting this work. The BrainMap database adopted for the creation of the non-ASD dataset may not correspond to the "real-world" distribution of brain disorders. Although there are no strong reasons to presume that

potential biases systematically impacted the reporting of experiments (Mancuso et al., 2020), one might argue against the generalizability and soundness of the findings. In addressing this, we performed the Fail-Safe analysis, which confirmed that our results are sound despite a substantial amount of contra-evidence data injection in both experimental datasets.

Although we assembled one of the largest VBM datasets, the design constraints of the original data hamper the possibility to discriminate possible differences related to clinical- or sex-stratified populations. In this regard, we point out that 36 out of 55 ASD experiments report findings associated with unspecified/mixed diagnoses. Also, over 84 % of the total experiments report a clinical sample composed of both male and female subjects. The meta-level approach embraced here was motivated by the interest in general neuroanatomical substrates of ASD in order to offer more reliable results in terms of generalization for the population of interest (Muller et al., 2018 Tahmasian et al., 2019).

Lastly, we note that 225 out of 849 VBM experiments report at least one focus of alteration in the cerebellum. Although no obvious biases were observed in our datasets (Table S5.10), we are unable to determine the amount of whole-brain published experiments where the cerebellum is neglected (entirely or in its inferior part) during the MRI scanning procedure. As this study demonstrates, the cerebellum plays a crucial role in the anatomy of brain disorders, and should be included in MRI scanning, as well as in subsequent analytic steps, in its entirety.

5.5. Conclusion

This study robustly pinpoints selective neuroanatomical patterns of alteration related to ASD in parietal, occipital and cerebellar brain regions. Considering the broad overlap between GM modifications associated with different brain disorders (Cauda et al., 2019b), this is a relevant result that may have potential clinical applications. Our results also objectively illustrate that the functional network associated with selective brain regions mainly corresponds with the DMN, further supporting the hypothesis that the alteration of posterior DMN components may be peculiar features of the ASD brain landscape (Liloia et al., 2021b). BACON can provide valuable insights into the understanding of ASD pathophysiology and, at the same time, opens new lines of research into the neuroanatomy of brain disorders.

5.6. Supplementary material

5.6.1. Supplementary methods

Data search strategy

A literature search was performed from inception to January 30, 2021, with no restrictions on publication year. First, BrainMap - VBM sector (http://brainmap.org/) (Vanasse et al., 2018) and MEDLINE (https://pubmed.ncbi.nlm.nih.gov/) databases were queried to identify voxel-based morphometry data related to subjects with autism spectrum disorder (ASD). The two searches were constructed as follow:

"ASD" BrainMap query (via Sleuth v.3.0.4 software package; Fox and Lancaster, 2002): (Diagnosis matches either is Autism spectrum disorders or is Asperger's Syndrome) "+" (Experiments context is disease effects) "+" (Experiments contrast is gray matter) "+" (Observed changes matches either controls > patients or controls < patients);

"ASD" MEDLINE query (via PubMed Advance Search Builder): ("Autism spectrum disorder" [title/abstract] OR "ASD" [title/abstract] OR "Autism" [title/abstract]) AND ("voxel-based morphometry" [title/abstract] OR "VBM" [title/abstract]);

Another standardized search was carried out on the BrainMap database to retrieve voxel-based morphometry data related to other conditions reporting appreciable gray matter changes and stored in the VBM sector (Vanasse et al., 2018).

"Non-ASD" BrainMap query (via Sleuth v.3.0.4 software package; Fox and Lancaster, 2002): (Diagnosis matches either is not Autism spectrum disorders or is not Asperger's Syndrome) "+" (Experiments context is disease effects) "+" (Experiments contrast is gray matter) "+" (Observed changes matches either controls > patients or controls < patients).

Of note, the search interface of the Sleuth software package organizes BrainMap's paradigm class entries in order to pool experiments of interest, rather than segregate them according to domain-specific keywords (Laird et al., 2009).

Fail-Safe analysis

The Fail-Safe is a statistical procedure that can be applied in both medical and psychological meta-analyses (Orwin, 1983). This technique has recently been adapted to the neuroimaging coordinate-based meta-analysis (CBMA) field in order to evaluate the robustness of results with regard to the "file-drawer" publication bias (Acar et al., 2018). The

Fail-Safe assumes the existence of unpublished experiments with opposite findings and estimates how many of contra-evidence results can be added to the CBMA before it is invalid. More specifically, the method makes increasing noise additions to the sample (i.e., unreported experiments) and evaluates the statistical robustness of the original result. In our case, the Fail-Safe has been employed to take into account the hypothesis that BrainMap does not store a quantity of contra-evidence experiments. We specifically applied the R code created by Acar et al. (2018) (https://github.com/NeuroStat/GenerateNull). Two phases form the analytic pipeline: noise generation and robustness estimation.

In the first phase, noise experiments are created. In doing this, the algorithm is limited by the distributions of x-y-z foci of alteration as well as by the number of the experimental subjects actually included in our sample. For example, if the experiments in our meta-analytic dataset reported between 1 and 30 foci, the noise experiments will also report between 1 and 30 foci. These constraints make the noise data more realistic. Subsequently, the foci positions are randomly derived from the same gray matter mask employed in the BACON analysis. This phase is independently repeated for every dataset (i.e., ASD and Non-ASD).

In the second phase, both the contra-evidence experiments and those of the original meta-analytic sample are combined and fed into the algorithm performing the activation likelihood estimation (ALE) (Eickhoff et al., 2016). Thus, this phase makes it possible to carry out CBMAs taking into consideration all the potential contrasting experiments that were not originally stored in our database. The procedure is repeated four times for every dataset of our study, each time by adding a greater amount of noise data (i.e., 6%, 10%, 20%, and 30%). For example, at 30% level, 17 and 239 noise experiments are added to the ASD dataset (55 experiments) and Non-ASD dataset (794 experiments), respectively. Subsequently, the couple of ALE maps obtained at each level are fed into BACON in order to understand the robustness of the findings, that is, to discover how much noise can be included before the peaks of alteration selectivity found by BACON vanish. To do so, a BACON map is finally calculated for every level of noise and compared with the original BACON map obtained before adding noise (a threshold of p $(ASD|alteration) \geq .90$ has been used for every map). In this way, the Fail-Safe permits assessment of the degree to which BACON results may be affected by a potential "file-drawer" publication bias.

5.6.2. Supplementary tables

Table S5.1. The evidence categories for the Bayes Factor (BF_{12}): Age-related contribution. Adapted from Jeffreys (1961).

BF_{12}	INTERPRETATION
>100	**Extreme evidence** for pediatric ($Group_1$)
30-100	**Very strong evidence** for pediatric ($Group_1$)
10-30	**Strong evidence** for pediatric ($Group_1$)
3-10	**Moderate evidence** for pediatric ($Group_1$)
1-3	**Anecdotal evidence** for pediatric ($Group_1$)
1	**No evidence**
1/3-1	**Anecdotal evidence** for adult ($Group_2$)
1/10-1/3	**Moderate evidence** for adult ($Group_2$)
1/30-1/10	**Strong evidence** for adult ($Group_2$)
1/100-1/30	**Very strong evidence** for adult ($Group_2$)
<1/100	**Extreme evidence** for adult ($Group_2$)

$Group_1$; ASD pediatric group (generated by grouping x-y-z foci related to ASD subjects with an age at scan < 18 years old); $Group_2$; ASD adult group (generated by grouping x-y-z foci related to ASD subjects with an age at scan ≥ 18 years old).

Table S5.2. The evidence categories for the Bayes Factor (BF_{12}): Alteration-related contribution. Adapted from Jeffreys (1961).

BF_{12}	INTERPRETATION
>100	**Extreme evidence** for GM decrease ($Group_1$)
30-100	**Very strong evidence** for GM decrease ($Group_1$)
10-30	**Strong evidence** for GM decrease ($Group_1$)
3-10	**Moderate evidence** for GM decrease ($Group_1$)
1-3	**Anecdotal evidence** for GM decrease ($Group_1$)
1	**No evidence**
1/3-1	**Anecdotal evidence** for GM increase ($Group_2$)
1/10-1/3	**Moderate evidence** for GM increase ($Group_2$)
1/30-1/10	**Strong evidence** for GM increase ($Group_2$)
1/100-1/30	**Very strong evidence** for GM increase ($Group_2$)
<1/100	**Extreme evidence** for GM increase ($Group_2$)

$Group_1$; ASD gray matter (GM) decrease group (generated by grouping x-y-z foci of GM decrease related to ASD subjects; ASD < Controls); $Group_2$; ASD gray matter (GM) increase group (generated by grouping x-y-z foci of GM increase related to ASD subjects; ASD > Controls).

Table S5.3. Experiments included in Bayes factor modeling analysis: ASD dataset.

ID	First Author	BrainMap or PMID ID	Medical Comorbidity	Age Group	Age, years (Range)	Subj (N)	Foci (N)
1	Abell et al. (1999)	12060002	0%	Mixed	29	15	9
2	Boddaert et al. (2004)	8060159	0%	Pediatric	9(7-15)	21	4
3	Bonilha et al. (2008)	11040085	25%	Pediatric	12(6-23)	12	69
4	Brieber et al. (2007)	10010005	0%	Pediatric	14(10-16)	15	8
5	Cai et al. (2018)	19120003	0%	Pediatric	10(5-16)	38	6
6	Calderoni et al. (2012)	12060003	0%	Pediatric	5(2-7)	38	1
7	Cheng et al. (2011)	12060004	0%	Pediatric	14(10-18)	11	17
8	Cheng et al. (2011)	12060004	0%	Pediatric	14(10-18)	12	4
9	Craig et al. (2007)	11080274	0%	Mixed	40	14	5
10	D'Mello et al. (2015)	25844317*	0%	Pediatric	10(8-13)	35	6
11	Ecker et al. (2010)	13100108	0%	Adult	27(18-42)	22	25
12	Ecker et al. (2012)	13100107	0%	Adult	26(18-43)	89	37
13	Eilam-Stock et al. (2016)	19120004	NR	Adult	27(18-64)	66	13
14	Foster et al. (2015)	19120005	0%	Pediatric	12(6-17)	38	47
15	Freitag et al. (2008)	19120006	0%	Mixed	18	15	1
16	Greimel et al. (2013)	19120006	4%	Mixed	21(10-50)	47	3
17	Hyde et al. (2010)	11040196	0%	Mixed	23(14-33)	15	11
18	Katz et al. (2017)	27105136*	0%	Adult	27(18-45)	23	2
19	Kaufman et al. (2013)	23117423*	0%	Mixed	15	10	3
20	Ke et al. (2008)	11040048	0%	Pediatric	9(6-14)	17	7
21	Kosaka et al. (2010)	10060044	0%	Mixed	24(17-32)	32	5
22	Kurth et al. (2011)	12060005	0%	Mixed	11(6-21)	52	1
23	Kwon et al. (2004)	8050081	0%	Pediatric	14(10-18)	11	3
24	Kwon et al. (2004)	8050081	0%	Pediatric	14(10-18)	9	2
25	Lai et al. (2013)	20070024	0%	Adult	28(18-49)	60	2
26	Lai et al. (2015)	25249409*	0%	Adult	24(18-41)	80	13
27	Lim et al. (2015)	19120014	0%	Pediatric	15	19	2
28	Lin et al. (2016)	27825394*	0%	Mixed	13(9-20)	18	1
29	McAlonan et al. (2002)	12060006	0%	Adult	32(18-49)	21	9
30	McAlonan et al. (2005)	12060007	0%	Pediatric	12(8-14)	17	13
31	McAlonan et al. (2008)	11040026	0%	Pediatric	12(7-16)	17	8
32	McAlonan et al. (2008)	11040026	0%	Pediatric	12(7-16)	16	4
33	Mengotti et al. (2011)	12060001	0%	Pediatric	7(4-14)	20	9
34	Muller et al. (2013)	19120018	0%	Mixed	36	12	14
35	Ni et al. (2018)	29129723*	0%	Pediatric	13(7-17)	53	9
36	Osipowicz et al. (2015)	25630444*	0%	Mixed	17(7-64)	531	17
37	Pappaianni et al. (2018)	28921735*	NR	Pediatric	10(8-12)	39	6
38	Pereira et al. (2018)	30042724*	0%	Mixed	18(14-25)	22	18
39	Radeloff et al. (2014)	25188200*	0%	Mixed	19(14-33)	34	5
40	Retico et al. (2016)	26788282*	0%	Pediatric	5(2-7)	76	9
41	Riddle et al. (2017)	26941174*	NR	Mixed	19	390	1

ID	First Author	BrainMap or PMID ID	Medical Comorbidity	Age Group	Age, years (Range)	Subj (N)	Foci (N)
42	Riedel et al. (2014)	24953998*	43% ///	Adult	35(21-52)	30	1
43	Riva et al. (2011)	12060008	0%	Pediatric	7(3-10)	21	12
44	Riva et al. (2013)	21700792*	0%	Pediatric	5(3-10)	26	13
45	Rojas et al. (2006)	17166273*	0%	Mixed	21(7-47)	24	13
46	Salmond et al. (2005)	8050117	0%	Pediatric	13(8-18)	14	18
47	Salmond et al. (2007)	12060009	0%	Pediatric	12(8-18)	26	10
48	Sato et al. (2018)	28824399*	0%	Adult	27(18-53)	36	19
49	Schmitz et al. (2006)	10060069	0%	Adult	38(18-50)	10	5
50	Toal et al. (2010)	12060010	0%	Mixed	32(16-59)	26	4
51	Toal et al. (2010)	12060010	0%	Mixed	30(16-59)	39	1
52	Waiter et al. (2004)	12060011	0%	Mixed	15(12-20)	16	14
53	Wang et al. (2017a)	19120023	0%	Pediatric	5(3-8)	31	2
54	Wilson et al. (2009)	30001226*	0%	Adult	30(22-47)	10	2
55	Yang et al. (2018)	19120025	NR	Pediatric	10	16	3

** For the articles non-included in the BrainMap, the PubMed identification number (PMID ID) was provided. ** For the articles including independent groups with the same main diagnosis, the specific subdiagnosis was provided.* ***ASD****, autism spectrum disorder;* ***Subj (N)****, number of subjects in the clinical group;* ***Foci (N)****, number of x-y-z coordinates of gray matter alteration.* ***NR****, data not reported. / 3 subjects with epileptic activity; // 1 subject with tic disorder; 1 subject with depressive disorder; /// 9 subjects with non-acute depression; 3 subjects with other psychiatric disorders (secondary to diagnosis of ASD).*

Table S5.4. Experiments included in Bayes factor modeling analysis: Non-ASD dataset.

ID	First Author	Year	BrainMap ID	Experimental group Diagnosis (vs. HC)*	Age, years (Range)	Subj (N)	Foci (N)
1	Abele M	2007	11040215	Spinocerebellar Ataxia	60	14	1
2	Adlam A L R	2006	8060152	Primary Progressive Aphasia	72(62-82)	7	6
3	Adleman N E	2012	17050001	Bipolar Disorder	14	55	3
4	Adler C M	2005	8050001	Bipolar Disorder	14	27	9
5	Adler C M	2007	8050002	Bipolar Disorder	20(13-41)	33	21
6	Agosta F	2007	8060153	Amyotrophic Lateral Sclerosis	54(27-75)	25	4
7	Agosta F	2010	13100084	Progressive Supranuclear Palsy	63(53-82)	20	16
8	Agosta F	2011	13100085	Alzheimer's Disease	75	23	32
9	Agosta F	2011	13100085	Mild Cognitive Impairment	70	15	1
10	Agostini A	2013	16030040	Crohn's Disease	32	18	4
11	Ahmed F	2012	14110027	Post-Traumatic Stress Disorder	16	21	3
12	Ahrendts J	2011	13100086	Attention Deficit Hyperactivity Disorder	31(18-55)	31	2
13	Alcauter S	2011	11080265	Spinocerebellar Ataxia	41(18-69)	9	65
14	Alemany S	2013	13120217	Major Depressive Disorder	34	12	4
15	Almeida J R C	2009	9050086	Bipolar Disorder	32	27	2
16	Alonso-Lana S	2016	17050002	Bipolar Disorder	46	28	1
17	Altena E	2010	11040009	Insomnia Disorder	60(52-74)	24	3
18	Ambrosi E	2013	14050011	Bipolar Disorder	42	20	3
19	Amico F	2011	11080296	Major Depressive Disorder	31	33	1
20	Ananth H	2002	8050004	Schizophrenia	38	20	13
21	Antonini G	2004	8050005	Myotonic Dystrophy	33(20-55)	22	21
22	Antonova E	2005	8060154	Schizophrenia	41	40	6
23	Arnone D	2009	13100002	Major Depressive Disorder	31	25	5
24	Arnone D	2013	14120037	Major Depressive Disorder	31	39	5
25	As-Sanie S	2012	13110201	Endometriosis (With Pain)	26	17	7
26	As-Sanie S	2012	13110201	Endometriosis (Without Pain)	26	15	4
27	As-Sanie S	2012	13110201	Chronic Pelvic Pain Syndrome	37	6	1
28	Asami T	2009	11040040	Panic Disorder	33	24	14
29	Ash S	2011	13100089	Dementia with Lewy Bodies	74	11	43
30	Ash S	2009	13100090	Progressive Non-Fluent Aphasia	71	6	3
31	Ash S	2009	13100090	Semantic Dementia	67	7	3
32	Ash S	2009	13100090	Frontotemporal Dementia	67	9	7
33	Aubert-Broche B	2011	16010003	Multiple Sclerosis	15(10-18)	30	4
34	Audoin B	2006	8050006	Multiple Sclerosis	36(27-55)	21	1
35	Audoin B	2010	10060033	Clinical Isolated Syndrome	29	62	26
36	Aydin K	2009	11040187	Subacute Sclerosing Panencephalitis	10(7-14)	17	11
37	Baldeweg T	2006	11080292	Sickle Cell Disease (With Lesions)	18	16	1
38	Baldeweg T	2006	11080292	Sickle Cell Disease (Without Lesions)	17	20	1
39	Barad M J	2013	16030041	Complex Regional Pain Syndrome	44(20-68)	15	9
40	Barbeau E	2008	11040158	Mild Cognitive Impairment (Normal DMS48 Performance)	72	12	17
41	Barbeau E	2008	11040158	Mild Cognitive Impairment	67	16	13

				(Impaired DMS48 Performance)			
ID	**First Author**	**Year**	**BrainMap ID**	**Experimental group Diagnosis (vs. HC)***	**Age, years (Range)**	**Subj (N)**	**Foci (N)**
42	Baron J C	2001	8050007	Alzheimer's Disease	73(63-85)	19	14
43	Barros-Loscertales A	2011	11080268	Substance Abuse	33	20	2
44	Bassitt D P	2007	8090152	Schizophrenia	32(18-50)	30	5
45	Baxter L C	2006	8050011	Alzheimer's Disease	76(64-91)	15	6
46	Beacher F D	2009	11040065	Neurocardiogenic Syncope	29	18	3
47	Beal D S	2007	11040010	Developmental Stuttering	30	26	5
48	Bell-McGinty S	2005	8060155	Mild Cognitive Impairment (Converters)	76(73-78)	9	7
49	Bell-McGinty S	2005	8060155	Mild Cognitive Impairment (Non-Converters)	72(66-78)	28	10
50	Belton E	2003	8060156	Verbal/Orofacial Dyspraxia	18(9-21)	10	9
51	Bergé D	2011	11080269	Schizophrenia	25	20	2
52	Berlingeri M	2008	12070013	Alzheimer's Disease	76	21	16
53	Bernasconi N	2004	8050013	Temporal Lobe Epilepsy (Left-Sided)	35(16-54)	45	26
54	Bernasconi N	2004	8050013	Temporal Lobe Epilepsy (Right-Sided)	35(16-54)	40	13
55	Bertsch K	2013	15090036	Antisocial Personality Disorder (With Borderline Personality Disorder)	29(18-54)	13	20
56	Bertsch K	2013	15090036	Antisocial Personality Disorder (Without Borderline Personality Disorder)	27(18-54)	12	30
57	Betting L E	2006	8050015	Idiopathic Generalized Epilepsy	32(18-63)	24	6
58	Betting L E	2010	11050260	Idiopathic Generalized Epilepsy	27(10-62)	17	44
59	Beyer M K	2007	8050016	Parkinson's Desease	77	16	18
60	Bitter T	2010	10060034	Anosmia	40(19-64)	17	35
61	Bitter T	2010	11040084	Hyposmia	43(18-55)	24	15
62	Bitter T	2010	11040084	Hyposmia (Sinunasal)	41	17	12
63	Bitter T	2011	11080271	Parosmia	54	22	1
64	Biundo R	2011	13100192	Parkinson's Disease	61	57	4
65	Boccardi M	2005	13100092	Frontotemporal Dementia	56	9	19
66	Boddaert N	2004	8050020	Smith Magenis Syndrome	13(12-17)	5	4
67	Bodini B	2009	11040159	Multiple Sclerosis	44	35	16
68	Boghi A	2011	13100004	Anorexia Nervosa	36(27-54)	21	19
69	Bonath B	2018	19120002	Attention Deficit Hyperactivity Disorder	13(11-17)	18	12
70	Bonavita S	2011	16030013	Multiple Sclerosis	41	36	24
71	Bonekamp D	2010	10030025	Mild Cognitive Impairment	73	10	1
72	Bonilha L	2004	8050021	Temporal Lobe Epilepsy (Right Lobe)	32(17-55)	21	14
73	Bonilha L	2004	8050021	Temporal Lobe Epilepsy (Left Lobe)	38(18-54)	22	20
74	Bonilha L	2008	11040111	Schizophrenia	40	13	9
75	Borgwardt S J	2007	13100005	At-Risk of Mental State	24	35	7
76	Borgwardt S J	2007	14010001	At-Risk of Mental State	25	12	9
77	Borgwardt S J	2010	13100093	Schizophrenia (With Family History)	38	28	11
78	Borgwardt S J	2010	13100093	Schizophrenia (Without Family History)	33	9	10
79	Borroni B	2008	11040066	Corticobasal Degeneration Syndrome	63	20	14
80	Bose S K	2009	13100094	Schizophrenia	40(27-65)	33	3
81	Bouilleret V	2008	11040160	Temporal Lobe Epilepsy	32(18-56)	12	12
82	Boxer A L	2003	8050023	Alzheimer's Disease	70	11	3
83	Boxer A L	2003	8050023	Semantic Dementia	66	11	4

ID	First Author	Year	BrainMap ID	Experimental group Diagnosis (vs. HC)*	Age, years (Range)	Subj (N)	Foci (N)
84	Boxer A L	2006	8060161	Corticobasal Degeneration Syndrome	65	14	11
85	Boxer A L	2006	8060161	Progressive Supranuclear Palsy	71	15	8
86	Bozzali M	2006	10010013	Alzheimer's Disease	70	22	19
87	Bozzali M	2006	10010013	Mild Cognitive Impairment (Converter)	68	14	14
88	Bozzali M	2006	10010013	Mild Cognitive Impairment (Non-converter)	71	8	2
89	Brambati S M	2004	8050024	Dyslexia	32(13-57)	10	9
90	Brambati S M	2009	14070012	Semantic Dementia (Left Temporal Lobe Variant)	65(35-95)	13	15
91	Brambati S M	2009	14070012	Semantic Dementia (Right Temporal Lobe Variant)	65(35-95)	6	15
92	Brazdil M	2009	10030016	Temporal Lobe Epilepsy	39(17-55)	20	9
93	Brenneis C	2004	8050025	Progressive Supranuclear Palsy	68	12	12
94	Brenneis C	2003	8050027	Multiple System Atrophy	62	12	16
95	Brenneis C	2006	8050028	Multiple-system Atrophy (Cerebellar Variant)	61	13	16
96	Brenneis C	2006	8050028	Spinocerebellar Ataxia	51	22	15
97	Brenneis C	2003	8050029	Spinocerebellar Ataxia	NR	9	15
98	Brenneis C	2004	8050030	Dementia with Lewy Bodies	70	10	7
99	Brenneis C	2004	8050030	Alzheimer's Disease	73	10	14
100	Brenneis C	2005	8050031	Narcolepsy	35	12	3
101	Brieber S	2007	10010005	Attention Deficit Hyperactivity Disorder	NA	15	15
102	Brooks S J	2011	13100007	Anorexia Nervosa	26	14	6
103	Brooks S J	2013	18100012	Obesity	75	59	1
104	Brown G G	2011	15080026	Schizophrenia	44(25-70)	17	9
105	Brown G G	2011	15080026	Bipolar Disorder	46(25-70)	17	19
106	Brown W E	2001	8050033	Dyslexia	24(18-40)	16	8
107	Brunner R	2010	11040043	Borderline Personality Disorder	17(14-18)	20	3
108	Brys M	2009	11040113	Alzheimer's Disease	70	8	9
109	Burton E J	2002	9010001	Dementia with Lewy Bodies	72	25	29
110	Burton E J	2004	11040044	Parkinson's Disease (With Dementia)	78	26	37
111	Burton E J	2004	11040044	Parkinson's Disease (Without Dementia)	75	31	8
112	Butler C R	2009	9050019	Amnesia	40	20	7
113	Cai Y	2015	15080027	Major Depressive Disorder	30(18-45)	23	1
114	Cai Y	2015	15080027	Bipolar Disorder	26(18-45)	23	2
115	Calhoun V D	2006	8050037	Schizophrenia	37	15	33
116	Camicioli R	2009	13100096	Parkinson's disease	71	43	3
117	Canessa N	2011	13100097	Obstructive Sleep Apnea	42	17	6
118	Canu E	2010	11080297	Alzheimer's Disease (Late Onset)	78	24	22
119	Canu E	2010	11080297	Alzheimer's Disease (Early Onset)	76	18	15
120	Carmona S	2005	8060164	Attention Deficit Hyperactivity Disorder	11	25	17
121	Caroli A	2007	15010013	Alzheimer's Disease	69(62-76)	9	5
122	Caroli A	2007	15010013	Mild Cognitive Impairment	69	14	2
123	Carrion V G	2009	13100098	Post-Traumatic Stress Disorder	NR(7-14)	24	4
124	Cascella N	2010	11040228	Schizophrenia (Deficit)	35	19	24
125	Cascella N	2010	11040228	Schizophrenia (Non-Deficit)	44	31	15
126	Castro-Fornieles J	2009	9050023	Anorexia Nervosa	15(11-17)	12	5

ID	First Author	Year	BrainMap ID	Experimental group Diagnosis (vs. HC)*	Age, years (Range)	Subj (N)	Foci (N)
127	Castro-Manglano P	2011	13100191	First-Episode Psychosis (Non-Affective)	19	10	13
128	Castro-Manglano P	2011	13100191	First-Episode Psychosis (Affective)	19	18	10
129	Ceccarelli A	2009	13100099	Multiple Sclerosis	50(38-73)	18	3
130	Ceccarelli A	2008	16030058	Multiple Sclerosis (Benign)	42	19	2
131	Ceccarelli A	2008	16030058	Multiple Sclerosis (Relapsing Remitting)	33	15	2
132	Ceko M	2013	16030043	Fibromyalgia (Older)	55(51-60)	14	14
133	Ceko M	2013	16030043	Fibromyalgia (Younger)	42(29-49)	14	9
134	Celle S	2010	11040114	Restless Legs Syndrome	66	17	3
135	Cerasa A	2013	16030014	Multiple Sclerosis (Without Cerebellar Signs)	39	14	2
136	Cerasa A	2013	16030014	Multiple Sclerosis (With Cerebellar Signs)	39	12	6
137	Chan C H	2006	8050038	Childhood Absence Epilepsy	18(9-27)	13	5
138	Chaney A	2014	14120038	Major Depressive Disorder	40(26-64)	17	4
139	Chang C C	2009	11040116	Multiple System Atrophy (Cerebellar Variant)	57	10	11
140	Chang C C	2009	11040116	Multiple System Atrophy (Parkinsonian Variant)	60	13	6
141	Chang J L	2005	8060166	Amyotrophic Lateral Sclerosis	49	20	14
142	Chang S E	2008	11040013	Childhood-Onset Fluency Disorder	11(9-12)	7	14
143	Chanraud S	2007	8050039	Substance Abuse	48	31	10
144	Chanraud S	2009	11040189	Substance Abuse	48	24	14
145	Chao L L	2012	14110028	Post-Traumatic Stress Disorder (Medicated)	35	17	3
146	Chao L L	2012	14110028	Post-Traumatic Stress Disorder (Unmedicated)	35	15	2
147	Chen S	2006	8050042	Post-Traumatic Stress Disorder	35	12	4
148	Chen S	2009	11040190	Post-Traumatic Stress Disorder	35	12	3
149	Chen X	2007	8050040	Bipolar Disorder (Family Hisory)	38(19-59)	24	2
150	Chen X	2007	8050040	Bipolar Disorder (Without Family Hisory)	38(19-59)	24	5
151	Chen Y	2012	14110029	Post-Traumatic Stress Disorder	41	10	1
152	Chen Z	2012	15080028	Bipolar Disorder	32	27	4
153	Cheng B	2015	16010005	Post-Traumatic Stress Disorder	26	30	3
154	Cheng Y	2010	13100014	Major Depressive Disorder	30	68	1
155	Chetelat G	2002	8050043	Mild Cognitive Impairment	71(55-87)	22	10
156	Chetelat G	2002	8050043	Alzheimer's Disease	72(63-85)	16	15
157	Christian C J	2008	9050025	Obsessive Compulsive Disorder	38	14	4
158	Chua S E	2007	11080293	First-Episode Psychosis	32	26	10
159	Chua S E	2007	11080293	Schizophrenia	32	26	10
160	Clausi S	2009	11040191	Right Cerebellar Damage	57(42-71)	8	9
161	Coan A C	2009	11040088	Temporal Lobe Epilepsy (Left-Sided)	37(16-49)	20	15
162	Coan A C	2009	11040088	Temporal Lobe Epilepsy (Right-Sided)	43(32-64)	13	11
163	Compta Y	2012	13100193	Parkinson's disease (With Dementia)	73(65-78)	15	12
164	Compta Y	2012	13100193	Parkinson's disease (Without dementia)	69(65-75)	18	5
165	Cooke M A	2008	11040068	Schizophrenia	38(19-61)	30	2
166	Corbo V	2005	8050044	Post-Traumatic Stress Disorder	33	14	5
167	Cordato N J	2005	8050045	Progressive Supranuclear Palsy	70	21	9
168	Cordato N J	2005	8050045	Parkinson's Desease	68	17	1
169	Cormack F	2005	8090163	Mesial Temporal Sclerosis (Left)	12(7-18)	20	9

ID	First Author	Year	BrainMap ID	Experimental group Diagnosis (vs. HC)*	Age, years (Range)	Subj (N)	Foci (N)
170	Cormack F	2005	8090163	Mesial Temporal Sclerosis (Right)	12(7-17)	10	7
171	Cosottini M	2012	13100102	Amyotrophic Lateral Sclerosis	58	20	21
172	Critchley H D	2003	8050046	Pure Autnomic Failure	62(42-79)	15	10
173	Cui L	2011	11080308	Bipolar Mania	28	24	9
174	Cui L	2011	11080308	Schizophrenia	25	23	3
175	Curie A	2009	9050026	Intellectual disability	33	5	3
176	D'Agata F	2011	13100103	Spinocerebellar Ataxia	48	12	19
177	Dalwani M	2011	15090038	Conduct Disorder	17(14-18)	25	5
178	Dash S K	2018	18100010	Multiple System Atrophy	54(48-60)	30	4
179	Dash S K	2018	18100010	Multiple System Atrophy (Without Cerebellar Atrophy)	56(51-61)	20	4
180	Davis K D	2007	16030044	Irritable Bowel Syndrome	NR(30-58)	9	2
181	De Araujo-Filho G M	2009	13100190	Juvenile Myoclonic Epilepsy	27	54	8
182	De Brito S A	2009	11040089	Conduct Disorder (Callous Traits)	11(10-13)	23	12
183	De Brito S A	2009	11040089	Conduct Disorder (Unemotional Traits)	11(10-13)	23	21
184	De Oliveira-Souza R	2008	11040185	Antisocial Personality Disorder	32	15	22
185	Della Nave R	2008	9050027	Friedreich's Ataxia	46	22	2
186	Della Nave R	2008	11040117	Spinocerebellar Ataxia (Type 1)	46	10	7
187	Della Nave R	2008	11040117	Spinocerebellar Ataxia (Type 2)	46	10	5
188	Delmaire C	2007	11080275	Dystonia	48	30	6
189	Deng M Y	2009	14070015	Schizophrenia	29	10	11
190	Dermody N	2016	20070016	Alzheimer's Desease	66	25	4
191	Dermody N	2016	20070016	Frontotemporal Dementia	63	24	1
192	Desgranges B	2007	12070014	Semantic Dementia (Without Hypometabolism)	66(54-79)	10	6
193	Desgranges B	2007	12070014	Semantic Dementia (With Hypometabolism)	66(54-79)	10	2
194	Di Paola M	2007	8090166	Alzheimer's Desease	64(46-77)	18	18
195	Dickstein D P	2005	8050048	Bipolar Disorder	13(9-18)	20	3
196	Doris A	2004	13100105	Bipolar Disorder	41	11	33
197	Douaud G	2007	11080276	Schizophrenia	16(13-18)	25	23
198	Draganski B	2006	8050051	Limb Amputation	42(18-68)	28	2
199	Draganski B	2003	8050052	Dystonia	44	10	8
200	Ebdrup B H	2010	13100017	Schizophrenia (Substance Abuse)	26(18-37)	38	2
201	Ebdrup B H	2010	13100017	Schizophrenia (Non-Substance Abuse)	26(18-37)	38	4
202	Eckart C	2011	13100106	Post-Traumatic Stress Disorder	36	20	5
203	Eckert M A	2005	8060170	Dyslexia	10	13	5
204	Eckert M A	2006	8060171	Williams Syndrome	31	8	34
205	Egger K	2007	11080277	Dystonia	40	31	9
206	Ellis C M	2001	13100109	Amyotrophic Lateral Sclerosis	55	16	3
207	Eshaghi A	2014	16030018	Multiple Sclerosis	43(39-47)	36	6
208	Etgen T	2005	8060172	Restless Legs Syndrome (Regensburg Sample)	53	28	4
209	Etgen T	2005	8060172	Restless Legs Syndrome (Munich Sample)	59	23	4
210	Etgen T	2006	10060056	Blepharospasm	67	16	3
211	Euler M	2009	11040070	Schizophrenia	43(22-63)	19	12
212	Fahim C	2012	20060011	Oppositional Defiant Disorder	8	18	2

ID	First Author	Year	BrainMap ID	Experimental group Diagnosis (vs. HC)*	Age, years (Range)	Subj (N)	Foci (N)
213	Fairchild G	2011	15090039	Conduct Disorder (Early-Onset)	18(16-21)	27	10
214	Fairchild G	2011	15090039	Conduct Disorder (Adolescent-Onset)	18(16-20)	27	9
215	Fallon N	2013	16030045	Fibromyalgia	38	16	4
216	Farrow T F D	2007	13100110	Alzheimer's Disease (Early-State)	78(69-88)	7	10
217	Farrow T F D	2007	13100110	Alzheimer's Disease (Elderly-State)	78(69-88)	7	10
218	Farrow T F D	2005	10010007	Schizophrenia	NR(13-25)	22	19
219	Farrow T F D	2005	10010007	Bipolar Disorder	NR(14-20)	8	12
220	Feldmann A	2008	11040163	Posterior Cortical Atrophy	57	1	7
221	Feldmann A	2008	11040163	Alzheimer's Disease	61	6	11
222	Focke N K	2011	13060001	Parkinson's Disease	65	21	2
223	Frangou S	2012	17050003	Bipolar Disorder (Relatives)	48	48	1
224	Frangou S	2012	17050003	Bipolar Disorder	46	47	1
225	Friedrich H C	2012	13100020	Anorexia Nervosa (Without Weight-Restored)	25	12	8
226	Friedrich H C	2012	13100020	Anorexia Nervosa (With Weight-Restored)	24	13	2
227	Frisoni G B	2002	8090170	Alzheimer's Disease	74(53-86)	29	34
228	Frodl T	2008	13100021	Major Depressive Disorder	46	38	65
229	Fusar-Poli P	2011	14010002	At-Risk of Mental State	24	15	4
230	Fusar-Poli P	2011	14010003	At-Risk of Mental State	25	39	5
231	Gale S D	2005	8050053	Traumatic Brain Injury	29	9	16
232	Gao W	2013	17050004	Bipolar Disorder	15	18	1
233	Garcia-Marti G	2008	9080091	Schizophrenia	36(21-42)	17	5
234	Garraux G	2004	8050054	Dystonia	53	36	7
235	Garraux G	2006	8060178	Tourette's Syndrome	32	31	3
236	Garrido L	2009	11040091	Developmental Prosopagnosia	31(20-46)	17	11
237	Gaudio S	2011	13100024	Anorexia Nervosa	15(12-18)	15	3
238	Gavazzi C	2007	8050055	Huntington's Disease	56(45-67)	9	4
239	Gee J	2003	8050056	Alzheimer's Disease	71	12	7
240	Gee J	2003	8050056	Frontotemporal Dementia	65	29	11
241	Geha P Y	2008	13100112	Complex Regional Pain Syndrome	NR	26	1
242	Geha P Y	2008	13100112	Complex Regional Pain Syndrome	NR	11	1
243	Ghosh B C	2012	14050007	Progressive Supranuclear Palsy	71	23	2
244	Gilbert A R	2008	9050032	Obsessive Compulsive Disorder	38(27-62)	25	9
245	Ginestroni A	2008	9050034	Spinocerebellar Ataxia	46	15	4
246	Giordano A	2013	14050008	Progressive Supranuclear Palsy	69	15	6
247	Giuliani N R	2005	13100025	Schizophrenia	39	34	17
248	Gobbi C	2014	16030020	Multiple Sclerosis (Non-Depressed)	42	54	56
249	Gobbi C	2014	16030020	Multiple Sclerosis (Depressed)	42	69	56
250	Gobbi C	2014	16030020	Multiple Sclerosis (Non-Fatigued)	41	59	56
251	Gobbi C	2014	16030020	Multiple Sclerosis (Fatigued)	42	64	56
252	Goel G	2011	13100114	Spinocerebellar Ataxia (Chromosome 1)	35	12	11
253	Goel G	2011	13100114	Spinocerebellar Ataxia (Chromosome 2)	33	9	12
254	Goel G	2011	13100114	Spinocerebellar Ataxia (Chromosome 3)	38	10	14
255	Gold B T	2010	11040071	Mild Cognitive Impairment	77(72-88)	12	4

ID	First Author	Year	BrainMap ID	Experimental group Diagnosis (vs. HC)*	Age, years (Range)	Subj (N)	Foci (N)
256	Gong Q	2011	15070023	Depressive Disorder (Refractory)	40	23	7
257	Gong Q	2011	15070023	Depressive Disorder (Non-Refractory)	39	23	9
258	Gorno-Tempini M L	2006	8060186	Progressive Nonfluent Aphasia (Mute)	69	6	11
259	Gorno-Tempini M L	2006	8060186	Progressive Nonfluent Aphasia (Non-Mute)	62	5	7
260	Granert O	2011	13100117	Dystonia	43(28-73)	11	7
261	Gregory S	2012	15090040	Antisocial Personality Disorder and Psychopathy	39(20-50)	17	18
262	Grieve S M	2013	14120039	Major Depressive Disorder	34(18-65)	102	41
263	Gross R G	2010	10060039	Corticobasal Degeneration Syndrome	67	20	6
264	Grosskreutz J	2006	8050063	Amyotrophic Lateral Sclerosis	61(34-77)	17	16
265	Grossman M	2004	9050035	Corticobasal Degeneration Syndrome	64	9	9
266	Grossman M	2004	9050035	Semantic Dementia	65	8	4
267	Grossman M	2004	9050035	Progressive Non-Fluent Aphasia	69	7	6
268	Grossman M	2004	9050035	Frontotemporal Dementia	65	14	5
269	Guedj E	2009	14080019	Mild Cognitive Impairment	69(60-78)	19	7
270	Guo W	2014	14120050	Major Depressive Disorder (First-Episode)	28	24	1
271	Guo W	2014	14120050	Major Depressive Disorder (Recurrent)	28	21	1
272	Guo X	2010	11040119	Alzheimer's Disease	72(58-81)	13	16
273	Gurling H	2006	11080294	Schizophrenia	41	13	2
274	Gustin S M	2011	11080299	Trigeminal Nuropathic Pain	55(42-75)	21	7
275	Gwilym S E	2010	11020004	Osteoarthritis	68	16	14
276	Ha T H	2010	11040045	Bipolar Disorder (Type I)	35	23	18
277	Ha T H	2010	11040045	Bipolar Disorder (Type II)	25	24	7
278	Ha T H	2004	11040072	Schizophrenia	28	35	16
279	Hajek T	2015	15080029	At-Risk of Mental State (Halifax Sample)	19(15-26)	30	1
280	Hajek T	2015	15080029	Bipolar Disorder (Halifax Sample)	21(15-30)	21	1
281	Hajek T	2015	15080029	At-Risk of Mental State (Prague Sample)	20(15-30)	20	1
282	Hajek T	2015	15080029	Bipolar Disorder (Prague Sample)	22(15-30)	15	1
283	Hakamata Y	2007	11040195	Post-Traumatic Stress Disorder	46	14	2
284	Haldane M	2008	13100119	Bipolar Disorder	43	44	19
285	Hall A M	2008	11040017	Alzheimer's Disease (Converted)	83	21	2
286	Hall A M	2008	11040017	Alzheimer's Disease (Non-Converted)	83	26	2
287	Haller S	2011	15080030	Bipolar Disorder	69	19	1
288	Halpern C H	2004	8060190	Corticobasal Degeneration Syndrome	67	5	4
289	Halpern C H	2004	8060190	Semantic Dementia	68	3	1
290	Hamalainen A	2007	9010002	Alzheimer's Disease	73	15	19
291	Hamalainen A	2007	9010002	Mild Cognitive Impairment	72	14	6
292	Hamalainen A	2007	14080024	Mild Cognitive Impairment (Progressive)	72(68-76)	13	29
293	Hamalainen A	2007	14080024	Mild Cognitive Impairment (Stable)	72(68-76)	43	35
294	Han X	2017	17070010	Multiple Sclerosis	40	20	11
295	He N	2015	19120007	Attention Deficit Hyperactivity Disorder	10(7-16)	37	4
296	Henley S M	2009	11040122	Huntington's Disease	49	40	27
297	Henry R G	2008	9080093	Multiple Sclerosis	37	41	15
298	Herold R	2009	9050036	Schizophrenia	29	18	38

ID	First Author	Year	BrainMap ID	Experimental group Diagnosis (vs. HC)*	Age, years (Range)	Subj (N)	Foci (N)
299	Herringa R	2012	14110033	Post-Traumatic Stress Disorder	29	13	4
300	Hirao K	2006	8050067	Alzheimer's Disease	71(48-87)	61	2
301	Hirao K	2008	9050037	Schizophrenia	37	20	6
302	Holzapfel M	2006	8060194	Turner's Syndrome	16(7-24)	10	8
303	Honea R A	2009	11040123	Alzheimer's Disease	73	60	13
304	Honea R A	2008	10010008	At-Risk of Mental State	36	213	15
305	Honea R A	2008	10010008	Schizophrenia Spectrum Disorder	36	169	32
306	Horn H	2010	10060041	Schizophrenia	30	20	2
307	Horn H	2009	11040124	Schizophrenia	30	13	12
308	Hornyak M	2007	8060195	Restless Legs Syndrome	50	14	4
309	Horstmann A	2010	10030029	Cardiac Arrest	51(21-74)	12	28
310	Huang W	2011	15070020	Generalized Seizure Disorder	26	31	12
311	Huebner T	2008	11040094	Conduct Disorder	15(12-17)	23	4
312	Huey E D	2009	11040125	Corticobasal Degeneration Syndrome	66	48	19
313	Hufner K	2009	11040020	Unilateral Vestibular Deafferentation Syndrome	58	16	12
314	Hüfner K	2007	11040021	Idiopathic Downbeat Nystagmus	65(45-84)	11	7
315	Hulshoff Pol H E	2001	8060196	Schizophrenia	36(16-68)	158	27
316	Hulshoff Pol H E	2004	8060197	Schizophrenia	34(16-68)	158	10
317	Hwang J	2010	13100029	Major Depressive Disorder	79	70	5
318	Iannaccone R	2015	19120008	Attention Deficit Hyperactivity Disorder	15(12-16)	18	5
319	Inkster B	2011	13100031	Major Depressive Disorder	48	148	1
320	Isaacs E B	2003	8060198	Preterm/Low Birthweight	16	11	4
321	Ishii K	2005	10060059	Alzheimer's Disease	60	30	3
322	Ivo R	2013	16030046	Chronic Low Back Pain	54(41-73)	14	16
323	Jacobson S	2010	11040022	At-Risk of Mental State	13(11-13)	11	5
324	Jagger-Rickels A C	2018	19120001	Attention Deficit Hyperactivity Disorder	10(8-12)	41	15
325	Jagger-Rickels A C	2018	19120001	Reading Disability	10(8-12)	17	12
326	Jang D P	2007	11080278	Substance Abuse	44	20	12
327	Janssen J	2008	11040219	Psychosis	16(11-18)	25	3
328	Janssen J	2008	11040219	Bipolar Disorder	17(15-18)	20	1
329	Janssen J	2008	11040219	Schizophrenia	15(12-18)	25	2
330	Jauhiainen A M	2008	14080025	Mild Cognitive Impairment	78(73-83)	7	4
331	Jayakumar P N	2005	10060060	Schizophrenia	24	18	10
332	Job D E	2003	8060202	Schizophrenia	21	36	6
333	Johnston B A	2014	19120009	Attention Deficit Hyperactivity Disorder	13	34	12
334	Joo E Y	2010	11040127	Obstructive Sleep Apnea	45(31-56)	36	27
335	Joos A	2010	10060042	Anorexia Nervosa	NR(18-25)	12	7
336	Joubert S	2006	8050072	Frontotemporal Dementia	64(59-73)	3	7
337	Jurkiewicz M T	2006	8050073	Spinal Cord Injury	33	17	2
338	Kanda T	2008	9050040	Alzheimer's Desease	65	20	7
339	Kanda T	2008	9050040	Frontotemporal Dementia	65	13	9
340	Kappel V	2014	19120010	Attention Deficit Hyperactivity Disorder (Adults)	10	16	5
341	Kappel V	2014	19120010	Attention Deficit Hyperactivity Disorder (Children)	23	14	8

ID	First Author	Year	BrainMap ID	Experimental group Diagnosis (vs. HC)*	Age, years (Range)	Subj (N)	Foci (N)
342	Karlsson H	2014	18090003	Obesity	46	23	7
343	Kasai K	2008	12070015	Post-Traumatic Stress Disorder	52	18	7
344	Kasparek T	2007	8050074	Schizophrenia	24	18	7
345	Kassubek J	2005	11040221	Huntington's Disease	45(25-66)	44	2
346	Kassubek J	2007	11080280	Kennedy Disease	50	18	10
347	Kassubek J	2002	8090174	Temporal Lobe Epilepsy	31(14-51)	7	8
348	Kassubek J	2004	8050075	Huntington's Disease	45(26-66)	44	17
349	Kassubek J	2007	12070016	Spastic Paraparesis (Complicated Hereditary)	29	12	7
350	Kassubek J	2007	12070016	Spastic Paraparesis (Pure Hereditary)	49	21	5
351	Kato S	2012	13110214	Parkinson's Disease	64	9	11
352	Kaufmann C	2002	8050076	Narcolepsy	36(22-65)	12	19
353	Kawachi T	2006	8050077	Alzheimer's Disease	67	32	14
354	Kawada R	2009	11040129	Schizophrenia	36	26	13
355	Kawasaki Y	2004	11080309	Schizotypal Personality Disorder	26(18-36)	25	4
356	Kawasaki Y	2007	8050078	Schizophrenia	25	30	9
357	Kawasaki Y	2004	11080309	Schizophrenia	26(18-36)	25	19
358	Kawasaki Y	2008	15010009	Schizophrenia	27(18-45)	30	3
359	Keller S S	2002	8060206	Temporal Lobe Epilepsy (Left)	32(15-48)	58	22
360	Keller S S	2002	8060206	Temporal Lobe Epilepsy (Right)	34(20-49)	58	21
361	Keller S S	2007	8090175	Temporal Lobe Epilepsy (Seizures Free-Post Surgery)	30	10	4
362	Keller S S	2007	8090175	Temporal Lobe Epilepsy (Persistent Post-Surgical Seizures)	33	12	3
363	Kempton M J	2009	11040049	Bipolar Disorder	39	30	3
364	Kesler S R	2008	11040096	Preterm/Low Birthweight	12	10	3
365	Khaleeli Z	2007	16030022	Multiple Sclerosis	44(19-65)	46	7
366	Kim D	2013	15080031	Bipolar Disorder	34	49	3
367	Kim E J	2007	13100035	Frontotemporal Lobar Degeneration (Tau Positive)	68	6	7
368	Kim E J	2007	13100035	Frontotemporal Lobar Degeneration (Tau Negative)	60	8	8
369	Kim J H	2008	9050043	Migraine	34(15-53)	20	20
370	Kim J H	2007	11080281	Juvenile Myoclonic Epilepsy	23(16-35)	25	7
371	Kim J J	2001	13100128	Obsessive Compulsive Disorder	27	25	10
372	Kim M J	2008	11040168	Major Depressive Disorder	39(21-55)	22	4
373	Kim S	2011	13100127	Alzheimer's Disease	70	61	10
374	Kim S J	2009	11040050	Narcolepsy	25(17-35)	17	29
375	Kirchner H	2011	13100129	Ataxia	70	31	21
376	Kobel M	2010	13100130	Attention Deficit Hyperactivity Disorder	11(9-11)	14	1
377	Koenig P	2008	11050243	Alzheimer's Disease	77	6	8
378	Koenigkam-Santos M	2008	9050084	Kennedy Disease	38(11-60)	21	7
379	Koprivova J	2009	11040051	Obsessive Compulsive Disorder	29	14	30
380	Koskenkorva P	2009	11040052	Unverricht-Lundborg Disease	33(16-51)	34	10
381	Kostic V S	2010	13100197	Parkinson's Disease (Depressed)	66(50-78)	16	15
382	Kostic V S	2010	13100197	Parkinson's Disease (Non-Depressed)	65(54-79)	24	15
383	Koutsouleris N	2008	9050044	Schizophrenia (Negative Symptoms)	33	59	26

ID	First Author	Year	BrainMap ID	Experimental group Diagnosis (vs. HC)*	Age, years (Range)	Subj (N)	Foci (N)
384	Koutsouleris N	2008	9050044	Schizophrenia (Positive Symptoms)	33	61	20
385	Koutsouleris N	2008	9050044	Schizophrenia (Disorganized Symptoms)	29	55	16
386	Kozicky J M	2013	15080032	Bipolar Disorder	23(17-35)	41	1
387	Kroes M C W	2010	16040061	Post-Traumatic Stress Disorder/Major Depressive Disorder	38(25-57)	53	3
388	Kronbichler M	2008	11080295	Dyslexia	16(14-16)	13	9
389	Kubicki M	2002	8050079	Psychosis	24	16	2
390	Kubicki M	2002	8050079	Schizophrenia	26	16	9
391	Kuchinad A	2007	13110205	Fibromyagia	52	10	5
392	Kumar U	2017	19120011	Attention Deficit Hyperactivity Disorder	9(7-13)	18	4
393	Labate A	2010	11040074	Temporal Lobe Epilepsy (Mild)	35	19	3
394	Labate A	2010	11040074	Temporal Lobe Epilepsy (Refractory)	38	19	1
395	Ladoucer C D	2008	13100036	Bipolar Disorder	13	20	1
396	Lagarde J	2013	14050009	Progressive Supranuclear Palsy	66	19	5
397	Lagarde J	2013	14050009	Frontotemporal Dementia	69	16	8
398	Lai C H	2012	16080066	Panic Disorder	47	21	1
399	Lai C H	2015	17050006	Panic Disorder	43	53	2
400	Lai C H	2012	13100132	Panic Disorder	47	30	4
401	Lai C H	2010	13100037	Major Depressive Disorder	38	16	12
402	Lai C H	2015	17050006	Major Depressive Disorder	43	53	6
403	Lazaro L	2009	11040025	Obsessive Compulsive Disorder	14(9-17)	15	3
404	Lee H Y	2011	13100133	Major Depressive Disorder	46	47	21
405	Lee J E	2013	13110212	Parkinson's disease (Mild Cognitive Impairment Converters)	73	15	8
406	Lee J E	2013	13110212	Parkinson's disease (Mild Cognitive Impairment Non-Converters)	71	36	3
407	Lentini E	2020	20070025	Klinefelter's Syndrome (XXY) (Male)	39(21-55)	33	16
408	Lentini E	2020	20070025	Klinefelter's Syndrome (XXY) (Female)	39(21-55)	33	12
409	Li C T	2010	13100039	Major Depressive Disorder (Non-Remiting)	47	19	3
410	Li C T	2010	13100039	Major Depressive Disorder (Remitting)	43	25	3
411	Li L	2006	8050084	Post-Traumatic Stress Disorder	35	12	4
412	Li M	2011	13100135	Bipolar Disorder	27	22	5
413	Li X	2015	19120024	Attention Deficit Hyperactivity Disorder	10(8-14)	30	2
414	Liao M	2013	20070026	Anxiety Disorder	17	26	1
415	Libon D J	2009	13100040	Progressive Non-Fluent Aphasia	69	11	13
416	Libon D J	2009	13100040	Semantic Dementia	66	10	7
417	Libon D J	2009	13100040	Frontotemporal Lobar Degeneration	61	51	13
418	Lim L	2013	19120012	Attention Deficit Hyperactivity Disorder	14(10-18)	29	3
419	Lin A	2013	16030024	Multiple Sclerosis	39(21-59)	11	5
420	Lin C H	2013	13100196	Essential Tremor	67	10	22
421	Lin C H	2013	13100196	Parkinson's Disease	63	10	24
422	Lin K	2009	11040169	Juvenile Myoclonic Epilepsy (With Photosensitivity)	23	19	10
423	Lin K	2009	11040169	Juvenile Myoclonic Epilepsy (Without Photosensitivity)	28	41	10
424	Liu C H	2014	14120042	Major Depressive Disorder (Current Diagnosis)	35(18-65)	19	2
425	Liu C H	2014	14120042	Major Depressive Disorder (Previous history)	38(20-62)	19	1

ID	First Author	Year	BrainMap ID	Experimental group Diagnosis (vs. HC)*	Age, years (Range)	Subj (N)	Foci (N)
426	Liu M	2011	15070021	Generalized Seizure Disorder	21(18-31)	10	6
427	Liu M	2011	15070021	Juvenile Myoclonic Epilepsy	21(17-32)	15	5
428	Lochhead R A	2004	8050085	Bipolar Disorder	38	11	8
429	Lu C	2010	11040053	Developmental Stuttering	25(19-31)	12	11
430	Ludolph A G	2006	8060209	Tourette Syndrome	13	14	4
431	Lui S	2009	11040222	Schizophrenia	22	10	15
432	Lui S	2009	12070017	Schizophrenia	24	68	3
433	Lyoo I K	2004	8050086	Bipolar Disorder	38	39	4
434	Maeda Y	2013	16030047	Carpal Tunnel Syndrome	48	28	1
435	Maier S	2016	19120015	Attention Deficit Hyperactivity Disorder	34	131	1
436	Mak A K	2009	11040133	Major Depressive Disorder	46	17	18
437	Mallik S	2015	16060063	Multiple Sclerosis (Relapsing-Remitting)	42(21-64)	51	7
438	Mallik S	2015	16060063	Multiple Sclerosis (Secondary Progressive)	53(36-65)	28	4
439	Maneru C	2003	10060046	Hypoxic-Ischemic Encephalopathy	16	13	9
440	Mannerkoski M K	2009	11040199	Mental Retardation	12(5-29)	26	5
441	Marcelis M	2003	8060212	Psychosis	31	31	7
442	Marti-Bonmati L	2007	11080300	Schizophrenia	39(21-51)	10	8
443	Martikainen I K	2013	16030048	Chronic Back Pain	38(20-50)	16	3
444	Martino D	2011	13100138	Primary Blespharospasm	65(46-78)	25	11
445	Massana G	2003	8050087	Panic Disorder	37	18	1
446	Massimo L	2009	11040200	Frontotemporal Lobar Degeneration (Apathyic Disturbance)	63	9	22
447	Massimo L	2009	11040200	Frontotemporal Lobar Degeneration (Disinhibition Disturbance)	64	5	24
448	Matsuda H	2002	8090180	Alzheimer's Disease	71(59-81)	15	13
449	Matsumoto R	2010	13100139	Obsessive Compulsive Disorder	33	16	4
450	Matsunari I	2007	9050048	Alzheimer's Disease	69	27	9
451	May A	1999	8050089	Headache	47(25-74)	25	1
452	Mazere J	2008	13100140	Alzheimer's Disease	81	8	6
453	McAlonan G M	2007	13100043	Attention Deficit Hyperactivity Disorder	10(6-13)	28	8
454	McDonald C	2005	9010003	Schizophrenia	37(24-55)	25	12
455	McIntosh A M	2004	8050090	Bipolar Disorder	41(22-64)	19	2
456	McIntosh A M	2004	8050090	Schizophrenia	37	26	4
457	McMillan A B	2004	8050091	Temporal Lobe Epilepsy (Left)	32	13	7
458	McMillan A B	2004	8050091	Temporal Lobe Epilepsy (Right)	32	12	15
459	Meda S A	2008	9080098	Schizophrenia (JHU Group)	42	133	51
460	Meda S A	2008	9080098	Schizophrenia (MPRC Group)	34	34	37
461	Meda S A	2008	9080098	Schizophrenia (WPIC Group)	41	21	31
462	Meisenzahl E M	2008	9080099	Schizophrenia (First-Episode)	28(18-49)	93	48
463	Meisenzahl E M	2008	9080099	Schizophrenia (Chronic)	36(19-65)	72	67
464	Meppelink A M	2011	13100199	Parkinson's Disease (Without Visual Hallucinations)	NR	13	13
465	Meppelink A M	2011	13100199	Parkinson's diease (With Visual Hallucinations)	NR	11	17
466	Mesaros S	2008	13100143	Multiple Sclerosis (Secondary Progressive)	47(30-63)	35	64
467	Mesaros S	2008	13100143	Multiple Sclerosis (Benign)	46(35-63)	60	31
468	Mesaros S	2008	9050051	Multiple Sclerosis	14(7-16)	28	2

ID	First Author	Year	BrainMap ID	Experimental group Diagnosis (vs. HC)*	Age, years (Range)	Subj (N)	Foci (N)
469	Mezzapesa D M	2007	9050052	Amyotrophic Lateral Sclerosis	59	16	13
470	Miettinen P S	2011	13100144	Alzheimer's Disease	75(63-83)	16	5
471	Miettinen P S	2011	13100144	Mild Cognitive Impairment	72(57-82)	18	5
472	Migliaccio R	2009	11050261	Alzheimer's Disease	61	16	18
473	Migliaccio R	2009	11050261	Progressive Non-Fluent Aphasia	64	10	18
474	Migliaccio R	2009	11050261	Posterior Cortical Atrophy	61	14	18
475	Milham M P	2005	8050094	Anxiety Disorder	13	17	6
476	Minnerop M	2007	10010002	Multiple System Atrophy (Cerebellar)	62	16	18
477	Minnerop M	2007	10010002	Multiple System Atrophy (Parkinsonian)	61	16	22
478	Minnerop M	2008	11040057	Dystonia	53	13	5
479	Molina V	2011	13100145	Bipolar Disorder	38	19	2
480	Molina V	2010	10030030	Schizophrenia	29	30	3
481	Molina V	2011	13100145	Schizophrenia	34	24	5
482	Molko N	2003	8090182	Turner Syndrome	25	14	4
483	Molko N	2004	8060217	Turner Syndrome	25(18-36)	14	25
484	Moorhead T W	2005	8090183	Learning Diability	NR	18	9
485	Moorhead T W	2005	8090183	Schizophrenia	NR	25	14
486	Mordasini L	2012	16030049	Chronic Pelvic Pain Syndrome	40(20-73)	20	3
487	Morgen K	2006	8060218	Multiple Sclerosis	32(22-46)	19	2
488	Morrell M J	2010	13100146	Obstructive Sleep Apnea	49	60	2
489	Mueller S G	2006	8050095	Mesial Temporal Sclerosis with Epilepsy	36(26-46)	26	28
490	Muhlau M	2013	16030026	Clinically Isolated Syndrome	37(18-68)	249	12
491	Muhlau M	2007	8050096	Huntington's Disease	44(24-68)	46	32
492	Muhlau M	2006	8060219	Tinnitus	40(26-53)	28	1
493	Muller-Vahl K R	2009	11040201	Tourette Syndrome	30(18-60)	19	14
494	Mummery C J	2000	8060220	Semantic Dementia	60(58-65)	6	17
495	Musen G	2006	9010005	Type 1 Diabetes	33	82	8
496	Na K S	2013	17050007	Panic Disorder (Without Agoraphobia)	37(18-65)	22	2
497	Na K S	2013	17050007	Panic Disorder (With Agoraphobia)	43(18-65)	12	7
498	Nagano-Saito A	2005	8050097	Parkinson's Disease	63	19	3
499	Nardo D	2010	11050255	Post-Traumatic Stress Disorder	40	21	5
500	Narita K	2011	15080033	Bipolar Disorder (With Rapid Cycling)	40	14	10
501	Narita K	2011	15080033	Bipolar Disorder (Without Rapid Cycling)	41	17	3
502	Neckelmann G	2006	10060062	Schizophrenia	NR(19-51)	12	3
503	Nestor P J	2003	8090184	Progressive Non-Fluent Aphasia	71	10	1
504	Niedtfeld I	2013	14110036	Borderline Personality Disorder	30	60	2
505	Nishio Y	2010	10060054	Parkinson's Disease	66(55-75)	40	36
506	Nosarti C	2008	11040058	Preterm/Low Birthweight	15	207	69
507	Nugent	2006	8050098	Bipolar Disorder (Unmedicated)	37(18-60)	21	9
508	Nugent	2006	8050098	Bipolar Disorder (Medicated)	41(18-60)	20	6
509	O'Daly O	2007	13100052	Schizophrenia	32	28	9
510	O'Muircheartaigh J	2011	13100150	Juvenile Myoclonic Epilepsy	34	28	2
511	Obermann M	2007	8060221	Blepharopasm	53(41-67)	11	9

ID	First Author	Year	BrainMap ID	Experimental group Diagnosis (vs. HC)*	Age, years (Range)	Subj (N)	Foci (N)
512	Obermann M	2007	8060221	Dystonia	58(43-63)	9	9
513	Obermann M	2013	16030050	Trigeminal Neuralgia	62(31-86)	60	14
514	Ohnishi T	2001	8050099	Alzheimer's Disease	72(59-79)	26	2
515	Ohnishi T	2006	13100053	Schizophrenia	45	19	19
516	Okada T	2004	8050100	Chronic Fatigue Syndrome	34(24-46)	16	2
517	Ortiz-Gil J	2011	13100151	Schizophrenia	40	23	1
518	Overmeyer S	2001	13100054	Attention Deficit Hyperactivity Disorder	10(7-14)	18	9
519	Padovani A	2006	8050102	Progress Supranuclear Palsy	73	14	22
520	Pail M	2010	11080301	Temporal Lobe Epilepsy (Left)	40	20	1
521	Pail M	2010	11080301	Temporal Lobe Epilepsy (Right)	40	20	1
522	Paillere-Martinot M L	2001	13100154	Schizophrenia	29(18-45)	20	9
523	Pan W J	2007	11040203	Blindness	47(39-58)	14	3
524	Pannacciulli N	2006	8050103	Obesity	32	24	13
525	Pantano P	2011	13100055	Dystonia	53	19	8
526	Pardini M	2009	11040175	Corticobasal Degeneration Syndrome	62	25	4
527	Pardini M	2009	11040175	Frontotemporal Dementia	60	22	5
528	Parisi L	2014	16030028	Multiple Sclerosis (Classic)	49	9	3
529	Parisi L	2014	16030028	Multiple Sclerosis (Cortical)	49	9	5
530	Peinemann A	2005	9010007	Huntington's Disease	44	25	7
531	Pell G S	2008	9050055	Temporal Lobe Epilepsy	39	19	18
532	Peng J	2010	10060048	Major Depressive Disorder	47	22	18
533	Penhune V B	2003	8090185	Deafness	29	12	2
534	Pennanen C	2005	8050105	Mild Cognitive Impairment	72	51	10
535	Pereira J B	2009	11040060	Parkinson's Disease	73	36	30
536	Pereira J M	2009	11050263	Alzheimer's Disease	65	3	1
537	Pereira J M	2009	11050263	Frontotemporal Dementia (With Tau Inclusions)	62	6	4
538	Pereira J M	2009	11050263	Frontotemporal Dementia (With Ubiquitin Inclusions)	64	9	3
539	Pereira J M	2009	11050263	Progressive Non-Fluent Aphasia	68	3	2
540	Pereira J M	2009	11050263	Semantic Dementia (With Tau Inclusions)	58	3	4
541	Pereira J M	2009	11050263	Semantic Dementia (With Ubiquitin Inclusions)	66	5	5
542	Pereira J M	2009	11050263	Frontotemporal Dementia (Behavioral Variant)	60	4	2
543	Perico C A M	2011	13120220	Bipolar Disorder	27	26	1
544	Perico C A M	2011	13120220	Major Depressive Disorder	30	20	2
545	Peterson E	2006	11080311	At-Risk of Mental State	40	23	19
546	Pleger B	2014	16030051	Complex Regional Pain Syndrome	41(22-53)	20	1
547	Pomarol-Clotet E	2010	11040138	Schizophrenia	42(28-60)	31	2
548	Prakash R S	2010	16030029	Multiple Sclerosis	44	21	12
549	Prell T	2013	16030052	Dystonia	52	24	15
550	Preziosa P	2016	17070011	Multiple Slerosis (Cognitively Impaired)	40	23	10
551	Preziosa P	2016	17070011	Multiple Sclerosis (Cognitively Preserved)	40	38	4
552	Prinster A	2006	8050107	Multiple Sclerosis	39(23-53)	51	8
553	Protopopescu X	2006	10060064	Panic Disorder	36(21-50)	10	1
554	Ptito M	2008	9050058	Blindness	36(20-54)	11	10

ID	First Author	Year	BrainMap ID	Experimental group Diagnosis (vs. HC)*	Age, years (Range)	Subj (N)	Foci (N)
555	Pujol J	2004	13100059	Obsessive Compulsive Disorder	30(18-60)	72	6
556	Qiu L	2014	14120051	Major Depressive Disorder	23	46	6
557	Qiu L	2011	13100155	Schizophrenia	35	29	23
558	Quarantelli M	2006	8050108	Facioscapulohumeral Dystrophy	44(20-72)	30	9
559	Quattrone A	2008	9080100	Essential Tremor (Arm)	62	43	1
560	Quattrone A	2008	9080100	Essential Tremor (Head)	71	50	3
561	Rabinovici G D	2007	11040099	Alzheimer's Disease	65	11	19
562	Rabinovici G D	2007	11040099	Frontotemporal Lobar Degeneration	63	18	38
563	Raji C A	2009	11040030	Alzheimer's Disease	83	33	41
564	Rami L	2009	11040232	Alzheimer's Disease	74	31	6
565	Rami L	2009	11040232	Mild Cognitive Impairment	73	14	5
566	Ramirez-Ruiz B	2007	13100195	Parkinson's Disease (Without Visual Hallucinations)	NR	20	2
567	Ramirez-Ruiz B	2007	13100195	Parkinson's Disease (With Visual Hallucinations)	NR	18	10
568	Redlich R	2014	15080035	Major Depressive Disorder	38	58	8
569	Redlich R	2014	15080035	Bipolar Disorder	38	58	8
570	Reetz K	2011	13100157	Spinocerebellar Ataxia	40	16	12
571	Reiss A L	2004	8060222	Williams Syndrome	29(12-50)	43	40
572	Remy F	2005	8090188	Alzheimer's Disease	72	8	21
573	Riccitelli G	2011	16030059	Multiple Sclerosis (Fatigued)	38	10	7
574	Riccitelli G	2011	16030059	Multiple Sclerosis (Non-Fatigued)	39	14	5
575	Riccitelli G	2012	13100158	Multiple Sclerosis	40(20-63)	78	42
576	Ridler K	2001	8090189	Tuberous Sclerosis	42	10	2
577	Riederer F	2012	16030053	Headache	41	29	26
578	Riederer F	2008	9050060	Temporal Lobe Epilepsy (Left)	38	9	15
579	Riederer F	2008	9050060	Temporal Lobe Epilepsy (Right)	38	13	7
580	Rocca M A	2015	16030034	Multiple Sclerosis	31(18-47)	37	3
581	Rocca M A	2015	16030034	Clinically Isolated Syndrome	31(18-47)	37	1
582	Rocca M A	2014	16030033	Multiple Sclerosis (Non-Fatigued)	40(27-58)	32	4
583	Rocca M A	2014	16030033	Multiple Sclerosis (Fatigued)	41(23-63)	31	12
584	Rocca M A	2006	8060223	Migraine (With Aura)	43(28-58)	7	9
585	Rocca M A	2006	8060223	Migraine (Without Aura)	43(28-58)	9	14
586	Rocha-Rego V	2012	14110031	Post-Traumatic Stress Disorder	43	16	2
587	Rodriguez-Raecke R	2009	13110208	Osteoarthritis	65	32	16
588	Rodriguez-Raecke R	2013	16030054	Osteoarthritis (Left Primary)	63	7	2
589	Rodriguez-Raecke R	2013	16030054	Osteoarthritis (Right Primary)	63	20	11
590	Roman-Urrestarazu A	2016	19120019	Attention Deficit Hyperactivity Disorder	22	49	2
591	Rosen H J	2002	8060224	Frontotemporal Lobar Degeneration	62(45-73)	20	8
592	Rossi R	2012	17050008	Borderline Personality Disorder	36	26	39
593	Rossi R	2006	8060225	White Matter Hyperintensity (Anterior)	58	39	10
594	Rossi R	2006	8060225	White Matter Hyperintensity (Posterior)	61	14	9
595	Rowan A	2007	8050111	Cerebral Infarction	9(7-12)	10	5
596	Rusch N	2004	8050112	Temporal Lobe Epilepsy	NR	24	4
597	Ruscheweyh R	2011	11080302	Chronic Back Pain	66	45	26

ID	First Author	Year	BrainMap ID	Experimental group Diagnosis (vs. HC)*	Age, years (Range)	Subj (N)	Foci (N)
598	Salgado-Pineda P	2003	8050114	Schizophrenia	24	13	21
599	Salgado-Pineda P	2004	8050115	Schizophrenia	25	14	38
600	Salgado-Pineda P	2011	13100159	Schizophrenia	37(22-56)	14	5
601	Salmond C H	2000	8050118	Amnesia	12	5	8
602	Salvadore G	2011	13100062	Major Depressive Disorder (Chronic)	39(20-60)	27	12
603	Salvadore G	2011	13100062	Major Depressive Disorder (Remitted)	40(18-61)	58	12
604	Sanchis-Segura C	2016	17070012	Multiple Sclerosis (Female)	41(20-60)	34	4
605	Sanchis-Segura C	2016	17070012	Multiple Sclerosis (Male)	39(23-60)	22	6
606	Santana M	2010	10060066	Temporal Lobe Epilepsy (Left)	38(18-59)	59	16
607	Santana M	2010	10060066	Temporal Lobe Epilepsy (Right)	36(20-62)	41	10
608	Saricicek A	2015	15080034	Bipolar Disorder	36(18-65)	28	4
609	Saricicek A	2015	15080034	At-Risk of Mental State	32(18-65)	25	5
610	Sasayama D	2010	13100160	Attention Deficit Hyperactivity Disorder	9(6-12)	10	9
611	Saykin A J	2006	8050119	Mild Cognitive Impairment (Cognitive Complaints)	73	40	12
612	Saykin A J	2006	8050119	Mild Cognitive Impairment (Non-Cognitive Complaints)	73	40	15
613	Schafer A	2010	10030031	Binge Eating Disorder	26	17	3
614	Schafer A	2010	10030031	Bulimia Nervosa	23	14	4
615	Scheuerecker J	2010	13100063	Major Depressive Disorder	38	13	18
616	Schiffer B	2007	8050120	Pedophilia	38(22-54)	18	5
617	Schiffer B	2013	15090044	Schizophrenia	36	25	15
618	Schmidt-Wilcke T	2006	8050122	Chronic Back Pain	50(34-59)	18	8
619	Schmidt-Wilcke T	2007	9050062	Fibromyalgia	54	20	6
620	Schmidt-Wilcke T	2005	11030006	Headache	34(15-70)	20	16
621	Schmidt-Wilcke T	2008	11030005	Migraine	32(18-49)	35	4
622	Schmidt-Wilcke T	2009	11040205	Mild Cognitive Impairment	66	18	4
623	Schmidt-Wilcke T	2010	10060067	Persistant Idiopathic Facial Pain	52	11	9
624	Schuster C	2012	13100064	Schizophrenia	60(50-82)	27	12
625	Schwartz D L	2010	10030032	Substance Abuse	33(20-63)	61	4
626	Schweinhardt P	2008	11030007	Vestibulodynia	26(19-36)	14	4
627	Seeley W W	2008	13100065	Frontotemporal Lobar Degeneration (CDR score of 0.5)	66	15	29
628	Seeley W W	2008	13100065	Frontotemporal Lobar Degeneration (CDR score of 1)	64	15	33
629	Seeley W W	2008	13100065	Frontotemporal Lobar Degeneration (CDR score of 2-3)	62	15	43
630	Seidman L J	2019	19120020	Attention Deficit Hyperactivity Disorder	37(18-59)	74	6
631	Seminowicz D A	2010	13100161	Irritable Bowel Syndrome	NR	56	26
632	Senda J	2011	14030006	Amyotrophic Lateral Sclerosis	61(40-78)	17	6
633	Sepulcre J	2006	8050123	Multiple Sclerosis	44	31	9
634	Serra-Blasco M	2013	13120218	Major Depressive Disorder (Chronic)	49	22	12
635	Serra-Blasco M	2013	13120218	Major Depressive Disorder (Remitted)	48	22	3
636	Sethi A	2017	19120021	Attention Deficit Hyperactivity Disorder	33	30	2
637	Shah P J	1998	13100067	Major Depressive Disorder	49	20	15
638	Shapleske J	2002	13100068	Schizophrenia (With Hallucinations)	35	32	7
639	Shapleske J	2002	13100068	Schizophrenia (Without Hallucinations)	32	31	2

ID	First Author	Year	BrainMap ID	Experimental group Diagnosis (vs. HC)*	Age, years (Range)	Subj (N)	Foci (N)
640	Shibata D K	2007	10010012	Deafness	21(18-27)	53	1
641	Shiino A	2006	9050064	Alzheimer's Desease	71	40	16
642	Shiino A	2006	9050064	Mild Cognitive Impairment	68	20	10
643	Shin S	2012	13110215	Parkinson's Disease (With Hallucinations)	71	46	20
644	Shin S	2012	13110215	Parkinson's Disease (Without Hallucinations)	71	64	1
645	Shott M E	2015	18100011	Obesity	29	18	8
646	Sigmundsson T	2001	13100165	Schizophrenia	35	27	4
647	Silani G	2005	8060227	Dyslexia	24	32	2
648	Silva C B	2013	14120053	Friedreich's Ataxia	29	22	6
649	Simon T J	2005	8090193	22q11.2 Deletion Syndrome	9(7-14)	18	8
650	Singh M K	2012	17050009	Bipolar Disorder	16	26	1
651	Smesny S	2010	10060070	Schizophrenia (First-Episode)	31	13	18
652	Smesny S	2010	10060070	Schizophrenia (Chronic)	46	11	38
653	Soria-Pastor S	2009	11040102	Preterm/Low Birthweight	9(8-10)	20	3
654	Soriano-Mas C	2011	13100069	Major Depressive Disorder	62(37-82)	70	2
655	Sowell E R	2001	8050125	Fetal Alcohol Syndrome	13	21	17
656	Spano B	2010	11040207	Multiple Sclerosis	45	10	12
657	Specht K	2003	8050127	Multiple-System Atrophy	59	14	1
658	Spencer M D	2006	8050129	Intellectually Disablility	16	63	2
659	Stanfield A C	2009	11040147	Bipolar Disorder	36	66	2
660	Steinbrink C	2008	9050065	Dyslexia	71(64-74)	7	2
661	Stevens M C	2019	19120016	Attention Deficit Hyperactivity Disorder	15(12-18)	24	2
662	Stratmann M	2014	14120045	Major Depressive Disorder	38(18-60)	132	5
663	Suchan B	2010	11040077	Anorexia Nervosa	27	15	2
664	Sui S G	2010	13100070	Post-Traumatic Stress Disorder	26(12-31)	11	11
665	Summerfield C	2005	8050131	Parkinson's Disease (Without Dementia)	73	13	3
666	Summerfield C	2005	8050131	Parkinson's Disease (With Dementia)	70	16	10
667	Suzuki M	2005	8090195	Schizophrenia	39	5	2
668	Suzuki M	2002	13100168	Schizophrenia	26	42	9
669	Szeszko P R	2008	11040103	Obsessive Compulsive Disorder	13	37	8
670	Tae W S	2006	8050133	Juvenile Myoclonic Epilepsy	23	19	6
671	Takahashi R	2010	13100171	Alzheimer's Disease	73	51	6
672	Takahashi R	2010	13100171	Lewy Body Dementia	73	43	6
673	Takahashi R	2011	13100172	Progressive Supranuclear Palsy	65	16	7
674	Tanabe J	2009	9050067	Substance Abuse	35	19	1
675	Tang L R	2014	14120054	Bipolar Disorder	32(20-57)	27	3
676	Tanskanen P	2010	13100173	Schizophrenia	33	54	7
677	Tavanti M	2012	13100174	Post-Traumatic Stress Disorder	38	25	26
678	Tavazzi E	2012	16020009	Amyotrophic Lateral Sclerosis	55	20	7
679	Tavazzi E	2012	16020009	Multiple Sclerosis	47	18	17
680	Tessitore A	2012	13100200	Parkinson's Disease	NR	12	2
681	Thivard L	2007	13100175	Amyotrophic Lateral Sclerosis	52(37-69)	15	19
682	Thomaes K	2010	13100176	Post-Traumatic Stress Disorder	35	31	5

ID	First Author	Year	BrainMap ID	Experimental group Diagnosis (vs. HC)*	Age, years (Range)	Subj (N)	Foci (N)
683	Tian L	2011	13100177	Schizophrenia	23	30	50
684	Tiihonen J	2008	9050069	Psychopathy	33	12	2
685	Tiihonen J	2008	9050069	Antisocial Personality Disorder	33	26	31
686	Tir M	2009	11040150	Multiple System Atrophy	64(44-77)	14	1
687	Tir M	2009	11040150	Parkinson's Desease	62(47-73)	19	2
688	Togao O	2010	13100178	Obsessive Compulsive Disorder	33	23	6
689	Tomelleri L	2009	11040063	Schizophrenia	40	25	2
690	Tomoda A	2009	11050264	Childhood Sexual Abuse	20	23	1
691	Torelli F	2011	13100179	Obstructive Sleep Apnea	56	16	1
692	Tost H	2010	15010004	Bipolar Disorder (With Psychotic Symptoms)	42(29-55)	30	6
693	Tost H	2010	15010004	Bipolar Disorder (With Persecutory Delusions)	46(34-58)	15	10
694	Tregallas J R	2007	9050070	Schizophrenia	40	32	9
695	Truong W	2013	14120046	Major Depressive Disorder	35	28	8
696	Tu C H	2010	11030008	Primary Dysmenorrhea	24	32	16
697	Tzarouchi L C	2010	11040064	Multiple System Atrophy	62(38-79)	11	31
698	Uchida R R	2008	9050085	Panic Disorder	37	19	4
699	Ung H	2012	16030055	Chronic Low Back Pain	37(19-60)	47	3
700	Valente A A Jr	2005	8060229	Obsessive Compulsive Disorder	33	7	6
701	Valet M	2009	11020003	Pain Disorder	51(28-68)	14	13
702	Valfre W	2008	9050072	Migraine	35	27	21
703	van de Pavert S H	2015	16030039	Multiple Sclerosis (Primary Progressive)	53	25	7
704	van de Pavert S H	2015	16030039	Multiple Sclerosis (Relapsing Remitting)	43	30	3
705	van de Pavert S H	2015	16030039	Multiple Sclerosis (Secondary Progressive)	53	25	10
706	van den Heuvel O A	2009	11040186	Obsessive Compulsive Disorder	34(19-54)	55	5
707	van Eijndhoven P	2013	14120049	Major Depressive Disorder	34(18-56)	20	5
708	van Haren N E	2007	11080259	Schizophrenia	32(17-56)	96	7
709	van Tol M J	2010	13100073	Anxiety Disorder	36	68	1
710	van Tol M J	2010	13100073	Major Depressive Disorder	37	88	2
711	van Wingen G	2013	19120027	Attention Deficit Hyperactivity Disorder (Without Cocaine Dependence)	32	14	4
712	van Wingen G	2013	19120027	Attention Deficit Hyperactivity Disorder (With Cocaine Dependence)	37	10	2
713	Vannorsdall T D	2010	11040211	Traumatic Brain Injury	44(25-64)	14	6
714	Vargha-Khadem F	2003	8090199	Hypoxic-Ischemic Encephalopathy	14(8-19)	11	9
715	Vartiainen N	2009	11040151	Herpes Simplex Virus	47(41-53)	8	7
716	Venkatasubramanian G	2008	9050073	Schizophrenia	NR	27	6
717	Voets N L	2008	9050074	Schizophrenia	16	25	9
718	von dem Hagen E A H	2005	8050141	Albinism	36(18-65)	19	2
719	Wagner G	2011	11080303	Major Depressive Disorder	37	30	9
720	Wang F	2011	13100182	Bipolar Disorder	17(10-21)	41	17
721	Wang J	2007	13100076	Attention Deficit Hyperactivity Disorder	13	12	6
722	Wang L	2019	19120013	Attention Deficit Hyperactivity Disorder	10(6-16)	30	3
723	Waragai M	2009	10030024	Alzheimer's Disease	71	15	2
724	Watkins K E	2002	8060231	Affected Speech and Language Disorder	NR(9-21)	10	20

ID	First Author	Year	BrainMap ID	Experimental group Diagnosis (vs. HC)*	Age, years (Range)	Subj (N)	Foci (N)
725	Watson D R	2012	13100183	Schizophrenia	29	25	18
726	Watson D R	2012	13100183	Bipolar Disorder	36	24	2
727	Wattendorf E	2009	15010006	Parkinson's Disease (Early)	60(44-71)	15	1
728	Wattendorf E	2009	15010006	Parkinson's Disease (Moderately Advanced)	62(46-69)	12	1
729	Weber Y G	2010	10060073	Myotonic Dystrophy (Type 1)	37	14	17
730	Weber Y G	2010	10060073	Myotonic Dystrophy (Type 2)	53	9	15
731	Weygandt M	2014	16030037	Multiple Sclerosis (Early Onset Pediatric)	12	16	7
732	Weygandt M	2014	16030037	Multiple Sclerosis (Late Onset Pediatric)	16	17	10
733	White N S	2003	8050143	Down Syndrome	42(34-52)	19	39
734	Whitford T J	2006	8050144	Schizophrenia	20(13-25)	41	28
735	Whitwell J L	2005	8090202	Frontotemporal Dementia (Ubiquitin-Positive)	61	9	3
736	Whitwell J L	2005	8090202	Pick Disease	52	7	6
737	Whitwell J L	2005	8090202	Frontotemporal Dementia (Ubiquitin-Negative)	61	5	2
738	Whitwell J L	2007	11080304	Frontotemporal Lobar Degeneration (With Hyperphagia)	63	7	2
739	Whitwell J L	2007	11080304	Frontotemporal Lobar Degeneration (With a Pathological Sweet Tooth)	62	9	13
740	Whitwell J L	2007	8050145	Alzheimer's Desease	65	38	1
741	Whitwell J L	2007	8050145	Posterior Cortical Atrophy	64	38	1
742	Whitwell J L	2013	14050010	Primary Progressive Apraxia	72	16	4
743	Whitwell J L	2013	14050010	Progressive Supranuclear Palsy	72	16	8
744	Whitwell J L	2009	11040214	Frontotemporal Dementia (IVS10+16 MAPT Mutation)	56(51-62)	4	1
745	Whitwell J L	2009	11040214	Various Neurodegenerative Diseases (IVS10+3 MAPT Mutation)	46(36-49)	3	1
746	Whitwell J L	2009	11040214	Frontotemporal Dementia (N279K MAPT Mutation)	49(43-51)	3	1
747	Whitwell J L	2009	11040214	Frontotemporal Dementia (P301L MAPT Mutation)	52(45-65)	4	1
748	Whitwell J L	2009	11040214	Frontotemporal Dementia (S305N MAPT Mutation)	36(34-37)	2	1
749	Whitwell J L	2009	11040214	Frontotemporal Dementia (V337M MAPT Mutation)	56(49-60)	3	1
750	Whitwell J L	2004	13100185	Frontotemporal Lobar Degeneration (Tau-Negative)	62	8	3
751	Whitwell J L	2004	13100185	Frontotemporal Lobar Degeneration (Tau-Positive)	52	9	10
752	Wiest R	2005	8090203	Temporal Lobe Epilepsy	36(29-53)	7	7
753	Wilke M	2001	8050146	Schizophrenia	33	48	16
754	Wilson L B	2009	11040152	Fragile X Syndrome	29(22-44)	10	5
755	Wilson S M	2009	13100186	Semantic Dementia	67	5	15
756	Woermann F G	2000	9080103	Temporal Lobe Epilepsy (With Intermittent Explosive Disorder)	27(18-49)	25	2
757	Woermann F G	2000	9080103	Temporal Lobe Epilepsy (Without Intermittent Explosive Disorder)	33(19-56)	25	1
758	Woermann F G	1999	15070022	Juvenile Myoclonic Epilepsy	25(15-37)	20	1
759	Wolf R C	2008	9050079	Schizophrenia	33	14	12
760	Wood P B	2009	11040235	Fibromyalgia	42	30	4
761	Xiao J X	2007	11080287	Amblyopia	6(4-8)	13	4
762	Xie S	2006	8090204	Alzheimer's Disease	72(62-82)	13	9
763	Xu L	2009	9090104	Schizophrenia	42(20-81)	120	55
764	Yamada M	2007	11080312	Schizophrenia	39	20	6
765	Yang F C	2013	16030056	Migraine (Left-Sided Attack)	35(20-55)	26	13

ID	First Author	Year	BrainMap ID	Experimental group Diagnosis (vs. HC)*	Age, years (Range)	Subj (N)	Foci (N)
766	Yang F C	2013	16030056	Migraine (Right-Sided Attack)	35(20-55)	23	33
767	Yang X	2017	20070035	Major Depressive Disorder	28	82	11
768	Yaouhi K	2009	11040106	Obstructive Sleep Apnea	55	16	7
769	Yasuda C L	2010	11040153	Temporal Lobe Epilepsy (With Negative Family History of Epilepsy)	36	29	13
770	Yasuda C L	2010	11040153	Temporal Lobe Epilepsy (With Positive Family History of Epilepsy)	33	40	13
771	Yasuda C L	2010	11040039	Temporal Lobe Epilepsy (Seizure Free)	34	34	23
772	Yasuda C L	2010	11040039	Temporal Lobe Epilepsy (With Worthwhile Improvement)	34	23	12
773	Yasuda C L	2010	11040039	Temporal Lobe Epilepsy (Without Improvement)	34	10	30
774	Yatham L N	2007	8050149	First-Episode Mania	36	15	3
775	Yoneyama E	2003	8090206	Schizotypal Personality Disorder	25(16-32)	14	3
776	Yoo H K	2005	8050150	Panic Disorder	33	18	7
777	Yoo S Y	2008	11040184	Obsessive Compulsive Disorder (Aggressive)	26	29	8
778	Yoo S Y	2008	11040184	Obsessive Compulsive Disorder (Contamination)	26	26	6
779	Yoon E J	2013	16030057	Spinal Cord Injury	39(31-53)	10	4
780	Yoshihara Y	2008	9050083	Schizophrenia	16	18	1
781	Younger J W	2010	10060053	Chronic Myofascial Temporomandibular Pain	38(23-61)	14	12
782	Yuan Y	2008	9050082	Depressive Disorder	67	19	4
783	Zahn R	2005	13100189	Alzheimer's Disease	67	10	4
784	Zahn R	2005	13100189	Progressive Non-Fluent Aphasia	65	5	4
785	Zamboni G	2008	11040079	Frontotemporal Dementia	60	62	11
786	Zhang J	2011	13100080	Post-Traumatic Stress Disorder	41	10	3
787	Zhang T	2009	13100079	Major Depressive Disorder	34(18-51)	15	10
788	Zhang X	2016	17070013	Multiple Sclerosis	38	39	4
789	Zhang X	2012	13120222	Depressive Disorder	20	30	2
790	Zhang X	2012	13120222	Major Depressive Disorder	21	33	2
791	Zhang X	2011	11080290	Smoke Addiction	31	48	2
792	Zhao Y	2019	19120026	Attention Deficit Hyperactivity Disorder	12(8-17)	36	6
793	Zou K	2010	13100081	Major Depressive Disorder	31(18-55)	23	2
794	Zubiaurre-Elorza L	2011	11080305	Preterm/Low Birthweight	9(6-14)	22	8

** For the articles including independent groups with the same main diagnosis, the specific subdiagnosis or clinical manifestation was provided.* ***Sub (N)****, number of subjects in the clinical group;* ***Foci (N)****, number of x-y-z coordinates of gray matter alteration;* ***NR****, meta-data not reported.*

Table S5.5. General distribution of the VBM meta-data included in both datasets.

BACON Datasets	VBM Experiments		Clinical Subjects		Foci x-y-z	
	N	%	N	%	N	%
ASD	55	6.4	2407	10.7	546	6.3
Non-ASD	794	93.6	19897	89.3	8035	93.7
Total	849	100	22304	100	8581	100

Table S5.6. Statistical distribution of the VBM meta-data included in the Non-ASD dataset.

Non-ASD Dataset	VBM Experiments		Clinical Subjects		Foci x-y-z	
	N	%	N	%	N	%
Neurologic	441	55.5	9366	47.1	4720	58.7
Psychiatric	327	41.2	9706	48.8	3079	38.4
Other	26	3.3	825	4.1	236	2.9
Total	794	100	19897	100	8035	100

Table S5.7. Age-related distribution of the VBM meta-data included in the ASD dataset.

ASD Dataset	VBM Experiments		ASD Subjects		Foci x-y-z	
	N	%	N	%	N	%
Pediatric	26	47.3	648	26.9	292	53.5
Adult	11	20.0	447	18.5	128	23.4
Mixed	18	32.7	1312	54.6	126	23.1
Total	55	100	2407	100	546	100

Table S5.8. Functional large-scale network decomposition results. For each threshold the number of volumes has been reported, as well as the relative percentages of alterations of the BACON map and network ROIs defined by the Yeo's parcellation (Buckner et al., 2011; Choi et al., 2012; Yeo et al., 2011).

(ASD ∣ Alt) p = .70	Volume (mm^3)	BACON Map (%)	(ASD ∣ Alt) p = .80	Volume (mm^3)	BACON Map (%)	(ASD ∣ Alt) p = .90	Volume (mm^3)	BACON Map (%)
Visual	17817	18.5	Visual	7323	19.2	Visual	944	30.3
SMN	10237	10.6	SMN	3780	9.9	SMN	0	0
DAN	1852	1.9	DAN	4678	12.3	DAN	0	0
SN/VAN	12815	13.3	SN/VAN	4998	13.1	SN/VAN	533	17.2
Limbic	6096	6.3	Limbic	1216	3.2	Limbic	0	0
FPN	16835	17.6	FPN	5696	14.9	FPN	273	8.8
DMN	30635	31.8	DMN	10422	27.4	DMN	1360	43.7
TOTAL	96287	100	**TOTAL**	38113	100	**TOTAL**	3110	100

Visual, visual network; SMN, sensorimotor network; DAN, dorsal attention network; SN/VAN, salience network/ventral attention network; Limbic, limbic network; FPN, frontoparietal network; DMN, default mode

network.

Table S5.9. Leave-one-out analysis of VBM experiments with subjects from ABIDE.

Discarded VBM Experiment	Right IOG	Left Lobule IX	Right Crus I	Left Crus II	Right PCUN	Right PCUN	Left PCUN	Right Lobule VIIIA
Eliam-Stock et al 2016	Yes	Yes	Yes	Yes	Yes	Yes	Yes	Yes
Osipowicz et al 2015	Yes	Yes	Yes	Yes	Yes	Yes	Yes	Yes
Pappaianni et al 2018	Yes	Yes	Yes	Yes	Yes	Yes	Yes	Yes
Riddle et al 2017	Yes	Yes	Yes	Yes	Yes	Yes	Yes	Yes

ABIDE, the autism brain imaging data exchange database; IOG, inferior occipital gyrus; PCUN, precuneus.

Table S5.10. Cerebellum-related distribution of the VBM meta-data included in both datasets.

BACON Datasets	VBM Experiments*		Foci x-y-z**	
	N	%	N	%
ASD	22	9.6	35	7.1
Non-ASD	205	90.4	455	92.9
Total	227	100	490	100

** Experiments with at least one focus of gray matter alteration in the cerebellum; ** Foci of gray matter alteration in the cerebellum.*

5.6.3. Supplementary figure

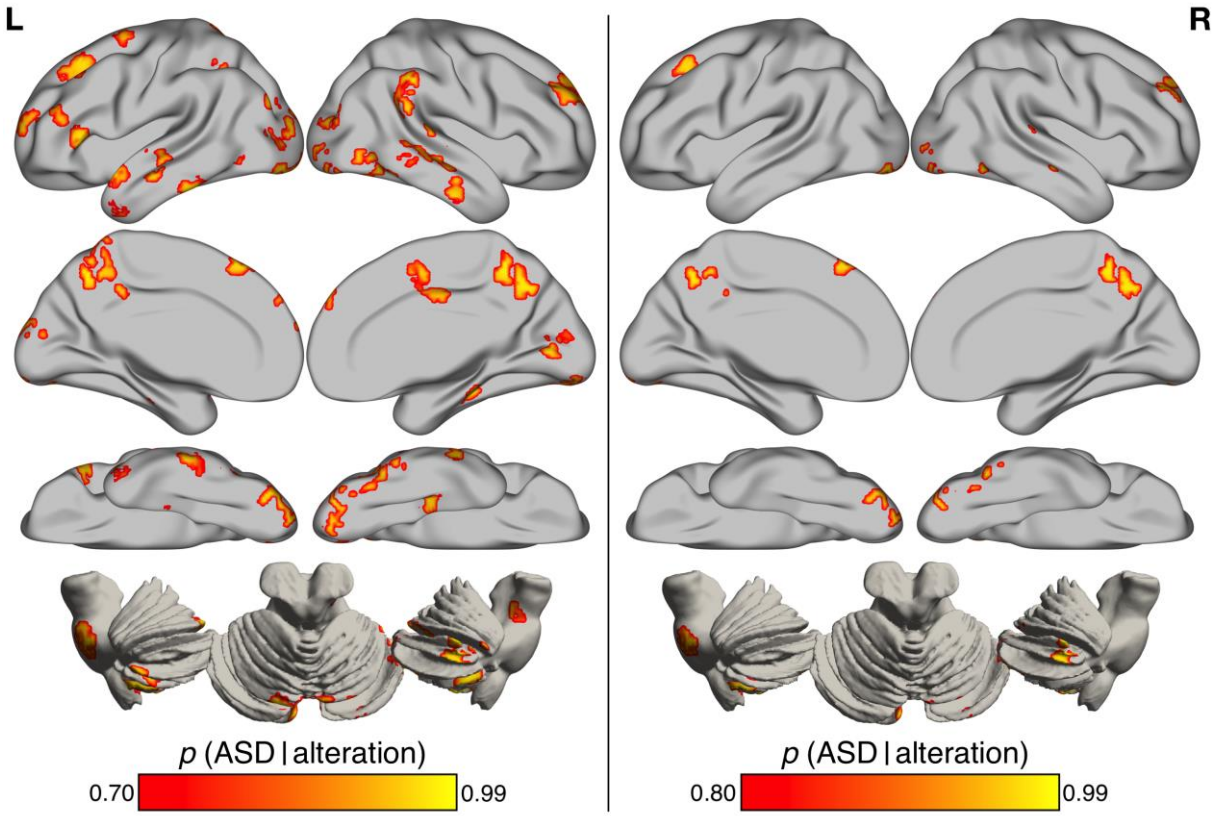

Figure S5.1. Brain clusters of selective gray matter alteration in autism spectrum disorder (ASD) derived from Bayes factor modeling (BACON) analysis, thresholded at $p(ASD|alteration) = 0.7$ (70%) - Left panel; and at $p(ASD|alteration) = 0.8$ (80%) - Right panel. BACON map is visualized as hemispheric and cerebellar surfaces (3-D cortical view). Templates are in neurological convention (L is left; R is right).

CHAPTER 6

Discussion and Conclusions

6.1. Thesis synopsis

The overarching theme of this thesis was the examination of the altered neuroanatomical substrate in major psychiatric disorders. To this end, I applied the neuroimaging coordinate-based meta-analysis (CBMA) approach, a well-established collection of computational techniques based on a solid and rigorous methodological background deriving from a long-running refinement of the human brain mapping community (Fox et al., 2014; Fox et al., 1985; Laird et al., 2009; Radua and Mataix-Cols, 2012a). Yet, I developed and applied novel CBMA- and Bayesian-based tools that allowed characterizing the gray matter substrate of autism spectrum disorder from a network-based and disorder-specific perspective, enhancing the ability to grasp the complex neuronal architecture of this group of neurodevelopmental conditions.

This concluding chapter recapitulates the main outcomes of the selected articles that compose the dissertation. It then presents some methodological considerations related to the CBMA approach in general and this project in particular. The Chapter also includes a discussion of possible directions for future CBMA research in the psychiatric context.

In Chapter 2, I examined the sequence of gray matter alteration patterns emerging from different stages of schizophrenia using a structural, functional, and behavioral CBMA approach. At the structural level, I employed the revised version of the activation likelihood estimation (ALE) algorithm (Eickhoff et al., 2017), stringent statistical procedures (Eickhoff et al., 2016), and field best-practice protocols (Müller et al., 2018). This state-of-the-art design has provided an unprecedented picture of the progressive neuronal damage of the disorder after its onset, which offers valuable insights that may potentially integrate the "neural component" into current pathophysiological models of schizophrenia. At the functional and behavioral level, I established a data-driven link between the identified neural structural damage and its functional behavior and psychological/cognitive functioning, by applying large-scale network decomposition (Biswal et al., 2010) and behavioral domain profiling analysis (Lancaster et al., 2012), respectively. These unbiased characterizations represent not only good practice to overcome the limitations of the usually qualitative interpretation of neuroimaging findings, but may also pave the way for future neuropsychological or functional interventions, for example, by applying meta-analytic

clusters as target areas for noninvasive brain stimulation sessions or as regions-of-interest for future functional magnetic resonance imaging research.

In Chapter 3, I presented the results of a CBMA replication study. The voxel-based morphometry (VBM) literature on dyslexia and attention-deficit hyperactivity disorder was used as a testing ground to provide a data-driven and real-world comparison between the recently developed PSI-SDM technique (Albajes-Eizagirre et al., 2019) and the ALE algorithm. A substantial spatial congruence was found between the two techniques demonstrating that, despite common neurobiological and environmental risk factors, no areas of gray matter decrease or increase overlapped in the two disorders. Specific clinical issues aside, I highlighted that the canonical design of CBMA techniques suffers from some drawbacks that do not enable to capture the whole spectrum of complexity underlying brain pathology.

In Chapter 4, I incorporated the graph theory framework into the ALE environment by manipulating the identified clusters of gray matter variation as *nodes* and their statistical co-occurrence across studies as *edges*. In this manner, it was possible to conceptualize the neuroanatomical alteration landscape of autism spectrum disorder (ASD) as a pathoconnectome (Rubinov and Bullmore, 2013). In light of this, I was able to directly measure the central role of each nodal area in the pathological network. Consistent with the notion that ASD is a syndrome resulting from perturbations of different spatially distributed neural systems (Ecker et al., 2016), a non-random and topologically defined network of co-alteration was found in the disorder, with a subset of multimodal areas significantly influencing the overall architecture of damage. As a further relevant note, the identified network-like pattern of co-alteration follows a biologically plausible distribution that resembles structural connectivity pathways. Taken together, these results offer a new outlook on the impact of clinical expression on brain structure that goes beyond the voxel-wise "static" picture of canonical neuroimaging approaches and opens attractive perspectives for future neuropsychiatric research.

Considering the non-negligible overlap of neuroanatomical alteration between brain disorders (Cauda et al., 2019b) and the limited inferential power of classical frequentist neuroimaging analysis (Poldrack et al., 2006), I proposed in Chapter 5 a posterior probability analysis to identify the selective profile of gray matter changes in ASD. To achieve this goal, I collected one of the largest CBMA-based datasets enriched with published VBM findings on

133 different clinical conditions, and I analyzed it employing the ALE and Bayes Factor (Jeffreys, 1961) methods. Findings revealed that in ASD there are brain areas with a high probability of alteration selectivity, mainly concentrated in the cerebellum and parietal territories that are forming part of the functionally defined default-mode network. The statistical approach applied here allowed to shed new light on the neuroanatomical profile of ASD demonstrating that Bayesian statistics can be a powerful tool to identify key regions that are selective for the alteration development of specific brain disorders. This provides essential information that could theoretically be useful to complement behavioral diagnosis, as well as to improve the assessment of treatment strategies.

6.2. Methodological considerations and future perspectives

The coordinate-based meta-analysis approach was introduced to human brain mapping research nearly two decades ago (Turkeltaub et al., 2002). Advances in its design, methodology, and statistical rigor have been ongoing since then, proving an unprecedented and multidisciplinary effort that has captured some core features of the healthy and pathological brain (Acar et al., 2018; Albajes-Eizagirre et al., 2019; Caspers et al., 2014; Eickhoff et al., 2012; Eickhoff et al., 2011; Eickhoff et al., 2009; Eickhoff et al., 2016; Fox et al., 2005; Fox et al., 2014; Laird et al., 2009; Laird et al., 2008; Laird et al., 2010; Lancaster et al., 2012; Manuello et al., 2022; Müller et al., 2018; Radua and Mataix-Cols, 2009; Radua and Mataix-Cols, 2012a; Radua et al., 2013; Salimi-Khorshidi et al., 2009; Tahmasian et al., 2019; Turkeltaub et al., 2012; Vanasse et al., 2018; Wager et al., 2007). By means of the analysis of tens of thousands of neuroimaging data published worldwide, recent CBMA advances now compute coactivation-based parcellation, independent component analysis, large-scale topological modeling, meta-analytic connectivity modeling, functional ontologies, meta-connectomics, and reverse inference analysis (Bzdok et al., 2013; Cauda et al., 2018b; Clos et al., 2013; Costa et al., 2021; Crossley et al., 2016; Crossley et al., 2014; Crossley et al., 2013; Kotkowski et al., 2018; Laird et al., 2011; Robinson et al., 2012; Robinson et al., 2010; Smith et al., 2009; Torta et al., 2013). Although CBMA is currently at the forefront of brain sciences research, some exciting challenges remain. Please note that general limitations of the CBMA environment (e.g., the limited spatial accuracy, cross-sectional design, and file drawer effect) have been extensively discussed in previous Chapters. Here, potential directions for future CBMA research are detailed.

Since their inception, CBMAs have provided a quantitative and data-driven synthesis of primary neuroimaging findings; however, a qualitative interpretation of the meta-analytic results obtained is traditionally given. In recent years, technological advances have opened great opportunities for objective integration of voxel-wise neuroimaging maps, including CBMA ones, with other types of experimental brain data. Among others, transcriptomics analysis pipelines are providing an unprecedented ability to statistically link brain-wide gene expression data and human brain mapping results of any sort (Arnatkeviciute et al., 2019a). Several software platforms have been developed (French and Paus, 2015; Larivière et al., 2022; Markello et al., 2021; Rizzo et al., 2016) with the same basic idea in mind, namely to capture spatial correlations between structural/functional brain maps and gene expression levels by using the Allen Human Brain Atlas transcriptome dataset (Hawrylycz et al., 2012), which consists of 20,737 measurements of gene expression taken from six adult human brains without known neurological disease history. This approach has yielded important research insights into the relationship between gene expression and normative brain connectivity (e.g., Goel et al., 2014; Richiardi et al., 2015; Vértes et al., 2016) or psychiatric and neurological neuronal substrate (e.g., Arnatkeviciute et al., 2022; McColgan et al., 2018; Romero-Garcia et al., 2019; Romme et al., 2017). However, its usage has been limited to primary functional and structural data; it has only recently been applied by my research group in the field of CBMA (Camasio et al., 2022; Cauda et al., 2018b; Liloia et al., 2021b). Interestingly, other methodological approaches are rapidly evolving to quantitatively enrich neuroimaging results with cytoarchitectonic properties. For example, a novel toolbox called BigBrainWarp (Larivière et al., 2022; Paquola et al., 2021) has been devised for integrating multimodal neuroimaging data with microstructural organization brain information derived from the *post mortem* ultrahigh-resolution histology dataset of Amunts et al. (2013). This toolbox could pave the way for molecular and cellular characterization of statistical brain maps that reveal, for example, a co-alteration pattern of a brain disorder under study. Given these considerations, future application in the field of clinical CBMA is warranted.

A more precise phenotypic characterization of the general CBMA findings remains a major challenge. In its current implementations, the CBMA framework does not finely manipulate important features of individual experimental subjects (e.g., biological sex, developmental stage, type of symptomatology, scores on clinical/psychological assessments, etc.). This is due to the fact that this secondary level of research is not able to model variables

better than individual primary studies (Fusar-Poli and Radua, 2018). Although the CBMA design can partially overcome this issue in psychiatric research by performing user-dependent subanalyses of clinical or socio-demographic interest (e.g., Fornito et al., 2009; Gray et al., 2020; Samea et al., 2019; Yan et al., 2021), data-driven CBMA tools conjointly using phenotypic and behavioral meta-data need to be developed. This may be particularly useful for meta-connectomics research, which computes the overall network of alteration in a given brain disorder taking exclusively into account the clinical diagnosis. However, in-depth characterization based on key variables may lead to the identification of peculiar sub-networks of alteration, paving the way for future personalized brain medicine interventions based on imaging pathoconnectomics (Fornito et al., 2017). Once again, the implementation of Bayesian statistics in CBMA could help us to address this issue. For example, the development of multinomial logistic regression and posterior predictive distribution approaches (Bishop and Nasrabadi, 2006) has the potential to identify specific co-alteration patterns by distinguishing between included clinical groups with different phenotypic characteristics.

Another critical issue that should be addressed in meta-connectomics research is the transition from undirected to directed brain co-alteration or co-activation networks. This methodological improvement has the potential to reveal the evolution of the damage fingerprint of a given brain disorder across the lifespan (Cauda et al., 2018b), target specific circuits for neurorehabilitation and pharmacological interventions (Fornito et al., 2017), as well as to discern disorder-specific pathophysiological mechanisms of alteration propagation underlying both psychiatric and neurological disorders (Fornito et al., 2015). Although efficient direction-oriented metrics have been proposed in MRI (Friston, 2011), their validity in the CBMA scenario needs to be further evaluated. For example, previous simulation (Patel et al., 2006; Smith et al., 2011) and experimental (Cauda et al., 2021; Mancuso et al., 2020) studies have shown that Patel's τ is a suitable high-order Bayesian statistic to infer effective connectivity (i.e., the directionality or causal influence exerted by a set of brain nodes on another) (Friston, 2011) in both the functional and structural connectome. However, the soundness of this method is still debated and its neurobiological basis remains unclear, especially in the context of fMRI research (Wang et al., 2017b).

6.3. Acknowledgements

First and foremost, I would like to express my deep gratitude to Prof. Tommaso Costa, my research supervisor, for his constant support during the last four years. His enormous knowledge and patient guidance have helped me improve not only as a neuroimager but also as a person. Thank you for bringing me to the dark (ahem…Bayesian) side of the Force!

Heartfelt thanks to Prof. Franco Cauda for routing me toward challenging research paths. It was a pleasure to discuss cutting-edge neuroimaging research (and post-punk new-wave music) with him.

I am grateful to my current and former mates in the FunctiOnal neuroimaging and Complex neUral Systems (FOCUS) Laboratory for our great time together.

I would like to express my sincere gratitude to the inspirational researchers with whom I have had the pleasure of collaborating on various research projects.

My wholehearted thanks to Prof. Monica Mazza and Prof. Igor Sotgiu for the time spent to revise the current dissertation.

Last but certainly not least, I would like to thank my family. Words cannot express the love I feel for Alessandra, Brian, Gerardo, Gioele, and Giuseppina. Without you I'm nothing.

BIBLIOGRAPHY

Abell, F., Krams, M., Ashburner, J., Passingham, R., Friston, K., Frackowiak, R., Happé, F., Frith, C., Frith, U., 1999. The neuroanatomy of autism: a voxel-based whole brain analysis of structural scans. NeuroReport 10, 1647-1651. doi:10.1097/00001756-199906030-00005

Acar, F., Seurinck, R., Eickhoff, S.B., Moerkerke, B., 2018. Assessing robustness against potential publication bias in Activation Likelihood Estimation (ALE) meta-analyses for fMRI. PloS one 13, e0208177. doi:10.1371/journal.pone.0208177

Adriano, F., Spoletini, I., Caltagirone, C., Spalletta, G., 2010. Updated meta-analyses reveal thalamus volume reduction in patients with first-episode and chronic schizophrenia. Schizophrenia research 123, 1-14. doi:10.1016/j.schres.2010.07.007

Aguirre, G.K., Feinberg, F.T., Farah, M., 2003. Functional imaging in behavioral neurology and cognitive neuropsychology, Behavioral neurology and cognitive neuropsychology. 2nd ed. Citeseer.

Ahrendts, J., Rüsch, N., Wilke, M., Philipsen, A., Eickhoff, S.B., Glauche, V., Perlov, E., Ebert, D., Hennig, J., van Elst, L.T., 2011. Visual cortex abnormalities in adults with ADHD: a structural MRI study. The world journal of biological psychiatry : the official journal of the World Federation of Societies of Biological Psychiatry 12, 260-270. doi:10.3109/15622975.2010.518624

Ajilore, O., Vizueta, N., Walshaw, P., Zhan, L., Leow, A., Altshuler, L.L., 2015. Connectome signatures of neurocognitive abnormalities in euthymic bipolar I disorder. J Psychiatr Res 68, 37-44. doi:10.1016/j.jpsychires.2015.05.017

Albajara Sáenz, A., Van Schuerbeek, P., Baijot, S., Septier, M., Deconinck, N., Defresne, P., Delvenne, V., Passeri, G., Raeymaekers, H., Slama, H., Victoor, L., Willaye, E., Peigneux, P., Villemonteix, T., Massat, I., 2020. Disorder-specific brain volumetric abnormalities in Attention-Deficit/Hyperactivity Disorder relative to Autism Spectrum Disorder. PLoS One 15, e0241856. doi:10.1371/journal.pone.0241856

Albajes-Eizagirre, A., Radua, J., 2018. What do results from coordinate-based meta-analyses tell us? NeuroImage 176, 550-553. doi:10.1016/j.neuroimage.2018.04.065

Albajes-Eizagirre, A., Solanes, A., Vieta, E., Radua, J., 2019. Voxel-based meta-analysis via permutation of subject images (PSI): Theory and implementation for SDM. NeuroImage 186, 174-184. doi:10.1016/j.neuroimage.2018.10.077

Albrecht, F., Bisenius, S., Neumann, J., Whitwell, J., Schroeter, M.L., 2019. Atrophy in midbrain & cerebral/cerebellar pedunculi is characteristic for progressive supranuclear palsy - A double-validation whole-brain meta-analysis. NeuroImage. Clinical 22, 101722. doi:10.1016/j.nicl.2019.101722

Alexander-Bloch, A., Giedd, J.N., Bullmore, E., 2013. Imaging structural co-variance between human brain regions. Nat Rev Neurosci 14, 322-336. doi:10.1038/nrn3465

Allen, G., Courchesne, E., 2001. Attention function and dysfunction in autism. Front Biosci 6, D105-119. doi:10.2741/allen

Allen, P., Stephan, K.E., Mechelli, A., Day, F., Ward, N., Dalton, J., Williams, S.C., McGuire, P., 2010. Cingulate activity and fronto-temporal connectivity in people with prodromal signs of psychosis. NeuroImage 49, 947-955. doi:10.1016/j.neuroimage.2009.08.038

Allman, J.M., Tetreault, N.A., Hakeem, A.Y., Manaye, K.F., Semendeferi, K., Erwin, J.M., Park, S., Goubert, V., Hof, P.R., 2010. The von Economo neurons in frontoinsular and anterior cingulate cortex in great apes and humans. Brain structure & function 214, 495-517. doi:10.1007/s00429-010-0254-0

Allman, J.M., Tetreault, N.A., Hakeem, A.Y., Manaye, K.F., Semendeferi, K., Erwin, J.M., Park, S., Goubert, V., Hof, P.R., 2011. The von Economo neurons in the frontoinsular and anterior cingulate cortex. Annals of the New York Academy of Sciences 1225, 59-71. doi:10.1111/j.1749-6632.2011.06011.x

Almeida Montes, L.G., Ricardo-Garcell, J., Barajas De La Torre, L.B., Prado Alcántara, H., Martínez García, R.B., Fernández-Bouzas, A., Avila Acosta, D., 2010. Clinical correlations of grey matter reductions in the caudate nucleus of adults with attention deficit hyperactivity disorder. Journal of psychiatry & neuroscience : JPN 35, 238-246. doi:10.1503/jpn.090099

Altamura, A.C., Buoli, M., Pozzoli, S., 2014. Role of immunological factors in the pathophysiology and diagnosis of bipolar disorder: comparison with schizophrenia. Psychiatry and clinical neurosciences 68, 21-36. doi:10.1111/pcn.12089

Amann, B.L., Canales-Rodriguez, E.J., Madre, M., Radua, J., Monte, G., Alonso-Lana, S., Landin-Romero, R., Moreno-Alcazar, A., Bonnin, C.M., Sarro, S., Ortiz-Gil, J., Gomar, J.J., Moro, N., Fernandez-Corcuera, P., Goikolea, J.M., Blanch, J., Salvador, R., Vieta, E.,

McKenna, P.J., Pomarol-Clotet, E., 2016. Brain structural changes in schizoaffective disorder compared to schizophrenia and bipolar disorder. Acta psychiatrica Scandinavica 133, 23-33. doi:10.1111/acps.12440

Ameis, S.H., Catani, M., 2015. Altered white matter connectivity as a neural substrate for social impairment in Autism Spectrum Disorder. Cortex 62, 158-181. doi:10.1016/j.cortex.2014.10.014

American Psychiatric Association, 2013. Diagnostic and Statistical Manual of Mental Disorders, Fifth Edition (DSM-5), 5th, ed. American Psychiatric Publishing, Arlington, VA.

Amico, F., Stauber, J., Koutsouleris, N., Frodl, T., 2011. Anterior cingulate cortex gray matter abnormalities in adults with attention deficit hyperactivity disorder: a voxel-based morphometry study. Psychiatry research 191, 31-35. doi:10.1016/j.pscychresns.2010.08.011

Anagnostou, E., Taylor, M.J., 2011. Review of neuroimaging in autism spectrum disorders: what have we learned and where we go from here. Molecular autism 2, 4. doi:10.1186/2040-2392-2-4

Amunts, K., Lepage, C., Borgeat, L., Mohlberg, H., Dickscheid, T., Rousseau, M., Bludau, S., Bazin, P.L., Lewis, L.B., Oros-Peusquens, A.M., Shah, N.J., Lippert, T., Zilles, K., Evans, A.C., 2013. BigBrain: an ultrahigh-resolution 3D human brain model. Science 340, 1472-1475. doi: 10.1126/science.1235381

Ananth, H., Popescu, I., Critchley, H.D., Good, C.D., Frackowiak, R.S., Dolan, R.J., 2002. Cortical and subcortical gray matter abnormalities in schizophrenia determined through structural magnetic resonance imaging with optimized volumetric voxel-based morphometry. The American journal of psychiatry 159, 1497-1505. doi:10.1176/appi.ajp.159.9.1497

Anderson, V.M., Goldstein, M.E., Kydd, R.R., Russell, B.R., 2015. Extensive gray matter volume reduction in treatment-resistant schizophrenia. The international journal of neuropsychopharmacology 18, pyv016. doi:10.1093/ijnp/pyv016

Anderson, K.K., Voineskos, A., Mulsant, B.H., George, T.P., McKenzie, K.J., 2014. The role of untreated psychosis in neurodegeneration: a review of hypothesized mechanisms of neurotoxicity in first-episode psychosis. Canadian journal of psychiatry. Revue canadienne de psychiatrie 59, 513-517 doi:10.1177/070674371405901003

Andreasen, N.C., 2010. The lifetime trajectory of schizophrenia and the concept of neurodevelopment. Dialogues in clinical neuroscience 12, 409-415. doi:10.31887/DCNS.2010.12.3/nandreasen

Andreou, C., Borgwardt, S., 2020. Structural and functional imaging markers for susceptibility to psychosis. Molecular psychiatry. doi:10.1038/s41380-020-0679-7

Andrews, D.S., Avino, T.A., Gudbrandsen, M., Daly, E., Marquand, A., Murphy, C.M., Lai, M.C., Lombardo, M.V., Ruigrok, A.N., Williams, S.C., Bullmore, E.T., The Mrc Aims, C., Suckling, J., Baron-Cohen, S., Craig, M.C., Murphy, D.G., Ecker, C., 2017. In Vivo Evidence of Reduced Integrity of the Gray-White Matter Boundary in Autism Spectrum Disorder. Cereb Cortex 27, 877-887. doi:10.1093/cercor/bhw404

Anderson, N.L., Anderson, N.G., 1998. Proteome and proteomics: new technologies, new concepts, and new words. Electrophoresis 19, 1853-1861. doi:10.1002/elps.1150191103

Anttila, V., Bulik-Sullivan, B., Finucane, H.K., Walters, R.K., Bras, J., Duncan, L., Escott-Price, V., Falcone, G.J., Gormley, P., Malik, R., Patsopoulos, N.A., Ripke, S., Wei, Z., Yu, D., Lee, P.H., Turley, P., Grenier-Boley, B., Chouraki, V., Kamatani, Y., Berr, C., Letenneur, L., Hannequin, D., Amouyel, P., Boland, A., Deleuze, J.-F., Duron, E., Vardarajan, B.N., Reitz, C., Goate, A.M., Huentelman, M.J., Kamboh, M.I., Larson, E.B., Rogaeva, E., St George-Hyslop, P., Hakonarson, H., Kukull, W.A., Farrer, L.A., Barnes, L.L., Beach, T.G., Demirci, F.Y., Head, E., Hulette, C.M., Jicha, G.A., Kauwe, J.S.K., Kaye, J.A., Leverenz, J.B., Levey, A.I., Lieberman, A.P., Pankratz, V.S., Poon, W.W., Quinn, J.F., Saykin, A.J., Schneider, L.S., Smith, A.G., Sonnen, J.A., Stern, R.A., Van Deerlin, V.M., Van Eldik, L.J., Harold, D., Russo, G., Rubinsztein, D.C., Bayer, A., Tsolaki, M., Proitsi, P., Fox, N.C., Hampel, H., Owen, M.J., Mead, S., Passmore, P., Morgan, K., Nöthen, M.M., Schott, J.M., Rossor, M., Lupton, M.K., Hoffmann, P., Kornhuber, J., Lawlor, B., McQuillin, A., Al-Chalabi, A., Bis, J.C., Ruiz, A., Boada, M., Seshadri, S., Beiser, A., Rice, K., van der Lee, S.J., De Jager, P.L., Geschwind, D.H., Riemenschneider, M., Riedel-Heller, S., Rotter, J.I., Ransmayr, G., Hyman, B.T., Cruchaga, C., Alegret, M., Winsvold, B., Palta, P., Farh, K.-H., Cuenca-Leon, E., Furlotte, N., Kurth, T., Ligthart, L., Terwindt, G.M., Freilinger, T., Ran, C., Gordon, S.D., Borck, G., Adams, H.H.H., Lehtimäki, T., Wedenoja, J., Buring, J.E., Schürks, M., Hrafnsdottir, M., Hottenga, J.-J., Penninx, B., Artto, V., Kaunisto, M., Vepsäläinen, S., Martin, N.G., Montgomery, G.W., Kurki, M.I., Hämäläinen, E., Huang, H., Huang, J.,

Sandor, C., Webber, C., Muller-Myhsok, B., Schreiber, S., Salomaa, V., Loehrer, E., Göbel, H., Macaya, A., Pozo-Rosich, P., Hansen, T., Werge, T., Kaprio, J., Metspalu, A., Kubisch, C., Ferrari, M.D., Belin, A.C., van den Maagdenberg, A.M.J.M., Zwart, J.-A., Boomsma, D., Eriksson, N., Olesen, J., Chasman, D.I., Nyholt, D.R., Anney, R., Avbersek, A., Baum, L., Berkovic, S., Bradfield, J., Buono, R.J., Catarino, C.B., Cossette, P., De Jonghe, P., Depondt, C., Dlugos, D., Ferraro, T.N., French, J., Hjalgrim, H., Jamnadas-Khoda, J., Kälviäinen, R., Kunz, W.S., Lerche, H., Leu, C., Lindhout, D., Lo, W., Lowenstein, D., McCormack, M., Møller, R.S., Molloy, A., Ng, P.-W., Oliver, K., Privitera, M., Radtke, R., Ruppert, A.-K., Sander, T., Schachter, S., Schankin, C., Scheffer, I., Schoch, S., Sisodiya, S.M., Smith, P., Sperling, M., Striano, P., Surges, R., Thomas, G.N., Visscher, F., Whelan, C.D., Zara, F., Heinzen, E.L., Marson, A., Becker, F., Stroink, H., Zimprich, F., Gasser, T., Gibbs, R., Heutink, P., Martinez, M., Morris, H.R., Sharma, M., Ryten, M., Mok, K.Y., Pulit, S., Bevan, S., Holliday, E., Attia, J., Battey, T., Boncoraglio, G., Thijs, V., Chen, W.-M., Mitchell, B., Rothwell, P., Sharma, P., Sudlow, C., Vicente, A., Markus, H., Kourkoulis, C., Pera, J., Raffeld, M., Silliman, S., Boraska Perica, V., Thornton, L.M., Huckins, L.M., William Rayner, N., Lewis, C.M., Gratacos, M., Rybakowski, F., Keski-Rahkonen, A., Raevuori, A., Hudson, J.I., Reichborn-Kjennerud, T., Monteleone, P., Karwautz, A., Mannik, K., Baker, J.H., O'Toole, J.K., Trace, S.E., Davis, O.S.P., Helder, S.G., Ehrlich, S., Herpertz-Dahlmann, B., Danner, U.N., van Elburg, A.A., Clementi, M., Forzan, M., Docampo, E., Lissowska, J., Hauser, J., Tortorella, A., Maj, M., Gonidakis, F., Tziouvas, K., Papezova, H., Yilmaz, Z., Wagner, G., Cohen-Woods, S., Herms, S., Julià, A., Rabionet, R., Dick, D.M., Ripatti, S., Andreassen, O.A., Espeseth, T., Lundervold, A.J., Steen, V.M., Pinto, D., Scherer, S.W., Aschauer, H., Schosser, A., Alfredsson, L., Padyukov, L., Halmi, K.A., Mitchell, J., Strober, M., Bergen, A.W., Kaye, W., Szatkiewicz, J.P., Cormand, B., Ramos-Quiroga, J.A., Sánchez-Mora, C., Ribasés, M., Casas, M., Hervas, A., Arranz, M.J., Haavik, J., Zayats, T., Johansson, S., Williams, N., Elia, J., Dempfle, A., Rothenberger, A., Kuntsi, J., Oades, R.D., Banaschewski, T., Franke, B., Buitelaar, J.K., Arias Vasquez, A., Doyle, A.E., Reif, A., Lesch, K.-P., Freitag, C., Rivero, O., Palmason, H., Romanos, M., Langley, K., Rietschel, M., Witt, S.H., Dalsgaard, S., Børglum, A.D., Waldman, I., Wilmot, B., Molly, N., Bau, C.H.D., Crosbie, J., Schachar, R., Loo, S.K., McGough, J.J., Grevet, E.H., Medland, S.E., Robinson, E., Weiss, L.A., Bacchelli, E., Bailey, A., Bal, V., Battaglia, A., Betancur, C., Bolton, P., Cantor, R., Celestino-Soper, P., Dawson, G., De Rubeis, S., Duque, F., Green, A., Klauck,

S.M., Leboyer, M., Levitt, P., Maestrini, E., Mane, S., De-Luca, D.M.-., Parr, J., Regan, R., Reichenberg, A., Sandin, S., Vorstman, J., Wassink, T., Wijsman, E., Cook, E., Santangelo, S., Delorme, R., Rogé, B., Magalhaes, T., Arking, D., Schulze, T.G., Thompson, R.C., Strohmaier, J., Matthews, K., Melle, I., Morris, D., Blackwood, D., McIntosh, A., Bergen, S.E., Schalling, M., Jamain, S., Maaser, A., Fischer, S.B., Reinbold, C.S., Fullerton, J.M., Grigoroiu-Serbanescu, M., Guzman-Parra, J., Mayoral, F., Schofield, P.R., Cichon, S., Mühleisen, T.W., Degenhardt, F., Schumacher, J., Bauer, M., Mitchell, P.B., Gershon, E.S., Rice, J., Potash, J.B., Zandi, P.P., Craddock, N., Ferrier, I.N., Alda, M., Rouleau, G.A., Turecki, G., Ophoff, R., Pato, C., Anjorin, A., Stahl, E., Leber, M., Czerski, P.M., Edenberg, H.J., Cruceanu, C., Jones, I.R., Posthuma, D., Andlauer, T.F.M., Forstner, A.J., Streit, F., Baune, B.T., Air, T., Sinnamon, G., Wray, N.R., MacIntyre, D.J., Porteous, D., Homuth, G., Rivera, M., Grove, J., Middeldorp, C.M., Hickie, I., Pergadia, M., Mehta, D., Smit, J.H., Jansen, R., de Geus, E., Dunn, E., Li, Q.S., Nauck, M., Schoevers, R.A., Beekman, A.T., Knowles, J.A., Viktorin, A., Arnold, P., Barr, C.L., Bedoya-Berrio, G., Bienvenu, O.J., Brentani, H., Burton, C., Camarena, B., Cappi, C., Cath, D., Cavallini, M., Cusi, D., Darrow, S., Denys, D., Derks, E.M., Dietrich, A., Fernandez, T., Figee, M., Freimer, N., Gerber, G., Grados, M., Greenberg, E., Hanna, G.L., Hartmann, A., Hirschtritt, M.E., Hoekstra, P.J., Huang, A., Huyser, C., Illmann, C., Jenike, M., Kuperman, S., Leventhal, B., Lochner, C., Lyon, G.J., Macciardi, F., Madruga-Garrido, M., Malaty, I.A., Maras, A., McGrath, L., Miguel, E.C., Mir, P., Nestadt, G., Nicolini, H., Okun, M.S., Pakstis, A., Paschou, P., Piacentini, J., Pittenger, C., Plessen, K., Ramensky, V., Ramos, E.M., Reus, V., Richter, M.A., Riddle, M.A., Robertson, M.M., Roessner, V., Rosário, M., Samuels, J.F., Sandor, P., Stein, D.J., Tsetsos, F., Van Nieuwerburgh, F., Weatherall, S., Wendland, J.R., Wolanczyk, T., Worbe, Y., Zai, G., Goes, F.S., McLaughlin, N., Nestadt, P.S., Grabe, H.-J., Depienne, C., Konkashbaev, A., Lanzagorta, N., Valencia-Duarte, A., Bramon, E., Buccola, N., Cahn, W., Cairns, M., Chong, S.A., Cohen, D., Crespo-Facorro, B., Crowley, J., Davidson, M., DeLisi, L., Dinan, T., Donohoe, G., Drapeau, E., Duan, J., Haan, L., Hougaard, D., Karachanak-Yankova, S., Khrunin, A., Klovins, J., Kučinskas, V., Lee Chee Keong, J., Limborska, S., Loughland, C., Lönnqvist, J., Maher, B., Mattheisen, M., McDonald, C., Murphy, K.C., Murray, R., Nenadic, I., van Os, J., Pantelis, C., Pato, M., Petryshen, T., Quested, D., Roussos, P., Sanders, A.R., Schall, U., Schwab, S.G., Sim, K., So, H.-C., Stögmann, E., Subramaniam, M., Toncheva, D., Waddington, J., Walters, J., Weiser, M., Cheng, W.,

Cloninger, R., Curtis, D., Gejman, P.V., Henskens, F., Mattingsdal, M., Oh, S.-Y., Scott, R., Webb, B., Breen, G., Churchhouse, C., Bulik, C.M., Daly, M., Dichgans, M., Faraone, S.V., Guerreiro, R., Holmans, P., Kendler, K.S., Koeleman, B., Mathews, C.A., Price, A., Scharf, J., Sklar, P., Williams, J., Wood, N.W., Cotsapas, C., Palotie, A., Smoller, J.W., Sullivan, P., Rosand, J., Corvin, A., Neale, B.M., 2018. Analysis of shared heritability in common disorders of the brain. Science 360, eaap8757. doi:10.1126/science.aap8757

Apps, M.A., Lockwood, P.L., Balsters, J.H., 2013. The role of the midcingulate cortex in monitoring others' decisions. Front Neurosci 7, 251. doi:10.3389/fnins.2013.00251

Arnatkeviciute, A., Fulcher, B.D., Bellgrove, M.A., Fornito, A., 2022. Imaging Transcriptomics of Brain Disorders. Biological psychiatry global open science 2, 319-331. doi: 10.1016/j.bpsgos.2021.10.002

Arnatkeviciute, A., Fulcher, B.D., Fornito, A., 2019a. A practical guide to linking brain-wide gene expression and neuroimaging data. Neuroimage 189, 353-367. doi:10.1016/j.neuroimage.2019.01.011

Arnatkeviciute, A., Fulcher, B.D., Fornito, A., 2019b. Uncovering the Transcriptional Correlates of Hub Connectivity in Neural Networks. Front Neural Circuits 13, 47. doi:10.3389/fncir.2019.00047

Asami, T., Bouix, S., Whitford, T.J., Shenton, M.E., Salisbury, D.F., McCarley, R.W., 2012. Longitudinal loss of gray matter volume in patients with first-episode schizophrenia: DARTEL automated analysis and ROI validation. NeuroImage 59, 986-996. doi:10.1016/j.neuroimage.2011.08.066

Ashburner, J., Friston, K.J., 2000. Voxel-based morphometry—the methods. NeuroImage 11, 805-821. doi:10.1006/nimg.2000.0582

Ashburner, J., Friston, K.J., 2001. Why voxel-based morphometry should be used. Neuroimage 14, 1238-1243. doi:10.1006/nimg.2001.0961

Ashe, P.C., Berry, M.D., Boulton, A.A., 2001. Schizophrenia, a neurodegenerative disorder with neurodevelopmental antecedents. Progress in neuro-psychopharmacology & biological psychiatry 25, 691-707. doi:10.1016/s0278-5846(01)00159-2

Avram, M., Brandl, F., Bäuml, J., Sorg, C., 2018. Cortico-thalamic hypo- and hyperconnectivity extend consistently to basal ganglia in schizophrenia.

Neuropsychopharmacology : official publication of the American College of Neuropsychopharmacology 43, 2239-2248. doi:10.1038/s41386-018-0059-z

Bachevalier, J., Loveland, K.A., 2006. The orbitofrontal-amygdala circuit and self-regulation of social-emotional behavior in autism. Neurosci Biobehav Rev 30, 97-117. doi:10.1016/j.neubiorev.2005.07.002

Baio, J., Wiggins, L., Christensen, D.L., Maenner, M.J., Daniels, J., Warren, Z., Kurzius-Spencer, M., Zahorodny, W., Robinson Rosenberg, C., White, T., Durkin, M.S., Imm, P., Nikolaou, L., Yeargin-Allsopp, M., Lee, L.C., Harrington, R., Lopez, M., Fitzgerald, R.T., Hewitt, A., Pettygrove, S., Constantino, J.N., Vehorn, A., Shenouda, J., Hall-Lande, J., Van Naarden Braun, K., Dowling, N.F., 2018. Prevalence of Autism Spectrum Disorder Among Children Aged 8 Years - Autism and Developmental Disabilities Monitoring Network, 11 Sites, United States, 2014. MMWR Surveill Summ 67, 1-23. doi:10.15585/mmwr.ss6706a1

Balardin, J.B., Comfort, W.E., Daly, E., Murphy, C., Andrews, D., Murphy, D.G., Ecker, C., Sato, J.R., 2015. Decreased centrality of cortical volume covariance networks in autism spectrum disorders. J Psychiatr Res 69, 142-149. doi:10.1016/j.jpsychires.2015.08.003

Barbi, C., Pizzini, F.B., Tamburin, S., Martini, A., Pedrinolla, A., Laginestra, F.G., Giuriato, G., Martignon, C., Schena, F., Venturelli, M., 2022. Brain Structural and Functional Alterations in Multiple Sclerosis-Related Fatigue: A Systematic Review. Neurology international 14, 506-535. doi:10.3390/neurolint14020042

Barnea-Goraly, N., Kwon, H., Menon, V., Eliez, S., Lotspeich, L., Reiss, A.L., 2004. White matter structure in autism: preliminary evidence from diffusion tensor imaging. Biol Psychiatry 55, 323-326. doi:10.1016/j.biopsych.2003.10.022

Baron-Cohen, S., Ring, H.A., Bullmore, E.T., Wheelwright, S., Ashwin, C., Williams, S.C., 2000. The amygdala theory of autism. Neurosci Biobehav Rev 24, 355-364. doi:10.1016/s0149-7634(00)00011-7.

Bassett, D.S., Bullmore, E.T., 2017. Small-World Brain Networks Revisited. The Neuroscientist : a review journal bringing neurobiology, neurology and psychiatry 23, 499-516. doi:10.1177/1073858416667720

Bassitt, D.P., Neto, M.R., de Castro, C.C., Busatto, G.F., 2007. Insight and regional brain volumes in schizophrenia. European archives of psychiatry and clinical neuroscience 257, 58-62. doi:10.1007/s00406-006-0685-z

Battaglia, S., Cardellicchio, P., Di Fazio, C., Nazzi, C., Fracasso, A., Borgomaneri, S., 2022. The Influence of Vicarious Fear-Learning in “Infecting” Reactive Action Inhibition. Frontiers in Behavioral Neuroscience 16. doi:10.3389/fnbeh.2022.946263

Beacher, F.D., Minati, L., Baron-Cohen, S., Lombardo, M.V., Lai, M.C., Gray, M.A., Harrison, N.A., Critchley, H.D., 2012. Autism attenuates sex differences in brain structure: a combined voxel-based morphometry and diffusion tensor imaging study. AJNR. American journal of neuroradiology 33, 83-89. doi:10.3174/ajnr.A2880

Becker, E.B., Stoodley, C.J., 2013. Autism spectrum disorder and the cerebellum. Int Rev Neurobiol 113, 1-34. doi:10.1016/B978-0-12-418700-9.00001-0

Beer, M.D., 1996. The dichotomies: psychosis/neurosis and functional/organic: a historical perspective. History of Psychiatry 7, 231-255. doi:10.1177/0957154X9600702603

Benetti, S., Pettersson-Yeo, W., Hutton, C., Catani, M., Williams, S.C., Allen, P., Kambeitz-Ilankovic, L.M., McGuire, P., Mechelli, A., 2013. Elucidating neuroanatomical alterations in the at risk mental state and first episode psychosis: a combined voxel-based morphometry and voxel-based cortical thickness study. Schizophrenia research 150, 505-511. doi:10.1016/j.schres.2013.08.030

Belyk, M., Brown, S., Lim, J., Kotz, S.A., 2017. Convergence of semantics and emotional expression within the IFG pars orbitalis. NeuroImage 156, 240-248. doi:10.1016/j.neuroimage.2017.04.020

Bennett, C.M., Wolford, G.L., Miller, M.B., 2009. The principled control of false positives in neuroimaging. Social cognitive and affective neuroscience 4, 417-422. doi:10.1093/scan/nsp053

Berlingeri, M., Devoto, F., Gasparini, F., Saibene, A., Corchs, S.E., Clemente, L., Danelli, L., Gallucci, M., Borgoni, R., Borghese, N.A., Paulesu, E., 2019. Clustering the Brain With "CluB": A New Toolbox for Quantitative Meta-Analysis of Neuroimaging Data. Frontiers in neuroscience 13, 1037. doi:10.3389/fnins.2019.01037

Bernard, J.A., Goen, J.R.M., Maldonado, T., 2017. A case for motor network contributions to schizophrenia symptoms: Evidence from resting-state connectivity. Human brain mapping 38, 4535-4545. doi:10.1002/hbm.23680

Bernhardt, B.C., Valk, S.L., Silani, G., Bird, G., Frith, U., Singer, T., 2014. Selective disruption of sociocognitive structural brain networks in autism and alexithymia. Cereb Cortex 24, 3258-3267. doi:10.1093/cercor/bht182

Berrios, G.E., Beer, D., 1994. The notion of unitary psychosis: a conceptual history. History of Psychiatry 5, 013-036. doi:10.1177/0957154X9400501702

Bethlehem, R.A.I., Romero-Garcia, R., Mak, E., Bullmore, E.T., Baron-Cohen, S., 2017. Structural Covariance Networks in Children with Autism or ADHD. Cereb Cortex 27, 4267-4276. doi:10.1093/cercor/bhx135

Bi, X.-a., Zhao, J., Xu, Q., Sun, Q., Wang, Z., 2018. Abnormal Functional Connectivity of Resting State Network Detection Based on Linear ICA Analysis in Autism Spectrum Disorder. Frontiers in physiology 9. doi:10.3389/fphys.2018.00475

Birur, B., Kraguljac, N.V., Shelton, R.C., Lahti, A.C., 2017. Brain structure, function, and neurochemistry in schizophrenia and bipolar disorder-a systematic review of the magnetic resonance neuroimaging literature. NPJ schizophrenia 3, 15. doi:10.1038/s41537-017-0013-9

Bishop, C.M., Nasrabadi, N.M., 2006. Pattern recognition and machine learning. Springer.

Biswal, B.B., Mennes, M., Zuo, X.N., Gohel, S., Kelly, C., Smith, S.M., Beckmann, C.F., Adelstein, J.S., Buckner, R.L., Colcombe, S., Dogonowski, A.M., Ernst, M., Fair, D., Hampson, M., Hoptman, M.J., Hyde, J.S., Kiviniemi, V.J., Kotter, R., Li, S.J., Lin, C.P., Lowe, M.J., Mackay, C., Madden, D.J., Madsen, K.H., Margulies, D.S., Mayberg, H.S., McMahon, K., Monk, C.S., Mostofsky, S.H., Nagel, B.J., Pekar, J.J., Peltier, S.J., Petersen, S.E., Riedl, V., Rombouts, S.A., Rypma, B., Schlaggar, B.L., Schmidt, S., Seidler, R.D., Siegle, G.J., Sorg, C., Teng, G.J., Veijola, J., Villringer, A., Walter, M., Wang, L., Weng, X.C., Whitfield-Gabrieli, S., Williamson, P., Windischberger, C., Zang, Y.F., Zhang, H.Y., Castellanos, F.X., Milham, M.P., 2010. Toward discovery science of human brain function. Proceedings of the National Academy of Sciences of the United States of America 107, 4734-4739. doi:10.1073/pnas.0911855107

Boddaert, N., Chabane, N., Gervais, H., Good, C.D., Bourgeois, M., Plumet, M.H., Barthelemy, C., Mouren, M.C., Artiges, E., Samson, Y., Brunelle, F., Frackowiak, R.S., Zilbovicius, M., 2004. Superior temporal sulcus anatomical abnormalities in childhood autism: a voxel-based morphometry MRI study. Neuroimage 23, 364-369. doi:10.1016/j.neuroimage.2004.06.016

Bolland, J.M., 1988. Sorting out centrality: An analysis of the performance of four centrality models in real and simulated networks. Social networks 10, 233-253. doi:10.1016/0378-8733(88)90014-7

Bonath, B., Tegelbeckers, J., Wilke, M., Flechtner, H.H., Krauel, K., 2018. Regional Gray Matter Volume Differences Between Adolescents With ADHD and Typically Developing Controls: Further Evidence for Anterior Cingulate Involvement. J Atten Disord 22, 627-638. doi:10.1177/1087054715619682

Bonelli, C., Mancuso, L., Manuello, J., Liloia, D., Costa, T., Cauda, F., 2022. Sex differences in brain homotopic co-activations: a meta-analytic study. Brain structure & function 227, 2839-2855. doi:10.1007/s00429-022-02572-0

Bonilha, L., Cendes, F., Rorden, C., Eckert, M., Dalgalarrondo, P., Li, L.M., Steiner, C.E., 2008. Gray and white matter imbalance--typical structural abnormality underlying classic autism? Brain & development 30, 396-401. doi:10.1016/j.braindev.2007.11.006

Bonner-Jackson, A., Haut, K., Csernansky, J.G., Barch, D.M., 2005. The influence of encoding strategy on episodic memory and cortical activity in schizophrenia. Biological psychiatry 58, 47-55. doi:10.1016/j.biopsych.2005.05.011

Boos, H.B., Aleman, A., Cahn, W., Hulshoff Pol, H., Kahn, R.S., 2007. Brain volumes in relatives of patients with schizophrenia: a meta-analysis. Archives of general psychiatry 64, 297-304. doi:10.1001/archpsyc.64.3.297

Bora, E., Akdede, B.B., Alptekin, K., 2017. The relationship between cognitive impairment in schizophrenia and metabolic syndrome: a systematic review and meta-analysis. Psychological medicine 47, 1030-1040. doi:10.1017/s0033291716003366

Bora, E., Fornito, A., Radua, J., Walterfang, M., Seal, M., Wood, S.J., Yucel, M., Velakoulis, D., Pantelis, C., 2011. Neuroanatomical abnormalities in schizophrenia: a multimodal

voxelwise meta-analysis and meta-regression analysis. Schizophrenia research 127, 46-57. doi:10.1016/j.schres.2010.12.020

Bora, E., Fornito, A., Yucel, M., Pantelis, C., 2012. The effects of gender on grey matter abnormalities in major psychoses: a comparative voxelwise meta-analysis of schizophrenia and bipolar disorder. Psychological medicine 42, 295-307. doi:10.1017/s0033291711001450

Borgwardt, S.J., McGuire, P.K., Aston, J., Berger, G., Dazzan, P., Gschwandtner, U., Pfluger, M., D'Souza, M., Radue, E.W., Riecher-Rossler, A., 2007a. Structural brain abnormalities in individuals with an at-risk mental state who later develop psychosis. The British journal of psychiatry 51, 69-75. doi:10.1192/bjp.191.51.s69

Borgwardt, S.J., McGuire, P.K., Aston, J., Gschwandtner, U., Pfluger, M.O., Stieglitz, R.D., Radue, E.W., Riecher-Rossler, A., 2008. Reductions in frontal, temporal and parietal volume associated with the onset of psychosis. Schizophrenia research 106, 108-114. doi:10.1016/j.schres.2008.08.007

Borgwardt, S.J., Picchioni, M.M., Ettinger, U., Toulopoulou, T., Murray, R., McGuire, P.K., 2010. Regional gray matter volume in monozygotic twins concordant and discordant for schizophrenia. Biological psychiatry 67, 956-964. doi:10.1016/j.biopsych.2009.10.026

Borgwardt, S.J., Riecher-Rossler, A., Dazzan, P., Chitnis, X., Aston, J., Drewe, M., Gschwandtner, U., Haller, S., Pfluger, M., Rechsteiner, E., D'Souza, M., Stieglitz, R.D., Radu, E.W., McGuire, P.K., 2007b. Regional gray matter volume abnormalities in the at risk mental state. Biological psychiatry 61, 1148-1156. doi:10.1016/j.biopsych.2006.08.009

Bos, D.J., Merchán-Naranjo, J., Martínez, K., Pina-Camacho, L., Balsa, I., Boada, L., Schnack, H., Oranje, B., Desco, M., Arango, C., Parellada, M., Durston, S., Janssen, J., 2015. Reduced Gyrification Is Related to Reduced Interhemispheric Connectivity in Autism Spectrum Disorders. J Am Acad Child Adolesc Psychiatry 54, 668-676. doi:10.1016/j.jaac.2015.05.011

Bourdenx, M., Koulakiotis, N.S., Sanoudou, D., Bezard, E., Dehay, B., Tsarbopoulos, A., 2017. Protein aggregation and neurodegeneration in prototypical neurodegenerative diseases: Examples of amyloidopathies, tauopathies and synucleinopathies. Progress in Neurobiology 155, 171-193. doi:10.1016/j.pneurobio.2015.07.003

Bourgeois-Gironde, S., 2010. Is neuroeconomics doomed by the reverse inference fallacy? Mind & Society 9, 229-249.

Bralten, J., Greven, C.U., Franke, B., Mennes, M., Zwiers, M.P., Rommelse, N.N., Hartman, C., van der Meer, D., O'Dwyer, L., Oosterlaan, J., Hoekstra, P.J., Heslenfeld, D., Arias-Vasquez, A., Buitelaar, J.K., 2016. Voxel-based morphometry analysis reveals frontal brain differences in participants with ADHD and their unaffected siblings. Journal of psychiatry & neuroscience : JPN 41, 272-279. doi:10.1503/jpn.140377

Brambati, S.M., Termine, C., Ruffino, M., Stella, G., Fazio, F., Cappa, S.F., Perani, D., 2004. Regional reductions of gray matter volume in familial dyslexia. Neurology 63, 742-745. doi:10.1212/01.wnl.0000134673.95020.ee

Breukelaar, I.A., Bryant, R.A., Korgaonkar, M.S., 2021. The functional connectome in posttraumatic stress disorder. Neurobiology of stress 14, 100321. doi:10.1016/j.ynstr.2021.100321

Brickman, A.M., Buchsbaum, M.S., Shihabuddin, L., Byne, W., Newmark, R.E., Brand, J., Ahmed, S., Mitelman, S.A., Hazlett, E.A., 2004. Thalamus size and outcome in schizophrenia. Schizophrenia research 71, 473-484. doi:10.1016/j.schres.2004.03.011

Brieber, S., Neufang, S., Bruning, N., Kamp-Becker, I., Remschmidt, H., Herpertz-Dahlmann, B., Fink, G.R., Konrad, K., 2007. Structural brain abnormalities in adolescents with autism spectrum disorder and patients with attention deficit/hyperactivity disorder. Journal of child psychology and psychiatry, and allied disciplines 48, 1251-1258. doi:10.1111/j.1469-7610.2007.01799.x

Brighenti, S., Schintu, S., Liloia, D., Keller, R., 2018. Neuropsychological aspects of Asperger Syndrome in adults: a review. Neuropsychological Trends, 63-95. doi:10.7358/neur-2018-024-brig

Brodmann, K., 2007. Brodmann's: Localisation in the cerebral cortex. Springer Science & Business Media.

Brown, R.W., Cheng, Y.-C.N., Haacke, E.M., Thompson, M.R., Venkatesan, R., 2014. Magnetic resonance imaging: physical principles and sequence design. John Wiley & Sons. doi:10.1002/9781118633953

Brown, G.G., Lee, J.S., Strigo, I.A., Caligiuri, M.P., Meloy, M.J., Lohr, J., 2011. Voxel-based morphometry of patients with schizophrenia or bipolar I disorder: a matched control study. Psychiatry research 194, 149-156. doi:10.1016/j.pscychresns.2011.05.005

Brown, W.E., Eliez, S., Menon, V., Rumsey, J.M., White, C.D., Reiss, A.L., 2001. Preliminary evidence of widespread morphological variations of the brain in dyslexia. Neurology 56, 781-783. doi:10.1212/wnl.56.6.781

Bruchhage, M.M.K., Bucci, M.P., Becker, E.B.E., 2018. Cerebellar involvement in autism and ADHD. Handbook of clinical neurology 155, 61-72. doi:10.1016/b978-0-444-64189-2.00004-4

Bruin, W.B., Taylor, L., Thomas, R.M., Shock, J.P., Zhutovsky, P., Abe, Y., Alonso, P., Ameis, S.H., Anticevic, A., Arnold, P.D., Assogna, F., Benedetti, F., Beucke, J.C., Boedhoe, P.S.W., Bollettini, I., Bose, A., Brem, S., Brennan, B.P., Buitelaar, J.K., Calvo, R., Cheng, Y., Cho, K.I.K., Dallaspezia, S., Denys, D., Ely, B.A., Feusner, J.D., Fitzgerald, K.D., Fouche, J.P., Fridgeirsson, E.A., Gruner, P., Gürsel, D.A., Hauser, T.U., Hirano, Y., Hoexter, M.Q., Hu, H., Huyser, C., Ivanov, I., James, A., Jaspers-Fayer, F., Kathmann, N., Kaufmann, C., Koch, K., Kuno, M., Kvale, G., Kwon, J.S., Liu, Y., Lochner, C., Lázaro, L., Marques, P., Marsh, R., Martínez-Zalacaín, I., Mataix-Cols, D., Menchón, J.M., Minuzzi, L., Moreira, P.S., Morer, A., Morgado, P., Nakagawa, A., Nakamae, T., Nakao, T., Narayanaswamy, J.C., Nurmi, E.L., O'Neill, J., Pariente, J.C., Perriello, C., Piacentini, J., Piras, F., Piras, F., Reddy, Y.C.J., Rus-Oswald, O.G., Sakai, Y., Sato, J.R., Schmaal, L., Shimizu, E., Simpson, H.B., Soreni, N., Soriano-Mas, C., Spalletta, G., Stern, E.R., Stevens, M.C., Stewart, S.E., Szeszko, P.R., Tolin, D.F., Venkatasubramanian, G., Wang, Z., Yun, J.Y., van Rooij, D., Thompson, P.M., van den Heuvel, O.A., Stein, D.J., van Wingen, G.A., 2020. Structural neuroimaging biomarkers for obsessive-compulsive disorder in the ENIGMA-OCD consortium: medication matters. Translational psychiatry 10, 342. doi:10.1038/s41398-020-01013-y

Brüne, M., Schöbel, A., Karau, R., Benali, A., Faustmann, P.M., Juckel, G., Petrasch-Parwez, E., 2010. Von Economo neuron density in the anterior cingulate cortex is reduced in early onset schizophrenia. Acta neuropathologica 119, 771-778. doi:10.1007/s00401-010-0673-2

Brüne, M., Schöbel, A., Karau, R., Faustmann, P.M., Dermietzel, R., Juckel, G., Petrasch-Parwez, E., 2011. Neuroanatomical correlates of suicide in psychosis: the possible role of von Economo neurons. PloS one 6, e20936. doi:10.1371/journal.pone.0020936

Bryńska, A., Wolak, T., Naumczyk, P., Srebnicki, T., Wolańczyk, T., 2021. Voxel-based morphometry in adolescents with autism spectrum disorder. Psychiatr. Pol. , 1-11.

Buckholtz, J.W., Meyer-Lindenberg, A., 2012. Psychopathology and the human connectome: toward a transdiagnostic model of risk for mental illness. Neuron 74, 990-1004. doi:10.1016/j.neuron.2012.06.002

Buckner, R.L., DiNicola, L.M., 2019. The brain's default network: updated anatomy, physiology and evolving insights. Nature Reviews Neuroscience 20, 593-608. doi:10.1038/s41583-019-0212-7

Buckner, R.L., Krienen, F.M., Castellanos, A., Diaz, J.C., Yeo, B.T., 2011. The organization of the human cerebellum estimated by intrinsic functional connectivity. J Neurophysiol 106, 2322-2345. doi:10.1152/jn.00339.2011

Buckner, R.L., Sepulcre, J., Talukdar, T., Krienen, F.M., Liu, H., Hedden, T., Andrews-Hanna, J.R., Sperling, R.A., Johnson, K.A., 2009. Cortical hubs revealed by intrinsic functional connectivity: mapping, assessment of stability, and relation to Alzheimer's disease. The Journal of neuroscience : the official journal of the Society for Neuroscience 29, 1860-1873. doi:10.1523/JNEUROSCI.5062-08.2009

Bulik-Sullivan, B., Finucane, H.K., Anttila, V., Gusev, A., Day, F.R., Loh, P.R., Duncan, L., Perry, J.R., Patterson, N., Robinson, E.B., Daly, M.J., Price, A.L., Neale, B.M., 2015. An atlas of genetic correlations across human diseases and traits. Nature genetics 47, 1236-1241. doi:10.1038/ng.3406

Bullmore, E., Sporns, O., 2012. The economy of brain network organization. Nat Rev Neurosci 13, 336-349. doi:10.1038/nrn3214

Buoli, M., Serati, M., Caldiroli, A., Cremaschi, L., Altamura, A.C., 2017. Neurodevelopmental Versus Neurodegenerative Model of Schizophrenia and Bipolar Disorder: Comparison with Physiological Brain Development and Aging. Psychiatria Danubina 29, 24-27. doi:10.24869/psyd.2017.24

Burrows, C.A., Laird, A.R., Uddin, L.Q., 2016. Functional connectivity of brain regions for self- and other-evaluation in children, adolescents and adults with autism. Developmental science 19, 564-580. doi:10.1111/desc.12400

Bush, G., Valera, E.M., Seidman, L.J., 2005. Functional neuroimaging of attention-deficit/hyperactivity disorder: a review and suggested future directions. Biological psychiatry 57, 1273-1284. doi:10.1016/j.biopsych.2005.01.034

Butti, C., Santos, M., Uppal, N., Hof, P.R., 2013. Von Economo neurons: clinical and evolutionary perspectives. Cortex; a journal devoted to the study of the nervous system and behavior 49, 312-326. doi:10.1016/j.cortex.2011.10.004

Button, K.S., Ioannidis, J.P.A., Mokrysz, C., Nosek, B.A., Flint, J., Robinson, E.S.J., Munafò, M.R., 2013. Power failure: why small sample size undermines the reliability of neuroscience. Nature Reviews Neuroscience 14, 365-376. doi:10.1038/nrn3475

Butts, C.T., 2009. Revisiting the foundations of network analysis. Science 325, 414-416. doi:10.1126/science.1171022

Byne, W., Buchsbaum, M.S., Kemether, E., Hazlett, E.A., Shinwari, A., Mitropoulou, V., Siever, L.J., 2001. Magnetic resonance imaging of the thalamic mediodorsal nucleus and pulvinar in schizophrenia and schizotypal personality disorder. Archives of general psychiatry 58, 133-140. doi:10.1001/archpsyc.58.2.133

Byne, W., Hazlett, E.A., Buchsbaum, M.S., Kemether, E., 2009. The thalamus and schizophrenia: current status of research. Acta neuropathologica 117, 347-368. doi:10.1007/s00401-008-0404-0

Bzdok, D., Laird, A.R., Zilles, K., Fox, P.T., Eickhoff, S.B., 2013. An investigation of the structural, connectional, and functional subspecialization in the human amygdala. Hum Brain Mapp 34, 3247-3266. doi: 10.1002/hbm.22138

Cai, J., Hu, X., Guo, K., Yang, P., Situ, M., Huang, Y., 2018. Increased Left Inferior Temporal Gyrus Was Found in Both Low Function Autism and High Function Autism. Frontiers in psychiatry 9. doi:10.3389/fpsyt.2018.00542

Calzavarini, F., Cevolani, G., 2022. Abductive reasoning in cognitive neuroscience: weak and strong reverse inference. Synthese 200, 1-26.

Camasio, A., Panzeri, E., Mancuso, L., Costa, T., Manuello, J., Ferraro, M., Duca, S., Cauda, F., Liloia, D., 2022. Linking neuroanatomical abnormalities in autism spectrum disorder with gene expression of candidate ASD genes: A meta-analytic and network-oriented approach. PLOS ONE 17, e0277466. doi: 10.1371/journal.pone.0277466

Cannon, T.D., Sun, F., McEwen, S.J., Papademetris, X., He, G., van Erp, T.G., Jacobson, A., Bearden, C.E., Walker, E., Hu, X., Zhou, L., Seidman, L.J., Thermenos, H.W., Cornblatt, B., Olvet, D.M., Perkins, D., Belger, A., Cadenhead, K., Tsuang, M., Mirzakhanian, H., Addington, J., Frayne, R., Woods, S.W., McGlashan, T.H., Constable, R.T., Qiu, M., Mathalon, D.H., Thompson, P., Toga, A.W., 2014. Reliability of neuroanatomical measurements in a multisite longitudinal study of youth at risk for psychosis. Human brain mapping 35, 2424-2434. doi:10.1002/hbm.22338

Canu, E., Agosta, F., Filippi, M., 2015. A selective review of structural connectivity abnormalities of schizophrenic patients at different stages of the disease. Schizophrenia research 161, 19-28. doi:10.1016/j.schres.2014.05.020

Cao, M., Shu, N., Cao, Q., Wang, Y., He, Y., 2014. Imaging functional and structural brain connectomics in attention-deficit/hyperactivity disorder. Molecular neurobiology 50, 1111-1123. doi:10.1007/s12035-014-8685-x

Cao, M., Wang, Z., He, Y., 2015. Connectomics in psychiatric research: advances and applications. Neuropsychiatr Dis Treat 11, 2801-2810. doi:10.2147/ndt.s63470

Cao, R., Yang, X., Luo, J., Wang, P., Meng, F., Xia, M., He, Y., Zhao, T., Li, Z., 2020. The effects of cognitive behavioral therapy on the whole brain structural connectome in unmedicated patients with obsessive-compulsive disorder. Prog Neuropsychopharmacol Biol Psychiatry 104, 110037. doi:10.1016/j.pnpbp.2020.110037

Cardon, G.J., Hepburn, S., Rojas, D.C., 2017. Structural Covariance of Sensory Networks, the Cerebellum, and Amygdala in Autism Spectrum Disorder. Front Neurol 8, 615. doi:10.3389/fneur.2017.00615

Carlisi, C.O., Norman, L.J., Lukito, S.S., Radua, J., Mataix-Cols, D., Rubia, K., 2017. Comparative Multimodal Meta-analysis of Structural and Functional Brain Abnormalities in Autism Spectrum Disorder and Obsessive-Compulsive Disorder. Biol Psychiatry 82, 83-102. doi:10.1016/j.biopsych.2016.10.006

Carmona, S., Vilarroya, O., Bielsa, A., Trèmols, V., Soliva, J.C., Rovira, M., Tomàs, J., Raheb, C., Gispert, J.D., Batlle, S., Bulbena, A., 2005. Global and regional gray matter reductions in ADHD: a voxel-based morphometric study. Neuroscience letters 389, 88-93. doi:10.1016/j.neulet.2005.07.020

Carp, J., 2012. The secret lives of experiments: methods reporting in the fMRI literature. Neuroimage 63, 289-300.

Carrera, E., Tononi, G., 2014. Diaschisis: past, present, future. Brain 137, 2408-2422. doi:10.1093/brain/awu101

Casanova, M.F., 2006. Neuropathological and genetic findings in autism: the significance of a putative minicolumnopathy. Neuroscientist 12, 435-441. doi:10.1177/1073858406290375

Cascella, N.G., Fieldstone, S.C., Rao, V.A., Pearlson, G.D., Sawa, A., Schretlen, D.J., 2010. Gray-matter abnormalities in deficit schizophrenia. Schizophrenia research 120, 63-70. doi:10.1016/j.schres.2010.03.039

Caspers, J., Zilles, K., Beierle, C., Rottschy, C., Eickhoff, S.B., 2014. A novel meta-analytic approach: mining frequent co-activation patterns in neuroimaging databases. Neuroimage 90, 390-402.

Caspi, A., Houts, R.M., Belsky, D.W., Goldman-Mellor, S.J., Harrington, H., Israel, S., Meier, M.H., Ramrakha, S., Shalev, I., Poulton, R., Moffitt, T.E., 2014. The p Factor:One General Psychopathology Factor in the Structure of Psychiatric Disorders? Clinical Psychological Science 2, 119-137. doi:10.1177/2167702613497473

Carlsson, T., Molander, F., Taylor, M.J., Jonsson, U., Bölte, S., 2020. Early environmental risk factors for neurodevelopmental disorders – a systematic review of twin and sibling studies. Development and Psychopathology 33, 1448-1495. doi:10.1017/S0954579420000620

Castellanos, F.X., 2002. Anatomic magnetic resonance imaging studies of attention-deficit/hyperactivity disorder. Dialogues in clinical neuroscience 4, 444-448.

Catani, M., Dell'Acqua, F., Budisavljevic, S., Howells, H., Thiebaut de Schotten, M., Froudist-Walsh, S., D'Anna, L., Thompson, A., Sandrone, S., Bullmore, E.T., Suckling, J., Baron-Cohen, S., Lombardo, M.V., Wheelwright, S.J., Chakrabarti, B., Lai, M.C., Ruigrok, A.N., Leemans, A., Ecker, C., Consortium, M.A., Craig, M.C., Murphy, D.G., 2016. Frontal networks in adults with autism spectrum disorder. Brain 139, 616-630. doi:10.1093/brain/awv351

Cauda, F., Costa, T., Nani, A., Fava, L., Palermo, S., Bianco, F., Duca, S., Tatu, K., Keller, R., 2017. Are schizophrenia, autistic, and obsessive spectrum disorders dissociable on the basis of neuroimaging morphological findings?: A voxel-based meta-analysis. Autism

research : official journal of the International Society for Autism Research. doi:10.1002/aur.1759

Cauda, F., Costa, T., Palermo, S., D'Agata, F., Diano, M., Bianco, F., Duca, S., Keller, R., 2014a. Concordance of white matter and gray matter abnormalities in autism spectrum disorders: A voxel-based meta-analysis study. Hum Brain Mapp 35, 2073-2098. doi:10.1002/hbm.22313

Cauda, F., Geda, E., Sacco, K., D'Agata, F., Duca, S., Geminiani, G., Keller, R., 2011. Grey matter abnormality in autism spectrum disorder: an activation likelihood estimation meta-analysis study. J Neurol Neurosurg Psychiatry 82, 1304-1313. doi:10.1136/jnnp.2010.239111

Cauda, F., Mancuso, L., Nani, A., Costa, T., 2019a. Heterogeneous neuroimaging findings, damage propagation and connectivity: an integrative view. Brain 142, e17-e17. doi:10.1093/brain/awz080

Cauda, F., Mancuso, L., Nani, A., Ficco, L., Premi, E., Manuello, J., Liloia, D., Gelmini, G., Duca, S., Costa, T., 2020a. Hubs of long-distance co-alteration characterize brain pathology. Hum Brain Mapp. doi:10.1002/hbm.25093

Cauda, F., Geminiani, G.C., Vercelli, A., 2014b. Evolutionary appearance of von Economo's neurons in the mammalian cerebral cortex. Frontiers in human neuroscience 8, 104. doi:10.3389/fnhum.2014.00104

Cauda, F., Nani, A., Costa, T., Palermo, S., Tatu, K., Manuello, J., Duca, S., Fox, P.T., Keller, R., 2018a. The morphometric co-atrophy networking of schizophrenia, autistic and obsessive spectrum disorders. Human brain mapping. doi:10.1002/hbm.23952

Cauda, F., Nani, A., Liloia, D., Gelmini, G., Mancuso, L., Manuello, J., Panero, M., Duca, S., Zang, Y.-F., Costa, T., 2021. Interhemispheric co-alteration of brain homotopic regions. Brain Structure and Function 226, 2181-2204. doi: 10.1007/s00429-021-02318-4

Cauda, F., Nani, A., Liloia, D., Manuello, J., Premi, E., Duca, S., Fox, P.T., Costa, T., 2020b. Finding specificity in structural brain alterations through Bayesian reverse inference. Human brain mapping. doi:10.1002/hbm.25105

Cauda, F., Nani, A., Manuello, J., Liloia, D., Tatu, K., Vercelli, U., Duca, S., Fox, P.T., Costa, T., 2019b. The alteration landscape of the cerebral cortex. NeuroImage 184, 359-371. doi:10.1016/j.neuroimage.2018.09.036

Cauda, F., Nani, A., Manuello, J., Premi, E., Palermo, S., Tatu, K., Duca, S., Fox, P.T., Costa, T., 2018b. Brain structural alterations are distributed following functional, anatomic and genetic connectivity. Brain 141, 3211-3232. doi:10.1093/brain/awy252

Cavanna, A.E., 2007. The precuneus and consciousness. CNS Spectr 12, 545-552. doi:10.1017/s1092852900021295

Cavanna, A.E., Trimble, M.R., 2006. The precuneus: a review of its functional anatomy and behavioural correlates. Brain 129, 564-583. doi:10.1093/brain/awl004

Chan, R.C., Di, X., McAlonan, G.M., Gong, Q.Y., 2011. Brain anatomical abnormalities in high-risk individuals, first-episode, and chronic schizophrenia: an activation likelihood estimation meta-analysis of illness progression. Schizophrenia bulletin 37, 177-188. doi:10.1093/schbul/sbp073

Chang, M., Womer, F.Y., Bai, C., Zhou, Q., Wei, S., Jiang, X., Geng, H., Zhou, Y., Tang, Y., Wang, F., 2016. Voxel-Based Morphometry in Individuals at Genetic High Risk for Schizophrenia and Patients with Schizophrenia during Their First Episode of Psychosis. PloS one 11, e0163749. doi:10.1371/journal.pone.0163749

Chang, J.C., Lin, H.Y., Lv, J., Tseng, W.I., Gau, S.S., 2021. Regional brain volume predicts response to methylphenidate treatment in individuals with ADHD. BMC psychiatry 21, 26. doi:10.1186/s12888-021-03040-5

Charlson, F.J., Ferrari, A.J., Santomauro, D.F., Diminic, S., Stockings, E., Scott, J.G., McGrath, J.J., Whiteford, H.A., 2018. Global Epidemiology and Burden of Schizophrenia: Findings From the Global Burden of Disease Study 2016. Schizophrenia bulletin 44, 1195-1203. doi:10.1093/schbul/sby058

Chen, X., Lu, B., Yan, C.G., 2018. Reproducibility of R-fMRI metrics on the impact of different strategies for multiple comparison correction and sample sizes. Human brain mapping 39, 300-318. doi:10.1002/hbm.23843

Chen, Z., Deng, W., Gong, Q., Huang, C., Jiang, L., Li, M., He, Z., Wang, Q., Ma, X., Wang, Y., Chua, S.E., McAlonan, G.M., Sham, P.C., Collier, D.A., McGuire, P., Li, T., 2014. Extensive brain structural network abnormality in first-episode treatment-naive patients with schizophrenia: morphometrical and covariation study. Psychological medicine 44, 2489-2501. doi:10.1017/s003329171300319x

Cheng, W., Rolls, E.T., Zhang, J., Sheng, W., Ma, L., Wan, L., Luo, Q., Feng, J., 2017. Functional connectivity decreases in autism in emotion, self, and face circuits identified by Knowledge-based Enrichment Analysis. Neuroimage 148, 169-178. doi:10.1016/j.neuroimage.2016.12.068

Cheng, Y., Chou, K.H., Fan, Y.T., Lin, C.P., 2011. ANS: aberrant neurodevelopment of the social cognition network in adolescents with autism spectrum disorders. PLoS One 6, e18905. doi:10.1371/journal.pone.0018905

Chiarotti, F., Venerosi, A., 2020. Epidemiology of Autism Spectrum Disorders: A Review of Worldwide Prevalence Estimates Since 2014. Brain Sciences 10, 274. doi:10.3390/brainsci10050274

Chiu, P.H., Kayali, M.A., Kishida, K.T., Tomlin, D., Klinger, L.G., Klinger, M.R., Montague, P.R., 2008. Self responses along cingulate cortex reveal quantitative neural phenotype for high-functioning autism. Neuron 57, 463-473. doi:10.1016/j.neuron.2007.12.020

Choi, E.Y., Yeo, B.T., Buckner, R.L., 2012. The organization of the human striatum estimated by intrinsic functional connectivity. J Neurophysiol 108, 2242-2263. doi:10.1152/jn.00270.2012

Choi, U.S., Kim, S.Y., Sim, H.J., Lee, S.Y., Park, S.Y., Jeong, J.S., Seol, K.I., Yoon, H.W., Jhung, K., Park, J.I., Cheon, K.A., 2015. Abnormal brain activity in social reward learning in children with autism spectrum disorder: an fMRI study. Yonsei Med J 56, 705-711. doi:10.3349/ymj.2015.56.3.705

Christensen, M.K., Lim, C.C.W., Saha, S., Plana-Ripoll, O., Cannon, D., Presley, F., Weye, N., Momen, N.C., Whiteford, H.A., Iburg, K.M., McGrath, J.J., 2020. The cost of mental disorders: a systematic review. Epidemiology and psychiatric sciences 29, e161. doi:10.1017/S204579602000075X

Chung, W., Jiang, S.-F., Paksarian, D., Nikolaidis, A., Castellanos, F.X., Merikangas, K.R., Milham, M.P., 2019. Trends in the Prevalence and Incidence of Attention-Deficit/Hyperactivity Disorder Among Adults and Children of Different Racial and Ethnic Groups. JAMA Network Open 2, e1914344-e1914344. doi:10.1001/jamanetworkopen.2019.14344

Cioli, C., Abdi, H., Beaton, D., Burnod, Y., Mesmoudi, S., 2014. Differences in human cortical gene expression match the temporal properties of large-scale functional networks. PLoS One 9, e115913. doi:10.1371/journal.pone.0115913

Çırak, M., Yağmurlu, K., Kearns, K.N., Ribas, E.C., Urgun, K., Shaffrey, M.E., Kalani, M.Y.S., 2020. The Caudate Nucleus: Its Connections, Surgical Implications, and Related Complications. World Neurosurg. doi:10.1016/j.wneu.2020.04.027

Clavaguera, F., Lavenir, I., Falcon, B., Frank, S., Goedert, M., Tolnay, M., 2013. "Prion-like" templated misfolding in tauopathies. Brain Pathol 23, 342-349. doi:10.1111/bpa.12044

Clos, M., Amunts, K., Laird, A.R., Fox, P.T., Eickhoff, S.B., 2013. Tackling the multifunctional nature of Broca's region meta-analytically: co-activation-based parcellation of area 44. Neuroimage 83, 174-188. doi: 10.1016/j.neuroimage.2013.06.041

Cole, M.W., Repovs, G., Anticevic, A., 2014. The frontoparietal control system: a central role in mental health. The Neuroscientist : a review journal bringing neurobiology, neurology and psychiatry 20, 652-664. doi:10.1177/1073858414525995

Collantoni, E., Alberti, F., Meregalli, V., Meneguzzo, P., Tenconi, E., Favaro, A., 2022. Brain networks in eating disorders: a systematic review of graph theory studies. Eating and weight disorders : EWD 27, 69-83. doi:10.1007/s40519-021-01172-x

Collin, G., Seidman, L.J., Keshavan, M.S., Stone, W.S., Qi, Z., Zhang, T., Tang, Y., Li, H., Anteraper, S.A., Niznikiewicz, M.A., McCarley, R.W., Shenton, M.E., Wang, J., Whitfield-Gabrieli, S., 2018. Functional connectome organization predicts conversion to psychosis in clinical high-risk youth from the SHARP program. Molecular psychiatry. doi:10.1038/s41380-018-0288-x

Collin, G., Sporns, O., Mandl, R.C., van den Heuvel, M.P., 2014. Structural and functional aspects relating to cost and benefit of rich club organization in the human cerebral cortex. Cereb Cortex 24, 2258-2267. doi:10.1093/cercor/bht064

Collin, G., van den Heuvel, M.P., Abramovic, L., Vreeker, A., de Reus, M.A., van Haren, N.E., Boks, M.P., Ophoff, R.A., Kahn, R.S., 2016. Brain network analysis reveals affected connectome structure in bipolar I disorder. Hum Brain Mapp 37, 122-134. doi:10.1002/hbm.23017

Colloby, S.J., O'Brien, J.T., Taylor, J.P., 2014. Patterns of cerebellar volume loss in dementia with Lewy bodies and Alzheimer′s disease: A VBM-DARTEL study. Psychiatry research 223, 187-191. doi:10.1016/j.pscychresns.2014.06.006

Compton, M.T., Lunden, A., Cleary, S.D., Pauselli, L., Alolayan, Y., Halpern, B., Broussard, B., Crisafio, A., Capulong, L., Balducci, P.M., Bernardini, F., Covington, M.A., 2018. The aprosody of schizophrenia: Computationally derived acoustic phonetic underpinnings of monotone speech. Schizophrenia research 197, 392-399. doi:10.1016/j.schres.2018.01.007

Contarino, V.E., Bulgheroni, S., Annunziata, S., Erbetta, A., Riva, D., 2016. Widespread Focal Cortical Alterations in Autism Spectrum Disorder with Intellectual Disability Detected by Threshold-Free Cluster Enhancement. AJNR. American journal of neuroradiology 37, 1721-1726. doi:10.3174/ajnr.A4779

Cooper, D., Barker, V., Radua, J., Fusar-Poli, P., Lawrie, S.M., 2014. Multimodal voxel-based meta-analysis of structural and functional magnetic resonance imaging studies in those at elevated genetic risk of developing schizophrenia. Psychiatry research 221, 69-77. doi:10.1016/j.pscychresns.2013.07.008

Coraci, D., Cevolani, G., 2022. L’analisi bayesiana dell’inferenza inversa in neuroscienza: una critica. Sistemi intelligenti 34, 209-234.

Corbetta, M., Kincade, J.M., Shulman, G.L., 2002. Neural systems for visual orienting and their relationships to spatial working memory. Journal of cognitive neuroscience 14, 508-523. doi:10.1162/089892902317362029

Costa, T., Manuello, J., Ferraro, M., Liloia, D., Nani, A., Fox, P.T., Lancaster, J., Cauda, F., 2021. BACON: A tool for reverse inference in brain activation and alteration. Human brain mapping. doi:10.1002/hbm.25452

Costafreda, S.G., David, A.S., Brammer, M.J., 2009. A parametric approach to voxel-based meta-analysis. Neuroimage 46, 115-122. doi:10.1016/j.neuroimage.2009.01.031

Courchesne, E., Pierce, K., 2005. Why the frontal cortex in autism might be talking only to itself: local over-connectivity but long-distance disconnection. Curr Opin Neurobiol 15, 225-230. doi:10.1016/j.conb.2005.03.001

Craig, M.C., Zaman, S.H., Daly, E.M., Cutter, W.J., Robertson, D.M., Hallahan, B., Toal, F., Reed, S., Ambikapathy, A., Brammer, M., Murphy, C.M., Murphy, D.G., 2007. Women with

autistic-spectrum disorder: magnetic resonance imaging study of brain anatomy. The British journal of psychiatry : the journal of mental science 191, 224-228. doi:10.1192/bjp.bp.106.034603

Cross-Disorder Group of the Psychiatric Genomics Consortium, 2013. Identification of risk loci with shared effects on five major psychiatric disorders: a genome-wide analysis. The Lancet 381, 1371-1379. doi:10.1016/S0140-6736(12)62129-1

Crossley, N.A., Fox, P.T., Bullmore, E.T., 2016. Meta-connectomics: human brain network and connectivity meta-analyses. Psychol Med 46, 897-907. doi:10.1017/s0033291715002895

Crossley, N.A., Mechelli, A., Scott, J., Carletti, F., Fox, P.T., McGuire, P., Bullmore, E.T., 2014. The hubs of the human connectome are generally implicated in the anatomy of brain disorders. Brain 137, 2382-2395. doi:10.1093/brain/awu132

Crossley, N.A., Mechelli, A., Vértes, P.E., Winton-Brown, T.T., Patel, A.X., Ginestet, C.E., McGuire, P., Bullmore, E.T., 2013. Cognitive relevance of the community structure of the human brain functional coactivation network. Proceedings of the National Academy of Sciences of the United States of America 110, 11583-11588. doi: 10.1073/pnas.1220826110

Crossley, N.A., Scott, J., Ellison-Wright, I., Mechelli, A., 2018. Neuroimaging distinction between neurological and psychiatric disorders. British Journal of Psychiatry 207, 429-434.

Cubillo, A., Halari, R., Smith, A., Taylor, E., Rubia, K., 2012. A review of fronto-striatal and fronto-cortical brain abnormalities in children and adults with Attention Deficit Hyperactivity Disorder (ADHD) and new evidence for dysfunction in adults with ADHD during motivation and attention. Cortex; a journal devoted to the study of the nervous system and behavior 48, 194-215. doi:10.1016/j.cortex.2011.04.007

Cuthbert, B.N., 2015. Research Domain Criteria: toward future psychiatric nosologies. Dialogues in clinical neuroscience 17, 89-97. doi:10.31887/DCNS.2015.17.1/bcuthbert

D'Mello, A.M., Crocetti, D., Mostofsky, S.H., Stoodley, C.J., 2015. Cerebellar gray matter and lobular volumes correlate with core autism symptoms. NeuroImage. Clinical 7, 631-639. doi:10.1016/j.nicl.2015.02.007

D'Mello, A.M., Moore, D.M., Crocetti, D., Mostofsky, S.H., Stoodley, C.J., 2016. Cerebellar gray matter differentiates children with early language delay in autism. Autism Res 9, 1191-1204. doi:10.1002/aur.1622

D'Mello, A.M., Stoodley, C.J., 2015. Cerebro-cerebellar circuits in autism spectrum disorder. Front Neurosci 9, 408. doi:10.3389/fnins.2015.00408

Dajani, D.R., Uddin, L.Q., 2016. Local brain connectivity across development in autism spectrum disorder: A cross-sectional investigation. Autism research : official journal of the International Society for Autism Research 9, 43-54. doi:10.1002/aur.1494

Darweesh, A.M., Elserogy, Y.M., Khalifa, H., Gabra, R.H., El-Ghafour, M.A., 2020. Psychiatric comorbidity among children and adolescents with dyslexia. Middle East current psychiatry 27, 1-9.

Davidson, L.L., Heinrichs, R.W., 2003. Quantification of frontal and temporal lobe brain-imaging findings in schizophrenia: a meta-analysis. Psychiatry research 122, 69-87. doi:10.1016/s0925-4927(02)00118-x

Davies, G., Hayward, M., Evans, S., Mason, O., 2020. A systematic review of structural MRI investigations within borderline personality disorder: Identification of key psychological variables of interest going forward. Psychiatry research 286, 112864. doi:10.1016/j.psychres.2020.112864

Davis, J., Moylan, S., Harvey, B.H., Maes, M., Berk, M., 2014. Neuroprogression in schizophrenia: Pathways underpinning clinical staging and therapeutic corollaries. The Australian and New Zealand journal of psychiatry 48, 512-529. doi:10.1177/0004867414533012

De Fossé, L., Hodge, S.M., Makris, N., Kennedy, D.N., Caviness Jr, V.S., McGrath, L., Steele, S., Ziegler, D.A., Herbert, M.R., Frazier, J.A., Tager-Flusberg, H., Harris, G.J., 2004. Language-association cortex asymmetry in autism and specific language impairment. Ann Neurol 56, 757-766. doi:10.1002/ana.20275

de Lange, S.C., Scholtens, L.H., van den Berg, L.H., Boks, M.P., Bozzali, M., Cahn, W., Dannlowski, U., Durston, S., Geuze, E., van Haren, N.E.M., Hillegers, M.H.J., Koch, K., Jurado, M., Mancini, M., Marqués-Iturria, I., Meinert, S., Ophoff, R.A., Reess, T.J., Repple, J., Kahn, R.S., van den Heuvel, M.P., 2019. Shared vulnerability for connectome alterations across psychiatric and neurological brain disorders. Nature human behaviour 3, 988-998. doi:10.1038/s41562-019-0659-6

Deco, G., Kringelbach, M.L., 2014. Great expectations: using whole-brain computational connectomics for understanding neuropsychiatric disorders. Neuron 84, 892-905. doi:10.1016/j.neuron.2014.08.034

Del Pinal, G., Nathan, M.J., 2013. There and up again: on the uses and misuses of neuroimaging in psychology. Cognitive neuropsychology 30, 233-252. doi:10.1080/02643294.2013.846254

Delvecchio, G., Lorandi, A., Perlini, C., Barillari, M., Ruggeri, M., Altamura, A.C., Bellani, M., Brambilla, P., 2017. Brain anatomy of symptom stratification in schizophrenia: a voxel-based morphometry study. Nordic journal of psychiatry 71, 348-354. doi:10.1080/08039488.2017.1300323

Dembler-Stamm, T., Fiebig, J., Heinz, A., Gallinat, J., 2018. Sexual Dysfunction in Unmedicated Patients with Schizophrenia and in Healthy Controls. Pharmacopsychiatry 51, 251-256. doi:10.1055/s-0044-100627

Depue, B.E., Burgess, G.C., Bidwell, L.C., Willcutt, E.G., Banich, M.T., 2010. Behavioral performance predicts grey matter reductions in the right inferior frontal gyrus in young adults with combined type ADHD. Psychiatry research 182, 231-237. doi:10.1016/j.pscychresns.2010.01.012

DeRamus, T.P., Kana, R.K., 2015. Anatomical likelihood estimation meta-analysis of grey and white matter anomalies in autism spectrum disorders. Neuroimage Clin 7, 525-536. doi:10.1016/j.nicl.2014.11.004

Derrfuss, J., Mar, R.A., 2009. Lost in localization: The need for a universal coordinate database. NeuroImage 48, 1-7. doi:10.1016/j.neuroimage.2009.01.053

Di Martino, A., O'Connor, D., Chen, B., Alaerts, K., Anderson, J.S., Assaf, M., Balsters, J.H., Baxter, L., Beggiato, A., Bernaerts, S., Blanken, L.M., Bookheimer, S.Y., Braden, B.B., Byrge, L., Castellanos, F.X., Dapretto, M., Delorme, R., Fair, D.A., Fishman, I., Fitzgerald, J., Gallagher, L., Keehn, R.J., Kennedy, D.P., Lainhart, J.E., Luna, B., Mostofsky, S.H., Müller, R.A., Nebel, M.B., Nigg, J.T., O'Hearn, K., Solomon, M., Toro, R., Vaidya, C.J., Wenderoth, N., White, T., Craddock, R.C., Lord, C., Leventhal, B., Milham, M.P., 2017. Enhancing studies of the connectome in autism using the autism brain imaging data exchange II. Scientific data 4, 170010. doi:10.1038/sdata.2017.10

Di Martino, A., Shehzad, Z., Kelly, C., Roy, A.K., Gee, D.G., Uddin, L.Q., Gotimer, K., Klein, D.F., Castellanos, F.X., Milham, M.P., 2009. Relationship between cingulo-insular functional connectivity and autistic traits in neurotypical adults. The American journal of psychiatry 166, 891-899. doi:10.1176/appi.ajp.2009.08121894

Di Martino, A., Yan, C.G., Li, Q., Denio, E., Castellanos, F.X., Alaerts, K., Anderson, J.S., Assaf, M., Bookheimer, S.Y., Dapretto, M., Deen, B., Delmonte, S., Dinstein, I., Ertl-Wagner, B., Fair, D.A., Gallagher, L., Kennedy, D.P., Keown, C.L., Keysers, C., Lainhart, J.E., Lord, C., Luna, B., Menon, V., Minshew, N.J., Monk, C.S., Mueller, S., Müller, R.A., Nebel, M.B., Nigg, J.T., O'Hearn, K., Pelphrey, K.A., Peltier, S.J., Rudie, J.D., Sunaert, S., Thioux, M., Tyszka, J.M., Uddin, L.Q., Verhoeven, J.S., Wenderoth, N., Wiggins, J.L., Mostofsky, S.H., Milham, M.P., 2014. The autism brain imaging data exchange: towards a large-scale evaluation of the intrinsic brain architecture in autism. Molecular psychiatry 19, 659-667. doi:10.1038/mp.2013.78

Diaz-de-Grenu, L.Z., Acosta-Cabronero, J., Chong, Y.F., Pereira, J.M., Sajjadi, S.A., Williams, G.B., Nestor, P.J., 2014. A brief history of voxel-based grey matter analysis in Alzheimer's disease. Journal of Alzheimer's disease : JAD 38, 647-659. doi:10.3233/JAD-130362

Doherty, J.L., Owen, M.J., 2014. Genomic insights into the overlap between psychiatric disorders: implications for research and clinical practice. Genome medicine 6, 29. doi:10.1186/gm546

Donohoe, G., Rose, E., Frodl, T., Morris, D., Spoletini, I., Adriano, F., Bernardini, S., Caltagirone, C., Bossu, P., Gill, M., Corvin, A.P., Spalletta, G., 2011. ZNF804A risk allele is associated with relatively intact gray matter volume in patients with schizophrenia. NeuroImage 54, 2132-2137. doi:10.1016/j.neuroimage.2010.09.089

Douaud, G., Smith, S., Jenkinson, M., Behrens, T., Johansen-Berg, H., Vickers, J., James, S., Voets, N., Watkins, K., Matthews, P.M., James, A., 2007. Anatomically related grey and white matter abnormalities in adolescent-onset schizophrenia. Brain 130, 2375-2386. doi:10.1093/brain/awm184

Dugré, J.R., Eickhoff, S.B., Potvin, S., 2022. Meta-analytical transdiagnostic neural correlates in common pediatric psychiatric disorders. Scientific reports 12, 4909. doi:10.1038/s41598-022-08909-3

Dukart, J., Smieskova, R., Harrisberger, F., Lenz, C., Schmidt, A., Walter, A., Huber, C., Riecher-Rossler, A., Simon, A., Lang, U.E., Fusar-Poli, P., Borgwardt, S., 2017. Age-related brain structural alterations as an intermediate phenotype of psychosis. Journal of psychiatry & neuroscience 42, 307-319. doi:10.1503/jpn.160179

Ecker, C., Andrews, D., Dell'Acqua, F., Daly, E., Murphy, C., Catani, M., Thiebaut de Schotten, M., Baron-Cohen, S., Lai, M.C., Lombardo, M.V., Bullmore, E.T., Suckling, J., Williams, S., Jones, D.K., Chiocchetti, A., Murphy, D.G., 2016. Relationship Between Cortical Gyrification, White Matter Connectivity, and Autism Spectrum Disorder. Cereb Cortex 26, 3297-3309. doi:10.1093/cercor/bhw098

Ecker, C., Bookheimer, S.Y., Murphy, D.G., 2015. Neuroimaging in autism spectrum disorder: brain structure and function across the lifespan. The Lancet. Neurology 14, 1121-1134. doi:10.1016/s1474-4422(15)00050-2

Ecker, C., Rocha-Rego, V., Johnston, P., Mourao-Miranda, J., Marquand, A., Daly, E.M., Brammer, M.J., Murphy, C., Murphy, D.G., 2010. Investigating the predictive value of whole-brain structural MR scans in autism: a pattern classification approach. Neuroimage 49, 44-56. doi:10.1016/j.neuroimage.2009.08.024

Ecker, C., Ronan, L., Feng, Y., Daly, E., Murphy, C., Ginestet, C.E., Brammer, M., Fletcher, P.C., Bullmore, E.T., Suckling, J., Baron-Cohen, S., Williams, S., Loth, E., Murphy, D.G., 2013. Intrinsic gray-matter connectivity of the brain in adults with autism spectrum disorder. Proc Natl Acad Sci U S A 110, 13222-13227. doi:10.1073/pnas.1221880110

Ecker, C., Suckling, J., Deoni, S.C., Lombardo, M.V., Bullmore, E.T., Baron-Cohen, S., Catani, M., Jezzard, P., Barnes, A., Bailey, A.J., Williams, S.C., Murphy, D.G., 2012. Brain anatomy and its relationship to behavior in adults with autism spectrum disorder: a multicenter magnetic resonance imaging study. Arch Gen Psychiatry 69, 195-209. doi:10.1001/archgenpsychiatry.2011.1251

Eckert, M.A., 2004. Neuroanatomical markers for dyslexia: a review of dyslexia structural imaging studies. The Neuroscientist : a review journal bringing neurobiology, neurology and psychiatry 10, 362-371. doi:10.1177/1073858404263596

Eckert, M.A., Berninger, V.W., Vaden, K.I., Jr., Gebregziabher, M., Tsu, L., 2016. Gray Matter Features of Reading Disability: A Combined Meta-Analytic and Direct Analysis Approach. eNeuro 3. doi:10.1523/eneuro.0103-15.2015

Eckert, M.A., Leonard, C.M., Wilke, M., Eckert, M., Richards, T., Richards, A., Berninger, V., 2005. Anatomical signatures of dyslexia in children: unique information from manual and voxel based morphometry brain measures. Cortex; a journal devoted to the study of the nervous system and behavior 41, 304-315. doi:10.1016/s0010-9452(08)70268-5

Egashira, K., Matsuo, K., Mihara, T., Nakano, M., Nakashima, M., Watanuki, T., Matsubara, T., Watanabe, Y., 2014. Different and shared brain volume abnormalities in late- and early-onset schizophrenia. Neuropsychobiology 70, 142-151. doi:10.1159/000364827

Eickhoff, S.B., Bzdok, D., Laird, A.R., Kurth, F., Fox, P.T., 2012. Activation likelihood estimation meta-analysis revisited. NeuroImage 59, 2349-2361. doi:10.1016/j.neuroimage.2011.09.017

Eickhoff, S.B., Bzdok, D., Laird, A.R., Roski, C., Caspers, S., Zilles, K., Fox, P.T., 2011. Co-activation patterns distinguish cortical modules, their connectivity and functional differentiation. NeuroImage 57, 938-949. doi:10.1016/j.neuroimage.2011.05.021

Eickhoff, S.B., Laird, A.R., Fox, P.M., Lancaster, J.L., Fox, P.T., 2017. Implementation errors in the GingerALE Software: Description and recommendations. Human brain mapping 38, 7-11. doi:10.1002/hbm.23342

Eickhoff, S.B., Laird, A.R., Grefkes, C., Wang, L.E., Zilles, K., Fox, P.T., 2009. Coordinate-based activation likelihood estimation meta-analysis of neuroimaging data: a random-effects approach based on empirical estimates of spatial uncertainty. Human brain mapping 30, 2907-2926. doi:10.1002/hbm.20718

Eickhoff, S.B., Nichols, T.E., Laird, A.R., Hoffstaedter, F., Amunts, K., Fox, P.T., Bzdok, D., Eickhoff, C.R., 2016. Behavior, sensitivity, and power of activation likelihood estimation characterized by massive empirical simulation. NeuroImage 137, 70-85. doi:10.1016/j.neuroimage.2016.04.072

Eilam-Stock, T., Wu, T., Spagna, A., Egan, L.J., Fan, J., 2016. Neuroanatomical Alterations in High-Functioning Adults with Autism Spectrum Disorder. Frontiers in neuroscience 10. doi:10.3389/fnins.2016.00237

Eisenberg, I.W., Wallace, G.L., Kenworthy, L., Gotts, S.J., Martin, A., 2015. Insistence on sameness relates to increased covariance of gray matter structure in autism spectrum disorder. Mol Autism 6, 54. doi:10.1186/s13229-015-0047-7

Ellison-Wright, I., Bullmore, E., 2010. Anatomy of bipolar disorder and schizophrenia: a meta-analysis. Schizophrenia research 117, 1-12. doi:10.1016/j.schres.2009.12.022

Ellison-Wright, I., Glahn, D.C., Laird, A.R., Thelen, S.M., Bullmore, E., 2008. The anatomy of first-episode and chronic schizophrenia: an anatomical likelihood estimation meta-analysis. The American journal of psychiatry 165, 1015-1023. doi:10.1176/appi.ajp.2008.07101562

Elnakib, A., Soliman, A., Nitzken, M., Casanova, M.F., Gimel'farb, G., El-Baz, A., 2014. Magnetic resonance imaging findings for dyslexia: a review. Journal of biomedical nanotechnology 10, 2778-2805. doi:10.1166/jbn.2014.1895

Enge, A., Friederici, A.D., Skeide, M.A., 2020. A meta-analysis of fMRI studies of language comprehension in children. NeuroImage 215, 116858. doi:10.1016/j.neuroimage.2020.116858

Eriksson, P.S., Perfilieva, E., Björk-Eriksson, T., Alborn, A.-M., Nordborg, C., Peterson, D.A., Gage, F.H., 1998. Neurogenesis in the adult human hippocampus. Nature medicine 4, 1313-1317. doi:10.1038/3305

Etkin, A., 2019. A Reckoning and Research Agenda for Neuroimaging in Psychiatry. The American journal of psychiatry 176, 507-511. doi:10.1176/appi.ajp.2019.19050521

Evans, A.C., Collins, D.L., Mills, S., Brown, E.D., Kelly, R.L., Peters, T.M., 1993. 3D statistical neuroanatomical models from 305 MRI volumes, 1993 IEEE conference record nuclear science symposium and medical imaging conference. IEEE, pp. 1813-1817.

Evans, A.C., 2013. Networks of anatomical covariance. Neuroimage 80, 489-504. doi:10.1016/j.neuroimage.2013.05.054

Evans, T.M., Flowers, D.L., Napoliello, E.M., Eden, G.F., 2014. Sex-specific gray matter volume differences in females with developmental dyslexia. Brain structure & function 219, 1041-1054. doi:10.1007/s00429-013-0552-4

Falkenberg, I., Valmaggia, L., Byrnes, M., Frascarelli, M., Jones, C., Rocchetti, M., Straube, B., Badger, S., McGuire, P., Fusar-Poli, P., 2015. Why are help-seeking subjects at ultra-high

risk for psychosis help-seeking? Psychiatry research 228, 808-815. doi:10.1016/j.psychres.2015.05.018

Fang, H., Wu, Q., Li, Y., Ren, Y., Li, C., Xiao, X., Xiao, T., Chu, K., Ke, X., 2020. Structural networks in children with autism spectrum disorder with regression: A graph theory study. Behav Brain Res 378, 112262. doi:10.1016/j.bbr.2019.112262

Farrow, T.F., Whitford, T.J., Williams, L.M., Gomes, L., Harris, A.W., 2005. Diagnosis-related regional gray matter loss over two years in first episode schizophrenia and bipolar disorder. Biological psychiatry 58, 713-723. doi:10.1016/j.biopsych.2005.04.033

Fatemi, S.H., Aldinger, K.A., Ashwood, P., Bauman, M.L., Blaha, C.D., Blatt, G.J., Chauhan, A., Chauhan, V., Dager, S.R., Dickson, P.E., Estes, A.M., Goldowitz, D., Heck, D.H., Kemper, T.L., King, B.H., Martin, L.A., Millen, K.J., Mittleman, G., Mosconi, M.W., Persico, A.M., Sweeney, J.A., Webb, S.J., Welsh, J.P., 2012. Consensus paper: pathological role of the cerebellum in autism. Cerebellum 11, 777-807. doi:10.1007/s12311-012-0355-9

Fernandes, H.M., Cabral, J., van Hartevelt, T.J., Lord, L.D., Gleesborg, C., Møller, A., Deco, G., Whybrow, P.C., Petrovic, P., James, A.C., Kringelbach, M.L., 2019. Disrupted brain structural connectivity in Pediatric Bipolar Disorder with psychosis. Sci Rep 9, 13638. doi:10.1038/s41598-019-50093-4

Ferri, F., Salone, A., Ebisch, S.J., De Berardis, D., Romani, G.L., Ferro, F.M., Gallese, V., 2012. Action verb understanding in first-episode schizophrenia: is there evidence for a simulation deficit? Neuropsychologia 50, 988-996. doi:10.1016/j.neuropsychologia.2012.02.005

Ferri, J., Ford, J.M., Roach, B.J., Turner, J.A., van Erp, T.G., Voyvodic, J., Preda, A., Belger, A., Bustillo, J., O'Leary, D., Mueller, B.A., Lim, K.O., McEwen, S.C., Calhoun, V.D., Diaz, M., Glover, G., Greve, D., Wible, C.G., Vaidya, J.G., Potkin, S.G., Mathalon, D.H., 2018. Resting-state thalamic dysconnectivity in schizophrenia and relationships with symptoms. Psychological medicine 48, 2492-2499. doi:10.1017/s003329171800003x

Fervaha, G., Remington, G., 2013. Neuroimaging findings in schizotypal personality disorder: a systematic review. Progress in neuro-psychopharmacology & biological psychiatry 43, 96-107. doi:10.1016/j.pnpbp.2012.11.014

Filippi, M., van den Heuvel, M.P., Fornito, A., He, Y., Hulshoff Pol, H.E., Agosta, F., Comi, G., Rocca, M.A., 2013. Assessment of system dysfunction in the brain through MRI-based connectomics. Lancet Neurol 12, 1189-1199. doi:10.1016/S1474-4422(13)70144-3

First, M.B., Drevets, W.C., Carter, C., Dickstein, D.P., Kasoff, L., Kim, K.L., McConathy, J., Rauch, S., Saad, Z.S., Savitz, J., Seymour, K.E., Sheline, Y.I., Zubieta, J.K., 2018. Clinical Applications of Neuroimaging in Psychiatric Disorders. The American journal of psychiatry 175, 915-916.

Fitzgerald, J., Johnson, K., Kehoe, E., Bokde, A.L., Garavan, H., Gallagher, L., McGrath, J., 2015. Disrupted functional connectivity in dorsal and ventral attention networks during attention orienting in autism spectrum disorders. Autism Res 8, 136-152. doi:10.1002/aur.1430

Floris, D.L., Chura, L.R., Holt, R.J., Suckling, J., Bullmore, E.T., Baron-Cohen, S., Spencer, M.D., 2013. Psychological correlates of handedness and corpus callosum asymmetry in autism: the left hemisphere dysfunction theory revisited. J Autism Dev Disord 43, 1758-1772. doi:10.1007/s10803-012-1720-8

Floris, D.L., Wolfers, T., Zabihi, M., Holz, N.E., Zwiers, M.P., Charman, T., Tillmann, J., Ecker, C., Dell'Acqua, F., Banaschewski, T., Moessnang, C., Baron-Cohen, S., Holt, R., Durston, S., Loth, E., Murphy, D., Marquand, A., Buitelaar, J.K., Beckmann, C.F., 2020. Atypical brain asymmetry in autism – a candidate for clinically meaningful stratification. Biological Psychiatry: Cognitive Neuroscience and Neuroimaging. doi:10.1016/j.bpsc.2020.08.008

Fornara, G.A., Papagno, C., Berlingeri, M., 2017. A neuroanatomical account of mental time travelling in schizophrenia: A meta-analysis of functional and structural neuroimaging data. Neuroscience and biobehavioral reviews 80, 211-222. doi:10.1016/j.neubiorev.2017.05.027

Fornito, A., Bullmore, E.T., 2015. Connectomics: a new paradigm for understanding brain disease. Eur Neuropsychopharmacol 25, 733-748. doi:10.1016/j.euroneuro.2014.02.011

Fornito, A., Bullmore, E.T., Zalesky, A., 2017. Opportunities and Challenges for Psychiatry in the Connectomic Era. Biol Psychiatry Cogn Neurosci Neuroimaging 2, 9-19. doi:10.1016/j.bpsc.2016.08.003

Fornito, A., Yucel, M., Patti, J., Wood, S.J., Pantelis, C., 2009. Mapping grey matter reductions in schizophrenia: an anatomical likelihood estimation analysis of voxel-based morphometry studies. Schizophrenia research 108, 104-113. doi:10.1016/j.schres.2008.12.011

Fornito, A., Yung, A.R., Wood, S.J., Phillips, L.J., Nelson, B., Cotton, S., Velakoulis, D., McGorry, P.D., Pantelis, C., Yucel, M., 2008. Anatomic abnormalities of the anterior cingulate cortex before psychosis onset: an MRI study of ultra-high-risk individuals. Biological psychiatry 64, 758-765. doi:10.1016/j.biopsych.2008.05.032

Fornito, A., Zalesky, A., Breakspear, M., 2015. The connectomics of brain disorders. Nat Rev Neurosci 16, 159-172. doi:10.1038/nrn3901

Fornito, A., Zalesky, A., Bullmore, E., 2016. Fundamentals of brain network analysis. Academic Press.

Foster, N.E., Doyle-Thomas, K.A., Tryfon, A., Ouimet, T., Anagnostou, E., Evans, A.C., Zwaigenbaum, L., Lerch, J.P., Lewis, J.D., Hyde, K.L., 2015. Structural Gray Matter Differences During Childhood Development in Autism Spectrum Disorder: A Multimetric Approach. Pediatric neurology 53, 350-359. doi:10.1016/j.pediatrneurol.2015.06.013

Fountoulakis, K.N., Dragioti, E., Theofilidis, A.T., Wikilund, T., Atmatzidis, X., Nimatoudis, I., Thys, E., Wampers, M., Hranov, L., Hristova, T., Aptalidis, D., Milev, R., Iftene, F., Spaniel, F., Knytl, P., Furstova, P., From, T., Karlsson, H., Walta, M., Salokangas, R.K.R., Azorin, J.M., Bouniard, J., Montant, J., Juckel, G., Haussleiter, I.S., Douzenis, A., Michopoulos, I., Ferentinos, P., Smyrnis, N., Mantonakis, L., Nemes, Z., Gonda, X., Vajda, D., Juhasz, A., Shrivastava, A., Waddington, J., Pompili, M., Comparelli, A., Corigliano, V., Rancans, E., Navickas, A., Hilbig, J., Bukelskis, L., Injac Stevovic, L., Vodopic, S., Esan, O., Oladele, O., Osunbote, C., Rybakowski, J., Wojciak, P., Domowicz, K., Figueira, M.L., Linhares, L., Crawford, J., Panfil, A.L., Smirnova, D., Izmailova, O., Lecic-Tosevski, D., Temmingh, H., Howells, F., Bobes, J., Garcia-Portilla, M.P., Garcia-Alvarez, L., Erzin, G., Karadag, H., De Sousa, A., Bendre, A., Hoschl, C., Bredicean, C., Papava, I., Vukovic, O., Pejuskovic, B., Russell, V., Athanasiadis, L., Konsta, A., Stein, D., Berk, M., Dean, O., Tandon, R., Kasper, S., De Hert, M., 2019. Staging of Schizophrenia With the Use of PANSS: An International Multi-Center Study. The international journal of neuropsychopharmacology 22, 681-697. doi:10.1093/ijnp/pyz053

Fountoulakis, K.N., Dragioti, E., Theofilidis, A.T., Wiklund, T., Atmatzidis, X., Nimatoudis, I., Thys, E., Wampers, M., Hranov, L., Hristova, T., Aptalidis, D., Milev, R., Iftene, F., Spaniel, F., Knytl, P., Furstova, P., From, T., Karlsson, H., Walta, M., Salokangas, R.K.R., Azorin, J.M., Bouniard, J., Montant, J., Juckel, G., Haussleiter, I.S., Douzenis, A., Michopoulos, I., Ferentinos, P., Smyrnis, N., Mantonakis, L., Nemes, Z., Gonda, X., Vajda, D., Juhasz, A., Shrivastava, A., Waddington, J., Pompili, M., Comparelli, A., Corigliano, V., Rancans, E., Navickas, A., Hilbig, J., Bukelskis, L., Stevovic, L.I., Vodopic, S., Esan, O., Oladele, O., Osunbote, C., Rybakowski, J., Wojciak, P., Domowicz, K., Figueira, M.L., Linhares, L., Crawford, J., Panfil, A.L., Smirnova, D., Izmailova, O., Lecic-Tosevski, D., Temmingh, H., Howells, F., Bobes, J., Garcia-Portilla, M.P., Garcia-Alvarez, L., Erzin, G., Karadag, H., De Sousa, A., Bendre, A., Hoschl, C., Bredicean, C., Papava, I., Vukovic, O., Pejuskovic, B., Russell, V., Athanasiadis, L., Konsta, A., Stein, D., Berk, M., Dean, O., Tandon, R., Kasper, S., De Hert, M., 2020. Modeling psychological function in patients with schizophrenia with the PANSS: an international multi-center study. CNS spectrums, 1-9. doi:10.1017/s1092852920001091

Fox, P.T., Laird, A.R., Fox, S.P., Fox, P.M., Uecker, A.M., Crank, M., Koenig, S.F., Lancaster, J.L., 2005. BrainMap taxonomy of experimental design: description and evaluation. Hum Brain Mapp 25, 185-198. doi:10.1002/hbm.20141

Fox, P.T., Lancaster, J.L., 2002. Opinion: Mapping context and content: the BrainMap model. Nature reviews. Neuroscience 3, 319-321. doi:10.1038/nrn789

Fox, P.T., Lancaster, J.L., Laird, A.R., Eickhoff, S.B., 2014. Meta-analysis in human neuroimaging: computational modeling of large-scale databases. Annual review of neuroscience 37, 409-434. doi:10.1146/annurev-neuro-062012-170320

Fox, P.T., Perlmutter, J.S., Raichle, M.E., 1985. A stereotactic method of anatomical localization for positron emission tomography. J Comput Assist Tomogr 9, 141-153. doi:10.1097/00004728-198501000-00025

Frahm, L., Cieslik, E.C., Hoffstaedter, F., Satterthwaite, T.D., Fox, P.T., Langner, R., Eickhoff, S.B., 2022. Evaluation of thresholding methods for activation likelihood estimation meta-analysis via large-scale simulations. Human Brain Mapping 43, 3987-3997. doi:10.1002/hbm.25898

Freeman, L.C., 1978. Centrality in social networks: conceptual clarification. Social networks 1, 215-239. doi:10.1016/0378-8733(78)90021-7

Freitag, C.M., Konrad, C., Häberlen, M., Kleser, C., von Gontard, A., Reith, W., Troje, N.F., Krick, C., 2008. Perception of biological motion in autism spectrum disorders. Neuropsychologia 46, 1480-1494. doi:10.1016/j.neuropsychologia.2007.12.025

French, L., Paus, T., 2015. A FreeSurfer view of the cortical transcriptome generated from the Allen Human Brain Atlas. Frontiers in neuroscience 9. doi: 10.3389/fnins.2015.00323

Friston, K.J., 2011. Functional and effective connectivity: a review. Brain connectivity 1, 13-36. doi: 10.1089/brain.2011.0008

Friston, K.J., Holmes, A.P., Worsley, K.J., Poline, J.P., Frith, C.D., Frackowiak, R.S., 1994a. Statistical parametric maps in functional imaging: a general linear approach. Human brain mapping 2, 189-210.

Friston, K.J., Penny, W., Phillips, C., Kiebel, S., Hinton, G., Ashburner, J., 2002. Classical and Bayesian inference in neuroimaging: theory. Neuroimage 16, 465-483. doi:10.1006/nimg.2002.1090

Friston, K.J., Worsley, K.J., Frackowiak, R.S., Mazziotta, J.C., Evans, A.C., 1994b. Assessing the significance of focal activations using their spatial extent. Hum Brain Mapp 1, 210-220. doi:10.1002/hbm.460010306

Frith, C., 2004. Is autism a disconnection disorder? Lancet Neurol 3, 577. doi:10.1016/s1474-4422(04)00875-0

Fusar-Poli, P., Bonoldi, I., Yung, A.R., Borgwardt, S., Kempton, M.J., Valmaggia, L., Barale, F., Caverzasi, E., McGuire, P., 2012. Predicting psychosis: meta-analysis of transition outcomes in individuals at high clinical risk. Archives of general psychiatry 69, 220-229. doi:10.1001/archgenpsychiatry.2011.1472

Fusar-Poli, P., Borgwardt, S., Crescini, A., Deste, G., Kempton, M.J., Lawrie, S., Mc Guire, P., Sacchetti, E., 2011a. Neuroanatomy of vulnerability to psychosis: a voxel-based meta-analysis. Neuroscience and biobehavioral reviews 35, 1175-1185. doi:10.1016/j.neubiorev.2010.12.005

Fusar-Poli, P., Broome, M.R., Woolley, J.B., Johns, L.C., Tabraham, P., Bramon, E., Valmaggia, L., Williams, S.C., McGuire, P., 2011b. Altered brain function directly related to structural abnormalities in people at ultra high risk of psychosis: longitudinal VBM-fMRI study. Journal of psychiatric research 45, 190-198. doi:10.1016/j.jpsychires.2010.05.012

Fusar-Poli, P., Crossley, N., Woolley, J., Carletti, F., Perez-Iglesias, R., Broome, M., Johns, L., Tabraham, P., Bramon, E., McGuire, P., 2011c. Gray matter alterations related to P300 abnormalities in subjects at high risk for psychosis: longitudinal MRI-EEG study. NeuroImage 55, 320-328. doi:10.1016/j.neuroimage.2010.11.075

Fusar-Poli, P., Radua, J., Frascarelli, M., Mechelli, A., Borgwardt, S., Di Fabio, F., Biondi, M., Ioannidis, J.P., David, S.P., 2015. Evidence of reporting biases in voxel-based morphometry (VBM) studies of psychiatric and neurological disorders. Hum Brain Mapp 35, 3052-3065. doi:10.1002/hbm.22384

Fusar-Poli, P., Smieskova, R., Kempton, M.J., Ho, B.C., Andreasen, N.C., Borgwardt, S., 2013. Progressive brain changes in schizophrenia related to antipsychotic treatment? A meta-analysis of longitudinal MRI studies. Neuroscience and biobehavioral reviews 37, 1680-1691. doi:10.1016/j.neubiorev.2013.06.001

Fusar-Poli, P., Smieskova, R., Serafini, G., Politi, P., Borgwardt, S., 2014. Neuroanatomical markers of genetic liability to psychosis and first episode psychosis: a voxelwise meta-analytical comparison. The world journal of biological psychiatry : the official journal of the World Federation of Societies of Biological Psychiatry 15, 219-228. doi:10.3109/15622975.2011.630408

Galvez-Contreras, A.Y., Campos-Ordonez, T., Gonzalez-Castaneda, R.E., Gonzalez-Perez, O., 2017. Alterations of Growth Factors in Autism and Attention-Deficit/Hyperactivity Disorder. Front Psychiatry 8. doi:10.3389/fpsyt.2017.00126

Gandal, M.J., Haney, J.R., Parikshak, N.N., Leppa, V., Ramaswami, G., Hartl, C., Schork, A.J., Appadurai, V., Buil, A., Werge, T.M., Liu, C., White, K.P., Horvath, S., Geschwind, D.H., Sestan, N., Vaccarino, F., Gerstein, M., Weissman, S., Pochareddy, S., State, M., Knowles, J., Farnham, P., Akbarian, S., Pinto, D., Van Baekl, H., Dracheva, S., Jaffe, A., Hyde, T., Zandi, P., Crawford, G., Sullivan, P., Thompson, W.K., Mortensen, P.B., Agerbo, E., Pedersen, M.G., Pedersen, C.B., Mors, O., Børglum, A.D., Nordentoft, M., Hougaard, D.M., Bybjerg-Grauholm, J., Bækvad-Hansen, M., Martin, A.R., Dumont, A., Stevens, C.,

Churchhouse, C., Howrigan, D.P., Palmer, D.S., Robinson, E.B., Satterstrom, K.F., Cerrato, F., Huang, H., Goldstein, J., Moran, J., Julian, J.M., Kimberly, M., Patrick, C., Turley, P., Walters, R., Belliveau, R., Ripke, S., Poterba, T., Daly, M.J., Neale, B., Fromer, M., Roussos, P., Johnson, J.S., Shah, H.R., Mahajan, M.C., Schadt, E., Haroutunian, V., Ruderfer, D.M., Buxbaum, J.D., Sieberts, S.K., Dang, K., Logsdon, B., Mangravite, L.M., Peters, M., Gur, R.E., Hahn, C.-G., Devlin, B., Klei, L.L., Lewis, D., Lipska, B., Hirai, K., Toyoshiba, H., Domenici, E., 2018. Shared molecular neuropathology across major psychiatric disorders parallels polygenic overlap. Science 359, 693-697. doi:10.1126/science.aad6469

Garcia, K.L., Yu, G., Nicolini, C., Michalski, B., Garzon, D.J., Chiu, V.S., Tongiorgi, E., Szatmari, P., Fahnestock, M., 2012. Altered balance of proteolytic isoforms of pro-brain-derived neurotrophic factor in autism. J Neuropathol Exp Neurol 71, 289-297. doi:10.1097/NEN.0b013e31824b27e4

Garcia-Marti, G., Aguilar, E.J., Lull, J.J., Marti-Bonmati, L., Escarti, M.J., Manjon, J.V., Moratal, D., Robles, M., Sanjuan, J., 2008. Schizophrenia with auditory hallucinations: a voxel-based morphometry study. Progress in neuro-psychopharmacology & biological psychiatry 32, 72-80. doi:10.1016/j.pnpbp.2007.07.014

Genovese, C.R., Lazar, N.A., Nichols, T., 2002. Thresholding of statistical maps in functional neuroimaging using the false discovery rate. Neuroimage 15, 870-878. doi:10.1006/nimg.2001.1037

Geschwind, D.H., Levitt, P., 2007. Autism spectrum disorders: developmental disconnection syndromes. Curr Opin Neurobiol 17, 103-111. doi:10.1016/j.conb.2007.01.009

Gibbard, C.R., Ren, J., Skuse, D.H., Clayden, J.D., Clark, C.A., 2018. Structural connectivity of the amygdala in young adults with autism spectrum disorder. Hum Brain Mapp 39, 1270-1282. doi:10.1002/hbm.23915

Girgis, R.R., Minshew, N.J., Melhem, N.M., Nutche, J.J., Keshavan, M.S., Hardan, A.Y., 2007. Volumetric alterations of the orbitofrontal cortex in autism. Prog Neuropsychopharmacol Biol Psychiatry 31, 41-45. doi:10.1016/j.pnpbp.2006.06.007

Giuliani, N.R., Calhoun, V.D., Pearlson, G.D., Francis, A., Buchanan, R.W., 2005. Voxel-based morphometry versus region of interest: a comparison of two methods for analyzing

gray matter differences in schizophrenia. Schizophrenia research 74, 135-147. doi:10.1016/j.schres.2004.08.019

Glahn, D.C., Laird, A.R., Ellison-Wright, I., Thelen, S.M., Robinson, J.L., Lancaster, J.L., Bullmore, E., Fox, P.T., 2008. Meta-analysis of gray matter anomalies in schizophrenia: application of anatomic likelihood estimation and network analysis. Biological psychiatry 64, 774-781. doi:10.1016/j.biopsych.2008.03.031

Glass, G.V., 1976. Primary, secondary, and meta-analysis of research. Educational researcher 5, 3-8.

Glenthoj, L.B., Kristensen, T.D., Wenneberg, C., Hjorthoj, C., Nordentoft, M., 2020. Experiential negative symptoms are more predictive of real-life functional outcome than expressive negative symptoms in clinical high-risk states. Schizophrenia research. doi:10.1016/j.schres.2020.01.012

Gnanavel, S., Sharma, P., Kaushal, P., Hussain, S., 2019. Attention deficit hyperactivity disorder and comorbidity: A review of literature. World journal of clinical cases 7, 2420-2426. doi:10.12998/wjcc.v7.i17.2420

Goedert, M., Clavaguera, F., Tolnay, M., 2010. The propagation of prion-like protein inclusions in neurodegenerative diseases. Trends Neurosci 33, 317-325. doi:10.1016/j.tins.2010.04.003

Goel, P., Kuceyeski, A., LoCastro, E., Raj, A., 2014. Spatial patterns of genome-wide expression profiles reflect anatomic and fiber connectivity architecture of healthy human brain. Hum Brain Mapp 35, 4204-4218. doi: 10.1002/hbm.22471

Goetz, M., Vesela, M., Ptacek, R., 2014. Notes on the role of the cerebellum in ADHD. Austin J Psychiatry Behav Sci 1, 1013.

Good, C.D., Johnsrude, I., Ashburner, J., Henson, R.N., Friston, K.J., Frackowiak, R.S., 2001a. Cerebral asymmetry and the effects of sex and handedness on brain structure: a voxel-based morphometric analysis of 465 normal adult human brains. Neuroimage 14, 685-700. doi:10.1006/nimg.2001.0857

Good, C.D., Johnsrude, I.S., Ashburner, J., Henson, R.N.A., Friston, K.J., Frackowiak, R.S.J., 2001b. A Voxel-Based Morphometric Study of Ageing in 465 Normal Adult Human Brains. NeuroImage 14, 21-36. doi:10.1006/nimg.2001.0786

Goodkind, M., Eickhoff, S.B., Oathes, D.J., Jiang, Y., Chang, A., Jones-Hagata, L.B., Ortega, B.N., Zaiko, Y.V., Roach, E.L., Korgaonkar, M.S., Grieve, S.M., Galatzer-Levy, I., Fox, P.T., Etkin, A., 2015. Identification of a common neurobiological substrate for mental illness. JAMA Psychiatry 72, 305-315. doi:10.1001/jamapsychiatry.2014.2206

Goradia, D.D., Vogel, S., Mohl, B., Khatib, D., Zajac-Benitez, C., Rajan, U., Robin, A., Rosenberg, D.R., Stanley, J.A., 2016. Distinct differences in striatal dysmorphology between attention deficit hyperactivity disorder boys with and without a comorbid reading disability. Psychiatry research. Neuroimaging 258, 30-36. doi:10.1016/j.pscychresns.2016.10.012

Gray, J.P., Müller, V.I., Eickhoff, S.B., Fox, P.T., 2020. Multimodal Abnormalities of Brain Structure and Function in Major Depressive Disorder: A Meta-Analysis of Neuroimaging Studies. The American journal of psychiatry 177, 422-434. doi:10.1176/appi.ajp.2019.19050560

Grecucci, A., Rubicondo, D., Siugzdaite, R., Surian, L., Job, R., 2016. Uncovering the Social Deficits in the Autistic Brain. A Source-Based Morphometric Study. Front Neurosci 10, 388. doi:10.3389/fnins.2016.00388

Green, M.F., Horan, W.P., Lee, J., 2019. Nonsocial and social cognition in schizophrenia: current evidence and future directions. World psychiatry : official journal of the World Psychiatric Association (WPA) 18, 146-161. doi:10.1002/wps.20624

Greicius, M., 2008. Resting-state functional connectivity in neuropsychiatric disorders. Current opinion in neurology 21, 424-430. doi:10.1097/WCO.0b013e328306f2c5

Greimel, E., Nehrkorn, B., Schulte-Rüther, M., Fink, G.R., Nickl-Jockschat, T., Herpertz-Dahlmann, B., Konrad, K., Eickhoff, S.B., 2013. Changes in grey matter development in autism spectrum disorder. Brain structure & function 218, 929-942. doi:10.1007/s00429-012-0439-9

Groen, W.B., Buitelaar, J.K., van der Gaag, R.J., Zwiers, M.P., 2011. Pervasive microstructural abnormalities in autism: a DTI study. Journal of psychiatry & neuroscience : JPN 36, 32-40.

Grolez, G., Moreau, C., Danel-Brunaud, V., Delmaire, C., Lopes, R., Pradat, P.F., El Mendili, M.M., Defebvre, L., Devos, D., 2016. The value of magnetic resonance imaging as a

biomarker for amyotrophic lateral sclerosis: a systematic review. BMC neurology 16, 155. doi:10.1186/s12883-016-0672-6

Grutzendler, J., Kasthuri, N., Gan, W.-B., 2002. Long-term dendritic spine stability in the adult cortex. Nature 420, 812-816. doi:10.1038/nature01276

Guo, F., Zhu, Y.Q., Li, C., Wang, X.R., Wang, H.N., Liu, W.M., Wang, L.X., Tian, P., Kang, X.W., Cui, L.B., Xi, Y.B., Yin, H., 2019. Gray matter volume changes following antipsychotic therapy in first-episode schizophrenia patients: A longitudinal voxel-based morphometric study. Journal of psychiatric research 116, 126-132. doi:10.1016/j.jpsychires.2019.06.009

Guo, W., Hu, M., Fan, X., Liu, F., Wu, R., Chen, J., Guo, X., Xiao, C., Quan, M., Chen, H., Zhai, J., Zhao, J., 2014. Decreased gray matter volume in the left middle temporal gyrus as a candidate biomarker for schizophrenia: a study of drug naive, first-episode schizophrenia patients and unaffected siblings. Schizophrenia research 159, 43-50. doi:10.1016/j.schres.2014.07.051

Guo, W., Liu, F., Xiao, C., Yu, M., Zhang, Z., Liu, J., Zhang, J., Zhao, J., 2015. Increased Causal Connectivity Related to Anatomical Alterations as Potential Endophenotypes for Schizophrenia. Medicine 94, e1493. doi:10.1097/md.0000000000001493

Guo, X., Li, J., Wei, Q., Fan, X., Kennedy, D.N., Shen, Y., Chen, H., Zhao, J., 2013. Duration of untreated psychosis is associated with temporal and occipitotemporal gray matter volume decrease in treatment naive schizophrenia. PloS one 8, e83679. doi:10.1371/journal.pone.0083679

Gupta, C.N., Calhoun, V.D., Rachakonda, S., Chen, J., Patel, V., Liu, J., Segall, J., Franke, B., Zwiers, M.P., Arias-Vasquez, A., Buitelaar, J., Fisher, S.E., Fernandez, G., van Erp, T.G.M., Potkin, S., Ford, J., Mathalon, D., McEwen, S., Lee, H.J., Mueller, B.A., Greve, D.N., Andreassen, O., Agartz, I., Gollub, R.L., Sponheim, S.R., Ehrlich, S., Wang, L., Pearlson, G., Glahn, D.C., Sprooten, E., Mayer, A.R., Stephen, J., Jung, R.E., Canive, J., Bustillo, J., Turner, J.A., 2014. Patterns of Gray Matter Abnormalities in Schizophrenia Based on an International Mega-analysis. Schizophrenia bulletin 41, 1133-1142.

Gusnard, D.A., Raichle, M.E., Raichle, M.E., 2001. Searching for a baseline: functional imaging and the resting human brain. Nature reviews. Neuroscience 2, 685-694. doi:10.1038/35094500

Hadjikhani, N., Chabris, C.F., Joseph, R.M., Clark, J., McGrath, L., Aharon, I., Feczko, E., Tager-Flusberg, H., Harris, G.J., 2004. Early visual cortex organization in autism: an fMRI study. Neuroreport 15, 267-270. doi:10.1097/00001756-200402090-00011

Hadjikhani, N., Joseph, R.M., Snyder, J., Tager-Flusberg, H., 2007. Abnormal activation of the social brain during face perception in autism. Human brain mapping 28, 441-449. doi:10.1002/hbm.20283

Hager, B.M., Keshavan, M.S., 2015. Neuroimaging Biomarkers for Psychosis. Current behavioral neuroscience reports 2015, 1-10. doi:10.1007/s40473-015-0035-4

Hagmann, P., Cammoun, L., Gigandet, X., Meuli, R., Honey, C.J., Wedeen, V.J., Sporns, O., 2008. Mapping the structural core of human cerebral cortex. PLoS Biol 6, e159. doi:10.1371/journal.pbio.0060159

Hardan, A.Y., Girgis, R.R., Lacerda, A.L., Yorbik, O., Kilpatrick, M., Keshavan, M.S., Minshew, N.J., 2006. Magnetic resonance imaging study of the orbitofrontal cortex in autism. J Child Neurol 21, 866-871. doi:10.1177/08830738060210100701

Hashemi, E., Ariza, J., Rogers, H., Noctor, S.C., Martínez-Cerdeño, V., 2017. The Number of Parvalbumin-Expressing Interneurons Is Decreased in the Prefrontal Cortex in Autism. Cereb Cortex 27, 1931-1943. doi:10.1093/cercor/bhw021

Hawrylycz, M.J., Lein, E.S., Guillozet-Bongaarts, A.L., Shen, E.H., Ng, L., Miller, J.A., van de Lagemaat, L.N., Smith, K.A., Ebbert, A., Riley, Z.L., Abajian, C., Beckmann, C.F., Bernard, A., Bertagnolli, D., Boe, A.F., Cartagena, P.M., Chakravarty, M.M., Chapin, M., Chong, J., Dalley, R.A., David Daly, B., Dang, C., Datta, S., Dee, N., Dolbeare, T.A., Faber, V., Feng, D., Fowler, D.R., Goldy, J., Gregor, B.W., Haradon, Z., Haynor, D.R., Hohmann, J.G., Horvath, S., Howard, R.E., Jeromin, A., Jochim, J.M., Kinnunen, M., Lau, C., Lazarz, E.T., Lee, C., Lemon, T.A., Li, L., Li, Y., Morris, J.A., Overly, C.C., Parker, P.D., Parry, S.E., Reding, M., Royall, J.J., Schulkin, J., Sequeira, P.A., Slaughterbeck, C.R., Smith, S.C., Sodt, A.J., Sunkin, S.M., Swanson, B.E., Vawter, M.P., Williams, D., Wohnoutka, P., Zielke, H.R., Geschwind, D.H., Hof, P.R., Smith, S.M., Koch, C., Grant, S.G.N., Jones, A.R., 2012.

An anatomically comprehensive atlas of the adult human brain transcriptome. Nature 489, 391-399. doi:10.1038/nature11405

Hawrylycz, M., Miller, J.A., Menon, V., Feng, D., Dolbeare, T., Guillozet-Bongaarts, A.L., Jegga, A.G., Aronow, B.J., Lee, C.K., Bernard, A., Glasser, M.F., Dierker, D.L., Menche, J., Szafer, A., Collman, F., Grange, P., Berman, K.A., Mihalas, S., Yao, Z., Stewart, L., Barabási, A.L., Schulkin, J., Phillips, J., Ng, L., Dang, C., Haynor, D.R., Jones, A., Van Essen, D.C., Koch, C., Lein, E., 2015. Canonical genetic signatures of the adult human brain. Nat Neurosci 18, 1832-1844. doi:10.1038/nn.4171

Haznedar, M.M., Buchsbaum, M.S., Wei, T.C., Hof, P.R., Cartwright, C., Bienstock, C.A., Hollander, E., 2000. Limbic circuitry in patients with autism spectrum disorders studied with positron emission tomography and magnetic resonance imaging. Am J Psychiatry 157, 1994-2001. doi:10.1176/appi.ajp.157.12.1994

He, N., Li, F., Li, Y., Guo, L., Chen, L., Huang, X., Lui, S., Gong, Q., 2015. Neuroanatomical deficits correlate with executive dysfunction in boys with attention deficit hyperactivity disorder. Neuroscience letters 600, 45-49. doi:10.1016/j.neulet.2015.05.062

Henderson, T.A., Cohen, P., van Lierop, M., Thornton, J., McLean, M.K., Uszler, J.M., Siow, Y.H., Cardaci, G., 2020a. A Reckoning to Keep Doing What We Are Already Doing With PET and SPECT Functional Neuroimaging. The American journal of psychiatry 177, 637-638. doi:10.1176/appi.ajp.2020.19080801

Henderson, T.A., van Lierop, M.J., McLean, M., Uszler, J.M., Thornton, J.F., Siow, Y.H., Pavel, D.G., Cardaci, J., Cohen, P., 2020b. Functional Neuroimaging in Psychiatry-Aiding in Diagnosis and Guiding Treatment. What the American Psychiatric Association Does Not Know. Frontiers in psychiatry 11, 276. doi:10.3389/fpsyt.2020.00276

Henson, R., 2006. Forward inference using functional neuroimaging: dissociations versus associations. Trends in cognitive sciences 10, 64-69. doi:10.1016/j.tics.2005.12.005

Henze, R., Brunner, R., Thiemann, U., Parzer, P., Richterich, A., Essig, M., Resch, F., Stieltjes, B., 2011. Gray matter alterations in first-admission adolescents with schizophrenia. Journal of neuroimaging : official journal of the American Society of Neuroimaging 21, 241-246. doi:10.1111/j.1552-6569.2010.00504.x

Hidese, S., Ota, M., Sasayama, D., Matsuo, J., Ishida, I., Hiraishi, M., Teraishi, T., Hattori, K., Kunugi, H., 2018. Manual dexterity and brain structure in patients with schizophrenia: A whole-brain magnetic resonance imaging study. Psychiatry research. Neuroimaging 276, 9-14. doi:10.1016/j.pscychresns.2018.04.003

Hirao, K., Miyata, J., Fujiwara, H., Yamada, M., Namiki, C., Shimizu, M., Sawamoto, N., Fukuyama, H., Hayashi, T., Murai, T., 2008. Theory of mind and frontal lobe pathology in schizophrenia: a voxel-based morphometry study. Schizophrenia research 105, 165-174. doi:10.1016/j.schres.2008.07.021

Hoeft, F., Meyler, A., Hernandez, A., Juel, C., Taylor-Hill, H., Martindale, J.L., McMillon, G., Kolchugina, G., Black, J.M., Faizi, A., Deutsch, G.K., Siok, W.T., Reiss, A.L., Whitfield-Gabrieli, S., Gabrieli, J.D., 2007. Functional and morphometric brain dissociation between dyslexia and reading ability. Proceedings of the National Academy of Sciences of the United States of America 104, 4234-4239. doi:10.1073/pnas.0609399104

Honea, R.A., Meyer-Lindenberg, A., Hobbs, K.B., Pezawas, L., Mattay, V.S., Egan, M.F., Verchinski, B., Passingham, R.E., Weinberger, D.R., Callicott, J.H., 2008. Is gray matter volume an intermediate phenotype for schizophrenia? A voxel-based morphometry study of patients with schizophrenia and their healthy siblings. Biological psychiatry 63, 465-474. doi:10.1016/j.biopsych.2007.05.027

Hoptman, M.J., Zuo, X.N., D'Angelo, D., Mauro, C.J., Butler, P.D., Milham, M.P., Javitt, D.C., 2012. Decreased interhemispheric coordination in schizophrenia: a resting state fMRI study. Schizophrenia research 141, 1-7. doi:10.1016/j.schres.2012.07.027

Horacek, J., Flegr, J., Tintera, J., Verebova, K., Spaniel, F., Novak, T., Brunovsky, M., Bubenikova-Valesova, V., Holub, D., Palenicek, T., Hoschl, C., 2012. Latent toxoplasmosis reduces gray matter density in schizophrenia but not in controls: voxel-based-morphometry (VBM) study. The world journal of biological psychiatry 13, 501-509. doi:10.3109/15622975.2011.573809

Horga, G., Bernacer, J., Dusi, N., Entis, J., Chu, K., Hazlett, E.A., Haznedar, M.M., Kemether, E., Byne, W., Buchsbaum, M.S., 2011. Correlations between ventricular enlargement and gray and white matter volumes of cortex, thalamus, striatum, and internal capsule in schizophrenia. European archives of psychiatry and clinical neuroscience 261, 467-476. doi:10.1007/s00406-011-0202-x

Howard, J.D., Reynolds, R., Smith, D.E., Voss, J.L., Schoenbaum, G., Kahnt, T., 2020. Targeted Stimulation of Human Orbitofrontal Networks Disrupts Outcome-Guided Behavior. Current biology : CB 30, 490-498.e494. doi:10.1016/j.cub.2019.12.007

Hu, M., Li, J., Eyler, L., Guo, X., Wei, Q., Tang, J., Liu, F., He, Z., Li, L., Jin, H., Liu, Z., Wang, J., Liu, F., Chen, H., Zhao, J., 2013. Decreased left middle temporal gyrus volume in antipsychotic drug-naive, first-episode schizophrenia patients and their healthy unaffected siblings. Schizophrenia research 144, 37-42. doi:10.1016/j.schres.2012.12.018

Hua, J., Blair, N.I.S., Paez, A., Choe, A., Barber, A.D., Brandt, A., Lim, I.A.L., Xu, F., Kamath, V., Pekar, J.J., van Zijl, P.C.M., Ross, C.A., Margolis, R.L., 2019. Altered functional connectivity between sub-regions in the thalamus and cortex in schizophrenia patients measured by resting state BOLD fMRI at 7T. Schizophrenia research 206, 370-377. doi:10.1016/j.schres.2018.10.016

Huang, P., Xi, Y., Lu, Z.L., Chen, Y., Li, X., Li, W., Zhu, X., Cui, L.B., Tan, Q., Liu, W., Li, C., Miao, D., Yin, H., 2015. Decreased bilateral thalamic gray matter volume in first-episode schizophrenia with prominent hallucinatory symptoms: A volumetric MRI study. Scientific reports 5, 14505. doi:10.1038/srep14505

Hulshoff Pol, H.E., Schnack, H.G., Mandl, R.C., Brans, R.G., van Haren, N.E., Baare, W.F., van Oel, C.J., Collins, D.L., Evans, A.C., Kahn, R.S., 2006. Gray and white matter density changes in monozygotic and same-sex dizygotic twins discordant for schizophrenia using voxel-based morphometry. NeuroImage 31, 482-488. doi:10.1016/j.neuroimage.2005.12.056

Hummer, T.A., Yung, M.G., Goñi, J., Conroy, S.K., Francis, M.M., Mehdiyoun, N.F., Breier, A., 2020. Functional network connectivity in early-stage schizophrenia. Schizophrenia research. doi:10.1016/j.schres.2020.01.023

Hutzler, F., 2014. Reverse inference is not a fallacy per se: cognitive processes can be inferred from functional imaging data. NeuroImage 84, 1061-1069. doi:10.1016/j.neuroimage.2012.12.075

Huys, Q.J., Maia, T.V., Frank, M.J., 2016. Computational psychiatry as a bridge from neuroscience to clinical applications. Nat Neurosci 19, 404-413. doi:10.1038/nn.4238

Hyde, K.L., Samson, F., Evans, A.C., Mottron, L., 2010. Neuroanatomical differences in brain areas implicated in perceptual and other core features of autism revealed by cortical

thickness analysis and voxel-based morphometry. Hum Brain Mapp 31, 556-566. doi:10.1002/hbm.20887

Iannaccone, R., Hauser, T.U., Ball, J., Brandeis, D., Walitza, S., Brem, S., 2015. Classifying adolescent attention-deficit/hyperactivity disorder (ADHD) based on functional and structural imaging. European child & adolescent psychiatry 24, 1279-1289. doi:10.1007/s00787-015-0678-4

Ingre, M., 2013. Why small low-powered studies are worse than large high-powered studies and how to protect against "trivial" findings in research: comment on Friston (2012). NeuroImage 81, 496-498. doi:10.1016/j.neuroimage.2013.03.030

Insel, T., Cuthbert, B., Garvey, M., Heinssen, R., Pine, D.S., Quinn, K., Sanislow, C., Wang, P., 2010. Research domain criteria (RDoC): toward a new classification framework for research on mental disorders. Am J Psychiatry 167, 748-751. doi:10.1176/appi.ajp.2010.09091379

Insel, T.R., 2014. The NIMH Research Domain Criteria (RDoC) Project: precision medicine for psychiatry. Am J Psychiatry 171, 395-397. doi:10.1176/appi.ajp.2014.14020138

Iorio-Morin, C., Sarica, C., Elias, G.J.B., Harmsen, I., Hodaie, M., 2022. Chapter 7 - Neuroimaging of psychiatric disorders, in: Chernov, M.F., Rzaev, J.A., Martínez-Álvarez, R. (Eds.), Progress in Brain Research. Elsevier, pp. 149-169.

Isobe, M., Miyata, J., Hazama, M., Fukuyama, H., Murai, T., Takahashi, H., 2016. Multimodal neuroimaging as a window into the pathological physiology of schizophrenia: Current trends and issues. Neuroscience research 102, 29-38. doi:10.1016/j.neures.2015.07.009

Itahashi, T., Yamada, T., Watanabe, H., Nakamura, M., Ohta, H., Kanai, C., Iwanami, A., Kato, N., Hashimoto, R., 2015. Alterations of local spontaneous brain activity and connectivity in adults with high-functioning autism spectrum disorder. Mol Autism 6, 30. doi:10.1186/s13229-015-0026-z

Iturria-Medina, Y., Evans, A.C., 2015. On the central role of brain connectivity in neurodegenerative disease progression. Front Aging Neurosci 7, 90. doi:10.3389/fnagi.2015.00090

Iturria-Medina, Y., Sotero, R.C., Toussaint, P.J., Evans, A.C., 2014. Epidemic spreading model to characterize misfolded proteins propagation in aging and associated neurodegenerative disorders. PLoS Comput Biol 10, e1003956. doi:10.1371/journal.pcbi.1003956

Jacobson, S., Kelleher, I., Harley, M., Murtagh, A., Clarke, M., Blanchard, M., Connolly, C., O'Hanlon, E., Garavan, H., Cannon, M., 2010. Structural and functional brain correlates of subclinical psychotic symptoms in 11-13 year old schoolchildren. NeuroImage 49, 1875-1885. doi:10.1016/j.neuroimage.2009.09.015

Jaeger, J., 2018. Digit Symbol Substitution Test: The Case for Sensitivity Over Specificity in Neuropsychological Testing. Journal of clinical psychopharmacology 38, 513-519. doi:10.1097/JCP.0000000000000941.

Jagger-Rickels, A.C., Kibby, M.Y., Constance, J.M., 2018. Global gray matter morphometry differences between children with reading disability, ADHD, and comorbid reading disability/ADHD. Brain and language 185, 54-66. doi:10.1016/j.bandl.2018.08.004

Jann, K., Hernandez, L.M., Beck-Pancer, D., McCarron, R., Smith, R.X., Dapretto, M., Wang, D.J., 2015. Altered resting perfusion and functional connectivity of default mode network in youth with autism spectrum disorder. Brain and behavior 5, e00358. doi:10.1002/brb3.358

Janssen, J., Reig, S., Parellada, M., Moreno, D., Graell, M., Fraguas, D., Zabala, A., Garcia Vazquez, V., Desco, M., Arango, C., 2008. Regional gray matter volume deficits in adolescents with first-episode psychosis. Journal of the American Academy of Child and Adolescent Psychiatry 47, 1311-1320. doi:10.1097/CHI.0b013e318184ff48

Jayakumar, P.N., Venkatasubramanian, G., Gangadhar, B.N., Janakiramaiah, N., Keshavan, M.S., 2005. Optimized voxel-based morphometry of gray matter volume in first-episode, antipsychotic-naive schizophrenia. Progress in neuro-psychopharmacology & biological psychiatry 29, 587-591. doi:10.1016/j.pnpbp.2005.01.020

Jbabdi, S., Sotiropoulos, S.N., Behrens, T.E., 2013. The topographic connectome. Current opinion in neurobiology 23, 207-215.

Jednoróg, K., Marchewka, A., Altarelli, I., Monzalvo Lopez, A.K., van Ermingen-Marbach, M., Grande, M., Grabowska, A., Heim, S., Ramus, F., 2015. How reliable are gray matter

disruptions in specific reading disability across multiple countries and languages? Insights from a large-scale voxel-based morphometry study. Hum Brain Mapp 36, 1741-1754. doi:10.1002/hbm.22734

Jeffreys, H., 1961. Theory of probability, 3rd ed. Clarendon, Oxford.

Jeong, B., Wible, C.G., Hashimoto, R., Kubicki, M., 2009. Functional and anatomical connectivity abnormalities in left inferior frontal gyrus in schizophrenia. Human brain mapping 30, 4138-4151. doi:10.1002/hbm.20835

Jessen, F., Scherk, H., Traber, F., Theyson, S., Berning, J., Tepest, R., Falkai, P., Schild, H.H., Maier, W., Wagner, M., Block, W., 2006. Proton magnetic resonance spectroscopy in subjects at risk for schizophrenia. Schizophrenia research 87, 81-88. doi:10.1016/j.schres.2006.06.011

Jiang, Y., Luo, C., Li, X., Duan, M., He, H., Chen, X., Yang, H., Gong, J., Chang, X., Woelfer, M., Biswal, B.B., Yao, D., 2018. Progressive Reduction in Gray Matter in Patients with Schizophrenia Assessed with MR Imaging by Using Causal Network Analysis. Radiology 287, 729. doi:10.1148/radiol.2018184005

Jiao, Y., Chen, R., Ke, X., Chu, K., Lu, Z., Herskovits, E.H., 2010. Predictive models of autism spectrum disorder based on brain regional cortical thickness. NeuroImage 50, 589-599. doi:10.1016/j.neuroimage.2009.12.047

Job, D.E., Whalley, H.C., McConnell, S., Glabus, M., Johnstone, E.C., Lawrie, S.M., 2003. Voxel-based morphometry of grey matter densities in subjects at high risk of schizophrenia. Schizophrenia research 64, 1-13. doi:10.1016/s0920-9964(03)00158-0

John, J.P., Lukose, A., Bagepally, B.S., Halahalli, H.N., Moily, N.S., Vijayakumari, A.A., Jain, S., 2015. A systematic examination of brain volumetric abnormalities in recent-onset schizophrenia using voxel-based, surface-based and region-of-interest-based morphometric analyses. Journal of negative results in biomedicine 14, 11. doi:10.1186/s12952-015-0030-z

Johnston, B.A., Mwangi, B., Matthews, K., Coghill, D., Konrad, K., Steele, J.D., 2014. Brainstem abnormalities in attention deficit hyperactivity disorder support high accuracy individual diagnostic classification. Hum Brain Mapp 35, 5179-5189. doi:10.1002/hbm.22542

Jou, R.J., Jackowski, A.P., Papademetris, X., Rajeevan, N., Staib, L.H., Volkmar, F.R., 2011. Diffusion tensor imaging in autism spectrum disorders: preliminary evidence of abnormal neural connectivity. Aust N Z J Psychiatry 45, 153-162. doi:10.3109/00048674.2010.534069

Jovicich, J., Czanner, S., Han, X., Salat, D., van der Kouwe, A., Quinn, B., Pacheco, J., Albert, M., Killiany, R., Blacker, D., Maguire, P., Rosas, D., Makris, N., Gollub, R., Dale, A., Dickerson, B.C., Fischl, B., 2009. MRI-derived measurements of human subcortical, ventricular and intracranial brain volumes: Reliability effects of scan sessions, acquisition sequences, data analyses, scanner upgrade, scanner vendors and field strengths. NeuroImage 46, 177-192. doi:10.1016/j.neuroimage.2009.02.010

Jung, W.H., Jang, J.H., Shin, N.Y., Kim, S.N., Choi, C.H., An, S.K., Kwon, J.S., 2012. Regional brain atrophy and functional disconnection in Broca's area in individuals at ultra-high risk for psychosis and schizophrenia. PloS one 7, e51975. doi:10.1371/journal.pone.0051975

Just, M.A., Cherkassky, V.L., Buchweitz, A., Keller, T.A., Mitchell, T.M., 2014. Identifying autism from neural representations of social interactions: neurocognitive markers of autism. PloS one 9, e113879. doi:10.1371/journal.pone.0113879

Kahn, R.S., Keefe, R.S., 2013. Schizophrenia is a cognitive illness: time for a change in focus. JAMA psychiatry 70, 1107-1112. doi:10.1001/jamapsychiatry.2013.155

Kakeda, S., Korogi, Y., 2010. The efficacy of a voxel-based morphometry on the analysis of imaging in schizophrenia, temporal lobe epilepsy, and Alzheimer's disease/mild cognitive impairment: a review. Neuroradiology 52, 711-721. doi:10.1007/s00234-010-0717-2

Kang, D.H., Son, J.H., Kim, Y.C., 2010. Neuroimaging studies of chronic pain. The Korean journal of pain 23, 159-165. doi:10.3344/kjp.2010.23.3.159

Kambeitz, J., Kambeitz-Ilankovic, L., Leucht, S., Wood, S., Davatzikos, C., Malchow, B., Falkai, P., Koutsouleris, N., 2015. Detecting neuroimaging biomarkers for schizophrenia: a meta-analysis of multivariate pattern recognition studies. Neuropsychopharmacology : official publication of the American College of Neuropsychopharmacology 40, 1742-1751. doi:10.1038/npp.2015.22

Kappel, V., Lorenz, R.C., Streifling, M., Renneberg, B., Lehmkuhl, U., Ströhle, A., Salbach-Andrae, H., Beck, A., 2015. Effect of brain structure and function on reward anticipation in

children and adults with attention deficit hyperactivity disorder combined subtype. Soc Cogn Affect Neurosci 10, 945-951. doi:10.1093/scan/nsu135

Kasarpalkar, N.J., Kothari, S.T., Dave, U.P., 2014. Brain-Derived Neurotrophic Factor in children with Autism Spectrum Disorder. Ann Neurosci 21, 129-133. doi:10.5214/ans.0972.7531.210403

Kasparek, T., Prikryl, R., Schwarz, D., Kucerova, H., Marecek, R., Mikl, M., Vanicek, J., Ceskova, E., 2009. Gray matter morphology and the level of functioning in one-year follow-up of first-episode schizophrenia patients. Progress in neuro-psychopharmacology & biological psychiatry 33, 1438-1446. doi:10.1016/j.pnpbp.2009.07.025

Kass, R.E., Raftery, A.E., 1995. Bayes factors. Journal of the american statistical association 90, 773-795.

Kay, S.R., Fiszbein, A., Opler, L.A., 1987. The positive and negative syndrome scale (PANSS) for schizophrenia. Schizophrenia bulletin 13, 261-276. doi:10.1093/schbul/13.2.261

Kaufmann, L., Zotter, S., Pixner, S., Starke, M., Haberlandt, E., Steinmayr-Gensluckner, M., Egger, K., Schocke, M., Weiss, E.M., Marksteiner, J., 2013. Brief report: CANTAB performance and brain structure in pediatric patients with Asperger syndrome. Journal of autism and developmental disorders 43, 1483-1490. doi:10.1007/s10803-012-1686-6

Ke, X., Hong, S., Tang, T., Zou, B., Li, H., Hang, Y., Zhou, Z., Ruan, Z., Lu, Z., Tao, G., Liu, Y., 2008. Voxel-based morphometry study on brain structure in children with high-functioning autism. Neuroreport 19, 921-925. doi:10.1097/WNR.0b013e328300edf3

Kebets, V., Holmes, A.J., Orban, C., Tang, S., Li, J., Sun, N., Kong, R., Poldrack, R.A., Yeo, B.T.T., 2019. Somatosensory-Motor Dysconnectivity Spans Multiple Transdiagnostic Dimensions of Psychopathology. Biological psychiatry 86, 779-791. doi:10.1016/j.biopsych.2019.06.013

Keller, R., Chieregato, S., Bari, S., Castaldo, R., Rutto, F., Chiocchetti, A., Dianzani, U., 2020. Autism in Adulthood: Clinical and Demographic Characteristics of a Cohort of Five Hundred Persons with Autism Analyzed by a Novel Multistep Network Model. Brain Sci 10. doi:10.3390/brainsci10070416

Kendler, K.S., 2012. The dappled nature of causes of psychiatric illness: replacing the organic-functional/hardware-software dichotomy with empirically based pluralism. Molecular psychiatry 17, 377-388. doi:10.1038/mp.2011.182

Kennedy, D.P., Courchesne, E., 2008. Functional abnormalities of the default network during self- and other-reflection in autism. Soc Cogn Affect Neurosci 3, 177-190. doi:10.1093/scan/nsn011

Kenneth Martin, A., Robinson, G., Reutens, D., Mowry, B., 2014. Cognitive and structural neuroimaging characteristics of schizophrenia patients with large, rare copy number deletions. Psychiatry research 224, 311-318. doi:10.1016/j.pscychresns.2014.10.006

Kemether, E.M., Buchsbaum, M.S., Byne, W., Hazlett, E.A., Haznedar, M., Brickman, A.M., Platholi, J., Bloom, R., 2003. Magnetic resonance imaging of mediodorsal, pulvinar, and centromedian nuclei of the thalamus in patients with schizophrenia. Archives of general psychiatry 60, 983-991. doi:10.1001/archpsyc.60.9.983

Kern, J.K., Geier, D.A., Sykes, L.K., Geier, M.R., Deth, R.C., 2015. Are ASD and ADHD a Continuum? A Comparison of Pathophysiological Similarities Between the Disorders. Journal of Attention Disorders 19, 805-827. doi:10.1177/1087054712459886

Keshavan, M.S., 1999. Development, disease and degeneration in schizophrenia: a unitary pathophysiological model. Journal of psychiatric research 33, 513-521. doi:10.1016/s0022-3956(99)00033-3

Keysers, C., Kaas, J.H., Gazzola, V., 2010. Somatosensation in social perception. Nature reviews. Neuroscience 11, 417-428. doi:10.1038/nrn2833

Khan, A.J., Nair, A., Keown, C.L., Datko, M.C., Lincoln, A.J., Muller, R.A., 2015. Cerebro-cerebellar Resting-State Functional Connectivity in Children and Adolescents with Autism Spectrum Disorder. Biol Psychiatry 78, 625-634. doi:10.1016/j.biopsych.2015.03.024

Kibby, M.Y., Kroese, J.M., Krebbs, H., Hill, C.E., Hynd, G.W., 2009. The pars triangularis in dyslexia and ADHD: A comprehensive approach. Brain and language 111, 46-54. doi:10.1016/j.bandl.2009.03.001

Killgore, W.D., Rosso, I.M., Gruber, S.A., Yurgelun-Todd, D.A., 2009. Amygdala volume and verbal memory performance in schizophrenia and bipolar disorder. Cognitive and

behavioral neurology : official journal of the Society for Behavioral and Cognitive Neurology 22, 28-37. doi:10.1097/WNN.0b013e318192cc67

Kim, H.J., Cho, M.H., Shim, W.H., Kim, J.K., Jeon, E.Y., Kim, D.H., Yoon, S.Y., 2017a. Deficient autophagy in microglia impairs synaptic pruning and causes social behavioral defects. Mol Psychiatry 22, 1576-1584. doi:10.1038/mp.2016.103

Kim, G.W., Kim, Y.H., Jeong, G.W., 2017b. Whole brain volume changes and its correlation with clinical symptom severity in patients with schizophrenia: A DARTEL-based VBM study. PloS one 12, e0177251. doi:10.1371/journal.pone.0177251

Kindler, J., Michel, C., Schultze-Lutter, F., Felber, G., Hauf, M., Schimmelmann, B.G., Kaess, M., Hubl, D., Walther, S., 2019. Functional and structural correlates of abnormal involuntary movements in psychosis risk and first episode psychosis. Schizophrenia research 212, 196-203. doi:10.1016/j.schres.2019.07.032

Klucharev, V., Hytönen, K., Rijpkema, M., Smidts, A., Fernández, G., 2009. Reinforcement learning signal predicts social conformity. Neuron 61, 140-151. doi:10.1016/j.neuron.2008.11.027

Kobel, M., Bechtel, N., Specht, K., Klarhöfer, M., Weber, P., Scheffler, K., Opwis, K., Penner, I.K., 2010. Structural and functional imaging approaches in attention deficit/hyperactivity disorder: does the temporal lobe play a key role? Psychiatry research 183, 230-236. doi:10.1016/j.pscychresns.2010.03.010

Kochunov, P., Thompson, P.M., Hong, L.E., 2019. Toward High Reproducibility and Accountable Heterogeneity in Schizophrenia Research. JAMA psychiatry 76, 680-681. doi:10.1001/jamapsychiatry.2019.0208

Koenders, L., Machielsen, M.W., van der Meer, F.J., van Gasselt, A.C., Meijer, C.J., van den Brink, W., Koeter, M.W., Caan, M.W., Cousijn, J., den Braber, A., van 't Ent, D., Rive, M.M., Schene, A.H., van de Giessen, E., Huyser, C., de Kwaasteniet, B.P., Veltman, D.J., de Haan, L., 2015. Brain volume in male patients with recent onset schizophrenia with and without cannabis use disorders. Journal of psychiatry & neuroscience : JPN 40, 197-206. doi:10.1503/jpn.140081

Kong, L., Herold, C.J., Zollner, F., Salat, D.H., Lasser, M.M., Schmid, L.A., Fellhauer, I., Thomann, P.A., Essig, M., Schad, L.R., Erickson, K.I., Schroder, J., 2015. Comparison of

grey matter volume and thickness for analysing cortical changes in chronic schizophrenia: a matter of surface area, grey/white matter intensity contrast, and curvature. Psychiatry research 231, 176-183. doi:10.1016/j.pscychresns.2014.12.004

Kong, X.-Z., Postema, M.C., Guadalupe, T., de Kovel, C., Boedhoe, P.S.W., Hoogman, M., Mathias, S.R., van Rooij, D., Schijven, D., Glahn, D.C., Medland, S.E., Jahanshad, N., Thomopoulos, S.I., Turner, J.A., Buitelaar, J., van Erp, T.G.M., Franke, B., Fisher, S.E., van den Heuvel, O.A., Schmaal, L., Thompson, P.M., Francks, C., 2020. Mapping brain asymmetry in health and disease through the ENIGMA consortium. Hum Brain Mapp n/a. doi:10.1002/hbm.25033

Korgaonkar, M.S., Fornito, A., Williams, L.M., Grieve, S.M., 2014. Abnormal structural networks characterize major depressive disorder: a connectome analysis. Biol Psychiatry 76, 567-574. doi:10.1016/j.biopsych.2014.02.018

Korth, C., 2012. Aggregated proteins in schizophrenia and other chronic mental diseases: DISC1opathies. Prion 6, 134-141. doi:10.4161/pri.18989

Kosaka, H., Omori, M., Munesue, T., Ishitobi, M., Matsumura, Y., Takahashi, T., Narita, K., Murata, T., Saito, D.N., Uchiyama, H., Morita, T., Kikuchi, M., Mizukami, K., Okazawa, H., Sadato, N., Wada, Y., 2010. Smaller insula and inferior frontal volumes in young adults with pervasive developmental disorders. Neuroimage 50, 1357-1363. doi:10.1016/j.neuroimage.2010.01.085

Koshino, H., Kana, R.K., Keller, T.A., Cherkassky, V.L., Minshew, N.J., Just, M.A., 2008. fMRI investigation of working memory for faces in autism: visual coding and underconnectivity with frontal areas. Cerebral cortex (New York, N.Y. : 1991) 18, 289-300. doi:10.1093/cercor/bhm054

Kotkowski, E., Price, L.R., Mickle Fox, P., Vanasse, T.J., Fox, P.T., 2018. The hippocampal network model: A transdiagnostic metaconnectomic approach. NeuroImage. Clinical 18, 115-129. doi: 10.1016/j.nicl.2018.01.002

Kotov, R., Krueger, R.F., Watson, D., Achenbach, T.M., Althoff, R.R., Bagby, R.M., Brown, T.A., Carpenter, W.T., Caspi, A., Clark, L.A., 2017. The Hierarchical Taxonomy of Psychopathology (HiTOP): A dimensional alternative to traditional nosologies. Journal of abnormal psychology 126, 454. doi:10.1037/abn0000258

Koutsouleris, N., Gaser, C., Jager, M., Bottlender, R., Frodl, T., Holzinger, S., Schmitt, G.J., Zetzsche, T., Burgermeister, B., Scheuerecker, J., Born, C., Reiser, M., Moller, H.J., Meisenzahl, E.M., 2008. Structural correlates of psychopathological symptom dimensions in schizophrenia: a voxel-based morphometric study. NeuroImage 39, 1600-1612. doi:10.1016/j.neuroimage.2007.10.029

Koutsouleris, N., Davatzikos, C., Borgwardt, S., Gaser, C., Bottlender, R., Frodl, T., Falkai, P., Riecher-Rossler, A., Moller, H.J., Reiser, M., Pantelis, C., Meisenzahl, E., 2014. Accelerated brain aging in schizophrenia and beyond: a neuroanatomical marker of psychiatric disorders. Schizophrenia bulletin 40, 1140-1153. doi:10.1093/schbul/sbt142

Kraguljac, N.V., McDonald, W.M., Widge, A.S., Rodriguez, C.I., Tohen, M., Nemeroff, C.B., 2021. Neuroimaging Biomarkers in Schizophrenia. The American journal of psychiatry 178, 509-521. doi:10.1176/appi.ajp.2020.20030340

Krause, M., Theiss, C., Brüne, M., 2017. Ultrastructural Alterations of Von Economo Neurons in the Anterior Cingulate Cortex in Schizophrenia. Anatomical record (Hoboken, N.J. : 2007) 300, 2017-2024. doi:10.1002/ar.23635

Kravitz, D.J., Saleem, K.S., Baker, C.I., Mishkin, M., 2011. A new neural framework for visuospatial processing. Nat Rev Neurosci 12, 217-230. doi:10.1038/nrn3008

Kronbichler, M., Wimmer, H., Staffen, W., Hutzler, F., Mair, A., Ladurner, G., 2008. Developmental dyslexia: gray matter abnormalities in the occipitotemporal cortex. Hum Brain Mapp 29, 613-625. doi:10.1002/hbm.20425

Kubicki, M., Shenton, M.E., Salisbury, D.F., Hirayasu, Y., Kasai, K., Kikinis, R., Jolesz, F.A., McCarley, R.W., 2002. Voxel-based morphometric analysis of gray matter in first episode schizophrenia. NeuroImage 17, 1711-1719. doi:10.1006/nimg.2002.1296

Kumar, A., Cook, I.A., 2002. White Matter Injury, Neural Connectivity and the Pathophysiology of Psychiatric Disorders. Developmental Neuroscience 24, 255-261.

Kumar, U., Arya, A., Agarwal, V., 2017. Neural alterations in ADHD children as indicated by voxel-based cortical thickness and morphometry analysis. Brain & development 39, 403-410. doi:10.1016/j.braindev.2016.12.002

Kurth, F., Gaser, C., Luders, E., 2015. A 12-step user guide for analyzing voxel-wise gray matter asymmetries in statistical parametric mapping (SPM). Nature protocols 10, 293-304. doi:10.1038/nprot.2015.014

Kurth, F., Narr, K.L., Woods, R.P., O'Neill, J., Alger, J.R., Caplan, R., McCracken, J.T., Toga, A.W., Levitt, J.G., 2011. Diminished gray matter within the hypothalamus in autism disorder: a potential link to hormonal effects? Biological psychiatry 70, 278-282. doi:10.1016/j.biopsych.2011.03.026

Kwon, H., Ow, A.W., Pedatella, K.E., Lotspeich, L.J., Reiss, A.L., 2004. Voxel-based morphometry elucidates structural neuroanatomy of high-functioning autism and Asperger syndrome. Developmental medicine and child neurology 46, 760-764. doi:10.1017/s0012162204001306

Labus, J.S., Naliboff, B., Kilpatrick, L., Liu, C., Ashe-McNalley, C., Dos Santos, I.R., Alaverdyan, M., Woodworth, D., Gupta, A., Ellingson, B.M., Tillisch, K., Mayer, E.A., 2016. Pain and Interoception Imaging Network (PAIN): A multimodal, multisite, brain-imaging repository for chronic somatic and visceral pain disorders. Neuroimage 124, 1232-1237. doi:10.1016/j.neuroimage.2015.04.018

Lahav, N., Ksherim, B., Ben-Simon, E., Maron-Katz, A., Cohen, R., Havlin, S., 2016. K-shell decomposition reveals hierarchical cortical organization of the human brain. New Journal of Physics 18, 083013. doi:10.1088/1367-2630/18/8/083013

Lahey, B.B., Krueger, R.F., Rathouz, P.J., Waldman, I.D., Zald, D.H., 2017. Validity and utility of the general factor of psychopathology. World Psychiatry 16, 142-144. doi:10.1002/wps.20410

Lai, M.C., Lombardo, M.V., Ecker, C., Chakrabarti, B., Suckling, J., Bullmore, E.T., Happé, F., Murphy, D.G., Baron-Cohen, S., 2015. Neuroanatomy of Individual Differences in Language in Adult Males with Autism. Cerebral cortex 25, 3613-3628. doi:10.1093/cercor/bhu211

Lai, M.C., Lombardo, M.V., Suckling, J., Ruigrok, A.N., Chakrabarti, B., Ecker, C., Deoni, S.C., Craig, M.C., Murphy, D.G., Bullmore, E.T., Baron-Cohen, S., 2013. Biological sex affects the neurobiology of autism. Brain 136, 2799-2815. doi:10.1093/brain/awt216

Laird, A., Eickhoff, S., Kurth, F., Fox, P., Uecker, A., Turner, J., Robinson, J., Lancaster, J., Fox, P., 2009. ALE meta-analysis workflows via the BrainMap database: progress towards a probabilistic functional brain atlas. Frontiers in Neuroinformatics 3. doi:10.3389/neuro.11.023.2009

Laird, A.R., Fox, P.M., Eickhoff, S.B., Turner, J.A., Ray, K.L., McKay, D.R., Glahn, D.C., Beckmann, C.F., Smith, S.M., Fox, P.T., 2011. Behavioral interpretations of intrinsic connectivity networks. J Cogn Neurosci 23, 4022-4037.

Laird, A.R., Fox, P.M., Price, C.J., Glahn, D.C., Uecker, A.M., Lancaster, J.L., Turkeltaub, P.E., Kochunov, P., Fox, P.T., 2005a. ALE meta-analysis: controlling the false discovery rate and performing statistical contrasts. Hum Brain Mapp 25, 155-164. doi:10.1002/hbm.20136

Laird, A.R., Lancaster, J.L., Fox, P.T., 2005b. BrainMap: the social evolution of a human brain mapping database. Neuroinformatics 3, 65-78. doi:10.1385/ni:3:1:065

Laird, A.R., Lancaster, J.L., Fox, P.T., 2008. Lost in localization? The focus is meta-analysis. Neuroimage 48, 18-20. doi:10.1016/j.neuroimage.2009.06.047

Laird, A.R., Robinson, J.L., McMillan, K.M., Tordesillas-Gutierrez, D., Moran, S.T., Gonzales, S.M., Ray, K.L., Franklin, C., Glahn, D.C., Fox, P.T., Lancaster, J.L., 2010. Comparison of the disparity between Talairach and MNI coordinates in functional neuroimaging data: validation of the Lancaster transform. Neuroimage 51, 677-683. doi:10.1016/j.neuroimage.2010.02.048

Laitin, D.D., Miguel, E., Alrababa'h, A., Bogdanoski, A., Grant, S., Hoeberling, K., Hyunjung Mo, C., Moore, D.A., Vazire, S., Weinstein, J., Williamson, S., 2021. Reporting all results efficiently: A RARE proposal to open up the file drawer. Proceedings of the National Academy of Sciences of the United States of America 118. doi:10.1073/pnas.2106178118

Lancaster, J.L., Laird, A.R., Eickhoff, S.B., Martinez, M.J., Fox, P.M., Fox, P.T., 2012. Automated regional behavioral analysis for human brain images. Frontiers in neuroinformatics 6, 23. doi:10.3389/fninf.2012.00023

Lancaster, J.L., Tordesillas-Gutierrez, D., Martinez, M., Salinas, F., Evans, A., Zilles, K., Mazziotta, J.C., Fox, P.T., 2007. Bias between MNI and Talairach coordinates analyzed using the ICBM-152 brain template. Human brain mapping 28, 1194-1205. doi:10.1002/hbm.20345

Lancaster, J.L., Woldorff, M.G., Parsons, L.M., Liotti, M., Freitas, C.S., Rainey, L., Kochunov, P.V., Nickerson, D., Mikiten, S.A., Fox, P.T., 2000. Automated Talairach atlas labels for functional brain mapping. Hum Brain Mapp 10, 120-131. doi:10.1002/1097-0193(200007)10:3<120::aid-hbm30>3.0.co;2-8

Lander, E.S., 1996. The new genomics: global views of biology. Science 274, 536-539.

Lange, N., Travers, B.G., Bigler, E.D., Prigge, M.B., Froehlich, A.L., Nielsen, J.A., Cariello, A.N., Zielinski, B.A., Anderson, J.S., Fletcher, P.T., Alexander, A.A., Lainhart, J.E., 2015. Longitudinal volumetric brain changes in autism spectrum disorder ages 6-35 years. Autism research : official journal of the International Society for Autism Research 8, 82-93. doi:10.1002/aur.1427

Langer, N., Benjamin, C., Becker, B.L.C., Gaab, N., 2019. Comorbidity of reading disabilities and ADHD: Structural and functional brain characteristics. Hum Brain Mapp 40, 2677-2698. doi:10.1002/hbm.24552

Larivière, S., Bayrak, Ş., de Wael, R.V., Benkarim, O., Herholz, P., Rodriguez-Cruces, R., Paquola, C., Hong, S.J., Misic, B., Evans, A.C., Valk, S.L., Bernhardt, B.C., 2022. BrainStat: a toolbox for brain-wide statistics and multimodal feature associations. Neuroimage, 119807. doi: 10.1016/j.neuroimage.2022.119807

Lawrie, S.M., 2018. Are structural brain changes in schizophrenia related to antipsychotic medication? A narrative review of the evidence from a clinical perspective. Therapeutic advances in psychopharmacology 8, 319-326. doi:10.1177/2045125318782306

Lazar, N.A., Luna, B., Sweeney, J.A., Eddy, W.F., 2002. Combining brains: a survey of methods for statistical pooling of information. Neuroimage 16, 538-550. doi:10.1006/nimg.2002.1107

Lee, P.H., Anttila, V., Won, H., Feng, Y.-C.A., Rosenthal, J., Zhu, Z., Tucker-Drob, E.M., Nivard, M.G., Grotzinger, A.D., Posthuma, D., Wang, M.M.J., Yu, D., Stahl, E.A., Walters, R.K., Anney, R.J.L., Duncan, L.E., Ge, T., Adolfsson, R., Banaschewski, T., Belangero, S., Cook, E.H., Coppola, G., Derks, E.M., Hoekstra, P.J., Kaprio, J., Keski-Rahkonen, A., Kirov, G., Kranzler, H.R., Luykx, J.J., Rohde, L.A., Zai, C.C., Agerbo, E., Arranz, M.J., Asherson, P., Bækvad-Hansen, M., Baldursson, G., Bellgrove, M., Belliveau, R.A., Buitelaar, J., Burton, C.L., Bybjerg-Grauholm, J., Casas, M., Cerrato, F., Chambert, K., Churchhouse, C.,

Cormand, B., Crosbie, J., Dalsgaard, S., Demontis, D., Doyle, A.E., Dumont, A., Elia, J., Grove, J., Gudmundsson, O.O., Haavik, J., Hakonarson, H., Hansen, C.S., Hartman, C.A., Hawi, Z., Hervás, A., Hougaard, D.M., Howrigan, D.P., Huang, H., Kuntsi, J., Langley, K., Lesch, K.-P., Leung, P.W.L., Loo, S.K., Martin, J., Martin, A.R., McGough, J.J., Medland, S.E., Moran, J.L., Mors, O., Mortensen, P.B., Oades, R.D., Palmer, D.S., Pedersen, C.B., Pedersen, M.G., Peters, T., Poterba, T., Poulsen, J.B., Ramos-Quiroga, J.A., Reif, A., Ribasés, M., Rothenberger, A., Rovira, P., Sánchez-Mora, C., Satterstrom, F.K., Schachar, R., Artigas, M.S., Steinberg, S., Stefansson, H., Turley, P., Walters, G.B., Werge, T., Zayats, T., Arking, D.E., Bettella, F., Buxbaum, J.D., Christensen, J.H., Collins, R.L., Coon, H., De Rubeis, S., Delorme, R., Grice, D.E., Hansen, T.F., Holmans, P.A., Hope, S., Hultman, C.M., Klei, L., Ladd-Acosta, C., Magnusson, P., Nærland, T., Nyegaard, M., Pinto, D., Qvist, P., Rehnström, K., Reichenberg, A., Reichert, J., Roeder, K., Rouleau, G.A., Saemundsen, E., Sanders, S.J., Sandin, S., St Pourcain, B., Stefansson, K., Sutcliffe, J.S., Talkowski, M.E., Weiss, L.A., Willsey, A.J., Agartz, I., Akil, H., Albani, D., Alda, M., Als, T.D., Anjorin, A., Backlund, L., Bass, N., Bauer, M., Baune, B.T., Bellivier, F., Bergen, S.E., Berrettini, W.H., Biernacka, J.M., Blackwood, D.H.R., Bøen, E., Budde, M., Bunney, W., Burmeister, M., Byerley, W., Byrne, E.M., Cichon, S., Clarke, T.-K., Coleman, J.R.I., Craddock, N., Curtis, D., Czerski, P.M., Dale, A.M., Dalkner, N., Dannlowski, U., Degenhardt, F., Di Florio, A., Elvsåshagen, T., Etain, B., Fischer, S.B., Forstner, A.J., Forty, L., Frank, J., Frye, M., Fullerton, J.M., Gade, K., Gaspar, H.A., Gershon, E.S., Gill, M., Goes, F.S., Gordon, S.D., Gordon-Smith, K., Green, M.J., Greenwood, T.A., Grigoroiu-Serbanescu, M., Guzman-Parra, J., Hauser, J., Hautzinger, M., Heilbronner, U., Herms, S., Hoffmann, P., Holland, D., Jamain, S., Jones, I., Jones, L.A., Kandaswamy, R., Kelsoe, J.R., Kennedy, J.L., Joachim, O.K., Kittel-Schneider, S., Kogevinas, M., Koller, A.C., Lavebratt, C., Lewis, C.M., Li, Q.S., Lissowska, J., Loohuis, L.M.O., Lucae, S., Maaser, A., Malt, U.F., Martin, N.G., Martinsson, L., McElroy, S.L., McMahon, F.J., McQuillin, A., Melle, I., Metspalu, A., Millischer, V., Mitchell, P.B., Montgomery, G.W., Morken, G., Morris, D.W., Müller-Myhsok, B., Mullins, N., Myers, R.M., Nievergelt, C.M., Nordentoft, M., Adolfsson, A.N., Nöthen, M.M., Ophoff, R.A., Owen, M.J., Paciga, S.A., Pato, C.N., Pato, M.T., Perlis, R.H., Perry, A., Potash, J.B., Reinbold, C.S., Rietschel, M., Rivera, M., Roberson, M., Schalling, M., Schofield, P.R., Schulze, T.G., Scott, L.J., Serretti, A., Sigurdsson, E., Smeland, O.B., Stordal, E., Streit, F., Strohmaier, J., Thorgeirsson, T.E., Treutlein, J., Turecki, G., Vaaler, A.E., Vieta, E., Vincent,

J.B., Wang, Y., Witt, S.H., Zandi, P., Adan, R.A.H., Alfredsson, L., Ando, T., Aschauer, H., Baker, J.H., Bencko, V., Bergen, A.W., Birgegård, A., Perica, V.B., Brandt, H., Burghardt, R., Carlberg, L., Cassina, M., Clementi, M., Courtet, P., Crawford, S., Crow, S., Crowley, J.J., Danner, U.N., Davis, O.S.P., Degortes, D., DeSocio, J.E., Dick, D.M., Dina, C., Docampo, E., Egberts, K., Ehrlich, S., Espeseth, T., Fernández-Aranda, F., Fichter, M.M., Foretova, L., Forzan, M., Gambaro, G., Giegling, I., Gonidakis, F., Gorwood, P., Mayora, M.G., Guo, Y., Halmi, K.A., Hatzikotoulas, K., Hebebrand, J., Helder, S.G., Herpertz-Dahlmann, B., Herzog, W., Hinney, A., Imgart, H., Jiménez-Murcia, S., Johnson, C., Jordan, J., Julià, A., Kaminská, D., Karhunen, L., Karwautz, A., Kas, M.J.H., Kaye, W.H., Kennedy, M.A., Kim, Y.-R., Klareskog, L., Klump, K.L., Knudsen, G.P.S., Landén, M., Le Hellard, S., Levitan, R.D., Li, D., Lichtenstein, P., Maj, M., Marsal, S., McDevitt, S., Mitchell, J., Monteleone, P., Monteleone, A.M., Munn-Chernoff, M.A., Nacmias, B., Navratilova, M., O'Toole, J.K., Padyukov, L., Pantel, J., Papezova, H., Rabionet, R., Raevuori, A., Ramoz, N., Reichborn-Kjennerud, T., Ricca, V., Roberts, M., Rujescu, D., Rybakowski, F., Scherag, A., Schmidt, U., Seitz, J., Slachtova, L., Slof-Op't Landt, M.C.T., Slopien, A., Sorbi, S., Southam, L., Strober, M., Tortorella, A., Tozzi, F., Treasure, J., Tziouvas, K., van Elburg, A.A., Wade, T.D., Wagner, G., Walton, E., Watson, H.J., Wichmann, H.E., Woodside, D.B., Zeggini, E., Zerwas, S., Zipfel, S., Adams, M.J., Andlauer, T.F.M., Berger, K., Binder, E.B., Boomsma, D.I., Castelao, E., Colodro-Conde, L., Direk, N., Docherty, A.R., Domenici, E., Domschke, K., Dunn, E.C., Foo, J.C., de. Geus, E.J.C., Grabe, H.J., Hamilton, S.P., Horn, C., Hottenga, J.-J., Howard, D., Ising, M., Kloiber, S., Levinson, D.F., Lewis, G., Magnusson, P.K.E., Mbarek, H., Middeldorp, C.M., Mostafavi, S., Nyholt, D.R., Penninx, B.W.J.H., Peterson, R.E., Pistis, G., Porteous, D.J., Preisig, M., Quiroz, J.A., Schaefer, C., Schulte, E.C., Shi, J., Smith, D.J., Thomson, P.A., Tiemeier, H., Uher, R., van der Auwera, S., Weissman, M.M., Alexander, M., Begemann, M., Bramon, E., Buccola, N.G., Cairns, M.J., Campion, D., Carr, V.J., Cloninger, C.R., Cohen, D., Collier, D.A., Corvin, A., DeLisi, L.E., Donohoe, G., Dudbridge, F., Duan, J., Freedman, R., Gejman, P.V., Golimbet, V., Godard, S., Ehrenreich, H., Hartmann, A.M., Henskens, F.A., Ikeda, M., Iwata, N., Jablensky, A.V., Joa, I., Jönsson, E.G., Kelly, B.J., Knight, J., Konte, B., Laurent-Levinson, C., Lee, J., Lencz, T., Lerer, B., Loughland, C.M., Malhotra, A.K., Mallet, J., McDonald, C., Mitjans, M., Mowry, B.J., Murphy, K.C., Murray, R.M., O'Neill, F.A., Oh, S.-Y., Palotie, A., Pantelis, C., Pulver, A.E., Petryshen, T.L., Quested, D.J., Riley, B., Sanders, A.R., Schall, U., Schwab, S.G., Scott, R.J.,

Sham, P.C., Silverman, J.M., Sim, K., Steixner, A.A., Tooney, P.A., van Os, J., Vawter, M.P., Walsh, D., Weiser, M., Wildenauer, D.B., Williams, N.M., Wormley, B.K., Zhang, F., Androutsos, C., Arnold, P.D., Barr, C.L., Barta, C., Bey, K., Bienvenu, O.J., Black, D.W., Brown, L.W., Budman, C., Cath, D., Cheon, K.-A., Ciullo, V., Coffey, B.J., Cusi, D., Davis, L.K., Denys, D., Depienne, C., Dietrich, A., Eapen, V., Falkai, P., Fernandez, T.V., Garcia-Delgar, B., Geller, D.A., Gilbert, D.L., Grados, M.A., Greenberg, E., Grünblatt, E., Hagstrøm, J., Hanna, G.L., Hartmann, A., Hedderly, T., Heiman, G.A., Heyman, I., Hong, H.J., Huang, A., Huyser, C., Ibanez-Gomez, L., Khramtsova, E.A., Kim, Y.K., Kim, Y.-S., King, R.A., Koh, Y.-J., Konstantinidis, A., Kook, S., Kuperman, S., Leventhal, B.L., Lochner, C., Ludolph, A.G., Madruga-Garrido, M., Malaty, I., Maras, A., McCracken, J.T., Meijer, I.A., Mir, P., Morer, A., Müller-Vahl, K.R., Münchau, A., Murphy, T.L., Naarden, A., Nagy, P., Nestadt, G., Nestadt, P.S., Nicolini, H., Nurmi, E.L., Okun, M.S., Paschou, P., Piras, F., Piras, F., Pittenger, C., Plessen, K.J., Richter, M.A., Rizzo, R., Robertson, M., Roessner, V., Ruhrmann, S., Samuels, J.F., Sandor, P., Schlögelhofer, M., Shin, E.-Y., Singer, H., Song, D.-H., Song, J., Spalletta, G., Stein, D.J., Stewart, S.E., Storch, E.A., Stranger, B., Stuhrmann, M., Tarnok, Z., Tischfield, J.A., Tübing, J., Visscher, F., Vulink, N., Wagner, M., Walitza, S., Wanderer, S., Woods, M., Worbe, Y., Zai, G., Zinner, S.H., Sullivan, P.F., Franke, B., Daly, M.J., Bulik, C.M., Lewis, C.M., McIntosh, A.M., O'Donovan, M.C., Zheutlin, A., Andreassen, O.A., Børglum, A.D., Breen, G., Edenberg, H.J., Fanous, A.H., Faraone, S.V., Gelernter, J., Mathews, C.A., Mattheisen, M., Mitchell, K.S., Neale, M.C., Nurnberger, J.I., Ripke, S., Santangelo, S.L., Scharf, J.M., Stein, M.B., Thornton, L.M., Walters, J.T.R., Wray, N.R., Geschwind, D.H., Neale, B.M., Kendler, K.S., Smoller, J.W., 2019. Genomic Relationships, Novel Loci, and Pleiotropic Mechanisms across Eight Psychiatric Disorders. Cell 179, 1469-1482.e1411. doi:10.1016/j.cell.2019.11.020

Lee, P.H., Feng, Y.-C.A., Smoller, J.W., 2021. Pleiotropy and Cross-Disorder Genetics Among Psychiatric Disorders. Biological psychiatry 89, 20-31. doi:10.1016/j.biopsych.2020.09.026

Lee, T.Y., Kim, S.N., Jang, J.H., Shim, G., Jung, W.H., Shin, N.Y., Kwon, J.S., 2013. Neural correlate of impulsivity in subjects at ultra-high risk for psychosis. Progress in neuro-psychopharmacology & biological psychiatry 45, 165-169. doi:10.1016/j.pnpbp.2013.04.008

Lee, J.S., Jung, S., Park, I.H., Kim, J.J., 2015. Neural Basis of Anhedonia and Amotivation in Patients with Schizophrenia: The Role of Reward System. Current neuropharmacology 13, 750-759. doi:10.2174/1570159x13666150612230333

Lei, W., Deng, W., Li, M., He, Z., Han, Y., Huang, C., Ma, X., Wang, Q., Guo, W., Li, Y., Jiang, L., Gong, Q., Hu, X., Zhang, N., Li, T., 2015. Gray matter volume alterations in first-episode drug-naive patients with deficit and nondeficit schizophrenia. Psychiatry research 234, 219-226. doi:10.1016/j.pscychresns.2015.09.015

Lei, W., Kirkpatrick, B., Wang, Q., Deng, W., Li, M., Guo, W., Liang, S., Li, Y., Zhang, C., Li, X., Zhang, P., Li, Z., Xiang, B., Chen, J., Hu, X., Zhang, N., Li, T., 2019. Progressive brain structural changes after the first year of treatment in first-episode treatment-naive patients with deficit or nondeficit schizophrenia. Psychiatry research. Neuroimaging 288, 12-20. doi:10.1016/j.pscychresns.2019.04.009

Li, C., Liu, W., Guo, F., Wang, X., Kang, X., Xu, Y., Xi, Y., Wang, H., Zhu, Y., Yin, H., 2019a. Voxel-based morphometry results in first-episode schizophrenia: a comparison of publicly available software packages. Brain imaging and behavior. doi:10.1007/s11682-019-00172-x

Li, J., Pan, P., Huang, R., Shang, H., 2012. A meta-analysis of voxel-based morphometry studies of white matter volume alterations in Alzheimer's disease. Neuroscience & Biobehavioral Reviews 36, 757-763. doi:10.1016/j.neubiorev.2011.12.001

Li, M., Li, X., Das, T.K., Deng, W., Li, Y., Zhao, L., Ma, X., Wang, Y., Yu, H., Meng, Y., Wang, Q., Palaniyappan, L., Li, T., 2019b. Prognostic Utility of Multivariate Morphometry in Schizophrenia. Frontiers in psychiatry 10, 245. doi:10.3389/fpsyt.2019.00245

Li, S., Hu, N., Zhang, W., Tao, B., Dai, J., Gong, Y., Tan, Y., Cai, D., Lui, S., 2019c. Dysconnectivity of Multiple Brain Networks in Schizophrenia: A Meta-Analysis of Resting-State Functional Connectivity. Frontiers in psychiatry 10, 482. doi:10.3389/fpsyt.2019.00482

Li, W.Q., Becker, B., Jiang, X., Zhao, Z., Zhang, Q., Yao, S., Kendrick, K.M., 2019d. Decreased interhemispheric functional connectivity rather than corpus callosum volume as a potential biomarker for autism spectrum disorder. Cortex 119, 258-266. doi:10.1016/j.cortex.2019.05.003

Li, T., Wang, Q., Zhang, J., Rolls, E.T., Yang, W., Palaniyappan, L., Zhang, L., Cheng, W., Yao, Y., Liu, Z., Gong, X., Luo, Q., Tang, Y., Crow, T.J., Broome, M.R., Xu, K., Li, C., Wang, J., Liu, Z., Lu, G., Wang, F., Feng, J., 2017. Brain-Wide Analysis of Functional Connectivity in First-Episode and Chronic Stages of Schizophrenia. Schizophrenia bulletin 43, 436-448. doi:10.1093/schbul/sbw099

Li, X., Alapati, V., Jackson, C., Xia, S., Bertisch, H.C., Branch, C.A., Delisi, L.E., 2012. Structural abnormalities in language circuits in genetic high-risk subjects and schizophrenia patients. Psychiatry research 201, 182-189. doi:10.1016/j.pscychresns.2011.07.017

Li, Y., Li, W.X., Xie, D.J., Wang, Y., Cheung, E.F.C., Chan, R.C.K., 2018. Grey matter reduction in the caudate nucleus in patients with persistent negative symptoms: An ALE meta-analysis. Schizophrenia research 192, 9-15. doi:10.1016/j.schres.2017.04.005

Liang, X., Zou, Q., He, Y., Yang, Y., 2013. Coupling of functional connectivity and regional cerebral blood flow reveals a physiological basis for network hubs of the human brain. Proc Natl Acad Sci U S A 110, 1929-1934. doi:10.1073/pnas.1214900110

Liao, J., Yan, H., Liu, Q., Yan, J., Zhang, L., Jiang, S., Zhang, X., Dong, Z., Yang, W., Cai, L., Guo, H., Wang, Y., Li, Z., Tian, L., Zhang, D., Wang, F., 2015. Reduced paralimbic system gray matter volume in schizophrenia: Correlations with clinical variables, symptomatology and cognitive function. Journal of psychiatric research 65, 80-86. doi:10.1016/j.jpsychires.2015.04.008

Liberati, A., Altman, D.G., Tetzlaff, J., Mulrow, C., Gotzsche, P.C., Ioannidis, J.P., Clarke, M., Devereaux, P.J., Kleijnen, J., Moher, D., 2009. The PRISMA statement for reporting systematic reviews and meta-analyses of studies that evaluate health care interventions: explanation and elaboration. J Clin Epidemiol 62, e1-34. doi:10.1016/j.jclinepi.2009.06.006

Liloia, D., Brasso, C., Cauda, F., Mancuso, L., Nani, A., Manuello, J., Costa, T., Duca, S., Rocca, P., 2021a. Updating and characterizing neuroanatomical markers in high-risk subjects, recently diagnosed and chronic patients with schizophrenia: A revised coordinate-based meta-analysis. Neuroscience & Biobehavioral Reviews 123, 83-103. doi:10.1016/j.dib.2018.10.142

Liloia, D., Cauda, F., Nani, A., Manuello, J., Duca, S., Fox, P.T., Costa, T., 2018. Low entropy maps as patterns of the pathological alteration specificity of brain regions: A meta-analysis dataset. Data in brief 21, 1483-1495. doi:10.1016/j.dib.2018.10.142

Liloia, D., Mancuso, L., Uddin, L.Q., Costa, T., Nani, A., Keller, R., Manuello, J., Duca, S., Cauda, F., 2021b. Gray matter abnormalities follow non-random patterns of co-alteration in autism: Meta-connectomic evidence. NeuroImage. Clinical 30, 102583. doi:10.1016/j.nicl.2021.102583

Lim, L., Marquand, A., Cubillo, A.A., Smith, A.B., Chantiluke, K., Simmons, A., Mehta, M., Rubia, K., 2013. Disorder-specific predictive classification of adolescents with attention deficit hyperactivity disorder (ADHD) relative to autism using structural magnetic resonance imaging. PLoS One 8, e63660. doi:10.1371/journal.pone.0063660

Lincoln, S.H., Hooker, C.I., 2014. Neural structure and social dysfunction in individuals at clinical high risk for psychosis. Psychiatry research 224, 152-158. doi:10.1016/j.pscychresns.2014.08.008

Linke, A.C., Olson, L., Gao, Y., Fishman, I., Müller, R.-A., 2017. Psychotropic Medication Use in Autism Spectrum Disorders May Affect Functional Brain Connectivity. Biological Psychiatry: Cognitive Neuroscience and Neuroimaging 2, 518-527.

Linkersdörfer, J., Lonnemann, J., Lindberg, S., Hasselhorn, M., Fiebach, C.J., 2012. Grey matter alterations co-localize with functional abnormalities in developmental dyslexia: an ALE meta-analysis. PLoS One 7, e43122. doi:10.1371/journal.pone.0043122

Liu, J., Yao, L., Zhang, W., Xiao, Y., Liu, L., Gao, X., Shah, C., Li, S., Tao, B., Gong, Q., Lui, S., 2017. Gray matter abnormalities in pediatric autism spectrum disorder: a meta-analysis with signed differential mapping. 26, 933-945. doi:10.1007/s00787-017-0964-4

Liu, L., You, W., Wang, W., Guo, X., Peng, D., Booth, J., 2013. Altered brain structure in Chinese dyslexic children. Neuropsychologia 51, 1169-1176. doi:10.1016/j.neuropsychologia.2013.03.010

Liu, L., Wang, Y.-P., Wang, Y., Zhang, P., Xiong, S., 2022. An enhanced multi-modal brain graph network for classifying neuropsychiatric disorders. Medical Image Analysis 81, 102550. doi:10.1016/j.media.2022.102550

Liu, Y., Guo, W., Zhang, Y., Lv, L., Hu, F., Wu, R., Zhao, J., 2018. Decreased Resting-State Interhemispheric Functional Connectivity Correlated with Neurocognitive Deficits in Drug-Naive First-Episode Adolescent-Onset Schizophrenia. The international journal of neuropsychopharmacology 21, 33-41. doi:10.1093/ijnp/pyx095

Lombardo, M.V., Eyler, L., Moore, A., Datko, M., Carter Barnes, C., Cha, D., Courchesne, E., Pierce, K., 2019. Default mode-visual network hypoconnectivity in an autism subtype with pronounced social visual engagement difficulties. Elife 8. doi:10.7554/eLife.47427

Long, Z., Duan, X., Mantini, D., Chen, H., 2016. Alteration of functional connectivity in autism spectrum disorder: effect of age and anatomical distance. Scientific reports 6, 26527. doi:10.1038/srep26527

Lorca-Puls, D.L., Gajardo-Vidal, A., White, J., Seghier, M.L., Leff, A.P., Green, D.W., Crinion, J.T., Ludersdorfer, P., Hope, T.M.H., Bowman, H., Price, C.J., 2018. The impact of sample size on the reproducibility of voxel-based lesion-deficit mappings. Neuropsychologia 115, 101-111. doi:10.1016/j.neuropsychologia.2018.03.014

Lord, C., Elsabbagh, M., Baird, G., Veenstra-Vanderweele, J., 2018. Autism spectrum disorder. Lancet 392, 508-520. doi:10.1016/s0140-6736(18)31129-2

Lord, L.D., Stevner, A.B., Deco, G., Kringelbach, M.L., 2017. Understanding principles of integration and segregation using whole-brain computational connectomics: implications for neuropsychiatric disorders. Philosophical transactions. Series A, Mathematical, physical, and engineering sciences 375. doi:10.1098/rsta.2016.0283

Lotze, M., Domin, M., Gerlach, F.H., Gaser, C., Lueders, E., Schmidt, C.O., Neumann, N., 2019. Novel findings from 2,838 Adult Brains on Sex Differences in Gray Matter Brain Volume. Scientific reports 9, 1671. doi:10.1038/s41598-018-38239-2

Lui, S., Deng, W., Huang, X., Jiang, L., Ma, X., Chen, H., Zhang, T., Li, X., Li, D., Zou, L., Tang, H., Zhou, X.J., Mechelli, A., Collier, D.A., Sweeney, J.A., Li, T., Gong, Q., 2009a. Association of cerebral deficits with clinical symptoms in antipsychotic-naive first-episode schizophrenia: an optimized voxel-based morphometry and resting state functional connectivity study. The American journal of psychiatry 166, 196-205. doi:10.1176/appi.ajp.2008.08020183

Lui, S., Deng, W., Huang, X., Jiang, L., Ouyang, L., Borgwardt, S.J., Ma, X., Li, D., Zou, L., Tang, H., Chen, H., Li, T., McGuire, P., Gong, Q., 2009b. Neuroanatomical differences between familial and sporadic schizophrenia and their parents: an optimized voxel-based morphometry study. Psychiatry research 171, 71-81. doi:10.1016/j.pscychresns.2008.02.004

Lukito, S., Norman, L., Carlisi, C., Radua, J., Hart, H., Simonoff, E., Rubia, K., 2020. Comparative meta-analyses of brain structural and functional abnormalities during cognitive control in attention-deficit/hyperactivity disorder and autism spectrum disorder. Psychol Med 50, 894-919. doi:10.1017/s0033291720000574

Lynch, C.J., Uddin, L.Q., Supekar, K., Khouzam, A., Phillips, J., Menon, V., 2013. Default mode network in childhood autism: posteromedial cortex heterogeneity and relationship with social deficits. Biol Psychiatry 74, 212-219. doi:10.1016/j.biopsych.2012.12.013

Machery, E., 2014. In defense of reverse inference. The British Journal for the Philosophy of Science 65, 251-267.

Madonna, D., Delvecchio, G., Soares, J.C., Brambilla, P., 2019. Structural and functional neuroimaging studies in generalized anxiety disorder: a systematic review. Revista brasileira de psiquiatria (Sao Paulo, Brazil : 1999) 41, 336-362. doi:10.1590/1516-4446-2018-0108

Maguire, E.A., Gadian, D.G., Johnsrude, I.S., Good, C.D., Ashburner, J., Frackowiak, R.S., Frith, C.D., 2000. Navigation-related structural change in the hippocampi of taxi drivers. Proceedings of the National Academy of Sciences of the United States of America 97, 4398-4403. doi:10.1073/pnas.070039597

Maier, S., Perlov, E., Graf, E., Dieter, E., Sobanski, E., Rump, M., Warnke, A., Ebert, D., Berger, M., Matthies, S., Philipsen, A., Tebartz van Elst, L., 2016. Discrete Global but No Focal Gray Matter Volume Reductions in Unmedicated Adult Patients With Attention-Deficit/Hyperactivity Disorder. Biological psychiatry 80, 905-915. doi:10.1016/j.biopsych.2015.05.012

Maisog, J.M., Einbinder, E.R., Flowers, D.L., Turkeltaub, P.E., Eden, G.F., 2008. A meta-analysis of functional neuroimaging studies of dyslexia. Annals of the New York Academy of Sciences 1145, 237-259. doi:10.1196/annals.1416.024

Mallikarjun, P.K., Lalousis, P.A., Dunne, T.F., Heinze, K., Reniers, R.L., Broome, M.R., Farmah, B., Oyebode, F., Wood, S.J., Upthegrove, R., 2018. Aberrant salience network functional connectivity in auditory verbal hallucinations: a first episode psychosis sample. Translational psychiatry 8, 69. doi:10.1038/s41398-018-0118-6

Mancuso, L., Costa, T., Nani, A., Manuello, J., Liloia, D., Gelmini, G., Panero, M., Duca, S., Cauda, F., 2019. The homotopic connectivity of the functional brain: a meta-analytic approach. Scientific reports 9, 3346. doi:10.1038/s41598-019-40188-3

Mancuso, L., Fornito, A., Costa, T., Ficco, L., Liloia, D., Manuello, J., Duca, S., Cauda, F., 2020. A meta-analytic approach to mapping co-occurrent grey matter volume increases and decreases in psychiatric disorders. Neuroimage, 117220. doi:10.1016/j.neuroimage.2020.117220

Mantel, N., 1967. The detection of disease clustering and a generalized regression approach. Cancer Res 27, 209-220.

Manuello, J., Costa, T., Cauda, F., Liloia, D., 2022. Six actions to improve detection of critical features for neuroimaging coordinate-based meta-analysis preparation. Neuroscience & Biobehavioral Reviews, 104659. doi.org/10.1016/j.neubiorev.2022.104659

Manuello, J., Nani, A., Premi, E., Borroni, B., Costa, T., Tatu, K., Liloia, D., Duca, S., Cauda, F., 2018. The Pathoconnectivity Profile of Alzheimer's Disease: A Morphometric Coalteration Network Analysis. Front Neurol 8. doi:10.3389/fneur.2017.00739

Marcelis, M., Suckling, J., Woodruff, P., Hofman, P., Bullmore, E., van Os, J., 2003. Searching for a structural endophenotype in psychosis using computational morphometry. Psychiatry research 122, 153-167. doi:10.1016/s0925-4927(02)00125-7

Marco, E.J., Hinkley, L.B., Hill, S.S., Nagarajan, S.S., 2011. Sensory processing in autism: a review of neurophysiologic findings. Pediatr Res 69, 48r-54r. doi:10.1203/PDR.0b013e3182130c54

Marek, K., Jennings, D., Lasch, S., Siderowf, A., Tanner, C., Simuni, T., Coffey, C., Kieburtz, K., Flagg, E., Chowdhury, S., Poewe, W., Mollenhauer, B., Klinik, P.-E., Sherer, T., Frasier, M., Meunier, C., Rudolph, A., Casaceli, C., Seibyl, J., Mendick, S., Schuff, N., Zhang, Y., Toga, A., Crawford, K., Ansbach, A., De Blasio, P., Piovella, M., Trojanowski, J., Shaw, L., Singleton, A., Hawkins, K., Eberling, J., Brooks, D., Russell, D., Leary, L., Factor, S., Sommerfeld, B., Hogarth, P., Pighetti, E., Williams, K., Standaert, D., Guthrie, S., Hauser, R., Delgado, H., Jankovic, J., Hunter, C., Stern, M., Tran, B., Leverenz, J., Baca, M., Frank, S., Thomas, C.-A., Richard, I., Deeley, C., Rees, L., Sprenger, F., Lang, E., Shill, H., Obradov, S., Fernandez, H., Winters, A., Berg, D., Gauss, K., Galasko, D., Fontaine, D.,

Mari, Z., Gerstenhaber, M., Brooks, D., Malloy, S., Barone, P., Longo, K., Comery, T., Ravina, B., Grachev, I., Gallagher, K., Collins, M., Widnell, K.L., Ostrowizki, S., Fontoura, P., Ho, T., Luthman, J., Brug, M.v.d., Reith, A.D., Taylor, P., 2011. The Parkinson Progression Marker Initiative (PPMI). Progress in Neurobiology 95, 629-635. doi:10.1016/j.pneurobio.2011.09.005

Margulies, D.S., Vincent, J.L., Kelly, C., Lohmann, G., Uddin, L.Q., Biswal, B.B., Villringer, A., Castellanos, F.X., Milham, M.P., Petrides, M., 2009. Precuneus shares intrinsic functional architecture in humans and monkeys. Proceedings of the National Academy of Sciences of the United States of America 106, 20069-20074. doi:10.1073/pnas.0905314106

Markello, R.D., Arnatkeviciute, A., Poline, J.B., Fulcher, B.D., Fornito, A., Misic, B., 2021. Standardizing workflows in imaging transcriptomics with the abagen toolbox. eLife 10. doi: 10.7554/eLife.72129

Marti-Bonmati, L., Lull, J.J., Garcia-Marti, G., Aguilar, E.J., Moratal-Perez, D., Poyatos, C., Robles, M., Sanjuan, J., 2007. Chronic auditory hallucinations in schizophrenic patients: MR analysis of the coincidence between functional and morphologic abnormalities. Radiology 244, 549-556. doi:10.1148/radiol.2442060727

Martinelli, C., Shergill, S.S., 2018. Everything you wanted to know about neuroimaging and psychiatry, but were afraid to ask. BJPsych Advances 21, 251-260.

Maslov, S., Sneppen, K., 2002. Specificity and Stability in Topology of Protein Networks. Science 296, 910-913. doi:10.1126/science.1065103

Matsuoka, K., Makinodan, M., Kitamura, S., Takahashi, M., Yoshikawa, H., Yasuno, F., Ishida, R., Kishimoto, N., Yasuda, Y., Hashimoto, R., Taoka, T., Miyasaka, T., Kichikawa, K., Kishimoto, T., 2020. Increased Dendritic Orientation Dispersion in the Left Occipital Gyrus is Associated with Atypical Visual Processing in Adults with Autism Spectrum Disorder. Cereb Cortex. doi:10.1093/cercor/bhaa121

McAlonan, G.M., Cheung, V., Cheung, C., Chua, S.E., Murphy, D.G., Suckling, J., Tai, K.S., Yip, L.K., Leung, P., Ho, T.P., 2007. Mapping brain structure in attention deficit-hyperactivity disorder: a voxel-based MRI study of regional grey and white matter volume. Psychiatry research 154, 171-180. doi:10.1016/j.pscychresns.2006.09.006

McAlonan, G.M., Cheung, V., Cheung, C., Suckling, J., Lam, G.Y., Tai, K.S., Yip, L., Murphy, D.G., Chua, S.E., 2005. Mapping the brain in autism. A voxel-based MRI study of volumetric differences and intercorrelations in autism. Brain 128, 268-276. doi:10.1093/brain/awh332

McAlonan, G.M., Daly, E., Kumari, V., Critchley, H.D., van Amelsvoort, T., Suckling, J., Simmons, A., Sigmundsson, T., Greenwood, K., Russell, A., Schmitz, N., Happe, F., Howlin, P., Murphy, D.G., 2002. Brain anatomy and sensorimotor gating in Asperger's syndrome. Brain 125, 1594-1606. doi:10.1093/brain/awf150

McAlonan, G.M., Suckling, J., Wong, N., Cheung, V., Lienenkaemper, N., Cheung, C., Chua, S.E., 2008. Distinct patterns of grey matter abnormality in high-functioning autism and Asperger's syndrome. Journal of child psychology and psychiatry, and allied disciplines 49, 1287-1295. doi:10.1111/j.1469-7610.2008.01933.x

McColgan, P., Gregory, S., Seunarine, K.K., Razi, A., Papoutsi, M., Johnson, E., Durr, A., Roos, R.A.C., Leavitt, B.R., Holmans, P., Scahill, R.I., Clark, C.A., Rees, G., Tabrizi, S.J., 2018. Brain Regions Showing White Matter Loss in Huntington's Disease Are Enriched for Synaptic and Metabolic Genes. Biological psychiatry 83, 456-465. doi: 10.1016/j.biopsych.2017.10.019

McDonald, C., Bullmore, E., Sham, P., Chitnis, X., Suckling, J., MacCabe, J., Walshe, M., Murray, R.M., 2005. Regional volume deviations of brain structure in schizophrenia and psychotic bipolar disorder: computational morphometry study. The British journal of psychiatry : the journal of mental science 186, 369-377. doi:10.1192/bjp.186.5.369

McDonald, C., Dineen, B., Hallahan, B., 2008. Meta-analysis of brain volumes in unaffected first-degree relatives of patients with schizophrenia overemphasizes hippocampal deficits. Archives of general psychiatry 65, 603-604; author reply 604-605. doi:10.1001/archpsyc.65.5.603

McGrath, L.M., Stoodley, C.J., 2019. Are there shared neural correlates between dyslexia and ADHD? A meta-analysis of voxel-based morphometry studies. Journal of neurodevelopmental disorders 11, 31. doi:10.1186/s11689-019-9287-8

McIntosh, A.M., Baig, B.J., Hall, J., Job, D., Whalley, H.C., Lymer, G.K., Moorhead, T.W., Owens, D.G., Miller, P., Porteous, D., Lawrie, S.M., Johnstone, E.C., 2007. Relationship of

catechol-O-methyltransferase variants to brain structure and function in a population at high risk of psychosis. Biological psychiatry 61, 1127-1134. doi:10.1016/j.biopsych.2006.05.020

McIntosh, A.M., Job, D.E., Moorhead, W.J., Harrison, L.K., Whalley, H.C., Johnstone, E.C., Lawrie, S.M., 2006. Genetic liability to schizophrenia or bipolar disorder and its relationship to brain structure. American journal of medical genetics. Part B, Neuropsychiatric genetics 141b, 76-83. doi:10.1002/ajmg.b.30254

McGorry, P.D., Hickie, I.B., Yung, A.R., Pantelis, C., Jackson, H.J., 2006. Clinical staging of psychiatric disorders: a heuristic framework for choosing earlier, safer and more effective interventions. The Australian and New Zealand journal of psychiatry 40, 616-622. doi:10.1080/j.1440-1614.2006.01860.x

McLennan, J.D., 2016. Understanding attention deficit hyperactivity disorder as a continuum. Canadian family physician Medecin de famille canadien 62, 979-982.

McTeague, L.M., Goodkind, M.S., Etkin, A., 2016. Transdiagnostic impairment of cognitive control in mental illness. J Psychiatr Res 83, 37-46. doi:10.1016/j.jpsychires.2016.08.001

McTeague, L.M., Huemer, J., Carreon, D.M., Jiang, Y., Eickhoff, S.B., Etkin, A., 2017. Identification of Common Neural Circuit Disruptions in Cognitive Control Across Psychiatric Disorders. The American journal of psychiatry 174, 676-685. doi:10.1176/appi.ajp.2017.16040400

McTeague, L.M., Rosenberg, B.M., Lopez, J.W., Carreon, D.M., Huemer, J., Jiang, Y., Chick, C.F., Eickhoff, S.B., Etkin, A., 2020. Identification of Common Neural Circuit Disruptions in Emotional Processing Across Psychiatric Disorders. The American journal of psychiatry 177, 411-421. doi:10.1176/appi.ajp.2019.18111271

Mechelli, A., Price, C.J., Friston, K.J., Ashburner, J., 2005. Voxel-based morphometry of the human brain: methods and applications. Current Medical Imaging 1, 105-113.

Mechelli, A., Riecher-Rossler, A., Meisenzahl, E.M., Tognin, S., Wood, S.J., Borgwardt, S.J., Koutsouleris, N., Yung, A.R., Stone, J.M., Phillips, L.J., McGorry, P.D., Valli, I., Velakoulis, D., Woolley, J., Pantelis, C., McGuire, P., 2011. Neuroanatomical abnormalities that predate the onset of psychosis: a multicenter study. Archives of general psychiatry 68, 489-495. doi:10.1001/archgenpsychiatry.2011.42

Meda, S.A., Giuliani, N.R., Calhoun, V.D., Jagannathan, K., Schretlen, D.J., Pulver, A., Cascella, N., Keshavan, M., Kates, W., Buchanan, R., Sharma, T., Pearlson, G.D., 2008. A large scale (N=400) investigation of gray matter differences in schizophrenia using optimized voxel-based morphometry. Schizophrenia research 101, 95-105. doi:10.1016/j.schres.2008.02.007

Meisenzahl, E.M., Koutsouleris, N., Bottlender, R., Scheuerecker, J., Jager, M., Teipel, S.J., Holzinger, S., Frodl, T., Preuss, U., Schmitt, G., Burgermeister, B., Reiser, M., Born, C., Moller, H.J., 2008a. Structural brain alterations at different stages of schizophrenia: a voxel-based morphometric study. Schizophrenia research 104, 44-60. doi:10.1016/j.schres.2008.06.023

Meisenzahl, E.M., Koutsouleris, N., Gaser, C., Bottlender, R., Schmitt, G.J., McGuire, P., Decker, P., Burgermeister, B., Born, C., Reiser, M., Moller, H.J., 2008b. Structural brain alterations in subjects at high-risk of psychosis: a voxel-based morphometric study. Schizophrenia research 102, 150-162. doi:10.1016/j.schres.2008.02.023

Mellet, E., Zago, L., Jobard, G., Crivello, F., Petit, L., Joliot, M., Mazoyer, B., Tzourio-Mazoyer, N., 2014. Weak language lateralization affects both verbal and spatial skills: An fMRI study in 297 subjects. Neuropsychologia 65, 56-62. doi:10.1016/j.neuropsychologia.2014.10.010

Mendrek, A., Mancini-Marïe, A., 2016. Sex/gender differences in the brain and cognition in schizophrenia. Neuroscience and biobehavioral reviews 67, 57-78. doi:10.1016/j.neubiorev.2015.10.013

Meng, L., Jiang, J., Jin, C., Liu, J., Zhao, Y., Wang, W., Li, K., Gong, Q., 2016. Trauma-specific Grey Matter Alterations in PTSD. Scientific reports 6, 33748. doi:10.1038/srep33748

Mengotti, P., D'Agostini, S., Terlevic, R., De Colle, C., Biasizzo, E., Londero, D., Ferro, A., Rambaldelli, G., Balestrieri, M., Zanini, S., Fabbro, F., Molteni, M., Brambilla, P., 2011. Altered white matter integrity and development in children with autism: a combined voxel-based morphometry and diffusion imaging study. Brain research bulletin 84, 189-195. doi:10.1016/j.brainresbull.2010.12.002

Menon, V., Uddin, L.Q., 2010. Saliency, switching, attention and control: a network model of insula function. Brain structure & function 214, 655-667. doi:10.1007/s00429-010-0262-0

Micai, M., Fulceri, F., Caruso, A., Guzzetta, A., Gila, L., Scattoni, M.L., 2020. Early behavioral markers for neurodevelopmental disorders in the first 3 years of life: An overview of systematic reviews. Neuroscience & Biobehavioral Reviews 116, 183-201. doi:10.1016/j.neubiorev.2020.06.027

Mier, D., Schirmbeck, F., Stoessel, G., Esslinger, C., Rausch, F., Englisch, S., Eisenacher, S., de Haan, L., Meyer-Lindenberg, A., Kirsch, P., Zink, M., 2019. Reduced activity and connectivity of left amygdala in patients with schizophrenia treated with clozapine or olanzapine. European archives of psychiatry and clinical neuroscience 269, 931-940. doi:10.1007/s00406-018-0965-4

Mikolas, P., Melicher, T., Skoch, A., Matejka, M., Slovakova, A., Bakstein, E., Hajek, T., Spaniel, F., 2016. Connectivity of the anterior insula differentiates participants with first-episode schizophrenia spectrum disorders from controls: a machine-learning study. Psychological medicine 46, 2695-2704. doi:10.1017/s0033291716000878

Miller, T.J., McGlashan, T.H., Rosen, J.L., Cadenhead, K., Cannon, T., Ventura, J., McFarlane, W., Perkins, D.O., Pearlson, G.D., Woods, S.W., 2003. Prodromal assessment with the structured interview for prodromal syndromes and the scale of prodromal symptoms: predictive validity, interrater reliability, and training to reliability. Schizophrenia bulletin 29, 703-715. doi:10.1093/oxfordjournals.schbul.a007040

Milward, E.A., Shahandeh, A., Heidari, M., Johnstone, D.M., Daneshi, N., Hondermarck, H., 2016. Transcriptomics, in: Bradshaw, R.A., Stahl, P.D. (Eds.), Encyclopedia of Cell Biology. Academic Press, Waltham, pp. 160-165.

Minshew, N.J., Williams, D.L., 2007. The new neurobiology of autism: cortex, connectivity, and neuronal organization. Arch Neurol 64, 945-950. doi:10.1001/archneur.64.7.945

Mitelman, S.A., Nikiforova, Y.K., Canfield, E.L., Hazlett, E.A., Brickman, A.M., Shihabuddin, L., Buchsbaum, M.S., 2009. A longitudinal study of the corpus callosum in chronic schizophrenia. Schizophrenia research 114, 144-153. doi:10.1016/j.schres.2009.07.021

Moher, D., Liberati, A., Tetzlaff, J., Altman, D.G., 2009. Preferred reporting items for systematic reviews and meta-analyses: the PRISMA statement. J Clin Epidemiol 62, 1006-1012. doi:10.1016/j.jclinepi.2009.06.005

Molina, V., Hernandez, J.A., Sanz, J., Paniagua, J.C., Hernandez, A.I., Martin, C., Matias, J., Calama, J., Bote, B., 2010a. Subcortical and cortical gray matter differences between Kraepelinian and non-Kraepelinian schizophrenia patients identified using voxel-based morphometry. Psychiatry research 184, 16-22. doi:10.1016/j.pscychresns.2010.06.006

Molina, V., Sanz, J., Villa, R., Perez, J., Gonzalez, D., Sarramea, F., Ballesteros, A., Galindo, G., Hernandez, J.A., 2010b. Voxel-based morphometry comparison between first episodes of psychosis with and without evolution to schizophrenia. Psychiatry research 181, 204-210. doi:10.1016/j.pscychresns.2009.09.003

Montagna, S., Wager, T., Barrett, L.F., Johnson, T.D., Nichols, T.E., 2018. Spatial Bayesian latent factor regression modeling of coordinate-based meta-analysis data. Biometrics 74, 342-353. doi:10.1111/biom.12713

Moreno-Alcázar, A., Ramos-Quiroga, J.A., Radua, J., Salavert, J., Palomar, G., Bosch, R., Salvador, R., Blanch, J., Casas, M., McKenna, P.J., Pomarol-Clotet, E., 2016. Brain abnormalities in adults with Attention Deficit Hyperactivity Disorder revealed by voxel-based morphometry. Psychiatry research. Neuroimaging 254, 41-47. doi:10.1016/j.pscychresns.2016.06.002

Morgan, J.T., Chana, G., Abramson, I., Semendeferi, K., Courchesne, E., Everall, I.P., 2012. Abnormal microglial-neuronal spatial organization in the dorsolateral prefrontal cortex in autism. Brain Res 1456, 72-81. doi:10.1016/j.brainres.2012.03.036

Mostofsky, S.H., Reiss, A.L., Lockhart, P., Denckla, M.B., 1998. Evaluation of Cerebellar Size in Attention-Deficit Hyperactivity Disorder. Journal of Child Neurology 13, 434-439. doi:10.1177/088307389801300904

Mucci, A., Merlotti, E., Ucok, A., Aleman, A., Galderisi, S., 2017. Primary and persistent negative symptoms: Concepts, assessments and neurobiological bases. Schizophrenia research 186, 19-28. doi:10.1016/j.schres.2016.05.014

Mueller, S., Keeser, D., Samson, A.C., Kirsch, V., Blautzik, J., Grothe, M., Erat, O., Hegenloh, M., Coates, U., Reiser, M.F., Hennig-Fast, K., Meindl, T., 2013. Convergent Findings of Altered Functional and Structural Brain Connectivity in Individuals with High Functioning Autism: A Multimodal MRI Study. PLoS One 8, e67329. doi:10.1371/journal.pone.0067329

Mukherjee, P., Whalley, H.C., McKirdy, J.W., Sprengelmeyer, R., Young, A.W., McIntosh, A.M., Lawrie, S.M., Hall, J., 2014. Altered amygdala connectivity within the social brain in schizophrenia. Schizophrenia bulletin 40, 152-160. doi:10.1093/schbul/sbt086

Mulert, C., Shenton, M.E., 2014. MRI in Psychiatry. Springer.

Müller, R.-A., 2014. Anatomical and functional connectivity in autism spectrum disorders. Comprehensive Guide to Autism. Springer New York, 49-75.

Müller, V.I., Cieslik, E.C., Laird, A.R., Fox, P.T., Radua, J., Mataix-Cols, D., Tench, C.R., Yarkoni, T., Nichols, T.E., Turkeltaub, P.E., Wager, T.D., Eickhoff, S.B., 2018. Ten simple rules for neuroimaging meta-analysis. Neuroscience and biobehavioral reviews 84, 151-161. doi:10.1016/j.neubiorev.2017.11.012

Müller, V.I., Cieslik, E.C., Serbanescu, I., Laird, A.R., Fox, P.T., Eickhoff, S.B., 2017. Altered Brain Activity in Unipolar Depression Revisited: Meta-analyses of Neuroimaging Studies. JAMA psychiatry 74, 47-55. doi:10.1001/jamapsychiatry.2016.2783

Mundy, P., 2018. A review of joint attention and social-cognitive brain systems in typical development and autism spectrum disorder. Eur J Neurosci 47, 497-514. doi:10.1111/ejn.13720

Naegel, S., Hagenacker, T., Theysohn, N., Diener, H.C., Katsarava, Z., Obermann, M., Holle, D., 2017. Short Latency Gray Matter Changes in Voxel-Based Morphometry following High Frequent Visual Stimulation. Neural plasticity 2017, 1397801. doi:10.1155/2017/1397801

Nakamura, K., Takahashi, T., Nemoto, K., Furuichi, A., Nishiyama, S., Nakamura, Y., Ikeda, E., Kido, M., Noguchi, K., Seto, H., Suzuki, M., 2013. Gray matter changes in subjects at high risk for developing psychosis and first-episode schizophrenia: a voxel-based structural MRI study. Frontiers in psychiatry 4, 16. doi:10.3389/fpsyt.2013.00016

Nani, A., Manuello, J., Liloia, D., Duca, S., Costa, T., Cauda, F., 2019. The Neural Correlates of Time: A Meta-analysis of Neuroimaging Studies. Journal of cognitive neuroscience, 1-31. doi:10.1162/jocn_a_01459

Nani, A., Manuello, J., Mancuso, L., Liloia, D., Costa, T., Vercelli, A., Duca, S., Cauda, F., 2021. The pathoconnectivity network analysis of the insular cortex: a morphometric fingerprinting. NeuroImage, 177481. doi:10.1016/j.neuroimage.2020.117481

Narr, K.L., Leaver, A.M., 2015. Connectome and schizophrenia. Current opinion in psychiatry 28, 229-235. doi:10.1097/YCO.0000000000000157

Nave, K.A., 2010. Myelination and the trophic support of long axons. Nat Rev Neurosci 11, 275-283. doi:10.1038/nrn2797

Nenadic, I., Dietzek, M., Langbein, K., Sauer, H., Gaser, C., 2017. BrainAGE score indicates accelerated brain aging in schizophrenia, but not bipolar disorder. Psychiatry research. Neuroimaging 266, 86-89. doi:10.1016/j.pscychresns.2017.05.006

Nenadic, I., Dietzek, M., Schonfeld, N., Lorenz, C., Gussew, A., Reichenbach, J.R., Sauer, H., Gaser, C., Smesny, S., 2015. Brain structure in people at ultra-high risk of psychosis, patients with first-episode schizophrenia, and healthy controls: a VBM study. Schizophrenia research 161, 169-176. doi:10.1016/j.schres.2014.10.041

Neniskyte, U., Gross, C.T., 2017. Errant gardeners: glial-cell-dependent synaptic pruning and neurodevelopmental disorders. Nat Rev Neurosci 18, 658-670. doi:10.1038/nrn.2017.110

Neugebauer, K., Hammans, C., Wensing, T., Kumar, V., Grodd, W., Mevissen, L., Sternkopf, M.A., Novakovic, A., Abel, T., Habel, U., Nickl-Jockschat, T., 2019. Nerve Growth Factor Serum Levels Are Associated With Regional Gray Matter Volume Differences in Schizophrenia Patients. Frontiers in psychiatry 10, 275. doi:10.3389/fpsyt.2019.00275

Ni, H.C., Lin, H.Y., Tseng, W.I., Chiu, Y.N., Wu, Y.Y., Tsai, W.C., Gau, S.S., 2018. Neural correlates of impaired self-regulation in male youths with autism spectrum disorder: A voxel-based morphometry study. Progress in neuro-psychopharmacology & biological psychiatry 82, 233-241. doi:10.1016/j.pnpbp.2017.11.008

Nichols, T.E., Das, S., Eickhoff, S.B., Evans, A.C., Glatard, T., Hanke, M., Kriegeskorte, N., Milham, M.P., Poldrack, R.A., Poline, J.B., Proal, E., Thirion, B., Van Essen, D.C., White, T., Yeo, B.T., 2017. Best practices in data analysis and sharing in neuroimaging using MRI. Nature neuroscience 20, 299-303. doi:10.1038/nn.4500

Nickl-Jockschat, T., Habel, U., Michel, T.M., Manning, J., Laird, A.R., Fox, P.T., Schneider, F., Eickhoff, S.B., 2012. Brain structure anomalies in autism spectrum disorder--a meta-analysis of VBM studies using anatomic likelihood estimation. Hum Brain Mapp 33, 1470-1489. doi:10.1002/hbm.21299

Nickl-Jockschat, T., Michel, T.M., 2011. The role of neurotrophic factors in autism. Mol Psychiatry 16, 478-490. doi:10.1038/mp.2010.103

Nickl-Jockschat, T., Schneider, F., Pagel, A.D., Laird, A.R., Fox, P.T., Eickhoff, S.B., 2011. Progressive pathology is functionally linked to the domains of language and emotion: meta-analysis of brain structure changes in schizophrenia patients. European archives of psychiatry and clinical neuroscience 261 Suppl 2, S166-171. doi:10.1007/s00406-011-0249-8

Niedtfeld, I., Schulze, L., Krause-Utz, A., Demirakca, T., Bohus, M., Schmahl, C., 2013. Voxel-based morphometry in women with borderline personality disorder with and without comorbid posttraumatic stress disorder. PLoS One 8, e65824. doi:10.1371/journal.pone.0065824

Nieto Del Rincón, P.L., 2008. Autism: alterations in auditory perception. Rev Neurosci 19, 61-78. doi:10.1515/revneuro.2008.19.1.61

Nomi, J.S., Uddin, L.Q., 2015. Developmental changes in large-scale network connectivity in autism. Neuroimage Clin 7, 732-741. doi:10.1016/j.nicl.2015.02.024

Noonan, S.K., Haist, F., Muller, R.A., 2009. Aberrant functional connectivity in autism: evidence from low-frequency BOLD signal fluctuations. Brain Res 1262, 48-63. doi:10.1016/j.brainres.2008.12.076

Norman, L.J., Carlisi, C., Lukito, S., Hart, H., Mataix-Cols, D., Radua, J., Rubia, K., 2016. Structural and Functional Brain Abnormalities in Attention-Deficit/Hyperactivity Disorder and Obsessive-Compulsive Disorder: A Comparative Meta-analysis. JAMA Psychiatry 73, 815-825. doi:10.1001/jamapsychiatry.2016.0700

Nunes, A.S., Vakorin, V.A., Kozhemiako, N., Peatfield, N., Ribary, U., Doesburg, S.M., 2020. Atypical age-related changes in cortical thickness in autism spectrum disorder. Scientific reports 10, 11067. doi:10.1038/s41598-020-67507-3

O'Rourke, K., 2007. An historical perspective on meta-analysis: dealing quantitatively with varying study results. Journal of the Royal Society of Medicine 100, 579-582. doi:10.1177/0141076807100012020

Oertel, V., Knochel, C., Rotarska-Jagiela, A., Schonmeyer, R., Lindner, M., van de Ven, V., Haenschel, C., Uhlhaas, P., Maurer, K., Linden, D.E., 2010. Reduced laterality as a trait marker of schizophrenia--evidence from structural and functional neuroimaging. The Journal

of neuroscience : the official journal of the Society for Neuroscience 30, 2289-2299. doi:10.1523/jneurosci.4575-09.2010

Oertel-Knöchel, V., Knochel, C., Matura, S., Rotarska-Jagiela, A., Magerkurth, J., Prvulovic, D., Haenschel, C., Hampel, H., Linden, D.E., 2012. Cortical-basal ganglia imbalance in schizophrenia patients and unaffected first-degree relatives. Schizophrenia research 138, 120-127. doi:10.1016/j.schres.2012.02.029

Oertel-Knöchel, V., Linden, D.E., 2011. Cerebral asymmetry in schizophrenia. The Neuroscientist : a review journal bringing neurobiology, neurology and psychiatry 17, 456-467. doi:10.1177/1073858410386493

Onnink, A.M., Zwiers, M.P., Hoogman, M., Mostert, J.C., Kan, C.C., Buitelaar, J., Franke, B., 2014. Brain alterations in adult ADHD: effects of gender, treatment and comorbid depression. European neuropsychopharmacology : the journal of the European College of Neuropsychopharmacology 24, 397-409. doi:10.1016/j.euroneuro.2013.11.011

Opel, N., Goltermann, J., Hermesdorf, M., Berger, K., Baune, B.T., Dannlowski, U., 2020. Cross-Disorder Analysis of Brain Structural Abnormalities in Six Major Psychiatric Disorders: A Secondary Analysis of Mega- and Meta-analytical Findings From the ENIGMA Consortium. Biological psychiatry 88, 678-686. doi:10.1016/j.biopsych.2020.04.027

Ortiz, B.B., Eden, F.D., de Souza, A.S., Teciano, C.A., de Lima, D.M., Noto, C., Higuchi, C.H., Cogo-Moreira, H., Bressan, R.A., Gadelha, A., 2017. New evidence in support of staging approaches in schizophrenia: Differences in clinical profiles between first episode, early stage, and late stage. Comprehensive psychiatry 73, 93-96. doi:10.1016/j.comppsych.2016.11.006

Ortiz-Gil, J., Pomarol-Clotet, E., Salvador, R., Canales-Rodriguez, E.J., Sarro, S., Gomar, J.J., Guerrero, A., Sans-Sansa, B., Capdevila, A., Junque, C., McKenna, P.J., 2011. Neural correlates of cognitive impairment in schizophrenia. The British journal of psychiatry 199, 202-210. doi:10.1192/bjp.bp.110.083600

Orwin, R.G., 1983. A fail-safe N for effect size in meta-analysis. Journal of educational statistics 8, 157-159.

Osipowicz, K., Bosenbark, D.D., Patrick, K.E., 2015. Cortical Changes Across the Autism Lifespan. Autism research : official journal of the International Society for Autism Research 8, 379-385. doi:10.1002/aur.1453

Overmeyer, S., Bullmore, E.T., Suckling, J., Simmons, A., Williams, S.C., Santosh, P.J., Taylor, E., 2001. Distributed grey and white matter deficits in hyperkinetic disorder: MRI evidence for anatomical abnormality in an attentional network. Psychological medicine 31, 1425-1435. doi:10.1017/s0033291701004706

Owen, M.J., Sawa, A., Mortensen, P.B., 2016. Schizophrenia. Lancet (London, England) 388, 86-97. doi:10.1016/s0140-6736(15)01121-6

Padmanabhan, A., Lynch, C.J., Schaer, M., Menon, V., 2017. The Default Mode Network in Autism. Biological Psychiatry: Cognitive Neuroscience and Neuroimaging 2, 476-486. doi:10.1016/j.bpsc.2017.04.004

Page, M.J., McKenzie, J.E., Bossuyt, P.M., Boutron, I., Hoffmann, T.C., Mulrow, C.D., Shamseer, L., Tetzlaff, J.M., Akl, E.A., Brennan, S.E., Chou, R., Glanville, J., Grimshaw, J.M., Hróbjartsson, A., Lalu, M.M., Li, T., Loder, E.W., Mayo-Wilson, E., McDonald, S., McGuinness, L.A., Stewart, L.A., Thomas, J., Tricco, A.C., Welch, V.A., Whiting, P., Moher, D., 2021. The PRISMA 2020 statement: an updated guideline for reporting systematic reviews. BMJ (Clinical research ed.) 372, n71.

Palande, S., Jose, V., Zielinski, B., Anderson, J., Fletcher, P.T., Wang, B., 2017. Revisiting Abnormalities in Brain Network Architecture Underlying Autism Using Topology-Inspired Statistical Inference. Connectomics Neuroimaging (2017) 10511, 98-107. doi:10.1007/978-3-319-67159-8_12

Palaniyappan, L., 2017. Progressive cortical reorganisation: A framework for investigating structural changes in schizophrenia. Neuroscience and biobehavioral reviews 79, 1-13. doi:10.1016/j.neubiorev.2017.04.028

Palaniyappan, L., Liddle, P.F., 2012. Does the salience network play a cardinal role in psychosis? An emerging hypothesis of insular dysfunction. Journal of psychiatry & neuroscience : JPN 37, 17-27. doi:10.1503/jpn.100176

Palmen, S.J., van Engeland, H., Hof, P.R., Schmitz, C., 2004. Neuropathological findings in autism. Brain 127, 2572-2583. doi:10.1093/brain/awh287

Pantelis, P.C., Byrge, L., Tyszka, J.M., Adolphs, R., Kennedy, D.P., 2015. A specific hypoactivation of right temporo-parietal junction/posterior superior temporal sulcus in response to socially awkward situations in autism. Social cognitive and affective neuroscience 10, 1348-1356. doi:10.1093/scan/nsv021

Pantelis, C., Velakoulis, D., McGorry, P.D., Wood, S.J., Suckling, J., Phillips, L.J., Yung, A.R., Bullmore, E.T., Brewer, W., Soulsby, B., Desmond, P., McGuire, P.K., 2003. Neuroanatomical abnormalities before and after onset of psychosis: a cross-sectional and longitudinal MRI comparison. Lancet 361, 281-288. doi:10.1016/s0140-6736(03)12323-9

Pantelis, C., Yucel, M., Wood, S.J., Velakoulis, D., Sun, D., Berger, G., Stuart, G.W., Yung, A., Phillips, L., McGorry, P.D., 2005. Structural brain imaging evidence for multiple pathological processes at different stages of brain development in schizophrenia. Schizophrenia bulletin 31, 672-696. doi:10.1093/schbul/sbi034

Pappaianni, E., Siugzdaite, R., Vettori, S., Venuti, P., Job, R., Grecucci, A., 2018. Three shades of grey: detecting brain abnormalities in children with autism using source-, voxel- and surface-based morphometry. Eur J Neurosci 47, 690-700. doi:10.1111/ejn.13704

Paquola, C., Royer, J., Lewis, L.B., Lepage, C., Glatard, T., Wagstyl, K., DeKraker, J., Toussaint, P.-J., Valk, S.L., Collins, L., Khan, A.R., Amunts, K., Evans, A.C., Dickscheid, T., Bernhardt, B., 2021. BigBrainWarp: Toolbox for integration of BigBrain 3D histology with multimodal neuroimaging. bioRxiv. doi:10.1101/2021.05.04.442563;

Paracampo, R., Tidoni, E., Borgomaneri, S., di Pellegrino, G., Avenanti, A., 2017. Sensorimotor Network Crucial for Inferring Amusement from Smiles. Cerebral cortex (New York, N.Y. : 1991) 27, 5116-5129. doi:10.1093/cercor/bhw294

Parenti, I., Rabaneda, L.G., Schoen, H., Novarino, G., 2020. Neurodevelopmental Disorders: From Genetics to Functional Pathways. Trends in Neurosciences 43, 608-621. doi:10.1016/j.tins.2020.05.004

Patel, R.S., Bowman, F.D., Rilling, J.K., 2006. A Bayesian approach to determining connectivity of the human brain. Hum Brain Mapp 27, 267-276. doi:10.1002/hbm.20182

Patriquin, M.A., DeRamus, T., Libero, L.E., Laird, A., Kana, R.K., 2016. Neuroanatomical and neurofunctional markers of social cognition in autism spectrum disorder. Hum Brain Mapp 37, 3957-3978. doi:10.1002/hbm.23288

Paulesu, E., Danelli, L., Berlingeri, M., 2014. Reading the dyslexic brain: multiple dysfunctional routes revealed by a new meta-analysis of PET and fMRI activation studies. Front Hum Neurosci 8, 830. doi:10.3389/fnhum.2014.00830

Pereira, A.M., Campos, B.M., Coan, A.C., Pegoraro, L.F., de Rezende, T.J.R., Obeso, I., Dalgalarrondo, P., da Costa, J.C., Dreher, J.-C., Cendes, F., 2018. Differences in Cortical Structure and Functional MRI Connectivity in High Functioning Autism. Frontiers in Neurology 9. doi:10.3389/fneur.2018.00539

Pereira-Sanchez, V., Castellanos, F.X., 2021. Neuroimaging in attention-deficit/hyperactivity disorder. Current opinion in psychiatry 34, 105-111. doi:10.1097/YCO.0000000000000669

Pergola, G., Selvaggi, P., Trizio, S., Bertolino, A., Blasi, G., 2015. The role of the thalamus in schizophrenia from a neuroimaging perspective. Neuroscience and biobehavioral reviews 54, 57-75. doi:10.1016/j.neubiorev.2015.01.013

Perlson, E., Maday, S., Fu, M.M., Moughamian, A.J., Holzbaur, E.L., 2010. Retrograde axonal transport: pathways to cell death? Trends Neurosci 33, 335-344. doi:10.1016/j.tins.2010.03.006

Pernet, C., Andersson, J., Paulesu, E., Demonet, J.F., 2009. When all hypotheses are right: a multifocal account of dyslexia. Hum Brain Mapp 30, 2278-2292. doi:10.1002/hbm.20670

Perry, A., Roberts, G., Mitchell, P.B., Breakspear, M., 2019. Connectomics of bipolar disorder: a critical review, and evidence for dynamic instabilities within interoceptive networks. Molecular psychiatry 24, 1296-1318. doi:10.1038/s41380-018-0267-2

Peterson, R.L., Pennington, B.F., Olson, R.K., 2013. Subtypes of developmental dyslexia: testing the predictions of the dual-route and connectionist frameworks. Cognition 126, 20-38. doi:10.1016/j.cognition.2012.08.007

Picci, G., Gotts, S.J., Scherf, K.S., 2016. A theoretical rut: revisiting and critically evaluating the generalized under/over-connectivity hypothesis of autism. Dev Sci 19, 524-549. doi:10.1111/desc.12467

Pierce, K., Haist, F., Sedaghat, F., Courchesne, E., 2004. The brain response to personally familiar faces in autism: findings of fusiform activity and beyond. Brain : a journal of neurology 127, 2703-2716. doi:10.1093/brain/awh289

Poeppl, T.B., Frank, E., Schecklmann, M., Kreuzer, P.M., Prasser, S.J., Rupprecht, R., Hajak, G., Langguth, B., Landgrebe, M., 2014. Amygdalohippocampal neuroplastic changes following neuroleptic treatment with quetiapine in first-episode schizophrenia. The international journal of neuropsychopharmacology 17, 833-843. doi:10.1017/s1461145713001739

Poldrack, R.A., 2006. Can cognitive processes be inferred from neuroimaging data? Trends in cognitive sciences 10, 59-63. doi:10.1016/j.tics.2005.12.004

Poldrack, R.A., 2008. The role of fMRI in cognitive neuroscience: where do we stand? Current opinion in neurobiology 18, 223-227. doi:10.1016/j.conb.2008.07.006

Poldrack, R.A., 2011. Inferring mental states from neuroimaging data: from reverse inference to large-scale decoding. Neuron 72, 692-697. doi:10.1016/j.neuron.2011.11.001

Poldrack, R.A., Yarkoni, T., 2016. From Brain Maps to Cognitive Ontologies: Informatics and the Search for Mental Structure. Annual review of psychology 67, 587-612. doi:10.1146/annurev-psych-122414-033729

Poletti, S., Vai, B., Smeraldi, E., Cavallaro, R., Colombo, C., Benedetti, F., 2016. Adverse childhood experiences influence the detrimental effect of bipolar disorder and schizophrenia on cortico-limbic grey matter volumes. Journal of affective disorders 189, 290-297. doi:10.1016/j.jad.2015.09.049

Pomarol-Clotet, E., Canales-Rodriguez, E.J., Salvador, R., Sarro, S., Gomar, J.J., Vila, F., Ortiz-Gil, J., Iturria-Medina, Y., Capdevila, A., McKenna, P.J., 2010. Medial prefrontal cortex pathology in schizophrenia as revealed by convergent findings from multimodal imaging. Molecular psychiatry 15, 823-830. doi:10.1038/mp.2009.146

Popescu, V., Schoonheim, M.M., Versteeg, A., Chaturvedi, N., Jonker, M., Xavier de Menezes, R., Gallindo Garre, F., Uitdehaag, B.M., Barkhof, F., Vrenken, H., 2016. Grey Matter Atrophy in Multiple Sclerosis: Clinical Interpretation Depends on Choice of Analysis Method. PLoS One 11, e0143942.

Postema, M.C., Van Rooij, D., Anagnostou, E., Arango, C., Auzias, G., Behrmann, M., Busatto Filho, G., Calderoni, S., Calvo, R., Daly, E., 2019. Altered structural brain asymmetry in autism spectrum disorder in a study of 54 datasets. Nat Commun 10, 1-12. doi:10.1038/s41467-019-13005-8

Poustka, L., Jennen-Steinmetz, C., Henze, R., Vomstein, K., Haffner, J., Sieltjes, B., 2012. Fronto-temporal disconnectivity and symptom severity in children with autism spectrum disorder. The world journal of biological psychiatry : the official journal of the World Federation of Societies of Biological Psychiatry 13, 269-280. doi:10.3109/15622975.2011.591824

Price, G., Cercignani, M., Chu, E.M., Barnes, T.R., Barker, G.J., Joyce, E.M., Ron, M.A., 2010. Brain pathology in first-episode psychosis: magnetization transfer imaging provides additional information to MRI measurements of volume loss. NeuroImage 49, 185-192. doi:10.1016/j.neuroimage.2009.07.037

Prieto, C., Risueno, A., Fontanillo, C., De las Rivas, J., 2008. Human gene coexpression landscape: confident network derived from tissue transcriptomic profiles. PLoS One 3, e3911. doi:10.1371/journal.pone.0003911

Prior, M.R., Bradshaw, J.L., 1979. Hemisphere functioning in autistic children. Cortex 15, 73-81. doi:10.1016/s0010-9452(79)80008-8

Puri, B.K., Counsell, S.J., Saeed, N., Bustos, M.G., Treasaden, I.H., Bydder, G.M., 2008. Regional grey matter volumetric changes in forensic schizophrenia patients: an MRI study comparing the brain structure of patients who have seriously and violently offended with that of patients who have not. BMC psychiatry 8 Suppl 1, S6. doi:10.1186/1471-244X-8-S1-S6

Qin, X.Y., Feng, J.C., Cao, C., Wu, H.T., Loh, Y.P., Cheng, Y., 2016. Association of Peripheral Blood Levels of Brain-Derived Neurotrophic Factor With Autism Spectrum Disorder in Children: A Systematic Review and Meta-analysis. JAMA Pediatr 170, 1079-1086. doi:10.1001/jamapediatrics.2016.1626

Qiu, A., Adler, M., Crocetti, D., Miller, M.I., Mostofsky, S.H., 2010. Basal ganglia shapes predict social, communication, and motor dysfunctions in boys with autism spectrum disorder. J Am Acad Child Adolesc Psychiatry 49, 539-551, 551.e531-534. doi:10.1016/j.jaac.2010.02.012

Qiu, H., Li, J., 2018. Major Depressive Disorder and Magnetic Resonance Imaging: A Mini-Review of Recent Progress. Current pharmaceutical design 24, 2524-2529. doi:10.2174/1381612824666180727111651

Rabinovici, G.D., Seeley, W.W., Kim, E.J., Gorno-Tempini, M.L., Rascovsky, K., Pagliaro, T.A., Allison, S.C., Halabi, C., Kramer, J.H., Johnson, J.K., Weiner, M.W., Forman, M.S., Trojanowski, J.Q., Dearmond, S.J., Miller, B.L., Rosen, H.J., 2007. Distinct MRI atrophy patterns in autopsy-proven Alzheimer's disease and frontotemporal lobar degeneration. American journal of Alzheimer's disease and other dementias 22, 474-488. doi:10.1177/1533317507308779

Radeloff, D., Ciaramidaro, A., Siniatchkin, M., Hainz, D., Schlitt, S., Weber, B., Poustka, F., Bölte, S., Walter, H., Freitag, C.M., 2014. Structural alterations of the social brain: a comparison between schizophrenia and autism. PLoS One 9, e106539. doi:10.1371/journal.pone.0106539

Radonjić, N.V., Hess, J.L., Rovira, P., Andreassen, O., Buitelaar, J.K., Ching, C.R.K., Franke, B., Hoogman, M., Jahanshad, N., McDonald, C., Schmaal, L., Sisodiya, S.M., Stein, D.J., van den Heuvel, O.A., van Erp, T.G.M., van Rooij, D., Veltman, D.J., Thompson, P., Faraone, S.V., 2021. Structural brain imaging studies offer clues about the effects of the shared genetic etiology among neuropsychiatric disorders. Molecular psychiatry. doi:10.1038/s41380-020-01002-z

Radua, J., Mataix-Cols, D., 2009. Voxel-wise meta-analysis of grey matter changes in obsessive-compulsive disorder. The British journal of psychiatry : the journal of mental science 195, 393-402. doi:10.1192/bjp.bp.108.055046

Radua, J., Mataix-Cols, D., 2012a. Meta-analytic methods for neuroimaging data explained. Biology of mood & anxiety disorders 2, 6. doi:10.1186/2045-5380-2-6

Radua, J., Mataix-Cols, D., Phillips, M.L., El-Hage, W., Kronhaus, D.M., Cardoner, N., Surguladze, S., 2012b. A new meta-analytic method for neuroimaging studies that combines reported peak coordinates and statistical parametric maps. European psychiatry : the journal of the Association of European Psychiatrists 27, 605-611. doi:10.1016/j.eurpsy.2011.04.001

Radua, J., Romeo, M., Mataix-Cols, D., Fusar-Poli, P., 2013. A general approach for combining voxel-based meta-analyses conducted in different neuroimaging modalities. Current medicinal chemistry 20, 462-466.

Radua, J., Rubia, K., Canales-Rodríguez, E.J., Pomarol-Clotet, E., Fusar-Poli, P., Mataix-Cols, D., 2014. Anisotropic kernels for coordinate-based meta-analyses of neuroimaging studies. Frontiers in psychiatry 5, 13. doi:10.3389/fpsyt.2014.00013

Raichle, M.E., MacLeod, A.M., Snyder, A.Z., Powers, W.J., Gusnard, D.A., Shulman, G.L., 2001. A default mode of brain function. Proceedings of the National Academy of Sciences of the United States of America 98, 676-682.

Raj, A., Kuceyeski, A., Weiner, M., 2012. A network diffusion model of disease progression in dementia. Neuron 73, 1204-1215. doi:10.1016/j.neuron.2011.12.040

Raj, A., Powell, F., 2018. Models of Network Spread and Network Degeneration in Brain Disorders. Biol Psychiatry Cogn Neurosci Neuroimaging 3, 788-797. doi:10.1016/j.bpsc.2018.07.012

Rajagopalan, V., Pioro, E.P., 2015. Disparate voxel based morphometry (VBM) results between SPM and FSL softwares in ALS patients with frontotemporal dementia: which VBM results to consider? BMC neurology 15, 32. doi:10.1186/s12883-015-0274-8

Rajagopalan, V., Yue, G.H., Pioro, E.P., 2014. Do preprocessing algorithms and statistical models influence voxel-based morphometry (VBM) results in amyotrophic lateral sclerosis patients? A systematic comparison of popular VBM analytical methods. Journal of magnetic resonance imaging : JMRI 40, 662-667. doi:10.1002/jmri.24415

Rametti, G., Junque, C., Bartres-Faz, D., Zubiaurre-Elorza, L., Catalan, R., Penades, R., Bargallo, N., Bernardo, M., 2010. Anterior cingulate and paracingulate sulci morphology in patients with schizophrenia. Schizophrenia research 121, 66-74. doi:10.1016/j.schres.2010.05.016

Reess, T.J., Rus, O.G., Schmidt, R., de Reus, M.A., Zaudig, M., Wagner, G., Zimmer, C., van den Heuvel, M.P., Koch, K., 2016. Connectomics-based structural network alterations in obsessive-compulsive disorder. Transl Psychiatry 6, e882. doi:10.1038/tp.2016.163

Reid, M.A., White, D.M., Kraguljac, N.V., Lahti, A.C., 2016. A combined diffusion tensor imaging and magnetic resonance spectroscopy study of patients with schizophrenia. Schizophrenia research 170, 341-350. doi:10.1016/j.schres.2015.12.003

Reiss, A.L., Eckert, M.A., Rose, F.E., Karchemskiy, A., Kesler, S., Chang, M., Reynolds, M.F., Kwon, H., Galaburda, A., 2004. An experiment of nature: brain anatomy parallels

cognition and behavior in Williams syndrome. Journal of Neuroscience 24, 5009-5015. doi:10.1523/JNEUROSCI.5272-03.2004

Ren, W., Lui, S., Deng, W., Li, F., Li, M., Huang, X., Wang, Y., Li, T., Sweeney, J.A., Gong, Q., 2013. Anatomical and functional brain abnormalities in drug-naive first-episode schizophrenia. The American journal of psychiatry 170, 1308-1316.

Retico, A., Giuliano, A., Tancredi, R., Cosenza, A., Apicella, F., Narzisi, A., Biagi, L., Tosetti, M., Muratori, F., Calderoni, S., 2016. The effect of gender on the neuroanatomy of children with autism spectrum disorders: a support vector machine case-control study. Molecular autism 7, 1-20. doi:10.1186/s13229-015-0067-3

Reynolds, E.H., 2018. Structure and Function in Neurology and Psychiatry. British Journal of Psychiatry 157, 481-490.

Ribeiro, L.G., Busatto, G.F., 2016. Voxel-based morphometry in Alzheimers disease and mild cognitive impairment: Systematic review of studies addressing the frontal lobe. Dementia & neuropsychologia 10, 104-112. doi:10.1590/S1980-5764-2016DN1002006

Ribolsi, M., Daskalakis, Z.J., Siracusano, A., Koch, G., 2014. Abnormal asymmetry of brain connectivity in schizophrenia. Frontiers in human neuroscience 8, 1010. doi:10.3389/fnhum.2014.01010

Richiardi, J., Altmann, A., Milazzo, A.C., Chang, C., Chakravarty, M.M., Banaschewski, T., Barker, G.J., Bokde, A.L., Bromberg, U., Büchel, C., Conrod, P., Fauth-Bühler, M., Flor, H., Frouin, V., Gallinat, J., Garavan, H., Gowland, P., Heinz, A., Lemaître, H., Mann, K.F., Martinot, J.L., Nees, F., Paus, T., Pausova, Z., Rietschel, M., Robbins, T.W., Smolka, M.N., Spanagel, R., Ströhle, A., Schumann, G., Hawrylycz, M., Poline, J.B., Greicius, M.D., 2015. BRAIN NETWORKS. Correlated gene expression supports synchronous activity in brain networks. Science 348, 1241-1244. doi: 10.1126/science.1255905

Richlan, F., Kronbichler, M., Wimmer, H., 2013. Structural abnormalities in the dyslexic brain: a meta-analysis of voxel-based morphometry studies. Hum Brain Mapp 34, 3055-3065. doi:10.1002/hbm.22127

Riedel, A., Maier, S., Ulbrich, M., Biscaldi, M., Ebert, D., Fangmeier, T., Perlov, E., Tebartz van Elst, L., 2014. No significant brain volume decreases or increases in adults with high-

functioning autism spectrum disorder and above average intelligence: a voxel-based morphometric study. Psychiatry research 223, 67-74. doi:10.1016/j.pscychresns.2014.05.013

Richlan, F., Kronbichler, M., Wimmer, H., 2009. Functional abnormalities in the dyslexic brain: a quantitative meta-analysis of neuroimaging studies. Hum Brain Mapp 30, 3299-3308. doi:10.1002/hbm.20752

Ridgway, G.R., Henley, S.M.D., Rohrer, J.D., Scahill, R.I., Warren, J.D., Fox, N.C., 2008. Ten simple rules for reporting voxel-based morphometry studies. NeuroImage 40, 1429-1435. doi:10.1016/j.neuroimage.2008.01.003

Rink, L., Pagel, T., Franklin, J., Baethge, C., 2016. Characteristics and heterogeneity of schizoaffective disorder compared with unipolar depression and schizophrenia - a systematic literature review and meta-analysis. Journal of affective disorders 191, 8-14. doi:10.1016/j.jad.2015.10.045

Riva, D., Annunziata, S., Contarino, V., Erbetta, A., Aquino, D., Bulgheroni, S., 2013. Gray matter reduction in the vermis and CRUS-II is associated with social and interaction deficits in low-functioning children with autistic spectrum disorders: a VBM-DARTEL Study. Cerebellum (London, England) 12, 676-685. doi:10.1007/s12311-013-0469-8

Riva, D., Bulgheroni, S., Aquino, D., Di Salle, F., Savoiardo, M., Erbetta, A., 2011. Basal forebrain involvement in low-functioning autistic children: a voxel-based morphometry study. AJNR. American journal of neuroradiology 32, 1430-1435. doi:10.3174/ajnr.A2527

Rizzo, G., Veronese, M., Expert, P., Turkheimer, F.E., Bertoldo, A., 2016. MENGA: A New Comprehensive Tool for the Integration of Neuroimaging Data and the Allen Human Brain Transcriptome Atlas. PLoS One 11, e0148744. doi: 10.1371/journal.pone.0148744

Robertson, C.E., Baron-Cohen, S., 2017. Sensory perception in autism. Nat Rev Neurosci 18, 671-684. doi:10.1038/nrn.2017.112

Rocha, E., Achaval, M., Santos, P., Rodnight, R., 1998. Lithium treatment causes gliosis and modifies the morphology of hippocampal astrocytes in rats. Neuroreport 9, 3971-3974.

Robinson, J.L., Laird, A.R., Glahn, D.C., Blangero, J., Sanghera, M.K., Pessoa, L., Fox, P.M., Uecker, A., Friehs, G., Young, K.A., Griffin, J.L., Lovallo, W.R., Fox, P.T., 2012. The functional connectivity of the human caudate: an application of meta-analytic connectivity

modeling with behavioral filtering. Neuroimage 60, 117-129. doi: 10.1016/j.neuroimage.2011.12.010

Robinson, J.L., Laird, A.R., Glahn, D.C., Lovallo, W.R., Fox, P.T., 2010. Metaanalytic connectivity modeling: delineating the functional connectivity of the human amygdala. Hum Brain Mapp 31, 173-184. doi: 10.1002/hbm.20854

Rojas, D.C., Peterson, E., Winterrowd, E., Reite, M.L., Rogers, S.J., Tregellas, J.R., 2006. Regional gray matter volumetric changes in autism associated with social and repetitive behavior symptoms. BMC psychiatry 6, 56. doi:10.1186/1471-244X-6-56

Rolls, E.T., 2019. The cingulate cortex and limbic systems for emotion, action, and memory. Brain Struct Funct 224, 3001-3018. doi:10.1007/s00429-019-01945-2

Rolls, E.T., Zhou, Y., Cheng, W., Gilson, M., Deco, G., Feng, J., 2020. Effective connectivity in autism. Autism research : official journal of the International Society for Autism Research 13, 32-44. doi:10.1002/aur.2235

Roman-Urrestarazu, A., Lindholm, P., Moilanen, I., Kiviniemi, V., Miettunen, J., Jääskeläinen, E., Mäki, P., Hurtig, T., Ebeling, H., Barnett, J.H., Nikkinen, J., Suckling, J., Jones, P.B., Veijola, J., Murray, G.K., 2016. Brain structural deficits and working memory fMRI dysfunction in young adults who were diagnosed with ADHD in adolescence. European child & adolescent psychiatry 25, 529-538. doi:10.1007/s00787-015-0755-8

Romero-Garcia, R., Warrier, V., Bullmore, E.T., Baron-Cohen, S., Bethlehem, R.A.I., 2019. Synaptic and transcriptionally downregulated genes are associated with cortical thickness differences in autism. Molecular psychiatry 24, 1053-1064. doi: 10.1038/s41380-018-0023-7

Romme, I.A.C., de Reus, M.A., Ophoff, R.A., Kahn, R.S., van den Heuvel, M.P., 2017. Connectome Disconnectivity and Cortical Gene Expression in Patients With Schizophrenia. Biological psychiatry 81, 495-502. doi:10.1016/j.biopsych.2016.07.012

Rose, E.J., Morris, D.W., Fahey, C., Cannon, D., McDonald, C., Scanlon, C., Kelly, S., Gill, M., Corvin, A., Donohoe, G., 2014. The miR-137 schizophrenia susceptibility variant rs1625579 does not predict variability in brain volume in a sample of schizophrenic patients and healthy individuals. American journal of medical genetics 165b, 467-471. doi:10.1002/ajmg.b.32249

Rubia, K., 2018. Cognitive Neuroscience of Attention Deficit Hyperactivity Disorder (ADHD) and Its Clinical Translation. Front Hum Neurosci 12, 100. doi:10.3389/fnhum.2018.00100

Rubinov, M., Bullmore, E., 2013. Fledgling pathoconnectomics of psychiatric disorders. Trends Cogn Sci 17, 641-647. doi:10.1016/j.tics.2013.10.007

Rubinov, M., Sporns, O., 2010. Complex network measures of brain connectivity: uses and interpretations. Neuroimage 52, 1059-1069. doi:10.1016/j.neuroimage.2009.10.003

Ruggero, C.J., Kotov, R., Hopwood, C.J., First, M., Clark, L.A., Skodol, A.E., Mullins-Sweatt, S.N., Patrick, C.J., Bach, B., Cicero, D.C., Docherty, A., Simms, L.J., Bagby, R.M., Krueger, R.F., Callahan, J.L., Chmielewski, M., Conway, C.C., De Clercq, B., Dornbach-Bender, A., Eaton, N.R., Forbes, M.K., Forbush, K.T., Haltigan, J.D., Miller, J.D., Morey, L.C., Patalay, P., Regier, D.A., Reininghaus, U., Shackman, A.J., Waszczuk, M.A., Watson, D., Wright, A.G.C., Zimmermann, J., 2019. Integrating the Hierarchical Taxonomy of Psychopathology (HiTOP) into clinical practice. Journal of consulting and clinical psychology 87, 1069-1084. doi:10.1037/ccp0000452

Saad, J.F., Griffiths, K.R., Kohn, M.R., Clarke, S., Williams, L.M., Korgaonkar, M.S., 2017. Regional brain network organization distinguishes the combined and inattentive subtypes of Attention Deficit Hyperactivity Disorder. NeuroImage. Clinical 15, 383-390. doi:10.1016/j.nicl.2017.05.016

Saarinen, A.I.L., Huhtaniska, S., Pudas, J., Bjornholm, L., Jukuri, T., Tohka, J., Grano, N., Barnett, J.H., Kiviniemi, V., Veijola, J., Hintsanen, M., Lieslehto, J., 2020. Structural and functional alterations in the brain gray matter among first-degree relatives of schizophrenia patients: A multimodal meta-analysis of fMRI and VBM studies. Schizophrenia research. doi:10.1016/j.schres.2019.12.023

Saeed, U., Lang, A.E., Masellis, M., 2020. Neuroimaging Advances in Parkinson's Disease and Atypical Parkinsonian Syndromes. Front Neurol 11, 572976. doi:10.3389/fneur.2020.572976

Salehi, A., Delcroix, J.-D., Mobley, W.C., 2003. Traffic at the intersection of neurotrophic factor signaling and neurodegeneration. Trends Neurosci 26, 73-80. doi:10.1016/S0166-2236(02)00038-3

Salem, H.A., Elsherbiny, N., Alzahrani, S., Alshareef, H.M., Abd Elmageed, Z.Y., Ajwah, S.M., Hamdan, A.M.E., Abdou, Y.S., Galal, O.O., El Azazy, M.K.A., Abu-Elfotuh, K., 2022. Neuroprotective Effect of Morin Hydrate against Attention-Deficit/Hyperactivity Disorder (ADHD) Induced by MSG and/or Protein Malnutrition in Rat Pups: Effect on Oxidative/Monoamines/Inflammatory Balance and Apoptosis. Pharmaceuticals 15, 1012.

Salimi-Khorshidi, G., Nichols, T.E., Smith, S.M., Woolrich, M.W., 2011. Using Gaussian-Process Regression for Meta-Analytic Neuroimaging Inference Based on Sparse Observations. IEEE Transactions on Medical Imaging 30, 1401-1416.

Salimi-Khorshidi, G., Smith, S.M., Keltner, J.R., Wager, T.D., Nichols, T.E., 2009. Meta-analysis of neuroimaging data: a comparison of image-based and coordinate-based pooling of studies. Neuroimage 45, 810-823.

Salgado-Pineda, P., Fakra, E., Delaveau, P., McKenna, P.J., Pomarol-Clotet, E., Blin, O., 2011. Correlated structural and functional brain abnormalities in the default mode network in schizophrenia patients. Schizophrenia research 125, 101-109. doi:10.1016/j.schres.2010.10.027

Salmond, C.H., Ashburner, J., Connelly, A., Friston, K.J., Gadian, D.G., Vargha-Khadem, F., 2005. The role of the medial temporal lobe in autistic spectrum disorders. The European journal of neuroscience 22, 764-772. doi:10.1111/j.1460-9568.2005.04217.x

Salmond, C.H., Ashburner, J., Vargha-Khadem, F., Connelly, A., Gadian, D.G., Friston, K.J., 2002. Distributional assumptions in voxel-based morphometry. Neuroimage 17, 1027-1030.

Salmond, C.H., Vargha-Khadem, F., Gadian, D.G., de Haan, M., Baldeweg, T., 2007. Heterogeneity in the patterns of neural abnormality in autistic spectrum disorders: evidence from ERP and MRI. Cortex; a journal devoted to the study of the nervous system and behavior 43, 686-699. doi:10.1016/s0010-9452(08)70498-2

Salomon, R., Progin, P., Griffa, A., Rognini, G., Do, K.Q., Conus, P., Marchesotti, S., Bernasconi, F., Hagmann, P., Serino, A., Blanke, O., 2020. Sensorimotor Induction of Auditory Misattribution in Early Psychosis. Schizophrenia bulletin. doi:10.1093/schbul/sbz136

Samartsidis, P., Montagna, S., Laird, A.R., Fox, P.T., Johnson, T.D., Nichols, T.E., 2020. Estimating the prevalence of missing experiments in a neuroimaging meta-analysis. Research Synthesis Methods. doi:10.1002/jrsm.1448

Samartsidis, P., Montagna, S., Nichols, T.E., Johnson, T.D., 2017. The coordinate-based meta-analysis of neuroimaging data. Statistical science : a review journal of the Institute of Mathematical Statistics 32, 580-599. doi:10.1214/17-STS624

Samea, F., Soluki, S., Nejati, V., Zarei, M., Cortese, S., Eickhoff, S.B., Tahmasian, M., Eickhoff, C.R., 2019. Brain alterations in children/adolescents with ADHD revisited: A neuroimaging meta-analysis of 96 structural and functional studies. Neuroscience and biobehavioral reviews 100, 1-8. doi:10.1016/j.neubiorev.2019.02.011

Samson, F., Mottron, L., Soulières, I., Zeffiro, T.A., 2012. Enhanced visual functioning in autism: an ALE meta-analysis. Human brain mapping 33, 1553-1581. doi:10.1002/hbm.21307

Sánchez-Morán, M., Hernández, J.A., Duñabeitia, J.A., Estévez, A., Bárcena, L., González-Lahera, A., Bajo, M.T., Fuentes, L.J., Aransay, A.M., Carreiras, M., 2018. Genetic association study of dyslexia and ADHD candidate genes in a Spanish cohort: Implications of comorbid samples. PLoS One 13, e0206431. doi:10.1371/journal.pone.0206431

Sans-Sansa, B., McKenna, P.J., Canales-Rodriguez, E.J., Ortiz-Gil, J., Lopez-Araquistain, L., Sarro, S., Duenas, R.M., Blanch, J., Salvador, R., Pomarol-Clotet, E., 2013. Association of formal thought disorder in schizophrenia with structural brain abnormalities in language-related cortical regions. Schizophrenia research 146, 308-313. doi:10.1016/j.schres.2013.02.032

Sarrazin, S., Poupon, C., Teillac, A., Mangin, J.-F., Polosan, M., Favre, P., Laidi, C., d'Albis, M.-A., Leboyer, M., Lledo, P.-M., 2019. Higher in vivo cortical intracellular volume fraction associated with lithium therapy in bipolar disorder: a multicenter NODDI study. Psychotherapy and Psychosomatics 88, 171-176. doi:10.1159/000498854

Sarro, S., Pomarol-Clotet, E., Canales-Rodriguez, E.J., Salvador, R., Gomar, J.J., Ortiz-Gil, J., Landin-Romero, R., Vila-Rodriguez, F., Blanch, J., McKenna, P.J., 2013. Structural brain changes associated with tardive dyskinesia in schizophrenia. The British journal of psychiatry 203, 51-57. doi:10.1192/bjp.bp.112.114538

Sasayama, D., Hayashida, A., Yamasue, H., Harada, Y., Kaneko, T., Kasai, K., Washizuka, S., Amano, N., 2010. Neuroanatomical correlates of attention-deficit-hyperactivity disorder accounting for comorbid oppositional defiant disorder and conduct disorder. Psychiatry and clinical neurosciences 64, 394-402. doi:10.1111/j.1440-1819.2010.02102.x

Sato, W., Kochiyama, T., Uono, S., Yoshimura, S., Kubota, Y., Sawada, R., Sakihama, M., Toichi, M., 2017. Reduced Gray Matter Volume in the Social Brain Network in Adults with Autism Spectrum Disorder. Front Hum Neurosci 11, 395. doi:10.3389/fnhum.2017.00395

Scardoni, G., Tosadori, G., Faizan, M., Spoto, F., Fabbri, F., Laudanna, C., 2014. Biological network analysis with CentiScaPe: centralities and experimental dataset integration. F1000Res 3, 139. doi:10.12688/f1000research.4477.2

Scarpazza, C., De Simone, M.S., 2016. Voxel-based morphometry: current perspectives. Neuroscience and Neuroeconomics 5, 19-35. doi:10.2147/NAN.S66439

Scarpazza, C., Ha, M., Baecker, L., Garcia-Dias, R., Pinaya, W.H.L., Vieira, S., Mechelli, A., 2020. Translating research findings into clinical practice: a systematic and critical review of neuroimaging-based clinical tools for brain disorders. Translational psychiatry 10, 107. doi:10.1038/s41398-020-0798-6

Scarpazza, C., Tognin, S., Frisciata, S., Sartori, G., Mechelli, A., 2015. False positive rates in Voxel-based Morphometry studies of the human brain: Should we be worried? Neuroscience & Biobehavioral Reviews 52, 49-55. doi:10.1016/j.neubiorev.2015.02.008

Schaefer, A., Kong, R., Gordon, E.M., Laumann, T.O., Zuo, X.N., Holmes, A.J., Eickhoff, S.B., Yeo, B.T.T., 2018. Local-Global Parcellation of the Human Cerebral Cortex from Intrinsic Functional Connectivity MRI. Cereb Cortex 28, 3095-3114. doi:10.1093/cercor/bhx179

Schaer, M., Ottet, M.-C., Scariati, E., Dukes, D., Franchini, M., Eliez, S., Glaser, B., 2013. Decreased frontal gyrification correlates with altered connectivity in children with autism. Front Hum Neurosci 7. doi:10.3389/fnhum.2013.00750

Schaufelberger, M.S., Lappin, J., Duran, F., Rosa, P., Uchida, R., Santos, L., Murray, R., McGuire, P., Scazufca, M., Menezes, P., 2011. Lack of progression of brain abnormalities in first-episode psychosis: a longitudinal magnetic resonance imaging study. Psychological medicine 41, 1677-1689.

Schaufelberger, M.S., Duran, F.L., Lappin, J.M., Scazufca, M., Amaro, E., Jr., Leite, C.C., de Castro, C.C., Murray, R.M., McGuire, P.K., Menezes, P.R., Busatto, G.F., 2007. Grey matter abnormalities in Brazilians with first-episode psychosis. The British journal of psychiatry. 51, 117-122.

Schiffer, B., Müller, B.W., Scherbaum, N., Forsting, M., Wiltfang, J., Leygraf, N., Gizewski, E.R., 2010. Impulsivity-related brain volume deficits in schizophrenia-addiction comorbidity. Brain : a journal of neurology 133, 3093-3103. doi:10.1093/brain/awq153

Schneider, K., Pauly, K.D., Gossen, A., Mevissen, L., Michel, T.M., Gur, R.C., Schneider, F., Habel, U., 2012. Neural correlates of moral reasoning in autism spectrum disorder. Social cognitive and affective neuroscience 8, 702-710. doi:10.1093/scan/nss051

Schröter, M., Paulsen, O., Bullmore, E.T., 2017. Micro-connectomics: probing the organization of neuronal networks at the cellular scale. Nature reviews. Neuroscience 18, 131-146. doi:10.1038/nrn.2016.182

Schulte-Rüther, M., Greimel, E., Markowitsch, H.J., Kamp-Becker, I., Remschmidt, H., Fink, G.R., Piefke, M., 2011. Dysfunctions in brain networks supporting empathy: an fMRI study in adults with autism spectrum disorders. Soc Neurosci 6, 1-21. doi:10.1080/17470911003708032

Schuster, C., Schuller, A.M., Paulos, C., Namer, I., Pull, C., Danion, J.M., Foucher, J.R., 2012. Gray matter volume decreases in elderly patients with schizophrenia: a voxel-based morphometry study. Schizophrenia bulletin 38, 796-802. doi:10.1093/schbul/sbq150

Scott-Wittenborn, N., Karadaghy, O.A., Piccirillo, J.F., Peelle, J.E., 2017. A methodological assessment of studies that use voxel-based morphometry to study neural changes in tinnitus patients. Hearing research 355, 23-32.

Sebastian, A., Jung, P., Krause-Utz, A., Lieb, K., Schmahl, C., Tüscher, O., 2014. Frontal dysfunctions of impulse control - a systematic review in borderline personality disorder and attention-deficit/hyperactivity disorder. Front Hum Neurosci 8, 698. doi:10.3389/fnhum.2014.00698

Seeley, W.W., Menon, V., Schatzberg, A.F., Keller, J., Glover, G.H., Kenna, H., Reiss, A.L., Greicius, M.D., 2007. Dissociable intrinsic connectivity networks for salience processing and

executive control. The Journal of neuroscience : the official journal of the Society for Neuroscience 27, 2349-2356. doi:10.1523/JNEUROSCI.5587-06.2007

Seidman, L.J., Biederman, J., Liang, L., Valera, E.M., Monuteaux, M.C., Brown, A., Kaiser, J., Spencer, T., Faraone, S.V., Makris, N., 2011. Gray matter alterations in adults with attention-deficit/hyperactivity disorder identified by voxel based morphometry. Biological psychiatry 69, 857-866. doi:10.1016/j.biopsych.2010.09.053

Seidman, L.J., Mirsky, A.F., 2017. Evolving Notions of Schizophrenia as a Developmental Neurocognitive Disorder. Journal of the International Neuropsychological Society : JINS 23, 881-892. doi:10.1017/s1355617717001114

Senjem, M.L., Gunter, J.L., Shiung, M.M., Petersen, R.C., Jack, C.R., Jr., 2005. Comparison of different methodological implementations of voxel-based morphometry in neurodegenerative disease. Neuroimage 26, 600-608. doi:10.1016/j.neuroimage.2005.02.005

Shafiei, G., Markello, R.D., Makowski, C., Talpalaru, A., Kirschner, M., Devenyi, G.A., Guma, E., Hagmann, P., Cashman, N.R., Lepage, M., Chakravarty, M.M., Dagher, A., Misic, B., 2020. Spatial Patterning of Tissue Volume Loss in Schizophrenia Reflects Brain Network Architecture. Biological psychiatry 87, 727-735. doi:10.1016/j.biopsych.2019.09.031

Shannon, C.E., 1948. A mathematical theory of communication. The Bell system technical journal 27, 379-423.

Shapleske, J., Rossell, S.L., Chitnis, X.A., Suckling, J., Simmons, A., Bullmore, E.T., Woodruff, P.W., David, A.S., 2002. A computational morphometric MRI study of schizophrenia: effects of hallucinations. Cerebral cortex 12, 1331-1341. doi:10.1093/cercor/12.12.1331

Sharda, M., Foster, N.E.V., Tryfon, A., Doyle-Thomas, K.A.R., Ouimet, T., Anagnostou, E., Evans, A.C., Zwaigenbaum, L., Lerch, J.P., Lewis, J.D., Hyde, K.L., 2017. Language Ability Predicts Cortical Structure and Covariance in Boys with Autism Spectrum Disorder. Cereb Cortex 27, 1849-1862. doi:10.1093/cercor/bhw024

Shaywitz, S.E., Escobar, M.D., Shaywitz, B.A., Fletcher, J.M., Makuch, R., 1992. Evidence That Dyslexia May Represent the Lower Tail of a Normal Distribution of Reading Ability. New England Journal of Medicine 326, 145-150. doi:10.1056/nejm199201163260301

Sheng, J., Zhu, Y., Lu, Z., Liu, N., Huang, N., Zhang, Z., Tan, L., Li, C., Yu, X., 2013. Altered volume and lateralization of language-related regions in first-episode schizophrenia. Schizophrenia research 148, 168-174. doi:10.1016/j.schres.2013.05.021

Shepherd, A.M., Laurens, K.R., Matheson, S.L., Carr, V.J., Green, M.J., 2012. Systematic meta-review and quality assessment of the structural brain alterations in schizophrenia. Neuroscience and biobehavioral reviews 36, 1342-1356. doi:10.1016/j.neubiorev.2011.12.015

Shim, G., Oh, J.S., Jung, W.H., Jang, J.H., Choi, C.H., Kim, E., Park, H.Y., Choi, J.S., Jung, M.H., Kwon, J.S., 2010. Altered resting-state connectivity in subjects at ultra-high risk for psychosis: an fMRI study. Behavioral and brain functions : BBF 6, 58. doi:10.1186/1744-9081-6-58

Shimizu, M., Fujiwara, H., Hirao, K., Namiki, C., Fukuyama, H., Hayashi, T., Murai, T., 2008. Structural abnormalities of the adhesio interthalamica and mediodorsal nuclei of the thalamus in schizophrenia. Schizophrenia research 101, 331-338. doi:10.1016/j.schres.2007.12.486

Siehl, S., Wicking, M., Pohlack, S., Winkelmann, T., Zidda, F., Steiger-White, F., King, J., Burgess, N., Flor, H., Nees, F., 2020. Structural white and gray matter differences in a large sample of patients with Posttraumatic Stress Disorder and a healthy and trauma-exposed control group: Diffusion tensor imaging and region-based morphometry. NeuroImage: Clinical 28, 102424. doi:10.1016/j.nicl.2020.102424

Sigmundsson, T., Suckling, J., Maier, M., Williams, S., Bullmore, E., Greenwood, K., Fukuda, R., Ron, M., Toone, B., 2001. Structural abnormalities in frontal, temporal, and limbic regions and interconnecting white matter tracts in schizophrenic patients with prominent negative symptoms. The American journal of psychiatry 158, 234-243. doi:10.1176/appi.ajp.158.2.234

Silani, G., Frith, U., Demonet, J.F., Fazio, F., Perani, D., Price, C., Frith, C.D., Paulesu, E., 2005. Brain abnormalities underlying altered activation in dyslexia: a voxel based morphometry study. Brain 128, 2453-2461. doi:10.1093/brain/awh579

Singh, S., Goyal, S., Modi, S., Kumar, P., Singh, N., Bhatia, T., Deshpande, S.N., Khushu, S., 2014. Motor function deficits in schizophrenia: an fMRI and VBM study. Neuroradiology 56, 413-422. doi:10.1007/s00234-014-1325-3

Singh, S., Modi, S., Goyal, S., Kaur, P., Singh, N., Bhatia, T., Deshpande, S.N., Khushu, S., 2015. Functional and structural abnormalities associated with empathy in patients with schizophrenia: An fMRI and VBM study. Journal of biosciences 40, 355-364. doi:10.1007/s12038-015-9509-5

Siok, W.T., Niu, Z., Jin, Z., Perfetti, C.A., Tan, L.H., 2008. A structural-functional basis for dyslexia in the cortex of Chinese readers. Proceedings of the National Academy of Sciences of the United States of America 105, 5561-5566. doi:10.1073/pnas.0801750105

Skåtun, K.C., Kaufmann, T., Brandt, C.L., Doan, N.T., Alnæs, D., Tønnesen, S., Biele, G., Vaskinn, A., Melle, I., Agartz, I., Andreassen, O.A., Westlye, L.T., 2018. Thalamo-cortical functional connectivity in schizophrenia and bipolar disorder. Brain imaging and behavior 12, 640-652. doi:10.1007/s11682-017-9714-y

Smallwood, R.F., Laird, A.R., Ramage, A.E., Parkinson, A.L., Lewis, J., Clauw, D.J., Williams, D.A., Schmidt-Wilcke, T., Farrell, M.J., Eickhoff, S.B., Robin, D.A., 2013. Structural brain anomalies and chronic pain: a quantitative meta-analysis of gray matter volume. J Pain 14, 663-675. doi:10.1016/j.jpain.2013.03.001

Smieskova, R., Fusar-Poli, P., Allen, P., Bendfeldt, K., Stieglitz, R.D., Drewe, J., Radue, E.W., McGuire, P.K., Riecher-Rössler, A., Borgwardt, S.J., 2010. Neuroimaging predictors of transition to psychosis--a systematic review and meta-analysis. Neuroscience and biobehavioral reviews 34, 1207-1222. doi:10.1016/j.neubiorev.2010.01.016

Smieskova, R., Marmy, J., Schmidt, A., Bendfeldt, K., Riecher-Rössler, A., Walter, M., Lang, U.E., Borgwardt, S., 2013. Do subjects at clinical high risk for psychosis differ from those with a genetic high risk?--A systematic review of structural and functional brain abnormalities. Current medicinal chemistry 20, 467-481. doi:10.2174/0929867311320030018

Smith, S.M., Beckmann, C.F., Ramnani, N., Woolrich, M.W., Bannister, P.R., Jenkinson, M., Matthews, P.M., McGonigle, D.J., 2005. Variability in fMRI: a re-examination of inter-session differences. Hum Brain Mapp 24, 248-257.

Smith, S.M., Fox, P.T., Miller, K.L., Glahn, D.C., Fox, P.M., Mackay, C.E., Filippini, N., Watkins, K.E., Toro, R., Laird, A.R., Beckmann, C.F., 2009. Correspondence of the brain's functional architecture during activation and rest. Proceedings of the National Academy of Sciences of the United States of America 106, 13040-13045.

Smith, S.M., Miller, K.L., Salimi-Khorshidi, G., Webster, M., Beckmann, C.F., Nichols, T.E., Ramsey, J.D., Woolrich, M.W., 2011. Network modelling methods for FMRI. Neuroimage 54, 875-891. doi:10.1016/j.neuroimage.2010.08.063

Spalletta, G., De Rossi, P., Piras, F., Iorio, M., Dacquino, C., Scanu, F., Girardi, P., Caltagirone, C., Kirkpatrick, B., Chiapponi, C., 2015. Brain white matter microstructure in deficit and non-deficit subtypes of schizophrenia. Psychiatry research 231, 252-261. doi:10.1016/j.pscychresns.2014.12.006

Spalthoff, R., Gaser, C., Nenadic, I., 2018. Altered gyrification in schizophrenia and its relation to other morphometric markers. Schizophrenia research 202, 195-202. doi:10.1016/j.schres.2018.07.014

Spreng, R.N., DuPre, E., Ji, J.L., Yang, G., Diehl, C., Murray, J.D., Pearlson, G.D., Anticevic, A., 2019. Structural Covariance Reveals Alterations in Control and Salience Network Integrity in Chronic Schizophrenia. Cerebral cortex (New York, N.Y. : 1991) 29, 5269-5284. doi:10.1093/cercor/bhz064

Sprooten, E., Rasgon, A., Goodman, M., Carlin, A., Leibu, E., Lee, W.H., Frangou, S., 2017. Addressing reverse inference in psychiatric neuroimaging: Meta-analyses of task-related brain activation in common mental disorders. Hum Brain Mapp 38, 1846-1864. doi:10.1002/hbm.23486

Sporns, O., 2013. The human connectome: origins and challenges. Neuroimage 80, 53-61. doi:10.1016/j.neuroimage.2013.03.023

Sporns, O., Honey, C.J., Kötter, R., 2007. Identification and classification of hubs in brain networks. PLoS One 2, e1049. doi:10.1371/journal.pone.0001049

Sporns, O., Tononi, G., Kötter, R., 2005. The human connectome: a structural description of the human brain. PLoS computational biology 1, e42. doi:10.1371/journal.pcbi.0010042

Stam, C.J., 2014. Modern network science of neurological disorders. Nat Rev Neurosci 15, 683-695. doi:10.1038/nrn3801

Steinbrink, C., Vogt, K., Kastrup, A., Müller, H.P., Juengling, F.D., Kassubek, J., Riecker, A., 2008. The contribution of white and gray matter differences to developmental dyslexia: insights from DTI and VBM at 3.0 T. Neuropsychologia 46, 3170-3178. doi:10.1016/j.neuropsychologia.2008.07.015

Stevens, F.L., Hurley, R.A., Taber, K.H., 2011. Anterior cingulate cortex: unique role in cognition and emotion. J Neuropsychiatry Clin Neurosci 23, 121-125. doi:10.1176/jnp.23.2.jnp121

Stoodley, C.J., 2014. Distinct regions of the cerebellum show gray matter decreases in autism, ADHD, and developmental dyslexia. Frontiers in Systems Neuroscience 8. doi:10.3389/fnsys.2014.00092

Stoodley, C.J., 2016. The Cerebellum and Neurodevelopmental Disorders. Cerebellum (London, England) 15, 34-37. doi:10.1007/s12311-015-0715-3

Su, G., Morris, J.H., Demchak, B., Bader, G.D., 2014. Biological network exploration with Cytoscape 3. Curr Protoc Bioinformatics 47, 8.13.11-24. doi:10.1002/0471250953.bi0813s47

Sugranyes, G., de la Serna, E., Romero, S., Sanchez-Gistau, V., Calvo, A., Moreno, D., Baeza, I., Diaz-Caneja, C.M., Sanchez-Gutierrez, T., Janssen, J., Bargallo, N., Castro-Fornieles, J., 2015. Gray Matter Volume Decrease Distinguishes Schizophrenia From Bipolar Offspring During Childhood and Adolescence. Journal of the American Academy of Child and Adolescent Psychiatry 54, 677-684.e672. doi:10.1016/j.jaac.2015.05.003

Sugranyes, G., Kyriakopoulos, M., Dima, D., O'Muircheartaigh, J., Corrigall, R., Pendelbury, G., Hayes, D., Calhoun, V.D., Frangou, S., 2012. Multimodal analyses identify linked functional and white matter abnormalities within the working memory network in schizophrenia. Schizophrenia research 138, 136-142. doi:10.1016/j.schres.2012.03.011

Sun, Y., Chen, Y., Collinson, S.L., Bezerianos, A., Sim, K., 2015. Reduced Hemispheric Asymmetry of Brain Anatomical Networks Is Linked to Schizophrenia: A Connectome Study. Cerebral Cortex 27, 602-615. doi:10.1093/cercor/bhv255

Supekar, K., Menon, V., 2015. Sex differences in structural organization of motor systems and their dissociable links with repetitive/restricted behaviors in children with autism. Molecular autism 6, 50. doi:10.1186/s13229-015-0042-z

Sutcubasi Kaya, B., Metin, B., Tas, Z.C., Buyukaslan, A., Soysal, A., Hatiloglu, D., Tarhan, N., 2018. Gray Matter Increase in Motor Cortex in Pediatric ADHD: A Voxel-Based Morphometry Study. J Atten Disord 22, 611-618. doi:10.1177/1087054716659139

Szucs, D., Ioannidis, J.P., 2020. Sample size evolution in neuroimaging research: An evaluation of highly-cited studies (1990-2012) and of latest practices (2017-2018) in high-impact journals. Neuroimage 221, 117164. doi:10.1016/j.neuroimage.2020.117164

Tahmasian, M., Sepehry, A.A., Samea, F., Khodadadifar, T., Soltaninejad, Z., Javaheripour, N., Khazaie, H., Zarei, M., Eickhoff, S.B., Eickhoff, C.R., 2019. Practical recommendations to conduct a neuroimaging meta-analysis for neuropsychiatric disorders. Human brain mapping. doi:10.1002/hbm.24746

Takahashi, T., Suzuki, M., 2018. Brain morphologic changes in early stages of psychosis: Implications for clinical application and early intervention. Psychiatry and clinical neurosciences 72, 556-571. doi:10.1111/pcn.12670

Takayanagi, Y., Kulason, S., Sasabayashi, D., Takahashi, T., Katagiri, N., Sakuma, A., Obara, C., Nakamura, M., Kido, M., Furuichi, A., Nishikawa, Y., Noguchi, K., Matsumoto, K., Mizuno, M., Ratnanather, J.T., Suzuki, M., 2017. Reduced Thickness of the Anterior Cingulate Cortex in Individuals With an At-Risk Mental State Who Later Develop Psychosis. Schizophrenia bulletin 43, 907-913. doi:10.1093/schbul/sbw167

Talairach, J., Tournoux, P., 1988. Co-planar stereotaxic atlas of the human brain. Thieme, New York.

Tamboer, P., Scholte, H.S., Vorst, H.C., 2015. Dyslexia and voxel-based morphometry: correlations between five behavioural measures of dyslexia and gray and white matter volumes. Annals of dyslexia 65, 121-141. doi:10.1007/s11881-015-0102-2

Tan, S., Zhao, Y., Fan, F., Zou, Y., Jin, Z., Zen, Y., Zhu, X., Yang, F., Tan, Y., Zhou, D., 2015. Brain Correlates of Self-Evaluation Deficits in Schizophrenia: A Combined Functional and Structural MRI Study. PloS one 10, e0138737. doi:10.1371/journal.pone.0138737

Tanaka, M., Spekker, E., Szabó, Á., Polyák, H., Vécsei, L., 2022. Modelling the neurodevelopmental pathogenesis in neuropsychiatric disorders. Bioactive kynurenines and their analogues as neuroprotective agents-in celebration of 80th birthday of Professor Peter Riederer. Journal of neural transmission (Vienna, Austria : 1996) 129, 627-642. doi:10.1007/s00702-022-02513-5

Tanaka, M., Tóth, F., Polyák, H., Szabó, Á., Mándi, Y., Vécsei, L., 2021. Immune Influencers in Action: Metabolites and Enzymes of the Tryptophan-Kynurenine Metabolic Pathway. Biomedicines 9, 734.

Tang, J., Liao, Y., Zhou, B., Tan, C., Liu, W., Wang, D., Liu, T., Hao, W., Tan, L., Chen, X., 2012. Decrease in temporal gyrus gray matter volume in first-episode, early onset schizophrenia: an MRI study. PloS one 7, e40247. doi:10.1371/journal.pone.0040247

Tardif, C.L., Collins, D.L., Pike, G.B., 2009. Sensitivity of voxel-based morphometry analysis to choice of imaging protocol at 3 T. Neuroimage 44, 827-838. doi:10.1016/j.neuroimage.2008.09.053

Tardif, C.L., Collins, D.L., Pike, G.B., 2010. Regional impact of field strength on voxel-based morphometry results. Hum Brain Mapp 31, 943-957. doi:10.1002/hbm.20908

Tatu, K., Costa, T., Nani, A., Diano, M., Quarta, D.G., Duca, S., Apkarian, A.V., Fox, P.T., Cauda, F., 2018. How do morphological alterations caused by chronic pain distribute across the brain? A meta-analytic co-alteration study. NeuroImage: Clinical 18, 15-30. doi:10.1016/j.nicl.2017.12.029

The ADHD-200 Consortium, 2012. The ADHD-200 Consortium: A Model to Advance the Translational Potential of Neuroimaging in Clinical Neuroscience. Front Syst Neurosci 6, 62. doi:10.3389/fnsys.2012.00062

Thomas, M.S.C., Davis, R., Karmiloff-Smith, A., Knowland, V.C.P., Charman, T., 2016. The over-pruning hypothesis of autism. Dev Sci 19, 284-305. doi:10.1111/desc.12303

Tench, C.R., Tanasescu, R., Constantinescu, C.S., Auer, D.P., Cottam, W.J., 2022. Easy to interpret coordinate based meta-analysis of neuroimaging studies: Analysis of brain coordinates (ABC). Journal of neuroscience methods 372, 109556.

Tian, L., Meng, C., Yan, H., Zhao, Q., Liu, Q., Yan, J., Han, Y., Yuan, H., Wang, L., Yue, W., Zhang, Y., Li, X., Zhu, C., He, Y., Zhang, D., 2011. Convergent evidence from multimodal imaging reveals amygdala abnormalities in schizophrenic patients and their first-degree relatives. PloS one 6, e28794. doi:10.1371/journal.pone.0028794

Thompson, P.M., Stein, J.L., Medland, S.E., Hibar, D.P., Vasquez, A.A., Renteria, M.E., Toro, R., Jahanshad, N., Schumann, G., Franke, B., Wright, M.J., Martin, N.G., Agartz, I., Alda, M., Alhusaini, S., Almasy, L., Almeida, J., Alpert, K., Andreasen, N.C., Andreassen,

O.A., Apostolova, L.G., Appel, K., Armstrong, N.J., Aribisala, B., Bastin, M.E., Bauer, M., Bearden, C.E., Bergmann, O., Binder, E.B., Blangero, J., Bockholt, H.J., Bøen, E., Bois, C., Boomsma, D.I., Booth, T., Bowman, I.J., Bralten, J., Brouwer, R.M., Brunner, H.G., Brohawn, D.G., Buckner, R.L., Buitelaar, J., Bulayeva, K., Bustillo, J.R., Calhoun, V.D., Cannon, D.M., Cantor, R.M., Carless, M.A., Caseras, X., Cavalleri, G.L., Chakravarty, M.M., Chang, K.D., Ching, C.R., Christoforou, A., Cichon, S., Clark, V.P., Conrod, P., Coppola, G., Crespo-Facorro, B., Curran, J.E., Czisch, M., Deary, I.J., de Geus, E.J., den Braber, A., Delvecchio, G., Depondt, C., de Haan, L., de Zubicaray, G.I., Dima, D., Dimitrova, R., Djurovic, S., Dong, H., Donohoe, G., Duggirala, R., Dyer, T.D., Ehrlich, S., Ekman, C.J., Elvsåshagen, T., Emsell, L., Erk, S., Espeseth, T., Fagerness, J., Fears, S., Fedko, I., Fernández, G., Fisher, S.E., Foroud, T., Fox, P.T., Francks, C., Frangou, S., Frey, E.M., Frodl, T., Frouin, V., Garavan, H., Giddaluru, S., Glahn, D.C., Godlewska, B., Goldstein, R.Z., Gollub, R.L., Grabe, H.J., Grimm, O., Gruber, O., Guadalupe, T., Gur, R.E., Gur, R.C., Göring, H.H., Hagenaars, S., Hajek, T., Hall, G.B., Hall, J., Hardy, J., Hartman, C.A., Hass, J., Hatton, S.N., Haukvik, U.K., Hegenscheid, K., Heinz, A., Hickie, I.B., Ho, B.C., Hoehn, D., Hoekstra, P.J., Hollinshead, M., Holmes, A.J., Homuth, G., Hoogman, M., Hong, L.E., Hosten, N., Hottenga, J.J., Hulshoff Pol, H.E., Hwang, K.S., Jack, C.R., Jr., Jenkinson, M., Johnston, C., Jönsson, E.G., Kahn, R.S., Kasperaviciute, D., Kelly, S., Kim, S., Kochunov, P., Koenders, L., Krämer, B., Kwok, J.B., Lagopoulos, J., Laje, G., Landen, M., Landman, B.A., Lauriello, J., Lawrie, S.M., Lee, P.H., Le Hellard, S., Lemaître, H., Leonardo, C.D., Li, C.S., Liberg, B., Liewald, D.C., Liu, X., Lopez, L.M., Loth, E., Lourdusamy, A., Luciano, M., Macciardi, F., Machielsen, M.W., Macqueen, G.M., Malt, U.F., Mandl, R., Manoach, D.S., Martinot, J.L., Matarin, M., Mather, K.A., Mattheisen, M., Mattingsdal, M., Meyer-Lindenberg, A., McDonald, C., McIntosh, A.M., McMahon, F.J., McMahon, K.L., Meisenzahl, E., Melle, I., Milaneschi, Y., Mohnke, S., Montgomery, G.W., Morris, D.W., Moses, E.K., Mueller, B.A., Muñoz Maniega, S., Mühleisen, T.W., Müller-Myhsok, B., Mwangi, B., Nauck, M., Nho, K., Nichols, T.E., Nilsson, L.G., Nugent, A.C., Nyberg, L., Olvera, R.L., Oosterlaan, J., Ophoff, R.A., Pandolfo, M., Papalampropoulou-Tsiridou, M., Papmeyer, M., Paus, T., Pausova, Z., Pearlson, G.D., Penninx, B.W., Peterson, C.P., Pfennig, A., Phillips, M., Pike, G.B., Poline, J.B., Potkin, S.G., Pütz, B., Ramasamy, A., Rasmussen, J., Rietschel, M., Rijpkema, M., Risacher, S.L., Roffman, J.L., Roiz-Santiañez, R., Romanczuk-Seiferth, N., Rose, E.J., Royle, N.A., Rujescu, D., Ryten, M., Sachdev, P.S.,

Salami, A., Satterthwaite, T.D., Savitz, J., Saykin, A.J., Scanlon, C., Schmaal, L., Schnack, H.G., Schork, A.J., Schulz, S.C., Schür, R., Seidman, L., Shen, L., Shoemaker, J.M., Simmons, A., Sisodiya, S.M., Smith, C., Smoller, J.W., Soares, J.C., Sponheim, S.R., Sprooten, E., Starr, J.M., Steen, V.M., Strakowski, S., Strike, L., Sussmann, J., Sämann, P.G., Teumer, A., Toga, A.W., Tordesillas-Gutierrez, D., Trabzuni, D., Trost, S., Turner, J., Van den Heuvel, M., van der Wee, N.J., van Eijk, K., van Erp, T.G., van Haren, N.E., van 't Ent, D., van Tol, M.J., Valdés Hernández, M.C., Veltman, D.J., Versace, A., Völzke, H., Walker, R., Walter, H., Wang, L., Wardlaw, J.M., Weale, M.E., Weiner, M.W., Wen, W., Westlye, L.T., Whalley, H.C., Whelan, C.D., White, T., Winkler, A.M., Wittfeld, K., Woldehawariat, G., Wolf, C., Zilles, D., Zwiers, M.P., Thalamuthu, A., Schofield, P.R., Freimer, N.B., Lawrence, N.S., Drevets, W., 2014. The ENIGMA Consortium: large-scale collaborative analyses of neuroimaging and genetic data. Brain imaging and behavior 8, 153-182. doi:10.1007/s11682-013-9269-5

Toal, F., Daly, E.M., Page, L., Deeley, Q., Hallahan, B., Bloemen, O., Cutter, W.J., Brammer, M.J., Curran, S., Robertson, D., Murphy, C., Murphy, K.C., Murphy, D.G., 2010. Clinical and anatomical heterogeneity in autistic spectrum disorder: a structural MRI study. Psychological medicine 40, 1171-1181. doi:10.1017/s0033291709991541

Tomasi, D., Wang, G.J., Volkow, N.D., 2013. Energetic cost of brain functional connectivity. Proceedings of the National Academy of Sciences of the United States of America 110, 13642-13647.

Torres, U.S., Duran, F.L., Schaufelberger, M.S., Crippa, J.A., Louza, M.R., Sallet, P.C., Kanegusuku, C.Y., Elkis, H., Gattaz, W.F., Bassitt, D.P., Zuardi, A.W., Hallak, J.E., Leite, C.C., Castro, C.C., Santos, A.C., Murray, R.M., Busatto, G.F., 2016. Patterns of regional gray matter loss at different stages of schizophrenia: A multisite, cross-sectional VBM study in first-episode and chronic illness. NeuroImage. Clinical 12, 1-15. doi:10.1016/j.nicl.2016.06.002

Torres, U.S., Portela-Oliveira, E., Borgwardt, S., Busatto, G.F., 2013. Structural brain changes associated with antipsychotic treatment in schizophrenia as revealed by voxel-based morphometric MRI: an activation likelihood estimation meta-analysis. BMC psychiatry 13, 342. doi:10.1186/1471-244x-13-342

Torta, D.M., Costa, T., Duca, S., Fox, P.T., Cauda, F., 2013. Parcellation of the cingulate cortex at rest and during tasks: a meta-analytic clustering and experimental study. Front Hum Neurosci 7, 275. doi: 10.3389/fnhum.2013.00275

Trautmann, S., Rehm, J., Wittchen, H.-U., 2016. The economic costs of mental disorders. EMBO reports 17, 1245-1249.

Tregellas, J.R., Shatti, S., Tanabe, J.L., Martin, L.F., Gibson, L., Wylie, K., Rojas, D.C., 2007. Gray matter volume differences and the effects of smoking on gray matter in schizophrenia. Schizophrenia research 97, 242-249. doi:10.1016/j.schres.2007.08.019

Turkeltaub, P.E., Coslett, H.B., 2010. Localization of sublexical speech perception components. Brain and language 114, 1-15. doi:10.1016/j.bandl.2010.03.008

Turkeltaub, P.E., Eden, G.F., Jones, K.M., Zeffiro, T.A., 2002. Meta-analysis of the functional neuroanatomy of single-word reading: method and validation. Neuroimage 16, 765-780. doi:10.1006/nimg.2002.1131

Turkeltaub, P.E., Eickhoff, S.B., Laird, A.R., Fox, M., Wiener, M., Fox, P., 2012. Minimizing within-experiment and within-group effects in Activation Likelihood Estimation meta-analyses. Human brain mapping 33, 1-13. doi:10.1002/hbm.21186

Tu, P.C., Hsu, J.W., Lan, C.C., Liu, C.C., Su, T.P., Chen, Y.S., 2016. Structural and functional correlates of a quantitative autistic trait measured using the social responsive scale in neurotypical male adolescents. Autism research : official journal of the International Society for Autism Research 9, 570-578. doi:10.1002/aur.1535

Turkeltaub, P.E., Eden, G.F., Jones, K.M., Zeffiro, T.A., 2002. Meta-analysis of the functional neuroanatomy of single-word reading: method and validation. Neuroimage 16, 765-780.

Turner, K.C., Frost, L., Linsenbardt, D., McIlroy, J.R., Müller, R.-A., 2006. Atypically diffuse functional connectivity between caudate nuclei and cerebral cortex in autism. Behavioral and Brain Functions 2, 34. doi:10.1186/1744-9081-2-34

Tyrer, P., 2018. A comparison of DSM and ICD classifications of mental disorder. Advances in Psychiatric Treatment 20, 280-285.

Uddin, L.Q., 2015. Salience processing and insular cortical function and dysfunction. Nature reviews. Neuroscience 16, 55-61. doi:10.1038/nrn3857

Uddin, L.Q., Dajani, D.R., Voorhies, W., Bednarz, H., Kana, R.K., 2017. Progress and roadblocks in the search for brain-based biomarkers of autism and attention-deficit/hyperactivity disorder. Translational psychiatry 7, e1218. doi:10.1038/tp.2017.164

Uddin, L.Q., Menon, V., Young, C.B., Ryali, S., Chen, T., Khouzam, A., Minshew, N.J., Hardan, A.Y., 2011. Multivariate searchlight classification of structural magnetic resonance imaging in children and adolescents with autism. Biological psychiatry 70, 833-841. doi:10.1016/j.biopsych.2011.07.014

Uddin, L.Q., Supekar, K., Menon, V., 2013. Reconceptualizing functional brain connectivity in autism from a developmental perspective. Front Hum Neurosci 7. doi:10.3389/fnhum.2013.00458

Uddin, L.Q., Yeo, B.T.T., Spreng, R.N., 2019. Towards a Universal Taxonomy of Macro-scale Functional Human Brain Networks. Brain topography 32, 926-942. doi:10.1007/s10548-019-00744-6

Valente, T.W., Coronges, K., Lakon, C., Costenbader, E., 2008. How correlated are network centrality measures? Connections (Toronto, Ont.) 28, 16.

Valk, S.L., Di Martino, A., Milham, M.P., Bernhardt, B.C., 2015. Multicenter mapping of structural network alterations in autism. Hum Brain Mapp 36, 2364-2373. doi:10.1002/hbm.22776

Van den Eynde, F., Suda, M., Broadbent, H., Guillaume, S., Van den Eynde, M., Steiger, H., Israel, M., Berlim, M., Giampietro, V., Simmons, A., Treasure, J., Campbell, I., Schmidt, U., 2012. Structural magnetic resonance imaging in eating disorders: a systematic review of voxel-based morphometry studies. European eating disorders review : the journal of the Eating Disorders Association 20, 94-105. doi:10.1002/erv.1163

van den Heuvel, M.P., Mandl, R.C., Stam, C.J., Kahn, R.S., Hulshoff Pol, H.E., 2010. Aberrant frontal and temporal complex network structure in schizophrenia: a graph theoretical analysis. J Neurosci 30, 15915-15926. doi:10.1523/jneurosci.2874-10.2010

van den Heuvel, M.P., Sporns, O., 2011. Rich-club organization of the human connectome. The Journal of neuroscience : the official journal of the Society for Neuroscience 31, 15775-15786. doi:10.1523/JNEUROSCI.3539-11.2011

van den Heuvel, M.P., Sporns, O., 2013. Network hubs in the human brain. Trends Cogn Sci 17, 683-696. doi:10.1016/j.tics.2013.09.012

van den Heuvel, M.P., Sporns, O., 2019. A cross-disorder connectome landscape of brain dysconnectivity. Nat Rev Neurosci 20, 435-446. doi:10.1038/s41583-019-0177-6

Van Essen, D.C., Smith, S.M., Barch, D.M., Behrens, T.E., Yacoub, E., Ugurbil, K., 2013. The WU-Minn Human Connectome Project: an overview. Neuroimage 80, 62-79. doi:10.1016/j.neuroimage.2013.05.041

Van Overwalle, F., Manto, M., Cattaneo, Z., Clausi, S., Ferrari, C., Gabrieli, J.D.E., Guell, X., Heleven, E., Lupo, M., Ma, Q., Michelutti, M., Olivito, G., Pu, M., Rice, L.C., Schmahmann, J.D., Siciliano, L., Sokolov, A.A., Stoodley, C.J., van Dun, K., Vandervert, L., Leggio, M., 2020. Consensus Paper: Cerebellum and Social Cognition. Cerebellum (London, England) 19, 833-868. doi:10.1007/s12311-020-01155-1

van Wingen, G.A., van den Brink, W., Veltman, D.J., Schmaal, L., Dom, G., Booij, J., Crunelle, C.L., 2013. Reduced striatal brain volumes in non-medicated adult ADHD patients with comorbid cocaine dependence. Drug and alcohol dependence 131, 198-203. doi:10.1016/j.drugalcdep.2013.05.007

van Tol, M.J., van der Meer, L., Bruggeman, R., Modinos, G., Knegtering, H., Aleman, A., 2014. Voxel-based gray and white matter morphometry correlates of hallucinations in schizophrenia: The superior temporal gyrus does not stand alone. NeuroImage. Clinical 4, 249-257. doi:10.1016/j.nicl.2013.12.008

Vanasse, T.J., Fox, P.M., Barron, D.S., Robertson, M., Eickhoff, S.B., Lancaster, J.L., Fox, P.T., 2018. BrainMap VBM: An environment for structural meta-analysis. Human brain mapping 39, 3308-3325. doi:10.1002/hbm.24078

Vanasse, T.J., Fox, P.T., Fox, P.M., Cauda, F., Costa, T., Smith, S.M., Eickhoff, S.B., Lancaster, J.L., 2021. Brain pathology recapitulates physiology: A network meta-analysis. Communications Biology 4, 301. doi:10.1038/s42003-021-01832-9

Velakoulis, D., Wood, S.J., McGorry, P.D., Pantelis, C., 2000. Evidence for progression of brain structural abnormalities in schizophrenia: beyond the neurodevelopmental model. The Australian and New Zealand journal of psychiatry 34 Suppl, S113-126. doi:10.1080/000486700231

Velakoulis, D., Wood, S.J., Wong, M.T., McGorry, P.D., Yung, A., Phillips, L., Smith, D., Brewer, W., Proffitt, T., Desmond, P., Pantelis, C., 2006. Hippocampal and amygdala volumes according to psychosis stage and diagnosis: a magnetic resonance imaging study of chronic schizophrenia, first-episode psychosis, and ultra-high-risk individuals. Archives of general psychiatry 63, 139-149. doi:10.1001/archpsyc.63.2.139

Venkatasubramanian, G., 2010. Neuroanatomical correlates of psychopathology in antipsychotic-naive schizophrenia. Indian journal of psychiatry 52, 28-36. doi:10.4103/0019-5545.58892

Verly, M., Verhoeven, J., Zink, I., Mantini, D., Peeters, R., Deprez, S., Emsell, L., Boets, B., Noens, I., Steyaert, J., Lagae, L., De Cock, P., Rommel, N., Sunaert, S., 2014. Altered functional connectivity of the language network in ASD: role of classical language areas and cerebellum. Neuroimage Clin 4, 374-382. doi:10.1016/j.nicl.2014.01.008

Vértes, P.E., Rittman, T., Whitaker, K.J., Romero-Garcia, R., Váša, F., Kitzbichler, M.G., Wagstyl, K., Fonagy, P., Dolan, R.J., Jones, P.B., Goodyer, I.M., Bullmore, E.T., 2016. Gene transcription profiles associated with inter-modular hubs and connection distance in human functional magnetic resonance imaging networks. Philosophical Transactions of the Royal Society B: Biological Sciences 371, 20150362. doi: 10.1098/rstb.2015.0362

Via, E., Radua, J., Cardoner, N., Happe, F., Mataix-Cols, D., 2011. Meta-analysis of gray matter abnormalities in autism spectrum disorder: should Asperger disorder be subsumed under a broader umbrella of autistic spectrum disorder? Arch Gen Psychiatry 68, 409-418. doi:10.1001/archgenpsychiatry.2011.27

Vijayakumari, A.A., Thirunavukkarasu, P., Lukose, A., Arunachalam, V., Saini, J., Jain, S., Kutty, B.M., John, J.P., 2015. Exploration of the effect of demographic and clinical confounding variables on results of voxel-based morphometric analysis in schizophrenia, Artificial Intelligence and Evolutionary Algorithms in Engineering Systems. Springer, pp. 139-149. doi:10.1007/978-81-322-2126-5_16

Villemonteix, T., De Brito, S.A., Kavec, M., Balériaux, D., Metens, T., Slama, H., Baijot, S., Mary, A., Peigneux, P., Massat, I., 2015a. Grey matter volumes in treatment naïve vs. chronically treated children with attention deficit/hyperactivity disorder: a combined approach. European neuropsychopharmacology : the journal of the European College of Neuropsychopharmacology 25, 1118-1127. doi:10.1016/j.euroneuro.2015.04.015

Villemonteix, T., De Brito, S.A., Slama, H., Kavec, M., Balériaux, D., Metens, T., Baijot, S., Mary, A., Peigneux, P., Massat, I., 2015b. Grey matter volume differences associated with gender in children with attention-deficit/hyperactivity disorder: A voxel-based morphometry study. Developmental cognitive neuroscience 14, 32-37. doi:10.1016/j.dcn.2015.06.001

Vinckenbosch, E., Robichon, F., Eliez, S., 2005. Gray matter alteration in dyslexia: converging evidence from volumetric and voxel-by-voxel MRI analyses. Neuropsychologia 43, 324-331. doi:10.1016/j.neuropsychologia.2004.06.023

Vita, A., De Peri, L., Deste, G., Barlati, S., Sacchetti, E., 2015. The Effect of Antipsychotic Treatment on Cortical Gray Matter Changes in Schizophrenia: Does the Class Matter? A Meta-analysis and Meta-regression of Longitudinal Magnetic Resonance Imaging Studies. Biological psychiatry 78, 403-412. doi:10.1016/j.biopsych.2015.02.008

Vitolo, E., Tatu, M.K., Pignolo, C., Cauda, F., Costa, T., Ando, A., Zennaro, A., 2017. White matter and schizophrenia: A meta-analysis of voxel-based morphometry and diffusion tensor imaging studies. Psychiatry research. Neuroimaging 270, 8-21. doi:10.1016/j.pscychresns.2017.09.014

Voets, N.L., Hough, M.G., Douaud, G., Matthews, P.M., James, A., Winmill, L., Webster, P., Smith, S., 2008. Evidence for abnormalities of cortical development in adolescent-onset schizophrenia. NeuroImage 43, 665-675. doi:10.1016/j.neuroimage.2008.08.013

von dem Hagen, E.A., Stoyanova, R.S., Baron-Cohen, S., Calder, A.J., 2013. Reduced functional connectivity within and between 'social' resting state networks in autism spectrum conditions. Soc Cogn Affect Neurosci 8, 694-701. doi:10.1093/scan/nss053

Voormolen, E.H., Wei, C., Chow, E.W., Bassett, A.S., Mikulis, D.J., Crawley, A.P., 2010. Voxel-based morphometry and automated lobar volumetry: the trade-off between spatial scale and statistical correction. NeuroImage 49, 587-596. doi:10.1016/j.neuroimage.2009.07.018

Waiter, G.D., Williams, J.H., Murray, A.D., Gilchrist, A., Perrett, D.I., Whiten, A., 2004. A voxel-based investigation of brain structure in male adolescents with autistic spectrum disorder. Neuroimage 22, 619-625. doi:10.1016/j.neuroimage.2004.02.029

Wager, T.D., Atlas, L.Y., Botvinick, M.M., Chang, L.J., Coghill, R.C., Davis, K.D., Iannetti, G.D., Poldrack, R.A., Shackman, A.J., Yarkoni, T., 2016. Pain in the ACC? Proceedings of the National Academy of Sciences of the United States of America 113, E2474-2475. doi:10.1073/pnas.1600282113

Wager, T.D., Kang, J., Johnson, T.D., Nichols, T.E., Satpute, A.B., Barrett, L.F., 2015. A Bayesian model of category-specific emotional brain responses. PLoS Comput Biol 11, e1004066. doi:10.1371/journal.pcbi.1004066

Wager, T.D., Lindquist, M., Kaplan, L., 2007. Meta-analysis of functional neuroimaging data: current and future directions. Social cognitive and affective neuroscience 2, 150-158.

Wagshal, D., Knowlton, B.J., Cohen, J.R., Bookheimer, S.Y., Bilder, R.M., Fernandez, V.G., Asarnow, R.F., 2015. Cognitive correlates of gray matter abnormalities in adolescent siblings of patients with childhood-onset schizophrenia. Schizophrenia research 161, 345-350. doi:10.1016/j.schres.2014.12.006

Wang, C., Ji, F., Hong, Z., Poh, J.S., Krishnan, R., Lee, J., Rekhi, G., Keefe, R.S., Adcock, R.A., Wood, S.J., Fornito, A., Pasternak, O., Chee, M.W., Zhou, J., 2016. Disrupted salience network functional connectivity and white-matter microstructure in persons at risk for psychosis: findings from the LYRIKS study. Psychological medicine 46, 2771-2783. doi:10.1017/s0033291716001410

Wang, A.T., Dapretto, M., Hariri, A.R., Sigman, M., Bookheimer, S.Y., 2004. Neural correlates of facial affect processing in children and adolescents with autism spectrum disorder. Journal of the American Academy of Child and Adolescent Psychiatry 43, 481-490. doi:10.1097/00004583-200404000-00015

Wang, A.T., Lee, S.S., Sigman, M., Dapretto, M., 2007. Reading affect in the face and voice: neural correlates of interpreting communicative intent in children and adolescents with autism spectrum disorders. Arch Gen Psychiatry 64, 698-708. doi:10.1001/archpsyc.64.6.698

Wang, H., Ma, Z.H., Xu, L.Z., Yang, L., Ji, Z.Z., Tang, X.Z., Liu, J.R., Li, X., Cao, Q.J., Liu, J., 2022. Developmental brain structural atypicalities in autism: a voxel-based morphometry

analysis. Child and adolescent psychiatry and mental health 16, 7. doi:10.1186/s13034-022-00443-4

Wang, Q., Zhang, J., Liu, Z., Crow, T.J., Zhang, K., Palaniyappan, L., Li, M., Zhao, L., Li, X., Deng, W., Guo, W., Ma, X., Cheng, W., Ma, L., Wan, L., Lu, G., Liu, Z., Wang, J., Feng, J., Li, T., 2019. "Brain Connectivity Deviates by Sex and Hemisphere in the First Episode of Schizophrenia"-A Route to the Genetic Basis of Language and Psychosis? Schizophrenia bulletin 45, 484-494. doi:10.1093/schbul/sby061

Wang, J., Fu, K., Chen, L., Duan, X., Guo, X., Chen, H., Wu, Q., Xia, W., Wu, L., Chen, H., 2016a. Increased Gray Matter Volume and Resting-State Functional Connectivity in Somatosensory Cortex and their Relationship with Autistic Symptoms in Young Boys with Autism Spectrum Disorder. Frontiers in physiology 8, 588. doi:10.3389/fphys.2017.00588

Wang, J., Zhou, L., Cui, C., Liu, Z., Lu, J., 2017a. Gray matter morphological anomalies in the cerebellar vermis in first-episode schizophrenia patients with cognitive deficits. BMC psychiatry 17, 374. doi:10.1186/s12888-017-1543-4

Wang, L., Alpert, K.I., Calhoun, V.D., Cobia, D.J., Keator, D.B., King, M.D., Kogan, A., Landis, D., Tallis, M., Turner, M.D., Potkin, S.G., Turner, J.A., Ambite, J.L., 2016b. SchizConnect: Mediating neuroimaging databases on schizophrenia and related disorders for large-scale integration. Neuroimage 124, 1155-1167. doi:10.1016/j.neuroimage.2015.06.065

Wang, X., Cheng, B., Luo, Q., Qiu, L., Wang, S., 2018. Gray Matter Structural Alterations in Social Anxiety Disorder: A Voxel-Based Meta-Analysis. Frontiers in psychiatry 9. doi:10.3389/fpsyt.2018.00449

Wang, Y., David, O., Hu, X., Deshpande, G., 2017b. Can Patel's τ accurately estimate directionality of connections in brain networks from fMRI? Magnetic Resonance in Medicine 78, 2003-2010. doi: 10.1002/mrm.26583

Ward, A.M., Schultz, A.P., Huijbers, W., Van Dijk, K.R., Hedden, T., Sperling, R.A., 2014. The parahippocampal gyrus links the default-mode cortical network with the medial temporal lobe memory system. Hum Brain Mapp 35, 1061-1073. doi:10.1002/hbm.22234

Warren, J.D., Rohrer, J.D., Schott, J.M., Fox, N.C., Hardy, J., Rossor, M.N., 2013. Molecular nexopathies: a new paradigm of neurodegenerative disease. Trends Neurosci 36, 561-569.

Waszczuk, M.A., Eaton, N.R., Krueger, R.F., Shackman, A.J., Waldman, I.D., Zald, D.H., Lahey, B.B., Patrick, C.J., Conway, C.C., Ormel, J., Hyman, S.E., Fried, E.I., Forbes, M.K., Docherty, A.R., Althoff, R.R., Bach, B., Chmielewski, M., DeYoung, C.G., Forbush, K.T., Hallquist, M., Hopwood, C.J., Ivanova, M.Y., Jonas, K.G., Latzman, R.D., Markon, K.E., Mullins-Sweatt, S.N., Pincus, A.L., Reininghaus, U., South, S.C., Tackett, J.L., Watson, D., Wright, A.G.C., Kotov, R., 2020. Redefining phenotypes to advance psychiatric genetics: Implications from hierarchical taxonomy of psychopathology. Journal of abnormal psychology 129, 143-161. doi:10.1037/abn0000486

Watkins, K.E., Paus, T., Lerch, J.P., Zijdenbos, A., Collins, D.L., Neelin, P., Taylor, J., Worsley, K.J., Evans, A.C., 2001. Structural asymmetries in the human brain: a voxel-based statistical analysis of 142 MRI scans. Cerebral cortex (New York, N.Y. : 1991) 11, 868-877.

Watson, D.R., Anderson, J.M., Bai, F., Barrett, S.L., McGinnity, T.M., Mulholland, C.C., Rushe, T.M., Cooper, S.J., 2012. A voxel based morphometry study investigating brain structural changes in first episode psychosis. Behavioural brain research 227, 91-99. doi:10.1016/j.bbr.2011.10.034

Weiner, M.W., Veitch, D.P., Aisen, P.S., Beckett, L.A., Cairns, N.J., Green, R.C., Harvey, D., Jack Jr., C.R., Jagust, W., Morris, J.C., Petersen, R.C., Salazar, J., Saykin, A.J., Shaw, L.M., Toga, A.W., Trojanowski, J.Q., Initiative, A.s.D.N., 2017. The Alzheimer's Disease Neuroimaging Initiative 3: Continued innovation for clinical trial improvement. Alzheimer's & Dementia 13, 561-571. doi:10.1016/j.jalz.2016.10.006

Wegiel, J., Flory, M., Kuchna, I., Nowicki, K., Ma, S.Y., Imaki, H., Wegiel, J., Cohen, I.L., London, E., Brown, W.T., Wisniewski, T., 2014. Brain-region-specific alterations of the trajectories of neuronal volume growth throughout the lifespan in autism. Acta Neuropathol Commun 2, 28. doi:10.1186/2051-5960-2-28

Weng, S.J., Wiggins, J.L., Peltier, S.J., Carrasco, M., Risi, S., Lord, C., Monk, C.S., 2010. Alterations of resting state functional connectivity in the default network in adolescents with autism spectrum disorders. Brain research 1313, 202-214. doi:10.1016/j.brainres.2009.11.057

Whitely, M., 2015. Attention deficit hyperactive disorder diagnosis continues to fail the reliability and validity tests. Australian & New Zealand Journal of Psychiatry 49, 497-498. doi:10.1177/0004867415579921

Whitford, T.J., Farrow, T.F., Gomes, L., Brennan, J., Harris, A.W., Williams, L.M., 2005. Grey matter deficits and symptom profile in first episode schizophrenia. Psychiatry research 139, 229-238. doi:10.1016/j.pscychresns.2005.05.010

Whitwell, J.L., 2009. Voxel-based morphometry: an automated technique for assessing structural changes in the brain. The Journal of neuroscience : the official journal of the Society for Neuroscience 29, 9661-9664.

Williams, L.M., Rush, A.J., Koslow, S.H., Wisniewski, S.R., Cooper, N.J., Nemeroff, C.B., Schatzberg, A.F., Gordon, E., 2011. International Study to Predict Optimized Treatment for Depression (iSPOT-D), a randomized clinical trial: rationale and protocol. Trials 12, 4. doi:10.1186/1745-6215-12-4

Williams, Z.J., He, J.L., Cascio, C.J., Woynaroski, T.G., 2020. A Review of Decreased Sound Tolerance in Autism: Definitions, Phenomenology, and Potential Mechanisms. Neurosci Biobehav Rev. doi:10.1016/j.neubiorev.2020.11.030

Wilson, L.B., Tregellas, J.R., Hagerman, R.J., Rogers, S.J., Rojas, D.C., 2009. A voxel-based morphometry comparison of regional gray matter between fragile X syndrome and autism. Psychiatry research 174, 138-145. doi:10.1016/j.pscychresns.2009.04.013

Winkler, A.M., Ridgway, G.R., Webster, M.A., Smith, S.M., Nichols, T.E., 2014. Permutation inference for the general linear model. NeuroImage 92, 381-397. doi:10.1016/j.neuroimage.2014.01.060

Witthaus, H., Kaufmann, C., Bohner, G., Ozgurdal, S., Gudlowski, Y., Gallinat, J., Ruhrmann, S., Brune, M., Heinz, A., Klingebiel, R., Juckel, G., 2009. Gray matter abnormalities in subjects at ultra-high risk for schizophrenia and first-episode schizophrenic patients compared to healthy controls. Psychiatry research 173, 163-169. doi:10.1016/j.pscychresns.2008.08.002

Wojtalik, J.A., Smith, M.J., Keshavan, M.S., Eack, S.M., 2017. A Systematic and Meta-analytic Review of Neural Correlates of Functional Outcome in Schizophrenia. Schizophrenia bulletin 43, 1329-1347. doi:10.1093/schbul/sbx008

Woo, C.W., Chang, L.J., Lindquist, M.A., Wager, T.D., 2017. Building better biomarkers: brain models in translational neuroimaging. Nature neuroscience 20, 365-377. doi:10.1038/nn.4478

Wood, S.J., Yung, A.R., McGorry, P.D., Pantelis, C., 2011. Neuroimaging and treatment evidence for clinical staging in psychotic disorders: from the at-risk mental state to chronic schizophrenia. Biological psychiatry 70, 619-625. doi:10.1016/j.biopsych.2011.05.034

Woodworth, D.C., Scambray, K.A., Phelan, M.J., Corrada, M.M., Kawas, C.H., Sajjadi, S.A., 2020. Distinct Patterns of Gray Matter Atrophy in Hippocampal Sclerosis of Aging and Alzheimer's Disease Neuropathology, 2020 Alzheimer's Association International Conference. ALZ.

Woodward, N.D., Cascio, C.J., 2015. Resting-State Functional Connectivity in Psychiatric Disorders. JAMA psychiatry 72, 743-744. doi:10.1001/jamapsychiatry.2015.0484

Worbe, Y., 2015. Neuroimaging signature of neuropsychiatric disorders. Curr Opin Neurol 28, 358-364. doi:10.1097/wco.0000000000000220

World Health Organization, 1992. The ICD-10 classification of mental and behavioural disorders : clinical descriptions and diagnostic guidelines. World Health Organization, Geneva.

Wright, I.C., McGuire, P.K., Poline, J.B., Travere, J.M., Murray, R.M., Frith, C.D., Frackowiak, R.S., Friston, K.J., 1995. A voxel-based method for the statistical analysis of gray and white matter density applied to schizophrenia. NeuroImage 2, 244-252. doi:10.1006/nimg.1995.1032

Wright, I.C., Rabe-Hesketh, S., Woodruff, P.W., David, A.S., Murray, R.M., Bullmore, E.T., 2000. Meta-analysis of regional brain volumes in schizophrenia. The American journal of psychiatry 157, 16-25. doi:10.1176/ajp.157.1.16

Wu, Y., Kang, R., Yan, Y., Gao, K., Li, Z., Jiang, J., Chi, X., Xia, L., 2018. Epidemiology of schizophrenia and risk factors of schizophrenia-associated aggression from 2011 to 2015. The Journal of international medical research 46, 4039-4049. doi:10.1177/0300060518786634

Wylie, K.P., Tregellas, J.R., 2010. The role of the insula in schizophrenia. Schizophrenia research 123, 93-104. doi:10.1016/j.schres.2010.08.027

Wylie, K.P., Tregellas, J.R., Bear, J.J., Legget, K.T., 2020. Autism Spectrum Disorder Symptoms are Associated with Connectivity Between Large-Scale Neural Networks and Brain Regions Involved in Social Processing. J Autism Dev Disord. doi:10.1007/s10803-020-04383-w

Xia, M., Wang, J., He, Y., 2013. BrainNet Viewer: a network visualization tool for human brain connectomics. PLoS One 8, e68910. doi:10.1371/journal.pone.0068910

Xia, Z., Hoeft, F., Zhang, L., Shu, H., 2016. Neuroanatomical anomalies of dyslexia: Disambiguating the effects of disorder, performance, and maturation. Neuropsychologia 81, 68-78. doi:10.1016/j.neuropsychologia.2015.12.003

Yahata, N., Kasai, K., Kawato, M., 2017. Computational neuroscience approach to biomarkers and treatments for mental disorders. Psychiatry Clin Neurosci 71, 215-237. doi:10.1111/pcn.12502

Yamada, M., Hirao, K., Namiki, C., Hanakawa, T., Fukuyama, H., Hayashi, T., Murai, T., 2007. Social cognition and frontal lobe pathology in schizophrenia: a voxel-based morphometric study. NeuroImage 35, 292-298. doi:10.1016/j.neuroimage.2006.10.046

Yan, H., Tian, L., Yan, J., Sun, W., Liu, Q., Zhang, Y.B., Li, X.M., Zang, Y.F., Zhang, D., 2012. Functional and anatomical connectivity abnormalities in cognitive division of anterior cingulate cortex in schizophrenia. PloS one 7, e45659. doi:10.1371/journal.pone.0045659

Yan, X., Jiang, K., Li, H., Wang, Z., Perkins, K., Cao, F., 2021. Convergent and divergent brain structural and functional abnormalities associated with developmental dyslexia. eLife 10. doi:10.7554/eLife.69523

Yang, P., Wang, P.N., Chuang, K.H., Jong, Y.J., Chao, T.C., Wu, M.T., 2008. Absence of gender effect on children with attention-deficit/hyperactivity disorder as assessed by optimized voxel-based morphometry. Psychiatry research 164, 245-253. doi:10.1016/j.pscychresns.2007.12.013

Yang, Q., Huang, P., Li, C., Fang, P., Zhao, N., Nan, J., Wang, B., Gao, W., Cui, L.B., 2018. Mapping alterations of gray matter volume and white matter integrity in children with autism spectrum disorder: evidence from fMRI findings. Neuroreport 29, 1188-1192. doi:10.1097/wnr.0000000000001094

Yang, Y.H., Yang, Y., Chen, B.G., Zhang, Y.W., Bi, H.Y., 2016. Anomalous Cerebellar Anatomy in Chinese Children with Dyslexia. Front Psychol 7, 324. doi:10.3389/fpsyg.2016.00324

Yang, Z.Y., Wang, S.K., Li, Y., Wang, Y., Wang, Y.M., Zhou, H.Y., Cai, X.L., Cheung, E.F.C., Shum, D.H.K., Ongur, D., Chan, R.C.K., 2019. Neural correlates of prospection

impairments in schizophrenia: Evidence from voxel-based morphometry analysis. Psychiatry research. Neuroimaging 293, 110987. doi:10.1016/j.pscychresns.2019.110987

Yankowitz, L.D., Yerys, B.E., Herrington, J.D., Pandey, J., Schultz, R.T., 2021. Dissociating regional gray matter density and gray matter volume in autism spectrum condition. NeuroImage: Clinical 32, 102888. doi:10.1016/j.nicl.2021.102888

Yarkoni, T., Poldrack, R.A., Nichols, T.E., Van Essen, D.C., Wager, T.D., 2011. Large-scale automated synthesis of human functional neuroimaging data. Nat Methods 8, 665-670. doi:10.1038/nmeth.1635

Yasuda, C.L., Betting, L.E., Cendes, F., 2010. Voxel-based morphometry and epilepsy. Expert review of neurotherapeutics 10, 975-984.

Yates, D., 2012. Neurodegenerative networking. Nature reviews. Neuroscience 13, 288. doi:10.1038/nrn3248

Yeh, F.C., Tseng, W.Y., 2011. NTU-90: a high angular resolution brain atlas constructed by q-space diffeomorphic reconstruction. Neuroimage 58, 91-99. doi:10.1016/j.neuroimage.2011.06.021

Yeh, F.C., Wedeen, V.J., Tseng, W.Y., 2010. Generalized q-sampling imaging. IEEE Trans Med Imaging 29, 1626-1635. doi:10.1109/tmi.2010.2045126

Yeo, B.T., Krienen, F.M., Sepulcre, J., Sabuncu, M.R., Lashkari, D., Hollinshead, M., Roffman, J.L., Smoller, J.W., Zollei, L., Polimeni, J.R., Fischl, B., Liu, H., Buckner, R.L., 2011. The organization of the human cerebral cortex estimated by intrinsic functional connectivity. J Neurophysiol 106, 1125-1165. doi:10.1152/jn.00338.2011

Yoshihara, Y., Sugihara, G., Matsumoto, H., Suckling, J., Nishimura, K., Toyoda, T., Isoda, H., Tsuchiya, K.J., Takebayashi, K., Suzuki, K., Sakahara, H., Nakamura, K., Mori, N., Takei, N., 2008. Voxel-based structural magnetic resonance imaging (MRI) study of patients with early onset schizophrenia. Annals of general psychiatry 7, 25. doi:10.1186/1744-859x-7-25

Yuan, B., Fang, Y., Han, Z., Song, L., He, Y., Bi, Y., 2017. Brain hubs in lesion models: Predicting functional network topology with lesion patterns in patients. Scientific reports 7, 17908. doi:10.1038/s41598-017-17886-x

Yung, A.R., Phillips, L.J., McGorry, P.D., McFarlane, C.A., Francey, S., Harrigan, S., Patton, G.C., Jackson, H.J., 1998. Prediction of psychosis. A step towards indicated prevention of schizophrenia. The British journal of psychiatry. Supplement 172, 14-20. doi:10.1192/S0007125000297602

Yung, A.R., Yuen, H.P., McGorry, P.D., Phillips, L.J., Kelly, D., Dell'Olio, M., Francey, S.M., Cosgrave, E.M., Killackey, E., Stanford, C., Godfrey, K., Buckby, J., 2005. Mapping the onset of psychosis: the Comprehensive Assessment of At-Risk Mental States. The Australian and New Zealand journal of psychiatry 39, 964-971. doi:10.1080/j.1440-1614.2005.01714.x

Zatorre, R.J., Fields, R.D., Johansen-Berg, H., 2012. Plasticity in gray and white: neuroimaging changes in brain structure during learning. Nature neuroscience 15, 528-536. doi:10.1038/nn.3045

Zhang, S., Li, C.S., 2012. Functional connectivity mapping of the human precuneus by resting state fMRI. Neuroimage 59, 3548-3562. doi:10.1016/j.neuroimage.2011.11.023

Zhang, Y., Zheng, J., Fan, X., Guo, X., Guo, W., Yang, G., Chen, H., Zhao, J., Lv, L., 2015. Dysfunctional resting-state connectivities of brain regions with structural deficits in drug-naive first-episode schizophrenia adolescents. Schizophrenia research 168, 353-359. doi:10.1016/j.schres.2015.07.031

Zhao, C., Zhu, J., Liu, X., Pu, C., Lai, Y., Chen, L., Yu, X., Hong, N., 2018. Structural and functional brain abnormalities in schizophrenia: A cross-sectional study at different stages of the disease. Progress in neuro-psychopharmacology & biological psychiatry 83, 27-32. doi:10.1016/j.pnpbp.2017.12.017

Zheng, K., Wang, H., Li, J., Yan, B., Liu, J., Xi, Y., Zhang, X., Yin, H., Tan, Q., Lu, H., Li, B., 2019. Structural networks analysis for depression combined with graph theory and the properties of fiber tracts via diffusion tensor imaging. Neurosci Lett 694, 34-40. doi:10.1016/j.neulet.2018.11.025

Zheng, W., Zhao, Z., Zhang, Z., Liu, T., Zhang, Y., Fan, J., Wu, D., 2020. Developmental pattern of the cortical topology in high-functioning individuals with autism spectrum disorder. Hum Brain Mapp n/a. doi:10.1002/hbm.25251

Zheng, Z., Zhang, L., Zhu, T., Huang, J., Qu, Y., Mu, D., 2016. Peripheral brain-derived neurotrophic factor in autism spectrum disorder: a systematic review and meta-analysis. Sci Rep 6, 31241. doi:10.1038/srep31241

Zhuo, C., Li, G., Lin, X., Jiang, D., Xu, Y., Tian, H., Wang, W., Song, X., 2019. The rise and fall of MRI studies in major depressive disorder. Translational psychiatry 9, 335. doi:10.1038/s41398-019-0680-6

Zhuo, C., Li, G., Lin, X., Jiang, D., Xu, Y., Tian, H., Wang, W., Song, X., 2021. Strategies to solve the reverse inference fallacy in future MRI studies of schizophrenia: a review. Brain imaging and behavior 15, 1115-1133. doi:10.1007/s11682-020-00284-9

Zhuo, C., Zhu, J., Wang, C., Qu, H., Ma, X., Tian, H., Liu, M., Qin, W., 2017. Brain structural and functional dissociated patterns in schizophrenia. BMC psychiatry 17, 45. doi:10.1186/s12888-017-1194-5

Zhou, J., Gennatas, E.D., Kramer, J.H., Miller, B.L., Seeley, W.W., 2012. Predicting regional neurodegeneration from the healthy brain functional connectome. Neuron 73, 1216-1227. doi:10.1016/j.neuron.2012.03.004

Zhou, X., Wu, R., Zeng, Y., Qi, Z., Ferraro, S., Xu, L., Zheng, X., Li, J., Fu, M., Yao, S., Kendrick, K.M., Becker, B., 2022. Choice of Voxel-based Morphometry processing pipeline drives variability in the location of neuroanatomical brain markers. Commun Biol 5, 913. doi:10.1038/s42003-022-03880-1

Zhou, Y., Shi, L., Cui, X., Wang, S., Luo, X., 2016. Functional Connectivity of the Caudal Anterior Cingulate Cortex Is Decreased in Autism. PLoS One 11, e0151879. doi:10.1371/journal.pone.0151879

Zielinski, B.A., Anderson, J.S., Froehlich, A.L., Prigge, M.B., Nielsen, J.A., Cooperrider, J.R., Cariello, A.N., Fletcher, P.T., Alexander, A.L., Lange, N., Bigler, E.D., Lainhart, J.E., 2012. scMRI reveals large-scale brain network abnormalities in autism. PLoS One 7, e49172. doi:10.1371/journal.pone.0049172

Zielinski, B.A., Prigge, M.B., Nielsen, J.A., Froehlich, A.L., Abildskov, T.J., Anderson, J.S., Fletcher, P.T., Zygmunt, K.M., Travers, B.G., Lange, N., Alexander, A.L., Bigler, E.D., Lainhart, J.E., 2014. Longitudinal changes in cortical thickness in autism and typical development. Brain : a journal of neurology 137, 1799-1812. doi:10.1093/brain/awu083

Zou, L., Ding, G., Abutalebi, J., Shu, H., Peng, D., 2012. Structural plasticity of the left caudate in bimodal bilinguals. Cortex; a journal devoted to the study of the nervous system and behavior 48, 1197-1206. doi:10.1016/j.cortex.2011.05.022